

# New therapeutic approaches for SARS-CoV-2/COVID-19

**Edited by**

Sergio Cimerman and Alfonso J. Rodriguez-Morales

**Coordinated by**

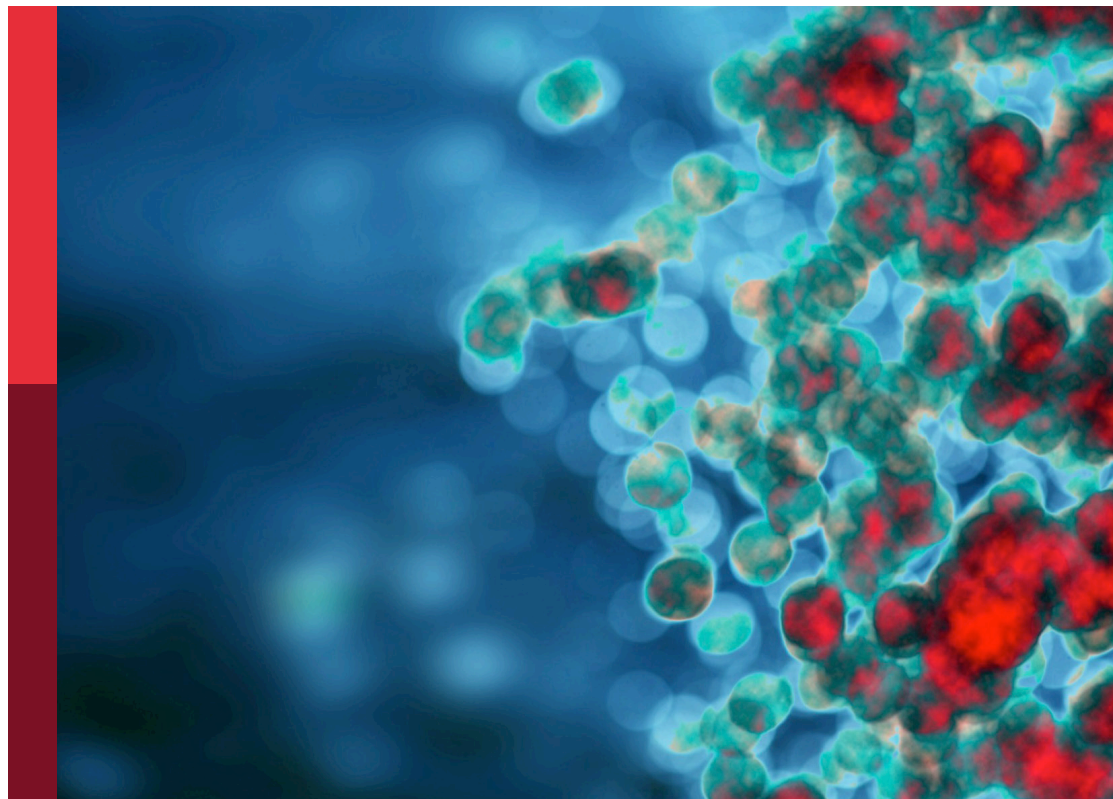
Alexandre Naime Barbosa

**Published in**

Frontiers in Immunology

Frontiers in Medicine

Frontiers in Physiology



## FRONTIERS EBOOK COPYRIGHT STATEMENT

The copyright in the text of individual articles in this ebook is the property of their respective authors or their respective institutions or funders. The copyright in graphics and images within each article may be subject to copyright of other parties. In both cases this is subject to a license granted to Frontiers.

The compilation of articles constituting this ebook is the property of Frontiers.

Each article within this ebook, and the ebook itself, are published under the most recent version of the Creative Commons CC-BY licence. The version current at the date of publication of this ebook is CC-BY 4.0. If the CC-BY licence is updated, the licence granted by Frontiers is automatically updated to the new version.

When exercising any right under the CC-BY licence, Frontiers must be attributed as the original publisher of the article or ebook, as applicable.

Authors have the responsibility of ensuring that any graphics or other materials which are the property of others may be included in the CC-BY licence, but this should be checked before relying on the CC-BY licence to reproduce those materials. Any copyright notices relating to those materials must be complied with.

Copyright and source acknowledgement notices may not be removed and must be displayed in any copy, derivative work or partial copy which includes the elements in question.

All copyright, and all rights therein, are protected by national and international copyright laws. The above represents a summary only. For further information please read Frontiers' Conditions for Website Use and Copyright Statement, and the applicable CC-BY licence.

ISSN 1664-8714  
ISBN 978-2-8325-3443-4  
DOI 10.3389/978-2-8325-3443-4

## About Frontiers

Frontiers is more than just an open access publisher of scholarly articles: it is a pioneering approach to the world of academia, radically improving the way scholarly research is managed. The grand vision of Frontiers is a world where all people have an equal opportunity to seek, share and generate knowledge. Frontiers provides immediate and permanent online open access to all its publications, but this alone is not enough to realize our grand goals.

## Frontiers journal series

The Frontiers journal series is a multi-tier and interdisciplinary set of open-access, online journals, promising a paradigm shift from the current review, selection and dissemination processes in academic publishing. All Frontiers journals are driven by researchers for researchers; therefore, they constitute a service to the scholarly community. At the same time, the *Frontiers journal series* operates on a revolutionary invention, the tiered publishing system, initially addressing specific communities of scholars, and gradually climbing up to broader public understanding, thus serving the interests of the lay society, too.

## Dedication to quality

Each Frontiers article is a landmark of the highest quality, thanks to genuinely collaborative interactions between authors and review editors, who include some of the world's best academicians. Research must be certified by peers before entering a stream of knowledge that may eventually reach the public - and shape society; therefore, Frontiers only applies the most rigorous and unbiased reviews. Frontiers revolutionizes research publishing by freely delivering the most outstanding research, evaluated with no bias from both the academic and social point of view. By applying the most advanced information technologies, Frontiers is catapulting scholarly publishing into a new generation.

## What are Frontiers Research Topics?

Frontiers Research Topics are very popular trademarks of the *Frontiers journals series*: they are collections of at least ten articles, all centered on a particular subject. With their unique mix of varied contributions from Original Research to Review Articles, Frontiers Research Topics unify the most influential researchers, the latest key findings and historical advances in a hot research area.

Find out more on how to host your own Frontiers Research Topic or contribute to one as an author by contacting the Frontiers editorial office: [frontiersin.org/about/contact](https://frontiersin.org/about/contact)



# New therapeutic approaches for SARS-CoV-2/COVID-19

## Topic editors

Sergio Cimerman — Institute of Infectology Emilio Ribas, Brazil  
Alfonso J. Rodriguez-Morales — Fundacion Universitaria Autónoma de las Américas, Colombia

## Topic Coordinator

Alexandre Naime Barbosa — São Paulo State University, Brazil

## Citation

Cimerman, S., Rodriguez-Morales, A. J., Barbosa, A. N., eds. (2023). *New therapeutic approaches for SARS-CoV-2/COVID-19*. Lausanne: Frontiers Media SA. doi: 10.3389/978-2-8325-3443-4

# Table of contents

- 05 **Editorial: New therapeutic approaches for SARS-CoV-2/COVID-19**  
Alfonso J. Rodriguez-Morales, Alexandre Naime Barbosa and Sergio Cimerman
- 09 **The efficiency of convalescent plasma in COVID-19 patients: A systematic review and meta-analysis of randomized controlled clinical trials**  
Zhenbei Qian, Zhijin Zhang, Haomiao Ma, Shuai Shao, Hanyujie Kang and Zhaohui Tong
- 23 **Interferon  $\alpha$ -2b spray shortened viral shedding time of SARS-CoV-2 Omicron variant: An open prospective cohort study**  
Nan Xu, Jinjin Pan, Li Sun, Cuimei Zhou, Siran Huang, Mingwei Chen, Junfei Zhang, Tiantian Zhu, Jiabin Li, Hong Zhang and Yufeng Gao
- 31 **Identifying potential pharmacological targets and mechanisms of vitamin D for hepatocellular carcinoma and COVID-19**  
Yongbiao Huang, Ye Yuan, Sheng Chen, Duo Xu, Lingyan Xiao, Xi Wang, Wan Qin and Bo Liu
- 45 **Discovering common pathogenetic processes between COVID-19 and sepsis by bioinformatics and system biology approach**  
Lu Lu, Le-Ping Liu, Rong Gui, Hang Dong, Yan-Rong Su, Xiong-Hui Zhou and Feng-Xia Liu
- 65 **A GABA-receptor agonist reduces pneumonitis severity, viral load, and death rate in SARS-CoV-2-infected mice**  
Jide Tian, Barbara J. Dillion, Jill Henley, Lucio Comai and Daniel L. Kaufman
- 78 **Circular RNAs as emerging regulators in COVID-19 pathogenesis and progression**  
Xiaojun Gao, Dan Fang, Yu Liang, Xin Deng, Ni Chen, Min Zeng and Mao Luo
- 97 **Cellular stress modulates severity of the inflammatory response in lungs *via* cell surface BiP**  
Gustavo Rico-Llanos, Óscar Porras-Perales, Sandra Escalante, Daniel B. Vázquez-Calero, Lucía Valiente, María I. Castillo, José Miguel Pérez-Tejeiro, David Baglietto-Vargas, José Becerra, José María Reguera, Ivan Duran and Fabiana Csukasi
- 114 **Oral GS-441524 derivatives: Next-generation inhibitors of SARS-CoV-2 RNA-dependent RNA polymerase**  
Zhonglei Wang, Liyan Yang and Xian-qing Song
- 130 **Computer-aided drug design combined network pharmacology to explore anti-SARS-CoV-2 or anti-inflammatory targets and mechanisms of Qingfei Paidu Decoction for COVID-19**  
Zixuan Wang, Jiuyu Zhan and Hongwei Gao

- 148 **Insights from comparison of the clinical presentation and outcomes of patients hospitalized with COVID-19 in an Italian internal medicine ward during first and third wave**  
Andrea Ticinesi, Alberto Parise, Antonio Nouvenne, Nicoletta Cerundolo, Beatrice Prati, Angela Guerra, Domenico Tuttolomondo, Nicola Gaibazzi and Tiziana Meschi
- 155 **Pharmacological potential of *Withania somnifera* (L.) Dunal and *Tinospora cordifolia* (Willd.) Miers on the experimental models of COVID-19, T cell differentiation, and neutrophil functions**  
Zaigham Abbas Rizvi, Prabhakar Babele, Upasna Madan, Srikanth Sadhu, Manas Ranjan Tripathy, Sandeep Goswami, Shailendra Mani, Madhu Dikshit and Amit Awasthi
- 175 **Novel ACE2 fusion protein with adapting activity against SARS-CoV-2 variants *in vitro***  
Latifa Zekri, Natalia Ruetalo, Mary Christie, Carolin Walker, Timo Manz, Hans-Georg Rammensee, Helmut R. Salih, Michael Schindler and Gundram Jung
- 184 **Tocilizumab-coated solid lipid nanoparticles loaded with cannabidiol as a novel drug delivery strategy for treating COVID-19: A review**  
Aleksandra Zielińska, Piotr Eder, Jacek Karczewski, Marlena Szalata, Szymon Hryhorowicz, Karolina Wielgus, Milena Szalata, Agnieszka Dobrowolska, Atanas G. Atanasov, Ryszard Słomski and Eliana B. Souto
- 204 **Bioinformatics and system biology approach to identify the influences among COVID-19, ARDS and sepsis**  
Peiyu Li, Tao Li, Zhiming Zhang, Xingui Dai, Bin Zeng, Zhen Li and Zhiwang Li
- 218 **Construction and application of prone position ventilation management scheme for severe COVID-19 patients**  
Xiuwen Chen, Cao Peng, Yao Xiao and Shiqing Liu
- 226 **SARS-CoV-2 neutralizing antibody bebtelovimab – a systematic scoping review and meta-analysis**  
Mabel Nyit Yi Liew, Kok Pim Kua, Shaun Wen Huey Lee and Kon Ken Wong



## OPEN ACCESS

EDITED AND REVIEWED BY

Pei-Hui Wang,  
Shandong University, China

\*CORRESPONDENCE

Alfonso J. Rodriguez-Morales  
✉ arodriguezmo@cientifica.edu.pe

RECEIVED 11 August 2023

ACCEPTED 18 August 2023

PUBLISHED 24 August 2023

## CITATION

Rodriguez-Morales AJ, Barbosa AN  
and Cimerman S (2023) Editorial:  
New therapeutic approaches  
for SARS-CoV-2/COVID-19.  
*Front. Immunol.* 14:1276279.  
doi: 10.3389/fimmu.2023.1276279

## COPYRIGHT

© 2023 Rodriguez-Morales, Barbosa and  
Cimerman. This is an open-access article  
distributed under the terms of the [Creative  
Commons Attribution License \(CC BY\)](#). The  
use, distribution or reproduction in other  
forums is permitted, provided the original  
author(s) and the copyright owner(s) are  
credited and that the original publication in  
this journal is cited, in accordance with  
accepted academic practice. No use,  
distribution or reproduction is permitted  
which does not comply with these terms.

# Editorial: New therapeutic approaches for SARS-CoV-2/COVID-19

Alfonso J. Rodriguez-Morales<sup>1,2\*</sup>, Alexandre Naime Barbosa<sup>3</sup>  
and Sergio Cimerman<sup>4</sup><sup>1</sup>Clinical Epidemiology and Biostatistics, Faculty of Health Sciences, Universidad Científica del Sur, Lima, Peru, <sup>2</sup>Gilbert and Rose-Marie Chagoury School of Medicine, Lebanese American University, Beirut, Lebanon, <sup>3</sup>Infectious Diseases Department, Botucatu School of Medicine, UNESP, Botucatu, Brazil, <sup>4</sup>Institute of Infectious Diseases Emilio Ribas, São Paulo, Brazil

## KEYWORDS

SARS-CoV-2, COVID-19, emerging, coronavirus, emerging infectious diseases, global health, therapy, pandemic

## Editorial on the Research Topic

## New therapeutic approaches for SARS-CoV-2/COVID-19

After three years and a half since the pandemic due to the Severe Acute Respiratory Syndrome coronavirus 2 (SARS-CoV-2) causing Coronavirus Disease 2019 (COVID-19) started (1), there has been an enormous impact in terms of morbidity and mortality due to this emerging pathogen (2). Up to August 9, 2023, there have been more than 769.37 million cases, with 6.95 million deaths, as reported to the World Health Organization (WHO) (Figure 1). Multiple advances during this time have been vital in controlling and ceasing the pandemic condition and the recent declaration to lift the international public health emergency in May 2023. One of them is undoubtedly related to the impact of preventing multiple outcomes (including deaths) of efficacious, safe and effective globally deployed vaccines against SARS-CoV-2 (3, 4). As of August 9, 2023, 13,492 million vaccine doses have been administered (Figure 1).

Although that cases of COVID-19 still occur, there is still a considerable risk to vulnerable populations presenting comorbidities, immunosuppression, and elderly, among other conditions prone to severe disease and even death, especially in low and middle-income countries (5–7). In addition, although for primary vaccination schemes, there was high vaccination coverage, especially in low and middle-income countries, subsequent boosters were less popular. Consequently, coverages for them (3<sup>rd</sup>, 4<sup>th</sup> and 5<sup>th</sup> doses) (8) were significantly lower compared to primary schemes (9). Even in Sub-Saharan Africa, such figures are worse. But also, in Latin America and Asia, there are multiple countries where 5<sup>th</sup> dose boosters are not yet available, despite the importance of the Omicron subvariants or lineages (Figure 1). Then, cases will continue and need medical management, including hospitalisation and sometimes admitting patients to the intensive care units for multiple reasons, requiring pharmaceutical evidence-based treatment (10, 11).

For those reasons, new efficacious, safe and effective therapeutical approaches for SARS-CoV-2/COVID-19 are still needed. In the current Research Topic (RT) about it, multiple studies and reviews unveiled different strategies for the management of infection

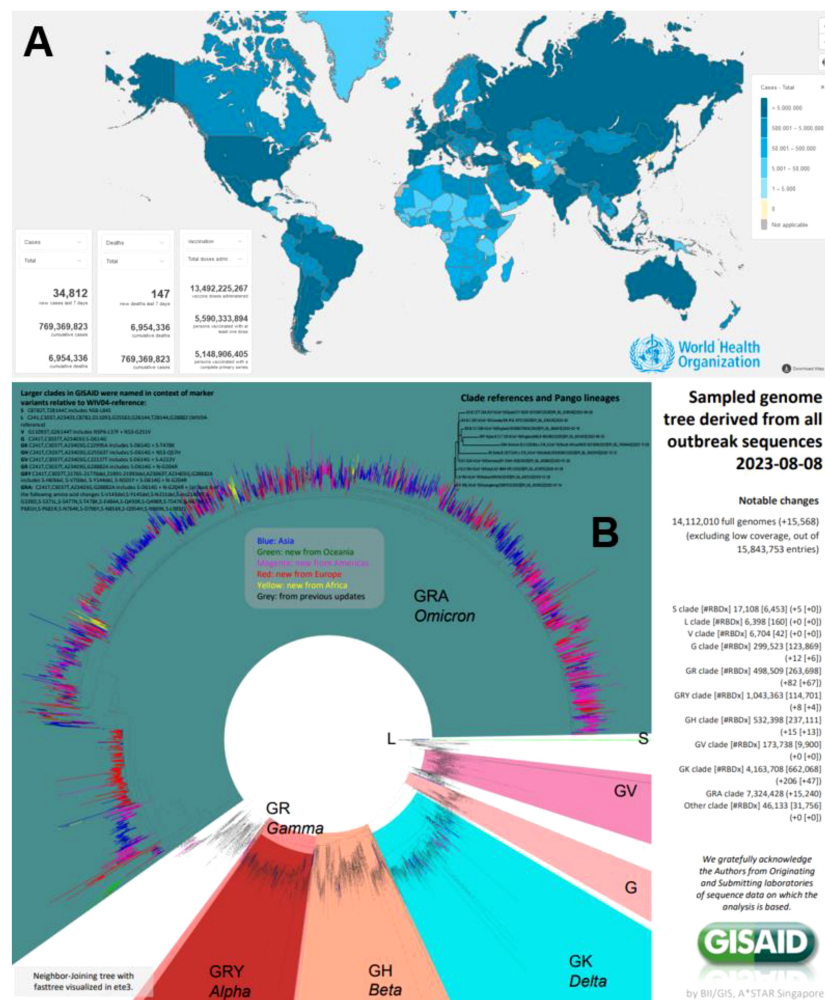


FIGURE 1

(A) COVID-19 global situation of cases, according to the WHO (<https://covid19.who.int/>). (B) Genomic distribution clades, lineages and variants of SARS-CoV-2 during 2020–2023 by GISAID (<https://gisaid.org/>).

and its associated complications. This RT includes 16 articles developed by authors from various countries (China, Germany, India, Italy, Malaysia, Poland, Spain, and the USA). Such articles covered original articles performing basic (Zekri et al.) and clinical studies (Ticinesi et al.), including animal models (Tian et al.), bioinformatics, observational and experimental designs (Wang Z. et al.), as well as systematic and scoping reviews, also with meta-analysis, during this Omicron times (Xu et al.). In addition to traditional therapeutic approaches, some of them discuss potential alternative therapies for COVID-19 (Rizvi et al.), primarily used in Asia (Wang Z. et al.), and also looking new potential pharmacological targets (Huang et al.). Focused on therapeutic potential, also some of the studies assess pathogenesis (Gao et al.) and physiopathological mechanisms (Lu et al.) related to different COVID-19 complications and therapeutic approaches (Liu et al.), performing comparisons with acute respiratory distress syndrome (ARDS) (Llanos et al.) and sepsis (Li et al.). Some studies focused on the usefulness of monoclonal antibodies (Liew et al.), including also new site-specific targeted drug delivery (Zielińska et al.).

Immunotherapies, such as convalescent plasma, are also included in this RT (Qian et al.).

The systematic review of Qian et al. from China on convalescent plasma for COVID-19 patients concluded that more double-blinded randomised clinical trials are needed to investigate the efficiency of convalescent plasma among patients in the initial stage of COVID-19, especially those who were within three days from symptoms onset and without detectable neutralising antibodies at enrolment.

Another systematic review on the topic, from Liew et al. from Malaysia and the USA concluded that the preclinical evidence suggests that bebtelovimab, a monoclonal antibody, would be a potential treatment for COVID-19 amidst viral evolution. Bebtlovimab has comparable efficacy to other COVID-19 therapies without evident safety concerns.

Another monoclonal antibody, tocilizumab, has been coated with solid lipid nanoparticles loaded with cannabidiol as a novel drug delivery strategy for treating COVID-19 and assessed in a review from Zielińska et al. from Poland, Bulgaria, Austria and Portugal.



Other immunomodulators, such as type I interferons (IFNs), inhibit the replication of both DNA and RNA viruses at different stages of their replication cycles and effect activating immune cell populations to clear infections; type I IFNs are directly antiviral agents and have been proposed for therapy in COVID-19. An open prospective cohort study from Xu et al. from China showed that IFN  $\alpha$ -2b spray shortened the viral shedding time of the Omicron SARS-CoV-2 variant when administrated within three days since the first positive test for SARS-CoV-2.

Further interventions, such as the gamma-aminobutyric acid (GABA)-receptor agonists, are promising, as an animal model in SARS-CoV-2-infected mice reduces pneumonitis severity, viral load, and death rate (Tian et al.), as shown by Tian et al. from USA.

At the molecular level, other articles assessing the expression and function of circular RNAs during severe acute COVID-19 showed their importance in the regulation of the inflammatory response, viral replication, immune evasion, and cytokines induced by SARS-CoV-2 infection (Gao et al.). An original study described the engineering of an optimised angiotensin-converting enzyme 2 (ACE2) fusion protein, designated ACE2-M, which comprises a human IgG1 Fc domain with abrogated Fc-receptor binding linked to a catalytically-inactive ACE2 extracellular domain that displays increased apparent affinity to the B.1 spike protein. The affinity and neutralisation capacity of ACE2-M is unaffected or even enhanced by mutations in the spike protein of viral variants. In contrast, a recombinant neutralising reference antibody and antibodies present in the sera of vaccinated individuals lose activity against such variants. With its potential to resist viral immune escape, ACE2-M appears to be particularly valuable in the context of pandemic preparedness towards newly emerging coronaviruses (Zekri et al.).

A review focused on oral GS-441524 derivatives (VV116, ATV006, and GS-621763; version 2.0, targeting highly conserved viral RdRp) that would be considered as game-changers in treating COVID-19 because oral administration has the potential to maximise clinical benefits, including decreased duration of COVID-19 and reduced post-acute sequelae of SARS-CoV-2 infection, as well as limited side effects such as hepatic accumulation (Wang Z. et al.). That review summarises the current research related to the oral derivatives of GS-441524 and provides essential insights into the potential factors underlying the controversial observations regarding the clinical efficacy of remdesivir; overall, it offers an effective launching pad for developing an oral version of GS-441524.

In physiopathology, original research investigated the role of cellular stress and binding-immunoglobulin protein (BiP) (Llanos et al.) in the modulation of the ARDS inflammatory response in samples from COVID-19 patients and a mouse model of ARDS. The authors demonstrate that BiP levels correlate with the severity of ARDS. Furthermore, they showed that the localisation of BiP on the cell surface is increased in the immune cell lineages during ARDS proportionally to the severity of the inflammatory response and identify a network of proteins that mediate this pathological process. Such results support using BiP as a prognosis biomarker of severe pneumonia and offer a new therapeutic strategy for diseases with ARDS, such as COVID-19.

ARDS is still a matter of concern in COVID-19 patients. Consequently, a bioinformatics study focused on understanding

the mutual differentially expressed genes (DEGs) for the patients with COVID-19, ARDS and sepsis for functional enrichment, pathway analysis, and candidate drugs analysis. Such candidate drugs in the study may contribute to effectively treating COVID-19 (Li et al.). Another similar bioinformatic study also reports similar findings. Based on enrichment analysis of common DEGs, many pathways closely related to inflammatory response were observed, such as the Cytokine-cytokine receptor interaction pathway and NF-kappa B signalling pathway. In addition, protein-protein interaction networks and gene regulatory networks of common DEGs were constructed, and the analysis results showed that the Integrin Subunit Alpha M (ITGAM) may be a potential key biomarker base on regulatory analysis. Furthermore, a disease diagnostic model and risk prediction nomogram for COVID-19 were constructed using machine learning methods. Finally, potential therapeutic agents, including progesterone and emetine, were screened through drug-protein interaction networks and molecular docking simulations (Lu et al.). Today, Computers are key in assessing potential therapies, including alternative medicine effects and traditional Chinese approaches. In another study, the authors used various network pharmacology methods combined with CADD techniques to reveal the diversity of potential targets and therapeutic pathways for QFPD against COVID-19. They found that RBP4, IL1RN, TTR, FYN, SFTPD, TP53, SRPK1, and AKT1 are highly related to COVID-19. QFPD could act on multiple pathways, including viral process, immunodeficiency, RNA polymerase, Sphingolipid signalling pathway, and taste transduction. The results showed that QFPD has “multi-component, multi-target, and multi-pathway” characteristics in regulating inflammation, viral infection, cellular damage, and immune responses (Wang Z. et al.).

Traditional but natural medicine also may provide potential therapeutic approaches. Because of this, an original study assessed the pharmacological potential of *Withania somnifera* (L.) Dunal (WS) and *Tinospora cordifolia* (Willd.) Miers on the experimental models of COVID-19, T cell differentiation, and neutrophil functions (Rizvi et al.). The results indicate that WS promoted the immunosuppressive environment in the hamster and hACE2 transgenic mice models and limited the worsening of the disease by reducing inflammation, suggesting that WS might be useful against other acute viral infections. That study thus provided preclinical efficacy data to demonstrate a robust protective effect of WS against COVID-19 through its broader immunomodulatory activity.

A molecular docking study (Huang et al.) showed that vitamin D possessed effective binding activity in COVID-19. Overall, the authors showed vitamin D's possible molecular mechanisms and pharmacological targets for treating COVID-19.

Finally, clinical studies are also included in the RT. One of them focused on comparing the characteristics and outcomes of patients admitted with confirmed COVID-19 in the same season during the first (March 2020) and the third pandemic wave (March 2021, dominance of SARS-CoV-2 B.1.1.7 lineage) in an internal medicine ward of a large teaching hospital in Italy (Ticinesi et al.). Despite the higher virulence of B.1.1.7 lineage, authors detected milder clinical presentation and improved mortality in patients hospitalised during the third COVID-19 wave, with the involvement of younger

subjects. The reasons for this discrepancy are unclear but could involve the population effect of vaccination campaigns conducted primarily in older frail subjects during the third wave. The second study (Liu et al.) constructed a prone ventilation management scheme for patients with severe coronavirus disease 2019 (COVID-19). It analysed its application effect, finding that its application can standardise and promote the implementation of prone ventilation, improve the quality of care, and improve the patient prognosis of COVID-19 patients.

## Author contributions

AR-M: Conceptualization, Data curation, Formal Analysis, Investigation, Methodology, Writing – original draft, Writing – review & editing. AB: Writing – original draft, Writing – review & editing. SC: Writing – original draft, Writing – review & editing.

## References

1. Zhu N, Zhang D, Wang W, Li X, Yang B, Song J, et al. A novel coronavirus from patients with pneumonia in China, 2019. *New Engl J Med* (2020) 382(8):727–33. doi: 10.1056/NEJMoa2001017
2. Rodríguez-Morales AJ, Cardona-Ospina JA, Gutiérrez-Ocampo E, Villamizar-Pena R, Holguín-Rivera Y, Escalera-Antezana JP, et al. Clinical, laboratory and imaging features of COVID-19: A systematic review and meta-analysis. *Travel Med Infect Dis* (2020) 34:101623. doi: 10.1016/j.tmaid.2020.101623
3. Solante R, Alvarez-Moreno C, Burhan E, Chariyalertsak S, Chiu NC, Chuenkitmongkol S, et al. Further implications on the global real-world vaccine effectiveness against SARS-CoV-2. *Expert Rev Vaccines* (2022) 21(9):1355–7. doi: 10.1080/14760584.2022.2110073
4. Solante R, Alvarez-Moreno C, Burhan E, Chariyalertsak S, Chiu NC, Chuenkitmongkol S, et al. Expert review of global real-world data on COVID-19 vaccine booster effectiveness and safety during the omicron-dominant phase of the pandemic. *Expert Rev Vaccines* (2023) 22(1):1–16. doi: 10.1080/14760584.2023.2143347
5. Cimerman S, Chebabo A, Cunha CAD, Rodríguez-Morales AJ. Deep impact of COVID-19 in the healthcare of Latin America: the case of Brazil. *Braz J Infect Dis* (2020) 24(2):93–5. doi: 10.1016/j.bjid.2020.04.005
6. Cimerman S, Chebabo A, Cunha CAD, Rodríguez-Morales AJ. One year after the arrival of COVID-19 in Latin America: what have we learned in Brazil and other countries? *Braz J Infect Dis* (2021) 25(2):101571. doi: 10.1016/j.bjid.2021.101571
7. Rodríguez-Morales AJ, Gallego V, Escalera-Antezana JP, Mendez CA, Zambrano LI, Franco-Paredes C, et al. COVID-19 in Latin America: The implications of the first confirmed case in Brazil. *Travel Med Infect Dis* (2020) 35:101613. doi: 10.1016/j.tmaid.2020.101613
8. Owusu-Dampare F, Bouchnita A. Equitable bivalent booster allocation strategies against emerging SARS-CoV-2 variants in US cities with large Hispanic communities: The case of El Paso County, Texas. *Infect Dis Model* (2023) 8(3):912–9. doi: 10.1016/j.idm.2023.07.009
9. Urrunaga-Pastor D, Bendezu-Quispe G, Herrera-Añazco P, Uyen-Cateriano A, Toro-Huamanchumo CJ, Rodríguez-Morales AJ, et al. Cross-sectional analysis of COVID-19 vaccine intention, perceptions and hesitancy across Latin America and the Caribbean. *Travel Med Infect Dis* (2021) 41:102059. doi: 10.1016/j.tmaid.2021.102059
10. Barbosa AN, Chebabo A, Starling C, Pérez C, Cunha CA, de Luna D, et al. Pan-American Guidelines for the treatment of SARS-CoV-2/COVID-19: a joint evidence-based guideline of the Brazilian Society of Infectious Diseases (SBI) and the Pan-American Association of Infectious Diseases (API). *Ann Clin Microbiol Antimicrob* (2023) 22(1):67. doi: 10.1186/s12941-023-00623-w
11. Saaavedra-Trujillo CH, Gutiérrez AB, Rodríguez-Morales AJ, Narváez Mejía AJ, García Peña AA, Giraldo Montoya AM, et al. Consenso Colombiano de atención, diagnóstico y manejo de la infección por SARS-COV-2/COVID-19 en establecimientos de atención de la salud - Recomendaciones basadas en consenso de expertos e informadas en la evidencia. *Infectio* (2020) 24(S3):1–102. doi: 10.22354/in.v24i3.851

## Conflict of interest

The authors declare that the research was conducted in the absence of any commercial or financial relationships that could be construed as a potential conflict of interest.

The authors declared that they were an editorial board member of Frontiers, at the time of submission. This had no impact on the peer review process and the final decision.

## Publisher's note

All claims expressed in this article are solely those of the authors and do not necessarily represent those of their affiliated organizations, or those of the publisher, the editors and the reviewers. Any product that may be evaluated in this article, or claim that may be made by its manufacturer, is not guaranteed or endorsed by the publisher.



## OPEN ACCESS

## EDITED BY

Alfonso J. Rodriguez-Morales,  
Fundacion Universitaria Autónoma de  
las Américas, Colombia

## REVIEWED BY

Alejandro Piscocoy,  
Hospital Guillermo Kaelin de la Fuente,  
Peru  
Morteza Arab-Zozani,  
Birjand University of Medical Sciences,  
Iran  
Constanza Martinez-Valdebenito,  
Pontificia Universidad Católica de  
Chile, Chile

## \*CORRESPONDENCE

Zhaohui Tong  
tongzhaohuicy@sina.com

<sup>†</sup>These authors have contributed  
equally to this work and share first  
authorship

## SPECIALTY SECTION

This article was submitted to  
Viral Immunology,  
a section of the journal  
Frontiers in Immunology

RECEIVED 08 June 2022

ACCEPTED 29 June 2022

PUBLISHED 28 July 2022

## CITATION

Qian Z, Zhang Z, Ma H, Shao S,  
Kang H and Tong Z (2022) The  
efficiency of convalescent plasma in  
COVID-19 patients: A systematic  
review and meta-analysis of  
randomized controlled clinical trials.  
*Front. Immunol.* 13:964398.  
doi: 10.3389/fimmu.2022.964398

## COPYRIGHT

© 2022 Qian, Zhang, Ma, Shao, Kang  
and Tong. This is an open-access article  
distributed under the terms of the  
Creative Commons Attribution License  
(CC BY). The use, distribution or  
reproduction in other forums is  
permitted, provided the original  
author(s) and the copyright owner(s)  
are credited and that the original  
publication in this journal is cited, in  
accordance with accepted academic  
practice. No use, distribution or  
reproduction is permitted which does  
not comply with these terms.

# The efficiency of convalescent plasma in COVID-19 patients: A systematic review and meta-analysis of randomized controlled clinical trials

Zhenbei Qian<sup>†</sup>, Zhijin Zhang<sup>†</sup>, Haomiao Ma<sup>†</sup>, Shuai Shao,  
Hanyujie Kang and Zhaohui Tong\*

Department of Respiratory and Critical Care Medicine, Beijing Institute of Respiratory Medicine,  
Beijing Chao-Yang Hospital, Capital Medical University, Beijing, China

The objective of this study was to assess whether convalescent plasma therapy could offer survival advantages for patients with novel coronavirus disease 2019 (COVID-19). An electronic search of Pubmed, Web of Science, Embase, Cochrane library and MedRxiv was performed from January 1st, 2020 to April 1st, 2022. We included studies containing patients with COVID-19 and treated with CCP. Data were independently extracted by two reviewers and synthesized with a random-effect analysis model. The primary outcome was 28-d mortality. Secondary outcomes included length of hospital stay, ventilation-free days, 14-d mortality, improvements of symptoms, progression of diseases and requirements of mechanical ventilation. Safety outcomes included the incidence of all adverse events (AEs) and serious adverse events (SAEs). The Cochrane risk-of-bias assessment tool 2.0 was used to assess the potential risk of bias in eligible studies. The heterogeneity of results was assessed by I<sup>2</sup> test and Q statistic test. The possibility of publication bias was assessed by conducting Begg and Egger test. GRADE (Grading of Recommendations Assessment, Development and Evaluation) method were used for quality of evidence. This study had been registered on PROSPERO, CRD42021273608. 32 RCTs comprising 21478 patients with Covid-19 were included. Compared to the control group, COVID-19 patients receiving CCP were not associated with significantly reduced 28-d mortality (CCP 20.0% vs control 20.8%; risk ratio 0.94; 95% CI 0.87-1.02; p = 0.16; I<sup>2</sup> = 8%). For all secondary outcomes, there were no significant differences between CCP group and control group. The incidence of AEs (26.9% vs 19.4%; risk ratio 1.14; 95% CI 0.99-01.31; p = 0.06; I<sup>2</sup> = 38%) and SAEs (16.3% vs 13.5%; risk ratio 1.03; 95% CI 0.87-1.20; p = 0.76; I<sup>2</sup> = 42%) tended to be higher in the CCP group compared to the control group, while the differences did not reach statistical significance. In all, CCP therapy was not related to significantly improved 28-d mortality or symptoms recovery, and should not be viewed as a routine treatment for COVID-19 patients.

**Trial registration number:** CRD42021273608. Registration on February 28, 2022

**Systematic review registration:** <https://www.crd.york.ac.uk/prospero/>, Identifier CRD42022313265.

#### KEYWORDS

convalescent plasma, COVID-19, SARS-CoV-2, antibodies, mortality, passive immunization

## 1 Introduction

The coronavirus disease 2019 (COVID-19), which was caused by the infection of Severe Acute Respiratory Syndrome Coronavirus 2 (SARS-COV-2), had become an acknowledged global pandemic and accounted for more than five hundred million confirmed cases and six million deaths (1), bringing a heavy burden to the healthcare system and serious threat to human beings. At present, the majority of treatments were still supportive, while few therapeutic strategies were confirmed for improved survival benefits.

Convalescent Plasma (CP) therapy, a form of passive immunization, had been widely applied in many viral infectious diseases like Middle East respiratory syndrome (MERS) (2) and Ebola (3). The specific antibodies in CP could accelerate clearance of virus (4), promote antibody-dependent cell-mediated cytotoxicity and complement activation (5). Results from previous studies suggested reduced mortality and improved symptoms in COVID-19 patients treated with COVID-19 convalescent plasma (CCP) (6, 7), and the FDA of the United States had approved the emergency use authorization (EUA) of CCP in COVID-19 patients (8). However, these studies were mainly retrospective and contained potential risk of bias, while the results from prospective studies suggested that administration of CCP could not result in reduced risk of mortality or improved symptoms (9–11). Recent meta-analysis which included results from RCTs (8, 12, 13) also indicated no significant improvements in the survival of COVID-19 who received CCP. The inconsistency of these studies made it controversial whether CCP should be regarded as a routine therapy for COVID-19 patients.

To further assess the efficiency of CCP, we conducted this meta-analysis to systematically evaluate whether COVID-19 patients could benefit from CCP therapy.

## 2 Methods

We reported this study according to the Preferred Reporting Items for Systematic Reviews and Meta-analyses (PRISMA)

guidelines (14). We have registered this study on PROSPERO (CRD42022313265) on February 28, 2022.

### 2.1 Inclusion and exclusion criteria

Studies were included if they fulfilled the following inclusion criteria: 1) Patients were confirmed at any clinical stage of COVID-19. 2) Patients  $\geq 18$  years old. 3) The intervention should be convalescent plasma. 4) The control group should include contemporaneous patients who didn't receive CCP or were treated with a placebo, including normal saline or standard plasma. 5) Only randomized controlled clinical trials were included. Exclusion criteria were defined as followed: 1) Animal or cell studies. 2) Editors, reviews, comments or abstracts. 3) Studies with unavailable full text. 4) Ineligible study designs, e.g. observational studies, retrospective studies, case reports, or case series studies. 5) Studies only contain the results that we were not interested in, including the changes in inflammatory factors (e.g. ferritin, IL-10 and D-Dimer) or biochemical factors (e.g. bilirubin, albumin and creatinine), the proportion of patients with negative nucleic acid test, time to the negative nucleic acid test, the proportion of patients with detectable endogenous antibodies after receiving CCP.

### 2.2 Search strategy

We performed a comprehensive search of the database including Pubmed, Web of Science, Embase, Cochrane library and medRxiv from January 1st, 2020 to April 1st, 2022. The keywords of "COVID-19" and "convalescent plasma" were used. No language restrictions were applied. Detailed systematic search strategy could be found in **Additional Table 1**. Reference lists of eligible studies were manually screened in case of loss of potentially relevant publications. The identification of potentially eligible studies was independently performed by two reviews (ZB Qian and S Shao). Any disagreement or discrepancy was eventually resolved by a third reviewer (ZH Tong).

## 2.3 Data collection and quality assessment

Two reviews (ZJ Zhang and HM Ma) conducted data collection independently. Any disagreement was resolved by the third reviewer (ZH Tong). For candidate literature, we designed a data collection form for temporary data management. The following information was extracted: name of the first author, publication year, study design, registration ID, inclusion criteria of subjects, the titer of neutralizing antibody and the dosage of CCP, type of control, sample size, details of baseline conditions and clinical outcomes. The incomplete data would be estimated by estimation or obtained by contacting the corresponding author. The Cochrane risk-of-bias assessment tool 2.0 (RoB 2.0) (15) was used to examine the potential risk of bias in eligible studies.

## 2.4 Outcomes

The selection and definition of outcomes referred to the previous meta-analysis (8, 12) and RCTs. The primary outcome was the 28-d mortality. Key secondary outcomes included 14-d mortality, the length of hospital stay (LOS), ventilation-free days, improvements of symptoms, progression of diseases and requirement of mechanical ventilation. The LOS was defined as the time from admission to hospital to discharge or death. Ventilation-free days were defined as the days without the support of ventilation. LOS and ventilation-free days were both assessed on day 28 (16). Improvements of symptoms were defined as improvements at least 2 grades on the WHO 7 symptom score within 28 days (17), while the progression of disease was defined as an exacerbation of the WHO 7 symptom score for at least 2 points or requirement for invasive ventilation or death. The safety outcomes included the incidence of all adverse events and serious adverse events. Severe adverse events referred to the adverse events that were assessed grade 3 or 4 (18).

## 2.5 Data synthesis

For continuous variables including LOS and ventilation-free days, the mean and standard deviation (SD) were extracted to calculate the mean difference (MD) with a 95% confidence interval (95% CI). For categorical variables like mortality, improvements of symptoms, progression of diseases, requirements of MV and incidence of AE, the risk ratio (RR) with 95% CI was calculated from frequencies and percentages. The statistical method was the inverse-variance method for continuous variables, while the Mantel-Haenszel method for categorical variables. All synthesis was based on the random-effects model and a two-tailed value of  $P$  less than 0.05 was considered statistically significant for all outcomes.  $I^2$  test and

$Q$  statistic test were performed to assess the inter-study heterogeneity, which was defined as moderate-to-high when  $P < 0.1$  in  $Q$  test and  $I^2 > 50\%$ . The possibility of publication bias was assessed by conducting a funnel plot and Egger or Begg test if more than 10 studies were included in the result, which was defined as high when the  $P$  value was lower than 0.1. The certainty of the evidence was assessed with the Grading of Recommendations Assessment, Development, and Evaluation tool (GRADE) Profiler version 3.6. Data synthesis was performed by using Review Manager Version 5.4 and Stata software (Stata Statistical Software, release 9.2).

## 2.6 Subgroup analysis and sensitivity analysis

In subgroup analysis, we stratified the eligible studies by (1) The status of publication (published in peer-reviewed publications or at preprint); (2) Patients' type (outpatients or inpatients); (3) The status of supplementary oxygenation at enrollment (requiring mechanical ventilation(MV), requiring non-invasive ventilation or not requiring oxygenation); (4) The serology of antibody at enrollment (antibody positive or antibody negative); (5) The titer of CCP (high titer CCP, low titer CCP or undivided titer of CCP): In terms of titer determination, we referred to the previous studies [12, 13]. The high titer CCP was defined as long as any of the followings was achieved: a. the titer of S-protein receptor binding domain specific antibody was more than 1:640; b. the titer of neutralizing antibody was more than 1:40; c. the PRNT50 of anti-S protein specific antibody was more than 1: 320; d. the ID50 of anti-S protein specific antibody was more than 1: 320; e. the signal-to-cutoff (S/C) value of anti-S protein specific antibody was more than 12 (6). The time from symptoms onset to enrollment (no more than 7 days or more than 7 days). The differences across subgroups were considered statistically significant when the  $P$  value of the interaction test was lower than 0.05. Forest plots were prepared to graphically visualize the heterogeneity and differences among subgroups. Sensitive analysis was conducted by screening the included studies to assess the impact on the outcomes when  $I^2 \geq 50\%$ .

## 3 Results

### 3.1 Literature search and study characteristics

The literature search yielded 17313 records in total, among which 6143 were excluded for duplicates. After the removal of 9533 and 1598 records for irrelevant studies and non-randomized trials, 39 articles were eligible for full-text assessment. Of these, 7 articles were respectively excluded for



lack of the results that we were interested in ( $n=3$ ) including 28-d mortality, changes in the progression of diseases and incidence of adverse events (19–21), lack of control group ( $n=2$ ) (22, 23), *post-hoc* analysis ( $n=1$ ) (9) and post-exposure prophylaxis ( $n=1$ ) (24). Finally, 32 RCTs (16–18, 24–52) with a total of 21478 patients were included in our analysis. A detailed flow chart was shown in Figure 1.

## 3.2 Baseline conditions

Among all the included studies, 4 studies (24, 28, 34, 48) were preprinted and 28 studies (16–18, 25–27, 29–33, 35–47, 49–52) were published in peer-reviewed journals. 10 studies (24, 26, 31, 38, 41, 43, 44, 46, 50, 51) were double-blind RCTs with placebo and 22 studies (16–18, 25, 27–30, 32–37, 39, 40, 42, 45, 47–49, 52) were designed as open-label trials. All trials included patients with confirmed Covid-19 except for the RECOVERY trial (35), which included both suspected and confirmed COVID-19 patients. 28 studies focused on the hospitalized patients with supplementary oxygenation (16–18, 25, 27–37, 39, 40, 42–52), and only 4 studies (24, 26, 38, 41) included outpatients. Most patients were older than 60 years and more than 60% were male. The median injection dose of convalescent plasma was 500ml (IQR 250–550). The majority of patients were enrolled more than 7 days after symptom onset. Serum status at enrollment was reported in 14 studies, while the percentage of patients with detectable neutralizing antibodies varied from 11.4% to 83.1% across eligible studies. More detailed information was shown in Additional Table 2.

The assessments of risk of bias were shown in Figure 2. 8 studies (26, 35, 38, 41, 43, 44, 46, 50) were regarded as low risk of bias, and 16 studies (16–18, 25, 27, 29, 30, 32, 37, 39, 40, 42, 45, 47, 49, 52) contained potential performance bias for the open-label design. 4 studies were considered as containing potential bias due to early termination (31, 33, 36, 51). Notably, although no high risks of bias in D1–D5, 4 studies (24, 28, 34, 48) were classified as high risk for pre-printed and lack of peer review.

## 3.3 Synthesis of results

### 3.3.1 Primary outcome

The 28-d mortality was reported in all included studies. In the overall population (Figure 3), the 28-d mortality was 20.0% (2228/11163) in CCP group and 20.8% (2149/10315) in control group, and the risk ratio was 0.94 (95% CI 0.87–1.02;  $p = 0.16$ ;  $I^2 = 8\%$ ). After excluding preprinted studies (Additional Figure 1), the 28-d mortality was 21.1% (2205/10474) in CCP group and 22.0% (2121/9628) in control group, without significant statistic differences (risk ratio 0.94; 95% CI 0.86–1.03;  $p = 0.18$ ;  $I^2 = 12\%$ ).

Subgroup analysis suggested potential differences between double-blinded RCTs and open-label RCTs (Additional Figure 2). Compared to the control group, double-blinded RCTs showed reduced 28-d mortality in COVID-19 patients treated with CCP (6.5%, 136/2084 vs. 7.0%, 129/1835; risk ratio 0.78; 95% CI 0.62–0.99;  $p = 0.04$ ;  $I^2 = 0\%$ ), while this association was not found in open-label RCTs (23.0%, 2092/9079 vs. 23.8%, 2020/8480; risk ratio 0.97; 95% CI 0.90–1.05;  $p = 0.48$ ;  $I^2 = 7\%$ ).

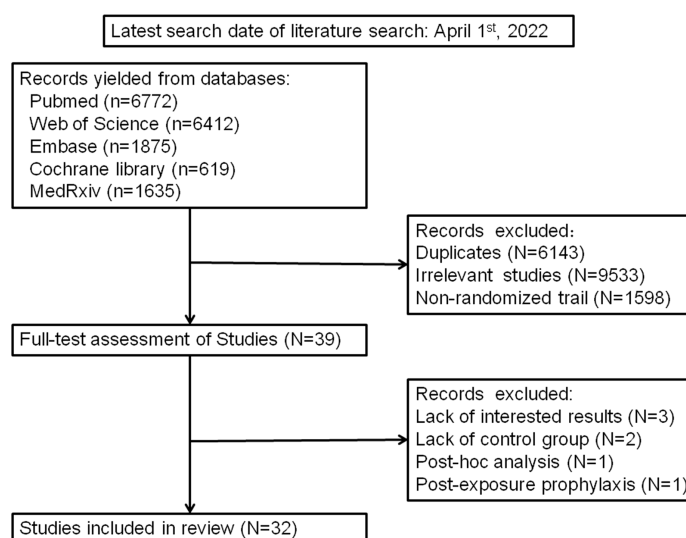


FIGURE 1  
The detailed flow chart of Literature search.

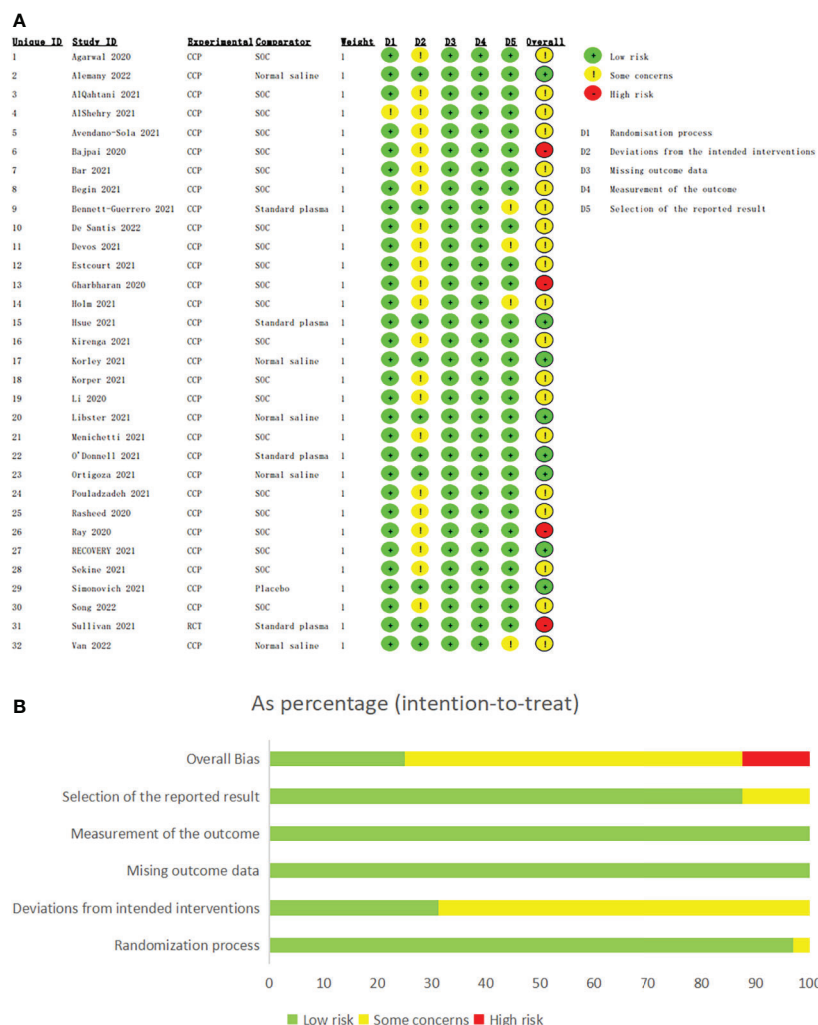


FIGURE 2

The assessments of risk of bias of eligible studies. The assessments of risk of bias of eligible studies. (A) The assessment of each eligible study. (B) The assessment of overall bias. Bajpai 2020, Gharbharan 2020, Ray 2020 and Sullivan 2021 were classified as high risk for pre-printed and lack of peer review although no high risks of bias in D1–D5.

Convalescent plasma neither reduced the risk for 28-d mortality in outpatients (0.6%, 7/1117 vs. 0.9%, 10/1111; risk ratio 0.63; 95% CI 0.14–2.95;  $p = 0.56$ ;  $I^2 = 42\%$ ), nor in inpatients (22.1%, 2217/10046 vs 23.3%, 2140/9204; risk ratio 0.94; 95% CI 0.86–1.02;  $p = 0.13$ ;  $I^2 = 11\%$ ). There were no significant differences between two subgroups (Additional Figure 3).

Compared to the control group, CCP therapy was not associated with significantly reduced 28-d mortality in patients requiring mechanical ventilation at enrollment (35.2%, 635/1802 vs 35.7%, 613/1717; risk ratio 0.95; 95% CI 0.81–1.10;  $p = 0.48$ ;  $I^2 = 40\%$ ). There was also no significant association between receiving CCP and lower 28-day mortality in patients who required non-invasive respiratory support at enrollment (20.9%, 1419/6779 vs 22.0%, 1372/6234; risk ratio 0.97; 95% CI 0.91–1.03;  $p = 0.34$ ;  $I^2 = 0\%$ ) or those who did not require

supplementary oxygenation at enrollment (3.9%, 58/1484 vs 5.1%, 76/1491; risk ratio 0.81; 95% CI 0.59–1.11;  $p = 0.19$ ;  $I^2 = 0\%$ ). (Additional Figure 4)

For antibody-seronegative patients, the 28-d mortality was 32.7% (791/2419) in CCP group and 34.1% (656/1926) in control group. While for antibody-seropositive patients, the 28-d mortality was 20.2% (794/3932) in CCP group and 19.2% (673/3510) in control group. Neither patients with detectable antibodies (risk ratio 1.00; 95% CI 0.85–1.18;  $p = 0.96$ ;  $I^2 = 40\%$ ) nor those without detectable antibodies (risk ratio 0.94; 95% CI 0.86–1.02;  $p = 0.14$ ;  $I^2 = 0\%$ ) at enrollment showed reduced 28-d mortality after receiving CCP. (Additional Figure 5)

For patients receiving high titer CCP, the 28-d mortality was 19.9% (1682/8461) in CCP group and 20.3% (1576/7779) in control group. Receiving high titer CCP was not related to lower

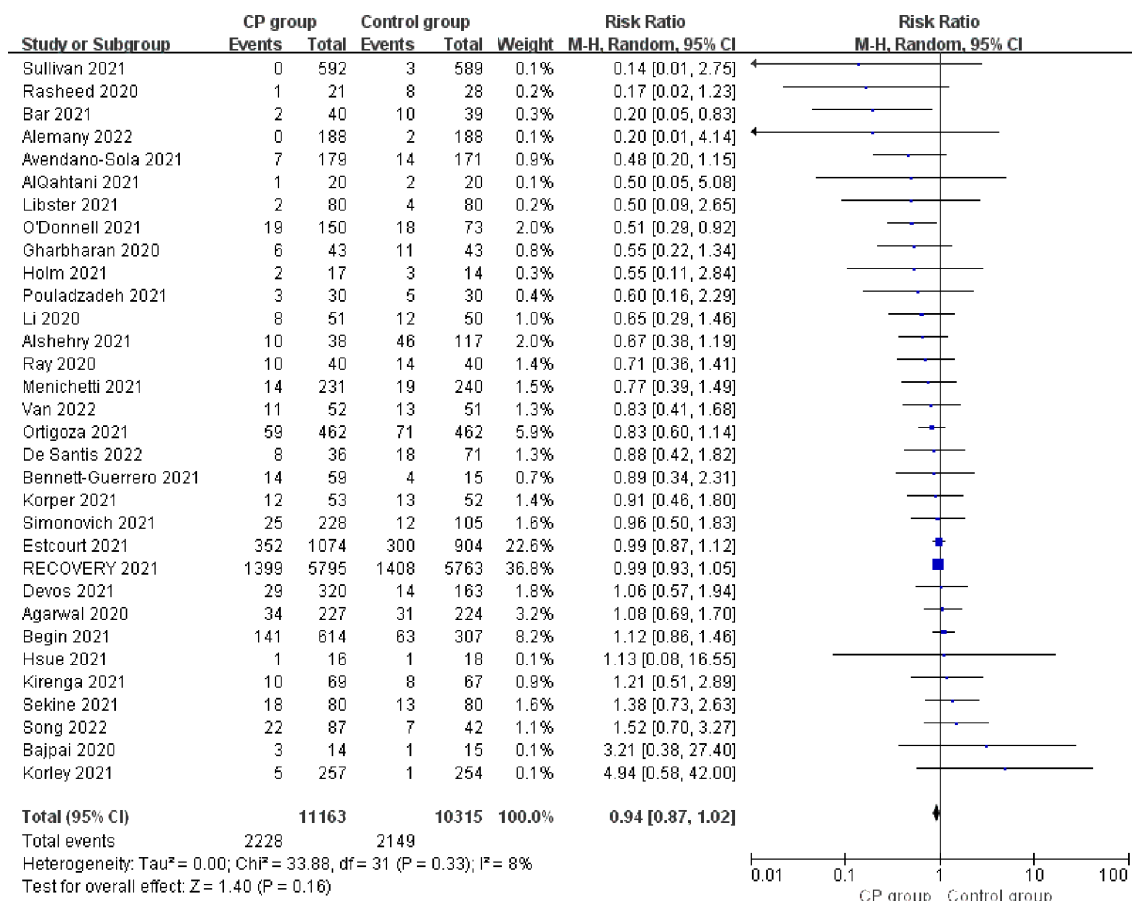


FIGURE 3

Forest plot of the risk ratio of 28-d mortality between CCP group and control group.

28-d mortality (risk ratio 0.99; 95% CI 0.94-1.06;  $p = 0.83$ ;  $I^2 = 0\%$ ). However, there was significantly reduced 28-d mortality for patients receiving low titer CCP (9.5%, 63/665 vs 13.1%, 77/587; risk ratio 0.68; 95% CI 0.55-0.92;  $p = 0.01$ ;  $I^2 = 0\%$ ) compared to the control group (Additional Figure 6).

In the patients whose median time from symptoms onset to enrollment was no more than 7 days, there were no significant differences in 28-d mortality in CCP group compared to control group (25.7%, 656/2553 vs 27.9%, 710/2549; risk ratio 0.92; 95% CI 0.84-1.01;  $p = 0.09$ ;  $I^2 = 0\%$ ). For patients with more than 7 days from symptoms onset, receiving CCP treatment did not show a significant reduction in 28-d mortality (21.3%, 820/3846 vs 20.9%, 781/3745; risk ratio 0.87; 95% CI 0.59-1.26;  $p = 0.45$ ;  $I^2 = 52\%$ ). There were no significant differences between the two subgroups ( $p = 0.45$ ; Additional Figure 7).

### 3.3.2 Secondary outcomes

The length of hospital stay was reported in 11 studies, with no significant differences between the CCP group and control group (MD 0.83; 95% CI -0.24-1.90;  $p = 0.13$ ;  $I^2 = 59\%$ )

(Additional Figure 8A). The ventilation-free days were assessed in 11 studies. Overall, the ventilation-free days were similar between the CCP group and control group (MD -0.04; 95% CI -0.74-0.67;  $p = 0.92$ ;  $I^2 = 35\%$ ). (Additional Figure 8B)

The 14-d mortality was assessed in 6 studies. Receiving CCP was not related to significantly reduced 14-d mortality compared to the control group (5.7%, 63/1098 vs 7.0%, 65/934; risk ratio 0.88; 95% CI 0.63-1.23;  $p = 0.45$ ;  $I^2 = 0\%$ ) (Additional Figure 9)

The deterioration and improvements of the diseases were respectively assessed in 8 studies and 9 studies. Overall, there were no significant differences in the improvement of symptoms (68.6%, 589/858 vs 65.7%, 353/537; risk ratio 1.00; 95% CI 0.94-1.07;  $p = 0.99$ ;  $I^2 = 0\%$ ) and progression of diseases (27.6%, 2101/7603 vs 27.7%, 2059/7436; risk ratio 0.96; 95% CI 0.85-1.08;  $p = 0.49$ ;  $I^2 = 46\%$ ) between the CCP group and control group. (Additional Figures 10A, B)

Initiation of mechanical ventilation was required in 20.4% (1159 of 5690) of patients receiving convalescent plasma and 21.2% (1107 of 5220) of patients with standard of care (RR 0.94, 95% CI 0.82-1.08,  $p = 0.38$ ). No significant differences between

CCP group and control group were observed. (Additional Figure 11)

### 3.3.3 Adverse events

Adverse events and serious adverse events were reported in 15 studies and 13 studies, respectively. Overall, the incidence of adverse events (26.9%, 570/2120 vs 19.4%, 374/1932; risk ratio 1.14; 95% CI 0.99-1.31;  $p = 0.06$ ;  $I^2 = 38\%$ ) and serious adverse events (16.3%, 590/3626 vs 13.5%, 370/2738; risk ratio 1.03; 95% CI 0.87-1.20;  $p = 0.76$ ;  $I^2 = 42\%$ ) tended to be higher in the CCP group compared to the control group, though the differences did not reach statistical significance (Figure 4A, B).

## 3.4 Quality of evidence

According to the GRADE assessment (Figure 5 and Additional File 1 Table 3), the evidence for the effect of CCP on 28-d mortality in all patients was high, which was mainly due to the large sample size and low level of heterogeneity despite publication bias. Similarly, the evidence for the effect of CCP on 28-d mortality in inpatients was high, while it downgraded to very low for outpatients for limited patients and moderate

heterogeneity. The evidence for the effect of CCP on patients receiving non-MV ventilation and high titer CCP was both moderate for publication bias (Additional Figure 12C). For other subgroup analysis on 28-mortality, the evidence for the effect of CCP ranged from low to very low. For secondary outcomes, the evidence for the effect of CCP on the improvements of symptoms was high, while the evidence for the effect of CCP on the ventilation-free days, 14-d mortality, progression and requirement of supplementary oxygenation was moderate due to the moderate heterogeneity, small size of included patients or publication bias (Additional Figures 12E, F). The evidence for the effect of CCP on length of hospital stay was low because of the serious heterogeneity of results. The evidence for the incidence of AE and SAE was low and moderate respectively due to moderate heterogeneity and publication bias (Additional Figures 12G, H).

## 4 Discussion

In this meta-analysis which included 32 RCTs and 21478 patients, we found that CCP therapy was not associated with significantly reduced 28-d mortality in COVID-19 patients.

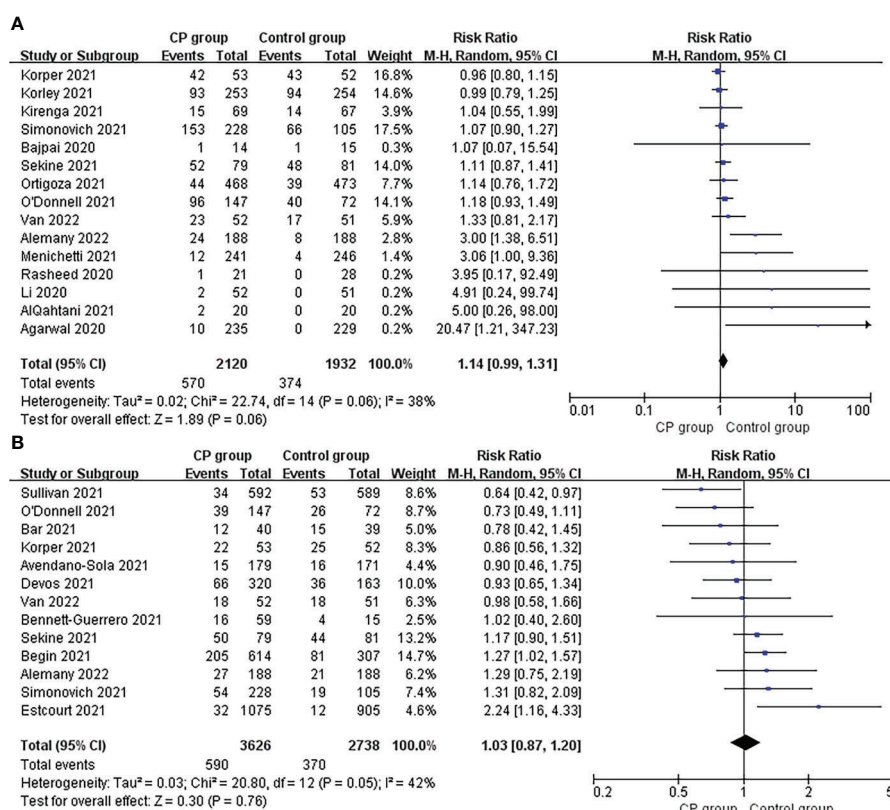


FIGURE 4

Forest plot of the risk ratio of (A) adverse events and (B) severe adverse between CCP group and control group.

**A****Primary outcome for CCP in COVID-19**

Patient or population: patients with COVID-19

Settings: COVID-19

Intervention: CCP

Outcomes	Illustrative comparative risks* (95% CI)		Relative effect (95% CI)	No of Participants (studies)	Quality of the evidence (GRADE)	Comments
	Assumed risk Control	Corresponding risk Primary outcome				
28-d mortality	Study population		RR 0.94 (0.87 to 1.02)	21478 (32 studies)	⊕⊕⊕⊕ high <sup>1,2</sup>	
	206 per 1000	196 per 1000 (181 to 213)				
	Moderate					
	167 per 1000	157 per 1000 (145 to 170)				

\*The basis for the assumed risk (e.g. the median control group risk across studies) is provided in footnotes. The corresponding risk (and its 95% confidence interval) is based on the assumed risk in the comparison group and the relative effect of the intervention (and its 95% CI).

CI: Confidence interval; RR: Risk ratio;

GRADE Working Group grades of evidence

High quality: Further research is very unlikely to change our confidence in the estimate of effect.

Moderate quality: Further research is likely to have an important impact on our confidence in the estimate of effect and may change the estimate.

Low quality: Further research is very likely to have an important impact on our confidence in the estimate of effect and is likely to change the estimate.

Very low quality: We are very uncertain about the estimate.

<sup>1</sup> Publication bias was suspected by Egger test and funnel plot<sup>2</sup> 32 studies with 21478 patients were included**B****Secondary outcomes for CCP in COVID-19**

Patient or population: patients with COVID-19

Settings: COVID-19

Intervention: CCP

Outcomes	Illustrative comparative risks* (95% CI)		Relative effect (95% CI)	No of Participants (studies)	Quality of the evidence (GRADE)	Comments
	Assumed risk Control	Corresponding risk Secondary outcomes				
Length of hospital stay		The mean length of hospital stay in the intervention groups was 0.83 higher (0.24 lower to 1.9 higher)		13762 (11 studies)	⊕⊕⊕⊕ low <sup>1</sup>	
Ventilation-free days		The mean ventilation-free days in the intervention groups was 0.04 lower (0.74 lower to 0.67 higher)		4224 (11 studies)	⊕⊕⊕⊕ moderate <sup>2</sup>	
14-d mortality	Study population		RR 0.88 (0.63 to 1.23)	2032 (6 studies)	⊕⊕⊕⊕ moderate <sup>3</sup>	
	70 per 1000	61 per 1000 (44 to 86)				
	Moderate					
	57 per 1000	50 per 1000 (36 to 70)				
Improvement of symptoms	Study population		RR 1 (0.94 to 1.07)	1395 (8 studies)	⊕⊕⊕⊕ high	
	657 per 1000	657 per 1000 (618 to 703)				
	Moderate					
	611 per 1000	611 per 1000 (574 to 654)				
Progression of diseases	Study population		RR 0.96 (0.85 to 1.08)	15039 (9 studies)	⊕⊕⊕⊕ moderate <sup>2</sup>	
	277 per 1000	266 per 1000 (235 to 299)				
	Moderate					
	288 per 1000	276 per 1000 (245 to 311)				
Requirement of supplementary oxygenation	Study population		RR 0.94 (0.82 to 1.08)	10910 (15 studies)	⊕⊕⊕⊕ moderate <sup>4</sup>	
	212 per 1000	199 per 1000 (174 to 229)				
	Moderate					
	229 per 1000	215 per 1000 (188 to 247)				

\*The basis for the assumed risk (e.g. the median control group risk across studies) is provided in footnotes. The corresponding risk (and its 95% confidence interval) is based on the assumed risk in the comparison group and the relative effect of the intervention (and its 95% CI).

CI: Confidence interval; RR: Risk ratio;

GRADE Working Group grades of evidence

High quality: Further research is very unlikely to change our confidence in the estimate of effect.

Moderate quality: Further research is likely to have an important impact on our confidence in the estimate of effect and may change the estimate.

Low quality: Further research is very likely to have an important impact on our confidence in the estimate of effect and is likely to change the estimate.

Very low quality: We are very uncertain about the estimate.

<sup>1</sup> High heterogeneity was observed<sup>2</sup> Moderate heterogeneity was observed<sup>3</sup> Limited studies and patients were included<sup>4</sup> Publication bias was suspected by Egger test and funnel plot**C****Safety outcomes**

Patient or population: patients with COVID-19

Settings: COVID-19

Intervention: CCP

Outcomes	Illustrative comparative risks* (95% CI)		Relative effect (95% CI)	No of Participants (studies)	Quality of the evidence (GRADE)	Comments
	Assumed risk Control	Corresponding risk Adverse events				
AE	Study population		RR 1.14 (0.89 to 1.31)	4052 (15 studies)	⊕⊕⊕⊕ low <sup>1,2</sup>	
	194 per 1000	221 per 1000 (192 to 254)				
	Moderate					
	83 per 1000	95 per 1000 (82 to 109)				
sAE	Study population		RR 1.03 (0.87 to 1.2)	6364 (13 studies)	⊕⊕⊕⊕ moderate <sup>1</sup>	
	135 per 1000	139 per 1000 (118 to 162)				
	Moderate					
	264 per 1000	272 per 1000 (230 to 317)				

\*The basis for the assumed risk (e.g. the median control group risk across studies) is provided in footnotes. The corresponding risk (and its 95% confidence interval) is based on the assumed risk in the comparison group and the relative effect of the intervention (and its 95% CI).

CI: Confidence interval; RR: Risk ratio;

GRADE Working Group grades of evidence

High quality: Further research is very unlikely to change our confidence in the estimate of effect.

Moderate quality: Further research is likely to have an important impact on our confidence in the estimate of effect and may change the estimate.

Low quality: Further research is very likely to have an important impact on our confidence in the estimate of effect and is likely to change the estimate.

Very low quality: We are very uncertain about the estimate.

<sup>1</sup> Moderate heterogeneity was observed<sup>2</sup> Publication bias was suspected by Egger test and funnel plot

FIGURE 5

The simplified Summary of Finding of outcomes. The simplified Summary of Finding for (A) Primary outcomes, (B) Secondary outcomes and (C) Safety outcomes. CCP, COVID-19 convalescent plasma; 95% CI, 95% confidence interval; RR, risk ratio.



Besides, receiving CCP was not related to improvements on other survival outcomes, including length of hospital stay, time without respiratory support, risk of symptoms progression and requirement of MV. In terms of safety, treatment with CCP presented a trend of higher incidence of adverse events, although the differences didn't reach statistical significance.

At present, several therapies have been recommended by WHO (53) and IDSA (54) to treat COVID-19. For mild patients, monoclonal antibodies such as Sotrovimab (55) could reduce the risk of hospitalization, while REGEN-CoV-2 (56) might reduce mortality in patients without detectable baseline antibodies. Antivirals such as remdesivir (57, 58), favipiravir (59), molnupiravir (60) and nirmatvir/ritonavir (61) could reduce the risk of ventilation as well as mortality in patients at high risk of hospitalization and release the symptoms. However, in low-income countries and regions, monoclonal antibodies and antivirals might not be readily available. IDSA recommended high titer and fully qualified CCP as an alternative to monoclonal antibodies and antivirals, which was opposite to WHO guidelines that strongly recommended against CCP in mild patients due to limited clinical benefits. For critically ill patients, treatments aiming to control unbalanced inflammation were preferred to reduce the risk of ventilation and mortality, including glucocorticoids (62, 63), IL-6 receptor inhibitors (64, 65), and Baricitinib (66). In addition, glucocorticoids could also improve ventilator-free days, while IL-6 and Baricitinib might play a role in reducing length of hospital stay. CCP was only recommended only in the context of clinical trials for severe COVID-19 patients, due to limited suppressive effect of CCP on inflammation and no significantly improved clinical outcomes.

Previously, there were studies suggesting the association between receiving CCP and lower 28-day mortality or less progression of diseases (67–70), while recent prospective studies and RCTs indicated that CCP could not lead to elevated antibody titer (71) or survival benefits in COVID-19 patients (72, 73). Our findings supported that COVID-19 patients might not benefit from the transfusion of CCP, which was consistent with the latest WHO and IDSA guideline (53, 54). These Inconsistencies of outcomes among these studies might be due to the heterogeneous baseline conditions of included patients (74) and the variations of interventions (75) between the CCP group and control group, especially in retrospective and observational studies. Severe COVID-19 patients were more likely to receive high titer and dosage of CCP beyond more frequent use of antiviral agents or corticosteroid, which might overestimate the efficiency of CCP.

Our study found that the administration of CCP was not related to significant improvements in 28-d mortality, length of hospital stays, ventilation-free days, or the progression of diseases. These could be due to several reasons: Firstly, most eligible studies were conducted between 2021 and 2022, when SARS-CoV-2 variants had spread widely around the world, like Delta and Omicron. Previous studies found that mutations in

spike proteins, including E484A and N501Y, made these variants more likely to escape from immune recognition (76, 77), reducing the efficiency of CCP (78). Additionally, according to the analysis focused on variables associated with CCP efficacy, CCP collected from certain locations and pandemic waves couldn't effectively neutralize the virus at other locations and waves (79). The chronological and epidemiological distance between plasma donors and receptors might lead to the mismatch in antibodies and circulating variants, resulting in further aggravation of the variants' resistance to antibodies. Therefore, considering the attempt to standardize the plasma centrally, the efficiency of CCP might be underestimated among studies that were carried out nationally and across multiple pandemic waves.

Secondly, the majority of eligible patients in our study were no less than 7 days from symptoms onset and suffering hypoxemia at enrollment, requiring at least one type of supplementary oxygenation. Results from subgroup analysis suggested that these patients could not benefit from the CCP therapy. Indeed, for patients at the end stage of COVID-19, the pathology of lung parenchyma was mainly characterized by inflammatory infiltration and fibrosis resulting from the unbalanced pro-inflammatory response and cytokine storm, while replication of SARS-CoV-2 contributed less to the damage (79, 80). The initial course of COVID-19 might be viewed as an optimal therapeutic window period for exogenous antibodies to maximize their neutralization effect (32, 81). However, our study found that there was no significantly lower 28-d mortality either in patients within 7 days from symptoms onset or those with more than 7 days. On the one hand, this could be due to the limited number of included patients in the early stages of COVID-19; on the other hand, 7 days might not be early enough to identify for potential benefit. In a multicenter retrospective study (74), administration of CCP within 3 days since symptoms onset, but not within 4 to 7 days, was related to a significantly reduced mortality. Therefore, what mattered to improve the efficiency of CCP at present was determining the appropriate therapeutic window period to identify the possible patients who might benefit from CCP therapy.

Thirdly, the variations in the standard of care among included studies might also be an important factor, especially the percentage of patients receiving corticosteroid or remdesivir which had been confirmed to be beneficial for survival. In the REMAP-CAP trial (52), up to 90% of patients in the study were treated with glucocorticoids, whereas in RECOVERY trial (35), less than 1% of patients received glucocorticoids. Similarly, the percentage of patients treated with remdesivir was more than 80% and less than 5% in the study of Bajpai et al. (28) and Agarwal et al. (25), respectively. In addition, we found that among the RCTs with placebo, receiving CCP was related to a lower risk of 28-d mortality, while this association was not observed among the open-label RCTs. Considering the

weakened control of performance bias, the lack of placebo might lead to the underestimation of CCP. More double-blinded RCTs were required for further assessment.

In addition to the reasons mentioned above, we noticed that receiving CCP was related to trend of elevated incidence of adverse events compared to the control group, although the difference was not statistically significant. This might be another essential factor that should be considered when applying CCP to COVID-19 patients. However, since the funnel plot and Egger test suggested potential publication bias, the evidentiary quality of this result was low. More studies were needed for the further assessment of the safety of CCP.

Notably, we found that CCP therapy did not significantly reduce 28-day mortality regardless of whether neutralizing antibodies were detectable at enrollment. Previous studies (82) found that hypogammaglobulinemia, regardless of causes, was associated with poor survival, and the immunoglobulin replacement therapy like CCP might be beneficial for elevating level of antibodies and alleviating viremia, thus reducing symptom duration, hospital stay, and mortality. However, this relationship was not shown in our study, which might be due to the limited number of included studies. Meanwhile, the antibody seronegativity was defined as the failed detection of IgG or IgM in the included studies (29, 35, 44, 52), while the ignorance of other subtypes of antibodies like IgA might result in the misclassification of seronegative patients.

Our results suggested receiving high titer CCP was not related to significantly reduced 28-d mortality. For one thing, the definition of high titer CCP remained controversial at present, which was mainly due to the inconsistent measurements across studies and the unclear cut-off value of high-and low-titer. According to the previous researches (8, 12), we defined the high titer CCP as the PRNT50 of anti-spike antibody  $\geq 1:320$  or the ID50 of anti-spike antibody  $\geq 1:320$ , apart from the titer of anti-spike antibody  $\geq 1:640$  and nAbs  $\geq 1:40$ . However, this was a preliminary stratification, while the CCP titer within each subgroup might vary a lot. In the high titer group, the CCP used in Holm 2021 (36) had a median nAbs titer of 1:116 (1:40-1:1160), while the median titer of nAbs of CCP used in Sekine 2021 (49) could reach 1:320 (1:160-1:960). For another, there were no significant improvements either in the composition of antibody profile or in the avidity of antibodies after high titer CCP transfusion (nAbs 1:160-1:640), which were more likely to be related to positive clinical outcomes rather than the titer of nAbs, according to the recent study focused on the severe COVID-19 patients (83). Besides, neutralizing antibody titer showed a sharp downward trend before the death of COVID-19 patients despite the previous administration of CCP, suggesting the limited effect of high titer CCP on the composition of antibodies and preventing the failure of the immune system at the end stage of COVID-19 (83).

Notably, during the data synthesis of 28-d mortality, we noticed that the RECOVERY trial and REMAP-CAP trial accounted for 30.5% and 21.5% of the weight respectively,

making our results to some extent dominated by these two studies. Previous study raised the concern that the impact of large studies might result in massive bias (81, 84), especially when the baseline conditions of patients could not be fully balanced in eligible studies. Therefore, we conducted the sensitivity analysis to assess the stability of our results, showing that the final conclusion would not be overturned even if these two RCTs were excluded simultaneously (RR 0.87; 95% CI, 0.76 to 1.00;  $P = 0.05$ ; Statistical difference was set as  $P < 0.05$ ). Coupled with the existence of publication bias, where both the funnel plot and Begg or Egger test had confirmed that more studies with risk ratio  $< 1$  were included, we were confident with the conclusion that CCP might not be regarded as an appropriate routine therapy for COVID-19, which was consistent with latest WHO guideline (53) and IDSA guideline (54).

There were several strengths in our study compared to previous meta-analysis (8, 12, 55, 85–88): 1. Our study was the latest meta-analysis with the data from latest RCTs; 2. More comprehensive subgroup analysis was performed, including the titer of CCP, the time from symptoms onset to enrollment and the type of control group (placebo+SOC or only SOC), which were not evaluated in previous studies; 3. We evaluated adverse events (AEs) and serious adverse events (SAEs) as the safety outcomes which were overlooked in previous studies; 4. The impact of large RCTs was weakened for larger number of eligible RCTs and patients. However, there were several limitations in our study. Firstly, although all the studies we included were RCTs, 50% of them were open-label designed, containing certain risk of bias. Subgroup analysis suggested potential differences in 28-d mortality between double-blinded RCTs and open-label RCTs, although the differences didn't reach statistical differences. Secondly, publication bias was observed in the 28-d mortality and adverse events, which might bring certain potential bias to the results. Thirdly, the eligible RCTs involved multiple time periods and different countries or regions, suggesting that patients might be infected with multiple variants. Fourthly, 90% of the included patients required supplementary oxygenation, while only 10% of the patients were outpatients. The assessment on mild patients was insufficient. Fifthly, our study mainly focused on COVID-19 patients with normal immunity, without evaluation on patients with immunodeficiency due to lack of data and giant heterogeneous baseline conditions from normal patients. Previous studies suggested reduced risk of mortality in immune-compromised patients receiving CCP (89). Future studies were needed for further assessment. Sixthly, we didn't assess the efficiency of CCP in low-income countries due to limited trials conducted in these countries. In fact, as a cost-effective treatment, CCP might be more suitable for these countries where antiviral and monoclonal antibodies were not readily available (54). Seventhly, the efficiency of CCP on post-exposure protection (90) was not assessed in our studies since the unconfirmed COVID-19 patients were not included

according to our exclusion criteria. Eighthly, we didn't assess the proportion of patients with negative nucleic acid test, time to the negative nucleic acid test, the proportion of patients with detectable endogenous antibodies after receiving CCP as our results. Lastly, a more comprehensive and advanced statistical modeling might be needed to better balance the baseline conditions among eligible studies, just as Troxel AB et al (12) did with a robust Bayesian framework.

## Conclusion

Compared to the control group, CCP therapy was not related to significantly improvements in 28-d mortality or other clinical outcomes in the overall COVID-19 patients. Considering the high quality of evidence, CCP should not be recognized as an appropriate routine treatment for clinicians. More double-blinded RCTs were needed to investigate the efficiency of CCP among patients in the initial stage of COVID-19, especially those who were within 3 days from symptoms onset and without detectable neutralizing antibodies at enrollment. Besides, the definition of high titer CCP required further determination.

## Data availability statement

The original contributions presented in the study are included in the article/**Supplementary Material**. Further inquiries can be directed to the corresponding author.

## Author contributions

ZQ developed the initial idea of this study and conducted a comprehensive search of databases. All authors have made their

contributions for writing articles. The manuscript was drafted by ZQ, ZZ, HM, and SS. HK and ZT reviewed this article and provided suggestions for it. All of the authors have carefully examined this manuscript and agreed with the ideas presented in the article.

## Funding

This study was supported by grant 2021YFC0863600 from the Ministry of Science and Technology of the People's Republic of China.

## Conflict of interest

The authors declare that the research was conducted in the absence of any commercial or financial relationships that could be construed as a potential conflict of interest.

## Publisher's note

All claims expressed in this article are solely those of the authors and do not necessarily represent those of their affiliated organizations, or those of the publisher, the editors and the reviewers. Any product that may be evaluated in this article, or claim that may be made by its manufacturer, is not guaranteed or endorsed by the publisher.

## Supplementary material

The Supplementary Material for this article can be found online at: <https://www.frontiersin.org/articles/10.3389/fimmu.2022.964398/full#supplementary-material>

## References

1. Organization WH. Weekly epidemiological update on COVID-19 - 18 may 2022. (2022). Available at: <https://www.who.int/publications/m/item/weekly-epidemiological-update-on-covid-19-18-may-2022>
2. Arabi YM, Hajeer AH, Luke T, Raviprakash K, Balkhy H, Johani S, et al. Feasibility of using convalescent plasma immunotherapy for MERS-CoV infection, Saudi Arabia. *Emerg Infect Dis* (2016) 22(9):1554–61. doi: 10.3201/eid2209.151164
3. Kraft CS, Hewlett AL, Koepsell S, Winkler AM, Kratochvil CJ, Larson L, et al. The use of TKM-100802 and convalescent plasma in 2 patients with Ebola virus disease in the united states. *Clin Infect Dis* (2015) 61(4):496–502. doi: 10.1093/cid/civ334
4. Lu CL, Murakowski DK, Bournazos S, Schoofs T, Sarkar D, Halper-Stromberg A, et al. Enhanced clearance of HIV-1-infected cells by broadly neutralizing antibodies against HIV-1 *in vivo*. *Science* (2016) 352(6288):1001–4. doi: 10.1126/science.aaf1279
5. Liu Q, Fan C, Li Q, Zhou S, Huang W, Wang L, et al. Antibody-dependent cellular-cytotoxicity-inducing antibodies significantly affect the post-exposure treatment of Ebola virus infection. *Sci Rep* (2017) 7:45552. doi: 10.1038/srep45552
6. Duan K, Liu B, Li C, Zhang H, Yu T, Qu J, et al. Effectiveness of convalescent plasma therapy in severe COVID-19 patients. *Proc Natl Acad Sci U S A* (2020) 117(17):9490–6. doi: 10.1073/pnas.2004168117
7. Liu STH, Lin HM, Baine I, Wajnberg A, Gumprecht JP, Rahman F, et al. Convalescent plasma treatment of severe COVID-19: a propensity score-matched control study. *Nat Med* (2020) 26(11):1708–13. doi: 10.1038/s41591-020-1088-9
8. Jorda A, Kussmann M, Kolenchery N, Siller-Matula JM, Zeitlinger M, Jilma B, et al. Convalescent plasma treatment in patients with covid-19: A systematic review and meta-analysis. *Front Immunol* (2022) 13:817829. doi: 10.3389/fimmu.2022.817829
9. Millat-Martinez P, Gharbharan A, Alemany A, Rokx C, Geurtsvankessel C, Papageorgiou G, et al. Convalescent plasma for outpatients with early COVID-19. *medRxiv* (2021) 2021:11.30.21266810. doi: 10.1101/2021.11.30.21266810
10. Koirala J, Gyanwali P, Gerzoff RB, Bhattarai S, Nepal B, Manandhar R, et al. Experience of treating COVID-19 with remdesivir and convalescent plasma in a resource-limited setting: A prospective, observational study. *Open Forum Infect Dis* (2021) 8(8):ofab391. doi: 10.1093/ofid/ofab391

11. Chauhan L, Pattee J, Ford J, Thomas C, Lesteberg K, Richards E, et al. A multi-center, prospective, observational-cohort controlled study of clinical outcomes following COVID-19 convalescent plasma therapy in hospitalized COVID-19 patients. *Clin Infect Dis* (2021) 21:ciab834. doi: 10.1101/2021.06.14.21258910
12. Troxel AB, Petkova E, Goldfeld K, Liu M, Tarpey T, Wu Y, et al. Association of convalescent plasma treatment with clinical status in patients hospitalized with COVID-19: A meta-analysis. *JAMA Netw Open* (2022) 5(1):e2147331. doi: 10.1001/jamanetworkopen.2021.47331
13. Janiaud P, Axfors C, Schmitt AM, Gloy V, Ebrahimi F, Hepprich M, et al. Association of convalescent plasma treatment with clinical outcomes in patients with COVID-19: A systematic review and meta-analysis. *JAMA* (2021) 325(12):1185–95. doi: 10.1001/jama.2021.2747
14. Moher D, Liberati A, Tetzlaff J, Altman DG. Preferred reporting items for systematic reviews and meta-analyses: the PRISMA statement. *PLoS Med* (2009) 6(7):e1000097. doi: 10.1371/journal.pmed.0060160
15. Sterne JAC, Savovic J, Page MJ, Elbers RG, Blencowe NS, Boutron I, et al. RoB 2: a revised tool for assessing risk of bias in randomised trials. *Bmj* (2019) 366:l4898. doi: 10.1136/bmj.l4898
16. AlShehry N, Zaidi SZA, AlAskar A, Al Odayani A, Alotaibi JM, AlSagheir A, et al. Safety and efficacy of convalescent plasma for severe COVID-19: Interim report of a multicenter phase II study from Saudi Arabia. *Saudi J Med Med Sci* (2021) 9(1):16–23. doi: 10.4103/sjms.sjms\_731\_20
17. Song ATW, Rocha V, Mendrone-Junior A, Calado RT, De Santis GC, Benites BD, et al. Treatment of severe COVID-19 patients with either low- or high-volume of convalescent plasma versus standard of care: A multicenter Bayesian randomized open-label clinical trial (COOP-COVID-19-MCTI). *Lancet Reg Health Am* (2022) 10:100216. doi: 10.1016/j.lana.2022.100216
18. Avendano-Sola C, Ramos-Martinez A, Munoz-Rubio E, Ruiz-Antoran B, Malo de Molina R, Torres F, et al. A multicenter randomized open-label clinical trial for convalescent plasma in patients hospitalized with COVID-19 pneumonia. *J Clin Invest* (2021) 131(20):e152740. doi: 10.1172/JCI152740
19. Ali S, Uddin SM, Shalim E, Sayeed MA, Anjum F, Saleem F, et al. Hyperimmune anti-COVID-19 IVIG (C-IVIG) treatment in severe and critical COVID-19 patients: A phase I/II randomized control trial. *EclinicalMedicine* (2021) 36:100926. doi: 10.1016/j.eclinm.2021.100926
20. Devos T, Geukens T, Schouwvlieghe A, Arien KK, Barbezange C, Cleeren M, et al. A randomized, multicenter, open-label phase II proof-of-concept trial investigating the clinical efficacy and safety of the addition of convalescent plasma to the standard of care in patients hospitalized with COVID-19: the donated antibodies working against nCoV (DAWN-plasma) trial. *Trials* (2020) 21(1):981. doi: 10.1186/s13063-020-04876-0
21. Hamdy Salman O, Ail Mohamed HS. Efficacy and safety of transfusing plasma from COVID-19 survivors to COVID-19 victims with severe illness: a double-blinded controlled preliminary study. *Egyptian J Anaesthesia* (2020) 36(1):264–72. doi: 10.1080/11101849.2020.1842087
22. Balcells ME, Rojas L, Le Corre N, Martinez-Valdebenito C, Ceballos ME, Ferrer M, et al. Early versus deferred anti-SARS-CoV-2 convalescent plasma in patients admitted for COVID-19: A randomized phase II clinical trial. *PLoS Med* (2021) 18(3):e1003415. doi: 10.1371/journal.pmed.1003415
23. Gonzalez JLB, González Gámez M, Mendoza Enciso EA, Esparza Maldonado RJ, Palacios DH, Campos SD, et al. Efficacy and safety of convalescent plasma and intravenous immunoglobulin in critically ill COVID-19 patients. *A Controlled Clin Trial* (2021) 2021:03.28.21254507. doi: 10.1101/2021.03.28.21254507
24. Sullivan DJ, Gebo KA, Shoham S, Bloch EM, Lau B, Shenoy AG, et al. Randomized controlled trial of early outpatient COVID-19 treatment with high-titer convalescent plasma. *medRxiv* (2021). doi: 10.1101/2021.12.10.21267485
25. Agarwal A, Mukherjee A, Kumar G, Chatterjee P, Bhatnagar T, Malhotra P, et al. Convalescent plasma in the management of moderate covid-19 in adults in India: open label phase II multicentre randomised controlled trial (PLACID trial). *BMJ* (2020) 371:m3939. doi: 10.1136/bmj.m3939
26. Alemany A, Millat-Martinez P, Corbacho-Monné M, Malchair P, Ouchi D, Ruiz-Comellas A, et al. High-titre methylene blue-treated convalescent plasma as an early treatment for outpatients with COVID-19: a randomised, placebo-controlled trial. *Lancet Respir Med* (2022) 10(3):278–88. doi: 10.1016/S2213-2600(21)00545-2
27. AlQahtani M, Abdulrahman A, Almadani A, Alali SY, Al Zamrooni AM, Hejab AH, et al. Randomized controlled trial of convalescent plasma therapy against standard therapy in patients with severe COVID-19 disease. *Sci Rep* (2021) 11(1):9927. doi: 10.1038/s41598-021-89444-5
28. Bajpai M, Kumar S, Maheshwari A, Chhabra K, Kale P, Gupta A, et al. Efficacy of convalescent plasma therapy compared to fresh frozen plasma in severely ill COVID-19 patients: A pilot randomized controlled trial. *medRxiv* (2020) 2020.10.25.20219337. doi: 10.1101/2020.10.25.20219337
29. Bar KJ, Shaw PA, Choi GH, Aqai N, Fesnak A, Yang JB, et al. A randomized controlled study of convalescent plasma for individuals hospitalized with COVID-19 pneumonia. *J Clin Invest* (2021) 131(24):e155114. doi: 10.1172/JCI155114
30. Begin P, Callum J, Jamula E, Cook R, Heddle NM, Tinmouth A, et al. Convalescent plasma for hospitalized patients with COVID-19: an open-label, randomized controlled trial. *Nat Med* (2021) 27(11):2012–24. doi: 10.1038/s41591-021-01488-2
31. Bennett-Guerrero E, Romeiser JL, Talbot LR, Ahmed T, Mamone LJ, Singh SM, et al. Severe acute respiratory syndrome coronavirus 2 convalescent plasma versus standard plasma in coronavirus disease 2019 infected hospitalized patients in new York: A double-blind randomized trial. *Crit Care Med* (2021) 49(7):1015–25. doi: 10.1097/CCM.0000000000005066
32. De Santis GC, Oliveira LC, Garibaldi PMM, Almado CEL, Croda J, Arcanjo GGA, et al. High-dose convalescent plasma for treatment of severe COVID-19. *Emerg Infect Dis* (2022) 28(3):548–55. doi: 10.3201/eid2803.212299
33. Devos T, Van Thillo Q, Compennolle V, Najdovski T, Romano M, Dauby N, et al. Early high antibody titre convalescent plasma for hospitalised COVID-19 patients: DAWN-plasma. *Eur Respir J* (2022) 59(2):2101724. doi: 10.1183/13993003.01724-2021
34. Gharbharan A, Jordans CCE, Geurtsvankessel C, den Hollander JG, Karim F, Mollema FPN, et al. Convalescent plasma for COVID-19. *A Randomized Clin Trial* (2020) 2020:07.01.20139857. doi: 10.1101/2020.07.01.20139857
35. Group RC. Convalescent plasma in patients admitted to hospital with COVID-19 (RECOVERY): a randomised controlled, open-label, platform trial. *Lancet* (2021) 397(10289):2049–59. doi: 10.1016/S0140-6736(21)00897-7
36. Holm K, Lundgren MN, Kjeldsen-Kragh J, Ljungquist O, Bottiger B, Wiken C, et al. Convalescence plasma treatment of COVID-19: results from a prematurely terminated randomized controlled open-label study in southern Sweden. *BMC Res Notes* (2021) 14(1):440. doi: 10.1186/s13104-021-05847-7
37. Kirenga B, Byakika-Kibwika P, Muttamba W, Kayongo A, Loryndah NO, Mugenyi L, et al. Efficacy of convalescent plasma for treatment of COVID-19 in Uganda. *BMJ Open Respir Res* (2021) 8(1):e001017. doi: 10.1136/bmjresp-2021-001017
38. Korley FK, Durkalski-Mauldin V, Yeatts SD, Schulman K, Davenport RD, Dumont LJ, et al. Early convalescent plasma for high-risk outpatients with covid-19. *N Engl J Med* (2021) 385(21):1951–60. doi: 10.1056/NEJMoa2103784
39. Korper S, Weiss M, Zickler D, Wiesmann T, Zacharowski K, Corman VM, et al. Results of the CAPSID randomized trial for high-dose convalescent plasma in patients with severe COVID-19. *J Clin Invest* (2021) 131(20):e152264. doi: 10.1172/JCI152264
40. Li L, Zhang W, Hu Y, Tong X, Zheng S, Yang J, et al. Effect of convalescent plasma therapy on time to clinical improvement in patients with severe and life-threatening COVID-19: A randomized clinical trial. *JAMA* (2020) 324(5):460–70. doi: 10.1001/jama.2020.10044
41. Libster R, Perez Marc G, Wappner D, Coviello S, Bianchi A, Braem V, et al. Early high-titer plasma therapy to prevent severe covid-19 in older adults. *N Engl J Med* (2021) 384(7):610–8. doi: 10.1056/NEJMoa2033700
42. Menichetti F, Popoli P, Puopolo M, Spila Alegiani S, Tiseo G, Bartoloni A, et al. Effect of high-titer convalescent plasma on progression to severe respiratory failure or death in hospitalized patients with COVID-19 pneumonia: A randomized clinical trial. *JAMA Netw Open* (2021) 4(11):e2136246. doi: 10.1001/jamanetworkopen.2021.36246
43. O'Donnell MR, Grinsztajn B, Cummings MJ, Justman JE, Lamb MR, Eckhardt CM, et al. A randomized double-blind controlled trial of convalescent plasma in adults with severe COVID-19. *J Clin Invest* (2021) 131(13):e150646. doi: 10.1172/JCI150646
44. Ortigoza MB, Yoon H, Goldfeld KS, Troxel AB, Daily JP, Wu Y, et al. Efficacy and safety of COVID-19 convalescent plasma in hospitalized patients: A randomized clinical trial. *JAMA Intern Med* (2022) 182(2):115–26. doi: 10.1001/jamainternmed.2021.6850
45. Pouladzadeh M, Safdarian M, Eshghi P, Abolghasemi H, Bavani AG, Sheibani B, et al. A randomized clinical trial evaluating the immunomodulatory effect of convalescent plasma on COVID-19-related cytokine storm. *Intern Emerg Med* (2021) 16(8):2181–91. doi: 10.1007/s11739-021-02734-8
46. Priscilla Hsue AL. Effects of COVID-19 convalescent plasma (CCP) on coronavirus-associated complications in hospitalized patients (CAPRI). clinicaltrials.gov. (2021). Available at: <https://clinicaltrials.gov/ct2/show/NCT04421404?term=Effects+of+COVID-19+convalescent+plasma+%28CCP%29+on+coronavirus-associated+complications+in+hospitalized+patients&draw=2&rank=1>
47. Rasheed AM, Fatah DF, Hashim HA, Maulood MF, Kabah KK, Almusawi YA, et al. The therapeutic potential of convalescent plasma therapy on treating critically-ill COVID-19 patients residing in respiratory care units in hospitals in Baghdad, Iraq. *Le Infezioni Med* (2020) 28(3):357–66.



48. Ray Y, Paul SR, Bhandopadhyay P, D'Rozario R, Sarif J, Lahiri A, et al. Clinical and immunological benefits of convalescent plasma therapy in severe COVID-19: insights from a single center open label randomised control trial. *medRxiv* (2020) 2020:11.25.20237883. doi: 10.1101/2020.11.25.20237883
49. Sekine L, Arns B, Fabro BR, Cipolatti MM, Machado RRG, Durigon EL, et al. Convalescent plasma for COVID-19 in hospitalised patients: an open-label, randomised clinical trial. *Eur Respir J* (2022) 59(2):2101471. doi: 10.1183/13993003.01471-2021
50. Simonovich VA, Burgos Pratz LD, Scibona P, Beruto MV, Vallone MG, Vazquez C, et al. A randomized trial of convalescent plasma in covid-19 severe pneumonia. *N Engl J Med* (2021) 384(7):619–29. doi: 10.1056/NEJMoa2031304
51. van den Berg K, Glatt TN, Vermeulen M, Little F, Swaneveldt R, Barrett C, et al. Convalescent plasma in the treatment of moderate to severe COVID-19 pneumonia: a randomized controlled trial (PROTECT-patient trial). *Sci Rep* (2022) 12(1):2552. doi: 10.1038/s41598-022-06221-8
52. Writing Committee for the R-CAP, Estcourt LJ, Turgeon AF, McQuilten ZK, McVerry BJ, Al-Beidh F, et al. Effect of convalescent plasma on organ support-free days in critically ill patients with COVID-19: A randomized clinical trial. *JAMA* (2021) 326(17):1690–702. doi: 10.1001/jama.2021.18178
53. Organization WH. *Therapeutics and COVID-19: Living guideline*, 22 April 2022. Geneva: World Health Organization (2022). (WHO/ 2019-nCoV/therapeutics/2022.3). Licence: CC BY-NC-SA 3.0 IGO.
54. America IDSo. IDSA guidelines on the treatment and management of patients with COVID-19. (2022). Available at: <https://www.idsociety.org/practice-guideline/covid-19-guideline-treatment-and-management/>
55. Siemieniuk RA, Bartoszko JJ, Diaz Martinez JP, Kum E, Qasim A, Zeraatkar D, et al. Antibody and cellular therapies for treatment of covid-19: a living systematic review and network meta-analysis. *BMJ* (2021) 374:n2231. doi: 10.1136/bmj.n2231
56. Group RC. Casirivimab and imdevimab in patients admitted to hospital with COVID-19 (RECOVERY): a randomised, controlled, open-label, platform trial. *Lancet (London England)* (2022) 399(10325):665–76. doi: 10.1016/S0140-6736(22)00163-5
57. Consortium WST. Remdesivir and three other drugs for hospitalised patients with COVID-19: final results of the WHO solidarity randomised trial and updated meta-analyses. *Lancet Infect Dis* (2022) 399(10339):1941–53. doi: 10.1016/S0140-6736(22)00519-0
58. Eastman RT, Roth JS, Brimacombe KR, Simeonov A, Shen M, Patnaik S, et al. Remdesivir: A review of its discovery and development leading to emergency use authorization for treatment of COVID-19. *ACS Cent Sci* (2020) 6(5):672–83. doi: 10.1021/acscentsci.0c00489
59. Hassanipour S, Arab-Zozani M, Amani B, Heidarzad F, Fathalipour M, Martinez-de-Hoyo R. The efficacy and safety of favipiravir in treatment of COVID-19: a systematic review and meta-analysis of clinical trials. *Sci Rep* (2021) 11(1):11022. doi: 10.1038/s41598-021-90551-6
60. Wen W, Chen C, Tang J, Wang C, Zhou M, Cheng Y, et al. Efficacy and safety of three new oral antiviral treatment (molnupiravir, fluvoxamine and paxlovid) for COVID-19: a meta-analysis. *Ann Med* (2022) 54(1):516–23. doi: 10.1080/07853890.2022.2034936
61. Drozdal S, Rosik J, Lechowicz K, Machaj F, Szostak B, Przybycinski J, et al. An update on drugs with therapeutic potential for SARS-CoV-2 (COVID-19) treatment. *Drug Resist Updat* (2021) 59:100794. doi: 10.1016/j.drup.2021.100794
62. Group WHOREAfC-TW, Sterne JAC, Murthy S, Diaz JV, Slutsky AS, Villar J, et al. Association between administration of systemic corticosteroids and mortality among critically ill patients with COVID-19: A meta-analysis. *JAMA* (2020) 324(13):1330–41. doi: 10.1001/jama.2020.17023
63. Cano EJ, Fonseca Fuentes X, Corsini Campioli C, O'Horo JC, Abu Saleh O, Odeyemi Y, et al. Impact of corticosteroids in coronavirus disease 2019 outcomes: Systematic review and meta-analysis. *Chest* (2021) 159(3):1019–40. doi: 10.1016/j.chest.2020.10.054
64. Group WHOREAfC-TW, Shankar-Hari M, Vale CL, Godolphin PJ, Fisher D, Higgins JPT, et al. Association between administration of IL-6 antagonists and mortality among patients hospitalized for COVID-19: A meta-analysis. *JAMA* (2021) 326(6):499–518. doi: 10.1001/jama.2021.11330
65. Investigators R-C, Gordon AC, Mouncey PR, Al-Beidh F, Rowan KM, Nichol AD, et al. Interleukin-6 receptor antagonists in critically ill patients with covid-19. *N Engl J Med* (2021) 384(16):1491–502. doi: 10.1056/NEJMoa2100433
66. Chen CX, Wang JJ, Li H, Yuan LT, Gale RP, Liang Y. JAK-inhibitors for coronavirus disease-2019 (COVID-19): a meta-analysis. *Leukemia* (2021) 35(9):2616–20. doi: 10.1038/s41375-021-01266-6
67. Allahyari A, Seddigh-Shamsi M, Mahmoudi M, Amel Jamehdar S, Amini M, Mozdourian M, et al. Efficacy and safety of convalescent plasma therapy in severe COVID-19 patients with acute respiratory distress syndrome. *Int Immunopharmacol* (2021) 93:107239. doi: 10.1016/j.intimp.2020.107239
68. De Silvestro G, Marson P, La Raja M, Cattelan AM, Guarnieri G, Monticelli J, et al. Outcome of SARS CoV-2 inpatients treated with convalescent plasma: One-year of data from the veneto region (Italy) registry. *Eur J Internal Med* (2022) 97:42–9. doi: 10.1016/j.ejim.2021.12.023
69. Lindemann M, Lenz V, Knop D, Klump H, Alt M, Aufderhorst UW, et al. Convalescent plasma treatment of critically ill intensive care COVID-19 patients. *Transfusion* (2021) 61(5):1394–403. doi: 10.1111/trf.16392
70. Sturek JM, Thomas TA, Gorham JD, Sheppard CA, Raymond AH, Petros De Guex K, et al. Convalescent plasma for preventing critical illness in COVID-19: a phase 2 trial and immune profile. *Microbiol Spectrum* (2022) 10(1):e0256021. doi: 10.1128/spectrum.02560-21
71. Bradfute SB, Hurwitz I, Yingling AV, Ye C, Cheng Q, Noonan TP, et al. Severe acute respiratory syndrome coronavirus 2 neutralizing antibody titers in convalescent plasma and recipients in new Mexico: An open treatment study in patients with coronavirus disease 2019. *J Infect Dis* (2020) 222(10):1620–8. doi: 10.1093/infdis/jiaa505
72. Baldeón ME, Maldonado A, Ochoa-Andrade M, Largo C, Pesantez M, Herdoiza M, et al. Effect of convalescent plasma as complementary treatment in patients with moderate COVID-19 infection. *Transfusion Med* (2022) 32(2):153–61. doi: 10.1111/tme.12851
73. Cho K, Keithly SC, Kurgansky KE, Madenci AL, Gerlovin H, Marucci-Wellman H, et al. Early convalescent plasma therapy and mortality among US veterans hospitalized with nonsevere COVID-19: An observational analysis emulating a target trial. *J Infect Dis* (2021) 224(6):967–75. doi: 10.1093/infdis/jiab330
74. Arnold Egloff SA, Junglen A, Restivo JS, Wongsakuluang M, Martin C, Doshi P, et al. Convalescent plasma associates with reduced mortality and improved clinical trajectory in patients hospitalized with COVID-19. *J Clin Invest* (2021) 131(20):e151788. doi: 10.1172/JCI151788
75. Shenoy AG, Hettlinger AZ, Fernandez SJ, Blumenthal J, Baez V. Early mortality benefit with COVID-19 convalescent plasma: a matched control study. *Br J Haematol* (2021) 192(4):706–13. doi: 10.1111/bjh.17272
76. Papanikolaou V, Chrysovergis A, Ragos V, Tsiambas E, Katsinis S, Manoli A, et al. From delta to omicron: S1-RBD/S2 mutation/deletion equilibrium in SARS-CoV-2 defined variants. *Gene* (2022) 814:146134. doi: 10.1016/j.gene.2021.146134
77. Shah M, Woo HG. Omicron: A heavily mutated SARS-CoV-2 variant exhibits stronger binding to ACE2 and potentially escapes approved COVID-19 therapeutic antibodies. *Front Immunol* (2021) 12:830527. doi: 10.3389/fimmu.2021.830527
78. Sheward DJ, Kim C, Ehling RA, Pankow A, Castro Dopico X, Dyrda R, et al. Neutralisation sensitivity of the SARS-CoV-2 omicron (B.1.1.529) variant: a cross-sectional study. *Lancet Infect Dis* (2022) 22(6):813–820. doi: 10.1016/S1473-3099(22)00129-3
79. Kunze KL, Johnson PW, van Helmond N, Senefeld JW, Petersen MM, Klassen SA, et al. Mortality in individuals treated with COVID-19 convalescent plasma varies with the geographic provenance of donors. *Nat Commun* (2021) 12(1):4864. doi: 10.1038/s41467-021-25113-5
80. Pirofski LA, Casadevall A. Pathogenesis of COVID-19 from the perspective of the damage-response framework. *mBio* (2020) 11(4):e01175–20. doi: 10.1128/mBio.01175-20
81. Focosi D, Casadevall A. High-dose convalescent plasma for treatment of severe COVID-19. *Emerg Infect Dis* (2022) 28(5):1083. doi: 10.3201/eid2805.220191
82. Scarpa R, Dell'Edera A, Felice C, Buso R, Muscianisi F, Finco Gambier R, et al. Impact of hypogammaglobulinemia on the course of COVID-19 in a non-intensive care setting: A single-center retrospective cohort study. *Front Immunol* (2022) 13:842643. doi: 10.3389/fimmu.2022.842643
83. Tang J, Grubbs G, Lee Y, Golding H, Khurana S. Impact of convalescent plasma therapy on severe acute respiratory syndrome coronavirus 2 (SARS-CoV-2) antibody profile in coronavirus disease 2019 (COVID-19) patients. *Clin Infect Dis* (2022) 74(2):327–34. doi: 10.1093/cid/ciab317
84. Focosi D, Franchini M, Pirofski LA, Burnouf T, Paneth N, Joyner MJ, et al. COVID-19 convalescent plasma and clinical trials: Understanding conflicting outcomes. *Clin Microbiol Rev* (2022):e0020021. doi: 10.1128/cmr.00200-21
85. Axfors C, Janiaud P, Schmitt AM, Van't Hooft J, Smith ER, Haber NA, et al. Association between convalescent plasma treatment and mortality in COVID-19: a collaborative systematic review and meta-analysis of randomized clinical trials. *BMC Infect Dis* (2021) 21(1):1170. doi: 10.1186/s12879-021-06829-7
86. Ling RR, Sim JLL, Tan FL, Tai BC, Syn N, Mucheli SS, et al. Convalescent plasma for patients hospitalized with coronavirus disease 2019: A meta-analysis with trial sequential analysis of randomized controlled trials. *Transfus Med Rev* (2022) 36(1):16–26. doi: 10.1016/j.tmr.2021.09.001



87. Snow TAC, Saleem N, Ambler G, Nastouli E, McCoy LE, Singer M, et al. Convalescent plasma for COVID-19: a meta-analysis, trial sequential analysis, and meta-regression. *Br J Anaesth* (2021) 127(6):834–44. doi: 10.1016/j.bja.2021.07.033
88. Yang P, Wang J, Zheng R, Tan R, Li X, Liu X, et al. Convalescent plasma may not be an effective treatment for severe and critically ill covid-19 patients: A systematic review & meta-analysis of randomized controlled trials. *Heart Lung* (2022) 53:51–60. doi: 10.1016/j.hrtlng.2022.01.019
89. Thompson MA, Henderson JP, Shah PK, Rubinstein SM, Joyner MJ, Choueiri TK, et al. Association of convalescent plasma therapy with survival in patients with hematologic cancers and COVID-19. *JAMA Oncol* (2021) 7(8):1167–75. doi: 10.1101/2021.02.05.21250953
90. Shoham S, Bloch EM, Casadevall A, Hanley D, Lau B, Gebo K, et al. Transfusing convalescent plasma as post-exposure prophylaxis against SARS-CoV-2 infection: a double-blinded, phase 2 randomized, controlled trial. *Clin Infect Dis* (2022) 17:ciac372. doi: 10.1093/cid/ciac372



## OPEN ACCESS

## EDITED BY

Alfonso J. Rodriguez-Morales,  
Fundacion Universitaria Autónoma de  
las Américas, Colombia

## REVIEWED BY

Piyush Baidara,  
University of Missouri, United States  
Enqiang Chen,  
Sichuan University, China  
Yan Huang,  
Central South University, China

## \*CORRESPONDENCE

Jiabin Li  
lijabin@ahmu.edu.cn  
Hong Zhang  
zhanghong20070703@163.com  
Yufeng Gao  
aygyf@ahmu.edu.cn

## SPECIALTY SECTION

This article was submitted to  
Viral Immunology,  
a section of the journal  
Frontiers in Immunology

RECEIVED 13 June 2022

ACCEPTED 18 July 2022

PUBLISHED 05 August 2022

## CITATION

Xu N, Pan J, Sun L, Zhou C, Huang S,  
Chen M, Zhang J, Zhu T, Li J, Zhang H  
and Gao Y (2022) Interferon  $\alpha$ -2b  
spray shortened viral shedding time of  
SARS-CoV-2 Omicron variant: An  
open prospective cohort study.  
*Front. Immunol.* 13:967716.  
doi: 10.3389/fimmu.2022.967716

## COPYRIGHT

© 2022 Xu, Pan, Sun, Zhou, Huang,  
Chen, Zhang, Zhu, Li, Zhang and Gao.  
This is an open-access article  
distributed under the terms of the  
Creative Commons Attribution License  
(CC BY). The use, distribution or  
reproduction in other forums is  
permitted, provided the original  
author(s) and the copyright owner(s)  
are credited and that the original  
publication in this journal is cited, in  
accordance with accepted academic  
practice. No use, distribution or  
reproduction is permitted which does  
not comply with these terms.

# Interferon $\alpha$ -2b spray shortened viral shedding time of SARS-CoV-2 Omicron variant: An open prospective cohort study

Nan Xu<sup>1</sup>, Jinjin Pan<sup>1</sup>, Li Sun<sup>2</sup>, Cuimei Zhou<sup>1</sup>, Siran Huang<sup>1</sup>,  
Mingwei Chen<sup>2</sup>, Junfei Zhang<sup>1</sup>, Tiantian Zhu<sup>3</sup>, Jiabin Li<sup>1\*</sup>,  
Hong Zhang<sup>1,3\*</sup> and Yufeng Gao<sup>1\*</sup>

<sup>1</sup>Department of Infectious Diseases, the First Affiliated Hospital of Anhui Medical University, Hefei, China, <sup>2</sup>Department of Endocrinology, the First Affiliated Hospital of Anhui Medical University, Hefei, China, <sup>3</sup>Department of Emergency, Anhui Public Health Clinical Centre, Hefei, China

**Background:** The Omicron SARS-CoV-2 variant has spread quickly worldwide due to its effects on virus transmission and vaccine effectiveness. Interferon (IFN) has been shown to have a protective effect against SARS-CoV because of its broad antiviral activity. This study aimed to analyze the treatment effects of IFN  $\alpha$ -2b spray in virus clearance of the Omicron SARS-CoV-2 variant.

**Methods:** We examined the effectiveness and safety of IFN  $\alpha$ -2b spray in Shanghai, China, with participants infected with the Omicron SARS-CoV-2 variant in an open, prospective cohort study from April 16th to May 5th, 2022.

**Results:** A total of 871 confirmed patients were enrolled in this study. Four hundred and thirteen patients were allocated to the IFN  $\alpha$ -2b spray group, and 458 patients were allocated to the control group. The viral shedding time was significantly different between experimental group and control group (11.90 vs. 12.58,  $P < 0.05$ ). In the experimental group, the median administration time since the first positive test for SARS-CoV-2 was three days, ranging from 0 to 15 days. There was no obvious adverse effect associated with the spray of IFN  $\alpha$ -2b. The univariate Cox regression analysis revealed that the administration time since the first positive test  $\leq 3$  days was a protective factor associated with viral shedding time (HR 0.81 95% CI 0.74-0.87,  $P < 0.05$ ). Subgroup analysis showed that the viral shedding time was 10.41 (4.00-16.00) days in the  $\leq 3$  days group, which was significantly less than that in the control group (12.58, 95% CI: 7.00-19.15,  $P < 0.0001$ ) and in the  $> 3$  days group (13.56, 95% CI: 7.00-22.25,  $P < 0.0001$ ).

**Conclusions:** IFN  $\alpha$ -2b spray shortened the viral shedding time of the Omicron SARS-CoV-2 variant when administrated within three days since the first positive test for SARS-CoV-2.

## KEYWORDS

SARS-CoV-2 Omicron variant, COVID-19, IFN  $\alpha$ -2b spray, viral shedding time, cohort study

## Introduction

Currently, the Omicron outpaces the other variants of SARS-CoV-2 to be the dominant circulating strain, sweeping across the world (1). Over 500,000 local Omicron infections have been reported in China between 1 March and 22 April 2022, with the majority occurring in Shanghai (about 93%) (2). The major Omicron sub-lineages that prevail among the local novel coronavirus pneumonia (COVID-19) outbreaks in China are BA.1 and BA.2 (3–5). Paxlovid (nirmatrelvir/ritonavir) was authorized by the Chinese National medical products administration in February 12, 2022 for cases with mild to moderate COVID-19. However, the potential for significant drug-drug interactions, the high cost and the low-accessibility limit clinical use. Globally, there are an increasing number of cases and deaths and very limited treatment options, so new effective antiviral drugs are urgently needed.

Considering that type I interferons (IFNs) inhibit the replication of both DNA and RNA viruses at different stages of their replication cycles and effect on activating immune cell populations to clear infections, type I IFNs are directly antiviral agents (6). Based on its character of broad antiviral activity, IFN has been shown to exert a protective effect against SARS-CoV infection (7). However, patients with Covid-19 who received IFN treatment had little effect, as indicated by their overall mortality, the start of ventilation, and the length of their hospital stay in multiple clinical studies (8–10). The possible reason was that SARS-CoV-2 was capable of avoiding or disabling many of interferon's effects (11). Nevertheless, a recent investigation revealed that Omicron variant has a lower ability to withstand host cell interferon responses. Further study showed that sequence variations in the SARS-CoV-2 IFN antagonists nsp3, nsp12, nsp13, nsp14, M protein, the nucleocapsid protein, and/or ORF3a may contribute to these differences (12, 13). As Omicron variant possesses a substantially enhanced IFN sensitivity, IFNs represent a promising option for the treatment of Omicron patients. Although a lot of meaningful exploration has been made, evidence of IFN effectiveness is mixed. Furthermore, the optimal route of administration and timing of IFN therapy to treat SARS-CoV-2 is not well documented.

Moreover, Nasal epithelium is thought to be one of the main entry points for SARS-CoV-2. The high transmissibility of SARS-CoV-2 is attributed to nasal epithelial tropism and efficient virus release from the nasopharynx. However, the main entrance of SARS-CoV-2, Angiotensin-converting enzyme 2 (ACE2), was expressed at very low protein levels in respiratory and olfactory epithelial cells. Another host factor, neuropilin-1 (NRP1) has been demonstrated as an entrance for SARS-CoV-2 infection (14). NRP1 represented as an ACE2 potentiating factor by promoting the interaction of the virus with ACE2 (15). A recent study analyzed the receptor-ligand interaction and found that the NRP1 coreceptor pathway may increase the infectivity of the

Omicron variant of SARS-CoV-2 (16). Nasal cells mount a robust innate antiviral response to SARS-CoV-2 dominated by paracrine IFN-I/III signaling. Upon exposure to exogenous IFN-I/III, these cells undergo a profound antiviral response (17). A new study by Imperial College London showed that Omicron replicates rapidly in human primary airway cultures, enabling Omicron to infect more cells in the respiratory epithelium, allowing it to be more infectious at lower exposure doses and resulting in enhanced intrinsic transmissibility (18). Similarly, another study identified that Omicron variant replicates more rapidly in the respiratory tract than all other SARS-CoV-2 variants, but less efficiently in the lungs, which may explain the reduced severity of Omicron that is now being reported in epidemiological studies (19). As the highest viral loads are detectable in the upper respiratory tract, reducing infectious viruses in the nasopharynx could lower viral shedding and, consequently, transmission by infected individuals (20).

IFN spray could act on respiratory epithelium, and directly exerts antiviral activity. According to the study from Gao, using IFN  $\alpha$ -2b for spray could effectively prevent respiratory infections caused by influenza viruses, para-influenza viruses, and adenoviruses (21). Therefore, IFN spray could be a potential prophylactic and therapeutic agent against SARS-CoV-2 Omicron variant. This study aimed to analyze the treatment effects of IFN  $\alpha$ -2b spray in virus clearance of Omicron SARS-CoV-2 variant in an open, prospective cohort.

## Methods

### Patients and study design

A total of 871 confirmed patients from Shanghai Temporary Hospital (Chongming District, Shanghai) were enrolled in this study from April 16th to May 5th, 2022. Four hundred and thirteen patients were allocated to the IFN  $\alpha$ -2b spray group, and 458 patients were allocated to the control group (Figure 1). None of the asymptomatic or mild participants underwent blood tests, limited by the temporary hospital. The study was registered in the ClinicalTrials.gov (Registry NO. ChiCTR2200058790) and has been approved by the ethic committee of the first affiliated hospital of Anhui medical university (PJ-2022-0408). All participants provided informed consent before enrollment and drug administration.

This open, prospective cohort study aims to evaluate the safety and viral shedding time (real-time PCR Ct value  $>35$  for both ORF1ab and N gene) of IFN  $\alpha$ -2b spray in treating Omicron SARS-CoV-2 variant from April 16th to May 5th, 2022. Patients aged between 18 and 60 years, with real-time PCR confirmed SARS-CoV-2 infection were enrolled. Exclusion criteria: 1) With history of IFN allergies; 2) co-morbidities such as chronic heart failure and respiratory failure, severe malnutrition, and immune deficiencies; 3) patients with a severe or critical COVID-19 diagnosis before intervention; 4) active bacterial, fungal, or viral infections besides COVID-19; 5)

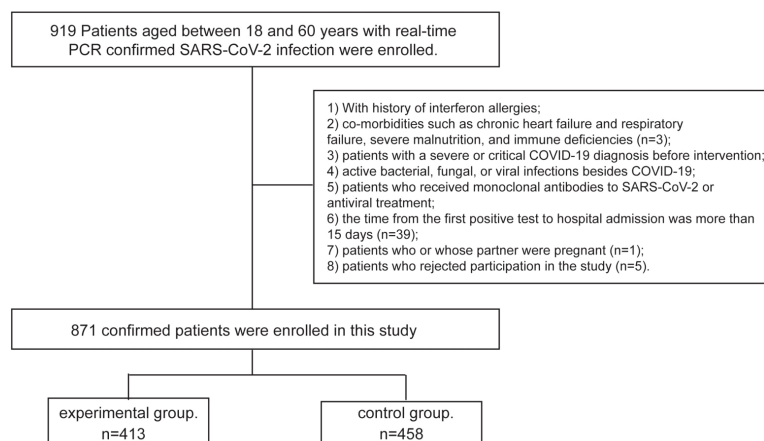


FIGURE 1

The flowchart of the study. Screening, enrolment and random classification of patients.

patients who received monoclonal antibodies to SARS-CoV-2 or antiviral treatment; 6) the time from the first positive test to hospital admission was more than 15 days; 7) patients who or whose partner were pregnant, nursing, or likely to become pregnant; 8) patients who rejected participation in the study.

## Interventions

Complete medical history was taken, including demographic information, chronic disease history, symptoms of COVID-19 illness and vaccination status at the baseline after receiving consent from every participant. In addition to an essential clinical assessment and examination, appropriate protective measures were taken for all participants. The participants were randomized into two groups with the control group and the experimental group.

In the experimental group, recombinant human IFN  $\alpha$ -2b were sprayed on the patients' posterior pharyngeal wall, bilateral tonsils and oral lesions every 6 hours for seven days (3 sprays/time, about 1.2 million IU/day, ANKE Biotechnology (Group) Co., Ltd., HEFEI, CHINA). After spraying, diet and water were prohibited for 15 minutes. The control group did not receive IFN  $\alpha$ -2b spray. All of the participants received symptomatic treatment based on their clinical manifestations, including non-steroidal anti-inflammatory drugs, cough mixtures and traditional Chinese medicine.

## Study definitions

Time to viral clearance was the primary outcome. SARS-CoV-2 RNA was tested daily in respiratory specimens from all patients until discharge. The nucleic acid test negative conversion was defined as two consecutive negative tests (Ct

value >35 for the ORF1ab and N gene). The viral shedding time was defined as the duration from the first positive nucleic acid test to the date of the first negative test (in two consecutive, more than 24 hours apart). For patients still shedding virus at the end of the study, the time from the date of confirmed diagnosis to the final follow-up date of May 15th, 2022 was used for the calculation of viral shedding time.

## Statistical analysis

Continuous variables were expressed as medians (Range) or means (Standard Deviation, SD) and compared using a non-parametric test. Categorical variables were expressed as numbers (%) and compared by the  $\chi^2$  test or Fisher's exact tests. The viral shedding time was compared between the two groups in both the primary and subgroup analyses. Hazard ratio (HR) and 95% confidence interval were calculated by Cox regression. A two-sided  $P < 0.05$  was considered statistically significant. Statistical analysis was performed using IBM SPSS 23.0 (IBM, Armonk, NY, USA).

## Results

Participant characteristics were generally similar between the two groups (Table 1) except for the sex ratio. The proportion of males in the experimental group (76.3%) was higher than that in the control group (67.2%). The average age was similar for both groups. There were 10 (2.4%) and 13 (2.8%) patients in the two groups who were obese. The experimental and control groups did not differ in smoking. Fewer cases of chronic

TABLE 1 The clinical characteristics of enrolled patients.

	Experimental(N=413)	Control(N=458)	P-value
Age, Mean± SD, years	39.0 ± 10.3	39.5 ± 10.3	0.463
Gender, n (%)			0.003
Female	98 (23.7)	150 (32.8)	
Male	315 (76.3)	308 (67.2)	
Obesity, n (%)			0.701
Normal	403 (97.6)	445 (97.2)	
Obesity	10 (2.4)	13 (2.8)	
Smoking, n (%)			0.165
Non-smoking	373 (90.3)	400 (87.3)	
Heavy smoking	40 (9.7)	58 (12.7)	
Chronic diseases, n (%)			0.162
Non-chronic diseases	356 (86.2%)	379 (82.8%)	
Chronic diseases	57 (13.8%)	79 (17.2%)	
Hypertension	48 (11.6)	68 (14.8)	
Diabetes	10 (2.4)	15 (3.3)	
Other	5 (1.2)	7 (1.5)	
Clinical classification, n(%)			0.690
Asymptomatic	185 (44.8)	199 (43.4)	
Symptomatic	228 (55.2)	259 (56.6)	
fever	186 (45.0)	165 (36.0)	
cough	184 (44.6)	208 (45.4)	
Sputum production	141 (34.1)	153 (33.4)	
Sore throat	128 (31.0)	156 (34.1)	
loss of gustation	25 (6.1)	37 (8.1)	
loss of olfaction	12 (2.9)	14 (3.1)	
Vaccination, n (%)			0.852
Unvaccinated	10 (2.4)	12 (2.6)	
Vaccinated	403 (97.6)	446 (97.4)	
Partially vaccinated	18 (4.5)	31 (7.0)	
Full vaccination	124 (30.8)	171 (38.3)	
Booster	261 (64.8)	244 (54.7)	
Admission time since the first positive test 0.120			
Median (range), days	3 (0-15)	3 (0-15)	
Mean ± SD, days	4.63 ± 3.94	3.86 ± 3.17	
Administration time since the first positive test			
≤3 days, n(%)	217 (52.5)	/	
>3 days, n(%)	196 (47.5)	/	
Median (range), days	3 (0-15)	/	
Mean ± SD, days	4.6 ± 3.9	/	

diseases were observed in the experimental group (13.8% vs. 17.2%) with no significance. Other chronic diseases included stable chronic bronchitis, asthma, hypothyroidism, and chronic hepatitis B also had no significant difference. The most frequently reported symptoms were fever (45.0% vs. 36.0%) and cough (44.6% vs. 45.4%) in both groups. There were no significant differences between vaccination status in the two groups, and both groups had high vaccination rates (97.6% vs. 97.4%,  $P=0.852$ ). There were 261 and 244 participants who

received the booster dose, respectively. In the experimental group, the median administration time since the first positive test for SARS-CoV-2 was three days, ranging from 0 to 15 days. There was no obvious adverse effect associated with spray of IFN  $\alpha$ -2b.

The univariate Cox regression analysis revealed that the administration time since the first positive test  $\leq 3$  days was a protective factor associated with the viral shedding time (Table 2, HR 0.81 95% CI 0.74-0.87,  $P < 0.05$ ). The viral



**TABLE 2** The hazard ratios, two-sided 95% confidence intervals, and P value were estimated with the use of Cox regression with the baseline stratification factors as covariates.

	Adjusted Hazard Ratio	P value
Administration time since the first positive test		
≤3 days	0.81 (0.74, 0.87)	0.000
>3 days	1.20 (1.02, 1.43)	0.031
Gender		
Male	0.96 (0.82,1.12)	0.540
Age	0.99 (0.99,1.00)	0.019
Obesity	1.44 (0.95,2.18)	0.088
Heavy smoking	0.97 (0.79,1.20)	0.805
Asymptomatic	1.00 (0.87,1.14)	0.980
Vaccination	0.83 (0.55,1.27)	0.397
Partially vaccinated	0.84 (0.55,1.29)	0.428
Full vaccination	1.03 (0.77,1.38)	0.836
Booster	1.03 (0.89,1.18)	0.741
Chronic diseases	0.87 (0.72,1.05)	0.137

shedding time was significantly different between experimental group and control group (11.90(5.00-20.00) vs.12.58(7.00-19.15),  $P = 0.024$ , **Table 3**). According to the median administration time since the first positive test for SARS-CoV-2, the experimental group was divided into ≤3 days group and >3 days group. Subgroup analysis showed that the viral shedding

time was 10.41 (4.00-16.00) days in the ≤3 days group and 13.56 (7.00-22.25) days in the >3 days group ( $P < 0.0001$ , **Table 3**). The subgroup analyses for vaccination, gender, obesity (BMI ≥30), heavy smoking (20 or more cigarettes per day), symptoms were performed. The effect of IFN  $\alpha$ -2b spray on virus clearance was significant among vaccinated, non-obese, smoking, and

**TABLE 3** Main groups and subgroups analysis of the differences of the viral shedding time.

Main groups and subgroups(95% CI)	IFN(n=413)	Control(n=458)	P-value
Main groups 11.90 (5.00-20.00) 12.58 (7.00-19.15)			0.024
Administration time since the first positive test			
≤3 days	10.41 (4.00-16.00) n=217	12.58 (7.00-19.15) n=458	<0.0001
>3 days	13.56 (7.00-22.25) n=196	12.58 (7.00-19.15) n=458	0.077
Vaccination			
Unvaccinated	11.80 (5.90-16.55) n=10	14.33 (9.55-22.15) n=12	0.192
Vaccinated	11.90 (5.00-20.00) n=403	12.53 (7.00-19.00) n=446	0.038
Partially vaccinated	10.33 (4.70-15.00) n=18	13.16 (8.00-19.00) n=31	0.013
Full vaccination	11.92 (5.15-20.00) n=124	12.49 (7.00-19.00) n=171	0.254
Booster	12.00 (5.00-21.00) n=261	12.48 (7.00-21.85) n=244	0.238
Gender			
Female	11.78 (5.00-20.15) n=98	12.47 (8.00-18.55) n=150	0.210
Male	11.93 (8.99-20.00) n=315	12.63 (6.00-21.00) n=308	0.056
Obesity			
Non-obesity	11.95 (3.00-20.00) n=403	12.60 (7.00-19.80) n=445	0.033
Obesity	9.80 (4.25-14.55) n=10	11.69 (7.00-14.60) n=13	0.205
Smoking			
Non-smoking	12.00 (5.00-20.40) n=373	12.49 (7.00-19.00) n=400	0.126
Heavy smoking	10.98 (4.00-15.20) n=40	13.22 (6.00-24.00) n=58	0.011
Symptoms			
Asymptomatic	11.95 (4.20-20.00) n=185	12.38 (6.00-19.00) n=199	0.375
Symptomatic	11.86 (5.35-20.00) n=228	12.73 (7.00-21.00) n=259	0.021

symptomatic patients (Table 3). The above results and the Kaplan-Meier curves indicated that viral shedding resolved sooner in individuals prescribed IFN  $\alpha$ -2b spray within three days of onset. The differences were statistically significant ( $P < 0.0001$ , Figure 2).

## Discussion

From February 26th to May 5th, 2022, there were 55,131 cumulative confirmed cases and 562,863 cumulative asymptomatic cases reported in the Omicron variant of SARS-CoV-2 epidemic wave (22). The emerging studies show that the Omicron variant became milder than the previous variants, the trend of increasing cases and admissions waves shifted with a higher and quicker peak but fewer patients were admitted to hospital, less clinically severe illnesses (23, 24). However, a recent study published in JAMA revealed that all-cause excess mortality in Massachusetts during the first eight weeks of the Omicron period was more than that during the entire 23-week Delta period (25). It presumably reflects a higher mortality product (i.e., a moderately lower infection fatality rate multiplied by a far higher infection rate). A predictive model study from China showed that immunity induced by the March 2022 vaccination campaign would not be sufficient to prevent an Omicron wave. The study also showed that the Omicron wave would cause a projected intensive care unit peak demand of 15.6 times the existing capacity and cause approximately 1.55 million deaths (26). As previously reported, the Omicron caused more infections but less severe ones or deaths, while constant outbreaks and a large population base still put a tremendous amount of strain on the system.

Some new drugs such as Paxlovid (nirmatrelvir/ritonavir) are developing and being tested in clinical trials, but still hard to widely used due to the high cost and side effects. Therefore, it is urgent to develop a simple and effective anti-viral drug for combating the Omicron variant of SARS-CoV-2 pandemics. In this study, all participants were asymptomatic and mild cases. IFN  $\alpha$ -2b spray significantly accelerated the viral shedding by 2–3 days when applied within three days since the first positive test for SARS-CoV-2. In addition, more than 97% of cases in experimental and control groups received the vaccine, which suggested that IFN  $\alpha$ -2b spray might benefit people who have already been vaccinated. Subgroup analysis revealed that vaccinated participants cleared viral infection faster regardless of when the first injection occurred. Notably, the same effect was observed in non-obese, smoking and symptomatic cases.

Innate immunity, in particular IFN-I, is the first line of defense against viral infection. IFN-I has an essential role in the pathogenesis of COVID-19 (27–29). Even though rapid induction of type I IFNs prevents viral propagation, a sustained increase in the levels of type I IFNs in the late phase of the infection results in aberrant inflammation and poor clinical outcome (29–32). A study from Domizio et al. showed that the cyclic GMP-AMP synthase (cGAS)–stimulator of interferon genes (STING) pathway, which controls immunity to cytosolic DNA, was a critical driver of aberrant type I IFN responses in COVID-19 (33). It has been reported that early administration of therapeutic IFN could correct the imbalanced IFN response with excessive cytokine production caused by repressed type I IFN expression in critically ill COVID-19 patients (34). However, ACE2 has been demonstrated as a type I and III interferon-stimulated gene in human airway epithelial cells (35), which suggested that IFN may promote viral entry and replication in those cells. A multicenter cohort

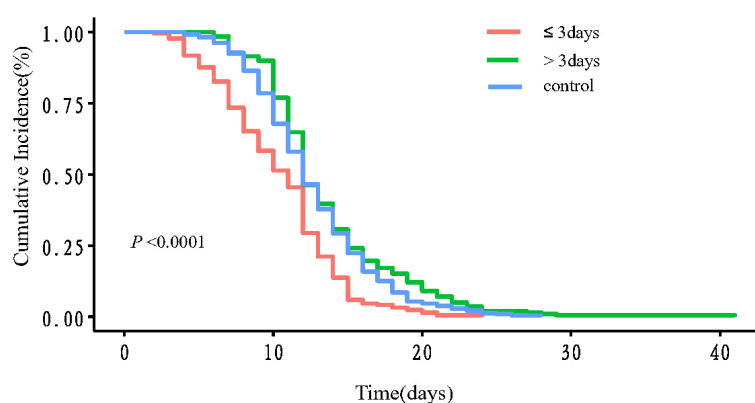


FIGURE 2

The Kaplan-Meier curve of the viral shedding time. Red line:  $\leq 3$  days group; green line:  $> 3$  days groups; blue line: control group.  $P < 0.0001$  between  $\leq 3$  days group and control group;  $P = 0.0176$  between  $> 3$  days group and control group;  $P < 0.0001$  between  $\leq 3$  days group and  $> 3$  days group.

study has shown no association of early IFN use with CT scan improvement in survived patients, and late IFN use was associated with slower CT scan improvement (36). Similarly, we found that early use of IFN  $\alpha$ -2b spray shortened viral shedding time, whereas delayed use may lead to prolonged viral shedding time. (Table 3, administration time since the first positive test 13.56 (7.00-22.25) vs. 12.58(7.00-19.15)).

Unlike other big proteins or molecules, Type I IFNs have been widely used as an anti-viral agent for a long time. Type I IFNs act through ubiquitously expressed IFN- $\alpha/\beta$  receptors (type I IFN receptor 1, IFNAR1 and IFNAR2), which are associated with tyrosine kinase 2 (TYK2) and Janus kinase 1 (JAK1), respectively (37). As the IFNAR receptors are generally widely expressed, the type I IFNs have a broad range of target cells, except red blood cells, phagocytes and kidney cells (38). However, the immunomodulatory action of IFN- $\alpha$  causes the release of a series of cytokines, including TNF- $\alpha$ , IL-1, IL-2, IL-6, and IFN- $\gamma$ , resulting in a cytokine storm that leads to adverse reactions such as fever, muscle soreness, chills and other transient flu-like symptoms (39, 40). In our study, we choose the aerosol instead of intramuscular injection to avoid the side effect. The application of IFN  $\alpha$ -2b spray had several advantages. First of all, the drug is commercially available, making it easier to apply than subcutaneous injections or atomized inhalations. Second, because the spray treatment can target the respiratory system directly, there is no need for systemic distribution. Third, as mentioned above, the use of IFN  $\alpha$ -2b spray in this study did not lead to noticeable side effects. Finally, in contrast with atomization inhalation, IFN  $\alpha$ -2b spray avoids droplet and aerosol transmission risks. However, there was a limitation in this study, the difference of viral shedding time between experimental and control group of unvaccinated patients had no significance. This may due to limited number of unvaccinated participants enrolled in this study.

In conclusion, our study is the first to evaluate the clinical function of IFN  $\alpha$ -2b spray, which was an inexpensive, easily available, few side effects drug to the Omicron SARS-CoV-2 variant. Furthermore, IFN  $\alpha$ -2b spray shortened the viral shedding time, and the administration time was within three days since the first positive test for SARS-CoV-2. However, the results of our study need to be further validated in other research before being clinically used in the future.

## Data availability statement

The raw data supporting the conclusions of this article will be made available by the authors, without undue reservation.

## Ethics statement

The studies involving human participants were reviewed and approved by The ethic committee of the first affiliated hospital of Anhui Medical University(PJ-2022-0408). The patients/participants provided their written informed consent to participate in this study.

## Author contributions

The study was designed and supervised by YG. The manuscript was written by NX, JP, SH. The data analysis was performed by LS, JZ, TZ. All authors were involved in critical revision of manuscript. All authors contributed to the article and approved the submitted version.

## Funding

This research was supported by the project of emergency scientific research of COVID-19 of Anhui Province (2022e07020078).

## Acknowledgments

We are grateful to all the patients who volunteered for this trial, as well as the personnel at the study sites. The authors thank Dr. Jiang Li for giving helpful comments on preparing manuscript. Study drug interferon  $\alpha$ -2b spray was donated by Anhui ANKE Biotechnology (Group) Co., Ltd.

## Conflict of interests

The authors declare that the research was conducted in the absence of any commercial or financial relationships that could be construed as a potential conflict of interest.

## Publisher's note

All claims expressed in this article are solely those of the authors and do not necessarily represent those of their affiliated organizations, or those of the publisher, the editors and the reviewers. Any product that may be evaluated in this article, or claim that may be made by its manufacturer, is not guaranteed or endorsed by the publisher.

## References

- Del Rio C, Omer SB, Malani PN. Winter of omicron-the evolving covid-19 pandemic. *Jama* (2022) 327(4):319–20. doi: 10.1001/jama.2021.24315
- The State Council Information Office PRCA. Press Conference Held on Situation Regarding Strict Prevention and Control of Covid-19 Epidemic. Available from: <http://www.gov.cn/xinwen/gwylflkjz193/index.htm>.
- Zhang D, Wu S, Ren Z, Sun Y, Dou X, Feng Z, et al. A local cluster of omicron variant covid-19 likely caused by internationally mailed document - Beijing municipality, China, January 2022. *China CDC Wkly* (2022) 4(14):302–4. doi: 10.46234/ccdcw2022.031
- Li K, Zheng Z, Zhao X, Zeng Q, Zhou T, Guo Q, et al. An imported case and an infected close contact of the omicron variant of sars-Cov-2 - guangdong province, China, December 13, 2021. *China CDC Wkly* (2022) 4(5):96–7. doi: 10.46234/ccdcw2021.265
- Guo Q, Ruhan A, Liang L, Zhao X, Deng A, Hu Y, et al. An imported case of Ba.2 lineage of omicron variant covid-19 - guangdong province, China, December 28, 2021. *China CDC Wkly* (2022) 4(5):98–9. doi: 10.46234/ccdcw2022.001
- Wang BX, Fish EN. Global virus outbreaks: Interferons as 1st responders. *Semin Immunol* (2019) 43:101300. doi: 10.1016/j.smim.2019.101300
- Haagmans BL, Kuiken T, Martina BE, Fouchier RA, Rimmelzwaan GF, van Amerongen G, et al. Pegylated interferon-alpha protects type 1 pneumocytes against sars coronavirus infection in macaques. *Nat Med* (2004) 10(3):290–3. doi: 10.1038/nm1001
- Pan H, Peto R, Henao-Restrepo AM, Preziosi MP, Sathiyamoorthy V, Abdool Karim Q, et al. Repurposed antiviral drugs for covid-19 - interim who solidarity trial results. *New Engl J Med* (2021) 384(6):497–511. doi: 10.1056/NEJMoa2023184
- Jagannathan P, Andrews JR, Bonilla H, Hedlin H, Jacobson KB, Balasubramanian V, et al. Peginterferon lambda-1a for treatment of outpatients with uncomplicated covid-19: A randomized placebo-controlled trial. *Nat Commun* (2021) 12(1):1967. doi: 10.1038/s41467-021-22177-1
- Kalil AC, Mehta AK, Patterson TF, Erdmann N, Gomez CA, Jain MK, et al. Efficacy of interferon beta-1a plus remdesivir compared with remdesivir alone in hospitalised adults with covid-19: A double-blind, randomised, placebo-controlled, phase 3 trial. *Lancet Respir Med* (2021) 9(12):1365–76. doi: 10.1016/s2213-2600(21)00384-2
- Oh SJ, Shin OS. Sars-Cov-2-Mediated evasion strategies for antiviral interferon pathways. *J Microbiol* (2022) 60(3):290–9. doi: 10.1007/s12275-022-1525-1
- Bojkova D, Widera M, Ciesek S, Wass MN, Michaelis M, Cinatl J Jr. Reduced interferon antagonism but similar drug sensitivity in omicron variant compared to delta variant of sars-Cov-2 isolates. *Cell Res* (2022) 32(3):319–21. doi: 10.1038/s41422-022-00619-9
- Bojkova D, Rothenburger T, Ciesek S, Wass MN, Michaelis M, Cinatl J Jr. Sars-Cov-2 omicron variant virus isolates are highly sensitive to interferon treatment. *Cell Discovery* (2022) 8(1):42. doi: 10.1038/s41421-022-00408-z
- Daly JL, Simonetti B, Klein K, Chen KE, Williamson MK, Antón-Plágaro C, et al. Neuropilin-1 is a host factor for sars-Cov-2 infection. *Science* (2020) 370(6518):861–5. doi: 10.1126/science.abd3072
- Wang HB, Zhang H, Zhang JP, Li Y, Zhao B, Feng GK, et al. Neuropilin 1 is an entry factor that promotes ebv infection of nasopharyngeal epithelial cells. *Nat Commun* (2015) 6:6240. doi: 10.1038/ncomms7240
- Baindara P, Roy D, Mandal SM, Schrum AG. Conservation and enhanced binding of sars-Cov-2 omicron spike protein to coreceptor neuropilin-1 predicted by docking analysis. *Infect Dis Rep* (2022) 14(2):243–9. doi: 10.3390/idr14020029
- Hatton CF, Botting RA, Dueñas ME, Haq IJ, Verdon B, Thompson BJ, et al. Delayed induction of type I and iii interferons mediates nasal epithelial cell permissiveness to sars-Cov-2. *Nat Commun* (2021) 12(1):7092. doi: 10.1038/s41467-021-27318-0
- Peacock TP, Brown JC, Zhou J, Thakur N, Newman J, Kugathasan R, et al. The sars-Cov-2 variant, omicron, shows rapid replication in human primary nasal epithelial cultures and efficiently uses the endosomal route of entry. *bioRxiv* (2022). doi: 10.1101/2021.12.31.474653
- Hui KPY, Ho JCW, Cheung MC, Ng KC, Ching RHH, Lai KL, et al. Sars-Cov-2 omicron variant replication in human bronchus and lung ex vivo. *Nature* (2022) 603(7902):715–20. doi: 10.1038/s41586-022-04479-6
- Bentley K, Stanton RJ. Hydroxypropyl methylcellulose-based sprays effectively inhibit in vitro sars-Cov-2 infection and spread. *Viruses* (2021) 13(12):2345. doi: 10.3390/v13122345
- Gao L, Yu S, Chen Q, Duan Z, Zhou J, Mao C, et al. A randomized controlled trial of low-dose recombinant human interferons alpha-2b spray to prevent acute viral respiratory infections in military recruits. *Vaccine* (2010) 28(28):4445–51. doi: 10.1016/j.vaccine.2010.03.062
- commission Smh. Daily Briefing on Covid-19 in Shanghai. Available from: <http://wsjkw.sh.gov.cn/xwfb/20220506/c682814657024377a49c7bc5745847d4.html>.
- Jassat W, Abdool Karim SS, Mudara C, Welch R, Ozougwu L, Groome MJ, et al. Clinical severity of covid-19 in patients admitted to hospital during the omicron wave in south Africa: A retrospective observational study. *Lancet Glob Health* (2022) 10(7):e961–9. doi: 10.1016/s2214-109x(22)00114-0
- Modes ME, Directo MP, Melgar M, Johnson LR, Yang H, Chaudhary P, et al. Clinical characteristics and outcomes among adults hospitalized with laboratory-confirmed sars-Cov-2 infection during periods of B.1.617.2 (Delta) and B.1.1.529 (Omicron) variant predominance - one hospital, California, July 15–September 23, 2021, and December 21, 2021–January 27, 2022. *MMWR Morb Mortal Wkly Rep* (2022) 71(6):217–23. doi: 10.15585/mmwr.mm7106e2
- Faust JS, Du C, Liang C, Mayes KD, Renton B, Panthagini K, et al. Excess mortality in Massachusetts during the delta and omicron waves of covid-19. *Jama* (2022) 328(1):74–6. doi: 10.1001/jama.2022.8045
- Cai J, Deng X, Yang J, Sun K, Liu H, Chen Z, et al. Modeling transmission of sars-Cov-2 omicron in China. *Nat Med* (2022) 28(7):1468–75. doi: 10.1038/s41591-022-01855-7
- Lucas C, Wong P, Klein J, Castro TBR, Silva J, Sundaram M, et al. Longitudinal analyses reveal immunological misfiring in severe covid-19. *Nature* (2020) 584(7821):463–9. doi: 10.1038/s41586-020-2588-y
- Nienhold R, Ciani Y, Koelzer VH, Tzankov A, Haslbauer JD, Menter T, et al. Two distinct immunopathological profiles in autopsy lungs of covid-19. *Nat Commun* (2020) 11(1):5086. doi: 10.1038/s41467-020-18854-2
- Park A, Iwasaki A. Type I and type iii interferons - induction, signaling, evasion, and application to combat covid-19. *Cell Host Microbe* (2020) 27(6):870–8. doi: 10.1016/j.chom.2020.05.008
- Hadadj J, Yatim N, Barnabei L, Corneau A, Boussier J, Smith N, et al. Impaired type I interferon activity and inflammatory responses in severe covid-19 patients. *Science* (2020) 369(6504):718–24. doi: 10.1126/science.abc6027
- Lee JS, Park S, Jeong HW, Ahn JY, Choi SJ, Lee H, et al. Immunophenotyping of covid-19 and influenza highlights the role of type I interferons in development of severe covid-19. *Sci Immunol* (2020) 5(49):eabd1554. doi: 10.1126/sciimmunol.abd1554
- Galani IE, Rovina N, Lampropoulou V, Triantafyllia V, Manioudaki M, Pavlos E, et al. Untuned antiviral immunity in covid-19 revealed by temporal type I/iii interferon patterns and flu comparison. *Nat Immunol* (2021) 22(1):32–40. doi: 10.1038/s41590-020-00840-x
- Domizio JD, Gulen MF, Saidoune F, Thacker VV, Yatim A, Sharma K, et al. The cgas-sting pathway drives type I ifn immunopathology in covid-19. *Nature* (2022) 603(7899):145–51. doi: 10.1038/s41586-022-04421-w
- Blanco-Melo D, Nilsson-Payant BE, Liu WC, Uhl S, Hoagland D, Möller R, et al. Imbalanced host response to sars-Cov-2 drives development of covid-19. *Cell* (2020) 181(5):1036–45.e9. doi: 10.1016/j.cell.2020.04.026
- Ziegler CGK, Allon SJ, Nyquist SK, Mbano IM, Miao VN, Tzouanas CN, et al. Sars-Cov-2 receptor Ace2 is an interferon-stimulated gene in human airway epithelial cells and is detected in specific cell subsets across tissues. *Cell* (2020) 181(5):1016–35.e19. doi: 10.1016/j.cell.2020.04.035
- Wang N, Zhan Y, Zhu L, Hou Z, Liu F, Song P, et al. Retrospective multicenter cohort study shows early interferon therapy is associated with favorable clinical responses in covid-19 patients. *Cell Host Microbe* (2020) 28(3):455–64.e2. doi: 10.1016/j.chom.2020.07.005
- Uzé G, Schreiber G, Piehler J, Pellegrini S. The receptor of the type I interferon family. *Curr Top Microbiol Immunol* (2007) 316:71–95. doi: 10.1007/978-3-540-71329-6\_5
- de Weerd NA, Nguyen T. The interferons and their receptors—distribution and regulation. *Immunol Cell Biol* (2012) 90(5):483–91. doi: 10.1038/icb.2012.9
- Taylor JL, Grossberg SE. The effects of interferon-alpha on the production and action of other cytokines. *Semin Oncol* (1998) 25(1 Suppl 1):23–9.
- Kirkwood JM, Bender C, Agarwala S, Tarhini A, Shipe-Spotloe J, Smelko B, et al. Mechanisms and management of toxicities associated with high-dose interferon Alfa-2b therapy. *J Clin Oncol* (2002) 20(17):3703–18. doi: 10.1200/jco.2002.03.052



## OPEN ACCESS

## EDITED BY

Alfonso J. Rodriguez-Morales,  
Fundacion Universitaria Autónoma de  
las Américas, Colombia

## REVIEWED BY

Oliver Joel Gona,  
Novartis Healthcare, India  
Yanni Lai,  
Guangzhou University of Chinese  
Medicine, China

## \*CORRESPONDENCE

Bo Liu  
bolu888@hotmail.com

<sup>†</sup>These authors have contributed  
equally to this work

## SPECIALTY SECTION

This article was submitted to  
Viral Immunology,  
a section of the journal  
Frontiers in Immunology

RECEIVED 04 July 2022

ACCEPTED 01 August 2022

PUBLISHED 17 August 2022

## CITATION

Huang Y, Yuan Y, Chen S, Xu D, Xiao L,  
Wang X, Qin W and Liu B (2022)  
Identifying potential pharmacological  
targets and mechanisms of vitamin D  
for hepatocellular carcinoma and  
COVID-19.  
*Front. Immunol.* 13:985781.  
doi: 10.3389/fimmu.2022.985781

## COPYRIGHT

© 2022 Huang, Yuan, Chen, Xu, Xiao,  
Wang, Qin and Liu. This is an open-  
access article distributed under the  
terms of the [Creative Commons  
Attribution License \(CC BY\)](#). The use,  
distribution or reproduction in other  
forums is permitted, provided the  
original author(s) and the copyright  
owner(s) are credited and that the  
original publication in this journal is  
cited, in accordance with accepted  
academic practice. No use,  
distribution or reproduction is  
permitted which does not comply with  
these terms.

# Identifying potential pharmacological targets and mechanisms of vitamin D for hepatocellular carcinoma and COVID-19

Yongbiao Huang<sup>1†</sup>, Ye Yuan<sup>2†</sup>, Sheng Chen<sup>3</sup>, Duo Xu<sup>1</sup>,  
Lingyan Xiao<sup>1</sup>, Xi Wang<sup>1</sup>, Wan Qin<sup>1</sup> and Bo Liu<sup>1\*</sup>

<sup>1</sup>Department of Oncology, Tongji Hospital, Tongji Medical College, Huazhong University of Science and Technology, Wuhan, China, <sup>2</sup>Department of Gastroenterology, Tongji Hospital, Tongji Medical College, Huazhong University of Science and Technology, Wuhan, China, <sup>3</sup>Department of general surgery, Shangrao People's Hospital, Shangrao, China

Coronavirus disease 2019 (COVID-19) is a severe pandemic that has posed an unprecedented challenge to public health worldwide. Hepatocellular carcinoma (HCC) is a common digestive system malignancy, with high aggressiveness and poor prognosis. HCC patients may be vulnerable to COVID-19. Since the anti-inflammatory, immunomodulatory and antiviral effects of vitamin D, we aimed to investigate the possible therapeutic effects and underlying action mechanisms of vitamin D in COVID-19 and HCC in this study. By using a range of bioinformatics and network pharmacology analyses, we identified many COVID-19/HCC target genes and analyzed their prognostic significance in HCC patients. Further, a risk score model with good predictive performance was developed to evaluate the prognosis of HCC patients with COVID-19 based on these target genes. Moreover, we identified seven possible pharmacological targets of vitamin D against COVID-19/HCC, including HMOX1, MB, TLR4, ALB, TTR, ACTA1 and RBP4. And we revealed the biological functions, signaling pathways and TF-miRNA coregulatory network of vitamin D in COVID-19/HCC. The enrichment analysis revealed that vitamin D could help in treating COVID-19/HCC effects through regulation of immune response, epithelial structure maintenance, regulation of chemokine and cytokine production involved in immune response and anti-inflammatory action. Finally, the molecular docking analyses were performed and showed that vitamin D possessed effective binding activity in COVID-19. Overall, we revealed the possible molecular mechanisms and pharmacological targets of vitamin D for treating COVID-19/HCC for the first time. But these findings need to be further validated in actual HCC patients with COVID-19 and need further investigation to confirm.

## KEYWORDS

COVID-19, hepatocellular carcinoma, vitamin D, network pharmacology, molecular docking, prognosis



## Introduction

Coronavirus disease 2019 (COVID-19), an ongoing global pandemic caused by severe acute respiratory syndrome coronavirus 2 (SARS-CoV-2), has posed a substantial challenge to healthcare systems around the world (1, 2). As of March 4, 2022, with 440,807,756 confirmed COVID-19 cases and 5,978,096 deaths reported globally (3). Although multiple COVID-19 vaccines have been developed and mass vaccinations have been undertaken, the number of infections is still continuously increasing (4). Besides, some antiviral drugs have been applied for treating COVID-19, such as remdesivir, but due to its high price and the need for intravenous administration, it has not been widely used (5). Thus, it is essential to screen effective, inexpensive and readily available drugs against COVID-19. Additionally, cancer patients, such as hepatocellular carcinoma (HCC), were reported to be at higher risk of COVID-19 infection and developing severe complications than those noncancer people (6–8). HCC is a common digestive system malignancy, with high aggressiveness and poor prognosis. Globally, HCC has the sixth highest incidence among all cancers, and the incidence has been continuously increasing in recent years (9, 10). HCC patients infected with COVID-19 will be very difficult to treat, because there is a lack of effective drugs that can improve immunity and against both COVID-19 and HCC. Therefore, screening effective therapeutic agents for such patients is important.

Vitamin D is a fat-soluble vitamin, including two major forms: vitamin D<sub>2</sub> and vitamin D<sub>3</sub>. The predominant source of vitamin D in humans is derived from skin synthesis (VD<sub>3</sub>) and dietary intake (VD<sub>2</sub> or VD<sub>3</sub>). To exert biological activity, vitamin D is converted to 25-hydroxyvitamin D (25(OH)D, circulating form) through hydroxylation in the liver, and then hydroxylated to the 1,25-dihydroxyvitamin D (1,25(OH)<sub>2</sub>D, active form) in the kidneys (11). The classical physiological function of vitamin D is to maintain calcium and phosphorus homeostasis and regulate bone metabolism (12). Recently, vitamin D has also been found to have multiple nonclassical functions including immunomodulation, anti-inflammation, anti-virus and anti-tumor (13–15). Numerous reports have indicated that vitamin D deficiency is associated with more severe COVID-19, and patients with low levels of vitamin D have higher mortality (16, 17). Vitamin D could inhibit NF- $\kappa$ B signaling, reduce the production of various pro-inflammatory cytokines, and thereby might help suppress cytokine storm in COVID-19 (18, 19). Furthermore, vitamin D exhibits anti-hepatocarcinogenic effects by inhibiting tumor cell proliferation, invasion and promoting apoptosis (20). However, the pharmacological targets and molecular mechanisms of vitamin D against COVID-19 in HCC patients are remain to be fully studied.

In this study, we used the network pharmacology and bioinformatics approaches to investigate the prognostic value of COVID-19 related genes in HCC patients, and further explore

the possible anti-COVID-19/HCC mechanisms of vitamin D. Our findings provide some new insights into vitamin D in the treatment of COVID-19/HCC.

The entire workflow of this study was summarized in a visible graphical abstract. (Figure 1).

## Materials and methods

### Data collection and identifying COVID-19/HCC related genes

This investigation was a retrospective cohort study, which was approved by The Medical Ethics Committee of Tongji Hospital, Tongji Medical College, Huazhong University of Science and Technology (TJ-IRB20200409). The transcriptome profiles and clinical data of HCC patients were downloaded from The Cancer Genome Atlas (TCGA) database, then the differentially expressed genes were identified using the 'edgeR' R package with  $|\log_2 \text{ fold change (FC)}| > 1.0$  and false discovery rate (FDR)  $< 0.05$  (21). Besides, the COVID-19 related genes were obtained from the Genecard database and NCBI gene module (22). Finally, we took the intersection of these genes and obtained the overlapping targets in HCC and COVID-19, and these overlapping genes were displayed in a volcano plot.

### Prognostic analysis of HCC and COVID-19 related genes

The association of COVID-19/HCC related genes with survival in HCC patients was analyzed using univariate Cox regression by the 'survival' R package, and the protein-protein interaction (PPI) network of the identified prognostic genes were explored in the STRING database (version 11.0). Moreover, a risk score model was further constructed based on multivariate Cox proportional hazards regression model, and the predictive ability of this model was evaluated through receiver operating characteristic (ROC) curves (10). Patients were divided into high-risk (n=171) and low-risk (n=171) groups based on the median risk score, and their overall survival rates were compared through the Kaplan–Meier method with the log-rank test. Additionally, the independent prognostic value of this risk model was analyzed using univariate analysis and multivariate regression analyses. Finally, we validated the performance of the prognostic model in an external validation set (ICGC, LIRI-JP project).

### Acquiring the pharmacological targets of vitamin D against COVID-19/HCC

We collected and screened all pharmacological targets of vitamin D<sub>3</sub> from freely accessible online databases designed to

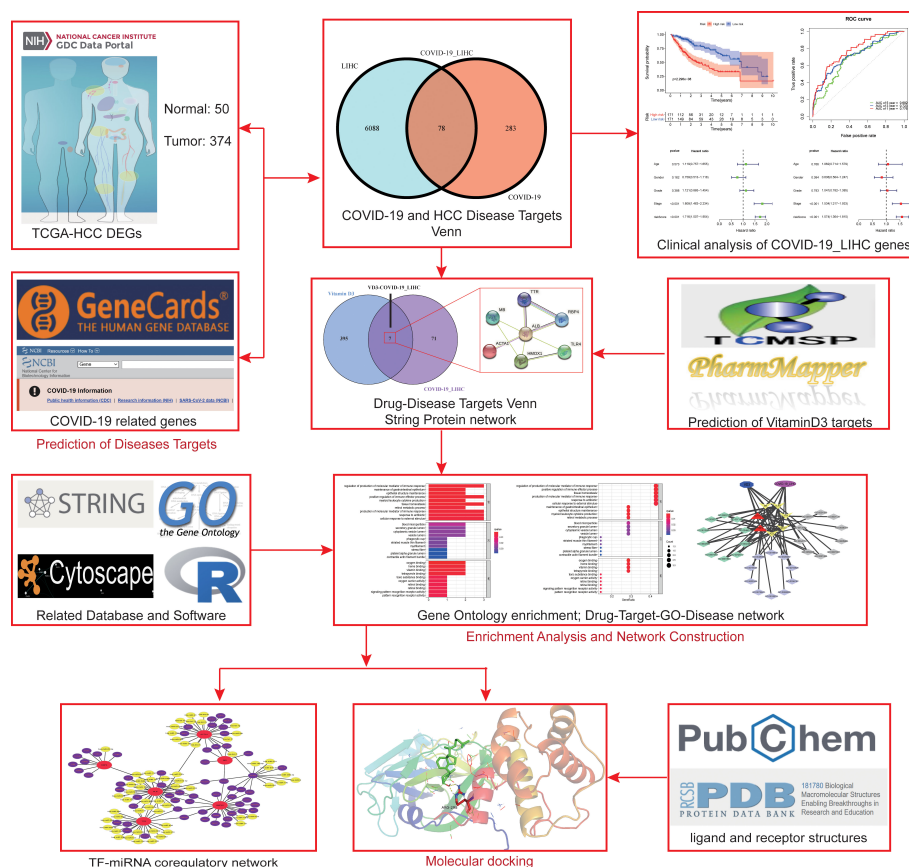


FIGURE 1  
Workflow of the whole study.

identify potential pharmacological targets for the given small molecules, including the Traditional Chinese Medicine Database and Analysis Platform (TCMSP) and PharmMapper Server (23, 24). The overlapping target genes of vitamin D3 in COVID-19/HCC were further acquired, and the PPI network was generated in the STRING database.

## Enrichment analysis and interaction network visualization

The gene ontology (GO) and KEGG enrichment analyses of the overlapping target genes of vitamin D in COVID-19/HCC was performed using the 'ClusterProfiler' R language package, and the enrichment results were visualized using the 'GPlot' R package, the p-value and q-value were set at 0.05 (25). The drug-target-GO function-disease interaction network was constructed using Cytoscape software (version 3.7.1) to illustrate the biological function of target genes of vitamin D treatment in COVID-19/HCC (26).

## TF-miRNA coregulatory network

TF-miRNA coregulatory interaction information was obtained from the RegNetwork repository, and the TF-miRNA coregulatory network was generated by using NetworkAnalyst (<https://dev.networkanalyst.ca>), and further visualized through Cytoscape software. NetworkAnalyst is a comprehensive platform for interaction network analysis, including protein-protein interactions, gene regulatory networks and gene coexpression networks (27).

## Molecular docking

The 2-dimensional molecular structure of vitamin D3 was obtained from the PubChem database (<https://pubchem.ncbi.nlm.nih.gov/>) (28), and its 3-dimensional structure was generated and optimized by the MM2 force field in ChemBioOffice software (version 2014) (29). Finally, the

output ligand file of vitamin D3 was saved as mol2 format. The protein structures of COVID-19 associated proteins were obtained from the PDB database (<http://www.rcsb.org/pdb>) (30). Then, all water molecules and ligands were removed from the structures using PyMOL software and saved as PDB files. The original protein receptor and ligand files were converted to PDBQT file format with AutoDockTools 1.5.6, which could be recognized by the Autodock Vina program for subsequent docking experiments (31). Finally, all docking results were displayed and analyzed by PyMOL software (32).

## Statistical analysis

Statistical analyses in this work were conducted by R software (version 3.6.3). The survival between different groups were compared through the Kaplan-Meier method with the log-rank test. Univariate and multivariate Cox regression were applied to compare the impact of the risk score model and other clinical characteristics on survival. The risk scores of subgroups classified by different clinical characteristics were compared with Wilcoxon test. The  $P < 0.05$  was regarded to have statistical significance.

## Results

### Identification of COVID-19/HCC targets

First, we identified 6166 HCC-associated differentially expressed genes (DEGs) in TCGA database. Meanwhile, 361 COVID-19 associated genes were collected from the Genecard and NCBI databases through network pharmacology. The intersection of these two gene clusters was shown in Figure 2A, and 78 common genes in HCC and COVID-19 were identified. Further, the differential expression of these common genes was checked, of which 27 genes were found to be upregulated and 61 genes were downregulated in HCC (Figure 2B).

### Prognostic value of COVID-19/HCC associated genes

To explore the correlation between COVID-19/HCC associated genes and the prognosis of COVID-19/HCC patients, univariate and multivariate Cox analyses were performed on the 78 DEGs. First, 19 genes significantly

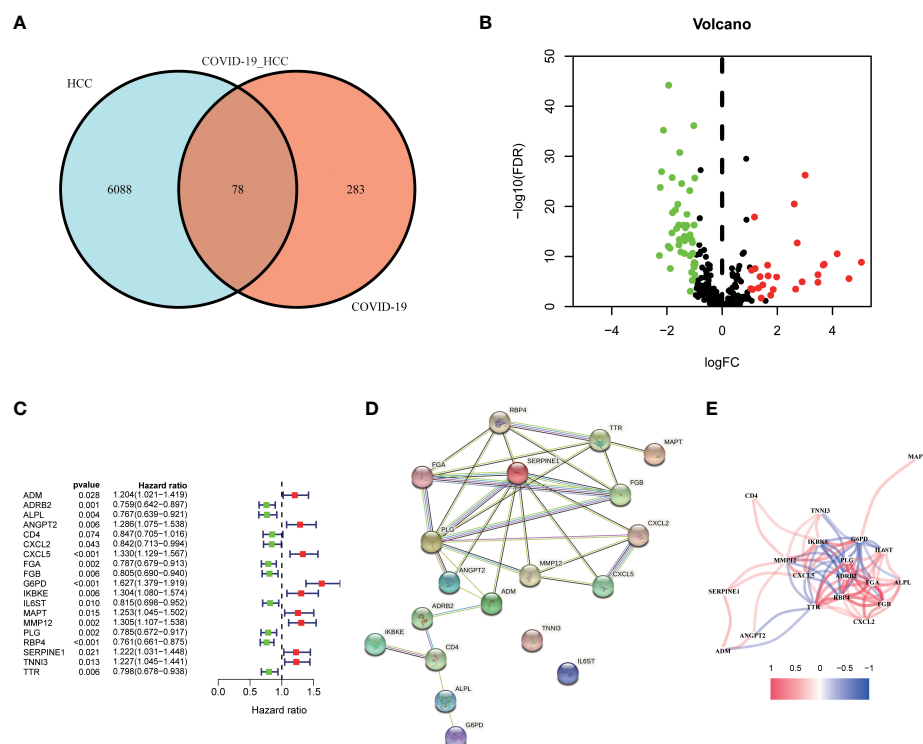


FIGURE 2

Identification of the candidate genes in COVID-19/HCC. (A) Venn diagram to identify the intersecting genes in COVID-19/HCC. (B) Volcano plot of the intersecting genes in HCC. (C) The results of the univariate Cox analysis presented in a forest plot. (D) The interaction network among the 19 COVID-19/HCC related genes. (E) The correlation network of the 19 COVID-19/HCC related genes.

associated with COVID-19/HCC were identified through univariate Cox analysis, including ADM, ADRB2, ALPL, ANGPT2, CD4, CXCL2, CXCL5, FGA, FGB, G6PD, IKBKE, IL6ST, MAPT, MMP12, PLG, RBP4, SERPINE1, TNNI3 and TTR ( $P < 0.05$ , Figure 2C and Table 1). The interaction network of these genes was presented in Figure 2D, and the correlations between them were showcased in Figure 2E. Thereafter, a six-gene signature containing ALPL, ANGPT2, CD4, G6PD, SERPINE1, and TNNI3 was developed through multivariate Cox regression analysis (Table 2). The patient's risk score was calculated based on the regression coefficient and expression of these six genes: Risk score =  $0.250 * \text{ANGPT2 Exp} + 0.436 * \text{G6PD Exp} + 0.211 * \text{SERPINE1 Exp} + 0.201 * \text{TNNI3 Exp} - 0.151 * \text{ALPL Exp} - 0.241 * \text{CD4 Exp}$ .

Then, according to the cut-off of the median risk score, the patients in TCGA cohort were stratified into high- and low-risk groups. In the Kaplan-Meier survival analysis, we found that patients in the high-risk group exhibited a significantly shorter overall survival compared with those in the low-risk group (Figure 3A). Time-dependent ROC curves of the six-gene signature were shown in Figure 3B, and the AUC values were 0.776 at 1 year, 0.723 at 3 years and 0.682 at 5 years. These results showed that the risk score could act as an effective prognostic indicator. Moreover, patients in high-risk group presented a higher probability of early death than those in the low-risk group (Figure 3C, D). Univariate and multivariate Cox analyses were applied among the available clinical characteristics to determine the independent prognostic value of the risk score for overall

survival. We observed that the risk score was significantly correlated with the survival of HCC patients in univariate Cox regression analysis (HR = 1.716, 95% CI = 1.507-1.954,  $P < 0.001$ ). Interestingly, after adjusting for other confounders, the risk score was still demonstrated as an independent predictor for survival in multivariate regression analysis (HR = 1.574, 95% CI = 1.364-1.815,  $P < 0.001$ ). Moreover, the risk scores of patients were calculated using the same formula in the ICGC cohort, and we obtained similar results with the TCGA cohort (Figure 4). These results demonstrated a robust predictive performance of the six-gene prognostic signature.

## Clinicopathological analysis of the risk score model

Furthermore, the clinicopathological analysis of the risk score indicated that the risk score was not related to age and gender in both TAGA and ICGC cohorts (Figures 5A, B, G, H). Whereas, patients with poor clinical outcomes usually had higher risk scores (Figure 5C, I). Additionally, the risk score was closely associated with higher pathological grade, more advanced stage and larger tumor size of HCC (Figures 5D-F, J). The further Kaplan-Meier survival analysis stratified by different clinicopathologic features showed that the high-risk patients had a poor prognosis in all subgroups (Figure 6). The results demonstrated that the risk score model

TABLE 1 Univariate Cox regression analysis of COVID-19/HCC related genes.

Symbol	HR	Lower 95% CI	Upper 95% CI	P-value
ADM	1.203567	1.020617	1.419311	0.027627
ADRB2	0.759201	0.642236	0.897468	0.00125
ALPL	0.767183	0.639181	0.920818	0.004431
ANGPT2	1.28599	1.07512	1.538218	0.005912
CD4	0.846686	0.705319	1.016386	0.074167
CXCL2	0.842264	0.713441	0.994348	0.042673
CXCL5	1.330195	1.129395	1.566696	0.000632
FGA	0.787212	0.679012	0.912653	0.001516
FGB	0.805357	0.689874	0.940173	0.006122
G6PD	1.626622	1.378565	1.919313	8.27e-09
IKBKE	1.303744	1.080161	1.573608	0.005722
IL6ST	0.815436	0.698339	0.952169	0.00989
MAPT	1.252519	1.044707	1.501668	0.014997
MMP12	1.304917	1.106879	1.538388	0.001529
PLG	0.784992	0.671732	0.917348	0.002326
RBP4	0.760531	0.660916	0.875159	0.000133
SERPINE1	1.221538	1.030646	1.447786	0.020992
TNNI3	1.227173	1.044765	1.441428	0.012655
TTR	0.797681	0.678232	0.938168	0.006312

HR, hazard ratio; CI, confidence interval.

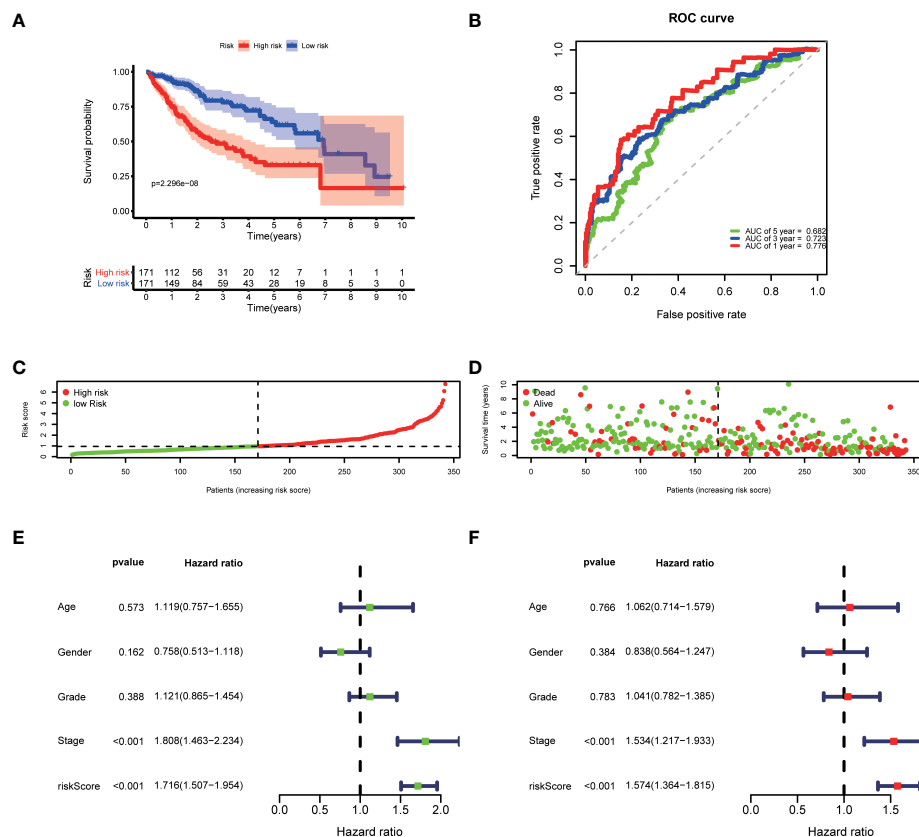


**FIGURE 3**  
Development of the prognostic model based on COVID-19/HCC associated genes in the TCGA cohort. **(A)** Kaplan-Meier survival analysis between the high- and low-risk patients. **(B)** Time-dependent ROC curves at 1,3,5-years. **(C)** Distribution of risk scores, **(D)** survival status of each patient. **(E)** Univariate and **(F)** multivariate Cox regression analyses.

could predict survival for HCC patients without considering clinicopathologic features.

## Identifying intersection targets of vitamin D against COVID-19 and HCC

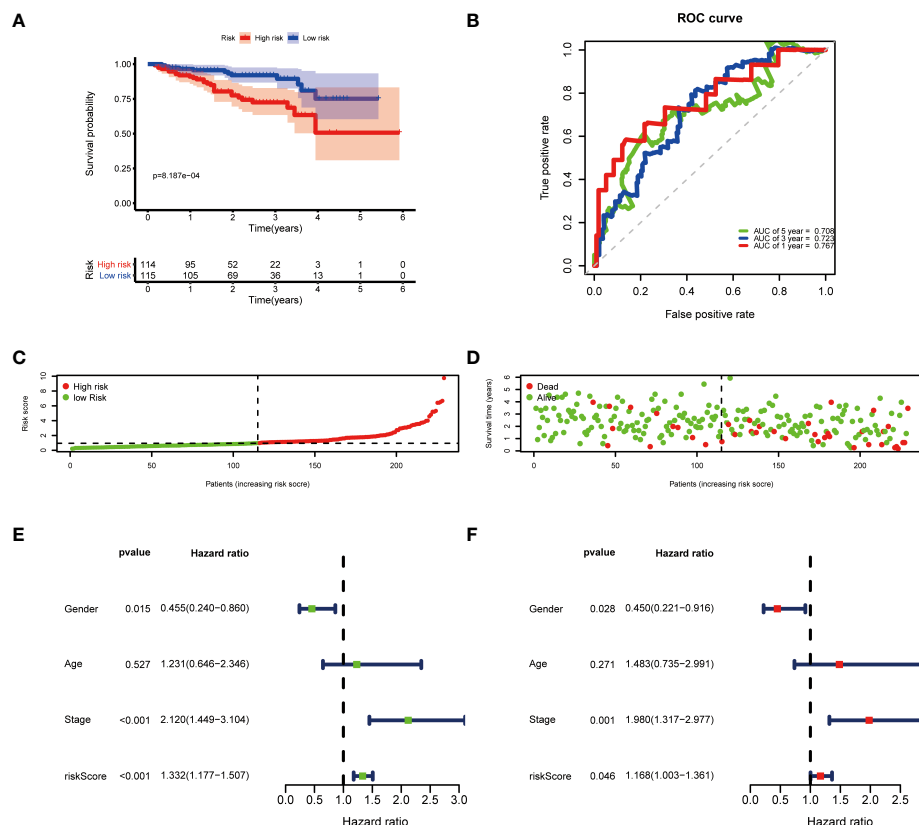
The pharmacological targets of vitamin D were determined by using TCMSP and PharmMapper databases, and 402 vitamin D-associated targets were identified. By taking the intersection of COVID-19/HCC genes and vitamin D-associated targets, we obtained seven overlapping genes (HMOX1, MB, TLR4, ALB, TTR, ACTA1 and RBP4) of vitamin D against COVID-19/HCC. Additionally, the PPI network of these intersection genes was constructed in the STRING database (Figure 7A). To explore the biological functions and pathways in which the seven intersection genes were involved, GO and KEGG enrichment analyses were conducted on these genes. The results indicated that vitamin D affects a series of biological processes, including

regulation of production of molecular mediator of immune response, maintenance of gastrointestinal epithelium, epithelial structure maintenance, positive regulation of immune effector process, myeloid leukocyte cytokine production, tissue homeostasis, retinol metabolic process, response to antibiotic, cellular response to external stimulus, positive regulation of chemokine production, positive regulation of cytokine biosynthetic process, regulation of cytokine production involved in immune response (Figures 7B, C and Table S1). Whereas in the KEGG pathway analysis, only thyroid hormone synthesis and HIF-1 signaling pathway were significantly enriched ( $P < 0.05$ , Figure S1).

## TF-miRNA coregulatory network

The TF-miRNA coregulatory network of the seven overlapping gene targets of vitamin D against COVID-19/HCC was analyzed using NetworkAnalyst. The TF-miRNA





coregulatory network analysis provided information about TFs and miRNAs interaction with these target genes. These interactions might be responsible for regulating the expression of these target genes. The TF-miRNA-gene interaction network contains a total of 125 nodes and 138 edges, 59 TFs and 59 miRNAs that interacted with these seven overlapping target genes. In the network, ALB is regulated by 13 TFs and 19 miRNAs, HMOX1 is regulated by 23 TFs and 3 miRNAs, ACTA1 is regulated by 11 TFs and 15 miRNAs, TTR is regulated by 7 TFs and 18 miRNAs, TLR4 is regulated by 5 TFs and 8 miRNAs, RBP4 is regulated by 9 TFs and 1 miRNA, and MB is regulated by 6 TFs (Figure 8).

## Binding of vitamin D to COVID-19 and potential intersection targets

To determine the possible binding of vitamin D with COVID-19 and the previously identified intersection targets,

molecular docking analysis was carried out. We obtained the crystal structure of the COVID-19 main protease (PDB ID 5R84) from the PDB database, for subsequent molecular docking with vitamin D. The docking results demonstrated that vitamin D possessed good binding activity with the COVID-19 main protease and formed two hydrogen bonds with the amino acid residue ARG-298 (2.0 Å and 2.3 Å) of protein 5R84 (Figure 9A). Next, we further analyzed the possible binding of vitamin D with the seven COVID-19/HCC targets (HMOX1, MB, TLR4, ALB, TTR, ACTA1 and RBP4) identified previously and found that vitamin D only binds to MB and RBP4. The crystal structures of MB and RBP4 were also gathered from the PDB database with PDB IDs 3RGK and 2WR6 respectively. We found that hydrogen bonding between vitamin D and the protein MB acted on the amino acid residue HIS-93 (2.6 Å) (Figure 9B). Furthermore, vitamin D bound to the RBP4 protein by forming hydrogen bonds with the amino acid residues LEU-37 (2.6 Å), LYS-29 (2.0 Å) and PHE-36 (1.5 Å) (Figure 9C). These results showed the high-affinity between vitamin D with MB and RBP4.

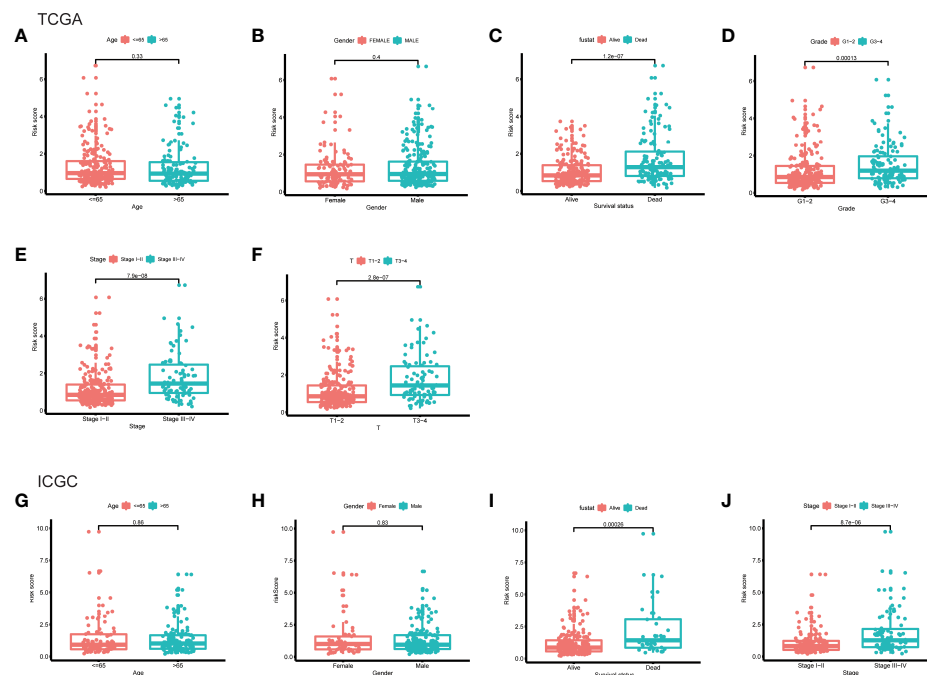


**FIGURE 5**  
The differences of risk score between subgroups stratified by different clinical characteristic in the TCGA and ICGC cohorts. (A) Age, (B) gender, (C) survival status, (D) grade, (E) stage, (F) T classification in the TCGA cohort. (G) Age, (H) gender, (I) survival status, (J) stage in the ICGC cohort.

## Discussion

COVID-19 is a serious, rapidly spreading infectious disease, that can be life-threatening (33). At this time of writing, with more than 400 million people infected with COVID-19 and more than 5.5 million died from COVID-19, and the numbers are still growing (3). The risk factors for COVID-19 infection and severe outcomes identified currently include male sex, older age, obesity, diabetes mellitus, cardiovascular disease and cancer (6, 8, 34). In particular, patients with cancer are more vulnerable to COVID-19 and contribute to adverse outcomes due to their low immunity and immunological dysfunction (7, 35). As per the latest global cancer statistics in 2020, the incidence of HCC ranks sixth, and the mortality ranks third among all cancers (9). Moreover, the COVID-19 pandemic is still raging, and HCC patients remain at an increased risk of COVID-19 infection. Thus, COVID-19 infection in HCC patients may lead to worse outcomes and amplify the risk of death.

In some previously published studies, vitamin D showed anti-proliferative and anti-invasive effects on HCC cells, which could inhibit HCC progression by inducing apoptosis, reducing oxidative stress and inflammation (36–39). Also, vitamin D is known to have direct antiviral and immunomodulatory properties (40, 41). Moreover, vitamin D deficiency is associated with an increased risk of both COVID-19 and HCC

(42). Thus, we hypothesize that vitamin D may exert potent pharmacological effects in HCC patients with COVID-19.

In the current study, we first collected 361 COVID-19 target genes and identified 6166 DEGs in HCC, and then further screened out 78 common genes of COVID-19 combined with HCC. Among these genes, 27 genes were upregulated and 61 genes were downregulated in HCC and/or COVID-19 patients. As per univariate and multivariate prognostic analyses, a few important genes, including ALPL, ANGPT2, CD4, G6PD, SERPINE1 and TNNT3, may serve as independent prognostic factors for HCC patients with COVID-19. Then, we developed a prognostic model based on the six genes to predict survival in patients with HCC and COVID-19, and the model exhibited good prediction capability in both independent cohorts without considering clinicopathologic features. Additionally, the prognostic model was significantly associated with HCC progression, which can be used to screen and characterize different stages of HCC patients with COVID-19. This prognostic model predicts survival independently of gender, age and tumor stage, and the gender, stage and risk score were all influential factors for survival. Until now, the TNM staging system is still a very important tool for predicting the survival of HCC patients. Due to the excellent predictive ability of this prognostic model, it may be used as a supplement to TNM staging system.

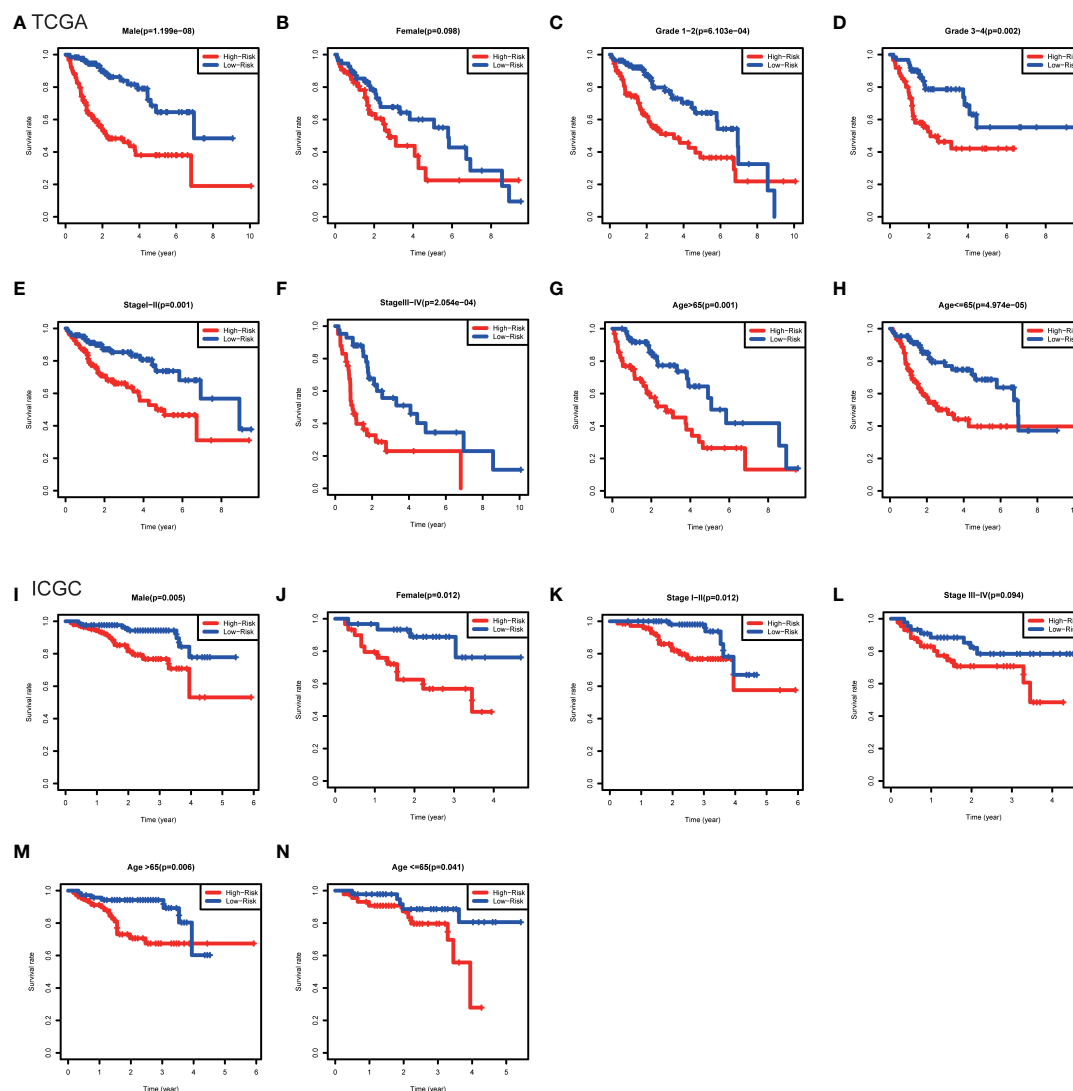


FIGURE 6

Kaplan-Meier survival analysis between subgroups stratified by different clinical characteristics in the TCGA and ICGC cohorts. (A) Male, (B) female, (C) grade 1-2, (D) grade 3-4, (E) stage I-II, (F) stage III-IV, (G) age>65, (H) age<=65 in the TCGA cohort. (I) male, (J) female, (K) stage I-II, (L) stage III-IV, (M) age>65, (N) age<=65 in the ICGC cohort.

Put together, these 78 intersection genes may be potential therapeutic targets of HCC and COVID-19. Further, we identified seven overlapping genes of vitamin D against HCC and COVID-19 using the network pharmacology approach, and the anti-COVID-19/HCC effects of vitamin D may be modulated by these molecules or genes, including HMOX1, MB, TLR4, ALB, TTR, ACTA1 and RBP4. There were significant differences in the expression of these genes. The HCC patients showed increased expression of MB and ACTA1, decreased expression of HMOX1, TLR4, ALB, TTR

and RBP4. Moreover, the decreased TTR and RBP4 expression was relevant for worse prognosis of HCC patients. The MB gene encodes myoglobin, an oxygen-binding hemoprotein, which was reported to be ectopically expressed in different human cancer cell lines and cancer tissues (43). ACTA1 was identified as a biomarker for head and neck squamous cell carcinoma and colorectal cancer (44, 45). HMOX1 encodes heme oxygenase 1, a stress-inducible enzyme, that plays an essential role in oxidative stress response. It is known to have anti-inflammatory and immunomodulatory effects, and it may be a promising target

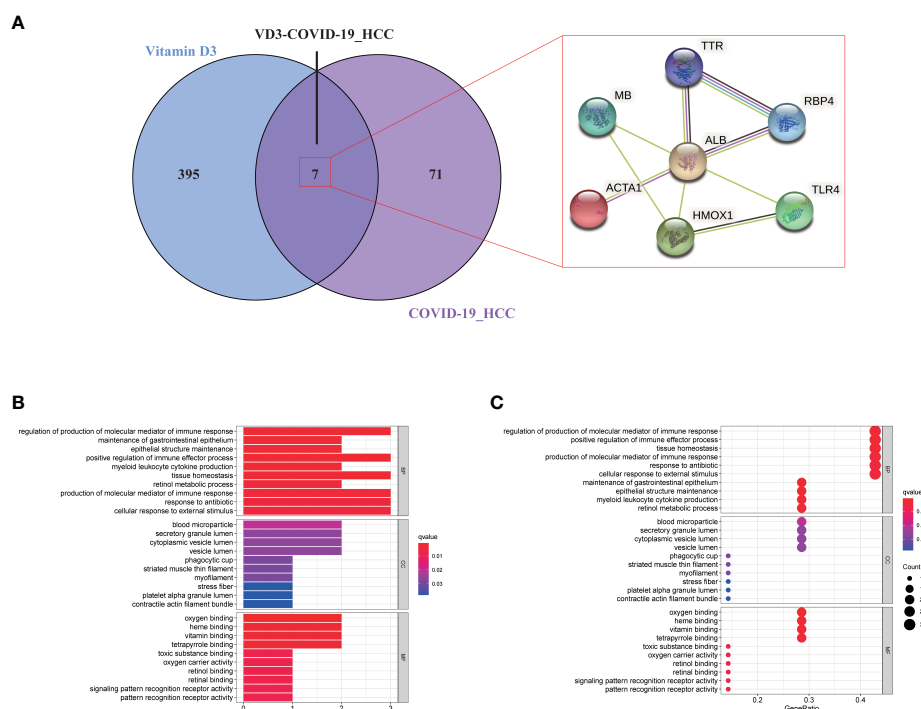


FIGURE 7

Functional enrichment analysis of vitamin D against COVID-19/HCC intersecting genes. **(A)** Venn diagram of vitamin D associated targets and COVID-19/HCC genes. **(B)** Bar plot and **(C)** bubble plot showing the results of GO enrichment analysis of vitamin D against COVID-19/HCC intersecting genes.

for the treatment of COVID-19 (46). ALB is a tumor suppressor in HCC that can inhibit the proliferation of HCC cells and regulate the cell cycle (47). Besides, ALB knockdown promoted the migration and invasion of HCC cells through the upregulation of uPAR, MMP2, and MMP9 (48). TTR was regarded as an independent prognostic factor for HCC patients, and the low serum TTR levels were associated with poor prognosis (49). RBP4 was considered a novel biomarker for predicting HCC prognosis, and decreased expression of RBP4 indicated a worse prognosis and correlated with immune infiltration in HCC (50). MB, TLR4 and ALB are involved in coronavirus biology, and are associated with COVID-19 prognosis (51–53). The serum myoglobin was an effective predictor of the prognosis in COVID-19 hospitalized patients, the higher serum myoglobin levels were related to poor prognosis of COVID-19 patients (54). TLR4 was reported to be able to directly interact with SARS-CoV-2 spike protein and activates related inflammatory responses, whilst the TLR4-specific inhibitor resatorvid could completely block the secretion of IL1B induced by SARS-CoV-2 (55). These findings further suggested that these seven intersection genes might be potent pharmacological targets of vitamin D against HCC and COVID-19.

The GO and KEGG enrichment analyses based on these seven intersection genes showed that vitamin D exerts the anti-COVID-19/HCC effects directly *via* regulation of immune response, epithelial structure maintenance, regulation of chemokine and cytokine production involved in immune response, anti-viral and anti-inflammatory actions, as well as regulation of the HIF-1 pathway. Cytokine storm caused by SARS-CoV-2 infection is the main cause of death in COVID-19 patients, thus, the inhibition of cytokine production may be an important screening condition of effective COVID-19 drugs (56). HIF-1 pathway is involved in the regulation of oxidative stress and inflammation, and the activity of HIF-1 pathway may promote SARS-CoV-2 infection and affect a variety of physiological functions (57, 58). Therefore, inhibiting the activity or activation of HIF-1 pathway may be used to prevent COVID-19.

Lastly, we identified good binding activities of vitamin D with the 5R84 structure in COVID-19, the 3RGK structure in the target MB and the 2WR6 structure in the target RBP4 through molecular docking analysis, suggesting that vitamin D can effectively bind to specific proteins associated with SARS-CoV-2, and that vitamin D may be able to act on the MB and RBP4 to target COVID-19. Therefore, we believe that vitamin D

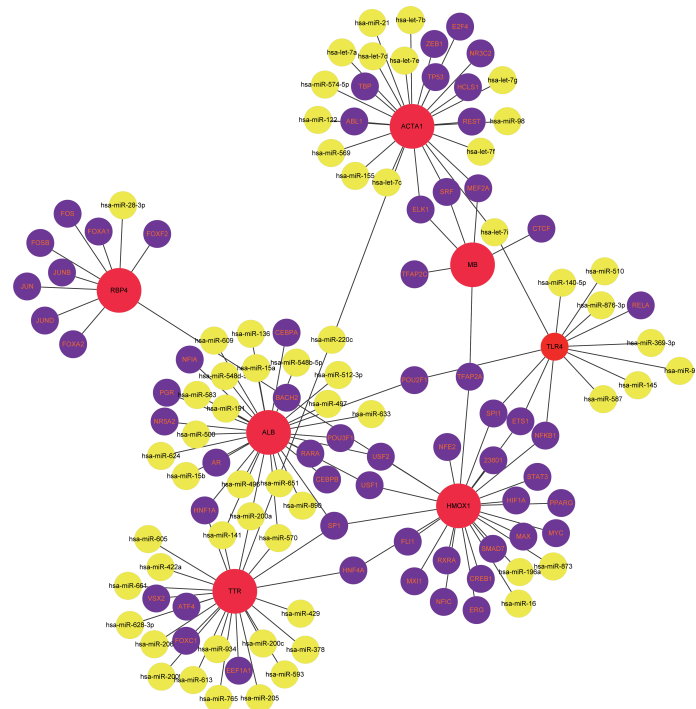


FIGURE 8 The TF-miRNA coregulatory network of vitamin D against COVID-19/HCC intersecting genes.

supplementation may improve the efficacy of current antiviral therapy and immunotherapy for the treatment of COVID-19, or the combination of HCC with COVID-19.

In summary, we identified many potential therapeutic targets of COVID-19/HCC and developed a reliable prognostic model for patients with HCC and COVID-19. Further, vitamin D may be used to treat COVID-19/HCC through the identified potential targets and pharmacological functions, including immunomodulation, anti-virus, anti-inflammation and so on (Figure 10). Moreover, the direct binding targets with high binding affinity of vitamin D against COVID-19/HCC were identified, which provided the evidence for the clinical application of vitamin D and rationale for subsequent clinical trials.

Strengths and limitations

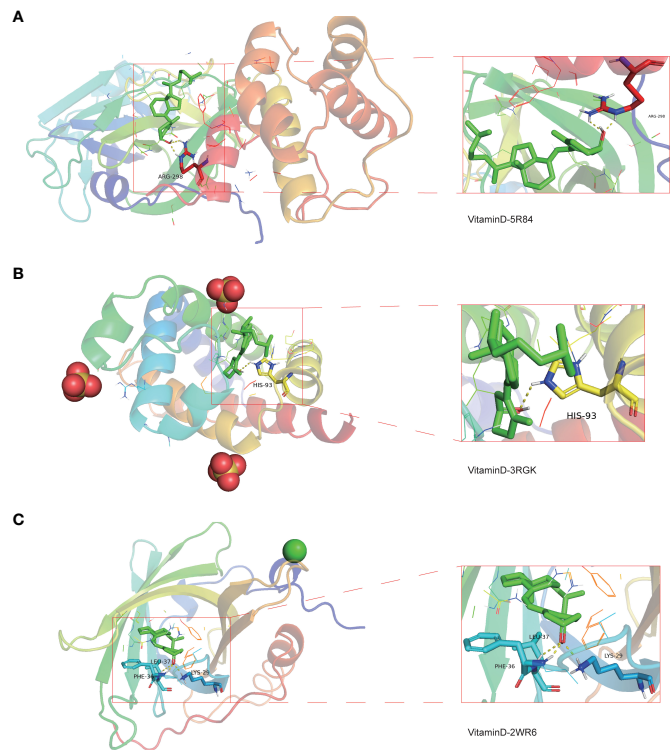
Notably, our study indicated the possible molecular mechanisms and potential pharmacological targets of vitamin D for treating COVID-19/HCC for the first time and provided some new insights into vitamin D in the treatment of COVID-19/HCC. Nevertheless, there remain a few limitations in our study need to be addressed. First, the findings of this study have not been validated in actual HCC patients with COVID-19; therefore, we need to collect real HCC patients with COVID-19 to verify these findings in the future. Second, the potential therapeutic use of vitamin D for COVID-19/HCC has not been validated experimentally, and further *in vivo* and *in vitro*

TABLE 2 Multivariate Cox proportional hazards regression model.

Symbol	Coefficient	HR	Lower 95% CI	Upper 95% CI	P-value
ALPL	-0.15074	0.860072	0.718649	1.029326	0.100051
ANGPT2	0.250202	1.284285	1.058391	1.558391	0.011247
CD4	-0.2413	0.785603	0.647798	0.952723	0.014202
G6PD	0.436329	1.547018	1.298831	1.842629	1.01E-06
SERPINE1	0.21077	1.234628	1.038959	1.467147	0.016662
TNNI3	0.200939	1.22255	1.022867	1.461214	0.027212

HR, hazard ratio; CI, confidence interval.





**FIGURE 9**  
Molecular docking analysis for the binding of vitamin D to COVID-19 and the targets MB and RBP4. **(A)** The binding of vitamin D with SARS-CoV-2 main protease (PDB ID 5R84). **(B)** The binding of vitamin D with the 3RGK protein of MB. **(C)** The binding of vitamin D with the 2WR6 protein of RBP4.

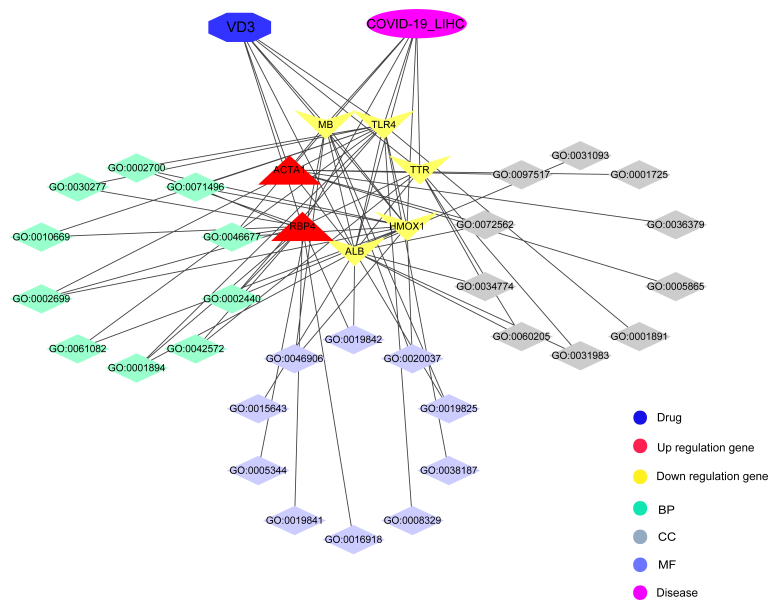


**FIGURE 10**  
Interaction network for pharmacological targets and biological functions of vitamin D against COVID-19/HCC.

experiments are needed to confirm the possible mechanisms and potential pharmacological targets.

## Data availability statement

The original contributions presented in the study are included in the article/Supplementary Material. Further inquiries can be directed to the corresponding author.

## Author contributions

YH and YY designed the study and wrote the manuscript. SC, DX, LX, XW, and WQ analyzed the results. BL helped to modified the manuscript. All authors contributed to the article and approved the submitted version.

## Funding

This work was supported by a grant from the National Natural Science Foundation of China (grant number 81902619).

## References

- Lai CC, Shih TP, Ko WC, Tang HJ, Hsueh PR. Severe acute respiratory syndrome coronavirus 2 (Sars-Cov-2) and coronavirus disease-2019 (Covid-19): The epidemic and the challenges. *Int J Antimicrob Agents* (2020) 55(3):105924. doi: 10.1016/j.ijantimicag.2020.105924
- Wang C, Horby PW, Hayden FG, Gao GF. A novel coronavirus outbreak of global health concern. *Lancet* (2020) 395(10223):470–3. doi: 10.1016/S0140-6736(20)30185-9
- WHO. Coronavirus (COVID-19) data. [cited 2022 March 4]. Available from: <https://www.who.int/data#reports>.
- Rabaan AA, Al-Ahmed SH, Sah R, Tiwari R, Yattoo MI, Patel SK, et al. Sars-Cov-2/Covid-19 and advances in developing potential therapeutics and vaccines to counter this emerging pandemic. *Ann Clin Microbiol Antimicrob* (2020) 19(1):40. doi: 10.1186/s12941-020-00384-v
- Wang Y, Zhang D, Du G, Du R, Zhao J, Jin Y, et al. Remdesivir in adults with severe covid-19: A randomised, double-blind, placebo-controlled, multicentre trial. *Lancet* (2020) 395(10236):1569–78. doi: 10.1016/S0140-6736(20)31022-9
- Chen N, Zhou M, Dong X, Qu J, Gong F, Han Y, et al. Epidemiological and clinical characteristics of 99 cases of 2019 novel coronavirus pneumonia in wuhan, China: A descriptive study. *Lancet* (2020) 395(10223):507–13. doi: 10.1016/S0140-6736(20)30211-7
- Dai M, Liu D, Liu M, Zhou F, Li G, Chen Z, et al. Patients with cancer appear more vulnerable to sars-Cov-2: A multicenter study during the covid-19 outbreak. *Cancer Discovery* (2020) 10(6):783–91. doi: 10.1158/2159-8290.CD-20-0422
- Tian J, Yuan X, Xiao J, Zhong Q, Yang C, Liu B, et al. Clinical characteristics and risk factors associated with covid-19 disease severity in patients with cancer in wuhan, China: A multicentre, retrospective, cohort study. *Lancet Oncol* (2020) 21(7):893–903. doi: 10.1016/S1470-2045(20)30309-0
- Sung H, Ferlay J, Siegel RL, Laversanne M, Soerjomataram I, Jemal A, et al. Global cancer statistics 2020: Globocan estimates of incidence and mortality worldwide for 36 cancers in 185 countries. *CA Cancer J Clin* (2021) 71(3):209–49. doi: 10.3322/caac.21660
- Huang Y, Chen S, Qin W, Wang Y, Li L, Li Q, et al. A novel rna binding protein-related prognostic signature for hepatocellular carcinoma. *Front Oncol* (2020) 10:580513. doi: 10.3389/fonc.2020.580513
- DeLuca HF. Vitamin d: Historical overview. *Vitam Horm* (2016) 100:1–20. doi: 10.1016/bs.vh.2015.11.001
- Reid IR, Bolland MJ, Grey A. Effects of vitamin d supplements on bone mineral density: A systematic review and meta-analysis. *Lancet* (2014) 383(9912):146–55. doi: 10.1016/S0140-6736(13)61647-5
- Bartley J. Vitamin d: Emerging roles in infection and immunity. *Expert Rev Anti Infect Ther* (2010) 8(12):1359–69. doi: 10.1586/eri.10.102
- Manson JE, Cook NR, Lee IM, Christen W, Bassuk SS, Mora S, et al. Vitamin d supplements and prevention of cancer and cardiovascular disease. *N Engl J Med* (2019) 380(1):33–44. doi: 10.1056/NEJMoa1809944
- Yin K, Agrawal DK. Vitamin d and inflammatory diseases. *J Inflammation Res* (2014) 7:69–87. doi: 10.2147/JIR.S63898
- Katz J, Yue S, Xue W. Increased risk for covid-19 in patients with vitamin d deficiency. *Nutrition* (2021) 84:111106. doi: 10.1016/j.nut.2020.111106
- Panagiotou G, Tee SA, Ihsan Y, Athar W, Marchitelli G, Kelly D, et al. Low serum 25-hydroxyvitamin d (25[OH]D) levels in patients hospitalized with covid-19 are associated with greater disease severity. *Clin Endocrinol (Oxf)* (2020) 93(4):508–11. doi: 10.1111/cen.14276
- Xu Y, Baylink DJ, Chen CS, Reeves ME, Xiao J, Lacy C, et al. The importance of vitamin d metabolism as a potential prophylactic, immunoregulatory and neuroprotective treatment for covid-19. *J Transl Med* (2020) 18(1):322. doi: 10.1186/s12967-020-02488-5
- Hadizadeh F. Supplementation with vitamin d in the covid-19 pandemic? *Nutr Rev* (2021) 79(2):200–8. doi: 10.1093/nutrit/nuaa081
- Adelani IB, Rotimi OA, Maduagwu EN, Rotimi SO. Vitamin d: Possible therapeutic roles in hepatocellular carcinoma. *Front Oncol* (2021) 11:642653. doi: 10.3389/fonc.2021.642653
- Robinson MD, McCarthy DJ, Smyth GK. Edger: A bioconductor package for differential expression analysis of digital gene expression data. *Bioinformatics* (2010) 26(1):139–40. doi: 10.1093/bioinformatics/btp616
- Li R, Li Y, Liang X, Yang L, Su M, Lai KP. Network pharmacology and bioinformatics analyses identify intersection genes of niacin and covid-19 as potential therapeutic targets. *Brief Bioinform* (2021) 22(2):1279–90. doi: 10.1093/bib/bbaa300

## Conflict of interest

The authors declare that the research was conducted in the absence of any commercial or financial relationships that could be construed as a potential conflict of interest.

## Publisher's note

All claims expressed in this article are solely those of the authors and do not necessarily represent those of their affiliated organizations, or those of the publisher, the editors and the reviewers. Any product that may be evaluated in this article, or claim that may be made by its manufacturer, is not guaranteed or endorsed by the publisher.

## Supplementary material

The Supplementary Material for this article can be found online at: <https://www.frontiersin.org/articles/10.3389/fimmu.2022.985781/full#supplementary-material>

23. Ru J, Li P, Wang J, Zhou W, Li B, Huang C, et al. Tcmsp: A database of systems pharmacology for drug discovery from herbal medicines. *J Cheminform* (2014) 6:13. doi: 10.1186/1758-2946-6-13
24. Wang X, Shen Y, Wang S, Li S, Zhang W, Liu X, et al. Phrammapper 2017 update: A web server for potential drug target identification with a comprehensive target pharmacophore database. *Nucleic Acids Res* (2017) 45(W1):W356–W60. doi: 10.1093/nar/gkx374
25. Yu G, Wang LG, Han Y, He QY. Clusterprofiler: An r package for comparing biological themes among gene clusters. *OMICS* (2012) 16(5):284–7. doi: 10.1089/omi.2011.0118
26. Shannon P, Markiel A, Ozier O, Baliga NS, Wang JT, Ramage D, et al. Cytoscape: A software environment for integrated models of biomolecular interaction networks. *Genome Res* (2003) 13(11):2498–504. doi: 10.1101/gr.1239303
27. Zhou G, Soufan O, Ewald J, Hancock REW, Basu N, Xia J. Networkanalyst 3.0: A visual analytics platform for comprehensive gene expression profiling and meta-analysis. *Nucleic Acids Res* (2019) 47(W1):W234–W41. doi: 10.1093/nar/gkz240
28. Wang Y, Bryant SH, Cheng T, Wang J, Gindulyte A, Shoemaker BA, et al. Pubchem bioassay: 2017 update. *Nucleic Acids Res* (2017) 45(D1):D955–D63. doi: 10.1093/nar/gkw1118
29. Kerwin SM. Chembiooffice ultra 2010 suite. *J Am Chem Soc* (2010) 132(7):2466–7. doi: 10.1021/ja1005306
30. Burley SK, Berman HM, Kleywegt GJ, Markley JL, Nakamura H, Velankar S. Protein data bank (Pdb): The single global macromolecular structure archive. *Methods Mol Biol* (2017) 1607:627–41. doi: 10.1007/978-1-4939-7000-1\_26
31. Trott O, Olson AJ. Autodock vina: Improving the speed and accuracy of docking with a new scoring function, efficient optimization, and multithreading. *J Comput Chem* (2010) 31(2):455–61. doi: 10.1002/jcc.21334
32. Seeliger D, de Groot BL. Ligand docking and binding site analysis with pymol and Autodock/Vina. *J Comput Aided Mol Des* (2010) 24(5):417–22. doi: 10.1007/s10822-010-9352-6
33. Yuki K, Fujiogi M, Koutsogiannaki S. Covid-19 pathophysiology: A review. *Clin Immunol* (2020) 215:108427. doi: 10.1016/j.clim.2020.108427
34. Huang C, Wang Y, Li X, Ren L, Zhao J, Hu Y, et al. Clinical features of patients infected with 2019 novel coronavirus in wuhan, China. *Lancet* (2020) 395(10223):497–506. doi: 10.1016/S0140-6736(20)30183-5
35. Pathania AS, Prathipati P, Abdul BA, Chava S, Katta SS, Gupta SC, et al. Covid-19 and cancer comorbidity: Therapeutic opportunities and challenges. *Theranostics* (2021) 11(2):731–53. doi: 10.7150/thno.51471
36. Huang J, Yang G, Huang Y, Kong W, Zhang S. 1,25(OH)<sub>2</sub>D<sub>3</sub> inhibits the progression of hepatocellular carcinoma Via downregulating Hdac2 and upregulating P21(Waf1/Cip1). *Mol Med Rep* (2016) 13(2):1373–80. doi: 10.3892/mmr.2015.4676
37. Fingas CD, Altinbas A, Schlattjan M, Beilfuss A, Sowa JP, Sydor S, et al. Expression of apoptosis- and vitamin d pathway-related genes in hepatocellular carcinoma. *Digestion* (2013) 87(3):176–81. doi: 10.1159/000348441
38. Adelani IB, Ogadi EO, Onuzulu C, Rotimi OA, Maduagwu EN, Rotimi SO. Dietary vitamin d ameliorates hepatic oxidative stress and inflammatory effects of diethylnitrosamine in rats. *Heliyon* (2020) 6(9):e04842. doi: 10.1016/j.heliyon.2020.e04842
39. Liu W, Zhang L, Xu HJ, Li Y, Hu CM, Yang JY, et al. The anti-inflammatory effects of vitamin d in tumorigenesis. *Int J Mol Sci* (2018) 19(9):2736. doi: 10.3390/ijms19092736
40. Beard JA, Bearden A, Striker R. Vitamin d and the anti-viral state. *J Clin Virol* (2011) 50(3):194–200. doi: 10.1016/j.jcv.2010.12.006
41. Dimitrov V, White JH. Species-specific regulation of innate immunity by vitamin d signaling. *J Steroid Biochem Mol Biol* (2016) 164:246–53. doi: 10.1016/j.jsmb.2015.09.016
42. Fedirko V, Duarte-Salles T, Bamia C, Trichopoulou A, Aleksandrova K, Trichopoulos D, et al. Prediagnostic circulating vitamin d levels and risk of hepatocellular carcinoma in European populations: A nested case-control study. *Hepatology* (2014) 60(4):1222–30. doi: 10.1002/hep.27079
43. Flonta SE, Arena S, Pisacane A, Micheli P, Bardelli A. Expression and functional regulation of myoglobin in epithelial cancers. *Am J Pathol* (2009) 175(1):201–6. doi: 10.2353/ajpath.2009.081124
44. Yang K, Zhang S, Zhang D, Tao Q, Zhang T, Liu G, et al. Identification of Serpine1, plau and Acta1 as biomarkers of head and neck squamous cell carcinoma based on integrated bioinformatics analysis. *Int J Clin Oncol* (2019) 24(9):1030–41. doi: 10.1007/s10147-019-01435-9
45. Liu J, Li H, Sun L, Wang Z, Xing C, Yuan Y. Aberrantly methylated-differentially expressed genes and pathways in colorectal cancer. *Cancer Cell Int* (2017) 17:75. doi: 10.1186/s12935-017-0444-4
46. Batra N, De Souza C, Batra J, Raetz AG, Yu AM. The Hmox1 pathway as a promising target for the treatment and prevention of sars-Cov-2 of 2019 (Covid-19). *Int J Mol Sci* (2020) 21(17):6412. doi: 10.3390/ijms21176412
47. Nojiri S, Joh T. Albumin suppresses human hepatocellular carcinoma proliferation and the cell cycle. *Int J Mol Sci* (2014) 15(3):5163–74. doi: 10.3390/ijms15035163
48. Fu X, Yang Y, Zhang D. Molecular mechanism of albumin in suppressing invasion and metastasis of hepatocellular carcinoma. *Liver Int* (2022) 42(3):696–709. doi: 10.1111/liv.15115
49. Shimura T, Shibata M, Kofunato Y, Okada R, Ishigame T, Kimura T, et al. Clinical significance of serum transthyretin level in patients with hepatocellular carcinoma. *ANZ J Surg* (2018) 88(12):1328–32. doi: 10.1111/ans.14458
50. Li M, Wang Z, Zhu L, Shui Y, Zhang S, Guo W. Down-regulation of Rbp4 indicates a poor prognosis and correlates with immune cell infiltration in hepatocellular carcinoma. *Biosci Rep* (2021) 41(4):BSR20210328. doi: 10.1042/BSR20210328
51. Aboudounya MM, Heads RJ. Covid-19 and toll-like receptor 4 (Tlr4): Sars-Cov-2 may bind and activate Tlr4 to increase Ace2 expression, facilitating entry and causing hyperinflammation. *Mediators Inflammation* (2021) 2021:8874339. doi: 10.1155/2021/8874339
52. Ali A, Noman M, Guo Y, Liu X, Zhang R, Zhou J, et al. Myoglobin and c-reactive protein are efficient and reliable early predictors of covid-19 associated mortality. *Sci Rep* (2021) 11(1):5975. doi: 10.1038/s41598-021-85426-9
53. Badawy MA, Yasseen BA, El-Messier RM, Abdel-Rahman EA, Elkhodiry AA, Kamel AG, et al. Neutrophil-mediated oxidative stress and albumin structural damage predict covid-19-Associated mortality. *Elife* (2021) 10:e69417. doi: 10.7554/eLife.69417
54. Rotondo C, Corrado A, Colia R, Maruotti N, Sciacca S, Lops L, et al. Possible role of higher serum level of myoglobin as predictor of worse prognosis in sars-cov 2 hospitalized patients. *A Monocentric Retrospective Study Postgrad Med* (2021) 133(6):688–93. doi: 10.1080/00325481.2021.1949211
55. Zhao Y, Kuang M, Li J, Zhu L, Jia Z, Guo X, et al. Sars-Cov-2 spike protein interacts with and activates Tlr4. *Cell Res* (2021) 31(7):818–20. doi: 10.1038/s41422-021-00495-9
56. Coperchini F, Chiovato L, Croce L, Magri F, Rotondi M. The cytokine storm in covid-19: An overview of the involvement of the Chemokine/Chemokine-receptor system. *Cytokine Growth Factor Rev* (2020) 53:25–32. doi: 10.1016/j.cytogfr.2020.05.003
57. Gheware A, Dholakia D, Kannan S, Panda L, Rani R, Pattnaik BR, et al. Adhatoda vasica attenuates inflammatory and hypoxic responses in preclinical mouse models: Potential for repurposing in covid-19-Like conditions. *Respir Res* (2021) 22(1):99. doi: 10.1186/s12931-021-01698-9
58. Tian M, Liu W, Li X, Zhao P, Shereen MA, Zhu C, et al. Hif-1 $\alpha$  promotes sars-Cov-2 infection and aggravates inflammatory responses to covid-19. *Signal Transduct Target Ther* (2021) 6(1):308. doi: 10.1038/s41392-021-00726-w



## OPEN ACCESS

## EDITED BY

Alfonso J. Rodriguez-Morales,  
Fundacion Universitaria Autónoma de  
las Américas, Colombia

## REVIEWED BY

Pier Maria Fornasari,  
Regenhealthsolutions, Italy  
Tao Chen,  
Huazhong University of Science and  
Technology, China

## \*CORRESPONDENCE

Feng-Xia Liu  
592111443@qq.com

<sup>†</sup>These authors have contributed  
equally to this work and share  
first authorship

## SPECIALTY SECTION

This article was submitted to  
Viral Immunology,  
a section of the journal  
Frontiers in Immunology

RECEIVED 22 June 2022

ACCEPTED 04 August 2022

PUBLISHED 31 August 2022

## CITATION

Lu L, Liu L-P, Gui R, Dong H, Su Y-R,  
Zhou X-H and Liu F-X (2022)  
Discovering common pathogenetic  
processes between COVID-19 and  
sepsis by bioinformatics and system  
biology approach.  
*Front. Immunol.* 13:975848.  
doi: 10.3389/fimmu.2022.975848

## COPYRIGHT

© 2022 Lu, Liu, Gui, Dong, Su, Zhou  
and Liu. This is an open-access article  
distributed under the terms of the  
[Creative Commons Attribution License](#)  
(CC BY). The use, distribution or  
reproduction in other forums is  
permitted, provided the original  
author(s) and the copyright owner(s)  
are credited and that the original  
publication in this journal is cited, in  
accordance with accepted academic  
practice. No use, distribution or  
reproduction is permitted which does  
not comply with these terms.

# Discovering common pathogenetic processes between COVID-19 and sepsis by bioinformatics and system biology approach

Lu Lu<sup>1†</sup>, Le-Ping Liu<sup>1,2†</sup>, Rong Gui<sup>1</sup>, Hang Dong<sup>1</sup>,  
Yan-Rong Su<sup>3</sup>, Xiong-Hui Zhou<sup>1</sup> and Feng-Xia Liu<sup>1\*</sup>

<sup>1</sup>Department of Blood Transfusion, The Third Xiangya Hospital of Central South University, Changsha, China, <sup>2</sup>Department of Pediatrics, The Third Xiangya Hospital, Central South University, Changsha, China, <sup>3</sup>Department of Laboratory Medicine, The Third Xiangya Hospital of Central South University, Changsha, China

Corona Virus Disease 2019 (COVID-19), an acute respiratory infectious disease caused by severe acute respiratory syndrome coronavirus-2 (SARS-CoV-2), has spread rapidly worldwide, resulting in a pandemic with a high mortality rate. In clinical practice, we have noted that many critically ill or critically ill patients with COVID-19 present with typical sepsis-related clinical manifestations, including multiple organ dysfunction syndrome, coagulopathy, and septic shock. In addition, it has been demonstrated that severe COVID-19 has some pathological similarities with sepsis, such as cytokine storm, hypercoagulable state after blood balance is disrupted and neutrophil dysfunction. Considering the parallels between COVID-19 and non-SARS-CoV-2 induced sepsis (hereafter referred to as sepsis), the aim of this study was to analyze the underlying molecular mechanisms between these two diseases by bioinformatics and a systems biology approach, providing new insights into the pathogenesis of COVID-19 and the development of new treatments. Specifically, the gene expression profiles of COVID-19 and sepsis patients were obtained from the Gene Expression Omnibus (GEO) database and compared to extract common differentially expressed genes (DEGs). Subsequently, common DEGs were used to investigate the genetic links between COVID-19 and sepsis. Based on enrichment analysis of common DEGs, many pathways closely related to inflammatory response were observed, such as Cytokine-cytokine receptor interaction pathway and NF-kappa B signaling pathway. In addition, protein-protein interaction networks and gene regulatory networks of common DEGs were constructed, and the analysis results showed that *ITGAM* may be a potential key biomarker base on regulatory analysis. Furthermore, a disease diagnostic model and risk prediction nomogram for COVID-19 were constructed using machine learning methods. Finally, potential therapeutic agents, including progesterone and emetine, were screened through drug-protein interaction networks and molecular docking simulations. We hope to provide new strategies for future research and

treatment related to COVID-19 by elucidating the pathogenesis and genetic mechanisms between COVID-19 and sepsis.

#### KEYWORDS

COVID-19, sepsis, differentially expressed gene (DEG), functional enrichment, gene ontology, protein–protein interaction (PPI), hub gene, drug molecule

## Introduction

The novel coronavirus, SARS-CoV-2, is the causative agent of an atypical respiratory disease that has caused a global pandemic since 2019. The World Health Organization defines the infectious disease caused by the virus as Corona Virus Disease 2019 (COVID-19) (1). Since the pandemic, the new coronavirus has undergone a variety of mutations, and it has now mutated to Omicron BA.4 and BA.5, which has a strong immune evasion ability. Data showed that as of 31 December 2021, over 287 million cases had occurred worldwide, including more than 5.4 million deaths (2). More than 80% of COVID-19 patients have mild disease, but the incidence of severe or high-risk disease varies among patient populations (3). Literature suggests that critical illness including respiratory failure, multi-organ damage or shock can occur in up to 5% of patients (2). Severe COVID-19 is often pathologically manifested by pulmonary and extrapulmonary organ dysfunction. Studies have shown that the lung is the organ most severely affected by SARS-CoV-2, manifesting as diffuse alveolar damage, exudation, and interstitial fibrosis, accompanied by a large number of immune cell infiltration and inflammatory factor expression (3–5). Extrapulmonary organs have different degrees of tissue damage and inflammatory response, manifested as multiple organ dysfunction and systemic inflammatory response (6). In terms of clinical symptoms, most severe COVID-19 patients eventually develop typical septic shock manifestations, including cold limbs, microcirculatory dysfunction, weak peripheral pulse, oxidative stress injury, and cytokine storm (7). In addition, in clinical care, the latest COVID-19 treatment guidelines, “surviving sepsis campaign”, have been adopted as treatment guidelines for critically ill patients (8). All in all, both in terms of clinical diagnosis and treatment, severe COVID-19 and sepsis have similarities, and the two can learn from each other.

Sepsis is a systemic inflammatory response syndrome (SIRS) caused by a variety of factors, including infection, trauma and surgery, and its mortality and morbidity are extremely high (5). Uncontrolled inflammation and overproduction of Reactive Oxygen and Nitrogen Species (RONS) are the hallmarks of sepsis, which in turn cause cell and tissue destruction, immune

system dysfunction, and marked hemopathology, ultimately leading to multiple organ failure syndrome Signs (MODS) (9–13). Part of the viral pneumonia caused by SARS-CoV-2 is a fulminant disease with similar manifestations to sepsis (14). Considering the similarities between COVID-19 and non-SARS-CoV-2 induced sepsis, it is necessary to understand the biological links and potential molecular mechanisms between the two to provide new insights into the pathogenesis of COVID-19 and to search for potential therapeutic agents for patients with COVID-19 or patients with COVID-19 secondary to sepsis.

With the development of science and technology, biology and computer technology are becoming more and more closely integrated. Bioinformatics is a discipline that uses computer algorithms to effectively analyze biological data, enabling a systematic approach to understanding the developmental process of organisms, classifying organisms, studying biomarkers of diseases, etc (15). Machine learning is a kind of algorithm of artificial intelligence, which can explore potential laws in massive data. It has high accuracy and has emerged in medical research and medical development (16). In recent years, machine learning and bioinformatics analysis have played an important role in medical research and application.

This study aims to understand the common pathogenesis between COVID-19 and sepsis, and to unearth potential drugs. First, datasets from the GEO database for COVID-19 and sepsis were analyzed to identify differentially expressed genes (DEGs) for these two diseases, and then further compared to obtain common DEGs. Based on the common DEGs, the enriched pathways and functions of these genes were analyzed to understand the biological processes they were involved in. Next, the protein–protein interaction (PPI) network was drawn to show the relationship between all DEGs, and the key genes with the highest degree of interaction were screened out from the Hub genes as potential biomolecules. The biological role of this key gene in COVID-19 was then analyzed to explore its potential mechanism in disease development and progression. In addition, a disease diagnosis model and risk prediction nomogram of COVID-19 were established using machine learning algorithms. Next, the transcriptional regulatory network of these common DEGs in COVID-19 was



analyzed. Finally, we predict drugs related to common DEGs, providing new ideas for the treatment of COVID-19. The sequential workflow of our research is presented in **Figure 1**.

## Materials and methods

### Transcriptomic data acquisition

To determine shared genetic interrelations between COVID-19 and sepsis, three RNA-Sequencing datasets were downloaded from the Gene Expression Omnibus (GEO) database of the National Center for Biotechnology Information (NCBI) (<https://www.ncbi.nlm.nih.gov/geo/>) (17). The GEO accession ID of the COVID-19 dataset was GSE147507, which included transcriptional profiling from 78 samples (23 COVID-19 samples and 55 healthy control samples) through high throughput sequencing Illumina NextSeq 500 platform for extracting RNA sequence (18). The sepsis dataset having association number GSE65682 was based on GPL13667 [HG-U219] Affymetrix Human Genome U219 Array platform, and contained 802 samples including healthy controls, non-sepsis critically ill patients and sepsis patients. Furthermore, the sepsis patients could be further categorized into pneumonia sepsis (n=192), abdominal sepsis (n=51) and others (n=443) based on infection site (19). According to some scholars, COVID-19 is a systemic infection, and its clinical manifestations range from asymptomatic to mild respiratory tract infection and influenza-like illness, to severe diseases with lung injury, multiple organ failure and death (20). However, the lung is thought to be the main site of SARS-CoV-2 infection and replication (14). Therefore, in our study, we screened 192 pneumonia sepsis samples and 42 healthy control samples from GSE65682 discovery dataset for further analysis. Besides, the GSE196822 discovery dataset was used as a

validation cohort for development of the COVID-19 diagnostic model. This second selected COVID-19 dataset consisted of 40 samples from COVID-19 subjects and 9 healthy controls, which were sequenced using microarrays called Illumina HiSeq 4000 platform. The summarized information of the datasets was shown in **Table S1**.

### Differential gene expression analysis

Firstly, the DEGs for the corresponding diseases were extracted from two mRNA datasets (GSE147507 and GSE65682). Specifically, the DEGs were identified by using the “limma” R package and the Benjamini–Hochberg false discovery rate method was used to discover genes which were statistically significant and limit false positives (21). Genes exhibiting an adjusted P-values of  $<0.05$  along with  $|\log_2FC| \geq 1.0$  were identified as statistically significant genes. The mutual DEGs of GSE147507 and GSE65682 was acquired through an online VENN analysis tool called Jvenn (<http://jvenn.toulouse.inra.fr/app/index.html>) (22).

### Functional insights into the differentially expressed genes

To clarify potential biological mechanisms between COVID-19 and sepsis, we attempted to investigate the gene ontology (GO) terms and Kyoto Encyclopedia of Genes and Genomes (KEGG) enrichment pathways base on common DEGs. KEGG is considered as a knowledge base for systematic analysis of gene functions, linking genomic information with higher order functional information (23).

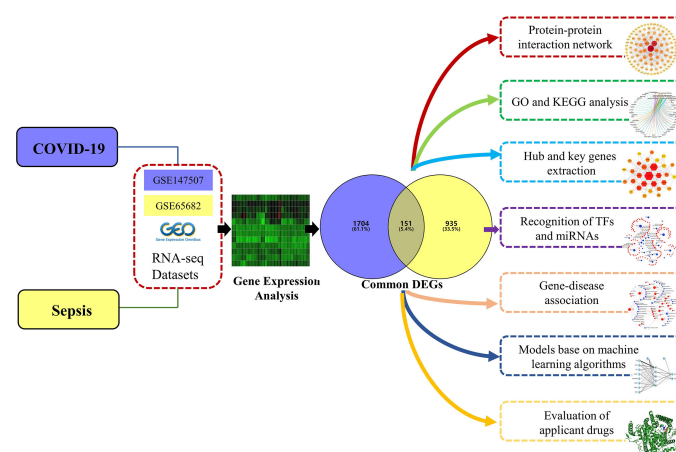


**FIGURE 1**  
Schematic illustration of the overall general workflow of this study.

Additionally, GO, a community-based bioinformatics resource, can provide information about gene product function by presenting biological knowledge as ontologies (24). GO analysis was classified into three subgroups, including molecular function (MF), biological process (BP) and cellular component (CC) (25). For quantifying the top listed functional items and pathways, a “clusterProfiler” R package was used to perform functional enrichment analysis, and a statistical threshold criterion with an adjusted P-value <0.05 was used to identify significant GO terms and KEGG pathways.

## Protein–protein interaction analysis and hub genes extraction

Proteins conclude their journey into a cell with a similar protein affiliation formed by a protein–protein network, which indicates the protein mechanisms (21). In this study, the protein subnetworks on common DEGs were identified to discover the associations between different diseases from the perspective of protein interactions. Specifically, an online analysis tool called STRING (<https://www.string-db.org/>) (version 11.5) was to insert common DEGs to generate PPI networks. Supported by Damian Szklarczyk, the STRING is a database which aims to integrate all known and predicted associations between proteins, including both physical interactions as well as functional associations (26). A combined score larger than 0.4 was used to construct the PPI network of frequent DEGs in this experiment. Then, the Cytoscape (version 3.9) was used for visual representation and further PPI network experimental studies. Furthermore, a Cytoscape plugin, CytoHubba (<https://apps.cytoscape.org/apps/cytohubba>), was put into practice to extract hub genes. Cytohubba is a significant Cytoscape application, which can rank and extract central or potential or targeted elements of a biological network based on various network features (21). Moreover, Cytohubba has 11 methods for investigating networks from various viewpoints, and Maximal Clique Centrality (MCC) is the best of them (27). The MCC function of Cytohubba was carried out to confirm the top 30 hub genes from the PPI network.

## Regulatory analysis of the key gene

Based on the analysis results of PPI network and Hub gene extraction, we further explored the biological function and possible mechanism of *ITGAM*, the most critical gene located at the core of the protein interaction network. First, the “limma” R package was used to implement differential expression analysis in GSE147507 discovery dataset to determine whether *ITGAM* differed between COVID-19 and healthy controls. Gene co-expression is a type of analysis method that uses a large

amount of gene expression data to construct correlations among genes and thus discover the function of genes (28). Next, based on gene co-expression analysis, *ITGAM*-related gene regulatory networks were constructed using gene expression data from COVID-19 dataset. In addition, to further explore the potential pathways and molecular biological functions that *ITGAM* may affect in COVID-19, gene set enrichment analysis (GSEA) for *ITGAM* was performed in GSE147507 discovery dataset. GSEA includes pathway analysis and gene ontology analysis, which plays an essential role in extracting biological insight from genome-scale experiments (29, 30). Furthermore, immune correlation analysis of *ITGAM* was conducted. Specifically, based on *ITGAM*’s expression data, the COVID-19 samples were divided into high- and low-expressed groups using the mean of *ITGAM* expression levels as a zero cut-off. Next, the difference for immune cell infiltration between the high- and low-expressed groups was analyzed using the “CIBERSORT” R package, and the correlation between *ITGAM* and immune cells was further explored (31). Finally, differences in the expression of immune checkpoints between the high- and low- expressed groups and the correlation between *ITGAM* and immune checkpoints were analyzed by the “corrplot” R package.

## Developing diagnostic signature and risk model for COVID-19

Based on the common DEGs obtained by differential expression and VENN analysis, machine learning methods were used to screen the features/key genes and further constructed the diagnostic model and risk prediction model for COVID-19. Specifically, random forests (RFs) were applied to screen diagnostic features in GSE147507 discovery dataset. RF is one type of very popular ensemble learning method in which numerous randomized decision trees are constructed and combined to form an RF that is then used for classification or regression (32). In this study, the DEGs with Gini index > 1.0 were considered characteristic variables. Next, using GSE147507 discovery dataset as training cohort, artificial neural networks (ANNs) were performed to construct COVID-19 diagnostic model based on the signature genes. ANNs are a set of technologies often encompassed with artificial intelligence that attempt to simulate the function of the human brain, and have been applied in almost every aspect of medicine (33, 34). Further, the GSE196822 discovery dataset was used as a validation cohort to evaluate the performance of the diagnostic model. Finally, a nomogram was developed based on the results of RF analysis to calculate the risk of COVID-19 for an individual patient by the points associated with the risk factors, and the performance of the nomogram was assessed by decision and calibration curve.

## Identification of transcription factors and miRNAs

To determine the major variation at the transcriptional level and gain a deeper understanding of the key protein regulatory molecules or common DEG, the DEG–miRNA (microRNA) interaction networks and transcription factor (TF)–DEG interaction networks were identified in our analysis. Specifically, the NetworkAnalyst platform was utilized to locate topologically credible TFs from the JASPAR database that tend to bind to the common DEGs (21). For DEG–miRNA network construction via NetworkAnalyst platform, the TarBase (35) and miRTarBase (36) databases were used to extract miRNAs with common DEGs focused on topological analysis (37).

## Gene–disease association analysis

DisGeNET is a knowledge management platform, which integrates and standardizes the data about disease associated genes and variants from multiple sources, including the scientific literature (38). The gene–disease relationship network was established through NetworkAnalyst platform to uncover associated diseases and their chronic complications related to the common DEGs (21).

## Evaluation of applicant drugs

In this analysis, the protein–drug interaction (PDI) and identified pharmacological molecules were predicted by using the common DEGs that COVID-19 shares with sepsis. The web portal of Enrichr and the Drug Signatures Database (DSigDB) were used to analyze the drug molecules based on the DEGs from both COVID-19 and sepsis. Enrichr (<http://amp.pharm.mssm.edu/Enrichr>) contains a large collection of diverse gene set libraries available for analysis and download, which can be used to explore gene-set enrichment across a genome-wide scale (39). DSigDB is a new gene set resource for gene set enrichment analysis, which related drugs/compounds and their target genes. The DSigDB database was accessed through Enrichr under the Diseases/Drugs function (40).

## Molecular docking simulation

Molecular docking that an established in silico structure-based method is widely used in drug discovery. Docking enables the identification of novel compounds of therapeutic interest, predicting ligand–target interactions at a molecular level, or delineating structure–activity relationships (SAR), without

knowing *a priori* the chemical structure of other target modulators (41). In our study, key targets of COVID-19 were obtained through literature search, including ACE2, 3CLpro, M<sup>pro</sup>, PLpro and RdRp. Next, the crystal structures of these key proteins were downloaded from the Protein Data Bank (<https://www.rcsb.org/>) for further molecular docking. The PDB codes for these five key proteins are shown below: 1R42 for ACE2, 6LU7 for 3CLpro, 5B60 for Mpro, 6Y2E for PLpro, 6NUS for RdRp. In addition, the molecular structures of potential drug molecules were obtained from the ZINC (<https://zinc.docking.org/>) database. The Autodock tools (version 1.5.4) was utilized in all the docking experiments, with the optimized model as the docking target. The screening method is restricted to molecular docking, and molecular dynamics simulation has not been carried. In addition, the results were shown with binding energy (BE), a weighted average of docking score, to assess the reliability and describe the accuracy of the ligand positioning. Pymol (PyMOL Molecular Visualization System 2020) was used for 3D visualization of the docking results.

## Results

### Identification of common transcriptional signatures between COVID-19 and sepsis

Patients with severe COVID-19 may develop a systemic inflammatory response syndrome (SIRS) that may progress to sepsis if inflammation worsens. To examine the interrelationships and implications between COVID-19 and sepsis, the human RNA-seq dataset and microarray datasets were analyzed from the GEO to identify the disrupting genes that trigger COVID-19 and sepsis. A total of 1855 DEGs were obtained from the COVID-19 dataset, including 1206 up-regulated DEGs and 649 down-regulated genes. In addition, a total of 1086 DEGs were identified in the sepsis blood dataset by differential expression analysis, of which 481 genes were up-regulated and 605 genes were down-regulated (Table S1). The two volcano plots in Figure 1 visually demonstrated the overall picture of transcribed gene expression for COVID-19 and sepsis, where red and blue dots indicated up- and down-regulated genes with significant differences, respectively (Figures 2A, B). Furthermore, we employed heatmaps to present the results of cluster analysis and expression analysis of the top 20 DEGs among different samples in COVID-19 and sepsis datasets, respectively (Figures 2C, D). The top 20 DEGs for COVID-19 included *HIST1H2AK*, *OLR1*, *SELL*, *ZBTB10*, *DUSP8*, *CREBRF*, *PLD6*, *BHLHE41*, *ZNF57*, *ZNF77*, *BCL2A1*, *IFITM2*, *ARRDC3*, *CLK1*, *HIST2H2BE*, *NFIL3*, *ZNF267*, *SERTAD2*, *ZNF292* and *ZNF12*. In sepsis discovery set, the top 20 DEGs were *ABLM1*, *LRRN3*, *EPHX2*, *NMT2*, *THEM4*, *GATA3*, *CD96*, *PLEKHA1*, *DYRK2*, *PID1*, *P2RY10*, *C2orf89*, *NELL2*, *LEF1*, *S100A8*, *S100A12*, *C5orf32*, *ARG1*, *C19orf59* and *ANXA3*. The identification of these genes with significant differential

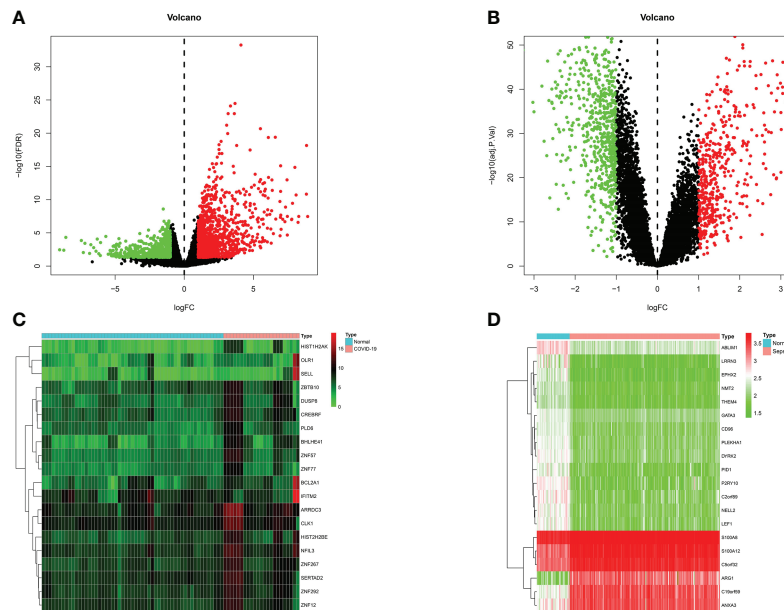


FIGURE 2

Volcano plots exhibit differentially expressed genes (DEGs) of (A) COVID-19 and (B) sepsis. Red dots indicated up-regulated genes, blue dots indicated down-regulated genes, and gray dots indicated non-DEGs, with  $FC \geq 1.0$  and  $P\text{-value} < 0.05$ . Heatmaps show the result of clustering analysis based on DEGs for (C) COVID-19 and (D) sepsis.

expression could help us to obtain a critical entry point for studying the development of diseases, which in turn could help to understand the underlying mechanisms of diseases and to obtain new therapeutic targets. After performing the cross-comparative analysis on the Jvenn, a reliable web portal for Venn analysis, a total of 151 common DEGs were identified from COVID-19 and sepsis datasets (Figure 4A). The results of differential expression analysis suggested that there were some mechanistic commonalities and interaction between COVID-19 and sepsis.

## Pathway enrichment and gene ontology analysis

To further understand the biological functions and signaling pathways involved in these common DEGs, we implemented KEGG pathway enrichment and GO functional analysis. The top 15 important pathways were displayed with bubble plots (Figure 3A). From the results of KEGG pathway analysis, these 151 common DEGs were mainly enriched in infectious/inflammatory disease-related and immune response-related pathways, for example, *Staphylococcus aureus* infection, Inflammatory bowel disease, Cytokine-cytokine receptor interaction pathway and NF-kappa B signaling pathway. It is well-known that both COVID-19 and sepsis are associated with inflammatory and immune responses in the body, which play an

important role in the development and progression of these two diseases, and are closely related to the therapeutic effect and prognosis of patients (3, 14, 42). Our pathway analysis results also showed that the immune-related pathway, Cytokine-cytokine receptor interaction, was the most significantly enriched pathway (Figure 3B), suggesting that these common DEGs may affect the progression of the disease through immune-related biological functions or signaling pathways.

GO analysis is divided into three parts: MF, BP and CC. Figure 3C presented the top 10 GO terms for MF, BP, and CC, respectively. Specific analysis revealed that the top 10 GO terms of BP were all associated with immune function, such as T cell activation, lymphocyte differentiation, mononuclear cell differentiation and negative regulation of cytokine production. Interestingly, most of the BP terms were associated with T cell immune function. In addition, the results of CC showed that these common DEGs were mainly involved in the formation or release of intracellular granules, for example, tertiary granule, specific granule, specific granule lumen and cytoplasmic lumen vesicle. Previous studies have suggested that tertiary granule and specific granule are associated with the function of human mature neutrophils, including differentiation and pro-inflammatory effect of neutrophils (43). During inflammation, neutrophils are activated and secrete part of the granular contents, which are cytotoxic and in part responsible for the collateral damage associated with neutrophil tissue infiltration (44). Furthermore, the results of MF analysis presented that MF

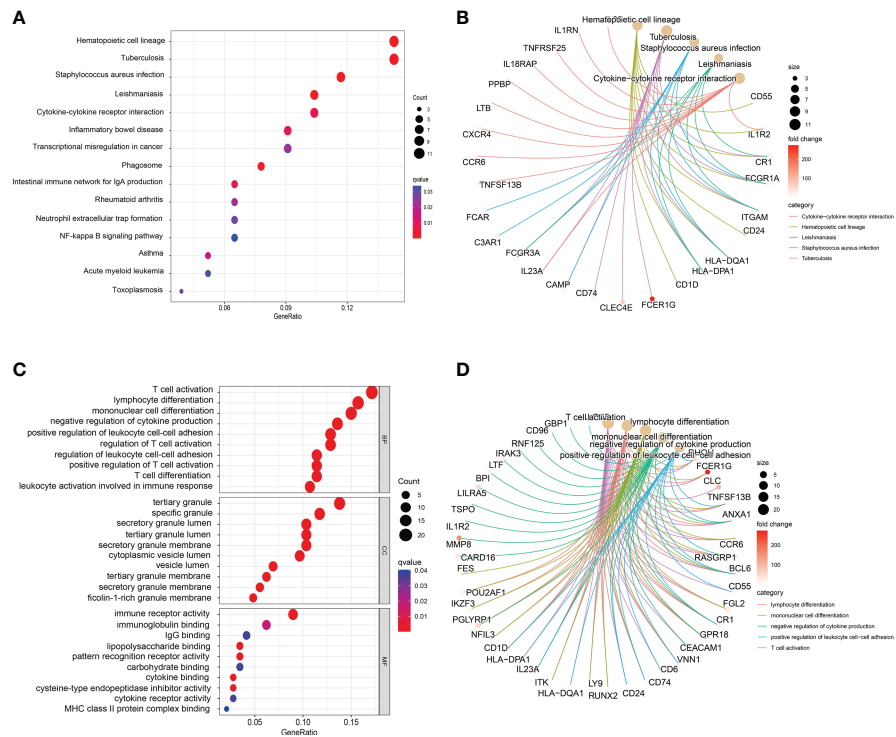


**FIGURE 3**  
Bubble graphs indicate the results for (A) Kyoto Encyclopedia of Genes and Genomes (KEGG) and (C) Gene Ontology (GO) analysis based on the common differentially expressed genes (DEGs). Loop graphs show the correlation between the five most important (B) pathways or (D) GO terms and the enriched DEGs.

terms were also mainly associated with immune responses, including immune receptor activity, immunoglobulin binding and IgG binding. Figure 3D shows the correlation between the five most important GO terms and the enriched DEGs, including lymphocyte differentiation negative regulation of cytokine production positive production regulation of leukocyte cell–cell adhesion T cell activation, all of which are immune-related molecular functions. Similar to the results suggested by KEGG analysis, these common DEGs may involve immune-related functions and pathways of the body, which in turn affect the disease progression of COVID-19.

## Protein–protein interaction network analysis and identification of hub genes

A PPI network was constructed using the common DEGs among COVID-19 and sepsis. The PPI network visually demonstrates the intercorrelations between different proteins, suggesting the underlying mechanisms by which proteins function. The assessment and analysis of PPI networks can help to obtain key proteins that influence the biological functions of cells and systems (45). Based on the online analysis website,

STRING, the PPI network of proteins derived from shared DEGs was constructed to portray functional and physical interactions between COVID-19 and sepsis. The PPI network of common DEGs included 151 nodes and 322 edges and was depicted in Figure 4C, with the PPI enrichment p-value < 0.001. As shown in the figure, the size and color depth of the circles indicated the degree of intercorrelation of the proteins, and the more connections to the central proteins, the stronger the relationship, suggesting its importance. By using cytoHubba package of Cytoscape, the top 30 (19.87%) DEGs were considered as the most influential genes. The top 30 influential genes included *ITGAM*, *FCGR3A*, *S100A12*, *FCER1G*, *FCGR1A*, *LY86*, *IL1RN*, *C3AR1*, *LCN2*, *BCL6*, *CAMP*, *RGS18*, *CXCR4*, *CLEC5A*, *SOC33*, *CD1D*, *FGL2*, *GPR29*, *AQP9*, *CLEC4D*, *CD74*, *TNFSF13B*, *CD24*, *LTF*, *HCST*, *MPEG*, *CR1*, *MMP8*, *MS4A4A* and *FCGR1B*, with specific information showing in Table S2. The identification of hub genes from common DEGs facilitates us to obtain more critical signatures in order to discover potential biomarkers. Since hub genes were potential, a submodule network was constructed by the Cytohubba plugin's aid to deeper understand their near connectivity and proximity (Figure 4B).

From the sub-module network of hub genes, *ITGAM* was shown to have the most edges, that is, the most proteins



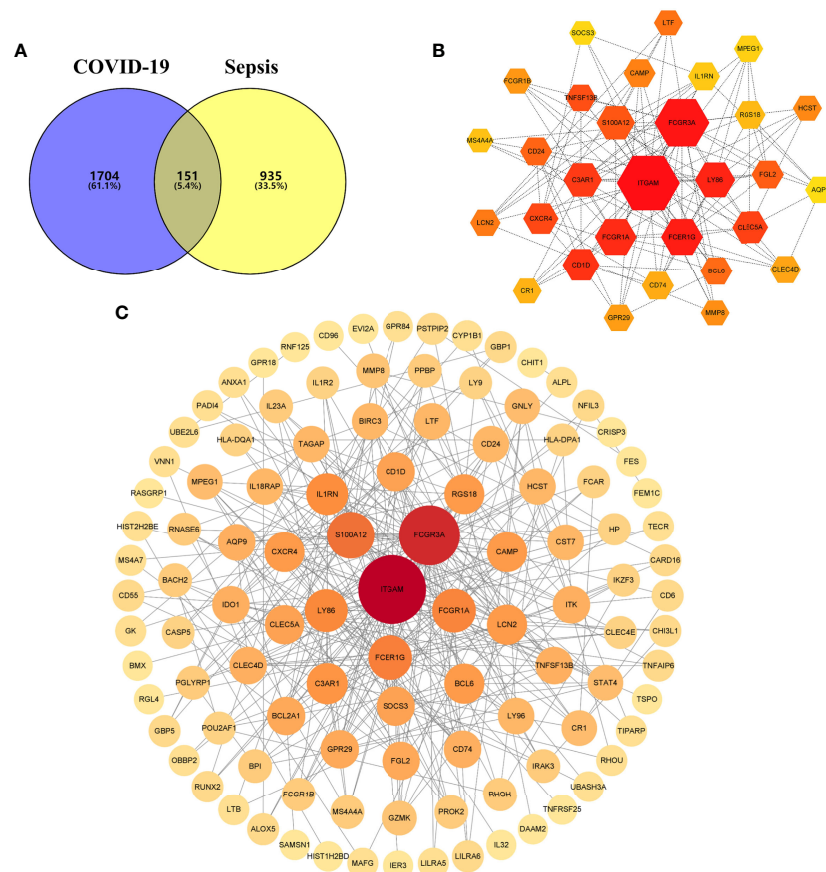


FIGURE 4

(A) The Venn diagram depicts the shared differentially expressed genes (DEGs) between COVID-19 and sepsis. (B) The top 30 hub gene was identified from the protein–protein interaction (PPI) network, and the hexagonal nodes represent DEGs and edges represent the interactions between nodes. (C) The (PPI) network of common DEGs among COVID-19 and RA, and the circle nodes represent DEGs and edges represent the interactions between nodes.

associated with it, so in further studies, the biological role of *ITGAM* in COVID-19 was focused to explore its potential mechanism in the development and progression of the disease. *ITGAM* encodes integrin- $\alpha$ M (CD11b +), molecule that combines with integrin- $\beta$ 2 to form a leucocyte-specific integrin, which associated with multiple immune disorders (46). The expression difference analysis indicated that the expression level of *ITGAM* was significantly different between COVID-19 and normal samples, with  $p$ -value < 0.01 (Figure 5A), suggesting that this signature may have an important role in COVID-19. In addition, a co-expression network of *ITGAM* with other genes was constructed by Gene Co-expression Network Analysis (GCNA) (Figure 5B). The GCNA results showed that *ITGAM* had a significant correlation with 156 genes ( $p$ -value < 0.05), and Figure 4B showed only the top 11 important genes, including *TGFBR3*, *NMNAT1*, *RHO*, *PLEKHG5*, *MAP3K8*, *ZCCHC17*, *DCAF6*, *CTNNBIP1*, *SRP9*, *F5*, and *S100A2*. Among them, *TGFBR3*,

*RHO*, *MAP3K8*, *SRP9* and *F5* were positively correlated with *ITGAM* expression, and the remaining six genes were negatively correlated with *ITGAM*. As a result of GCNA, the co-expressed genes mediated the expression and function of *ITGAM* through different pathways, and *ITGAM* played multiple biological roles *in vivo*. Furthermore, GSEA enrichment analysis was implemented to interrogate the function and pathway of *ITGAM*. Among the GO terms, the GSEA analysis in the GSE147507 dataset revealed that the samples of highly expressed *ITGAM* were mainly enriched in an important immune-related biological process, adaptive immune response. Other GO terms involved included cornification, epidermal cell differentiation, epidermis development and keratinization (Figure 5C). Among the KEGG pathways, the top 5 signaling pathways influenced by highly expressed *ITGAM* were cytokine-cytokine receptor interaction, graft versus host disease, leishmania infection, systemic lupus erythematosus and type I diabetes mellitus (Figure 5D). In addition, based on the average

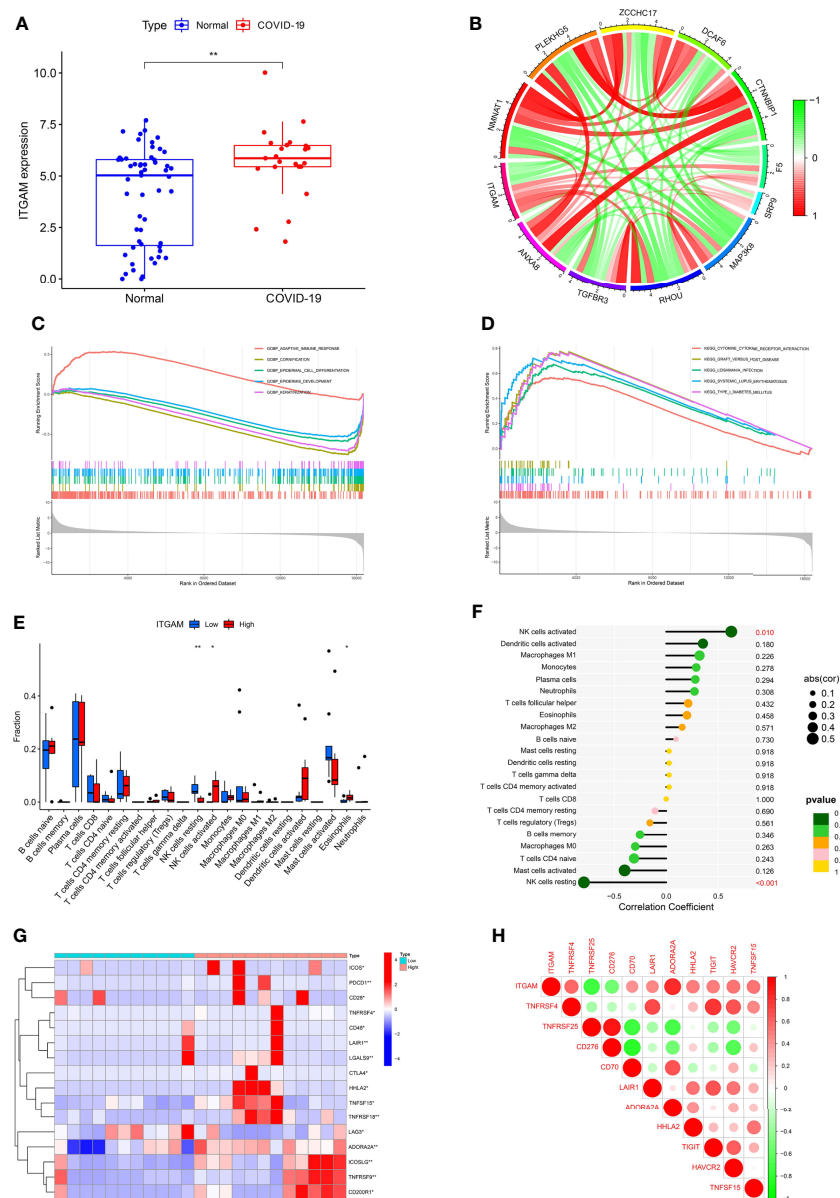


FIGURE 5

(A) The differential expression levels of *ITGAM* between COVID-19 and healthy controls. (B) The construction of a co-expression network for *ITGAM* with other genes in COVID-19. Gene set enrichment analysis (GSEA) for *ITGAM* in COVID-19, including (C) gene ontology analysis and (D) pathway analysis. (E) The difference for immune cell infiltration between *ITGAM* high- and low-expressed groups in COVID-19. \* $p < 0.05$ ; \*\* $p < 0.01$ . (F) Plots of immune cells associated with *ITGAM* in COVID-19. (G) The clustering analysis for differentially expressed immune checkpoints between *ITGAM* high- and low-expressed groups in COVID-19. (H) Heatmap of immune checkpoints associated with *ITGAM* in COVID-19.

expression level of *ITGAM*, the COVID-19 samples from the GSE14750 dataset were divided into high- expressed and low-expressed groups. In order to explore the degree of immune cell infiltration between the high and low *ITGAM* expression groups to understand the potential immune mechanism, the infiltration levels of 22 immune cells were analyzed between the two groups using the “CIBERSORT” R package. The results of

“CIBERSORT” analysis showed that there were significant differences in resting NK cells, activated NK cells and Eosinophils between the *ITGAM* high-expressed and the low-expressed groups (Figure 5E). Interestingly, our results showed that *ITGAM* was positively correlated with activated NK cells, but negatively correlated with resting NK cells, with a  $p$ -value  $< 0.01$  (Figure 5F). Finally, the expression levels of immune

checkpoints were analyzed between the *ITGAM* high-expressed and the low-expressed groups and found that a total of 16 immune checkpoint genes were differentially expressed, including *ICOS*, *PDCD1*, *CD28*, *TNFRSF4*, *CD48*, *LAIR1*, *LGALS9*, *CTLA4*, *HHLA2*, *TNFSF15*, *TNFRSF18*, *LAG3*, *ADORA2A*, *ICOSLG*, *TNFRSF9* and *CD200R1* (Figure 5G). Among them, the study results suggested that 14 immune checkpoints (*TNFRSF4*, *CD48*, *TNFRSF18*, *CD70*, *HHLA2*, *BTLA*, *ICOSLG*, *TNFRSF9*, *CTLA4*, *LGALS9*, *PDCD1*, *TNFSF15*, *LAIR1*, *ADORA2A*) were positively correlated with *ITGAM*, while *CD276* and *TNFRSF25* were negatively correlated with *ITGAM* (Figure 5H). The results of the above analysis help us to preliminarily understand the immune mechanism of *ITGAM* in COVID-19, which in turn taps its potential biological functions.

## Construction of disease diagnosis and risk model based on common DEGs

Through the above analysis, it was found that the common DEGs of COVID-19 and sepsis may affect the disease process of COVID-19 through different functions and pathways, therefore, based on 151 common DEGs, we screened and constructed a diagnostic model and risk model of COVID-19 using machine learning algorithms. Specifically, the RF analysis was implemented to select key DEGs, and selected the top eight important DEGs for model construction according to the variable importance ranking, with a Gini index > 1.0 (Figures 6A, B). Figure 6C visually showed the expression levels of these eight key genes in COVID-19 and normal samples. Next, based on eight key signatures, a disease diagnostic model for COVID-19 was constructed in the training set, with an AUC = 0.998 (Figures 6D, E). In addition, the GSE196822 dataset was used as a validation cohort to further assess the performance of this ANN model and found that it performed well in the validation set (Figure 6F). The above diagnostic model has a good discriminatory ability for COVID-19 and hopes to be applied in clinical practice to assist the clinical diagnosis of COVID-19. Furthermore, a nomogram for COVID-19 disease risk assessment was successfully established by using the above eight key signatures for easier use (Figure 6G). Then, the accuracy of this nomogram was preliminarily assessed using the calibration curve, and the results showed that the Bias-corrected curve coincided well with the Ideal curve (Figure 6H). Furthermore, both the DCA curve and clinical impact curve (Figures 6I, J) indicated that the risk model had good performance ability. Specifically, it can be seen from the above figure that the model can achieve a higher net benefit rate at a threshold around 0.6.

## Construction of regulatory networks at transcriptional level

To identify substantial changes happening at the transcriptional level and get insights into the common DEGs, a network-based approach was employed to decode the regulatory TFs and miRNAs. The DEG-TFs interactions network was identified by using TarBase and miRTarBase bases and displayed in Figure 7. Circles represented common DEGs, while diamonds were TFs. The size of the circular or rhombus node depends on the degree of the node. The degree of a node is the number of connections the node has with other nodes in the network. Nodes with a higher degree are considered as important hubs of the network. From the Figure 7, *FCGR1B*, *BCL6*, *CD1D*, *MS4A4A* and *LTF* were more among more highly expressed DEGs as these genes have a higher degree in the TF-gene interactions network. TFs such as *FOXC1*, *YY1*, *GATA2*, *PPARG* and *FOXL1* were more significant than others as presented in the same figure. Again, the Figure 8 represented the interactions of miRNAs regulators with common DEGs. In the Figure 8, red squares represented miRNA s, while blue circles represented DEGs. Our results showed that *SOC3*, *BCL6*, *CXCR4*, and *TNFSF13B* were the hub genes of this network, with the five genes most involved in miRNAs. Besides, the significant hub miRNAs were detected from the miRNAs-gene interaction network, namely *hsa-mir-27a-3p*, *hsa-mir-26a-5p*, *hsa-mir-124-3p*, *hsa-mir-146a-5p* and *hsa-mir-20a-5p*.

## Identification of disease association

The circumstances in which different diseases can be correlated or associated are that they must usually have one or more similar genes (21). Therapeutic design strategies for disorders begin with deciphering the relationship between genes and disease (40). From the analysis of the gene-disease association base on the DisGeNET platform, it was noticed that liver Cirrhosis, rheumatoid arthritis, hypertensive disease, allergic contact dermatitis, lupus erythematosus systemic, anemia, hypersensitivity and Influenza were most coordinated to our reported hub genes, and even in COVID-19 (Figure 9). Interestingly, the study results suggested that most of the diseases mentioned above were related to inflammation or immune response in the body. The gene-disease association suggests that certain diseases may have the same molecular mechanism in progression, which has implications for our development of new therapeutic strategies for COVID-19.

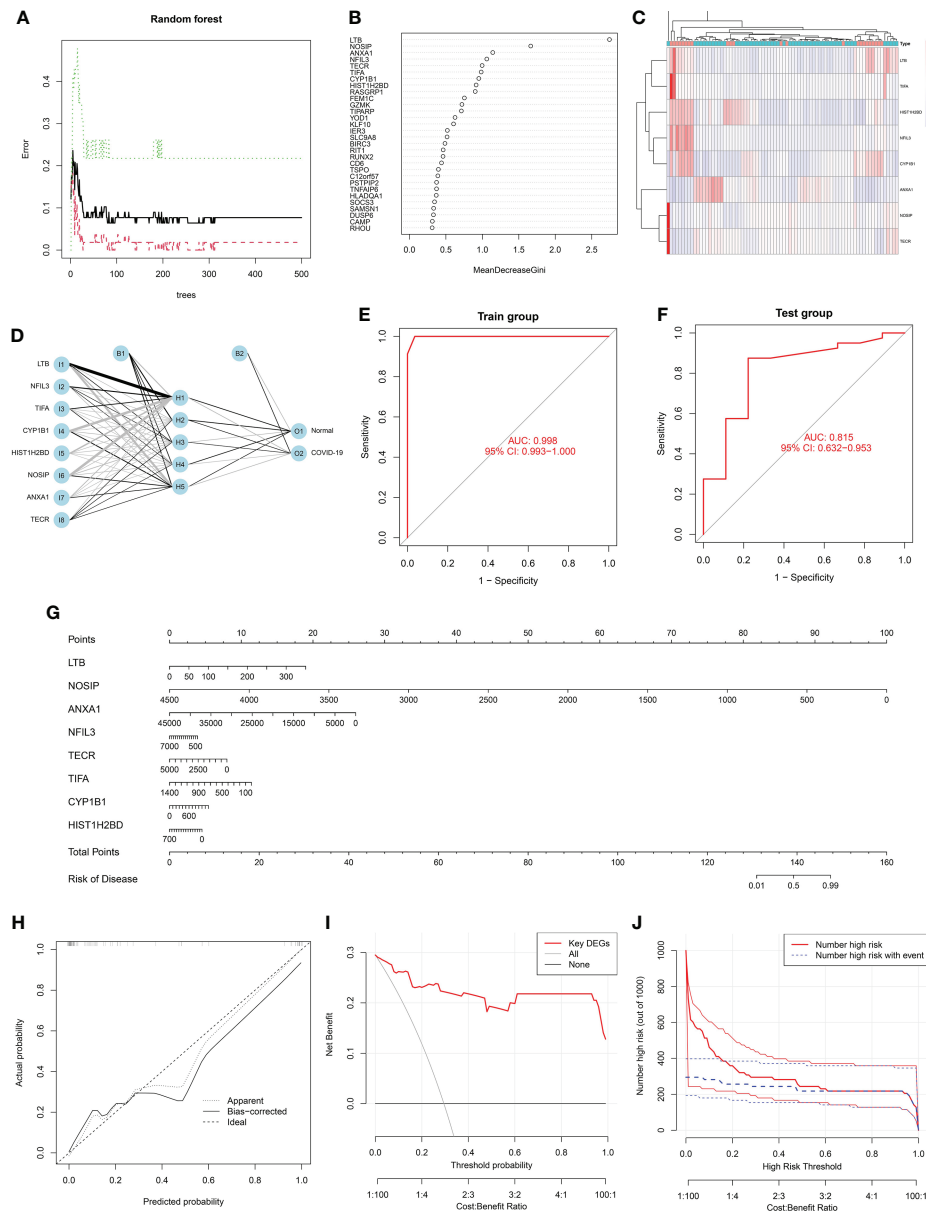


FIGURE 6

Screening feature genes from common differentially expressed genes (DEGs) using random forest (RF): (A) The random forest trees; (B) The importance rankings of features. (C) Heatmap shows the clustering analysis results for feature genes in COVID-19. Red represented up-regulated genes and blue represented down-regulated genes. (D) Graph represents the disease diagnosis model constructed by artificial neural network (ANN). Receiver operating characteristic (ROC) curve analysis of the model's performance for (E) training set and (F) validation set, respectively. (G) A constructed nomogram for risk prediction of COVID-19. (H) The calibration curve, (I) decision curve analysis (DCA) curve and (J) clinical impact curve for assessing the nomogram's performance.

## Identification of candidate drugs and target–chemical interaction in COVID-19

A chemical–protein interaction network is an important research tool for understanding the function of proteins, which is helpful for advancing drug discovery (29). In the aspects of common DEGs as potential drug targets in COVID-

19 and sepsis, the candidate drugs were identified by using Enrichr based on transcriptome signatures from the DSigDB database. The top 10 drug molecules selected based on p-value were considered as potential compounds that could be used for COVID-19 treatment and subsequent analysis. These 10 possible drug molecules included cephaline, mebendazole, tretinoin, progesterone, emetine, digitoxigenin, trichostatin A,

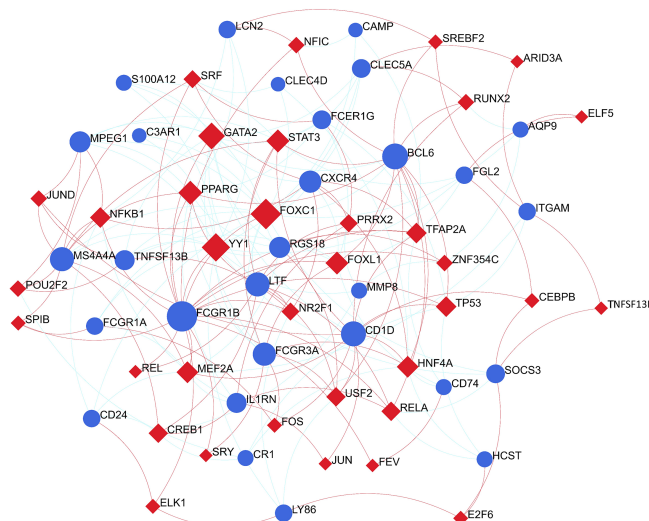


**FIGURE 7**  
The construction of an interconnected regulatory interaction network for DEG-TFs. In this figure, circles represent common differentially expressed genes (DEGs), while diamonds are transcription factors (TFs).

piperlongumine, terfenadine and strophanthidin (Table 1). These potential drugs were recommended for use in the common DEGs, which was a common compound for the treatment of two diseases.

Furthermore, molecular docking was implemented to predict the binding mode of these 10 potential compounds

with five different targets from COVID-19, including ACE2, 3CLpro, M<sup>Pro</sup>, PLpro and RdRp. It is generally believed that the lower the stabilization energy of ligand binding to the receptor, the greater the possibility of action, and the binding energy in screening criteria was changed to  $\leq -5.0$  kcal/mol (-20 kJ/mol) in this study. The results of molecular docking analysis were shown

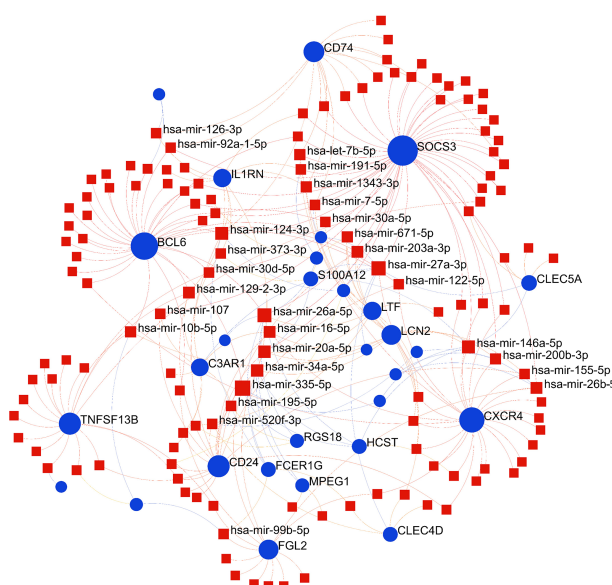


**FIGURE 8**  
The construction of an interconnected regulatory interaction network for DEGs-miRNAs. In this figure, square nodes indicate miRNAs and circle nodes represent common differentially expressed genes (DEGs).



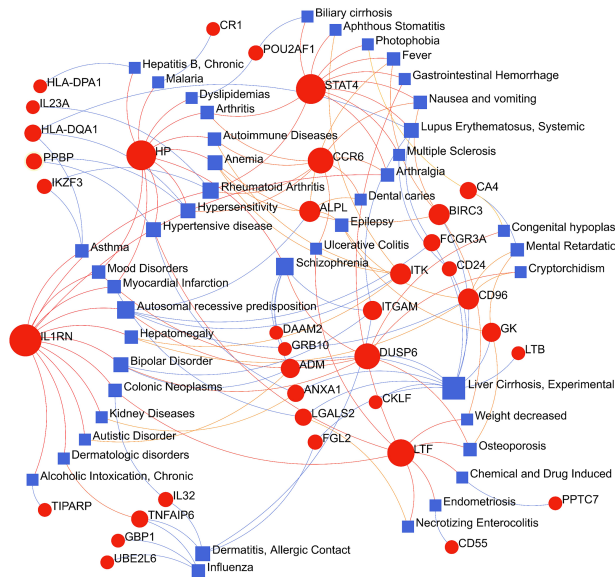


**FIGURE 9**  
The gene-disease association network represents diseases associated with common differentially expressed genes (DEGs). The disorder is depicted by the square node and also its subsequent DEGs are defined by the circle node.

in Table 2, and the binding energy of most compounds met the criteria. Figure 10 demonstrated the binding differences of the top 3 potential compounds that bind to these 5 COVID-19 targets. The bioactive compounds, progesterone, emetine, and digitoxigenin, were the most promising compounds on ACE2, and emetine, progesterone and cephaeline were the most active on 3CLpro. For the main protease ( $M^{Pro}$ ), the most promising compounds included progesterone, cephaeline and emetine. Besides, the most potential compounds binding to PLpro were progesterone, cephaeline and terfenadine, while progesterone, emetine and tretinoin were the most active on RdRp. Interestingly, emetine was found to have lower stabilization energy at binding sites to four targets (ACE2, 3CLpro,  $M^{Pro}$ , and RdRp), while progesterone could stably bind to all COVID-19 targets, with all binding energy  $\leq -6.5$  kcal/mol. Therefore,

these two drugs may be the most potential compounds for the treatment of COVID-19, and further studies on the pharmacological effects of these two compounds are needed.

## Discussion

From the COVID-19 pandemic to the present, research on COVID-19 has become more and more in-depth, and it has been found that COVID-19 has many unique characteristics, and many manifestations are very similar to sepsis (47). For example, both cytokines and chemokines are elevated in the serum of severe COVID-19 patients, and similar manifestations are seen in sepsis patients. Severely ill COVID-19 patients have clinical manifestations of shock without hypotension. At the same time, a hypercoagulable state is present in both diseases. At present, many pathological studies believe that sepsis is caused by the imbalance between the body's pro-inflammatory response and anti-inflammatory response (48). According to some scholars, treating COVID-19 as viral sepsis, using effective antiviral therapy for patients, regulating innate and adaptive immune responses, and limiting their damage to tissues will help improve the treatment outcome (7). The focus of this study is to explore the correlation between COVID-19 and sepsis, and to explore the common mechanisms that may be involved between the two, so as to provide a theoretical basis for the classification and treatment of COVID-19.

The enrichment analysis of pathways and functions helps us to understand the regulatory effects and specific mechanisms of

TABLE 1 Candidate drugs (top ten) identified from gene–drug interaction enrichment analysis.

Name	Adjusted P-value	Chemical Formula
cephaeline	4.94E-10	C <sub>28</sub> H <sub>38</sub> N <sub>2</sub> O <sub>4</sub>
mebendazole	9.95E-10	C <sub>16</sub> H <sub>13</sub> N <sub>3</sub> O <sub>3</sub>
tretinoin	1.64E-09	C <sub>20</sub> H <sub>28</sub> O <sub>2</sub>
progesterone	8.06E-09	C <sub>21</sub> H <sub>30</sub> O <sub>2</sub>
emetine	8.28E-09	C <sub>29</sub> H <sub>40</sub> N <sub>2</sub> O <sub>4</sub>
digitoxigenin	2.71E-06	C <sub>23</sub> H <sub>34</sub> O <sub>4</sub>
trichostatin A	2.71E-06	C <sub>17</sub> H <sub>22</sub> N <sub>2</sub> O <sub>3</sub>
piperlongumine	3.62E-06	C <sub>17</sub> H <sub>19</sub> NO <sub>5</sub>
terfenadine	7.43E-06	C <sub>32</sub> H <sub>41</sub> NO <sub>2</sub>
strophanthidin	1.67E-05	C <sub>23</sub> H <sub>32</sub> O <sub>6</sub>

**TABLE 2** The binding sites and energies for key drug targets of COVID-19 were evaluated through AutoDock calculations.

Drug targets	Amino acid	Binding energy
<b>ACE2</b>		
cephaeline	ALA-348, ASP-350	-7.40
mebendazole	TYR-158, SER-254	-4.52
tretinoin	UNK-914, UNK-915, UNK-916, UNK-917	-5.90
progesterone	TYR-158	-8.08
emetine	GLU-140, GLU-150	-7.97
digitoxigenin	UNK-920, UNK-922	-7.48
trichostatin A	ASP-350, ARG-393, LYS-562	-4.51
piperlongumine	ASN-210	-5.28
terfenadine	GLU-564	-6.43
strophanthidin	SER-170, UNK-951	-5.13
<b>3CLpro</b>		
cephaeline	PRO-108, ASP-245	-6.59
mebendazole	GLU-166, PRO-168	-3.80
tretinoin	LYS-97	-6.01
progesterone	LYS-236, LEU-287	-7.00
emetine	PRO-108, ASP-245	-7.02
digitoxigenin	LYS-137, LEU-272, LEU-287	-6.55
trichostatin A	LYS-97, ASN-119, GLY-120	-3.79
piperlongumine	GLU-166, PRO-168	-5.45
terfenadine	ASP-33	-5.41
strophanthidin	LYS-137, LEU-287	-5.06
<b>M<sup>Pro</sup></b>		
cephaeline	ALA-115, GLU-49, ASP-241	-7.15
mebendazole	ALA-189, ASP-191	-4.86
tretinoin	SER-253	-6.60
progesterone	ARG-251	-7.52
emetine	GLU-20	-7.05
digitoxigenin	ALA-115	-6.17
trichostatin A	GLY-215, GLN-224	-3.38
piperlongumine	ASP-241	-4.90
terfenadine	GLU-20	-5.87
strophanthidin	GLY-93	-5.58
<b>PLpro</b>		
cephaeline	HIS-163, GLU-166, GLN-189	-7.22
mebendazole	TYR-239, MET-276, GLY-278, ALA-285	-4.94
tretinoin	LYS-97	-5.87
progesterone	GLU-166	-7.57
emetine	GLY-120	-6.45
digitoxigenin	ASN-142, GLU-166	-6.96
trichostatin A	ARG-298, GLN-299	-4.24
piperlongumine	THR-26, GLY-143	-4.93
terfenadine	GLU-166, LEU-141, SER-144	-7.03
strophanthidin	GLU-240, HIS-246	-5.71
<b>RdRp</b>		
cephaeline	ASP-284, ASP-291	-6.06

(Continued)

**TABLE 2** Continued

Drug targets	Amino acid	Binding energy
mebendazole	THR-141	-3.69
tretinoin	LYS-391	-6.56
progesterone	SER-709	-7.36
emetine	LYS-288, ASP-291	-7.20
digitoxigenin	ILE-266, THR-319	-6.42
trichostatin A	ASP-336	-3.05
piperlongumine	LYS-603	-3.56
terfenadine	SER-709	-4.24
strophanthidin	ASP-284, ASP-291, GLN-292, TYR-294	-3.05

genes on the body. In this study, firstly, the 151 common DEGs were obtained by expression profile differential analysis and VENN analysis, then functional enrichment analysis was performed on them. The results of enrichment analysis showed that these DEGs were mainly enriched in infection and inflammation-related pathways and functions, such as Cytokine-cytokine receptor interaction pathway and NF-kappa B signaling pathway. Cytokines play critical roles in the pathogenesis of COVID-19 and sepsis. Much evidence suggests that cytokine storm is associated with the severity of COVID-19 patients and is a key factor in the death of COVID-19 patients (49). Studies have shown that bacteria-related molecules are recognized by Toll-like receptors of body cells and will cause a series of intracellular signaling pathways, which together activate nuclear factor  $\kappa$ -light-chain-enhancer of activated B cell (NF- $\kappa$ B), eventually leading to the expression of pro-inflammatory mediators (cytokines, chemokines, oxygen free radicals) (50). In the bioinformatics analysis of COVID-19, studies have also shown that the genes related to COVID-19 and herpes zoster are also involved in the Cytokine-cytokine receptor interaction pathway and the IL-17 signaling pathway (51). The pathway analysis results presented that these common DEGs were enriched in pathway associated with bacterial infections, staphylococcus aureus infection. Studies have shown that Staphylococcus aureus bacteremia is associated with high mortality in hospitalized patients with COVID-19 (52). In addition, these common DEGs may also be involved in certain chronic inflammatory diseases, such as Inflammatory bowel disease (IBD). Interestingly, some studies have also found that ACE2 is up-regulated in the inflamed intestinal mucosa of IBD patients, indicating that IBD patients are theoretically more susceptible to COVID-19 infection (53). However, in clinical studies, there is no data showing that the IBD population is more susceptible to COVID-19 infection, so further research is needed to determine the correlation between the two (54).

In this study, GO terms of CC indicate that these common DEGs also involve a variety of intracellular granule formation- and secretion-related pathways, including example, tertiary

granule, specific granule, cytoplasmic granule lumen and cytoplasmic vesicle lumen, which have all been shown to be closely related to the function of neutrophils. It has been shown that neutrophils also play an important role in COVID-19, and their main function is phagocytosis of pathogens and debris (55). Barnes found extensive neutrophil infiltration in the pulmonary capillaries of a COVID-19 patient (56). In addition, the neutrophil-to-lymphocyte ratio (NLR) is increased in patients with COVID-19, and the neutrophil count and NLR are also the highest in critically ill patients admitted to the ICU (57). Importantly, the number and activation of neutrophils correlates with the severity of the disease (58). Furthermore, current evidence suggests that immunopathology resulting from neutrophil dysfunction is one of the important mechanisms in the pathogenesis of COVID-19 (58, 59). Typically, neutrophils can suppress and inactivate viruses through specific immune effects (release of NETs) (60, 61). Specifically, neutrophils can construct a complex network of DNA and proteins, neutrophil extracellular traps (NETs), which is a release of histone-encapsulated nucleic acid networks that retain viral particles (62). Granules, in addition to being associated with neutrophil differentiation and maturation, can also be released upon cell death and is associated with NETs (63, 64). Notably, granules embedded in NETs has been reported to have a critical pathological role in atherosclerosis, thrombosis, or tumor development (43). Data showed that circulating neutrophils exhibited an activated phenotype in COVID-19 cases and molecules associated with NETs were significantly upregulated in severe COVID-19 cases (58). In addition, Skendros discovered that complement activation enhances the platelet/NET/tissue factor/thrombin axis in COVID-19 patients (65). Nicolai noted that fibrin- and platelet-related NETs are contained in inflammatory microvascular thrombi in the kidneys, lungs, and hearts of COVID-19 patients (66). These suggest that we can disrupt the vicious cycle of thrombosis/thrombotic inflammation in COVID-19 patients by activating neutrophils and promoting the formation of NETs.

Based on the results of PPI network and hub gene extraction, *ITGAM* interacts with other genes to the strongest extent, and is probably the most important gene between COVID-19 and sepsis. In studies on COVID-19 and Guillain-Barré syndrome, it was also found that *ITGAM* is an important factor in the gene regulatory network associated with the two diseases (67). *ITGAM* is a protective factor expressed during inflammatory injury. Some studies have found that in patients with COVID-19, the expression of *ITGAM* in females is lower than that in males, indicating that different genders have different mechanisms for regulating inflammation (68). The integrin CD11b encoded by *ITGAM* is expressed on the surface of macrophages and is involved in adhesion, migration and cell-mediated

cytotoxicity (69). Studies have found that CD11b can mediate thrombus formation in COVID-19, so *ITGAM* plays an important role in thrombus formation in COVID-19 patients (70). Another study found that *ITGAM* also plays an important role in methicillin-resistant *Staphylococcus aureus* (MRSA)-induced sepsis. After mice were infected with MRSA, the mortality rate of *ITGAM* knockout mice was significantly higher than that of control mice (69). In a scoring system established with *ITGAM* and two other immune genes, patients with low-risk scores showed better response to immune checkpoint therapy (71). Our analysis also found significant differences in the degree of certain immune cell infiltration and immune checkpoint expression levels between COVID-19 patients with high and low *ITGAM* expression. Furthermore, our study suggested that *ITGAM* was significantly associated with some immune cells (NK cells, activated NK cells and Eosinophils) and many immune checkpoints. This also suggests that we can genotype patients with COVID-19 or patients with sepsis secondary to COVID-19 to explore which type of patients is more effective for immune checkpoint therapy.

In order to understand how common DEGs regulate COVID-19 (or sepsis) at the transcriptional level, the interactions among TFs, miRNAs and genes were investigated *via* web tools. Our results showed that the regulatory relationship between TFs (FOXC1, YY1, GATA2, PPARG and FOXL1) and genes (FCGR1B, BCL6, CD1D, MS4A4A and LTF), as well as miRNAs (hsa-mir-27a-3p, hsa-mir-26a-5p, hsa-mir-124-3p, hsa-mir-146a-5p and hsa-mir-20a-5p) and genes (SOCS3, BCL6, CXCR4, and *TNFSF13B*) that may play important roles in COVID-19 and sepsis. In previous bioinformatics analysis, Ahmed (72) and Islam et al. (73) both found that FOXC1, YY1, GATA2, and FOXL1 are important TFs for COVID-19. Some network pharmacology studies (74, 75) also found that PPARG may be a key therapeutic target for COVID-19. In addition, hsa-mir-27a-3p may be related to the malignant biological behavior of glioma cells (76), and may also be an important molecular feature in esophageal cancer (77). In the serum of lactating mothers with type 1 diabetes, hsa-mir-26a-5p was upregulated and was shown to be significantly associated with inflammatory responses and cytokine- and chemokine-mediated signaling pathways (78). Hsa-mir-124-3p and hsa-mir-20a-5p were also considered as potential therapeutic targets for COVID-19 in previous bioinformatics analysis (79–82). Although many previous studies have suggested that these TFs and miRNAs may have important therapeutic effects, these analytical results require further experiments to confirm their validity and authenticity.

Based on common DEGs, a gene-disease relationship network was established to understand the correlation between these genes and diseases, and these results can inspire us to develop potential drugs to treat COVID-19

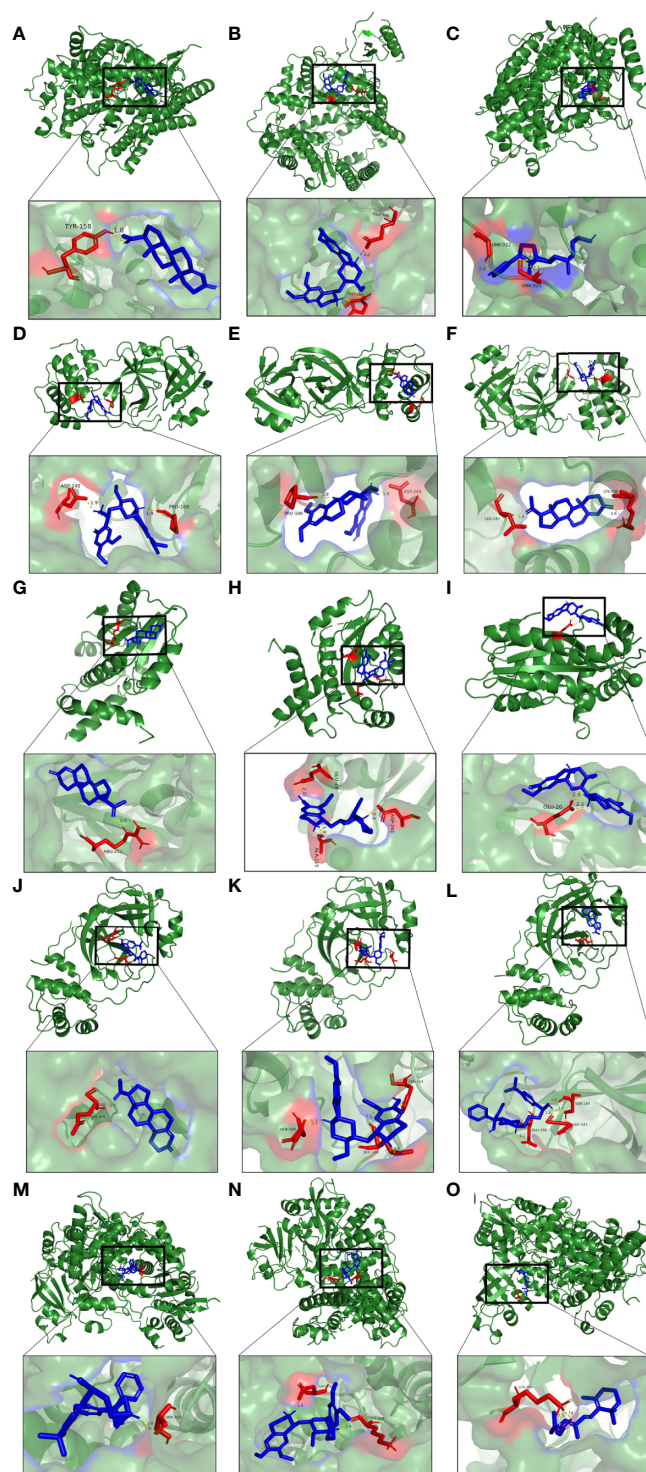


FIGURE 10

Molecular docking patterns for (A) progesterone, (B) emetine, (C) digitoxigenin with the ACE2, respectively. Molecular docking patterns for (D) emetine, (E) progesterone, (F) cephaeline with the 3CLpro, respectively. Molecular docking patterns for (G) progesterone, (H) cephaeline, (I) emetine with the M<sup>pro</sup>, respectively. Molecular docking patterns for (J) progesterone, (K) cephaeline, (L) terfenadine with the PLpro, respectively. Molecular docking patterns for (M) progesterone, (N) emetine, (O) tretinoin with the RdRp respectively.



with reference to the occurrence, development and treatment of these diseases. Diseases enriched by these DEGs include: liver Cirrhosis, rheumatoid arthritis, lupus erythematosus systemic and other immune and inflammation-related diseases. Recent studies have found that approximately one-third of patients with cirrhosis die within 10 days of being diagnosed with COVID-19, and two-thirds of patients with cirrhosis die before admission to the intensive care unit due to pulmonary insufficiency (83). In patients with rheumatoid arthritis, older age and comorbidities are risk factors for severe COVID-19. Glucocorticoids, appear to increase the worsening of COVID-19 outcomes (84). COVID-19 shares similarities with autoimmune diseases in clinical manifestations, immune responses, and pathogenic mechanisms. Both cause organ damage due to an excessive immune response. Autoantibodies that are hallmarks of autoimmune disease can also be detected in COVID-19 patients. Meanwhile, some COVID-19 patients have been reported to have secondary autoimmune diseases, such as Guillain-Barré syndrome or systemic lupus erythematosus (85). It appears that there are some similarities between these two diseases in terms of pathogenesis, which means that COVID-19 can be studied from this perspective.

Our drug prediction and molecular docking results suggest that emetine and progesterone can bind to multiple key targets of COVID-19 and may become new potential therapeutic drugs. Emetine is an isoquinoline alkaloid that is highly enriched in the lungs, and it has been found to have a certain inhibitory effect on the novel coronavirus in the *in vitro* environment. A real-world study showed that low-dose emetine combined with conventional antiviral drugs improved symptoms in patients with COVID-19 (86). There are also studies showing that the synergy between remdesivir and emetine can inhibit viral growth (87). Studies have found that emetine not only has a certain antiviral effect, but also can reduce the inflammatory response of patients by inhibiting the activity of NF- $\kappa$ B through I $\kappa$ B $\alpha$  phosphorylation, and can also reduce pulmonary hypertension by regulating various cellular processes (88). Progesterone is a sex hormone, and it also has some anti-inflammatory properties. When the novel coronavirus is infected, it can help the body control blood pressure, inhibit the formation of blood clots, and inhibit the growth of the virus. It can also regulate the body's immune response (89).

## Conclusions

The transcriptome data of COVID-19 and sepsis versus normal controls was downloaded from public databases and then used to find DEGs for both diseases, respectively. The top 30 hub genes were screened from 151 shared DEGs. Based on

these 151 DEGs, KEGG pathways and GO functions commonly involved in both diseases were explored. The results showed that they were mainly involved in infection and immune-related pathways and functions. To understand the interactions between common genes, the PPI network was delineated to show how these 151 DEGs interacted. Based on the results of hub gene extraction, ITGAM is considered to have the highest degree of interaction with other genes, and it may be potentially the most critical gene in both diseases. In order to verify our conjecture, the functional annotation and immune analysis were performed of ITGAM-related genes, and results showed that it does play a key role in immune regulation. The related genes are involved in immune-related pathways such as cytokines, anti-host transplantation disease, and infection. At the same time, it is also related to the infiltration degree of NK cells and eosinophils. In addition, there are 16 immune checkpoints associated with them, which are potential targets for the treatment of novel coronavirus and sepsis. Then these DEGs were used for screening out 8 key genes to establish an artificial neural network prediction model for COVID-19, and its AUC was as high as 0.998, indicating that the model performed very well. At the same time, a nomogram was built to predict the risk of COVID-19. To understand the role of these DEGs at the transcriptional level, TF-gene interaction network and miRNA-gene interaction network for DEGs were established to discover key TFs and miRNAs. Then the diseases most related to these DEGs were learned, mainly immune-related diseases, which suggests that we can mine effective information related to the treatment of novel coronavirus from the perspective of the development of these diseases.

## Data availability statement

Publicly available datasets were analyzed in this study. The data could be download from the GEO database of the National Center for Biotechnology Information (NCBI) (<https://www.ncbi.nlm.nih.gov/geo/>), accession numbers GSE147507, GSE65682 and GSE196822.

## Author contributions

FX-L conceived and designed the study. LL and LP-L provided equal contributions to research design, data analysis and article writing. RG revised the manuscript. HD, YR-S and XH-Z helped to write the manuscript. All authors contributed to the article and approved the submitted version.

## Funding

This work was supported by the Natural Science Foundation of Hunan Province (No. 2020JJ4840) and the Postgraduate



Research and Innovation Project of Central South University (No. 2021zzts1093).

## Acknowledgments

The authors would like to acknowledge the GEO database for providing their platforms and those contributors for uploading their valuable datasets.

## Conflict of interest

The authors declare that the research was conducted in the absence of any commercial or financial relationships that could be construed as a potential conflict of interest.

## References

- Pollard CA, Morran MP, Nestor-Kalinoski AL. The COVID-19 pandemic: a global health crisis. *Physiol Genomics* (2020) 52:549–57. doi: 10.1152/physiolgenomics.00089.2020
- Long B, Carius BM, Chavez S, Liang SY, Brady WJ, Koefman A, et al. Clinical update on COVID-19 for the emergency clinician: Presentation and evaluation. *Am J Emerg Med* (2022) 54:46–57. doi: 10.1016/j.ajem.2022.01.028
- Lopez-Collazo E, Avendano-Ortiz J, Martin-Quiros A, Aguirre LA. Immune response and COVID-19: A mirror image of sepsis. *Int J Biol Sci* (2020) 16:2479–89. doi: 10.7150/ijbs.48400
- Remy KE, Brakenridge SC, Francois B, Daix T, Deutschman CS, Monneret G, et al. Immunotherapies for COVID-19: lessons learned from sepsis. *Lancet Respir Med* (2020) 8:946–49. doi: 10.1016/S2213-2600(20)30217-4
- Chen L, Huang Q, Zhao T, Sui L, Wang S, Xiao Z, et al. Nanotherapies for sepsis by regulating inflammatory signals and reactive oxygen and nitrogen species: New insight for treating COVID-19. *Redox Biol* (2021) 45:102046. doi: 10.1016/j.redox.2021.102046
- Yao XH, Luo T, Shi Y, He ZC, Tang R, Zhang PP, et al. A cohort autopsy study defines COVID-19 systemic pathogenesis. *Cell Res* (2021) 31:836–46. doi: 10.1038/s41422-021-00523-8
- Li H, Liu L, Zhang D, Xu J, Dai H, Tang N, et al. SARS-CoV-2 and viral sepsis: observations and hypotheses. *Lancet* (2020) 395:1517–20. doi: 10.1016/S0140-6736(20)30920-X
- Alhazzani, Moller, Arabi, Loeb, Gong, Fan, et al. Surviving Sepsis Campaign: guidelines on the management of critically ill adults with Coronavirus Disease 2019 (COVID-19). *Intensive Care Med* (2020) 46:854–87. doi: 10.1007/s00134-020-06022-5
- Crunkhorn S. A new route to sepsis therapy. *Nat Rev Drug Discovery* (2019) 8:d41573-019-00034-7. doi: 10.1038/d41573-019-00034-7
- Cecconi M, Evans L, Levy M, Rhodes A. Sepsis and septic shock. *Lancet* (2018) 392:75–87. doi: 10.1016/S0140-6736(18)30696-2
- Toledo AG, Golden G, Campos AR, Cuello H, Sorrentino J, Lewis N, et al. Proteomic atlas of organ vasculopathies triggered by staphylococcus aureus sepsis. *Nat Commun* (2019) 10:4656. doi: 10.1038/s41467-019-12672-x
- Olwal CO, Nganyewo NN, Tapela K, Djomkam Zune AL, Owoicho O, Bediako Y, et al. Parallels in sepsis and COVID-19 conditions: Implications for managing severe COVID-19. *Front Immunol* (2021) 12:602848. doi: 10.3389/fimmu.2021.602848
- Singer M, Deutschman CS, Seymour CW, Shankar-Hari M, Annane D, Bauer M, et al. The third international consensus definitions for sepsis and septic shock (sepsis-3). *JAMA* (2016) 315:801–10. doi: 10.1001/jama.2016.0287
- Wiersinga WJ, Rhodes A, Cheng A, Peacock SJ, Prescott HC. Pathophysiology, transmission, diagnosis, and treatment of coronavirus disease 2019 (covid-19): a review. *JAMA* (2020) 324:782–93. doi: 10.1001/jama.2020.12839
- Ma L, Li H, Lan J, Hao X, Liu H, Wang X, et al. Comprehensive analyses of bioinformatics applications in the fight against COVID-19 pandemic. *Comput Biol Chem* (2021) 95:107599. doi: 10.1016/j.compbiolchem.2021.107599
- MacEachern SJ, Forkert ND. Machine learning for precision medicine. *Genome* (2021) 64:416–25. doi: 10.1139/gen-2020-0131
- Barrett T, Wilhite SE, Ledoux P, Evangelista C, Kim IF, Tomashevsky M, et al. NCBI GEO: archive for functional genomics data sets—update. *Nucleic Acids Res* (2013) 41:D991–5. doi: 10.1093/nar/gks1193
- Blanco-Melo D, Nilsson-Payant BE, Liu WC, Uhl S, Hoagland D, Moller R, et al. Imbalanced host response to SARS-CoV-2 drives development of COVID-19. *Cell* (2020) 181:1036–45 e9. doi: 10.1016/j.cell.2020.04.026
- Zhang Z, Chen L, Xu P, Xing L, Hong Y, Chen P. Gene correlation network analysis to identify regulatory factors in sepsis. *J Transl Med* (2020) 18:381. doi: 10.1186/s12967-020-02561-z
- Synowiec A, Szczepanski A, Barreto-Duran E, Lie LK, Pyrc K. Severe acute respiratory syndrome coronavirus 2 (SARS-CoV-2): a systemic infection. *Clin Microbiol Rev* (2021) 34:e00133-20. doi: 10.1128/CMR.00133-20
- Mahmud SMH, Al-Mustanjid MD, Akter F, Rahman MDS, Ahmed K, Rahman MDH, et al. Bioinformatics and system biology approach to identify the influences of SARS-CoV-2 infections to idiopathic pulmonary fibrosis and chronic obstructive pulmonary disease patients. *Brief Bioinform* (2021) 22:bbab115. doi: 10.1093/bib/bbab115
- Bardou P, Mariette J, Escudie F, Djemiel C, Klopp C. Jvenn: an interactive Venn diagram viewer. *BMC Bioinf* (2014) 15:293. doi: 10.1186/1471-2105-15-293
- Kanehisa M, Goto S. KEGG: kyoto encyclopedia of genes and genomes. *Nucleic Acids Res* (2000) 28:27–30. doi: 10.1093/nar/28.1.27
- Gene Ontology Consortium. Gene Ontology Consortium: going forward. *Nucleic Acids Res* (2015) 43:D1049–56. doi: 10.1093/nar/gku1179
- Wang C, Liu H, Yang M, Bai Y, Ren H, Zou Y, et al. RNA-Seq based transcriptome analysis of endothelial differentiation of bone marrow mesenchymal stem cells. *Eur J Vasc Endovasc Surg* (2020) 59:834–42. doi: 10.1016/j.ejvs.2019.11.003
- Szklarczyk D, Gable AL, Nastou KC, Lyon D, Kirsch R, Pyysalo S, et al. The STRING database in 2021: customizable protein-protein networks, and functional characterization of user-uploaded gene/measurement sets. *Nucleic Acids Res* (2021) 49:D605–D12. doi: 10.1093/nar/gkaa1074
- Chin CH, Chen SH, Wu SH, Ho CW, Ko MT, Lin CY. cytoHubba: identifying hub objects and sub-networks from complex interactome. *BMC Syst Biol* (2014) 8 Suppl 4:S11. doi: 10.1186/1752-0509-8-S4-S11
- van Dam S, Vosa U, van der Graaf A, Franke L, de Magalhaes JP. Gene co-expression analysis for functional classification and gene-disease predictions. *Brief Bioinform* (2018) 19:575–92. doi: 10.1093/bib/bbw139

## Publisher's note

All claims expressed in this article are solely those of the authors and do not necessarily represent those of their affiliated organizations, or those of the publisher, the editors and the reviewers. Any product that may be evaluated in this article, or claim that may be made by its manufacturer, is not guaranteed or endorsed by the publisher.

## Supplementary material

The Supplementary Material for this article can be found online at: <https://www.frontiersin.org/articles/10.3389/fimmu.2022.975848/full#supplementary-material>

29. Xia J, Chen S, Li Y, Li H, Gan M, Wu J, et al. Immune response is key to genetic mechanisms of sars-cov-2 infection with psychiatric disorders based on differential gene expression pattern analysis. *Front Immunol* (2022) 13:798538. doi: 10.3389/fimmu.2022.798538
30. Bu D, Luo H, Huo P, Wang Z, Zhang S, He Z, et al. KOBAS-i: intelligent prioritization and exploratory visualization of biological functions for gene enrichment analysis. *Nucleic Acids Res* (2021) 49:W317–W25. doi: 10.1093/nar/gkab447
31. Newman AM, Liu CL, Green MR, Gentles AJ, Feng W, Xu Y, et al. Robust enumeration of cell subsets from tissue expression profiles. *Nat Methods* (2015) 12:453–7. doi: 10.1038/nmeth.3337
32. Wang Y, Xia ST, Tang Q, Wu J, Zhu X. A novel consistent random forest framework: Bernoulli random forests. *IEEE Trans Neural Netw Learn Syst* (2018) 29:3510–23. doi: 10.1109/TNNLS.2017.2729778
33. Azimi P, Mohammadi HR, Benzel EC, Shahzadi S, Azhari S, Montazeri A. Artificial neural networks in neurosurgery. *J Neurol Neurosurg Psychiatry* (2015) 86:251–6. doi: 10.1136/jnnp-2014-307807
34. Huang YT, Kangas LJ, Rasco BA. Applications of artificial neural networks (ANNs) in food science. *Crit Rev Food Sci Nutr* (2007) 47:113–26. doi: 10.1080/10408390600626453
35. Sethupathy P, Corda B, Hatzigeorgiou AG. TarBase: A comprehensive database of experimentally supported animal microRNA targets. *RNA* (2006) 12:192–7. doi: 10.1261/rna.2239606
36. Hsu SD, Lin FM, Wu WY, Liang C, Huang WC, Chan WL, et al. miRTarBase: a database curates experimentally validated microRNA-target interactions. *Nucleic Acids Res* (2011) 39:D163–9. doi: 10.1093/nar/gkq1107
37. Auwal MR, Rahman MR, Gov E, Shahjahan M, Moni MA. Bioinformatics and machine learning approach identifies potential drug targets and pathways in COVID-19. *Brief Bioinform* (2021) 22:bbab120. doi: 10.1093/bib/bbab120
38. Pinero P, Ramirez-Anguita JM, Sauch-Pitarch J, Ronzano F, Centeno E, Sanz F, et al. The DisGeNET knowledge platform for disease genomics: 2019 update. *Nucleic Acids Res* (2020) 48:D845–D55. doi: 10.1093/nar/gkz1021
39. Kuleshov MV, Jones MR, Rouillard AD, Fernandez NF, Duan Q, Wang Z, et al. Enrichr: a comprehensive gene set enrichment analysis web server 2016 update. *Nucleic Acids Res* (2016) 44:W90–7. doi: 10.1093/nar/gkw377
40. Hu H, Tang N, Zhang F, Li L, Li L. Bioinformatics and system biology approach to identify the influences of COVID-19 on rheumatoid arthritis. *Front Immunol* (2022) 13:860676. doi: 10.3389/fimmu.2022.860676
41. Pinzi P, Rastelli G. Molecular docking: Shifting paradigms in drug discovery. *Int J Mol Sci* (2019) 20:4331. doi: 10.3390/ijms20184331
42. Schultze JL, Aschenbrenner AC. COVID-19 and the human innate immune system. *Cell* (2021) 184:1671–92. doi: 10.1016/j.cell.2021.02.029
43. Cassatella MA, Ostberg NK, Tamassia N, Soehnlein O. Biological roles of neutrophil-derived granule proteins and cytokines. *Trends Immunol* (2019) 40:648–64. doi: 10.1016/j.it.2019.05.003
44. Segel GB, Halterman MW, Lichtman MA. The paradox of the neutrophil's role in tissue injury. *J Leukoc Biol* (2011) 89:359–72. doi: 10.1189/jlb.0910538
45. Chen B, Fan W, Liu J, Wu FX. Identifying protein complexes and functional modules—from static PPI networks to dynamic PPI networks. *Brief Bioinform* (2014) 15:177–94. doi: 10.1093/bib/bbt039
46. Zhou M, Wang X, Shi Y, Ding Y, Li X, Xie T, et al. Deficiency of ITGAM attenuates experimental abdominal aortic aneurysm in mice. *J Am Heart Assoc* (2021) 10:e019900. doi: 10.1161/JAHA.120.019900
47. Kocak Tufan Z, Kayaaslan B, Mer M. COVID-19 and sepsis. *Turk J Med Sci* (2021) 51:3301–11. doi: 10.3906/sag-2108-239
48. Rello J, Valenzuela-Sanchez F, Ruiz-Rodriguez M, Moyano S. Sepsis: A review of advances in management. *Adv Ther* (2017) 34:2393–411. doi: 10.1007/s12325-017-0622-8
49. Hu B, Huang S, Yin L. The cytokine storm and COVID-19. *J Med Virol* (2021) 93:250–56. doi: 10.1002/jmv.26232
50. Kumar V. Toll-like receptors in sepsis-associated cytokine storm and their endogenous negative regulators as future immunomodulatory targets. *Int Immunopharmacol* (2020) 89:107087. doi: 10.1016/j.intimp.2020.107087
51. Yu X, Li L, Chan MTV, Wu WKK. Bioinformatic analyses suggest augmented interleukin-17 signaling as the mechanism of COVID-19-associated herpes zoster. *Environ Sci Pollut Res Int* (2021) 28:65769–75. doi: 10.1007/s11356-021-15567-x
52. Cusumano JA, Dupper AC, Malik Y, Gavioli EM, Banga J, Berbel Caban A, et al. *Staphylococcus aureus* bacteremia in patients infected with COVID-19: A case series. *Forum Infect Dis* (2020) 7:ofaa518. doi: 10.1093/ofid/ofaa518
53. Monteleone G, Ardizzone S. Are patients with inflammatory bowel disease at increased risk for covid-19 infection? *J Crohns Colitis* (2020) 14:1334–36. doi: 10.1093/ecco-jcc/jjaa061
54. Sultan K, Mone A, Durbin L, Khuwaja S, Swaminath A. Review of inflammatory bowel disease and COVID-19. *World J Gastroenterol* (2020) 26:5534–42. doi: 10.3748/wjg.v26.i37.5534
55. Rosales C. Neutrophils at the crossroads of innate and adaptive immunity. *J Leukoc Biol* (2020) 108:377–96. doi: 10.1002/JLB.4MIR0220-574RR
56. Huang C, Wang Y, Li X, Ren L, Zhao J, Hu Y, et al. Clinical features of patients infected with 2019 novel coronavirus in wuhan, China. *Lancet* (2020) 395:497–506. doi: 10.1016/S0140-6736(20)30183-5
57. Sun S, Cai X, Wang H, He G, Lin Y, Lu B, et al. Abnormalities of peripheral blood system in patients with COVID-19 in wenzhou, China. *Clin Chim Acta* (2020) 507:174–80. doi: 10.1016/j.cca.2020.04.024
58. Masso-Silva JA, Moshensky A, Lam MTY, Odish MF, Patel A, Xu L, et al. Increased peripheral blood neutrophil activation phenotypes and neutrophil extracellular trap formation in critically ill coronavirus disease 2019 (COVID-19) patients: A case series and review of the literature. *Clin Infect Dis* (2022) 74:479–89. doi: 10.1093/cid/ciab437
59. Li CH, Chiou HY, Lin MH, Kuo CH, Lin YC, Lin YC, et al. Immunological map in COVID-19. *J Microbiol Immunol Infect* (2021) 54:547–56. doi: 10.1016/j.jmii.2021.04.006
60. Lamichhane PP, Samarasinghe AE. The role of innate leukocytes during influenza virus infection. *J Immunol Res* (2019) 2019:8028725. doi: 10.1155/2019/8028725
61. Barr FD, Ochsenbauer C, Wira CR, Rodriguez-Garcia M. Neutrophil extracellular traps prevent HIV infection in the female genital tract. *Mucosal Immunol* (2018) 11:1420–28. doi: 10.1038/s41385-018-0045-0
62. Jenne CN, Wong CHY, Zemp FJ, McDonald B, Rahman MM, Forsyth PA, et al. Neutrophils recruited to sites of infection protect from virus challenge by releasing neutrophil extracellular traps. *Cell Host Microbe* (2013) 13:169–80. doi: 10.1016/j.chom.2013.01.005
63. Lim CH, Adav SS, Sze SK, Choong YK, Saravanan R, Schmidtchen A. Thrombin and plasmin alter the proteome of neutrophil extracellular traps. *Front Immunol* (2018) 9:1554. doi: 10.3389/fimmu.2018.01554
64. Urban CF, Ermer D, Schmid M, Abu-Abed U, Goosmann C, Nacken W, et al. Neutrophil extracellular traps contain calprotectin, a cytosolic protein complex involved in host defense against candida albicans. *PLoS Pathog* (2009) 5:e1000639. doi: 10.1371/journal.ppat.1000639
65. Skendros P, Mitsios A, Chrysanthopoulou A, Mastellos DC, Metallidis S, Rafailidis P, et al. Complement and tissue factor-enriched neutrophil extracellular traps are key drivers in COVID-19 immunothrombosis. *J Clin Invest* (2020) 130:6151–57. doi: 10.1172/JCI141374
66. Nicolai L, Leunig A, Brambs S, Kaiser R, Weinberger T, Weigand M, et al. Immunothrombotic dysregulation in covid-19 pneumonia is associated with respiratory failure and coagulopathy. *Circulation* (2020) 142:1176–89. doi: 10.1161/CIRCULATIONAHA.120.048488
67. Li Z, Huang Z, Li X, Huang C, Shen J, Li S, et al. Bioinformatic analyses hinted at augmented T helper 17 cell differentiation and cytokine response as the central mechanism of COVID-19-associated Guillain-Barre syndrome. *Cell Prolif* (2021) 54:e13024. doi: 10.1111/cpr.13024
68. Freire PP, Marques AH, Baiocchi GC, Schimke LF, Fonseca DL, Salgado RC, et al. The relationship between cytokine and neutrophil gene network distinguishes SARS-CoV-2-infected patients by sex and age. *JCI Insight* (2021) 6:e147535. doi: 10.1172/jci.insight.147535
69. Sim H, Jeong D, Kim HY, Pak S, Thapa B, Kwon HJ, et al. CD11b deficiency exacerbates methicillin-resistant staphylococcus aureus-induced sepsis by upregulating inflammatory responses of macrophages. *Immune Netw* (2021) 21:e13. doi: 10.4110/in.2021.21.e13
70. Das D, Podder S. Unraveling the molecular crosstalk between atherosclerosis and COVID-19 comorbidity. *Comput Biol Med* (2021) 134:104459. doi: 10.1016/j.combiomed.2021.104459
71. Liang T, Chen J, Xu G, Zhang H, Xue J, Zeng H, et al. TYROBP, TLR4 and ITGAM regulated macrophages polarization and immune checkpoints expression in osteosarcoma. *Sci Rep* (2021) 11:19315. doi: 10.1038/s41598-021-98637-x
72. Ahmed FF, Reza MS, Sarker MS, Islam MS, Mosharaf MP, Hasan S, et al. Identification of host transcriptome-guided repurposable drugs for SARS-CoV-1 infections and their validation with SARS-CoV-2 infections by using the integrated bioinformatics approaches. *PLoS One* (2022) 17:e0266124. doi: 10.1371/journal.pone.0266124
73. Islam T, Rahman MR, Aydin B, Beklen H, Arga KY, Shahjahan M. Integrative transcriptomics analysis of lung epithelial cells and identification of repurposable drug candidates for COVID-19. *Eur J Pharmacol* (2020) 887:173594. doi: 10.1016/j.ejphar.2020.173594
74. Wang WX, Zhang YR, Luo SY, Zhang YS, Zhang Y, Tang C. Chlorogenic acid, a natural product as potential inhibitor of COVID-19: virtual screening experiment based on network pharmacology and molecular docking. *Nat Prod Res* (2022) 36:2580–84. doi: 10.1080/14786419.2021.1904923

75. Li H, You J, Yang X, Wei Y, Zheng L, Zhao Y, et al. Glycyrrhetic acid: A potential drug for the treatment of COVID-19 cytokine storm. *Phytomedicine* (2022) 102:154153. doi: 10.1016/j.phymed.2022.154153
76. Chen Q, Wang W, Wu Z, Chen S, Chen X, Zhuang S, et al. Over-expression of lncRNA TMEM161B-AS1 promotes the malignant biological behavior of glioma cells and the resistance to temozolomide via up-regulating the expression of multiple ferroptosis-related genes by sponging hsa-miR-27a-3p. *Cell Death Discovery* (2021) 7:311. doi: 10.1038/s41420-021-00709-4
77. Lu M, Li J, Fan X, Xie F, Fan J, Xiong Y. Novel immune-related ferroptosis signature in esophageal cancer: An informatics exploration of biological processes related to the TMEM161B-AS1/hsa-miR-27a-3p/GCH1 regulatory network. *Front Genet* (2022) 13:829384. doi: 10.3389/fgene.2022.829384
78. Frorup C, Mirza AH, Yarani R, Nielsen LB, Mathiesen ER, Damm P, et al. Plasma exosome-enriched extracellular vesicles from lactating mothers with type 1 diabetes contain aberrant levels of miRNAs during the postpartum period. *Front Immunol* (2021) 12:744509. doi: 10.3389/fimmu.2021.744509
79. Wicik Z, Eyileten C, Jakubik D, Simoes SN, Martins DC, Pavao R, et al. ACE2 interaction networks in COVID-19: A physiological framework for prediction of outcome in patients with cardiovascular risk factors. *J Clin Med* (2020) 9:3743. doi: 10.3390/jcm9113743
80. Prasad K, Alasmari AF, Ali N, Khan R, Alghamdi A, Kumar V. Insights into the SARS-CoV-2-Mediated alteration in the stress granule protein regulatory networks in humans. *Pathogens* (2021) 10:1459. doi: 10.3390/pathogens10111459
81. Li C, Hu X, Li L, Li JH. Differential microRNA expression in the peripheral blood from human patients with COVID-19. *J Clin Lab Anal* (2020) 34:e23590. doi: 10.1002/jcla.23590
82. Sardar R, Satish D, Gupta D. Identification of novel SARS-CoV-2 drug targets by host MicroRNAs and transcription factors Co-regulatory interaction network analysis. *Front Genet* (2020) 11:571274. doi: 10.3389/fgene.2020.571274
83. Sansoe G, Aragno M, Wong F. COVID-19 and liver cirrhosis: Focus on the nonclassical renin-angiotensin system and implications for therapy. *Hepatology* (2021) 74:1074–80. doi: 10.1002/hep.31728
84. D'Silva KM, Wallace ZS. COVID-19 and rheumatoid arthritis. *Curr Opin Rheumatol* (2021) 33:255–61. doi: 10.1097/BOR.0000000000000786
85. Liu Y, Sawalha AH, Lu Q. COVID-19 and autoimmune diseases. *Curr Opin Rheumatol* (2021) 33:155–62. doi: 10.1097/BOR.0000000000000776
86. Fan S, Zhen Q, Chen C, Wang W, Wu Q, Ma H, et al. Clinical efficacy of low-dose emetine for patients with COVID-19: a real-world study. *J BioX Res* (2021) 4:53–9. doi: 10.1097/JBR.0000000000000076
87. Choy KT, Wong AY, Kaewpreedee P, Sia SF, Chen K, Hui KPY, et al. Remdesivir, lopinavir, emetine, and homoharringtonine inhibit SARS-CoV-2 replication in vitro. *Antiviral Res* (2020) 178:104786. doi: 10.1016/j.antiviral.2020.104786
88. Valipour M. Different aspects of emetine's capabilities as a highly potent SARS-CoV-2 inhibitor against COVID-19. *ACS Pharmacol Transl Sci* (2022) 5:387–99. doi: 10.1021/acspstsci.2c00045
89. Shah SB. COVID-19 and progesterone: Part 1. SARS-CoV-2, progesterone and its potential clinical use. *Endocrine and Metabolic Science* (2021) 5:100109. doi: 10.1016/j.endmts.2021.100109



## OPEN ACCESS

## EDITED BY

Alfonso J. Rodríguez-Morales,  
Fundación Universitaria Autónoma de  
las Américas, Colombia

## REVIEWED BY

Stephen Rawlings,  
Maine Health, United States  
Andrea Gabriela Rodríguez Morales,  
CSR Salvador Allende, Chile

## \*CORRESPONDENCE

Daniel Kaufman  
dkaufman@mednet.ucla.edu  
Jide Tian  
jtian@mednet.ucla.edu

## SPECIALTY SECTION

This article was submitted to  
Viral Immunology,  
a section of the journal  
Frontiers in Immunology

RECEIVED 31 July 2022

ACCEPTED 07 October 2022

PUBLISHED 25 October 2022

## CITATION

Tian J, Dillion BJ, Henley J, Comai L  
and Kaufman DL (2022) A GABA-  
receptor agonist reduces pneumonitis  
severity, viral load, and death rate in  
SARS-CoV-2-infected mice.  
*Front. Immunol.* 13:1007955.  
doi: 10.3389/fimmu.2022.1007955

## COPYRIGHT

© 2022 Tian, Dillion, Henley, Comai and  
Kaufman. This is an open-access article  
distributed under the terms of the  
[Creative Commons Attribution License](#)  
(CC BY). The use, distribution or  
reproduction in other forums is  
permitted, provided the original  
author(s) and the copyright owner(s)  
are credited and that the original  
publication in this journal is cited, in  
accordance with accepted academic  
practice. No use, distribution or  
reproduction is permitted which does  
not comply with these terms.

# A GABA-receptor agonist reduces pneumonitis severity, viral load, and death rate in SARS-CoV-2-infected mice

Jide Tian<sup>1\*</sup>, Barbara J. Dillion<sup>2</sup>, Jill Henley<sup>3</sup>, Lucio Comai<sup>3</sup>  
and Daniel L. Kaufman<sup>1\*</sup>

<sup>1</sup>Department of Molecular and Medical Pharmacology, University of California, Los Angeles, CA, United States, <sup>2</sup>High Containment Program, University of California, Los Angeles, CA, United States, <sup>3</sup>Department of Molecular Microbiology and Immunology, Keck School of Medicine of the University of Southern California, Los Angeles, CA, United States

Gamma-aminobutyric acid (GABA) and GABA-receptors (GABA-Rs) form a major neurotransmitter system in the brain. GABA-Rs are also expressed by 1) cells of the innate and adaptive immune system and act to inhibit their inflammatory activities, and 2) lung epithelial cells and GABA-R agonists/potentiators have been observed to limit acute lung injuries. These biological properties suggest that GABA-R agonists may have potential for treating COVID-19. We previously reported that GABA-R agonist treatments protected mice from severe disease induced by infection with a lethal mouse coronavirus (MHV-1). Because MHV-1 targets different cellular receptors and is biologically distinct from SARS-CoV-2, we sought to test GABA therapy in K18-hACE2 mice which develop severe pneumonitis with high lethality following SARS-CoV-2 infection. We observed that GABA treatment initiated immediately after SARS-CoV-2 infection, or 2 days later near the peak of lung viral load, reduced pneumonitis severity and death rates in K18-hACE2 mice. GABA-treated mice had reduced lung viral loads and displayed shifts in their serum cytokine/chemokine levels that are associated with better outcomes in COVID-19 patients. Thus, GABA-R activation had multiple effects that are also desirable for the treatment of COVID-19. The protective effects of GABA against two very different beta coronaviruses (SARS-CoV-2 and MHV-1) suggest that it may provide a generalizable off-the-shelf therapy to help treat diseases induced by new SARS-CoV-2 variants and novel coronaviruses that evade immune responses and antiviral medications. GABA is inexpensive, safe for human use, and stable at room temperature, making it an attractive candidate for testing in clinical trials. We also discuss the potential of GABA-R agonists for limiting COVID-19-associated neuroinflammation.

## KEYWORDS

GABA, GABA-receptors, COVID-19, SARS-CoV-2, antiviral, long-covid, neuroinflammation, homotaurine



## Introduction

Despite the great success of vaccines to reduce serious illness due to COVID-19, this approach has limitations due to breakthrough infections, vaccine hesitancy, viral variants, and novel coronaviruses. Antiviral drugs can greatly help reduce the risk for severe disease and mortality due to COVID-19, however, these drugs may not become readily available in developing countries and they may be less effective against coronaviruses that emerge in the future. The identification of additional therapeutics that have established safety records, are inexpensive, and do not have special storage requirements could be especially helpful for reducing COVID-19-associated morbidity and mortality worldwide.

Gamma-aminobutyric acid type A receptors (GABA<sub>A</sub>-Rs) are a family of ligand-gated chloride channels which play key roles in neurodevelopment and neurotransmission in the central nervous system (CNS) (1–3). GABA<sub>A</sub>-Rs are also expressed by cells of the human and murine immune systems [e.g. (4–9)]. The activation of GABA<sub>A</sub>-Rs on innate immune system cells such as macrophages, dendritic, and natural killer (NK) cells reduces their inflammatory activities and shifts them toward anti-inflammatory phenotypes (7, 8, 10–17). Moreover, GABA<sub>A</sub>-R agonists inhibit the inflammatory activities of human and rodent Th17 and Th1 CD4<sup>+</sup> T cells and cytotoxic CD8<sup>+</sup> T cells (7, 18–22) while also promoting CD4<sup>+</sup> and CD8<sup>+</sup> Treg responses (18, 20, 23, 24). These properties have enabled treatments with GABA-R agonists to inhibit the progression of a diverse array of autoimmune diseases that occur in mice with different genetic backgrounds, including models of type 1 diabetes (T1D), multiple sclerosis (MS), rheumatoid arthritis, Sjogren's syndrome, as well as inflammation in type 2 diabetes (11, 12, 15, 19, 20, 23–26). Relevant to the treatment of COVID-19, GABA inhibits human immune cell secretion of many pro-inflammatory cytokines and chemokines associated with cytokine storms in individuals with COVID-19 (5, 7, 27–31).

Airway epithelial cells, including type II alveolar epithelial cells, also express GABA<sub>A</sub>-Rs which modulate the intracellular ionic milieu and help maintain alveolar fluid homeostasis (32–35). GABA and GABA<sub>A</sub>-R positive allosteric modulators (PAMs) reduce inflammation and improve alveolar fluid clearance and lung functional recovery in different rodent models of acute lung injury (36–43), and limit pulmonary inflammatory responses and improve clinical outcomes in ventilated human patients (44–46). GABA decreases the secretion of inflammatory factors by human bronchial epithelial cells *in vitro* (37) and GABA<sub>A</sub>-R PAMs reduce macrophage infiltration and inflammatory cytokine levels in bronchoalveolar lavage fluid and reduce rodent and human macrophage inflammatory responses (10, 13, 33, 42, 47–49). Moreover, GABA<sub>A</sub>-R ligands inhibit human neutrophil activation (50) and platelet aggregation (51), which are

potentially important because pulmonary thrombosis often occurs in critically ill COVID-19 patients. Finally, lower levels of plasma GABA are detected in hospitalized COVID-19 patients and associated with the pathogenesis of COVID-19 (52, 53), although the basis for this observation is not understood. Together, the multiple actions of GABA<sub>A</sub>-R modulators on various immune cells and lung epithelial cells, along with their safety for clinical use, make them candidates for limiting dysregulated immune responses, severe pneumonia, and lung damage due to coronavirus infection.

In a previous study, we began to assess whether GABA-R agonists had therapeutic potential for treating coronavirus infections by studying A/J mice that were inoculated with mouse hepatitis virus (MHV-1) (54). MHV-1 is a pneumotropic beta-coronavirus that induces a highly lethal pneumonitis in A/J mice (55–60). We observed that oral administration of GABA or the GABA<sub>A</sub>-R-specific agonist homotaurine, but not a GABA<sub>B</sub>-R-specific agonist, effectively inhibited MHV-1-induced pneumonitis, and reduced disease severity, and death rates when given before or after the onset of symptoms (54). GABA treatment also modestly reduced MHV-1 viral load in their lungs.

While MHV-1 and SARS-CoV-2 are both beta coronaviruses, they bind different cellular receptors (CEACAM1 vs. ACE2, respectively), differ antigenically, and are quite biologically distinct. Moreover, the host's response to respiratory infections varies greatly between different virus strains and mouse strains (60). To more stringently test the therapeutic potential of GABA as a therapy for COVID-19, we assessed the ability of GABA treatment to limit the disease process in SARS-CoV-2-infected human ACE2 transgenic K18-hACE2 mice, which provide a widely used acute and lethal model of COVID-19 (61–66). We found that GABA-Rs are a new druggable target for limiting disease severity, lung viral load, pneumonitis, and death in SARS-CoV-2 infected mice. We also discuss the potential of GABA<sub>A</sub>-R agonists for limiting COVID-19-associated neuroinflammation.

## Results

GABA treatment protects SARS-CoV-2-infected K18-hACE2 transgenic mice from severe illness and death. K18-ACE2 mice were inoculated with SARS-CoV-2 intranasally and placed in cages with water bottles containing 0, 0.2, or 2.0 mg/mL GABA, as described in Methods. The mice were maintained on these treatments for the entire study. Their body weights, behavior, and activity were monitored and scored for the onset and severity of the disease twice daily. There was no statistically significant difference in longitudinal body weights or the amounts of water consumed among the different groups of mice (Supplementary Figure 1). The SARS-CoV-2 infected control mice that received plain water developed overt signs of illness beginning around day 5 post-infection, which increased



in severity and often necessitated humane euthanasia prior to the end of the study (Figures 1A, B), similar to previous observations in this model (64). In contrast, the mice receiving GABA displayed significantly reduced illness scores compared to the control mice (Figure 1A). Only 20% of control mice survived until the pre-determined end of the studies 7–8 days post-infection. In contrast, 80% of the mice that received GABA at 0.2 or 2 mg/mL were surviving on days 7–8 post-infection (Figure 1B,  $p=0.004$  and  $p=0.018$ , respectively vs. the control).

At the time of euthanasia, each animal's lungs were excised and weighed. The ratio of lung weight to total body weight (i.e., the lung coefficient index) reflects the extent of inflammation in the lung. We observed a significant reduction in the lung coefficient index scores in the group treated with 2.0 mg/mL GABA (Figure 1C), indicating reduced lung inflammation. Together, these studies demonstrate that GABA treatment reduces disease severity, inflammation, and death rates in SARS-CoV-2 infected mice.

## GABA treatment reduces SARS-CoV-2 titers in the lungs of infected K18-hACE2 mice

We next asked whether GABA's protective mechanism could be due in part to reducing viral replication in their lungs. K18-hACE2 mice were infected with SARS-CoV-2 (2,000 TCID<sub>50</sub> intranasally) and placed on plain water (control) or water containing GABA (2 mg/mL) for the rest of the study. Three days post-infection, which should be near to the peak of viral load in the lungs (64), we harvested their lung tissues to determine viral load by TCID<sub>50</sub> assay using Vero E6 cells. We found that SARS-CoV-2 titers in the lungs of GABA-treated mice were on average a 1.36 log<sub>10</sub> (23-fold) lower than that in the lungs of mice that received plain water ( $p<0.0001$ , Figure 2). Thus, GABA treatment inhibited the replication of SARS-CoV-2 in the lungs of K18-hACE2 mice.

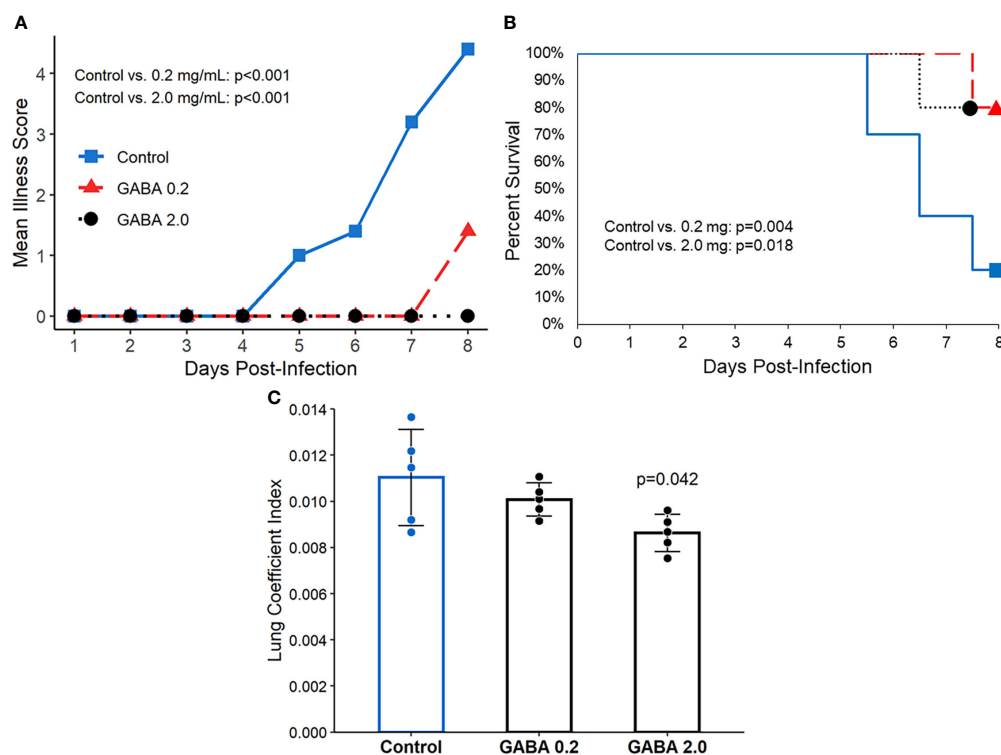


FIGURE 1

GABA treatment limits disease severity and mortality in SARS-CoV-2 infected K18-hACE2 mice. Following SARS-CoV-2 inoculation the mice were placed on plain water (blue line with squares), 0.2 mg/mL GABA (red line with triangles), or 2.0 mg/mL GABA (black dotted line with circles). (A) Longitudinal mean illness scores. Disease severity was scored in one of the studies and compared between groups by fitting mixed-effect linear regression models with group and time as fixed effects (to compare means), and with group, time and group by time interaction as fixed effects (to compare slopes). Mouse ID was used as a random effect.  $N=5$  mice/group. (B) Combined percent surviving mice from two independent studies with 5 mice/group which followed the mice for 7 or 8 days post-infection ( $n=10$  mice/group total). Survival curves were estimated using the Kaplan-Meier method and statistically analyzed by the log-rank test. (C) Mice that reached an illness score of 5 or survived to the end of the observation period were euthanized. Their lungs were dissected and weighed to calculate the lung coefficient index (the ratio of lung weight to body weight). The data shown are the mean lung coefficient index  $\pm$  SEM/ $N=5$  mice/group. The  $p$ -value was determined by Student's  $t$ -test.

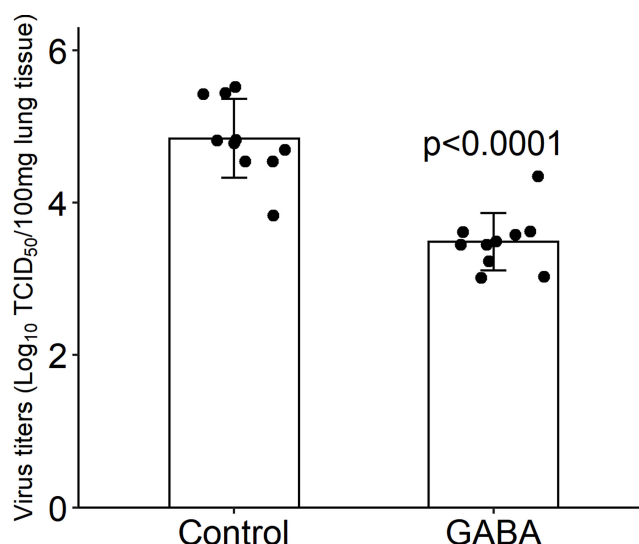


FIGURE 2

GABA treatment reduces SARS-CoV-2 titers in the lungs. Three days post-infection the right lung was harvested from each mouse and homogenized. The viral titer in lung tissue (100 mg) were determined by TCID<sub>50</sub> assay using Vero E6 cells. Black dots show viral titers for individual mice (determined in quadruplicate). The data shown are the mean virus titer (Log<sub>10</sub> TCID<sub>50</sub>/100 mg lung tissue)  $\pm$  SD in mice given plain water (control) or GABA. N=10 mice/group. The p-value was determined by Student's t-test.

## GABA treatment modulates early cytokine and chemokine responses to SARS-CoV-2 infection

We next asked whether GABA treatment could modulate serum cytokine and chemokine levels in SARS-CoV-2 infected mice. Serum samples were collected three days post-infection from the same mice that were used to study lung viral load and were analyzed using a multiplex bead kit designed to detect 13 cytokines and chemokines. We did not detect any statistically significant difference in the levels of serum IFN $\alpha$ , IFN $\beta$ , IFN $\gamma$ , IL-12, or GM-CSF between SARS-CoV-2 infected mice that did or did not receive GABA treatment (Figure 3). There was, however, some suggestion that GABA treatment elevated type I interferons in some mice because only 1/10 mice in the healthy control (HC) and in the SARS-CoV-2-infected control (SC) group had a detectable level of IFN $\beta$ , while 3/10 of the infected mice which received GABA (G) had detectable IFN $\beta$  levels and these were greater in magnitude than that found in the other groups (Figure 3). The median and the mean levels of IFN $\alpha$  were also slightly elevated in the GABA treated vs. untreated SARS-CoV-2 infected group (Figure 3). Conversely, 3/10 mice in the SC group displayed high levels of IFN $\gamma$  vs 1/10 mice in the G group and the median and mean IFN $\gamma$  levels were reduced in the GABA-treated vs. untreated SARS-CoV-2 infected mice (Figure 3,  $p=0.25$ ).

Analysis of pro-inflammatory and anti-inflammatory cytokines revealed that SARS-CoV-2 infection significantly

increased the levels of serum TNF $\alpha$  in the SC group ( $p<0.001$ , Figure 3) as in previous studies of SARS-CoV-2-infected K18-hACE2 mice (64, 66–68). GABA treatment significantly mitigated TNF $\alpha$  production following infection ( $p<0.001$ ). There was no statistically significant difference in the levels of serum IL-1 $\beta$  and IL-6 although the levels of serum IL-1 $\beta$  and IL-6 in the GABA-treated group were slightly reduced compared with the SC group (Figure 3). SARS-CoV-2 infection significantly increased the levels of serum IL-10, as in past studies of K-18-hACE2 mice (64, 66, 68). GABA treatment further significantly elevated the serum IL-10 levels above that in untreated SARS-CoV-2 infected mice ( $p<0.001$ ).

Analysis of serum chemokines revealed that untreated SARS-CoV-2 infected mice, but not the GABA-treated SARS-CoV-2 infected mice, displayed significantly higher levels of CCL2 relative to healthy controls ( $p<0.05$ ), with the levels of CCL2 tending to be lower in GABA-treated vs. untreated-infected mice ( $p=0.07$ ). Moreover, GABA treatment led to significantly reduced levels of IP-10 (CXCL10) compared to that in untreated SARS-CoV-2 infected mice ( $p<0.001$ , Figure 3). We observed no statistically significant difference in the levels of serum CXCL1 and CCL5 among these groups of mice. Thus, GABA treatment shifted systemic cytokine and chemokine responses towards those associated with less risk for developing severe COVID-19 by increasing early type I IFN responses in some mice, significantly reducing the levels of TNF $\alpha$  and IP-10, tending to reduce CCL2 levels, but enhancing IL-10 production in SARS-CoV-2 infected mice.

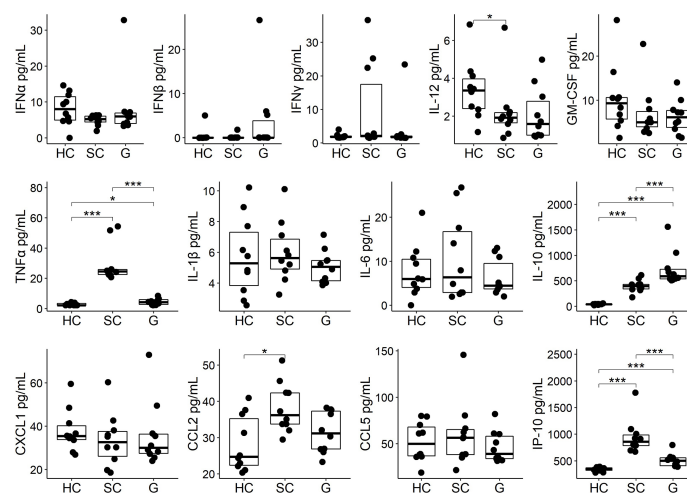


FIGURE 3

GABA treatment modulates circulating cytokines and chemokines in SARS-CoV-2-infected K18-hACE2 mice. Three days post-infection sera from individual SARS-CoV-2 infected control (SC) mice that were untreated, or were GABA treated (G), were collected and frozen at  $-80^{\circ}\text{C}$  until analysis by a multiplex assay as described in Methods. In addition, sera from age-matched healthy control (HC) B6 mice were studied. The non-normally distributed data are shown in boxplots with the borders of the box indicating 1st and 3rd quartile of each group ( $n=10$ ), the bolded line indicating the median. The data were analyzed by Wilcoxon rank-sum tests. \* $p<0.05$ , \*\*\* $p<0.001$ .

## GABA treatment protects SARS-CoV-2-infected mice from severe illness and pneumonitis when treatment is initiated near the peak of viral load in the lungs

We next examined whether GABA treatment could be also beneficial when treatment was initiated at a later stage of the disease process. K18-hACE2 mice were infected with SARS-CoV-2 as above and GABA treatment (2 mg/mL) was initiated at 2 days post-infection, near the peak of viral load in the lungs. Compared to untreated control mice, GABA-treated mice displayed reduced longitudinal mean illness scores (overall  $p=0.002$ , Figure 4A). At the end of the study on day 7, only 22% of control mice survived, while 88% of GABA-treated mice had survived ( $p=0.004$ , Figure 4B). GABA-treated mice also had a reduced lung coefficient index ( $p<0.001$ , Figure 4C).

Consistent with the reduced lung coefficient index, histological evaluation of lung sections from these mice revealed that while many inflammatory infiltrates, several hyaline-like membranes, severe diffused hemorrhage, and large areas of inflammatory consolidation were observed in the lungs of GABA-untreated mice, these pathological changes were obviously mitigated in the lungs of GABA-treated mice (Figures 5A, B). Quantitative analysis revealed that the pneumonitis scores in the mice which received GABA at 2 days post-infection were significantly less than that in the control mice (Figure 5C,  $p=0.027$ ). Thus, GABA treatment limited SARS-CoV-2-induced pneumonitis and lung damages in mice.

## Discussion

Our studies demonstrated that GABA administration initiated immediately, or two-day post-SARS-CoV-2 infection, reduced the lung coefficient index, lung viral load, pneumonitis, and death rate in SARS-CoV-2-infected K18-hACE2 mice. These results, along with our previous findings in the MHV-1 infected A/J mice, are the first reports of GABA administration modulating the outcome of viral infections. The ability of GABA treatment to limit the disease severity following infection with two biologically distinct and lethal coronaviruses in different mouse strains suggests that GABA-R activation may be a generalizable therapeutic strategy to help reduce the severity of coronavirus infections, at least in mice.

Our observations are surprising in a number of ways. First, based on GABA's anti-inflammatory actions in models of autoimmune disease, cancer, and parasitic infection, it was highly possible that early GABA treatment could have exacerbated the disease in SARS-CoV-2 infected mice by limiting or delaying the innate immune responses to the viral infection. However, SARS-CoV-2-infected mice that received GABA treatment at the time of infection, or 2-days post-infection, fared much better than their untreated SARS-CoV-2-infected counterparts.

Second, GABA's ability to modestly reduce viral load in the lungs was surprising. This indicates that GABA-R mediated changes in the intracellular ionic milieu modulate processes involved in SARS-CoV-2 entry, replication, and/or egress. We know from large-scale screens of drug libraries that GABA-R

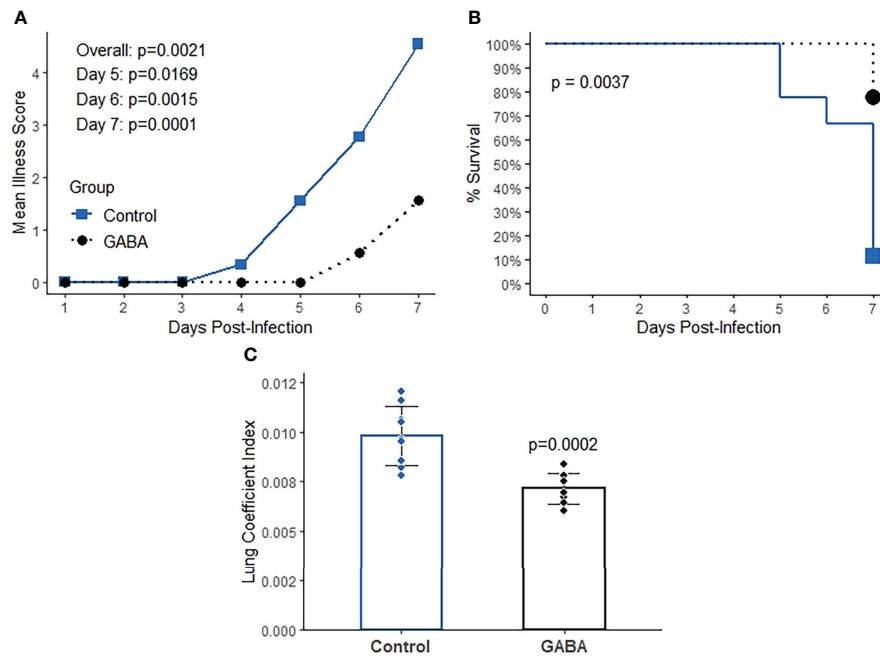


FIGURE 4

GABA treatment initiated near the peak of lung viral load has protective effects in SARS-CoV-2 infected K18-hACE2 mice. Mice were infected with SARS-CoV-2 and two days later mice received GABA through their drinking water (2 mg/mL), or were maintained on plain water for the remainder of the study. **(A)** Longitudinal mean illness scores. The data were analyzed by fitting mixed-effect linear regression models with group and time as fixed effects (to compare means), and with group, time and group by time interaction as fixed effects (to compare slopes). Mouse ID was used as a random effect. **(B)** Percent surviving mice. The data were analyzed by Kaplan-Meier survival curves and the log-rank test. **(C)** Lung coefficient index. The data were analyzed by Student t-test.  $N=9$  mice/group.

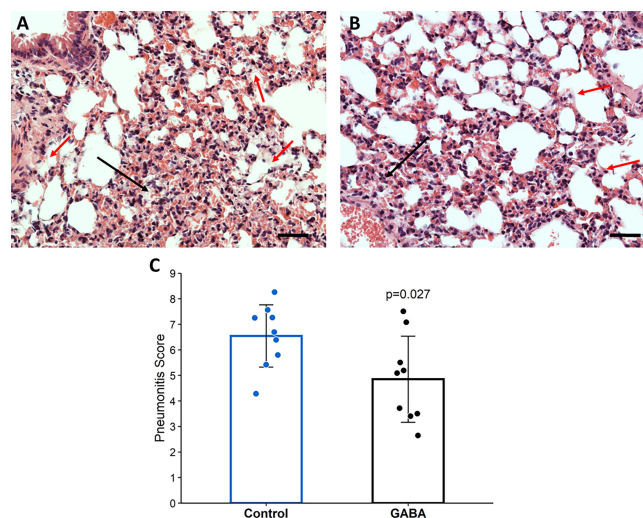


FIGURE 5

GABA treatment initiated 2-days post-infection reduces pneumonitis in SARS-CoV-2-infected mice. At the time of euthanasia, the lungs of mice studied in Figure 4 were removed and processed for histological examination as described in Methods. Representative images of H&E-stained lung sections (magnification  $\times 200$ ) from **(A)** untreated mice and **(B)** GABA-treated mice. Red arrows point to hyaline-like membranes and black arrows indicate local consolidation. The scale bar is 50  $\mu\text{m}$ ; **(C)** Quantitative analysis of the degrees of pneumonitis in the lungs. Data are expressed as the mean pneumonitis score  $\pm$  SD of each group. The data were analyzed by Student t-test.  $N=9$  mice per group.

agonists do not interfere with SARS-CoV-2 binding to ACE2 or its internalization into cultured Vero E6 cells (69). Notably, GABA<sub>A</sub>-Rs are expressed by lung bronchial and alveolar cells (32, 33, 70) and it is possible that GABA<sub>A</sub>-R activation led to changes in intracellular ion levels that made the environment less favorable for viral replication. While the activation of neuronal GABA<sub>A</sub>-Rs leads to Cl<sup>-</sup> influx and hyperpolarization, the activation of GABA<sub>A</sub>-Rs on other types of cells, such as alveolar ATII cells, causes Cl<sup>-</sup> efflux and depolarization (32, 33). Many viruses, including some coronaviruses, can promote Ca<sup>2+</sup> influx into their host cell to enhance their replication (71, 72). The activation of GABA<sub>A</sub>-Rs on infected cells could promote Cl<sup>-</sup> efflux which would oppose Ca<sup>2+</sup> influx and reduce Ca<sup>2+</sup> contents, limiting SARS-CoV-2 replication. Indeed, calcium blockers have been shown to reduce SARS-CoV-2 replication *in vitro*, but whether they confer beneficial effects to COVID-19 patients has been controversial (73–75). The activation of GABA<sub>A</sub>-Rs on alveolar and large airway epithelial cells may also have altered 1) the secretion of inflammatory signaling molecules from infected cells, 2) alveolar surfactant production/absorption, and/or 3) altered inflammatory responses and autophagy processes (17) in ways that limited virus infection and replication.

Third, while there has been some characterization of GABA's effects on immune cell cytokine and chemokine secretion in models of autoimmune disease and cancer, little is known about GABA's effects on anti-viral responses. We observed that GABA treatment shifted some cytokine and chemokine levels in directions that are expected to be beneficial if extended to COVID-19 treatment. Early GABA treatment elevated type 1 interferons in some mice. Since delayed or reduced type I interferon responses are a risk factor for developing severe COVID-19 (76), such tendencies could be beneficial. GABA treatment significantly reduced circulating TNF $\alpha$  levels in infected mice, extending previous observations that GABA inhibits the NF- $\kappa$ B activation in mouse and human immune cells (7, 21). As a result, GABA treatment slightly decreased mean serum IL-6 from 10.7 to 6.3 pg/mL. Since TNF $\alpha$  and IL-6 are important pro-inflammatory mediators, the decreased levels of circulating TNF $\alpha$  and IL-6 indicated that GABA treatment suppressed innate immune responses, which is likely to have contributed to its protective effects.

GABA-treated mice also had reduced levels of serum IP-10, a pro-inflammatory chemokine that attracts the migration of CXCR3<sup>+</sup> macrophages/monocytes, T cells, and NK cells (77). Elevated levels of IP-10 are consistently detected in severely ill COVID-19 patients and may provide a predictive marker of patient outcome (78–81). IP-10 production is induced by IFN $\gamma$ , NF- $\kappa$ B activation and other stimulators in several types of cells (82). Consistent with the reduced IP-10 levels, we also found that the serum mean IFN $\gamma$  level in the GABA-treated mice was about

half that in the untreated SARS-CoV-2 infected mice (4.0 vs. 9.8 pg/mL). These data suggest that early GABA treatment reduced IFN $\gamma$  production and together with its inhibition of NF- $\kappa$ B activation, led to decreased IP-10 secretion. Given that IP-10 functions to recruit inflammatory cell infiltration into lesions and modulates cell survival, the lower levels of circulating IP-10 in GABA-treated mice are likely to have limited the migration of macrophages, monocytes, and NK cells into the pulmonary lesions and helped to protect the mice from death. Similarly, we also observed that GABA treatment slightly reduced the levels of serum CCL2 which may have contributed to protecting mice from death since high levels of CCL2 are associated with high mortality in COVID-19 patients (83).

GABA treatment also enhanced IL-10 levels in SARS-CoV-2 infected mice. IL-10 is generally regarded as an anti-inflammatory cytokine, however, it can be immunostimulatory in certain contexts and elevated levels of IL-10 are associated with the development of severe COVID-19 (84, 85). If the elevation of IL-10 levels in GABA-treated SARS-CoV-2 infected mice had counter-therapeutic effects, it is evident that GABA's beneficial actions were functionally dominant leading to improved outcomes. Conceivably, the enhanced levels of IL-10 levels due to GABA treatment may have been therapeutic by 1) its classical anti-inflammatory actions, 2) exhausting immune cells, 3) reducing tissue damage in the lungs, or 4) other yet to be identified actions.

Initiating GABA treatment 2-days after SARS-CoV-2 infection, near the peak of viral loads in the lungs, was essentially just as effective as initiating the treatment immediately post-infection in terms of limiting disease severity and death rates during the observation period. Coinciding with those observations, the lungs of mice treated with GABA 2 days-post infection displayed reduced histopathological damage relative to untreated controls. It will be of interest to further test the efficacy of GABA when initiated at even later time points post-infection—however, the current findings clearly indicate GABA to be an excellent candidate therapeutic for COVID-19 and due to the inherent imperfections of any animal model, the ultimate test of this treatment will require human clinical trials.

Besides expressing the hACE2 transgene in lung cell epithelial cells, K18-hACE2 mice express hACE2 ectopically in their CNS leading to the spreading of SARS-CoV-2 infection to their CNS at late stages of the disease process (64, 66, 67). Because GABA does not pass through the blood-brain barrier (BBB), it is unlikely that GABA treatment directly exerted beneficial effects in the CNS. However, the decreased levels of circulating proinflammatory cytokines and chemokines in GABA-treated mice may have also reduced their entry into the CNS. While SARS-CoV-2 is thought not to efficiently replicate in the human CNS (86), some COVID-19 patients experience cognitive impairments (or “brain fog”). Histological studies of



the brains from COVID-19 patients have observed immune cell infiltrates and increased frequencies of glial cells with inflammatory phenotypes which are indicative of neuroinflammatory responses (86–93). In previous studies, we have shown that treatment with homotaurine, a GABA<sub>A</sub>-R-specific agonist that can pass through the BBB, reduced the spreading of inflammatory T cell responses within the CNS, limited the pro-inflammatory activity of antigen-presenting cells, and ameliorated disease in mouse models of multiple sclerosis (15, 20). Since microglia and astrocytes express GABA<sub>A</sub>-Rs which act to down-regulate their inflammatory activities (94), homotaurine treatment may have also limited glial inflammation. Homotaurine was as effective as GABA in protecting MHV-1-infected A/J mice from severe illness, pointing to GABA<sub>A</sub>-Rs as the major mediators of GABA's beneficial effects in this model (54). These observations suggest that homotaurine treatment may provide a new strategy to both reduce the deleterious effects of coronavirus infection in the periphery and limit inflammation in the CNS. Homotaurine (also known as Tramiprosate) was found to physically interfere with amyloid aggregation *in vitro*, leading to its testing as a treatment for Alzheimer's disease in a large long-term phase III clinical study (95–97). While this treatment failed to meet primary endpoints, the treatment appeared to be very safe and follow-up studies suggested some disease-modifying effect (98, 99).

Finally, it is worth noting that circulating GABA levels are significantly reduced in hospitalized patients with COVID-19 (52, 53). This clinical finding, independent of our results presented here, raises the question of whether GABA therapy could be beneficial for COVID-19 patients.

It is likely that SARS-CoV-2 variants and novel coronaviruses will constantly arise that will be insufficiently controlled by available vaccines and antiviral medications. Developing new vaccines against these new viruses will be much slower than the spread of these new viruses among the world population. Our findings suggest that GABA-R agonists may provide inexpensive off-the-shelf agents to help lessen the severity of disease caused by these new viruses. Because GABA's mechanisms of action are unlike that of other coronavirus treatments, combination treatments could have enhanced benefits.

GABA is regarded as safe for human use and is available as a dietary supplement in the USA, China, Japan, and much of Europe (100). In other countries, because GABA is a non-protein amino acid, it is regulated as a medicinal agent or drug (e.g., in the UK, Canada, and Australia). In our studies, GABA at 2.0 and 0.2 mg/mL were equally effective at protecting SARS-CoV-2 infected mice from death (Figure 1B). The human equivalent dose of GABA at 0.2 mg/mL [assuming consumption of 3.5 mL/day water, see Supplemental Figure 1 and calculated as

per (101)] is 0.68 g/day for a 70 kg person, which is well within the level known to be safe (100). While our preclinical observations indicate that GABA-R agonists are promising candidates to help treat coronavirus infections, information on their dosing and the time window during which their effects might be beneficial or deleterious during a coronavirus infection in humans are lacking and clinical trials are needed to assess their therapeutic potential.

## Limitations of this study

There are a number of major limitations of this study. First, the K18-hACE2 mouse model imperfectly models SARS-CoV-2 infection and immune responses in humans. Second, GABA's impact on immune cells and lung cells may differ in important ways between mice and humans. Third, GABA treatment may only be beneficial during a specific time window of the disease process and at other times may be deleterious. Accordingly, careful clinical trials are needed to determine the time window and dosage, if any, that GABA-R agonist treatment has a beneficial effect in COVID-19 patients.

## Materials and methods

### Virus

SARS-CoV-2 (USA-WA1/2020) was obtained from the Biodefense and Emerging Infections Resources of the National Institute of Allergy and Infectious Diseases. All *in vivo* studies of SARS-CoV-2 infection were conducted within a Biosafety Level 3 facility at UCLA or USC. SARS-CoV-2 stocks were generated by infection of Vero-E6 cells (American Type Culture Collection (ATCC CRL1586)) cultured in DMEM growth media containing 10% fetal bovine serum, 2 mM L-glutamine, penicillin (100 units/mL), streptomycin (100 units/mL), and 10 mM HEPES. The cells were incubated at 37°C with 5% CO<sub>2</sub> and virus titers were determined as described below for titrating virus in lung homogenates.

### Mice and GABA treatments

Female K18-hACE2 mice (8 weeks in age) were purchased from the Jackson Laboratory. The first survival study was conducted within USC's BSL3 Core facility and all following studies were conducted in the UCLA ABSL3 Core Facility. One week after arrival, they were inoculated with SARS-Cov-2 (2,000 PFU or 2,000 TCID<sub>50</sub> (as per (64) at USC and UCLA, respectively) in 20 µL Dulbecco's modified Eagle's medium. The mice were randomized into groups of 5–9 mice and were placed on water bottles containing 0, 0.2, or 2.0 mg/mL GABA

(Millipore-Sigma (stock #A2129), St. Louis, MO, USA) immediately, or 2 days post-infection (as indicated) and maintained on those treatments for the remainder of each study. These studies were carried out in accordance with the recommendations of the Guide for the Care and Use of Laboratory Animals of the National Institutes of Health. The protocols for all experiments using vertebrate animals were approved by the Animal Research Committee at UCLA (Protocol ID: ARC #2020-122; 8/25/20-8/24/2023) or USC (IACUC protocol # 21258; 1/28/2021-1/27/2024) and were carried out in compliance with the ARRIVE guidelines.

## Illness scoring and lung index score

Individual mice were monitored by two observers twice daily for their illness development and progression which were scored on the following scale: 0) no symptoms, 1) slightly ruffled fur and altered hind limb posture; 2) ruffled fur and mildly labored breathing; 3) ruffled fur, inactive, moderately labored breathing; 4) ruffled fur, inactive, obviously labored breathing, hunched posture; 5) moribund or dead.

The percent survival of each group of mice was determined longitudinally. Mice with a disease score of 5 were weighed, euthanized, and their lungs removed and weighed for calculation of lung coefficient index (the ratio of lung weight to total body weight, which reflects the extent of edema and inflammation in the lungs). On day 7 or 8 post-infection, the surviving animals were weighed, euthanized, and their lungs were removed and weighed for determination of the lung coefficient index.

## Histology

Individual mice were infected intranasally with SARS-CoV-2 virus and two days later, they were randomized to receive plain water, or water containing GABA (2 mg/mL) for the remainder of the study. On days 5-7 post infection, those mice which met euthanasia criteria or survived until the end of the study on day 7, were euthanized and their lungs were dissected. The left lung from each mouse was fixed in 10% neutral buffered formalin and embedded in paraffin. The lung tissue sections (4  $\mu$ m) were routine-stained with hematoxylin and eosin. Five images from each mouse were captured under a light microscope at 200  $\times$  magnification. The degrees of pathological changes were scored, as in our previous report (54). Briefly, the degrees of pathological changes were scored, based on the number of hyaline-like membranes, % of pulmonary areas with obvious inflammatory infiltrates in lung parenchyma, and the % of area with inflammatory consolidation within the total area of the section. The total numbers of hyaline-like membranes with, or without, cell debris or hyaline-like deposition in alveoli of the lung tissue

section were scored as 0: none detectable; 1: 1-5; 2: 6-10; 3: >10. The areas of lung inflammation and hemorrhage in one lung section were estimated and the severity of inflammation and hemorrhage in the section was scored as 1: mild; 2: moderate; 3: marked; 4: severe. Accordingly, an inflammatory score in each mouse was obtained by % of lung areas  $\times$  severity score. The areas of lung inflammatory consolidation were estimated in the lung section and scored as 1:  $\leq$ 10%; 2: 11-25%; 3: 26-50%; 4: >50%. Finally, the pneumonitis score of individual mice = inflammation score + lung consolidation score + hyaline membrane score with a maximum score of 11.

## Viral titers in lungs

Female K18-ACE2 mice (9 weeks in age) were intranasally inoculated with 2,000 TCID<sub>50</sub> SARS-Cov-2 and placed on plain water or water containing GABA (2 mg/mL) for the rest of the study. Three days post-infection, the mice were euthanized and individual blood samples were collected for preparing serum samples. A portion of their lower right lung was weighed and about 100 mg of wet lung tissue from each mouse was homogenized into 1 mL of ice-cold DMEM with 10% fetal calf serum (FBS) with 1 mm glass beads using a Minilys homogenizer at 50 Hz for 90 seconds, followed by centrifugation. Their supernatants were collected for virus titrating. Vero E6 cells ( $1 \times 10^4$  cells/well) were cultured in DMEM medium supplemented with 10% FBS in 96-well plates overnight to reach 80% of confluency and infected in quintuplicate with a series of diluted mouse lung homogenates in 100  $\mu$ l of FBS-free DMEM medium at 37°C for four days. The percentages of viral cytopathic effect areas were determined. The SARS-CoV-2 titers were calculated by the Reed and Muench method (102).

## Simultaneous detection of multiple cytokines and chemokines by flow cytometry

Blood samples were collected from the same mice that were used to study viral loads in the lungs at three days post-infection. Sera from individual mice were prepared and stored at -80°C. The levels of serum cytokines and chemokines were determined by a bead-based multiplex assay using the LEGENDplex mouse anti-virus response panel (13-plex) kit (#740622, Biolegend, San Diego, USA), according to the manufacturer's instructions. Briefly, the control and experimental groups of serum samples were diluted at 1:2 and tested in duplicate simultaneously. After being washed, the fluorescent signals in each well were analyzed by flow cytometry in an ATTUNE NxT flow cytometer (ThermoFisher). The data were analyzed using the LEGENDplex™ Data Analysis Software Suite (Biolegend) and the levels of each cytokine or chemokine in serum

samples were calculated, according to the standard curves established using the standards provided.

## Statistics

Statistical methods are described in each figure legend. A p-value of  $<0.05$  was considered statistically significant.

## Data availability statement

The raw data supporting the conclusions of this article will be made available by the authors, without undue reservation.

## Ethics statement

The animal study was reviewed and approved by Animal Research Committee at UCLA (Protocol ID: ARC #2020-122; Date 8/25/20-8/24/2023 and BUA-2021-071-001) and USC (IACUC protocol # 21258 (1/28/2021-1/27/2024), IBC: BUA 20-0030/20-0033).

## Author contributions

Conceived and designed the experiments: JT and DK; Performed the experiments: JT, BD, and JH; Supervised work and assessed data quality in the ABSL3 labs BD, LC. Analyzed the data: JT, DLK. Wrote the paper: JT, DLK. DLK and JT are guarantors of this work and, as such, had full access to all the data in the study and take responsibility for the integrity of the data and the accuracy of the data analysis. All authors contributed to the article and approved the submitted version.

## Funding

This work was supported by a grant to DK from the UCLA DGSOM-Broad Stem Cell Research Center COVID-19 Research Award (ORC #21-93), DK's unrestricted funds, JT's unrestricted funds, funds from the Department of Molecular and Medical Pharmacology, and the Immunotherapeutics Research Fund. Work in the Hasting Foundation and the Wright Foundation BSL3 lab at the Keck School of Medicine of USC was supported by a grant from the COVID-19 Keck Research Fund to LC.

Statistical analysis was supported by a grant from the NCATS, UCLA CTSI Grant Number UL1TR001881.

## Acknowledgments

We would like to thank Dr. Vaithilingaraja Arumugaswami for his kind provision of virus stock and Drs. Jennifer Hahn, Orian Shirihi, Anton Petcherski, Theodoros Kelesidis, and Joanne L. Zahorsky-Reeves, as well as Madhav Sharma, Melanie Ciampaglia, Tomoko Yamada, and Lenore Kaufman for their help. We thank Lucia Chen, Dr. Jeffery Gornbein, and Dr. Alexandra Klomhaus for statistical analysis and figure preparation, and Miss. Salem Haile in the Janice Gorgi Flow Cytometry Center for FACS analysis. We thank Jeremy Marshall and Philip Sell for their support in the ABSL3 lab at USC.

## Conflict of interest

DLK and JT are inventors of GABA-related patents. DLK serves on the Scientific Advisory Board of Diamyd Medical. DLK gifted the Immunotherapeutics Research Fund.

The remaining authors declare that the research was conducted in the absence of any commercial or financial relationships that could be construed as a potential conflict of interest.

## Publisher's note

All claims expressed in this article are solely those of the authors and do not necessarily represent those of their affiliated organizations, or those of the publisher, the editors and the reviewers. Any product that may be evaluated in this article, or claim that may be made by its manufacturer, is not guaranteed or endorsed by the publisher.

## Supplementary material

The Supplementary Material for this article can be found online at: <https://www.frontiersin.org/articles/10.3389/fimmu.2022.1007955/full#supplementary-material>

## References

- Olsen RW, Sieghart W. GABA<sub>A</sub> receptors: subtypes provide diversity of function and pharmacology. *Neuropharmacology* (2009) 56(1):141–8. doi: 10.1016/j.neuropharm.2008.07.045
- Ben-Ari Y. Excitatory actions of gaba during development: the nature of the nurture. *Nat Rev Neurosci* (2002) 3(9):728–39. doi: 10.1038/nrn920
- Deidda G, Bozarth IF, Cancedda L. Modulation of GABAergic transmission in development and neurodevelopmental disorders: investigating physiology and pathology to gain therapeutic perspectives. *Front Cell Neurosci* (2014) 8:119. doi: 10.3389/fncel.2014.00119
- Tian J, Chau C, Hales TG, Kaufman DL. GABA(A) receptors mediate inhibition of T cell responses. *J Neuroimmunol* (1999) 96(1):21–8. doi: 10.1016/s0165-5728(98)00264-1
- Bhandage AK, Jin Z, Korol SV, Shen Q, Pei Y, Deng Q, et al. GABA regulates release of inflammatory cytokines from peripheral blood mononuclear cells and CD4(+) T cells and is immunosuppressive in type 1 diabetes. *EBioMedicine* (2018) 30:283–94. doi: 10.1016/j.ebiom.2018.03.019
- Tian J, Middleton B, Lee VS, Park HW, Zhang Z, Kim B, et al. GABAB-receptor agonist-based immunotherapy for type 1 diabetes in NOD mice. *Biomedicine* (2021) 9(1). doi: 10.3390/biomedicine9010043
- Zhang B, Vogelzang A, Miyajima M, Sugiura Y, Wu Y, Chamoto K, et al. B cell-derived GABA elicits IL-10(+) macrophages to limit anti-tumour immunity. *Nature* (2021) 599(7885):471–6. doi: 10.1038/s41586-021-04082-1
- Bhandage AK, Barragan A. GABAergic signaling by cells of the immune system: more the rule than the exception. *Cell Mol Life Sci* (2021) 78(15):5667–79. doi: 10.1007/s00018-021-03881-z
- Mendu SK, Bhandage A, Jin Z, Birnir B. Different subtypes of GABA-a receptors are expressed in human, mouse and rat T lymphocytes. *PLoS One* (2012) 7(8):e42959. doi: 10.1371/journal.pone.0042959
- Januzi L, Poirier JW, Maksoud MJE, Xiang YY, Veldhuizen RAW, Gill SE, et al. Autocrine GABA signaling distinctively regulates phenotypic activation of mouse pulmonary macrophages. *Cell Immunol* (2018) 332:7–23. doi: 10.1016/j.cellimm.2018.07.001
- Tian J, Yong J, Dang H, Kaufman DL. Oral GABA treatment downregulates inflammatory responses in a mouse model of rheumatoid arthritis. *Autoimmunity* (2011) 44:465–70. doi: 10.3109/08916934.2011.571223
- Bhat R, Axtell R, Mitra A, Miranda M, Lock C, Tsien RW, et al. Inhibitory role for GABA in autoimmune inflammation. *Proc Natl Acad Sci U S A* (2010) 107(6):2580–5. doi: 10.1073/pnas.0915139107
- Wheeler DW, Thompson AJ, Corletto F, Reckless J, Loke JC, Lapaque N, et al. Anaesthetic impairment of immune function is mediated via GABA(A) receptors. *PLoS One* (2011) 6(2):e17152. doi: 10.1371/journal.pone.0017152
- Reyes-Garcia MG, Hernandez-Hernandez F, Hernandez-Tellez B, Garcia-Tamayo F. GABA (A) receptor subunits RNA expression in mice peritoneal macrophages modulate their IL-6/IL-12 production. *J Neuroimmunol* (2007) 188(1–2):64–8. doi: 10.1016/j.jneuroim.2007.05.013
- Tian J, Song M, Kaufman DL. Homotaurine limits the spreading of T cell autoreactivity within the CNS and ameliorates disease in a model of multiple sclerosis. *Sci Rep* (2021) 11(1):5402. doi: 10.1038/s41598-021-84751-3
- Bhandage AK, Friedrich LM, Kanatani S, Jakobsson-Bjorken S, Escrig-Larena JJ, Wagner AK, et al. GABAergic signaling in human and murine NK cells upon challenge with toxoplasma gondii. *J Leukoc Biol* (2021) 10:617–28. doi: 10.1002/jlb.3H10720-431R
- Kim JK, Kim YS, Lee HM, Jin HS, Neupane C, Kim S, et al. GABAergic signaling linked to autophagy enhances host protection against intracellular bacterial infections. *Nat Commun* (2018) 9(1):4184. doi: 10.1038/s41467-018-06487-5
- Tian J, Dang H, Nguyen AV, Chen Z, Kaufman DL. Combined therapy with GABA and proinsulin/album acts synergistically to restore long-term normoglycemia by modulating T-cell autoimmunity and promoting beta-cell replication in newly diabetic NOD mice. *Diabetes* (2014) 63(9):3128–34. doi: 10.2337/db13-1385
- Tian J, Dang H, O'Laco K, Song M, Tiu B-C, Gilles S, et al. Homotaurine treatment enhances CD4+ and CD8+ treg responses and synergizes with low-dose anti-CD3 to enhance diabetes remission in type 1 diabetic mice. *ImmuoHorizons* (2019) 3(10):498–510. doi: 10.4049/immunohorizons.1900019
- Tian J, Dang H, Wallner M, Olsen R, Kaufman DL. Homotaurine, a safe blood-brain barrier permeable GABA<sub>A</sub>-specific agonist, ameliorates disease in mouse models of multiple sclerosis. *Sci Rep* (2018) 8(1):16555. doi: 10.1038/s41598-018-32733-3
- Prud'homme GJ, Glinka Y, Hasilo C, Paraskevas S, Li X, Wang Q. GABA protects human islet cells against the deleterious effects of immunosuppressive drugs and exerts immunoinhibitory effects alone. *Transplantation* (2013) 96(7):616–23. doi: 10.1097/TP.0b013e31829c24be
- Mendu SK, Akesson L, Jin Z, Edlund A, Cilio C, Lernmark A, et al. Increased GABA(A) channel subunits expression in CD8(+) but not in CD4(+) T cells in BB rats developing diabetes compared to their congenic littermates. *Mol Immunol* (2011) 48(4):399–407. doi: 10.1016/j.molimm.2010.08.005
- Soltani N, Qiu H, Aleksic M, Glinka Y, Zhao F, Liu R, et al. GABA exerts protective and regenerative effects on islet beta cells and reverses diabetes. *Proc Natl Acad Sci U S A* (2011) 108(28):11692–7. doi: 10.1073/pnas.1102715108
- Tian J, Dang HN, Yong J, Chui WS, Dizon MP, Yaw CK, et al. Oral treatment with gamma-aminobutyric acid improves glucose tolerance and insulin sensitivity by inhibiting inflammation in high fat diet-fed mice. *PLoS One* (2011) 6(9):e25338. doi: 10.1371/journal.pone.0025338
- Tian J, Lu Y, Zhang H, Chau CH, Dang HN, Kaufman DL. Gamma-aminobutyric acid inhibits T cell autoimmunity and the development of inflammatory responses in a mouse type 1 diabetes model. *J Immunol* (2004) 173(8):5298–304. doi: 10.4049/jimmunol.173.8.5298
- Song M, Tian J, Middleton B, Nguyen CQ, Kaufman DL. GABA administration ameliorates sjogren's syndrome in two different mouse models. *Biomedicine* (2022) 10(1). doi: 10.3390/biomedicine10010129
- Vabret N, Britton GJ, Gruber C, Hegde S, Kim J, Kuksin M, et al. Immunology of COVID-19: Current state of the science. *Immunity* (2020) 52(6):910–41. doi: 10.1016/j.immuni.2020.05.002
- Lucas C, Wong P, Klein J, Castro TBR, Silva J, Sundaram M, et al. Longitudinal analyses reveal immunological misfiring in severe COVID-19. *Nature* (2020) 584(7821):463–9. doi: 10.1038/s41586-020-2588-y
- Channappanavar R, Perlman S. Pathogenic human coronavirus infections: causes and consequences of cytokine storm and immunopathology. *Semin Immunopathol* (2017) 39(5):529–39. doi: 10.1007/s00281-017-0629-x
- Sariol A, Perlman S. Lessons for COVID-19 immunity from other coronavirus infections. *Immunity* (2020) 53(2):248–63. doi: 10.1016/j.immuni.2020.07.005
- Grant RA, Morales-Nebreda L, Markov NS, Swaminathan S, Querrey M, Guzman ER, et al. Circuits between infected macrophages and T cells in SARS-CoV-2 pneumonia. *Nature* (2021) 590(7847):635–41. doi: 10.1038/s41586-020-03148-w
- Jin N, Kolliputi N, Gou D, Weng T, Liu L. A novel function of ionotropic gamma-aminobutyric acid receptors involving alveolar fluid homeostasis. *J Biol Chem* (2006) 281(47):36012–20. doi: 10.1074/jbc.M606895200
- Xiang YY, Chen X, Li J, Wang S, Faclier G, Macdonald JF, et al. Isoflurane regulates atypical type-a gamma-aminobutyric acid receptors in alveolar type II epithelial cells. *Anesthesiology* (2013) 118(5):1065–75. doi: 10.1097/ALN.0b013e31828e180e
- Xiang YY, Wang S, Liu M, Hirota JA, Li J, Ju W, et al. A GABAergic system in airway epithelium is essential for mucus overproduction in asthma. *Nat Med* (2007) 13(7):862–7. doi: 10.1038/nm1604
- Barrios J, Kho AT, Aven L, Mitchel JA, Park JA, Randell SH, et al. Pulmonary neuroendocrine cells secrete gamma-aminobutyric acid to induce goblet cell hyperplasia in primate models. *Am J Respir Cell Mol Biol* (2019) 60(6):687–94. doi: 10.1165/rcmb.2018-0179OC
- Huang T, Zhang Y, Wang C, Gao J. Propofol reduces acute lung injury by up-regulating gamma-aminobutyric acid type a receptors. *Exp Mol Pathol* (2019) 110:104295. doi: 10.1016/j.yexmp.2019.104295
- Fortis S, Spieth PM, Lu WY, Parotto M, Haisma JJ, Slutsky AS, et al. Effects of anesthetic regimes on inflammatory responses in a rat model of acute lung injury. *Intensive Care Med* (2012) 38(9):1548–55. doi: 10.1007/s00134-012-2610-4
- Chintagari NR, Liu L. GABA receptor ameliorates ventilator-induced lung injury in rats by improving alveolar fluid clearance. *Crit Care* (2012) 16(2):R55. doi: 10.1186/cc11298
- Jin S, Merchant ML, Ritzenthaler JD, McLeish KR, Lederer ED, Torres-Gonzalez E, et al. Baclofen, a GABABR agonist, ameliorates immune-complex mediated acute lung injury by modulating pro-inflammatory mediators. *PLoS One* (2015) 10(4):e0121637. doi: 10.1371/journal.pone.0121637
- Voigtsberger S, Lachmann RA, Leutert AC, Schlapfer M, Booy C, Reyes L, et al. Sevoflurane ameliorates gas exchange and attenuates lung damage in experimental lipopolysaccharide-induced lung injury. *Anesthesiology* (2009) 111(6):1238–48. doi: 10.1097/ALN.0b013e31824bdf87
- Faller S, Strosing KM, Ryter SW, Buerkle H, Loop T, Schmidt R, et al. The volatile anesthetic isoflurane prevents ventilator-induced lung injury via phosphoinositide 3-kinase/Akt signaling in mice. *Anesth Analg* (2012) 114(4):747–56. doi: 10.1213/ANE.0b013e31824762f0
- Taniguchi T, Yamamoto K, Ohmoto N, Ohta K, Kobayashi T. Effects of propofol on hemodynamic and inflammatory responses to endotoxemia in rats. *Crit Care Med* (2000) 28(4):1101–6. doi: 10.1097/00003246-200004000-00032



43. Lin X, Ju YN, Gao W, Li DM, Guo CC. Desflurane attenuates ventilator-induced lung injury in rats with acute respiratory distress syndrome. *BioMed Res Int* (2018) 2018:7507314. doi: 10.1155/2018/7507314
44. Mahmoud K, Ammar A. Immunomodulatory effects of anesthetics during thoracic surgery. *Anesthesiol Res Pract* (2011) 2011:317410. doi: 10.1155/2011/317410
45. De Conno E, Steurer MP, Wittlinger M, Zalunardo MP, Weder W, Schneider D, et al. Anesthetic-induced improvement of the inflammatory response to one-lung ventilation. *Anesthesiology* (2009) 110(6):1316–26. doi: 10.1097/ALN.0b013e3181a10731
46. Schilling T, Kozian A, Kretschmar M, Huth C, Welte T, Buhling F, et al. Effects of propofol and desflurane anaesthesia on the alveolar inflammatory response to one-lung ventilation. *Br J Anaesth* (2007) 99(3):368–75. doi: 10.1093/bja/aem184
47. Kochiyama T, Li X, Nakayama H, Kage M, Yamane Y, Takamori K, et al. Effect of propofol on the production of inflammatory cytokines by human polarized macrophages. *Mediators Inflammation* (2019) 2019:1919538. doi: 10.1155/2019/1919538
48. Forkuo GS, Nieman AN, Kodali R, Zahn NM, Li G, Rashid Roni MS, et al. A novel orally available asthma drug candidate that reduces smooth muscle constriction and inflammation by targeting GABAA receptors in the lung. *Mol Pharm* (2018) 15(5):1766–77. doi: 10.1021/acs.molpharmaceut.7b01013
49. Boost KA, Leipold T, Scheiermann P, Hoegl S, Sadik CD, Hofstetter C, et al. Sevoflurane and isoflurane decrease TNF-alpha-induced gene expression in human monocyte THP-1 cells: potential role of intracellular IkappaBalpha regulation. *Int J Mol Med* (2009) 23(5):665–71. doi: 10.3892/ijmm.00000178
50. Bredthauer A, Geiger A, Gruber M, Pfahler SM, Petermichl W, Bitzinger D, et al. Propofol ameliorates exaggerated human neutrophil activation in a LPS sepsis model. *J Inflammation Res* (2021) 14:3849–62. doi: 10.2147/JIR.S314192
51. Lin KH, Lu WJ, Wang SH, Fong TH, Chou DS, Chang CC, et al. Characteristics of endogenous gamma-aminobutyric acid (GABA) in human platelets: functional studies of a novel collagen glycoprotein VI inhibitor. *J Mol Med (Berl)* (2014) 92(6):603–14. doi: 10.1007/s00109-014-1140-7
52. Masoodi M, Peschka M, Schmiedel S, Haddad M, Frye M, Maas C, et al. Disturbed lipid and amino acid metabolisms in COVID-19 patients. *J Mol Med (Berl)* (2022) 100(4):555–68. doi: 10.1007/s00109-022-02177-4
53. Karu N, Kindt A, van Gammeren AJ, Ermens AAM, Harms AC, Portengen L, et al. Severe COVID-19 is characterised by perturbations in plasma amines correlated with immune response markers, and linked to inflammation and oxidative stress. *Metabolites* (2022) 12(7). doi: 10.3390/metabo12070618
54. Tian J, Middleton B, Kaufman DL. GABAA-receptor agonists limit pneumonitis and death in murine coronavirus-infected mice. *Viruses* (2021) 13(6). doi: 10.3390/v13060966
55. De Albuquerque N, Baig E, Ma X, Zhang J, He W, Rowe A, et al. Murine hepatitis virus strain 1 produces a clinically relevant model of severe acute respiratory syndrome in A/J mice. *J Virol* (2006) 80(21):10382–94. doi: 10.1128/JVI.00747-06
56. Khanolkar A, Hartwig SM, Haag BA, Meyerholz DK, Epping LL, Haring JS, et al. Protective and pathologic roles of the immune response to mouse hepatitis virus type 1: implications for severe acute respiratory syndrome. *J Virol* (2009) 83(18):9258–72. doi: 10.1128/JVI.00355-09
57. Khanolkar A, Hartwig SM, Haag BA, Meyerholz DK, Hart JT, Varga SM. Toll-like receptor 4 deficiency increases disease and mortality after mouse hepatitis virus type 1 infection of susceptible C3H mice. *J Virol* (2009) 83(17):8946–56. doi: 10.1128/JVI.01857-08
58. Khanolkar A, Fulton RB, Epping LL, Pham NL, Tifrea D, Varga SM, et al. T Cell epitope specificity and pathogenesis of mouse hepatitis virus-1-induced disease in susceptible and resistant hosts. *J Immunol* (2010) 185(2):1132–41. doi: 10.4049/jimmunol.0902749
59. Caldera-Crespo LA, Paidas MJ, Roy S, Schulman CI, Kenyon NS, Daunert S, et al. Experimental models of COVID-19. *Front Cell Infect Microbiol* (2021) 11:792584. doi: 10.3389/fcimb.2021.792584
60. Korner RW, Majjouti M, Alcazar MAA, Mahabir E. Of mice and men: The coronavirus MHV and mouse models as a translational approach to understand SARS-CoV-2. *Viruses* (2020) 12(8). doi: 10.3390/v12080880
61. McCray PB Jr., Pewe L, Wohlford-Lenane C, Hickey M, Manzel L, Shi L, et al. Lethal infection of K18-hACE2 mice infected with severe acute respiratory syndrome coronavirus. *J Virol* (2007) 81(2):813–21. doi: 10.1128/JVI.02012-06
62. Moreau GB, Burgess SL, Sturek JM, Donlan AN, Petri WA, Mann BJ. Evaluation of K18-hACE2 mice as a model of SARS-CoV-2 infection. *Am J Trop Med Hyg* (2020) 103(3):1215–9. doi: 10.4269/ajtmh.20-0762
63. Rathnasinghe R, Strohmeier S, Amanat F, Gillespie VL, Krammer F, Garcia-Sastre A, et al. Comparison of transgenic and adenovirus hACE2 mouse models for SARS-CoV-2 infection. *Emerg Microbes Infect* (2020) 9(1):2433–45. doi: 10.1080/22221751.2020.1838955
64. Golden JW, Cline CR, Zeng X, Garrison AR, Carey BD, Mucker EM, et al. Human angiotensin-converting enzyme 2 transgenic mice infected with SARS-CoV-2 develop severe and fatal respiratory disease. *JCI Insight* (2020) 5(19). doi: 10.1172/jci.insight.142032
65. Winkler ES, Bailey AL, Kafai NM, Nair S, McCune BT, Yu J, et al. SARS-CoV-2 infection in the lungs of human ACE2 transgenic mice causes severe inflammation, immune cell infiltration, and compromised respiratory function. *bioRxiv* (2020). doi: 10.1101/2020.07.09.196188
66. Oladunni FS, Park JG, Pino PA, Gonzalez O, Akhter A, Allue-Guardia A, et al. Lethality of SARS-CoV-2 infection in K18 human angiotensin-converting enzyme 2 transgenic mice. *Nat Commun* (2020) 11(1):6122. doi: 10.1038/s41467-020-19891-7
67. Zheng J, Wong LR, Li K, Verma AK, Ortiz ME, Wohlford-Lenane C, et al. COVID-19 treatments and pathogenesis including anosmia in K18-hACE2 mice. *Nature* (2021) 589(7843):603–7. doi: 10.1038/s41586-020-2943-z
68. Winkler ES, Bailey AL, Kafai NM, Nair S, McCune BT, Yu J, et al. SARS-CoV-2 infection of human ACE2-transgenic mice causes severe lung inflammation and impaired function. *Nat Immunol* (2020) 21(11):1327–35. doi: 10.1038/s41590-020-0778-2
69. NCATS COVID-19 OpenData portal. Available at: <https://opendata.ncats.nih.gov/covid19/databrowser>.
70. Zhang X, Zhang R, Zheng Y, Shen J, Xiao D, Li J, et al. Expression of gamma-aminobutyric acid receptors on neoplastic growth and prediction of prognosis in non-small cell lung cancer. *J Transl Med* (2013) 11:102. doi: 10.1186/1479-5876-11-102
71. Bai D, Fang L, Xia S, Ke W, Wang J, Wu X, et al. Porcine deltacoronavirus (PDCoV) modulates calcium influx to favor viral replication. *Virology* (2020) 539:38–48. doi: 10.1016/j.virol.2019.10.011
72. Kraefft SK, Chen DS, Li HP, Chen LB, Lai MM. Mouse hepatitis virus infection induces an early, transient calcium influx in mouse astrocytoma cells. *Exp Cell Res* (1997) 237(1):55–62. doi: 10.1006/excr.1997.3768
73. Loas G, Van de Borne P, Darquennes G, Le Corre P. Association of amlodipine with the risk of in-hospital death in patients with COVID-19 and hypertension: A reanalysis on 184 COVID-19 patients with hypertension. *Pharm (Basel)* (2022) 15(3). doi: 10.3390/ph15030380
74. Sadeghpour S, Ghasemnejad-Berenji H, Pashapour S, Ghasemnejad-Berenji M. Using of calcium channel blockers in patients with COVID-19: a magic bullet or a double-edged sword? *J Basic Clin Physiol Pharmacol* (2021) 33(1):117–9. doi: 10.1515/jbcp-2021-0334
75. Zhang LK, Sun Y, Zeng H, Wang Q, Jiang X, Shang WJ, et al. Calcium channel blocker amlodipine besylate therapy is associated with reduced case fatality rate of COVID-19 patients with hypertension. *Cell Discovery* (2020) 6(1):96. doi: 10.1038/s41421-020-00235-0
76. Blanco-Melo D, Nilsson-Payant BE, Liu WC, Uhl S, Hoagland D, Moller R, et al. Imbalanced host response to SARS-CoV-2 drives development of COVID-19. *Cell* (2020) 181(5):1036–45.e9. doi: 10.1016/j.cell.2020.04.026
77. Karimabad MN, Kounis NG, Hassanshahi G, Hassanshahi F, Mplani V, Koniari I, et al. The involvement of CXCL10 motif chemokine ligand 10 (CXCL10) and its related chemokines in the pathogenesis of coronary artery disease and in the COVID-19 vaccination: A narrative review. *Vaccines (Basel)* (2021) 9(11). doi: 10.3390/vaccines9111224
78. Blot M, Jacquier M, Aho Gle LS, Beltramo G, Nguyen M, Bonniaud P, et al. CXCL10 could drive longer duration of mechanical ventilation during COVID-19 ARDS. *Crit Care* (2020) 24(1):632. doi: 10.1186/s13054-020-03328-0
79. Ravindran R, McReynolds C, Yang J, Hammock BD, Ikram A, Ali A, et al. Immune response dynamics in COVID-19 patients to SARS-CoV-2 and other human coronaviruses. *PloS One* (2021) 16(7):e0254367. doi: 10.1371/journal.pone.0254367
80. Kwon JS, Kim JY, Kim MC, Park SY, Kim BN, Bae S, et al. Factors of severity in patients with COVID-19: Cytokine/Chemokine concentrations, viral load, and antibody responses. *Am J Trop Med Hyg* (2020) 103(6):2412–8. doi: 10.4269/ajtmh.20-1110
81. Tripathy AS, Vishwakarma S, Trimbake D, Gurav YK, Potdar VA, Mokashi ND, et al. Pro-inflammatory CXCL-10, TNF-alpha, IL-1beta, and IL-6: biomarkers of SARS-CoV-2 infection. *Arch Virol* (2021) 166(12):3301–10. doi: 10.1007/s00705-021-05247-z
82. Liu M, Guo S, Hibbert JM, Jain V, Singh N, Wilson NO, et al. CXCL10/IP-10 in infectious diseases pathogenesis and potential therapeutic implications. *Cytokine Growth Factor Rev* (2011) 22(3):121–30. doi: 10.1016/j.cytogr.2011.06.001
83. Abers MS, Delmonte OM, Ricotta EE, Fintzi J, Fink DL, de Jesus AAA, et al. An immune-based biomarker signature is associated with mortality in COVID-19 patients. *JCI Insight* (2021) 6(1). doi: 10.1172/jci.insight.144455
84. Han H, Ma Q, Li C, Liu R, Zhao L, Wang W, et al. Profiling serum cytokines in COVID-19 patients reveals IL-6 and IL-10 are disease severity predictors. *Emerg Microbes Infect* (2020) 9(1):1123–30. doi: 10.1080/22221751.2020.1770129



85. Zhao Y, Qin L, Zhang P, Li K, Liang L, Sun J, et al. Longitudinal COVID-19 profiling associates IL-1RA and IL-10 with disease severity and RANTES with mild disease. *JCI Insight* (2020) 5(13). doi: 10.1172/jci.insight.139834
86. Yang AC, Kern F, Losada PM, Agam MR, Maat CA, Schmartz GP, et al. Dysregulation of brain and choroid plexus cell types in severe COVID-19. *Nature* (2021) 595(7868):565–71. doi: 10.1038/s41586-021-03710-0
87. Douaud G, Lee S, Alfaro-Almagro F, Arthofer C, Wang C, McCarthy P, et al. SARS-CoV-2 is associated with changes in brain structure in UK biobank. *Nature* (2022) 604(7907):697–707. doi: 10.1038/s41586-022-04569-5
88. Frere JJ, Serafini RA, Pryce KD, Zazhytska M, Oishi K, Golyner I, et al. SARS-CoV-2 infection results in lasting and systemic perturbations post recovery. *Biorxiv* (2022). doi: 10.1101/2022.01.18.476786
89. Crunfli F, Carregari CC, Veras FP, Henrique Vendramini P, Valença AGF, Antunes ASLM, et al. Morphological, cellular and molecular basis of brain infection in COVID-19 patients. *MedRxiv* (2020) 16. doi: 10.1101/2020.10.09.20207464
90. Virhammar J, Naas A, Fallmar D, Cunningham JL, Klang A, Ashton NJ, et al. Biomarkers for central nervous system injury in cerebrospinal fluid are elevated in COVID-19 and associated with neurological symptoms and disease severity. *Eur J Neurol* (2021) 28(10):3324–31. doi: 10.1111/ene.14703
91. Kanberg N, Ashton NJ, Andersson LM, Yilmaz A, Lindh M, Nilsson S, et al. Neurochemical evidence of astrocytic and neuronal injury commonly found in COVID-19. *Neurology* (2020) 95(12):e1754–e9. doi: 10.1212/WNL.0000000000001011
92. Lee MH, Perl DP, Nair G, Li W, Maric D, Murray H, et al. Microvascular injury in the brains of patients with covid-19. *N Engl J Med* (2021) 384(5):481–3. doi: 10.1056/NEJMc2033369
93. Johansson A, Mohamed MS, Moulin TC, Schioth HB. Neurological manifestations of COVID-19: A comprehensive literature review and discussion of mechanisms. *J Neuroimmunol* (2021) 358:577658. doi: 10.1016/j.jneuroim.2021.577658
94. Lee M, Schwab C, McGeer PL. Astrocytes are GABAergic cells that modulate microglial activity. *Glia* (2011) 59(1):152–65. doi: 10.1002/glia.21087
95. Manzano S, Agüera L, Aguilar M, Olazarán J. A review on tramiprosate (Homotaurine) in alzheimer's disease and other neurocognitive disorders. *Front Neurol* (2020) 11:614. doi: 10.3389/fneur.2020.00614
96. Aisen PS, Gauthier S, Ferris SH, Saumier D, Haine D, Garceau D, et al. Tramiprosate in mild-to-moderate alzheimer's disease - a randomized, double-blind, placebo-controlled, multi-centre study (the alphase study). *Arch Med Sci* (2010) 7(1):102–11. doi: 10.5114/aoms.2011.20612
97. Tsolaki M. Future strategies of management of alzheimer's disease. the role of homotaurine. *Hell J Nucl Med* (2019) 22 Suppl:82–94.
98. Gauthier S, Aisen PS, Ferris SH, Saumier D, Duong A, Haine D, et al. Effect of tramiprosate in patients with mild-to-moderate alzheimer's disease: exploratory analyses of the MRI sub-group of the alphase study. *J Nutr Health Aging* (2009) 13(6):550–7. doi: 10.1007/s12603-009-0106-x
99. Bossù P, Salani F, Ciaramella A, Sacchinelli E, Mosca A, Banaj N, et al. Anti-inflammatory effects of homotaurine in patients with amnesic mild cognitive impairment. *Front Aging Neurosci* (2018) 210:285. doi: 10.3389/fnagi.2018.00285
100. Oketch-Rabah HA, Madden EF, Roe AL, Betz JM. United states pharmacopeia (USP) safety review of gamma-aminobutyric acid (GABA). *Nutrients* (2021) 13(8). doi: 10.3390/nu13082742
101. Nair AB, Jacob S. A simple practice guide for dose conversion between animals and human. *J Basic Clin Pharm* (2016) 7(2):27–31. doi: 10.4103/0976-0105.177703
102. Reed L, Muench H. A simple method of estimating fifty per cent endpoints. *Am J Hyg* (1938) 27:493–7.



## OPEN ACCESS

## EDITED BY

Alfonso J. Rodriguez-Morales,  
Fundacion Universitaria Autónoma de  
las Américas, Colombia

## REVIEWED BY

Daniela Cardozo,  
State University of Campinas, Brazil  
Shetty Ravi Dyavar,  
Adicet Bio, Inc., United States

## \*CORRESPONDENCE

Min Zeng  
zengminlz@163.com  
Mao Luo  
luomao20050908@163.com

†These authors have contributed  
equally to this work

## SPECIALTY SECTION

This article was submitted to  
Viral Immunology,  
a section of the journal  
Frontiers in Immunology

RECEIVED 28 June 2022

ACCEPTED 19 October 2022

PUBLISHED 09 November 2022

## CITATION

Gao X, Fang D, Liang Y, Deng X,  
Chen N, Zeng M and Luo M (2022)  
Circular RNAs as emerging regulators  
in COVID-19 pathogenesis and  
progression.  
*Front. Immunol.* 13:980231.  
doi: 10.3389/fimmu.2022.980231

## COPYRIGHT

© 2022 Gao, Fang, Liang, Deng, Chen,  
Zeng and Luo. This is an open-access  
article distributed under the terms of  
the [Creative Commons Attribution  
License \(CC BY\)](#). The use, distribution  
or reproduction in other forums is  
permitted, provided the original  
author(s) and the copyright owner(s)  
are credited and that the original  
publication in this journal is cited, in  
accordance with accepted academic  
practice. No use, distribution or  
reproduction is permitted which does  
not comply with these terms.

# Circular RNAs as emerging regulators in COVID-19 pathogenesis and progression

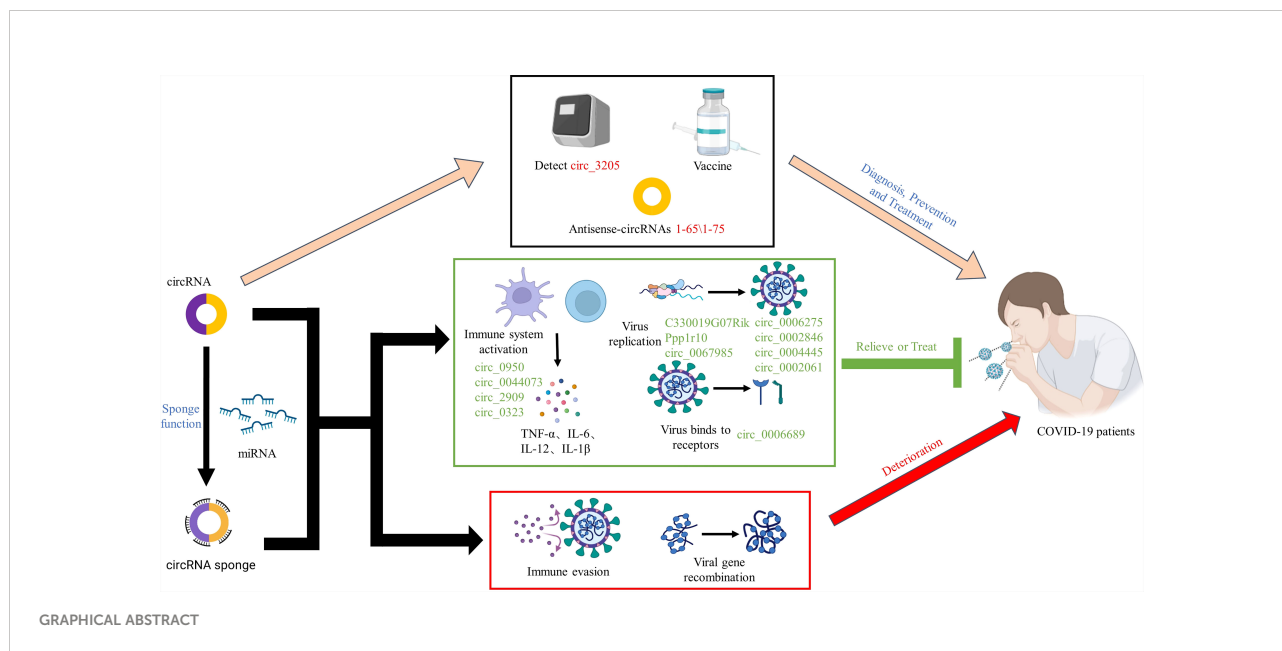
Xiaojun Gao<sup>1,2†</sup>, Dan Fang<sup>1,2†</sup>, Yu Liang<sup>3†</sup>, Xin Deng<sup>1,2</sup>,  
Ni Chen<sup>1,2</sup>, Min Zeng<sup>4\*</sup> and Mao Luo<sup>1,2,3\*</sup>

<sup>1</sup>Key Laboratory of Medical Electrophysiology, Ministry of Education, Drug Discovery Research Center, Southwest Medical University, Luzhou, Sichuan, China, <sup>2</sup>Laboratory for Cardiovascular Pharmacology, Department of Pharmacology, School of Pharmacy, Southwest Medical University, Luzhou, Sichuan, China, <sup>3</sup>College of Integrated Traditional Chinese and Western Medicine, Affiliated Hospital of Traditional Chinese Medicine, Southwest Medical University, Luzhou, Sichuan, China, <sup>4</sup>Department of Pharmacy, the Affiliated Hospital of Southwest Medical University, Luzhou, Sichuan, China

Coronavirus disease 2019 (COVID-19), an infectious acute respiratory disease caused by a newly emerging RNA virus, is a still-growing pandemic that has caused more than 6 million deaths globally and has seriously threatened the lives and health of people across the world. Currently, several drugs have been used in the clinical treatment of COVID-19, such as small molecules, neutralizing antibodies, and monoclonal antibodies. In addition, several vaccines have been used to prevent the spread of the pandemic, such as adenovirus vector vaccines, inactivated vaccines, recombinant subunit vaccines, and nucleic acid vaccines. However, the efficacy of vaccines and the onset of adverse reactions vary among individuals. Accumulating evidence has demonstrated that circular RNAs (circRNAs) are crucial regulators of viral infections and antiviral immune responses and are heavily involved in COVID-19 pathologies. During novel coronavirus infection, circRNAs not only directly affect the transcription process and interfere with viral replication but also indirectly regulate biological processes, including virus-host receptor binding and the immune response. Consequently, understanding the expression and function of circRNAs during severe acute respiratory syndrome coronavirus 2 (SARS-CoV-2) infection will provide novel insights into the development of circRNA-based methods. In this review, we summarize recent progress on the roles and underlying mechanisms of circRNAs that regulate the inflammatory response, viral replication, immune evasion, and cytokines induced by SARS-CoV-2 infection, and thus highlighting the diagnostic and therapeutic challenges in the treatment of COVID-19 and future research directions.

## KEYWORDS

COVID-19, circRNAs, inflammatory response, biological regulator, vaccine



## Introduction

Coronavirus disease 2019 (COVID-19) is an infectious acute respiratory disease caused by severe acute respiratory syndrome coronavirus 2 (SARS-CoV-2) (1). As of 18 July 2022, the cumulative number of cases reported globally is now over 500 million, and the cumulative number of deaths exceeds 6 million. The rapid spread of the provirus strain of SARS-CoV-2 has seriously threatened the lives and health of people across the world, and it certainly caught most of the population completely off-guard and forever changed their lives (2). In times of global pandemic, there is an urgent need for prophylactic vaccines and therapeutic drugs to protect individuals from COVID-19 and to help abate the growing epidemic (1). Currently, several drugs have been used in the clinical treatment of COVID-19, including small molecules (SARS-CoV-2 Mpro inhibitors), neutralizing antibodies (casirivimab and imdevimab), and monoclonal antibodies (tocilizumab) (3–6). In addition, some vaccines have been used to prevent the spread of the pandemic, such as adenovirus vector vaccines (VAXZEVRIA, COVISHIELD™), inactivated vaccines (inactivated COVID-19 vaccine (Vero Cell), CoronaVac), recombinant subunit vaccines (COVOVAX™), and nucleic acid vaccines (COMIRNATY®). However, the efficacy of vaccines and the onset of adverse reactions vary among individuals (7). Therefore, it is desperately important to develop safe and effective drugs and vaccines to prevent, diagnose and treat COVID-19.

Circular RNAs (circRNAs) are a large class of abundant, stable and ubiquitous noncoding RNA molecules having a covalently closed loop structure generated from back-splicing

of pre-mRNA transcripts. By acting as microRNA (miRNA) sponges, RNA-binding protein sponges, regulating transcription and translating to proteins, circRNAs have recently shown huge capabilities as gene regulators at transcriptional or post-transcriptional levels in the pathogenesis of various diseases, such as viral infections. Accumulating evidence indicates that circRNAs are crucial regulators of viral infections and antiviral immune responses and are heavily involved in COVID-19 pathologies (8–20). During novel coronavirus infection, circRNAs not only directly affect the transcription process and interfere with viral replication but also indirectly regulate biological processes, such as virus-host receptor binding and the immune response (21). However, the characteristics and functional mechanisms of circRNAs in COVID-19 remain unclear. This review focuses on the roles of circRNAs in regulation of the inflammatory response, viral replication, immune evasion, and cytokines induced by SARS-CoV-2 infection, exploring the underlying regulatory mechanisms, and thus highlighting the prospects and challenges in circRNA applications.

## Pathogenesis of SARS-CoV-2 and regulation of related circRNAs

### Structure and pathogenesis of SARS-CoV-2

Coronaviruses (CoVs) are the largest, enveloped, single-stranded positive-sense RNA virus belonging to the Coronaviridae family (22, 23) and have been divided into four

genera:  $\alpha$ -coronavirus,  $\beta$ -coronavirus,  $\gamma$ -coronavirus, and  $\delta$ -coronavirus. Additionally,  $\beta$ -coronavirus is further subdivided into four different lineages: A, B, C, and D (24, 25). Genetic sequence analysis has revealed that SARS-CoV-2 and SARS-CoV-1 can be classified into the B lineage, while the Middle East respiratory syndrome coronavirus (MERS-CoV) with lower homology belongs to the C lineage (26, 27). Furthermore, these CoVs possess cis-acting secondary RNA structures flanked by 5' and 3' untranslated regions, which are essential for RNA synthesis (28). At the 5'-terminal region, two-thirds of the genomic RNA constitutes two open reading frames (ORF1a and ORF1b), which are involved in encoding nonstructural proteins (nsps) in the viral life cycle. One-third of the genome RNAs of the 3'-end are involved in encoding structural proteins, including spike (S), envelope (E), membrane (M), and nucleocapsid (N) proteins, as well as eight accessory proteins (28–30). Although SARS-CoV-1, MERS-CoV, and SARS-CoV-2 share a large number of similarities in cytopathic effects on host cells, there are fundamental differences in their structures and modes of replication due to sequence divergence. The S protein mediates attachment of the virus to host cell surface receptors and is the first and essential step in CoV infection. However, both SARS-CoV-1 and SARS-CoV-2 enter host cells by using membrane-bound angiotensin-converting enzyme 2 (ACE2) as a primary receptor, while MERS-CoV enters host cells by binding to the dipeptidyl peptidase 4 (DPP4) receptor (31). Furthermore, in addition to relying on cell-surface transmembrane serine protease 2 (TMPRSS2), SARS-CoV-1 entry into host cells also relies on the assistance of cysteine cathepsin B (CatB) and cysteine cathepsin L (CatL), while the invasion of SARS-CoV-2 depends only on TMPRSS2 (32, 33). Moreover, several studies have found that SARS-CoV-1 mainly enters cells by binding to the ACE2 receptor in the lower respiratory tract tissue of the host, whereas SARS-CoV-2 mainly replicates in the upper respiratory tract epithelium (34, 35).

Recent studies have shown that ciliated bronchial epithelial cells and type II alveolar cells are the primary targets of SARS-CoV-2 (36). As shown in Figure 1, when SARS-CoV-2 attaches to host cells, its S1 protein binds to the ACE2 receptor on the surface of the host cells. At the same time, the master regulator of endocytosis, AP2-associated kinase 1 (AAK1), triggers endocytosis for smooth virus entry into host cells. However, loss of AAK1 leads to interruption of virus particle assembly and entry of the virus into susceptible host cells (36). After entering cells, SARS-CoV-2 hijacks the endogenous transcriptional machinery of host cells to replicate and disseminate within the host. First, the RNA of SARS-CoV-2 encodes 2 long polyproteins and 4 structural proteins, of which the polyproteins are hydrolysed by proteases to generate short nsps, which promote viral replication and induce rapid cellular decay (37, 50). The major histocompatibility complex (MHC) class I-mediated antigen presentation is an ubiquitous process by which cells present endogenous proteins to CD8+ T lymphocytes during immune surveillance and response and plays a critical role in antiviral

immunity. A recent study by Yoo J et al. showed that the MHC class I pathway is targeted by SARS-CoV-2 (39). Moreover, the induction of the MHC class I pathway is inhibited by SARS-CoV-2 infection. MHC class I contributes towards antiviral immunity by facilitating the presentation of viral antigens to CD8 cytotoxic T cells. Consequently, activated CD8 cytotoxic T cells specifically eliminate virus-infected cells (40–43). In addition, the ability of B lymphocytes to capture external antigens and present them as peptide fragments, loaded on MHC class II molecules, to CD4+ T cells is a crucial part of the adaptive immune response. The ability to activate CD4+ T cells is restricted to antigen-presenting cells that are endocytosed and processed in lysosomes for presentation on MHC class II molecules, which can transduce signals required for B-cell activation. Moreover, MHC class II antigen presentation by B lymphocytes is a multistep process involving in the presentation of MHC II-peptide complexes to CD4+ T cells (44–47). Although the host's innate immune system works against the virus particles in this process, a small number of viruses still escape, and the RNAs released by these viruses are captured and identified by toll-like receptors (TLRs). Subsequently, activated TLRs further induce cellular autoimmunity, resulting in a series of immune response processes, such as protein complex formation, transcription factor (TF) migration to the nucleus, and proinflammatory cytokine expression (48, 49, 51). Furthermore, several recent studies have demonstrated that SARS-CoV-2 not only directly damages lung tissue but also triggers a cytokine storm, which leads to a sharp increase in cytokines and hyperactivation of immune cells, causing diffuse alveolar damage and exacerbating respiratory failure in patients and even potentially causing uncontrollable systemic inflammatory responses (SIRS) (52).

## Differential expression of related circRNAs

Increasing studies have shown that circRNAs can be used as biomarkers and therapeutic targets in multiple viral diseases, as their abnormal levels may be considered to indicate the stage of pathology and prognosis (53, 54). CircRNAs encoded by viruses might play an important role in host-virus interactions by regulating viral and host gene expression. The study of changes in the expression levels of circRNAs will help us to further understand the mechanism of CoV entry into host cells and how to prevent and treat any secondary symptoms. CircRNAs encoded by CoVs are essential components of the CoV transcriptome and have the potential ability to encode circRNAs exerting different functions in host cells. The dynamic expression of these circRNAs may regulate host gene expression at different times to influence virus pathogenicity. For example, Cai Z et al. (15) identified 28754, 720, and 3437 virus-encoded circRNAs from Calu-3 cells infected with MERS-CoV, SARS-CoV-1, and SARS-CoV-2, respectively. Moreover, the expression levels of

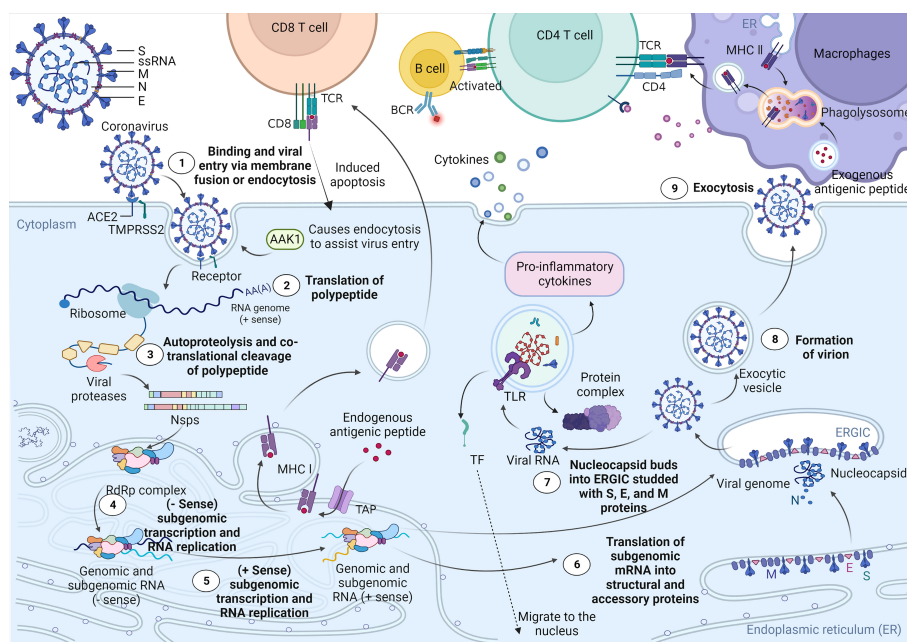


FIGURE 1

Cell entry mechanism and life cycle of SARS-CoV-2. SARS-CoV-2 virions consist of structural proteins, including spike (S), envelope (E), membrane (M), and nucleocapsid (N) proteins. When in contact with host cells, the S protein of SARS-CoV-2 specifically interacts with cellular receptors [such as angiotensin-converting enzyme 2 (ACE2)] and host factors [such as the cell surface serine protease TMPRSS2 and major endocytosis regulator AP2-related protein kinase 1 (AAK1)] to promote viral uptake and fusion at the cellular or endosomal membranes (37, 38). Following entry, viral genomic RNA is released into the cytoplasm and translated into polypeptides, which are subsequently hydrolysed and cotranslationally cleaved by proteases to generate nonstructural proteins (nsps). nsps further form RNA-dependent RNA polymerase (RdRP) complexes in the endoplasmic reticulum. Subsequently, the RdRP complex is involved in the transcription and RNA replication of the -sense subgenome and the +sense subgenome. Translation of the -sense and +sense subgenomes further enables the synthesis of structural and accessory proteins at the endoplasmic reticulum membrane. At the same time, the nucleocapsid buds into an ER-Golgi intermediate compartment (ERGIC) filled with S, E, and M proteins. Finally, virions are secreted from infected cells via exocytosis. As a result, MHC class I contributes towards antiviral immunity by facilitating the presentation of viral antigens to CD8 cytotoxic T cells. Moreover, the ability of antigen-presenting cells to capture external antigens and present them as peptide fragments, loaded on MHC class II molecules, which can transduce signals required for B-cell activation, to CD4+ T cells is a crucial part of the adaptive immune response (39–47). In addition, the RNA released by the virus is captured and recognized by the pattern recognition receptor (TLR) located on the endosomal membrane. Subsequently, TLR activates and induces further self-immunity of cells, resulting in the formation of protein complexes, the migration of transcription factors (TFs) to the nucleus, and the expression of proinflammatory cytokines (48, 49).

MERS-CoV-encoded circRNAs were significantly higher than those encoded by SARS-CoV-1 and SARS-CoV-2 circRNAs. The results revealed that the expression level of certain circRNAs was increased in the late stage of viral infection compared to the early stage. Interestingly, another study came to a different conclusion. Yang S et al. (17) predicted 351, 224, and 2764 circRNAs derived from SARS-CoV-2, SARS-CoV, and Middle East respiratory syndrome coronavirus, respectively. Moreover, 75 potential SARS-CoV-2 circRNAs were identified from RNA samples extracted from SARS-CoV-2-infected Vero E6 cells. These results suggest that virus-encoded circRNAs have strong cell and tissue specificity and play critical roles in autoimmune diseases and viral pathogenesis.

Currently, multiple studies based on bioanalysis have found a variety of dynamically expressed host-encoded circRNAs associated with SARS-CoV-2 infection. Yang M et al. (16)

found 42 host-encoded circRNAs that were significantly dysregulated, of which 17 were upregulated and 25 were downregulated in SARS-CoV-2-infected human lung epithelial cells. Dysregulated circRNAs can regulate mRNA stability, immunity, and cell death by binding specific proteins and indirectly regulate gene expression by absorbing their targeted miRNAs. Notably, this result is consistent with that obtained by Zhang X et al. (18) who demonstrated that the proportion of differentially expressed (DE) circRNAs was very low (4/35056, 0.01%) at 6 hpi and was significantly increased (1567/46569, 3.4%) at 24 hpi in MERS-CoV-infected vs. mock-infected Calu-3 cells. Moreover, 1267 DE circRNAs were identified when comparing MERS-CoV-infected samples at 6 and 24 hpi. These results suggest that the DE circRNAs have potential biological functions during CoV infection, especially in the late stage of CoV infection. Additionally, Wu Y et al. (11) identified 570 DE



circRNAs, of which 155 were upregulated and 415 were downregulated, in the peripheral blood of COVID-19 patients. Further analysis showed that these circRNAs could negatively affect the normal physiological activities of the body by regulating host cell immunity and inflammation, substance and energy metabolism, cell cycle progression and apoptosis. Collectively, both virus-encoded circRNAs and host-encoded circRNAs are progressively expressed during virus infection, thereby affecting the infection process, but the specific roles and mechanisms remain unclear. As shown in **Supplementary Table 1**, we summarize the key viral and host cell circRNAs and role in COVID-19, SARS and MERS pathogenesis to provide a theoretical basis for further understanding the changes in the expression level of CoV-associated circRNAs and their roles in pathogenesis and virus replication.

## Potential mechanisms of circRNAs in SARS-COV-2 infection

### Sponging of miRNAs by circRNAs affects viral replication

CircRNAs are highly evolutionarily conserved across species with cell-specific and tissue-specific characteristics (57–60). As

an integral part of the competing endogenous RNA (ceRNA) network, circRNAs containing miRNA-responsive elements can regulate downstream target gene expression by acting as microRNA (miRNA) sponges to quickly bind the respective miRNAs and release the inhibitory effect of miRNAs on messenger RNA (mRNA) translation. Remarkably, circRNAs containing miRNA-responsive elements can act as miRNA sponges through the ceRNA network to prevent miRNA-mediated regulation of target genes (61, 62). Moreover, the sponge functions of circRNAs have been confirmed to be more efficient than those of linear miRNAs and long noncoding RNA (lncRNA) transcripts (63, 64). A recent study by Arora S et al. (65) identified a ceRNA network consisting of one miRNA (MMU-miR-124-3p), one lncRNA (Gm26917), one TF (Stat2), one mRNA (Ddx58), and two circRNAs (Ppp1r10, C330019G07Rik) in SARS-CoV-1-infected cells. As shown in **Figure 2A**, the RIG-I/Ddx58 receptor in the ceRNA network has a helicase domain that interacts with SARS-CoV-1 nsp13 and initiates the viral life cycle. In addition, Ddx58 is involved in the mRNA splicing process and miRNA biogenesis, and its upregulation leads to reprogramming of miRNA splicing events, thereby downregulating the miRNA expression. Overexpression of miR-124-3p leads to the degradation of Ddx58, resulting in a reduction in viral replication. Furthermore, miR-124-3p has been shown to modulate TLR-

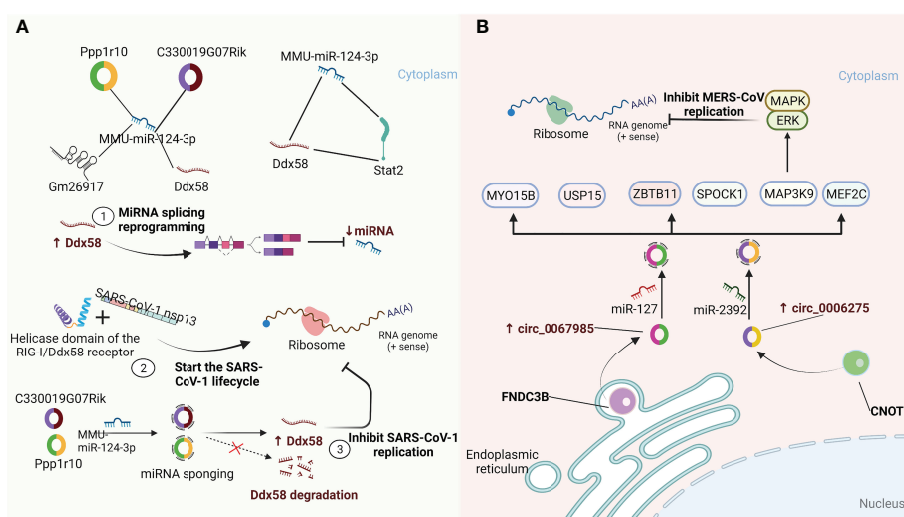


FIGURE 2

CircRNAs function as miRNA sponges to influence viral replication. **(A)** A quintuple ceRNA network exists in SARS-CoV-1 infection that includes one miRNA (MMU-miR-124-3p), one lncRNA (Gm26917), one TF (Stat2), one mRNA (Ddx58) and two circRNAs (Ppp1r10, C330019G07Rik). They form a closed 3-node miRNA feed-forward loop and a 4-node ceRNA network, respectively. Upregulation of Ddx58 leads to reprogramming of miRNA splicing events, resulting in downregulation of miRNA expression. Meanwhile, the helicase domain of the RIG-I/Ddx58 receptor can interact with SARS-CoV-1 nonstructural protein 13 (NSP13) to initiate the viral life cycle. Furthermore, Ppp1r10 and C330019G07Rik act as sponges for miR-124-3p, inhibiting miR-124-3p expression, which in turn impedes Ddx58 degradation and further inhibits SARS-CoV-1 replication (65). **(B)** circ\_0067985 derived from the FNDC3B gene and circ\_0006275 derived from the CNOT1 gene serve as miR-127 and miR-2392 sponges, respectively, to regulate the downstream expression of MAP3K9, MYO15B, SPOCK1, MEF2C, USP15 and ZBTB11. Of these, the upstream regulator of the MAPK pathway, MAP3K9, further regulates the downstream ERK/MAPK pathway to inhibit MERS-CoV replication (18).

mediated innate immune responses by targeting Stat3 and reducing IL-6 and TNF- $\alpha$  expression (66). These results suggest that miR-124-3p may also play a similar role in regulating Stat2 to affect the viral life cycle. Importantly, in this ceRNA regulatory network, two circRNAs (Ppp1r10 and C330019G07Rik) play vital regulatory roles as sponges of miR-124-3p to hinder the degradation of Ddx58, which in turn affects the replication of SARS-CoV-1. In addition, Zhang X et al. (18) found that host circRNAs mainly function as sponges of miRNAs to affect MERS-CoV replication. As shown in **Figure 2B**, hsa\_circ\_0067985 is derived from the gene FNDC3B and acts as a sponge of hsa-miR-1275, and hsa\_circ\_0006275 is derived from the gene CNOT1 and serves as a sponge of hsa-miR-2392, both of which are significantly upregulated in MERS-CoV infection and thus regulate the expression of representative downstream targets, including MAP3K9, MYO15B, SPOCK1, MEF2C, USP15, and ZBTB11. Collectively, these results provide new insights into the regulation of circRNAs and their related signalling pathways as host-targeted antiviral strategies against SARS-CoV-2 infection.

## CircRNAs in regulation of the immune response in SARS-CoV-2 infection by affecting cytokines

CircRNAs can effectively prevent the virus from damaging the body by mediating the immune response process of the host-virus interaction (67). A study by Li X et al. (9) found that NF90/NF110 produced from human interleukin-enhanced binding factor 3 (ILF3) directly regulate back-splicing and coordinate with circRNA production in response to viral infection. The nuclear export of NF90/NF110 upon viral infection contributed in part to a decrease in circRNA production. Moreover, NF90/NF110-circRNP accumulation in the cytoplasm may influence the host immune response. The findings also indicated that circRNAs compete with viral mRNAs for binding to NF90/NF110, and circRNAs may act as a molecular reservoir of NF90/NF110 for a prompt immune response upon viral infection (9, 68). In addition, Chen YG et al. (69) found that circRNAs composed of self-splicing introns can bind to the receptor retinoic acid-inducible gene I (RIG-I) to effectively activate immune signal transduction in the context of viral infection. A recent study also indicated that the overexpressed hsa\_circ\_0000479 in COVID-19 patients may regulate the expression of IL-6 and RIG-I by sponging hsa-miR-149-5p (55). Additionally, regulation of immune responses by circRNAs generally involves the transduction of signalling pathways and the production of cytokines. A recent comprehensive protein transcription analysis indicated that epidermal growth factor receptor (ErbB), hypoxia-inducible factor-1 (HIF-1), mammalian leukaemia target of rapamycin

(mTOR) and tumour necrosis factor (TNF) signalling pathways, among others, were markedly modulated during the course of SARS-CoV-2 infection (70). The parental genes of DE circRNAs enriched in these pathways are associated with numerous antiviral signalling pathways, such as interferon (IFN), chemokines, mitogen-activated protein kinases (MAPKs), and RIG-I-like receptors (58), indicating that circRNAs play regulatory roles in cell signal transduction and immune-inflammatory response during SARS-CoV-2 infection.

Cytokines are small molecular polypeptides or glycoproteins synthesized and secreted by a variety of cell types, participating in many physiological processes including the regulation of immune and inflammatory responses. Cytokines have been shown to act as immunomodulators involved in autocrine, paracrine and endocrine signaling, and play important roles in the immune response to host-viral infection (71, 72). Moreover, viral infection can lead to the production of cytokines that have a crucial role in control of the immune response and anti-viral defence, as well as in the capacity of target cells to support virus replication (73). Several recent studies have found that SARS-CoV-2 infection triggers an autoimmune response by activating certain immune factors, such as 2'-5' oligoadenylate synthase (OAS1-3), interferon-inducible protein (Ifit1-3), and the T helper cell type 1 (Th1) chemokines CXCL9/10/11, and reducing the transcription of ribosomal proteins (74). A previous study showed that the activation of OAS requires the participation of viral genome dsRNA, which combines to generate 2'-5' oligoadenylate (2'-5'A). Furthermore, 2'-5'A exerts antiviral effects by significantly increasing the activity of RNase L to degrade viral RNA and interfere with viral protein synthesis (75). Liu CX et al. (76) found that endogenous circRNAs tend to form imperfect short (16–26 bp) RNA duplexes and act as inhibitors of dsRNA-activated Protein Kinase R (PKR) associated with innate immunity. Moreover, circRNAs can be globally degraded by the endonuclease RNase L to activate the PKR antiviral pathway. As shown in **Figure 3**, these results indicate that circRNAs may modulate the immune response in SARS-CoV-2 infection by affecting cytokines.

## Potential mechanism of action of circRNAs in inflammation

Inflammation involves a set of biologic mechanisms that evolved in multicellular organisms to contain invasive pathogens and resolve injuries by activating innate and adaptive immune responses, which require a balance between sufficient cytokine production to eliminate pathogens and avoidance of a hyperinflammatory response that causes collateral damage (77). Remarkably, cytokine storm is closely associated with overproduction of a series of proinflammatory cytokines and poor prognosis, which is related to inflammatory signalling in the pathway regulated by circRNAs, as shown in

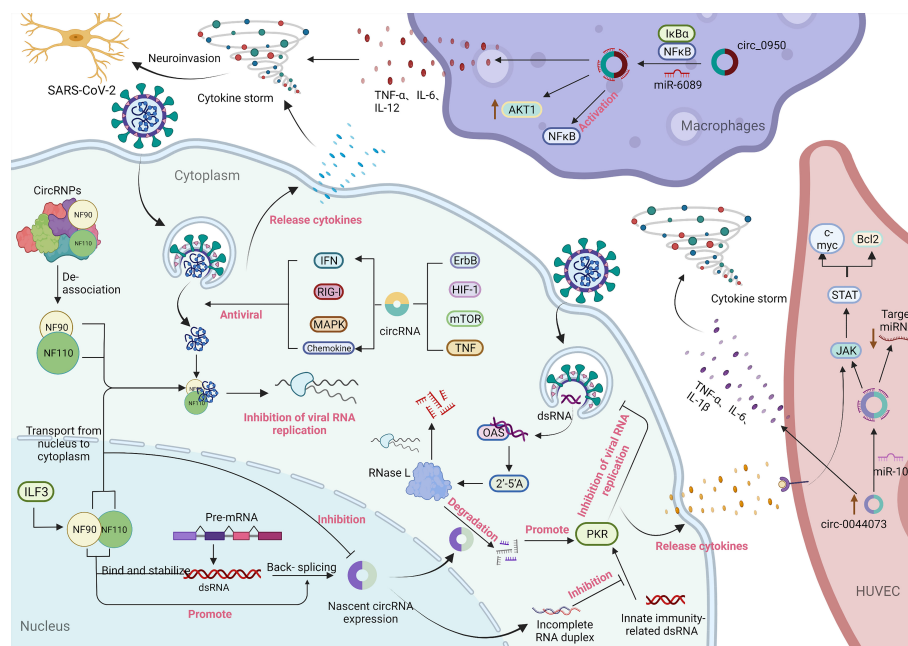


FIGURE 3

Immune response involving circRNAs in SARS-CoV-2 infection and the potential mechanism of circRNAs in inflammation. During virus infection, nuclear factor 90 (NF90) and its 110 (NF110) isoform produced by interleukin-enhanced binding factor 3 (ILF3) bind to viral mRNA to inhibit virus replication through two pathways: transport from the nucleus to the cytoplasm and decoupling from the circRNA-protein complex (CircRNPs) in the cytoplasm. Among them, the transport of NF90/NF110 from the nucleus to the cytoplasm can reduce the expression of circRNAs. In contrast, the binding of NF90/NF110 to dsRNA formed during pre-mRNA processing can not only stabilize the RNA duplex but also promote reverse splicing to form circRNA (57). 2'-5' Oligoadenylate (2'-5'A) is generated by the combination of 2'-5' oligoadenylate synthase (OAS) and viral genome dsRNA and plays an antiviral effect by significantly increasing the activity of RNase L to degrade viral RNA and interfere with viral protein synthesis. Endogenous circRNAs often form incomplete RNA duplexes and act as inhibitors of PKR activation by dsRNAs associated with innate immunity. Meanwhile, circRNAs can be globally degraded by the endonuclease RNase L to activate the PKR antiviral pathway (77). In addition, parental genes enriched for differentially expressed circRNAs in signalling pathways that are significantly regulated upon SARS-CoV-2 infection are associated with multiple antiviral signalling pathways (16, 74, 78). The generation of a cytokine storm is related to the overproduction of proinflammatory cytokines mediated by circRNAs. In macrophages, circ\_09505 acts as a sponge of miR-6089 through the IκBα/NFκB signalling pathway, on the one hand, promoting the expression of AKT1 in macrophages and the activation of NF-κB, and on the other hand, promoting the production of the proinflammatory cytokines TNF-α, IL-6 and IL-12 (79). Furthermore, circ\_0044073 in HUVECs functions as a miR-107 sponge to downregulate the expression levels of target mRNAs, while activation of the JAK/STAT signalling pathway enhanced the expression of the downstream proteins Bcl2 and c-myc. Moreover, circ\_0044073 significantly upregulated the levels of the proinflammatory cytokines IL-1β, IL-6 and TNF-α (80). In addition, the occurrence of a cytokine storm disrupts the balance of proinflammatory and anti-inflammatory mechanisms, thereby invading the patient's nervous system (81, 82).

**Figure 3.** A study by Yang J et al. (83) demonstrated that the expression of circ\_09505 in arthritic (RA) mice was positively correlated with the life cycle of macrophages. Circ\_09505 sponges miR-6089 to promote the expression of AKT1 and activate nuclear factor-κB (NF-κB) in macrophages through the IκBα/NFκB signalling pathway, thereby promoting macrophage inflammation. Furthermore, circ\_09505 functions as a sponge of miR-6089 in macrophages to promote the production of proinflammatory cytokines, such as TNF-α, IL-6, and IL-12. Numerous studies have demonstrated that activation of the NF-κB pathway plays a pivotal regulatory role in the development of SARS-CoV-2-induced inflammation (84–88). Collectively, these findings may provide novel insights into the mechanism underlying circRNAs in the regulation of the IκBα/NFκB signalling

pathway as a potential therapeutic target for the initial symptoms of inflammation in COVID-19 patients.

Additionally, a study by Shen L et al. (79) found that circ\_0044073 was upregulated in chronic inflammation of the arterial vessel wall and promoted the proliferation of human vascular cells by acting as a sponge for miR-107. The study further found that overexpressed circ\_0044073 in vascular cells reduced the expression levels of miR-107 target mRNAs and activated the JAK/STAT signalling pathway, thereby enhancing the expression of downstream proteins, such as Bcl2 and c-myc. The JAK/STAT pathway has been shown to be activated downstream of various cytokines during cytokine storms and that is involved in promoting inflammation, proliferation, migration, and adhesion of vascular cells (80). Furthermore, circ\_0044073 can significantly increase the levels of

proinflammatory cytokines, such as IL-1 $\beta$ , IL-6, and TNF- $\alpha$ . These findings suggested that SARS-CoV-2 disrupts the balance between proinflammatory and anti-inflammatory mechanisms by promoting the occurrence of a cytokine storm *via* the specific regulations of circRNAs pathways, which in turn leads to cardiovascular inflammation in patients with COVID-19.

## Regulatory roles of circRNAs in immune evasion

The innate immune response can effectively prevent the virus from invading the host. However, the virus has evolved the ability to evade the host immune response. As shown in **Figure 4**, viral nucleic acid intermediates and released genomic RNAs during the proliferation of SARS-CoV-2 can be recognized by TLRs and RIG-I-like receptors (RLRs), thereby activating the body's immune pathways to produce immune factors, such as IFN-I, IFN-III, and numerous ISGs. ISGs have general antiviral effects, however, the proviral effects of ISG15 may lead to the generation of autocrine loops that ultimately induce viral drug resistance by amplifying and prolonging their secretion (89, 94).

In addition, a study by Arora S et al. (65) demonstrated that SARS-CoV-1 may reprogram splicing events by inducing the cytoplasmic translocation of DROSHA (an enzyme involved in miRNA biogenesis) to generate another circRNA that can act as a sponge for miR-124-3p and hinder its degradation of Ddx58, thereby evading ISG-mediated antiviral effects (90). Furthermore, SARS-CoV-1 can enhance viral replication by confiscating the helicase in Ddx58 independent of interferon-related pathways.

Several recent studies have found that SARS-CoV-2 can further evade immune responses by mutating its S protein on the basis of its S protein shielding immune factor clearance, which can greatly promote the spread of SARS-CoV-2 in the population (91, 95). Recent studies have shown that circRNAs play a key role in the immune evasion and replication of SARS-CoV-2. For example, Zaffagni M et al. (92, 96) found that SARS-CoV-2 Nsp14 mediates the effects of viral infection on the host cell transcriptome. Nsp14 altered the splicing of more than 1000 genes and resulted in a dramatic increase in the number of circRNAs that were linked to innate immunity. Furthermore, a recent study by Hassanin A et al. (97) indicated that viral circRNAs are involved in the mechanism of genome recombination, which may cause virion mutation leading to

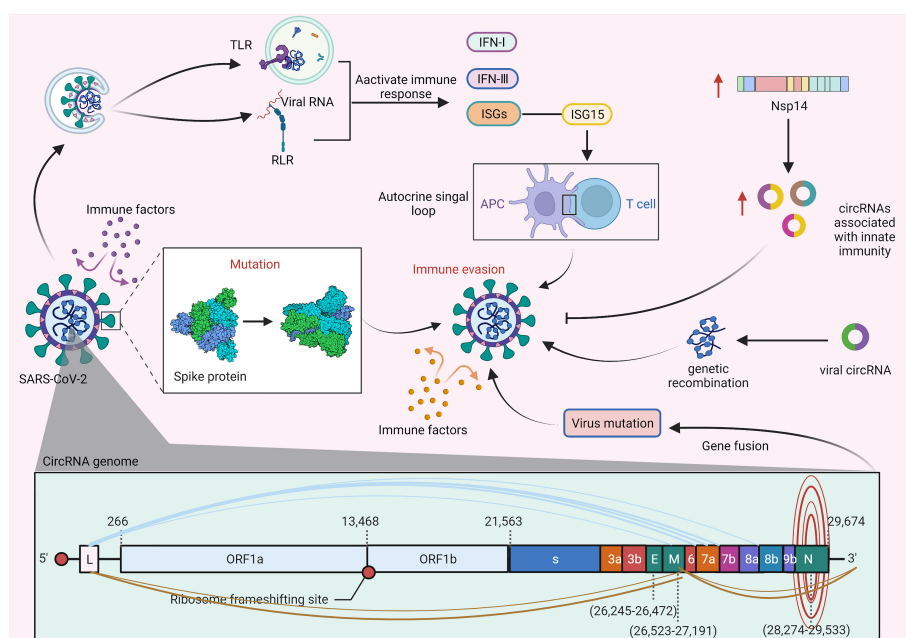


**FIGURE 4**

CircRNAs regulate immune evasion of SARS-CoV-2. During SARS-CoV-2 proliferation, genomic RNAs are recognized by TLR receptors and pattern recognition receptors (RLRs) and subsequently activate immune responses. The proviral action of the immune factor ISG15 leads to the generation of an autocrine loop, which amplifies and prolongs autocrine signalling and ultimately induces viral drug resistance (89, 90). Furthermore, the S protein of SARS-CoV-2 can prevent the virus from being cleared by immune factors, and mutation of the S protein will further enhance the ability of the virus to evade immune responses (91, 92). In addition, the expression of viral nsp14 can upregulate the levels of circRNAs related to innate immunity, thereby inhibiting viral replication and immune evasion (93). Likewise, viral circRNAs may be involved in the mechanism of genome recombination, resulting in mutation of virions leading to immune evasion. There are various types of gene fusions in the circRNA genome of SARS-CoV-2, which may cause the virus to mutate and evade immunity.



immune evasion. In addition, a study by Yang S et al. (17, 98) found that abundant and diverse circRNAs are generated by SARS-CoV-2, SARS-CoV and MERS-CoV and represent a novel type of circRNA that differs from circRNAs encoded by DNA genomes, and forward splice junctions (FSJs) representing noncanonical “splicing” events were detected in these circRNA genome sequences. Furthermore, the study also reported the existence of alternative back-splicing events in SARS-CoV-2 circRNAs that share either 5' or 3' breakpoints. Several studies have reported that gene fusion is closely related to the occurrence and development of various diseases, and thus, fused genes may be potential drug targets. Accordingly, atypical fusions in the SARS-CoV-2 transcriptome may provide conditions for the generation of viral mutation as well as viral survival and immune evasion in infected tissues.

## Prospects of the clinical application of circRNAs in COVID-19

### CircRNAs as diagnostic biomarkers for COVID-19 detection

CircRNAs are resistant to RNase R degradation and have a longer half-life, and their expression patterns are affected by viral infection. Several studies have demonstrated that circRNAs are abundant in the circulatory system of COVID-19 patients and may be reliable biomarkers of disease progression or prognosis (15–17). A study by Wu Y et al. (11) found that 114 DE circRNAs in SARS-CoV-2-infected peripheral blood were associated with exosomes, which could not only promote infection but also activate the body's immune response (99, 100). Moreover, recent studies have demonstrated that exosomes may be a key factor in the recurrence of COVID-19 (101). Importantly, since exosomes can reflect the pathological state of the cells from which they originate, they can be used as diagnostic markers of various diseases. Thus, identification and isolation of exosome-related circRNAs may be helpful for the diagnosis of COVID-19.

In addition, a recent study found that virus-encoded circRNAs in SARS-CoV-2 infection downregulated genes related to cholesterol, alcohol, sterol, and fatty acid metabolic processes and upregulated genes associated with cellular responses to oxidative stress at the later stage of virus infection (15). Barbagallo D et al. (56) found that circ\_3205 encoded by SARS-CoV-2 serves as a sponge of hsa-miR-298, thereby targeting downstream KCNMB4 and PRKCE mRNAs to promote the development of COVID-19. Furthermore, circ\_3205 was only expressed in positive samples, and its expression was positively correlated with S protein mRNA and SARS-CoV-2 viral load, suggesting that circ\_3205 could be used as a diagnostic marker for COVID-19. More importantly, the

dysregulation of circRNAs may reflect physiological and pathological changes in each human body. For example, host circRNAs formed by nonsequential back-splicing in SARS-CoV-2-infected Calu-3 cells are widely and abundantly expressed in human lung epithelial cells compared to normal Calu-3 cells (16, 102). Zhang X et al. (18) found that differential expression of circRNAs in the circRNA-miRNA-mRNA network leads to the disturbance of a series of biological processes in MERS-CoV-infected Calu-3 and HFL cells. Overall, it is suggested that monitoring the expression level of circRNAs may provide a new reference index for diagnosis and prognosis determination in COVID-19 patients (103).

### CircRNAs as potential therapeutic targets for COVID-19

Since the outbreak of COVID-19, a wealth of studies have shown that angiotensin-converting enzyme 2 (ACE2) is a recognized receptor for SARS-CoV-2 entry into host cells. Therefore, regulating the ACE2 gene promoter to interfere with the transcription and production of ACE2 may be a new approach to preventing the virus from binding to host cells to prevent COVID-19. Previous studies have shown that sex-determining region Y (SRY) can inhibit ACE2 promoter activity, thus increasing angiotensinogen, renin, and ACE gene promoter activity (104). Furthermore, a recent study by Wang D et al. (105) indicated that there are 24 common transcription factor binding sites in the conserved region of the ACE2 gene promoter, including SRY, HNF-1, IRF, AP-1, YY1, and c-Jun. Previous studies have revealed that SRY transcripts mainly exist in the form of circRNA molecules, which account for more than 90% of all SRY transcripts (106, 107). Moreover, recent studies have also demonstrated that circRNAs can participate in the regulation of SRY-box transcription factors through the ceRNA network thereby regulating the expression of downstream target genes (108–110). Remarkably, several studies have found significant gender differences in the incidence of COVID-19, with males having significantly higher rates than females. Consequently, circRNAs may affect the transcription process of ACE2 by regulating SRY-related genes, thus mediating the infection of SARS-CoV-2 to the host. However, no research has focused on circRNAs involved in the regulation of ACE2 through modulation of the SRY gene. In addition, recent studies have revealed that AXL receptor tyrosine kinase (AXL), a founding member of the TAM family of receptor tyrosine kinases (RTKs), is a novel candidate receptor for SARS-CoV-2 to invade host cells. AXL can specifically interact with the N-terminal domain of the SARS-CoV-2 genome to mediate its entry into host cells without the involvement of ACE2, suggesting that AXL may be a potential target for future treatment of COVID-19 (111). Notably, a recent study has found that hsa\_circ\_0006689 regulates the



transmembrane receptor protein tyrosine kinase signal transduction pathway by targeting hsa-miR-1255a (112), indicating that hsa\_circ\_0006689 may participate in the invasion of SARS-CoV-2 by mediating the expression of AXL. Taken together, circRNAs may be therapeutic targets against COVID-19 by regulating the binding of SARS-CoV-2 to relevant host receptors.

Immunity induced by a viral infection can protect cellular functions, resist viral invasion, clear viruses, and clear infections. However, excessive activation of immune responses may cause serious damage to the host (113). For example, over-recruitment of immune cells and uncontrolled proinflammatory cytokines can lead to systemic inflammation that can cause extensive damage to tissues and organs. Numerous studies have shown that TNF and IL-1 $\beta$  can stimulate the production of IL-6, which can serve as a biomarker of disease severity and a prognostic indicator of cytokine storm (114, 115). Interestingly, IL-6 is involved in the activation of the NF- $\kappa$ B pathway, and subsequently, NF- $\kappa$ B positively regulates HIF-1 $\alpha$ , which in turn enhances the regulatory effect of HIF-1 $\alpha$  on the expression of downstream proinflammatory factors. Meanwhile, HIF-1 $\alpha$  plays a key role in the synthesis of IL-1 $\beta$  (116–120). A recent study by Tian M et al. (121) found that the ORF3a protein of SARS-CoV-2 in patients with COVID-19 can promote the production of HIF-1 $\alpha$ , which regulates the expression of inflammatory cytokines, such as IFN- $\beta$ , IL-6, and IL-1 $\beta$ , to promote virus replication and infection. Noticeably, Yang YW et al. (122) found that two circRNAs (circ\_2909 and circ\_0323) could promote the expression of HIF-1 $\alpha$  and inducible nitric oxide synthase (NOS2) by acting as sponges for miRNAs. Furthermore, Demirci YM et al. (123) reported DE miRNAs during SARS-CoV-2 infection and found that ORF3a protein is a viral target of human miRNAs. The study further found that among 2498 miRNAs with predicted targets, 2448 had more targets in circRNAs. Therefore, regulatory network of circRNA-miRNA-mRNA contributes to regulating the expression of downstream HIF-1 pathway genes and that may become a new approach to treating COVID-19.

Currently, CoVs have evolved to the point where they can evade a complex system of sensors and signalling molecules to suppress host immunity. Papain-like protease (PLpro) is an enzyme in CoVs that regulates viral spread and innate immune responses (124, 125). Several recent studies have demonstrated that SARS-CoV-2-PLpro is a multifunctional enzyme with deubiquitination and de-ISG activities *via* regulating multiple signalling pathways, such as STING, NF- $\kappa$ B, and TGF- $\beta$ , to block immune responses (126), suggesting that PLpro can serve as an important therapeutic target against COVID-19. Remarkably, previous studies have indicated that MERS-CoV-PLpro has deubiquitination activity and participates in the proteolysis of viral polyproteins during viral replication (127, 128). A study by Zhang X et al. (18) found that

ubiquitin-mediated proteolysis was significantly disturbed after MERS-CoV infection, and DE circRNAs related to ubiquitin-mediated proteolysis could affect MERS-CoV replication by regulating downstream target genes. For example, knockout of hsa\_circ\_0067985 or hsa\_circ\_0006275 significantly reduced the expression of MAP3K9, thereby regulating the extracellular signal-regulated kinase (ERK)/MAPK pathway associated with MERS-CoV replication (129). In addition, heterogeneous nuclear ribonucleoprotein C (hnRNP C) is an upstream regulator of multiple proviral circRNAs and can bind and obscure Alu on pre-mRNA and protect against Alu exonation to regulate circRNA biogenesis (130, 131). A recent study by Zhang X et al. (19) found that hnRNP C was able to regulate MERS-CoV replication by targeting the CRK-mTOR signalling pathway. Furthermore, this study also confirmed that hnRNP C is a key modulator of the expression of MERS-CoV-perturbed circRNAs, such as hsa\_circ\_0002846, hsa\_circ\_0002061 and hsa\_circ\_0004445, and the data further demonstrated that hnRNP C regulates the expression of these circRNAs through direct physical binding. The correlation analysis of circRNAs and their parental genes as potential biomarkers and therapeutic targets for the diagnosis of SARS-CoV-2 is summarized in [Supplementary Table 2](#), which suggests that circRNAs play a key role in the occurrence of COVID-19.

## Discussion

In summary, circRNAs are emerging as important players in regulating virus-mediated infection and subsequent disease status. With the rapid development of high-throughput sequencing technology and bioinformatics, it has been demonstrated that a large number of circRNAs are DE in COVID-19 patients and that circRNAs play a key role in the process of virus-host interaction. On the one hand, the host directly regulates immune response factors during virus infection *via* circRNAs and indirectly regulates the expression of downstream target genes through the ceRNA network to inhibit virus replication. On the other hand, viruses trigger molecular expression through host-encoded and self-encoded circRNAs, generating new circRNAs that interfere with the host's innate immune response and that may create a suitable microenvironment for the virus to replicate or mutate in cells. Moreover, conserved circRNAs are widely involved in cell proliferation, differentiation, and apoptosis. Furthermore, these circRNAs act as key targeted therapies for SARS-CoV-2-infected cells, including blocking the binding of the virus to host receptors, inducing host-specific immune responses, interfering with gene transcription, and hindering protein translation. Current studies clearly show that circRNAs are evolutionarily conserved and closely involved in the process of SARS-CoV-2 infection, which paves the way for further studies on how circRNAs regulate host-virus dynamics in CoV-involved

TABLE 1 Status of COVID-19 vaccines within WHO Emergency Use Listing (EUL)/Prequalification (PQ).

Vaccine	WHO EUL Holder	National Regulatory System (NRA) of record	Recommendation issued	Suitable age	Type of vaccine	Working principle	Disadvantages	Reference
COMIRNATY®	BioNTech Manufacturing GmbH	European Medicines Agency Food and Drug Administration	16-Jul-21	aged 5 years and older	Nucleic acid vaccine	mRNA encoding SARS-CoV-2 spike protein	broken down shortly after vaccination myocarditis pericarditis erythema multiforme Allergic reactions	(132)
VAXZEVRIA	AstraZeneca AB / SK Bioscience Co. Ltd	European Medicines Agency European Medicines Agency Ministry of Health, Labour and Welfare	15-Feb-21 15-Apr-21 09-Jul-21	aged 18 years and older	Adenovirus vector vaccine	Adenovirus recombinantly containing a gene for the production of SARS-CoV-2 spike-in protein	Thrombosis in combination with thrombocytopenia (TTS), Guillain-Barré syndrome, angioedema, capillary leak syndrome, Allergic reactions	(133)
	AstraZeneca AB	Therapeutic Goods Administration Health Canada COFEPRIS (DP) ANMAT (DS)	09-Jul-21					
COVISHIELD™	Serum Institute of India Pvt. Ltd	Central Drugs Standard Control Organization	15-Feb-21	aged 18 years and older	Adenovirus vector vaccine	Adenovirus recombinantly containing a gene for the production of SARS-CoV-2 spike-in protein	Thrombosis in combination with thrombocytopenia (TTS), Allergic reactions	(134)
Ad26.COV2-S [recombinant]	Janssen-Cilag International NV	European Medicines Agency	12-Mar-21	aged 18 years and older	Adenovirus vector vaccine	encoding a full-length and stabilized SARS-CoV-2 spike protein	thrombosis with thrombocytopenia syndrome [TTS], capillary leak syndrome, and Guillain-Barré syndrome	(135)
SPIKEVAX	Moderna Biotech ModernaTX, Inc	European Medicines Agency Ministry of Food and Drug Safety (MFDS) Food and Drug Administration	30-Apr-21	aged 12 years and older	Nucleic acid vaccine	mRNA encoding SARS-CoV-2 spike protein	broken down shortly after vaccination, erythema multiforme, Allergic reactions	(136)
Inactivated COVID-19 Vaccine (Vero Cell)	Beijing Institute of Biological Products Co., Ltd. (BIBP)	National Medicinal Products Association		18 to 59 years of age	Inactivated vaccine	The antibodies against the SARS-CoV-2 can be produced after vaccination	local injection site reactions	(137)
CoronaVac	Sinovac Life Sciences Co., Ltd	National Medical Products Administration	01-Jun-21	18 to 59 years of age	Inactivated vaccine	The antibodies against the SARS-CoV-2 can be	local injection site reactions	(138)

(Continued)

TABLE 1 Continued

Vaccine	WHO EUL Holder	National Regulatory System (NRA) of record	Recommendation issued	Suitable age	Type of vaccine	Working principle	Disadvantages	Reference
COVAXIN®	Bharat Biotech International Ltd	Central Drugs Standard Control Organization	03-Nov-21	aged 18 years and older	Inactivated vaccine	produced after vaccination The antibodies against the SARS-CoV-2 can be produced after vaccination	Headaches, Fever	(139)
COVOVAX™	Serum Institute of India Pvt. Ltd	Central Drugs Standard Control Organization		aged 18 years and older	Recombinant subunit vaccine	The antibodies against the SARS-CoV-2 can be produced after vaccination	local injection site reactions	(140)
NUVAXOVID™	Novavax CZ a.s.	European Medicines Agency		aged 18 years and older	Recombinant subunit vaccine	The antibodies against the SARS-CoV-2 can be produced after vaccination	local injection site reactions	(140)
Sputnik V	Russian Direct Investment Fund	Russian NRA	/	aged 18 years and older	Adenovirus vector vaccine	The antibodies against the SARS-CoV-2 can be produced after vaccination	Localised pain, weakness, headaches and joint pain	(141)
Inactivated SARS-CoV-2 Vaccine (Vero Cell)	Wuhan Institute of Biological Products Co Ltd	National Medicinal Products Association	/	18 to 59 years of age	Inactivated vaccine	The antibodies against the SARS-CoV-2 can be produced after vaccination	local injection site reactions	(142)
Ad5-nCoV	CanSinoBIO	National Medicinal Products Association	/	/	Recombinant subunit vaccine	Adenovirus recombinantly containing a gene for the production of SARS-CoV-2 spike-in protein	local injection site reactions, Headache, Drowsiness and Muscle aches	(143)
CoV2 preS dTM-AS03 vaccine	SANOFI	European Medicines Agency	/	/	Adjuvanted soluble protein vaccines	robust induction of antibody responses	local injection site reactions, Headaches, Fever	(144)
SCB-2019	Clover Biopharmaceuticals	National Medicinal Products Association	/	/	Recombinant subunit vaccine	The antibodies against the SARS-CoV-2 can be produced after vaccination	local injection site reactions	(145)
Recombinant Novel Coronavirus Vaccine (CHO Cell)	Zhifei Longcom, China	National Medicinal Products Association	/	/	Recombinant subunit vaccine	The antibodies against the SARS-CoV-2 can be produced after vaccination	local injection site reactions	(146)

(Continued)

TABLE 1 Continued

Vaccine	WHO EUL Holder	National Regulatory System (NRA) of record	Recommendation issued	Suitable age	Type of vaccine	Working principle	Disadvantages	Reference
Zorecimeran (INN) concentrate and solvent for dispersion for injection; Company code: CVnCoV/ CV07050101	Curevac	European Medicines Agency	/	/	Nucleic acid vaccine	mRNA-based vaccine encapsulated in lipid nanoparticle (LNP)	Headache, fatigue, chills and pain at the injection site	(147)
EpiVacCorona	Vector State Research Centre of Virology and Biotechnology	Russian NRA	/	/	Adenovirus vector vaccine	The immune system is stimulated to neutralize the virus by peptides-short fragments of viral protein	/	(148)
SARS-CoV-2 Vaccine, Inactivated (Vero Cell)	IMBCAMS, China	National Medicinal Products Association	/	18 to 59 years of age	Inactivated vaccine	The antibodies against the SARS-CoV-2 can be produced after vaccination	Redness and swelling at the injection site, induration and fever at the injection site	(142)
Soberana 01, Soberana 02, Soberana Plus, Abdala	BioCubaFarma - Cuba	CECMED	/	/	Conjugate protein vaccines	SARS-CoV-2 spike protein conjugated chemically to meningococcal B or tetanus toxoid or Aluminum	/	(149)

diseases. However, the lack of research on clinical effectiveness has greatly increased the challenges in the clinical application of circRNAs.

By far, the new mutated strain of SARS-CoV-2, Omicron, has once again caused a global panic. At this stage, vaccination is the most promising way to end the COVID-19 pandemic. However, the efficacy of vaccines and the onset of adverse reactions vary among individuals. Information on COVID-19 vaccines that have been certified for emergency use by the WHO and are in the process of being evaluated is summarized in Table 1 (132–149). Traditional vaccines and nucleic acid vaccines against SARS-CoV-2 have been extensively developed. Among them, an mRNA vaccine was the first to be officially approved by the FDA for use in the COVID-19 pandemic due to its advantages of rapid production, low cost, and rapid response to SARS-CoV-2 infection. However, in the face of rapidly mutating virus strains, alternative vaccines with high efficacy, high design flexibility, and fast production have not yet been developed. With the development of RNA vaccines, improving RNA stability has become a huge challenge.

Fortunately, prior to this challenge, circRNAs showed great potential. Unlike linear mRNA, circRNA is highly stable and has a long half-life because its covalently closed-loop structure protects it from exonuclease-mediated degradation (150–152). However, only a few endogenous circRNAs have been demonstrated to serve as templates for protein translation, but several studies have shown that m6A modifications introduced into the ribosomal entry site (IRES) or 5'-untranslated region *via* artificial engineering can promote the extensive translation of circRNAs (110, 153–155). Recently, Liang Qu et al. (10) rapidly synthesized a highly stable circRNA-RBD vaccine (a circRNA vaccine that encodes the receptor-binding domain (RBD) of the SARS-CoV-2 S protein trimer) through *in vitro* transcription and found that the vaccine was capable of inducing potent and sustained anti-SARS-CoV-2-RBD neutralizing antibodies and Th1-biased T-cell responses in mice. Furthermore, the production of highly active neutralizing antibodies of the corresponding Beta variant was successfully induced in mice by using the circRNA vaccine encoding the RBD variant (K417N-E484K-501Y). Moreover, the latest research results

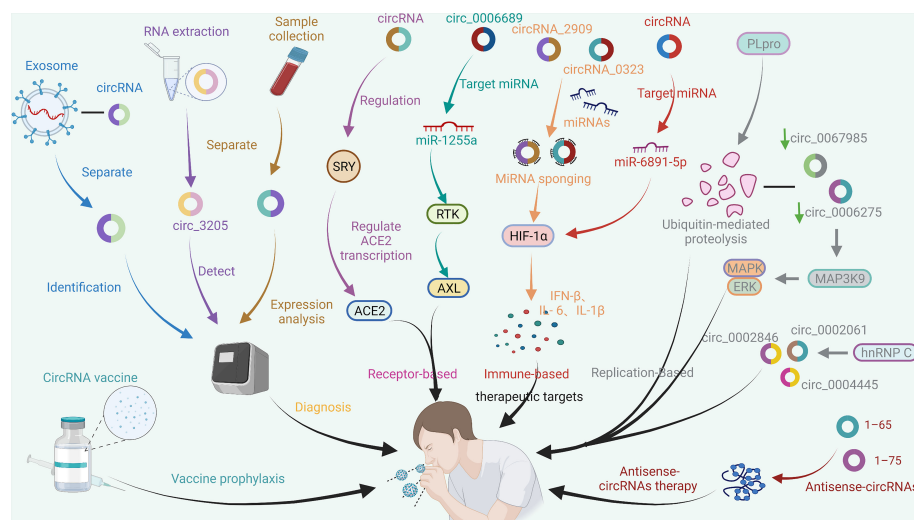


FIGURE 5

Potential application of circRNAs in the treatment of COVID-19. CircRNAs are a new class of regulatory factors that mediate host–virus interactions. The identification and isolation of exosome-associated circRNAs, virus-encoded circRNAs, and significantly DE circRNAs after SARS-CoV-2 infection may be helpful in the diagnosis of COVID-19. In addition, circRNAs may serve as potential therapeutic targets against COVID-19 by indirectly regulating the expression of host receptors, such as ACE2 and AXL, that bind to SARS-CoV-2; HIF-1 $\alpha$  and other signalling pathways related to the immune response; and multiple signalling pathways related to SARS-CoV-2 replication. Additionally, vaccines based on circRNAs and antisense circRNAs have shown initial effectiveness in preventing and inhibiting SARS-CoV-2. The coloured arrows in the figure are only for the convenience of differentiation and have no special meaning.

have revealed that circRNA-RBD-Delta can elicit high levels of neutralizing antibodies against the Delta and Omicron variants compared to the circRNA-RBD-Omicron vaccine, which only induces effective neutralizing antibodies against Omicron. In addition, Seephetdee C et al. (20) found that SARS-CoV-2 circRNA vaccine VFLIP-X induces humoral and cellular immune responses that provide broad immune responses against emerging SARS-CoV-2 variants in mice. The results showed that circRNA vaccines can not only effectively prevent SARS-CoV-2 infection but can also quickly adapt to emerging SARS-CoV-2 mutant strains. Additionally, compared with the preparation method for conventional inactivated vaccines, which requires obtaining virus strains and then expanding and culturing live viruses, circRNA technology allows rapid development of new vaccines by only obtaining virus sequences or mutated sequences. CircRNA vaccines have the advantages of strong stability, immunogen coding ability, self-adjuvant, rapid mass production *in vitro*, and no needed nucleotide modification. CircRNAs can also be used to express nanobodies or ACE2 decoys to neutralize SARS-CoV-2 pseudovirus (10). Recently, Breuer J et al. (156) found that artificial circRNAs can bypass the cellular RNA sensors and that are not recognized by the innate immune system. Moreover, the antisense circRNAs 1–65 and 1–75 designed by Pfafenrot C et al. (14) significantly inhibited viral replication by specifically targeting specific 5'-UTR regions and sgRNAs of the SARS-CoV-2 genome. The potential applications of circRNAs for the

diagnosis, treatment and prognosis of COVID-19 are shown in Figure 5, which indicates that circRNAs have very good application prospects in the fight against SARS-CoV-2 variant viruses, and circRNA vaccines and artificial circRNAs can be used as new vaccines and therapeutic platforms in the COVID-19 pandemic.

In general, circRNAs are highly resistant to RNase R due to their unique ring structure and are more conservative and stable than lncRNAs and miRNAs. CircRNAs can exist stably in cells or tissues and have become the star molecules in the field of ncRNA. Furthermore, circRNAs have the potential to be molecular markers of viral infectious diseases, which can provide a scientific basis for early diagnosis of diseases and the search for potential therapeutic targets. Taking circRNAs as an entry point to study the interaction between viral infection and the host will help clarify the function of circRNAs and thus the pathogenic mechanism of coronaviruses. Therefore, circRNAs may prove to be helpful as diagnostic markers and therapeutic agents against COVID-19.

## Author contributions

XG, DF, YL and ML conceived the idea, analysis of literature, and writing of the manuscript; XG, XD and NC collected and read the literature and revised the article; MZ and ML read through and corrected the manuscript. All authors contributed to the article and approved the submitted version.



## Funding

This work was supported by the National Natural Science Foundation of China [grant numbers 81800434], Grant of Sichuan Province Science and Technology Agency Grant [2019YJ0487].

## Acknowledgments

Figures were created with ©BioRender - [biorender.com](https://biorender.com).

## Conflict of interest

The authors declare that the research was conducted in the absence of any commercial or financial relationships that could be construed as a potential conflict of interest.

## References

1. Aleem A, Akbar Samad AB, Slenker AK. *Emerging variants of SARS-CoV-2 and novel therapeutics against coronavirus (COVID-19)*. StatPearls. Treasure Island (FL: StatPearls Publishing Copyright © 2022, StatPearls Publishing LLC (2022).
2. Torjesen I. Covid-19: Delta variant is now UK's most dominant strain and spreading through schools. *BMJ (Clin Res ed)* (2021) 373:n1445. doi: 10.1136/bmj.n1445
3. Jorgensen SCJ, Kebriaei R, Dresser LD. Remdesivir: Review of pharmacology, pre-clinical data, and emerging clinical experience for COVID-19. *Pharmacotherapy* (2020) 40(7):659–71. doi: 10.1002/phar.2429
4. Gupta A, Gonzalez-Rojas Y, Juarez E, Crespo Casal M, Moya J, Falci DR, et al. Early treatment for covid-19 with SARS-CoV-2 neutralizing antibody sotrovimab. *N Engl J Med* (2021) 385(21):1941–50. doi: 10.1056/NEJMoa2107934
5. Lan SH, Lai CC, Huang HT, Chang SP, Lu LC, Hsueh PR. Tocilizumab for severe COVID-19: a systematic review and meta-analysis. *Int J Antimicrob Agents*. (2020) 56(3):106103. doi: 10.1016/j.ijantimicag.2020.106103
6. Tomazini BM, Maia IS, Cavalcanti AB, Berwanger O, Rosa RG, Veiga VC, et al. Effect of dexamethasone on days alive and ventilator-free in patients with moderate or severe acute respiratory distress syndrome and COVID-19: The CoDEX randomized clinical trial. *Jama* (2020) 324(13):1307–16. doi: 10.1001/jama.2020.17021
7. Christie A, Brooks JT, Hicks LA, Sauber-Schatz EK, Yoder JS, Honein MA. Guidance for implementing COVID-19 prevention strategies in the context of varying community transmission levels and vaccination coverage. *MMWR Morb Mortal Wkly Rep* (2021) 70(30):1044–7. doi: 10.15585/mmwr.mm7030e2
8. Awan FM, Yang BB, Naz A, Hanif A, Ikram A, Obaid A. The emerging role and significance of circular RNAs in viral infections and antiviral immune responses: possible implication as theranostic agents. *RNA Biol* (2021) 18(1):1–15. doi: 10.1080/15476286.2020.1790198
9. Li X, Liu CX, Xue W, Zhang Y, Jiang S, Yin QF, et al. Coordinated circRNA biogenesis and function with NF90/NF110 in viral infection. *Mol Cell* (2017) 67(2):214–27.e7. doi: 10.1016/j.molcel.2017.05.023
10. Qu L, Yi Z, Shen Y, Lin L, Chen F, Xu Y, et al. Circular RNA vaccines against SARS-CoV-2 and emerging variants. *Cell* (2022) 185(10):1728–44.e16. doi: 10.1016/j.cell.2022.03.044
11. Wu Y, Zhao T, Deng R, Xia X, Li B, Wang X. A study of differential circRNA and lncRNA expressions in COVID-19-infected peripheral blood. *Sci Rep* (2021) 11(1):7991. doi: 10.1038/s41598-021-86134-0
12. Chen YG, Chen R, Ahmad S, Verma R, Kasturi SP, Amaya L, et al. N6-methyladenosine modification controls circular RNA immunity. *Mol Cell* (2019) 76(1):96–109.e9. doi: 10.1016/j.molcel.2019.07.016
13. Yan L, Chen YG. Circular RNAs in immune response and viral infection. *Trends Biochem Sci* (2020) 45(12):1022–34. doi: 10.1016/j.tibs.2020.08.006

## Publisher's note

All claims expressed in this article are solely those of the authors and do not necessarily represent those of their affiliated organizations, or those of the publisher, the editors and the reviewers. Any product that may be evaluated in this article, or claim that may be made by its manufacturer, is not guaranteed or endorsed by the publisher.

## Supplementary material

The Supplementary Material for this article can be found online at: <https://www.frontiersin.org/articles/10.3389/fimmu.2022.980231/full#supplementary-material>

14. Pfaffenrot C, Schneider T, Müller C. Inhibition of SARS-CoV-2 coronavirus proliferation by designer antisense-circRNAs. *Nucleic Acids Res* (2021) 49(21):12502–16. doi: 10.1093/nar/gkab1096
15. Cai Z, Lu C, He J, Liu L, Zou Y, Zhang Z, et al. Identification and characterization of circRNAs encoded by MERS-CoV, SARS-CoV-1 and SARS-CoV-2. *Briefings Bioinf* (2021) 22(2):1297–308. doi: 10.1093/bib/bbaa334
16. Yang M, Qi M, Xu L, Huang P, Wang X, Sun J, et al. Differential host circRNA expression profiles in human lung epithelial cells infected with SARS-CoV-2. *Infect Genet Evol J Mol Epidemiol evol. Genet Infect Dis*. (2021) 93:104923. doi: 10.1016/j.meegid.2021.104923
17. Yang S, Zhou H, Liu M, Jaiyyan D, Cruz-Cosme R, Ramasamy S, et al. SARS-CoV-2, SARS-CoV, and MERS-CoV encode circular RNAs of spliceosome-independent origin. *J Med virol*. (2022) 94(7):3203–22. doi: 10.1002/jmv.27734
18. Zhang X, Chu H, Wen L, Shuai H, Yang D, Wang Y, et al. Competing endogenous RNA network profiling reveals novel host dependency factors required for MERS-CoV propagation. *Emerg Microbes Infect* (2020) 9(1):733–46. doi: 10.1080/22221751.2020.1738277
19. Zhang X, Chu H. hnRNP c modulates MERS-CoV and SARS-CoV-2 replication by governing the expression of a subset of circRNAs and cognitive mRNAs. *Emerg Microbes Infect* (2022) 11(1):519–31. doi: 10.1080/22221751.2022.2032372
20. Seephetdee C, Bhukhai K, Buasri N, Leelukkanaveera P, Lerdwattanasombat P, Manopwisedjaroen S, et al. A circular mRNA vaccine prototype producing VFLIP-X spike confers a broad neutralization of SARS-CoV-2 variants by mouse sera. *Antiviral Res* (2022) 204:105370. doi: 10.1016/j.antiviral.2022.105370
21. Zhou Z, Sun B, Huang S, Zhao L. Roles of circular RNAs in immune regulation and autoimmune diseases. *Cell Death Dis* (2019) 10(7):503. doi: 10.1038/s41419-019-1744-5
22. Rahman N, Basharat Z. Virtual screening of natural products against type II transmembrane serine protease (TMPRSS2), the priming agent of coronavirus 2 (SARS-CoV-2). *Molecules* (2020) 25(10):2271. doi: 10.3390/molecules25102271
23. Cheever FS, Daniels JB, Pappenheimer AM, Bailey OT. A murine virus (JHM) causing disseminated encephalomyelitis with extensive destruction of myelin. *J Exp Med* (1949) 90(3):181–210. doi: 10.1084/jem.90.3.181
24. Yang Y, Xiao Z, Ye K, He X, Sun B, Qin Z, et al. SARS-CoV-2: characteristics and current advances in research. *Virol J* (2020) 17(1):117. doi: 10.1186/s12985-020-01369-z
25. Fehr AR, Perlman S. Coronaviruses: an overview of their replication and pathogenesis. *Methods Mol Biol (Clifton NJ)* (2015) 1282:1–23. doi: 10.1007/978-1-4939-2438-7\_1
26. Zhou P, Yang X-L, Wang X-G, Hu B, Zhang L, Zhang W, et al. Discovery of a novel coronavirus associated with the recent pneumonia outbreak in humans and its potential bat origin. *bioRxiv preprint server Biol* (2020) 22:914952. doi: 10.1101/2020.01.22.914952

27. Cascella M, Rajnik M, Aleem A, Dulebohn SC, Di Napoli R. *Features, evaluation, and treatment of coronavirus (COVID-19)*. StatPearls. Treasure Island (FL: StatPearls Publishing Copyright © 2022, StatPearls Publishing LLC (2022).
28. Lu R, Wang Y, Wang W, Nie K, Zhao Y, Su J, et al. Complete genome sequence of middle East respiratory syndrome coronavirus (MERS-CoV) from the first imported MERS-CoV case in China. *Genome announc* (2015) 3(4):e00818–15. doi: 10.1128/genomeA.00818-15
29. Wu A, Peng Y, Huang B, Ding X, Wang X, Niu P, et al. Genome composition and divergence of the novel coronavirus (2019-nCoV) originating in China. *Cell Host Microbe* (2020) 27(3):325–8. doi: 10.1016/j.chom.2020.02.001
30. van Boheemen S, de Graaf M, Lauber C, Bestebroer TM, Raj VS, Zaki AM, et al. Genomic characterization of a newly discovered coronavirus associated with acute respiratory distress syndrome in humans. *mBio* (2012) 3(6):e00473–12. doi: 10.1128/mBio.00473-12
31. Wan Y, Shang J, Graham R, Baric RS, Li F. Receptor recognition by the novel coronavirus from wuhan: an analysis based on decade-long structural studies of SARS coronavirus. *J Virol* (2020) 94(7):e00127–20. doi: 10.1128/jvi.00127-20
32. Gierer S, Bertram S, Kaup F, Wrensch F, Heurich A, Krämer-Kühl A, et al. The spike protein of the emerging betacoronavirus EMC uses a novel coronavirus receptor for entry, can be activated by TMPRSS2, and is targeted by neutralizing antibodies. *J virol.* (2013) 87(10):5502–11. doi: 10.1128/jvi.00128-13
33. Shang J, Wan Y, Luo C, Ye G, Geng Q, Auerbach A. Cell entry mechanisms of SARS-CoV-2. *Proc Natl Acad Sci U S A* (2020) 117(21):11727–34. doi: 10.1073/pnas.2003138117
34. Leung GM, Hedley AJ, Ho LM, Chau P, Wong IO, Thach TQ, et al. The epidemiology of severe acute respiratory syndrome in the 2003 Hong Kong epidemic: an analysis of all 1755 patients. *Ann Internal Med* (2004) 141(9):662–73. doi: 10.7326/0003-4819-141-9-200411020-00006
35. Wölfel R, Corman VM, Guggemos W, Seilmaier M, Zange S, Müller MA, et al. Virological assessment of hospitalized patients with COVID-2019. *Nature* (2020) 581(7809):465–9. doi: 10.1038/s41586-020-2196-x
36. Richardson P, Griffin I, Tucker C, Smith D, Oechsle O, Phelan A, et al. Baricitinib as potential treatment for 2019-nCoV acute respiratory disease. *Lancet (London England)* (2020) 395(10223):e30–1. doi: 10.1016/s0140-6736(20)30304-4
37. Owen DR, Allerton CMN. An oral SARS-CoV-2 m(pro) inhibitor clinical candidate for the treatment of COVID-19. *Science* (2021) 374(6575):1586–93. doi: 10.1126/science.abl4784
38. V'kovski P, Kratzel A, Steiner S, Stalder H. Coronavirus biology and replication: implications for SARS-CoV-2. *Nat Rev Microbiol* (2021) 19(3):155–70. doi: 10.1038/s41579-020-00468-6
39. Yoo JS, Sasaki M. SARS-CoV-2 inhibits induction of the MHC class I pathway by targeting the STAT1-IRF1-NLRC5 axis. *Nat Commun* (2021) 12(1):6602. doi: 10.1038/s41467-021-26910-8
40. Rha MS, Jeong HW, Ko JH, Choi SJ, Seo IH, Lee JS, et al. PD-1-Expressing SARS-CoV-2-Specific CD8(+) T cells are not exhausted, but functional in patients with COVID-19. *Immunity* (2021) 54(1):44–52.e3. doi: 10.1016/j.immuni.2020.12.002
41. Saini SK, Hersby DS, Tamhane T. SARS-CoV-2 genome-wide T cell epitope mapping reveals immunodominance and substantial CD8(+) T cell activation in COVID-19 patients. *Sci Immunol* (2021) 6(58):eabf7550. doi: 10.1126/sciimmunol.abf7550
42. Aschman T, Schneider J, Greuel S, Meinhardt J, Streit S, Goebel HH, et al. Association between SARS-CoV-2 infection and immune-mediated myopathy in patients who have died. *JAMA Neurol* (2021) 78(8):948–60. doi: 10.1001/jamaneurol.2021.2004
43. Poluektov Y, George M, Daftarian P, Delcommenne MC. Assessment of SARS-CoV-2 specific CD4(+) and CD8(+) T cell responses using MHC class I and II tetramers. *Vaccine* (2021) 39(15):2110–6. doi: 10.1016/j.vaccine.2021.03.008
44. Taher I, Almaeen A, Ghazy A, Abu-Farha M, Mohamed Channanath A, Elsa John S, et al. Relevance between COVID-19 and host genetics of immune response. *Saudi J Biol Sci* (2021) 28(11):6645–52. doi: 10.1016/j.sjbs.2021.07.037
45. Sáez JJ, Lennon-Duménil AM, Yuseff MI. Studying MHC class II presentation of immobilized antigen by b lymphocytes. *Methods Mol Biol (Clifton NJ)*. (2019) 1988:419–37. doi: 10.1007/978-1-4939-9450-2\_29
46. Obermair FJ, Renoux F, Heer S. High-resolution profiling of MHC II peptide presentation capacity reveals SARS-CoV-2 CD4 T cell targets and mechanisms of immune escape. *Sci Adv* (2022) 8(17):eabf5394. doi: 10.1126/sciadv.abf5394
47. Hyun YS, Lee YH, Jo HA, Baek IC, Kim SM, Sohn HJ, et al. Comprehensive analysis of CD4(+) T cell response cross-reactive to SARS-CoV-2 antigens at the single allele level of HLA class II. *Front Immunol* (2021) 12:774491. doi: 10.3389/fimmu.2021.774491
48. Hur S. Double-stranded RNA sensors and modulators in innate immunity. *Annu Rev Immunol* (2019) 37:349–75. doi: 10.1146/annurev-immunol-042718-041356
49. Fung SY, Yuen KS. A tug-of-war between severe acute respiratory syndrome coronavirus 2 and host antiviral defence: lessons from other pathogenic viruses. *Emerg Microbes Infect* (2020) 9(1):558–70. doi: 10.1080/22221751.2020.1736644
50. Meyer B, Chiaravalli J, Gellenoncourt S. Characterising proteolysis during SARS-CoV-2 infection identifies viral cleavage sites and cellular targets with therapeutic potential. *Nat Commun* (2021) 12(1):5553. doi: 10.1038/s41467-021-25796-w
51. Upton JW, Chan FK. Staying alive: cell death in antiviral immunity. *Mol Cell* (2014) 54(2):273–80. doi: 10.1016/j.molcel.2014.01.027
52. Hui DSC, Zumla A. Severe acute respiratory syndrome: Historical, epidemiologic, and clinical features. *Infect Dis Clinics N Am* (2019) 33(4):869–89. doi: 10.1016/j.idc.2019.07.001
53. Du WW, Fang L, Yang W, Wu N, Awan FM, Yang Z, et al. Induction of tumor apoptosis through a circular RNA enhancing Foxo3 activity. *Cell Death Differ* (2017) 24(2):357–70. doi: 10.1038/cdd.2016.133
54. Zhang X, Yang T, Xiao J. Circular RNAs: Promising biomarkers for human diseases. *EBioMedicine* (2018) 34:267–74. doi: 10.1016/j.ebiom.2018.07.036
55. Firoozi Z, Mohammadisoleimani E. Hsa\_circ\_0000479/Hsa-miR-149-5p/RIG-I, IL-6 axis: A potential novel pathway to regulate immune response against COVID-19. *Can J Infect Dis Med Microbiol* (2022) 2022:2762582. doi: 10.1155/2022/2762582
56. Barbagallo D, Palermo CI, Barbagallo C, Battaglia R, Caponnetto A, Spina V, et al. Competing endogenous RNA network mediated by circ\_3205 in SARS-CoV-2 infected cells. *Cell Mol Life Sci CMLS* (2022) 79(2):75. doi: 10.1007/s00018-021-04119-8
57. Barrett SP, Wang PL, Salzman J. Circular RNA biogenesis can proceed through an exon-containing lariat precursor. *eLife* (2015) 4:e07540. doi: 10.7554/eLife.07540
58. Jeck WR, Sharpless NE. Detecting and characterizing circular RNAs. *Nat Biotechnol* (2014) 32(5):453–61. doi: 10.1038/nbt.2890
59. Salzman J, Chen RE, Olsen MN, Wang PL, Brown PO. Cell-type specific features of circular RNA expression. *PloS Genet* (2013) 9(9):e1003777. doi: 10.1371/journal.pgen.1003777
60. You X, Vlatkovic I, Babic A, Will T, Epstein I, Tushev G, et al. Neural circular RNAs are derived from synaptic genes and regulated by development and plasticity. *Nat Neurosci* (2015) 18(4):603–10. doi: 10.1038/nn.3975
61. Hansen TB, Jensen TI, Clausen BH, Bramsen JB, Finsen B, Damgaard CK, et al. Natural RNA circles function as efficient microRNA sponges. *Nature* (2013) 495(7441):384–8. doi: 10.1038/nature11993
62. Salmena L, Poliseno L, Tay Y, Kats L, Pandolfi PP. A ceRNA hypothesis: the Rosetta stone of a hidden RNA language? *Cell* (2011) 146(3):353–8. doi: 10.1016/j.cell.2011.07.014
63. Memczak S, Jens M, Elefsinioti A, Torti F, Krueger J, Rybak A, et al. Circular RNAs are a large class of animal RNAs with regulatory potency. *Nature* (2013) 495(7441):333–8. doi: 10.1038/nature11928
64. Thomas LF, Sætrom P. Circular RNAs are depleted of polymorphisms at microRNA binding sites. *Bioinf (Oxford England)* (2014) 30(16):2243–6. doi: 10.1093/bioinformatics/btu257
65. Arora S, Singh P, Dohare R, Jha R, Ali Syed M. Unravelling host-pathogen interactions: ceRNA network in SARS-CoV-2 infection (COVID-19). *Gene* (2020) 762:145057. doi: 10.1016/j.gene.2020.145057
66. Qin Z, Wang PY, Su DF, Liu X. miRNA-124 in immune system and immune disorders. *Front Immunol* (2016) 7:406. doi: 10.3389/fimmu.2016.00406
67. Cadena C, Hur S. Antiviral immunity and circular RNA: No end in sight. *Mol Cell* (2017) 67(2):163–4. doi: 10.1016/j.molcel.2017.07.005
68. Wang M, Yu F, Wu W, Zhang Y, Chang W, Ponnusamy M, et al. Circular RNAs: A novel type of non-coding RNA and their potential implications in antiviral immunity. *Int J Biol Sci* (2017) 13(12):1497–506. doi: 10.7150/ijbs.22531
69. Chen YG, Kim MV, Chen X, Batista PJ, Aoyama S, Wilusz JE, et al. Sensing self and foreign circular RNAs by intron identity. *Mol Cell* (2017) 67(2):228–38.e5. doi: 10.1016/j.molcel.2017.05.022
70. Appelberg S, Gupta S, Svensson Akusjärvi S, Ambikan AT, Mikaeloff F, Saccon E, et al. Dysregulation in Akt/mTOR/HIF-1 signaling identified by proteo-transcriptomics of SARS-CoV-2 infected cells. *Emerg Microbes Infect* (2020) 9(1):1748–60. doi: 10.1080/22221751.2020.1799723
71. Fajgenbaum DC, June CH. Cytokine storm. (2020) 383(23):2255–73. doi: 10.1056/NEJMra2026131
72. Coperchini F, Chiovato L, Croce L, Magri F, Rotondi M. The cytokine storm in COVID-19: An overview of the involvement of the chemokine/chemokine-

receptor system. *Cytokine Growth Factor Rev* (2020) 53:25–32. doi: 10.1016/j.cytogfr.2020.05.003

73. Alcamí A. Viral mimicry of cytokines, chemokines and their receptors. *Nat Rev Immunol* (2003) 3(1):36–50. doi: 10.1038/nri980

74. Lieberman NAP, Peddu V. *In vivo* antiviral host transcriptional response to SARS-CoV-2 by viral load, sex, and age. *PLoS Biol* (2020) 18(9):e3000849. doi: 10.1371/journal.pbio.3000849

75. Hertzog PJ. Overview. type I interferons as primers, activators and inhibitors of innate and adaptive immune responses. immunology and cell biology. *Immunol Cell Biol* (2012) 90(5):471–3. doi: 10.1038/icb.2012.15

76. Liu CX, Li X, Nan F, Jiang S, Gao X, Guo SK, et al. Structure and degradation of circular RNAs regulate PKR activation in innate immunity. *Cell* (2019) 177(4):865–80.e21. doi: 10.1016/j.cell.2019.03.046

77. Chousterman BG, Swirski FK, Weber GF. Cytokine storm and sepsis disease pathogenesis. *Semin Immunopathol* (2017) 39(5):517–28. doi: 10.1007/s00281-017-0639-8

78. Fagone P, Ciurleo R, Lombardo SD, Iacobello C, Palermo CI, Shoenfeld Y, et al. Transcriptional landscape of SARS-CoV-2 infection dismantles pathogenic pathways activated by the virus, proposes unique sex-specific differences and predicts tailored therapeutic strategies. *Autoimmun Rev* (2020) 19(7):102571. doi: 10.1016/j.autrev.2020.102571

79. Shen L, Hu Y, Lou J, Yin S, Wang W, Wang Y, et al. CircRNA-0044073 is upregulated in atherosclerosis and increases the proliferation and invasion of cells by targeting miR-107. *Mol Med Rep* (2019) 19(5):3923–32. doi: 10.3892/mmr.2019.10011

80. Wang R, Zhang Y, Xu L, Lin Y, Yang X, Bai L, et al. Protein inhibitor of activated STAT3 suppresses oxidized LDL-induced cell responses during atherosclerosis in apolipoprotein e-deficient mice. *Sci Rep* (2016) 6:36790. doi: 10.1038/srep36790

81. García-Howard M, Herranz-Aguirre M, Moreno-Galarraga L, Urretavizcaya-Martinez M, Alegria-Echauri J, Gorriá-Redondo N, et al. Case report: Benign infantile seizures temporally associated with COVID-19. *Front Pediatr* (2020) 8:507. doi: 10.3389/fped.2020.00507

82. McClelland S, Dubé CM, Yang J, Baram TZ. Epileptogenesis after prolonged febrile seizures: mechanisms, biomarkers and therapeutic opportunities. *Neurosci Letters* (2011) 497(3):155–62. doi: 10.1016/j.neulet.2011.02.032

83. Yang J, Cheng M, Gu B, Wang J, Yan S, Xu D. CircRNA\_09505 aggravates inflammation and joint damage in collagen-induced arthritis mice via miR-6089/AKT1/NF- $\kappa$ B axis. *Cell Death Dis* (2020) 11(10):833. doi: 10.1038/s41419-020-03038-z

84. Khan S, Shafiei MS, Longoria C, Schoggins JW. SARS-CoV-2 spike protein induces inflammation via TLR2-dependent activation of the NF- $\kappa$ B pathway. *Elife* (2021) 10. doi: 10.7554/eLife.68563

85. Wu Y, Ma L, Cai S, Zhuang Z, Zhao Z, Jin S. RNA-Induced liquid phase separation of SARS-CoV-2 nucleocapsid protein facilitates NF- $\kappa$ B hyper-activation and inflammation. *Signal Transduct Target Ther* (2021) 6(1):167. doi: 10.1038/s41392-021-00575-7

86. Ma Q, Li R, Pan W, Huang W, Liu B, Xie Y, et al. Phyllyrin (KD-1) exerts anti-viral and anti-inflammatory activities against novel coronavirus (SARS-CoV-2) and human coronavirus 229E (HCoV-229E) by suppressing the nuclear factor kappa b (NF- $\kappa$ B) signaling pathway. *Phytomedicine* (2020) 78:153296. doi: 10.1016/j.phymed.2020.153296

87. Neufeldt CJ, Cerikan B, Cortese M, Frankish J, Lee JY, Plociennikowska A, et al. SARS-CoV-2 infection induces a pro-inflammatory cytokine response through cGAS-STING and NF- $\kappa$ B. *Commun Biol* (2022) 5(1):45. doi: 10.1038/s42003-021-02983-5

88. Giron LB, Peluso MJ, Ding J, Kenny G, Zilberstein NF, Koshy J, et al. Markers of fungal translocation are elevated during post-acute sequelae of SARS-CoV-2 and induce NF- $\kappa$ B signaling. *JCI Insight* (2022) 7(18):e164813. doi: 10.1172/jci.insight.160989

89. Li G, Fan Y. Coronavirus infections and immune responses. (2020) 92(4):424–32. doi: 10.1002/jmv.25685

90. Shapiro JS, Schmid S, Aguado LC, Sabin LR, Yasunaga A, Shim JV, et al. Droscha as an interferon-independent antiviral factor. *Proc Natl Acad Sci U S A* (2014) 111(19):7108–13. doi: 10.1073/pnas.1319635111

91. Weisblum Y, Schmidt F. Escape from neutralizing antibodies by SARS-CoV-2 spike protein variants. *Elife* (2020) 9:e61312. doi: 10.7554/eLife.61312

92. Zaffagni M, Harris JM, Patop IL, Pamudurti NR, Nguyen S, Kadener S. SARS-CoV-2 Nsp14 mediates the effects of viral infection on the host cell transcriptome. bioRxiv : the preprint server for biology. *bioRxiv [Preprint]* (2022) 2021.07.02.450964. doi: 10.1101/2021.07.02.450964

93. Ogando NS, Zevenhoven-Dobbe JC, van der Meer Y, Bredenbeek PJ, Posthuma CC. The enzymatic activity of the nsp14 exoribonuclease is critical for replication of MERS-CoV and SARS-CoV-2. (2020) 94(23):93. doi: 10.1128/jvi.01246-20

94. Medzhitov R. Toll-like receptors and innate immunity. *Nat Rev Immunol* (2001) 1(2):135–45. doi: 10.1038/35100529

95. Guan H, Wang Y, Perčulija V, Saeed A, Liu Y, Li J, et al. Cryo-electron microscopy structure of the swine acute diarrhea syndrome coronavirus spike glycoprotein provides insights into evolution of unique coronavirus spike proteins. *J Virol* (2020) 94(22):e01301–20. doi: 10.1128/jvi.01301-20

96. Zaffagni M, Harris JM, Patop IL, Pamudurti NR, Nguyen S, Kadener S. SARS-CoV-2 Nsp14 mediates the effects of viral infection on the host cell transcriptome. (2022) 11:e71945. doi: 10.7554/eLife.71945

97. Hassanin A, Rambaud O, Klein D. Genomic bootstrap barcodes and their application to study the evolution of sarbecoviruses. *Viruses* (2022) 14(2):440. doi: 10.3390/v14020440

98. Yang S, Zhou H. Circular RNA profiling reveals abundant and diverse circRNAs of SARS-CoV-2, SARS-CoV and MERS-CoV origin. *bioRxiv [Preprint]* (2020) 2020.12.07.415422. doi: 10.1101/2020.12.07.415422

99. Liu Z, Zhang X, Yu Q, He JJ. Exosome-associated hepatitis c virus in cell cultures and patient plasma. *Biochem Biophys Res Commun* (2014) 455(3-4):218–22. doi: 10.1016/j.bbrc.2014.10.146

100. Kerr CH, Dalwadi U, Scott NE. Transmission of cricket paralysis virus via exosome-like vesicles during infection of drosophila cells. *Sci Rep* (2018) 8(1):17353. doi: 10.1038/s41598-018-35717-5

101. Elrashdy F, Aljaddawi AA, Redwan EM. On the potential role of exosomes in the COVID-19 reinfection/reactivation opportunity. *J Biomol Struct Dyn* (2021) 39(15):5831–42. doi: 10.1080/07391102.2020.1790426

102. Sun J, Ye F, Wu A, Yang R, Pan M, Sheng J, et al. Comparative transcriptome analysis reveals the intensive early stage responses of host cells to SARS-CoV-2 infection. *Front Microbiol* (2020) 11:593857. doi: 10.3389/fmicb.2020.593857

103. Xu Z, Shi L, Wang Y, Zhang J, Huang L, Zhang C, et al. Pathological findings of COVID-19 associated with acute respiratory distress syndrome. *Lancet Respir Med* (2020) 8(4):420–2. doi: 10.1016/s2213-2600(20)30076-x

104. Milsted A, Underwood AC, Dunmire J, DelPuerto HL, Martins AS, Ely DL, et al. Regulation of multiple renin-angiotensin system genes by sry. *J Hypertens* (2010) 28(1):59–64. doi: 10.1097/HJH.0b013e3283232b8d

105. Wang D LD. Bioinformatics analysis of ACE2 gene promoter Region, SARS-CoV-2 key receptor. *J Natural Sci Hunan Normal Univ* (2020) 43(5):30. doi: 10.7612/j.jssn.2096-5281.2020.05.005

106. Capel B, Swain A, Nicolis S, Hacker A, Walter M, Koopman P, et al. Circular transcripts of the testis-determining gene sry in adult mouse testis. *Cell* (1993) 73(5):1019–30. doi: 10.1016/0092-8674(93)90279-y

107. Granados-Riveron JT, Aquino-Jarquín G. Does the linear sry transcript function as a ceRNA for miR-138? the sense of antisense. *F1000Research* (2014) 3:90. doi: 10.12688/f1000research.3872.2

108. Li S, Liu J, Liu S, Jiao W, Wang X. Mesenchymal stem cell-derived extracellular vesicles prevent the development of osteoarthritis via the circHIPK3/miR-124-3p/MYH9 axis. *J Nanobiotechnol* (2021) 19(1):194. doi: 10.1186/s12951-021-00940-2

109. Zhang W, Zhang H, Zhao X. circ\_0005273 promotes thyroid carcinoma progression by SOX2 expression. *Endocr-related Cancer* (2020) 27(1):11–21. doi: 10.1530/erc-19-0381

110. Zhang P, Li J. Down-regulation of circular RNA hsa\_circ\_0007534 suppresses cell growth by regulating miR-219a-5p/SOX5 axis in osteosarcoma. *J Bone Oncol* (2021) 27:100349. doi: 10.1016/j.jbo.2021.100349

111. Bohan D, Van Ert H. Phosphatidylserine receptors enhance SARS-CoV-2 infection. *PLoS Pathog* (2021) 17(11):e1009743. doi: 10.1371/journal.ppat.1009743

112. Wei Y LWY, Fan RG, Hou W, Wen SJ, Lin YK. Preliminary study on the molecular mechanism of circRNA hsa-circ-0006689 in systemic lupus erythematosus. *J Guangxi Med Univ* (2021) 38(3):486–92. doi: 10.16190/j.cnki.45-1211/r.2021.03.011

113. Getts DR, Chastain EM, Terry RL, Miller SD. Virus infection, antiviral immunity, and autoimmunity. *Immunol Rev* (2013) 255(1):197–209. doi: 10.1111/immr.12091

114. Xue M, Del Bigio MR. Intracortical hemorrhage injury in rats : relationship between blood fractions and brain cell death. *Stroke* (2000) 31(7):1721–7. doi: 10.1161/01.str.31.7.1721

115. Tanaka T, Narazaki M, Masuda K, Kishimoto T. Regulation of IL-6 in immunity and diseases. *Adv Exp Med Biol* (2016) 941:79–88. doi: 10.1007/978-94-024-0921-5\_4

116. van den Berg DF, Te Velde AA. Severe COVID-19: NLRP3 inflammasome dysregulated. *Front Immunol* (2020) 11:1580. doi: 10.3389/fimmu.2020.01580

117. Hariharan A, Hakeem AR. The role and therapeutic potential of NF-kappa-B pathway in severe COVID-19 patients. *Inflammopharmacology* (2021) 29(1):91–100. doi: 10.1007/s10787-020-00773-9



118. Kircheis R, Haasbach E, Lueftenegger D, Heyken WT, Ocker M, Planz O. NF- $\kappa$ B pathway as a potential target for treatment of critical stage COVID-19 patients. *Front Immunol* (2020) 11:598444. doi: 10.3389/fimmu.2020.598444
119. Cai X, Huang Y, Zhang X, Wang S, Zou Z, Wang G, et al. Cloning, characterization, hypoxia and heat shock response of hypoxia inducible factor-1 (HIF-1) from the small abalone *haliotis diversicolor*. *Gene* (2014) 534(2):256–64. doi: 10.1016/j.gene.2013.10.048
120. Sheu SY, Hong YW, Sun JS, Liu MH, Chen CY, Ke CJ. Radix scrophulariae extracts (harpagoside) suppresses hypoxia-induced microglial activation and neurotoxicity. *BMC complement Altern Med* (2015) 15:324. doi: 10.1186/s12906-015-0842-x
121. Tian M, Liu W, Li X, Zhao P, Shereen MA, Zhu C, et al. HIF-1 $\alpha$  promotes SARS-CoV-2 infection and aggravates inflammatory responses to COVID-19. *Signal Transduct Target Ther* (2021) 6(1):308. doi: 10.1038/s41392-021-00726-w
122. Yang YW, Meng X, Meng YY, Tang HK, Cheng MH, Zhang ZQ, et al. ceRNA regulatory network of FIH inhibitor as a radioprotector for gastrointestinal toxicity by activating the HIF-1 pathway. *Mol Ther Nucleic Acids* (2021) 25:173–85. doi: 10.1016/j.omtn.2021.05.008
123. Demirci YM, Saçar Demirci MD. Circular RNA-MicroRNA-mRNA interaction predictions in SARS-CoV-2 infection. *J Integr Bioinf* (2021) 18(1):45–50. doi: 10.1515/jib-2020-0047
124. Harcourt BH, Jukneliene D, Kanjanahaluethai A, Bechill J, Severson KM, Smith CM, et al. Identification of severe acute respiratory syndrome coronavirus replicase products and characterization of papain-like protease activity. *J virol* (2004) 78(24):13600–12. doi: 10.1128/jvi.78.24.13600-13612.2004
125. Lim KP, Ng LF, Liu DX. Identification of a novel cleavage activity of the first papain-like proteinase domain encoded by open reading frame 1a of the coronavirus avian infectious bronchitis virus and characterization of the cleavage products. *J virol* (2000) 74(4):1674–85. doi: 10.1128/jvi.74.4.1674-1685.2000
126. Mahmoudvand S, Shokri S. Interactions between SARS coronavirus 2 papain-like protease and immune system: A potential drug target for the treatment of COVID-19. *Scand J Immunol* (2021) 94(4):e13044. doi: 10.1111/sji.13044
127. Bailey-Elkin BA, Knaap RC, Johnson GG, Dalebout TJ, Ninaber DK, van Kasteren PB, et al. Crystal structure of the middle East respiratory syndrome coronavirus (MERS-CoV) papain-like protease bound to ubiquitin facilitates targeted disruption of deubiquitinating activity to demonstrate its role in innate immune suppression. *J Biol Chem* (2014) 289(50):34667–82. doi: 10.1074/jbc.M114.609644
128. Ratia K, Saikatendu KS, Santarsiero BD, Barretto N, Baker SC, Stevens RC, et al. Severe acute respiratory syndrome coronavirus papain-like protease: structure of a viral deubiquitinating enzyme. *Proc Natl Acad Sci United States America*. (2006) 103(15):5717–22. doi: 10.1073/pnas.0510851103
129. Kindrachuk J, Ork B, Hart BJ, Mazur S. Antiviral potential of ERK/MAPK and PI3K/AKT/mTOR signaling modulation for middle East respiratory syndrome coronavirus infection as identified by temporal kinase analysis. *Antimicrob Agents Chemother* (2015) 59(2):1088–99. doi: 10.1128/aac.03659-14
130. Di Liddo A, de Oliveira Freitas Machado C, Fischer S, Ebersberger S, Heumüller AW, Weigand JE, et al. A combined computational pipeline to detect circular RNAs in human cancer cells under hypoxic stress. *J Mol Cell Biol* (2019) 11(10):829–44. doi: 10.1093/jmcb/mjz094
131. Zarnack K, König J, Tajnik M, Martincorena I, Eustermann S, Stévant I, et al. Direct competition between hnRNP c and U2AF65 protects the transcriptome from the exonization of alu elements. *Cell* (2013) 152(3):453–66. doi: 10.1016/j.cell.2012.12.023
132. Meißner T. MMW fortschritte der medizin. (2021) 163(14):64. doi: 10.1007/s15006-021-0196-x
133. Sprute R, Schumacher S, Pauls M, Pauls W, Cornely OA. Delayed cutaneous hypersensitivity reaction to vaxzevria (ChAdOx1-s) vaccine against SARS-CoV-2. *Drugs RD* (2021) 21(4):371–4. doi: 10.1007/s40268-021-00358-z
134. Knoll MD, Wonodi C. Oxford-AstraZeneca COVID-19 vaccine efficacy. *Lancet (London England)* (2021) 397(10269):72–4. doi: 10.1016/s0140-6736(20)32623-4
135. Sadoff J, Le Gars M, Shukarev G, Heerwegh D, Truysers C, de Groot AM, et al. Interim results of a phase 1-2a trial of Ad26. COV2.S Covid-19 Vaccine (2021) 384(19):1824–35. doi: 10.1056/NEJMoa2034201
136. Hammerschmidt SI, Thurm C, Bošnjak B, Bernhardt G. Robust induction of neutralizing antibodies against the SARS-CoV-2 delta variant after homologous spikevax or heterologous vaxzevria-spikevax vaccination. (2022) 52(2):356–9. doi: 10.1002/eji.202149645
137. Wang H, Zhang Y, Huang B, Deng W, Quan Y, Wang W, et al. Development of an inactivated vaccine candidate, BBIBP-CorV, with potent protection against SARS-CoV-2. *Cell* (2020) 182(3):713–21.e9. doi: 10.1016/j.cell.2020.06.008
138. Sharma O, Sultan AA, Ding H, Triggler CR. A review of the progress and challenges of developing a vaccine for COVID-19. *frontiers in immunology. Front Immunol* (2020) 11:585354. doi: 10.3389/fimmu.2020.585354
139. Thiagarajan K. What do we know about india's covaxin vaccine? *BMJ* (2021) 373:n997. doi: 10.1136/bmj.n997
140. Chung YH, Beiss V, Fiering SN, Steinmetz NF. COVID-19 vaccine frontrunners and their nanotechnology design. *ACS Nano* (2020) 14(10):12522–37. doi: 10.1021/acsnano.0c07197
141. Jones I, Roy P, Sputnik V COVID-19 vaccine candidate appears safe and effective. *Lancet (London England)* (2021) 397(10275):642–3. doi: 10.1016/s0140-6736(21)00191-4
142. Akova M, Unal S. A randomized, double-blind, placebo-controlled phase III clinical trial to evaluate the efficacy and safety of SARS-CoV-2 vaccine (inactivated, vero cell): a structured summary of a study protocol for a randomised controlled trial. *Trials* (2021) 22(1):276. doi: 10.1186/s13063-021-05180-1
143. Wu S, Huang J, Zhang Z, Wu J, Zhang J, Hu H, et al. Safety, tolerability, and immunogenicity of an aerosolised adenovirus type-5 vector-based COVID-19 vaccine (Ad5-nCoV) in adults: preliminary report of an open-label and randomised phase 1 clinical trial. *Lancet Infect Dis* (2021) 21(12):1654–64. doi: 10.1016/s1473-3099(21)00396-0
144. Francica JR, Flynn BJ, Foulds KE, Noe AT, Werner AP, Moore IN, et al. Vaccination with SARS-CoV-2 spike protein and AS03 adjuvant induces rapid anamnestic antibodies in the lung and protects against virus challenge in nonhuman primates. *bioRxiv preprint server Biol* (2021). doi: 10.1101/2021.03.02.433390
145. Ambrosino D, Han HH, Hu B, Liang J, Clemens R, Johnson M, et al. Immunogenicity of SCB-2019 coronavirus disease 2019 vaccine compared with 4 approved vaccines. *J Infect Dis* (2022) 225(2):327–31. doi: 10.1093/infdis/jiab574
146. Liu H, Zhou C, An J, Song Y, Yu P, Li J, et al. Development of recombinant COVID-19 vaccine based on CHO-produced, prefusion spike trimer and alum/CpG adjuvants. *Vaccine* (2021) 39(48):7001–11. doi: 10.1016/j.vaccine.2021.10.066
147. Baker N, Dolgin E. Coronapod: CureVac disappoints in COVID vaccine trial. *Nature* (2021). doi: 10.1038/d41586-021-01694-5
148. Hadj Hassine I. Covid-19 vaccines and variants of concern: A review. *Rev Med Virol* (2021) 32(4):e2313. doi: 10.1002/rmv.2313
149. Aguilar-Guerra TL, Fajardo-Díaz EM. Cuba's national regulatory authority & COVID-19: Olga lidia jacobó-casanueva MS director, center for state control of medicines and medical devices (CECMED). *MEDICC Rev* (2021) 23(3-4):9–14. doi: 10.37757/mr2021.v23.n3.3
150. Patiño C, Haenni AL, Urcuqui-Inchima S. NF90 isoforms, a new family of cellular proteins involved in viral replication? *Biochimie* (2015) 108:20–4. doi: 10.1016/j.biochi.2014.10.022
151. Kristensen LS, Andersen MS, Stagsted LVW, Ebbesen KK, Hansen TB. The biogenesis, biology and characterization of circular RNAs. *Nat Rev Genet* (2019) 20(11):675–91. doi: 10.1038/s41576-019-0158-7
152. Enuke Y, Lauriola M, Feldman ME, Sas-Chen A, Ulitsky I, Yarden Y. Circular RNAs are long-lived and display only minimal early alterations in response to a growth factor. *Nucleic Acids Res* (2016) 44(3):1370–83. doi: 10.1093/nar/gkv1367
153. Pamudurti NR, Bartok O, Jens M, Ashwal-Fluss R, Stottmeister C, Ruhe L, et al. Translation of CircRNAs. *Mol Cell* (2017) 66(1):9–21.e7. doi: 10.1016/j.molcel.2017.02.021
154. Wesselhoeft RA, Kowalski PS, Anderson DG. Engineering circular RNA for potent and stable translation in eukaryotic cells. *Nat Commun* (2018) 9(1):2629. doi: 10.1038/s41467-018-05096-6
155. Yang Y, Fan X, Mao M, Song X, Wu P, Zhang Y, et al. Extensive translation of circular RNAs driven by N(6)-methyladenosine. *Cell Res* (2017) 27(5):626–41. doi: 10.1038/cr.2017.31
156. Breuer J, Barth P, Noe Y, Shalamova L, Goesmann A, Weber F, et al. What goes around comes around: Artificial circular RNAs bypass cellular antiviral responses. *Mol Ther Nucleic Acids* (2022) 28:623–35. doi: 10.1016/j.omtn.2022.04.017

## Glossary

COVID-19	coronavirus disease 2019
RNase R	ribonuclease R
SARS-CoV-2	severe acute respiratory syndrome coronavirus 2
CoVs	coronaviruses
PKR	Protein Kinase R
RNase L	ribonuclease L
NF90	nuclear factor 90
NF110	nuclear factor 110
Calu-3	human lung adenocarcinoma cells
SARS-CoV-1	severe acute respiratory syndrome coronavirus 1
MERS-CoV	middle east respiratory syndrome coronavirus
ORF	open reading frame
nsps	nonstructural proteins
S	spike
E	envelope
M	membrane
N	nucleocapsid
ACE2	angiotensin-converting enzyme 2
DPP4	dipeptidyl peptidase 4
TMPRSS2	transmembrane serine protease 2
CatB	cathepsin B
CatL	cathepsin L
AAK1	AP2-associated kinase 1
TLRs	toll-like receptors
TF	transcription factor
SIRs	systemic inflammatory responses
IL-6	interleukin-6
ncRNAs	non-coding RNAs
hpi	hours post-infection
ecircRNA	exonic circRNA
ciRNA	intronic circRNA

(Continued)

## Continued

ELciRNA	exon-intronic circRNA
ceRNA	competing endogenous RNA
miRNA	microRNA
lncRNA	long noncoding RNA
mRNA	messenger RNA
HFL-I	human embryonic lung fibroblast cell
ILF3	human interleukin-enhanced binding factor 3
dsRNA	double-stranded RNA
CircRNPs	circRNA-protein complexes
RIG-I	retinoic acid inducible gene-I
HIF-1	hypoxia-inducible factor-1
mTOR	mammalian leukemia target of pamycin
TNF	tumor necrosis factor
MAPK	mitogen-activated protein kinase
ISG	interferon-stimulated gene
IFN	interferon
OAS1-3	2'-5' oligoadenylate synthase
Ifit1-3	interferon-inducible protein
Th1	T helper cell type 1
2'-5'A	2'-5' oligoadenylate
PKR	Protein Kinase R
RA	arthritic
HUVSMCs	human vascular smooth muscle cells
HUVECs	human vascular endothelial cells
RLRs	RIG-I-like receptors
FSJs	forward splicing junctions
SRY	sex-determining region Y
AXL	AXL receptor tyrosine kinase
RTK	receptor tyrosine kinase
NF-kB	nuclear factor-kB
NOS2	inducible nitric oxide synthase
PLpro	papain-like protease
ERK	extracellular signal-regulated kinase
RBD	receptor-binding domain





## OPEN ACCESS

## EDITED BY

Alfonso J. Rodríguez-Morales,  
Fundación Universitaria Autónoma de  
las Américas, Colombia

## REVIEWED BY

Zhonglei Wang,  
Qufu Normal University, China  
Pedro Xavier-Elsas,  
Federal University of Rio de  
Janeiro, Brazil

## \*CORRESPONDENCE

Ivan Duran  
ijduran@uma.es

†These authors have contributed  
equally to this work and share  
last authorship

## SPECIALTY SECTION

This article was submitted to  
Viral Immunology,  
a section of the journal  
Frontiers in Immunology

RECEIVED 27 September 2022

ACCEPTED 27 October 2022

PUBLISHED 18 November 2022

## CITATION

Rico-Llanos G, Porras-Perales Ó,  
Escalante S, Vázquez-Calero DB,  
Valiente L, Castillo MI, Pérez-  
Tejeiro JM, Baglietto-Vargas D,  
Becerra J, Reguera JM, Duran I and  
Csukasi F (2022) Cellular stress  
modulates severity of the  
inflammatory response in lungs *via* cell  
surface BiP.  
*Front. Immunol.* 13:1054962.  
doi: 10.3389/fimmu.2022.1054962

## COPYRIGHT

© 2022 Rico-Llanos, Porras-Perales,  
Escalante, Vázquez-Calero, Valiente,  
Castillo, Pérez-Tejeiro, Baglietto-Vargas,  
Becerra, Reguera, Duran and Csukasi.  
This is an open-access article  
distributed under the terms of the  
Creative Commons Attribution License  
(CC BY). The use, distribution or  
reproduction in other forums is  
permitted, provided the original  
author(s) and the copyright owner(s)  
are credited and that the original  
publication in this journal is cited, in  
accordance with accepted academic  
practice. No use, distribution or  
reproduction is permitted which does  
not comply with these terms.

# Cellular stress modulates severity of the inflammatory response in lungs *via* cell surface BiP

Gustavo Rico-Llanos<sup>1,2</sup>, Óscar Porras-Perales<sup>2,3</sup>,  
Sandra Escalante<sup>2,4</sup>, Daniel B. Vázquez-Calero<sup>2,5</sup>,  
Lucía Valiente<sup>2,3</sup>, María I. Castillo<sup>2</sup>,  
José Miguel Pérez-Tejeiro<sup>2,4</sup>, David Baglietto-Vargas<sup>4,6,7</sup>,  
José Becerra<sup>1,2,4</sup>, José María Reguera<sup>2,3</sup>, Ivan Duran<sup>1,2,4,8\*†</sup>  
and Fabiana Csukasi<sup>1,2,4†</sup>

<sup>1</sup>Networking Biomedical Research Center in Bioengineering, Biomaterials, and Nanomedicine (CIBER-BBN), Andalusian Centre for Nanomedicine and Biotechnology, Málaga, Spain, <sup>2</sup>Laboratory of Precision Medicine in Musculoskeletal and Inflammatory Diseases, IBIMA-Bionand Platform, Málaga, Spain, <sup>3</sup>Infectious Disease Unit, Hospital Regional de Málaga, Málaga, Spain, <sup>4</sup>Department of Cell Biology, Genetics, and Physiology, Faculty of Sciences, University of Málaga, Málaga, Spain, <sup>5</sup>Veterinary clinic of exotic pets ARACAVIA, Málaga, Spain, <sup>6</sup>Networking Biomedical Research Center in Neurodegenerative Disease (CIBER-NED), Madrid, Spain, <sup>7</sup>Institute for Memory Impairments and Neurological Disorders, University of California, Irvine, Irvine, CA, United States, <sup>8</sup>Department of Orthopaedic Surgery, University of California-Los Angeles, Los Angeles, CA, United States

Inflammation is a central pathogenic feature of the acute respiratory distress syndrome (ARDS) in COVID-19. Previous pathologies such as diabetes, autoimmune or cardiovascular diseases become risk factors for the severe hyperinflammatory syndrome. A common feature among these risk factors is the subclinical presence of cellular stress, a finding that has gained attention after the discovery that BiP (GRP78), a master regulator of stress, participates in the SARS-CoV-2 recognition. Here, we show that BiP serum levels are higher in COVID-19 patients who present certain risk factors. Moreover, early during the infection, BiP levels predict severe pneumonia, supporting the use of BiP as a prognosis biomarker. Using a mouse model of pulmonary inflammation, we observed increased levels of cell surface BiP (cs-BiP) in leukocytes during inflammation. This corresponds with a higher number of neutrophils, which show naturally high levels of cs-BiP, whereas alveolar macrophages show a higher than usual exposure of BiP in their cell surface. The modulation of cellular stress with the use of a clinically approved drug, 4-PBA, resulted in the amelioration of the lung hyperinflammatory response, supporting the anti-stress therapy as a valid therapeutic strategy for patients developing ARDS. Finally, we identified stress-modulated proteins that shed light into the mechanism underlying the cellular stress-inflammation network in lungs.

## KEYWORDS

COVID-19, acute respiratory distress syndrome, binding-immunoglobulinprotein (BiP/GRP78/HSPA5), cytokine storm, cell surface GRP78 (csGRP78), cellular stress, 4-PBA, TNFα

## Introduction

The COVID-19 pandemic has challenged our understanding of the inflammatory response. COVID-19 is an infectious disease that becomes severe and lethal through a poorly known mechanism whose output is barely prognosed by risk factors and comorbidities (1, 2). Since the first wave in 2020, we have learned that the *severe acute respiratory syndrome coronavirus 2* (SARS-CoV-2) is able to induce a hyperinflammatory response commonly known as *cytokine storm*, with consequences that are very similar to other diseases with a *cytokine release syndrome* (CRS). Although COVID-19 is considered a systemic disease, the respiratory system is the most affected, where the CRS is better defined as *acute respiratory distress syndrome* (ARDS).

A major problem with COVID-19 has been the inability to predict which patients could develop a severe disease and the most accurate method to predict the outcome of the infection has been the measurement of interleukin-6 (IL-6) (1, 3–5). However, IL-6 can only be detected after the development of acute symptoms, leaving clinical risk factors as our only way of prognosis (6, 7). Risk factors correlated with COVID-19 include age (median > 62), sex (with increased tendency in men), and chronic pathologies such as diabetes, chronic liver disease, hypertension, immunodeficiency, chronic obstructive pulmonary disease (COPD), smoking history, among others (8–11), and while they have been useful for early follow-up of symptoms, they are not accurate predicting severity and they do not include subclinical manifestations that also cause severe CRS.

The cytokine profile of COVID-19 has been studied since the beginning of the pandemic concluding that it does not differ much from other forms of ARDS and sepsis (1). There is plenty of evidence that elevated levels of different cytokines like IFN- $\gamma$ , IL-6, IL-1 $\beta$ , IL-10 and MCP-1 are higher in COVID-19 patients. There is also a clear association between others such as IP-10, MCP-1, MIP-1 $\alpha$ , TNF- $\alpha$  and IL-6 and COVID-19 severity when comparing ICU-patients with non-ICU patients (1, 3–5). However, they do not predict the severity outcome of the disease and they cannot be used reliably to explain why some patients develop a severe response to the infection.

The binding-immunoglobulin protein (BiP), also called Grp78, and encoded by the gene *Hspa5*, is an endoplasmic reticulum (ER) chaperone that acts as a master regulator of the unfolded protein response (UPR) and ER-stress signaling pathways (12, 13). Increased levels of BiP have been found in several pathological conditions such as liver disease (14), metabolic disorders and atherosclerosis (15, 16), cardiovascular diseases (17), diabetes (18), cancer (19, 20), acute lung injury (ALI) (21), autoimmune disorders (22, 23), different forms of subclinical inflammation (24, 25), aging (26) and neurodegenerative diseases (27). Many of these pathologies are risk factors for COVID-19. Although the main fraction of BiP in the cell is dedicated to regulate the UPR and the secretory pathway, BiP has also been found to translocate to other compartments upon stress stimulus (cytoplasm, mitochondria, extracellular matrix and

cell surface) (28, 29). Cellular surface BiP (csBiP or csGRP78) acts as a co-receptor for different signaling pathways (PI3K, CD109, Cripto, CD44v, alpha2M, caspases 7 and 8 and clathrin dependent pathways) modulating cell proliferation, differentiation, survival and apoptosis (30, 31). It is therefore considered a key protein in the crosstalk between multiple signaling pathways, working as a sensor of various cellular stresses to maintain homeostasis (20). Moreover, BiP has been found to participate in many viral infections including COVID-19 (32, 33), Ebola, Zika, Dengue, Japanese Encephalitis Virus, Cocksackievirus A9, Borna Disease Virus and the Middle-East Respiratory Syndrome coronavirus (MERS) (33–39). However, even when there is solid evidence that dysregulated levels of both intracellular and csBiP are linked to these diseases, much work is needed to fully understand the mechanism by which this protein modulates inflammation in response to the stress signals that increase its expression or promote its localization to the cell membrane. Nonetheless, BiP is a multifunctional chaperone that goes beyond the ER compartment when the cell is under any type of cellular stress (infection, hypoxia, heat shock, ER and oxidative stress) (40–44).

After BiP was found to act as a co-receptor of Angiotensin converting enzyme-2 (ACE2) for SARS-CoV-2 virus (33) BiP has been hypothesized to favor virus entry into the cell, however, evidence from other pathologies in which BiP acts as co-receptor indicate that this role goes beyond virus recognition or replication. For example, BiP has been related as an immunomodulatory factor interacting with the Jak/STAT system and possibly with other cytokine intracellular signaling components, including IL-6 (45, 46). From all this evidence, our group and others have suggested that BiP and the cellular stress must have a modulatory effect on the hyper-inflammatory response produced after infection with SARS-CoV-2 and its clinical outcome (47, 48).

Here, we investigated the role of cellular stress and BiP in the modulation of the ARDS inflammatory response in samples from COVID-19 patients and a mouse model of ARDS. We demonstrate that BiP levels correlate with the severity of ARDS. Furthermore, we show that the localization of BiP on the cell surface is increased in the immune cell lineages during ARDS proportionally to the severity of the inflammatory response and identify a network of proteins that mediate this pathological process. Our results support the use of BiP as a prognosis biomarker of severe pneumonia and offer a new therapeutic strategy for diseases with ARDS such as COVID-19.

## Results

### BiP levels in blood serum correlate with COVID-19 comorbidities and severity

Besides being a SARS-CoV-2 coreceptor, BiP is increased in several pathologies identified as risk factors of COVID-19, however, no study has investigated the connection of BiP with

the risk factors of severe COVID-19. To correlate BiP with COVID-19 severity we measured BiP levels in blood serum from 194 patients of the first wave of the pandemic (March–June 2020), obtained at the beginning of the SARS-CoV-2 infection during the first medical evaluation. All patients were confirmed PCR-positive. This cohort included patients with different degree of clinical severity, from asymptomatic to lethal COVID-19. Thirty healthy blood donors, without infection or any detectable pathology, were used as a control of BiP levels (see [Supplementary document 1](#) about blood donor selection/exclusion criteria). We established that 95% of the healthy control population has levels of BiP in serum below 181 pg/ml. Thus, we considered high levels of BiP those above 181 pg/ml. The average BiP level was higher in patients compared to control although it did not reach significance ( $P$  value = 0.0789). We detected high levels of BiP in the blood serum of 35 out of the 194 COVID-19 patients (18.04%) ([Figure 1A](#)). To determine which risk factors and comorbidities were present in patients with increased BiP, we analyzed how BiP levels correlated with 43 clinical parameters ([Figure 1](#) and [S1](#)). BiP levels were higher in male patients and individuals above 60 years old, a group particularly vulnerable to suffer severe COVID-19 disease ([Figures 1B, C](#)). Among previous conditions, BiP was also elevated in patients with a history of hypertension, diabetes, immunosuppression and previous respiratory pathologies ([Figures 1D–G](#)). Within previous respiratory pathologies we were able to determine that increased BiP levels in blood correlated specifically with previous history of chronic obstructive pulmonary disease (COPD) ([Figure 1H](#)). These results indicate that increased BiP levels correlate to several risk factors of COVID-19 patients with a strong significance with the presence of previous respiratory pathologies.

To determine the predictive potential of circulating BiP we analyzed the relationship between BiP serum levels and respiratory parameters corresponding with a severe COVID-19 like development of pneumonia. To categorize severity in pneumonia, patients were clinically classified into 5 groups according with the need for oxygen saturation, tachypnea and mechanic ventilation (Table S1). We observed a solid correlation between BiP and pneumonia severity groups “high” and “very high” ([Figure 1I](#)), which includes patients with oxygen saturation below 90%, possible tachypnea and in need for mechanical ventilation. Supporting this correlation, BiP levels were also significantly elevated in patients presenting pulmonary consolidations, a radiological finding typical of severe pneumonia ([Figure 1J](#)). From this data, we determined the distinctive threshold of BiP levels above which all patients developed severe pneumonia under these two categories. Thus, any patient with BiP levels 300pg/ml or higher during the initial stages of the infection developed severe pneumonia and needed high flow mechanical ventilation ([Figure 1K](#)). These results suggest that serum levels of BiP are a useful biomarker of the severe pneumonia output.

Next, we studied the correlation between BiP and IL-6 levels, the most widely used inflammation and severity marker for COVID-19. Our data showed a significant correlation between systemic BiP and IL-6 ([Figure 1L](#)), which confirms not only the association between BiP and COVID-19 severity but also suggests a connection between cellular stress and inflammation in the COVID-19 mechanism of disease. No other relevant changes were observed in blood values in correlation with BiP serum levels ([Figure S2](#)).

To further evaluate the predictive character of BiP in serum, we compared BiP levels with severity indexes for COVID-19. Systemic BiP was correlated with COVID-19 severity measured by its specific scale: Brescia-COVID-19 Respiratory Severity Scale (49) that scored respiratory fatigue, respiratory rate  $>22$ ,  $\text{PaO}_2 <65$  mmHg,  $\text{SpO}_2 <90\%$  and significantly worsening Chest X-Ray. More precisely, BiP levels were significantly elevated in patients with a Brescia index  $\geq 2$  ([Figure 1M](#)). Interestingly, above this score, patients in our cohort were considered for Tocilizumab (Anti IL-6) treatment which accordingly correlated the selection criteria of high IL-6 with high levels of BiP in serum ([Figure 1N](#)). Given the association between BiP levels and respiratory parameters, we also analyzed other pneumonia scores such as Pneumonia Outcomes Research Team (PORT) or the Pneumonia Severity Score CURB65. However, while PORT showed a weak association to BiP levels, CURB65 showed no change regarding to the stress marker ([Figure S2](#)).

Altogether, these results indicate that the levels of BiP in serum, measured at the time of hospital admission, correlate with a variety of general pre-existing comorbidities and could be used as a biomarker of the severity output that is especially relevant in relation with respiratory pathologies.

## Treatment with 4-PBA ameliorates the severity of the hyperinflammatory response in ARDS

Given the association between the stress marker BiP and the cytokine IL-6, we next studied the connection between this UPR regulator and other markers of the inflammatory response to determine which factors could be modulated by cellular stress. As the respiratory conditions are among the most relevant correlations with the levels of BiP in serum, we used an inflammation mouse model of acute respiratory distress syndrome (ARDS) that consists on the intranasal administration of lipopolysaccharide (LPS) from *E. Coli*. To determine whether cellular stress is involved in the inflammatory response, we also studied the effect of the application of the molecular chaperone 4-PBA after LPS challenge, an approved drug for several pathologies (50–54) that reduces cellular stress and inflammation (55–57). Hemograms performed after administration of LPS revealed a systemic neutrophilia,

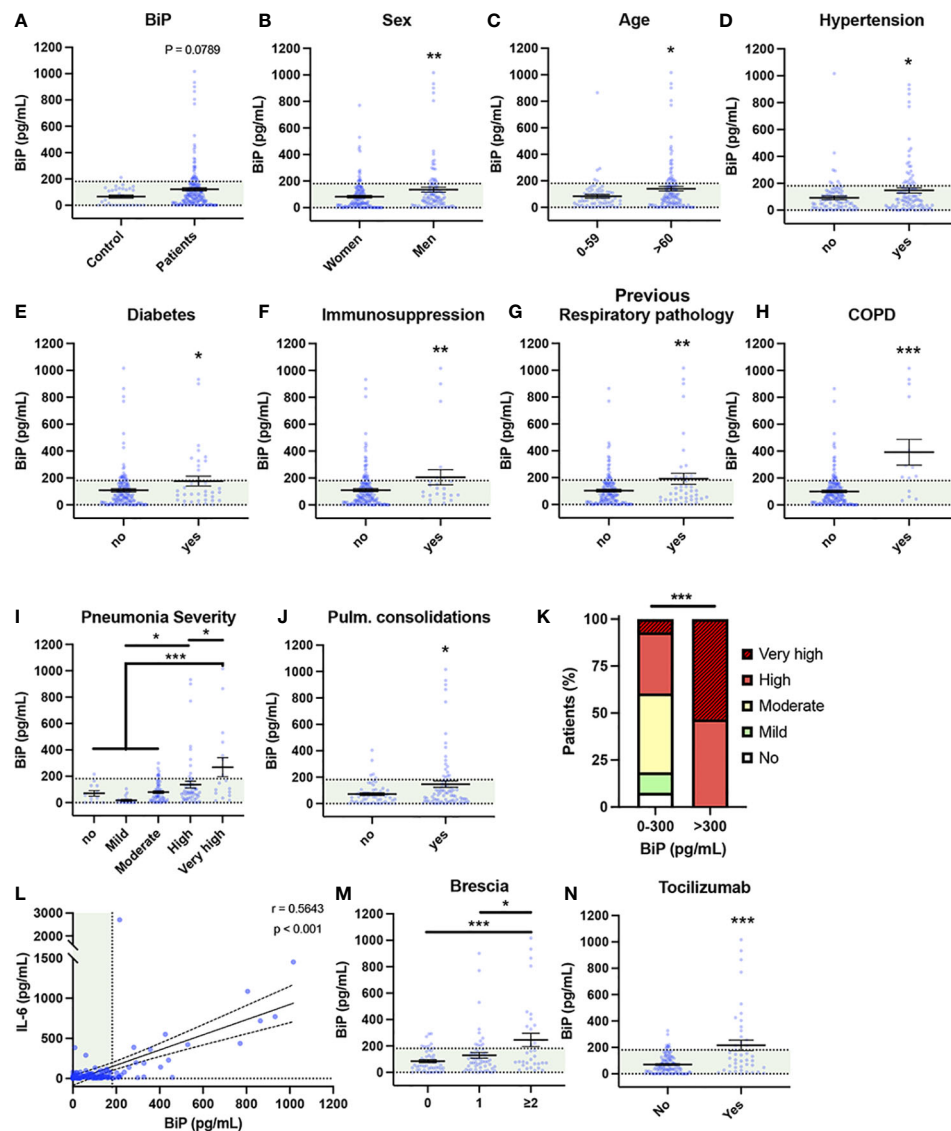


FIGURE 1

Serum BiP levels are increased in certain groups of COVID-19 patients. (A–L) Serum BiP levels classified by group of patients/donors. Black lines and whiskers denote the mean  $\pm$  SEM of every data set. Green areas represent normal BiP levels in serum (0 and 181 pg/mL, respectively) defined between 5<sup>th</sup> and 95<sup>th</sup> percentiles of healthy donor's data set. General BiP levels in total cohort: healthy control patients (n=30) versus COVID-19 patients (n=194) (A); BiP levels classified by Sex (B), Age (C), and previous comorbidities (D–H). (I) Serum BiP in patients classified by pneumonia severity in 5 levels depending on oxygen saturation, Tachypnea and need for mechanic ventilation. (J) BiP levels analyzed by radiological presence of pneumonia pulmonary consolidations developed during COVID-19. (K) Stacked bar plot showing percentage of patients with BiP levels below or above the selected critical threshold (300 pg/mL) who developed severe pneumonia (denoted by color code in legend). (L) Scatter plot showing a positive correlation between BiP levels versus IL-6 levels in blood serum tested by Pearson's correlation coefficient. (M) BiP levels analyzed by Brescia-COVID Respiratory Severity Scale. (N) BiP levels analyzed by application of Tocilizumab treatment. \* $P < 0.05$ , \*\* $P < 0.01$ , \*\*\* $P < 0.001$  indicate statistical significant differences between indicated samples for a Two-Tailed unpaired t-Test (A–H, J, N), One-Way ANOVA with a Tukey's multiple comparisons test (I, M) and Chi-square test (K).

lymphopenia and monocytosis, mimicking the human response to SARS-CoV-2 infection. 4-PBA treatment seemed to partially rescue the blood parameters, however, these changes were not statistically significant at the systemic level except for the monocyte numbers that increased with LPS and were significantly rescued with 4-PBA (Figure S3).

To study in depth the inflammatory response in lungs we measured 14 cytokines in the bronchoalveolar lavage fluid (BALF), selected by its relevance in lung tissues during the COVID-19 and/or cytokine storm syndrome. Among these, changes in IL-6, IL-1 $\beta$  and TNF- $\alpha$  levels were the best documented in the hyperinflammatory response associated to



COVID-19 and ARDS. LPS challenge induced a significant increase in all the cytokines included in this study (IL-1 $\beta$ , TNF- $\alpha$ , IL-6, IFN- $\gamma$ , IL-17a, MIP-1 $\alpha$ , MCP-3, GM-CSF, IP-10, RANTES, MIG, IL-18 and MCP-3) except for IL-12p70 whose increase was not statistically significant (Figures 2A–N). Nor PBS instillation (C-) neither 4-PBA alone induced any changes in the cytokine levels. These data validated our mouse model induced by LPS instillation and established a well-characterized response of acute lung inflammation (ALI) at the cytokine level.

When animals challenged with LPS were treated with 4-PBA to reduce cellular stress we observed a significant rescue of several cytokine values. Among these, we observed a significant decrease in the three best documented general pro-inflammatory markers in COVID-19: IL-6, IL-1 $\beta$  and TNF- $\alpha$  (Figure 2A–C). These cytokines have been extensively related with bad prognosis in COVID-19 patients, being IL-6, as we aforementioned, one of the most important markers of deterioration of clinical profile and even associated with higher mortality rates (1, 58). Other rescued cytokine values were detected in the macrophagic inducer IFN- $\gamma$  (Figure 2D) and IL-17a, synthesized predominantly by CD4<sup>+</sup> lymphocytes, strongly related with ARDS and responsible for neutrophil chemotaxis (Figure 2E). MIP-1 $\alpha$  and MCP-3, produced initially by lung endothelial and epithelial cells at the beginning of the infection and by M $\phi$  in later stages, also showed a reduction after treatment with 4-PBA (Figures 2F, G). Only one cytokine, GM-CSF, a myeloid growth factor associated with alveolar M $\phi$  maturation, showed an increase after application of LPS and 4-PBA combined (Figure 2H). The remaining cytokines analyzed showed a slight decrease with LPS + 4-PBA compared to LPS alone without reaching statistical significance (Figures 2I–N).

In summary, the modulation of cellular stress with the use of 4-PBA showed changes in the levels of several cytokines associated with monocytic/macrophagic activation and neutrophilia (IL-17a), suggesting a connection between cellular stress and certain immune lineages through the inflammatory response.

## The severity of the inflammatory response in ARDS is correlated with increased BiP in the alveolar space

As patient-derived data showed that increased BiP levels are correlated to risk factors and comorbidities of severe COVID-19, we next analyzed this stress marker in our ARDS mouse model. Results showed that LPS treatment increased BiP levels in the secretions of the alveolar space, and that this increase was ameliorated by 4-PBA treatment (Figure 3A). Furthermore, BiP levels had a significant and positive correlation with 12 of the 14 cytokines measured, including MCP-3, TNF- $\alpha$ , MIP-1 $\alpha$ , IL-6 and IL-1 $\beta$ , all the cytokines that were modulated by treatment with 4-PBA (Figure 2), further supporting that the

hyper-inflammatory lung milieu is associated with the ER stress response with participation of BiP.

To study how BiP could be linked with the severity of the ARDS, we analyzed cytokines levels from each animal individually to detect which mice suffered a stronger response to the LPS challenge and to determine responsiveness to the 4-PBA treatment. From this analysis, we created a Severity Index, calculated from the average value from the cytokines in each animal (Figures 3B–D). This severity index is, therefore, an indicative score of how strong the overall inflammatory response was by individual animals. Figure 3B shows how the majority of the cytokine highest values were found in LPS-treated mice, a group that included 13 of the 14 cytokine maximum levels in this experimental group. These qualitative observations were confirmed by the calculated Severity Index which was significantly higher in LPS challenged animals while significantly ameliorated by 4-PBA treatment (Figure 3C). Finally, we found a statistically significant correlation between increased levels of BiP in BALF with the Severity Index (Figure 3C and Table S1). Together, our data suggest a link between the severity of the inflammatory response and the ER stress state evidenced by increased BiP levels in BALF which can be modulated by the treatment with 4-PBA.

## Cell surface exposure of BiP is promoted in cell lineages responsible for the hyperinflammatory response

After we established that BiP is linked to inflammation and the severity of ARDS, we further studied the role of this chaperone in the immune cell environment responsible for the hyperinflammatory response. As previously mentioned, although BiP mostly resides in the ER, stress factors induce a translocation of BiP to the cell surface (59). Furthermore, csBiP was shown to act as a coreceptor of several virus infections, including SARS-CoV-2 (32, 33). Therefore, we decided to evaluate the participation of pan-BiP or csBiP in ARDS. We first evaluated the mRNA expression and the protein levels of pan-BiP in lung tissues from our ARDS mouse model. Although we had detected an increase of available BiP in the alveolar space in response to LPS (Figure 3B), neither *Hspa5* gene expression (Figure S4A) nor whole protein abundance was significantly altered (Figures S4B, C), which suggests that the changes observed in BiP human serum and in the mice bronchoalveolar space are not correlated to changes in canonical ER stress.

Then, we looked into the cell surface BiP from lung tissue and since BiP-correlated cytokines pattern during inflammatory response in lungs is mainly orchestrated by neutrophils and monocytic lineages, we analyzed these cell populations from whole lung tissues (Figures 4A–L and Figure S5) and measured the levels of csBiP in all of them. At first glance, whole leukocyte



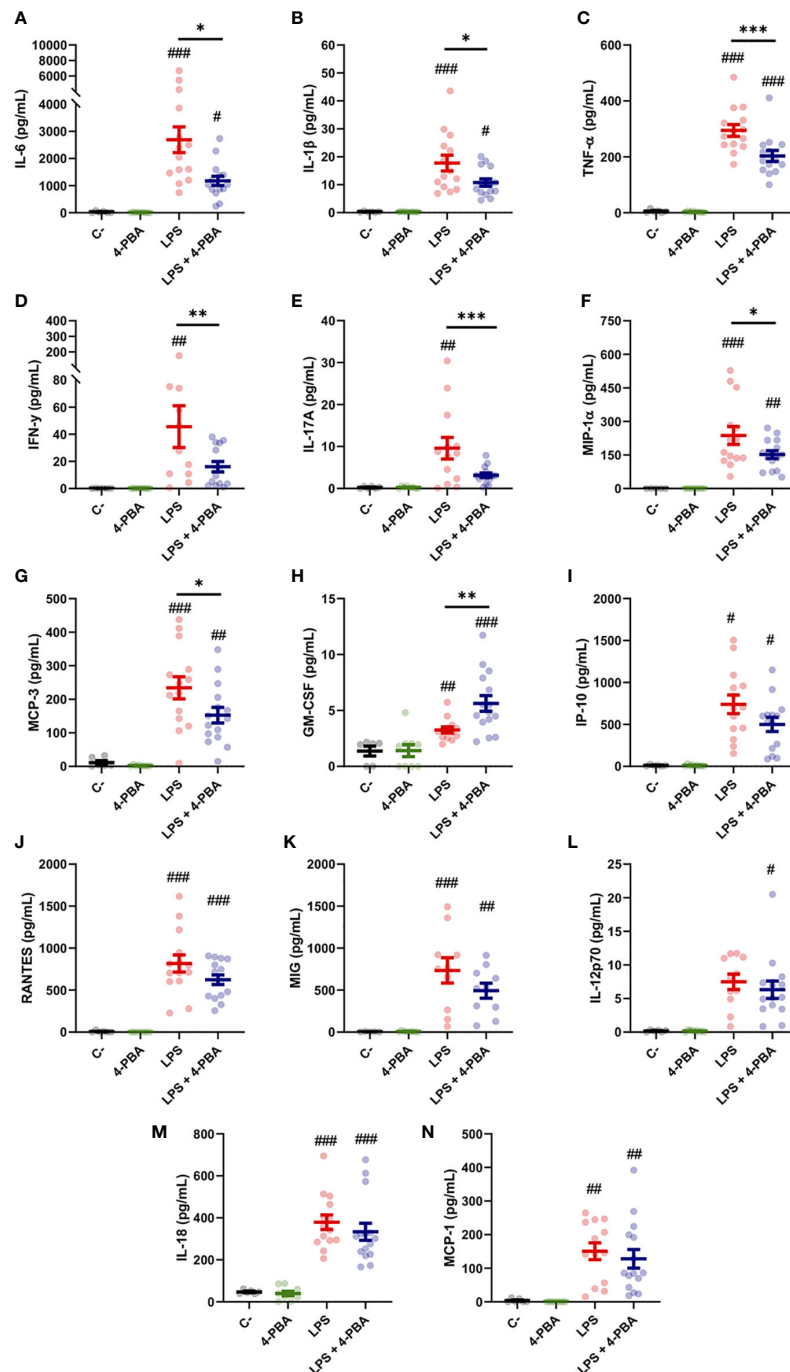


FIGURE 2

Bronchoalveolar cytokine profile after LPS challenge and 4-PBA treatment in ARDS model. (A–N) Levels of cytokines IL-6, IL-1 $\beta$ , TNF- $\alpha$ , IFN- $\gamma$ , IL-17A, MIP-1 $\alpha$ , MCP-3, GM-CSF, IP-10, RANTES, MIG, IL-12p70, IL-18 and MCP-1 in BALF from mice challenged with LPS without 4-PBA treatment (LPS,  $n=14$ , graphed in red) and with 4-PBA treatment (LPS + 4-PBA,  $n=15$ , graphed in blue). Groups of unchallenged mice without 4-PBA (C-,  $n=6$ , graphed in black) and with 4-PBA treatment (4-PBA,  $n=9$ ; graphed in green) were also evaluated. Colored lines and whiskers denote mean  $\pm$  SEM for every data set. Hash marks indicate significant difference versus non-LPS challenge conditions ( $\#P < 0.05$ ,  $\##P < 0.01$ ,  $\###P < 0.001$ ) and a straight line between LPS and LPS + 4-PBA ( $*P < 0.05$ ,  $**P < 0.01$ ,  $***P < 0.001$ ) by Two-way ANOVA followed by Tukey's post-hoc test.

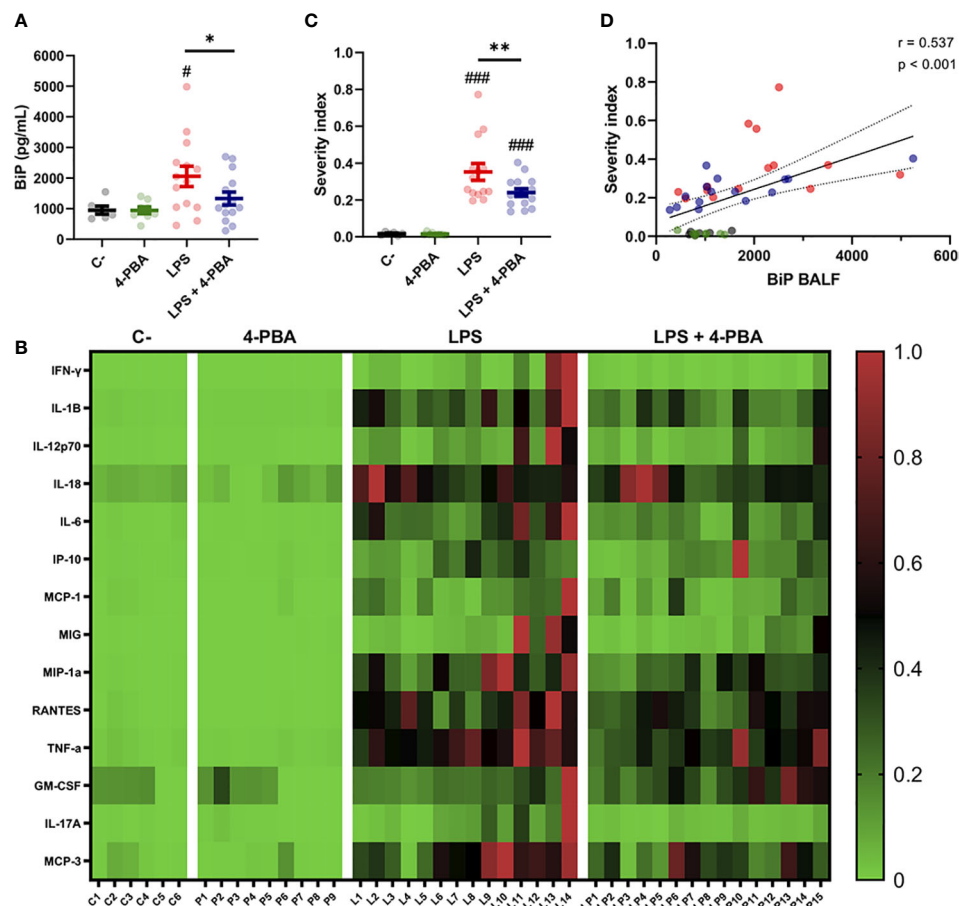


FIGURE 3

BiP levels correlate with ARDS severity. (A) BiP levels in BALF from control mice, 4-PBA treatment, challenged with LPS with and without 4-PBA treatment. Colored lines and whiskers denote mean  $\pm$  SEM for every data set. Hash marks indicate significant difference versus non-LPS challenge conditions ( $^{\#}P < 0.05$ ) and a straight line between LPS and LPS + 4-PBA ( $^*P < 0.05$ ,  $^{**}P < 0.01$ ) by Two-way ANOVA followed by Tukey's *post-hoc* test. (B) Heatmap showing levels for all measured cytokines for every single mouse (In the X axis: C = C-; P = 4-PBA; L = LPS and LP = LPS + 4-PBA with numbers indicating replicate number). Normalized cytokine values are depicted on a low-to-high scale (green-black-red). (C) Severity Index calculated as an average of normalized values for all cytokine by every single animal. Values near to 1 indicate more severe outcome whereas values tend to zero a milder response. Colored lines and whiskers denote mean  $\pm$  SEM for every data set. Hash marks indicate significant difference versus non-LPS challenge conditions ( $^{###}P < 0.001$ ) and a straight line between LPS and LPS + 4-PBA by Two-way ANOVA followed by Tukey's *post-hoc* test. (D) Scatter plot showing a positive correlation between BiP levels in mice BALF and the calculated Severity Index tested by Pearson's correlation coefficient.

population (CD45<sup>+</sup> cells) did not change in number during the inflammatory process (Figure 4M Top), however, they showed a significant increase of csBiP (Figure 4M Bottom).

When we analyzed each population independently, we found that neutrophil lung population (CD45<sup>+</sup> Ly6G<sup>+</sup>) increased upon LPS stimulation, rising from 11.51% to 65.74% of the leukocyte population (Figure 4N Top). Interestingly, neutrophils showed the highest expression of csBiP amongst all the studied hematopoietic populations, although these levels of csBiP were not responsive to LPS stimulation (Figure 4N Bottom), indicating that they are naturally elevated in this cell population.

On the other hand, the non-neutrophilic population (Ly6G<sup>-</sup> cells) showed lower basal levels of csBiP but a significant

responsiveness to LPS stimulation, which increased 3 to 4 times compared to non-stimulated cells (Figure 4O). Within this non-neutrophilic population, we analyzed the monocyte subset identified as CD11b<sup>+</sup> CD11c<sup>low</sup>, formed mainly by interstitial Mφ and residential monocytes (60) (Figure 4I-L; purple square), whose population increased upon stimulation with LPS (Figure 4P Top). More importantly, this population showed increased levels of csBiP, when treated with LPS (Figure 4P Bottom). Finally, we analyzed the CD11c<sup>+</sup> population formed by alveolar Mφ and dendritic cells (DCs). These cells did not increase in numbers with LPS treatment (Figures 4I-L, green squares, and Q Top) but similarly to monocytes, alveolar Mφ showed a significant increase in csBiP after LPS challenge (Figure 4Q Bottom).

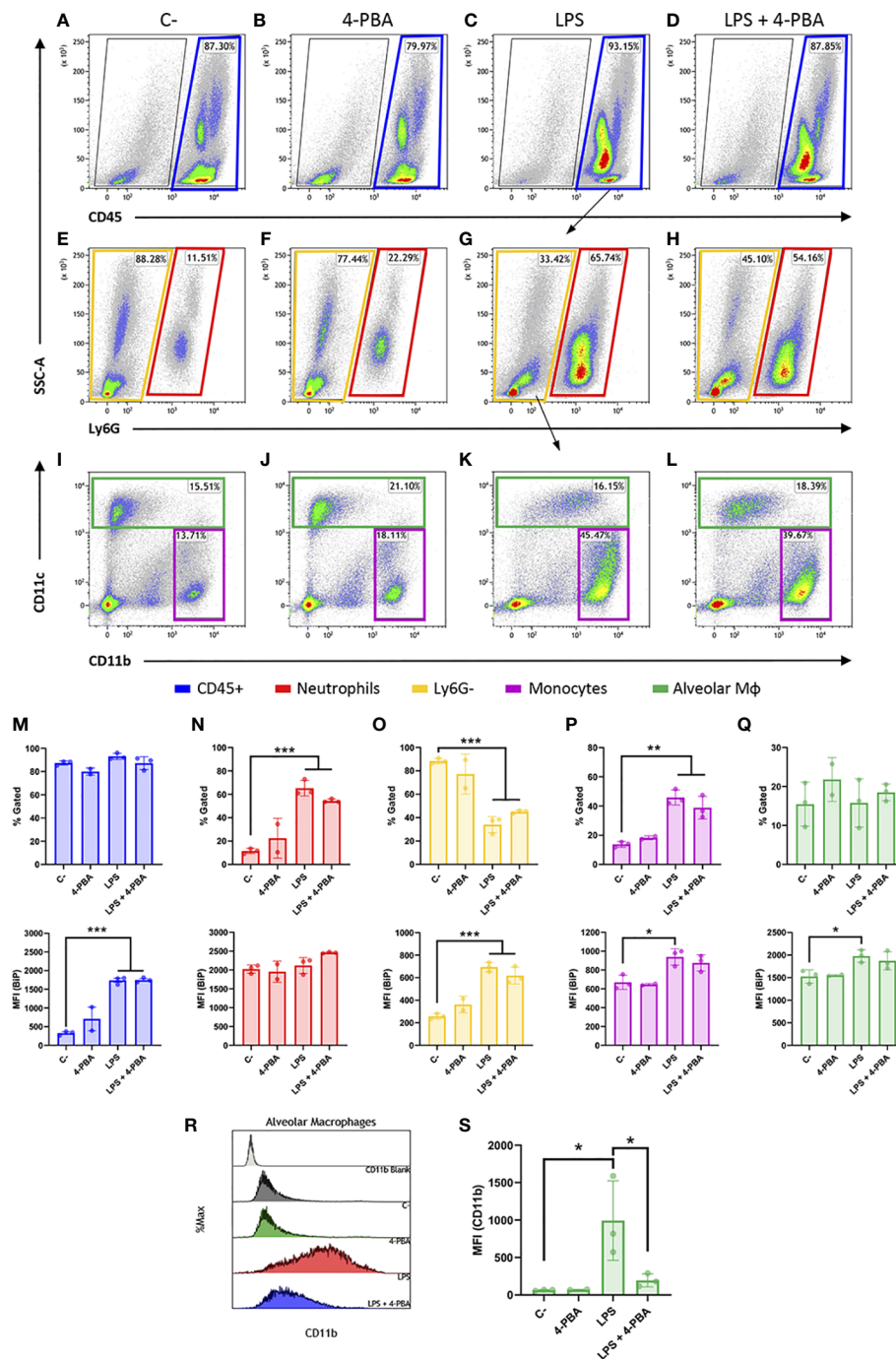


FIGURE 4

Cell surface BiP levels in immune lineages during the hyperinflammatory response. (A–D) Representative flow cytometry plots for CD45<sup>+</sup> cells in blue squares. (E–H) Neutrophils are defined as CD45<sup>+</sup> Ly6G<sup>+</sup> in red squares. (I–L) Among the CD45<sup>+</sup> Ly6G<sup>-</sup> population in yellow squares, we defined alveolar macrophages and DCs (CD45<sup>+</sup> Ly6G<sup>-</sup> CD11c<sup>+</sup>) in green squares and monocytes as well as other myeloid phenotypes (CD45<sup>+</sup> Ly6G<sup>-</sup> CD11b<sup>+</sup> CD11c<sup>-/low</sup>) in purple squares (n=3 mice per group, n=2 for “4-PBA” group). (M–Q) Percentage of gated cells and cell surface BiP levels measured by Median Fluorescence Intensity (MFI) of tagged csBiP antibody are represented in bar plots for every defined population. (R, S) Histogram graph show the intensity distribution of CD11b marker among Alveolar Mφ population (R) also represented as the average of its correspondent MFI in a bar plot (S). All bar plots show mean ± SD for every treatment into the defined population. \**P* < 0.05, \*\**P* < 0.01, \*\*\**P* < 0.001 indicate statistically significant differences versus C- samples for a One-Way ANOVA with a Tukey’s multiple comparisons test.

Regarding LPS + 4-PBA treatments, even though we registered certain changes, there was no significant amelioration in the number of cells or csBiP translocation. Then, we wondered if 4-PBA modulated the immune activation state in any of these myeloid populations. For this, we analyzed CD11b expression levels, which is known to increase upon alveolar M $\phi$  activation (61) and we observed that this alveolar M $\phi$  population was highly activated by LPS challenge while 4-PBA treatment rescued values of CD11b to normal levels (Figures 4R, S).

These results suggest that csBiP is associated to the modulation of the inflammatory response and that the two elevated immune cell populations increased in COVID-19 and ARSD, neutrophil and macrophages, are naturally elevated or have the ability to increase csBiP, further supporting their importance in the mediation of cellular stress during the hyperinflammatory response.

## A network of ER stress related proteins is altered during ARDS and crosstalk with pro-inflammatory factors

After establishing that BiP is involved in the ARDS mechanism of disease, we next analyzed the proteomic profile of lung tissue challenged with LPS and/or treated with 4-PBA to identify pathways and components that link BiP and cellular stress with the hyperinflammatory response. In LPS challenged lungs, we detected significant changes ( $p < 0.05$  and Fold change  $> 1.5$ ) in 159 proteins of the 3628 detected compared to negative control mice. String protein clustering identified four major clusters defined by GO term association (Figure S6A). Three of the four clusters identified were relatively expected: the first cluster contained proteins related to inflammation GO terms (37 proteins, Figure S6B); the second cluster included proteins related to interferon response (22 proteins, Figure S6C) and a third cluster included proteins from a more heterogeneous group related to cell metabolism and mitochondrial oxidative response (15 proteins, Figure S6D). More interestingly, the unsupervised algorithm also grouped a fourth cluster with 11 proteins classified under UPR and cellular stress GO-terms (Figure S6E). The existence of this differentially expressed cluster in the ARDS model suggests a solid participation of UPR-stress signaling in the mechanism of disease. Within this cluster, we did not find BiP, which showed no significant change in the proteomic analysis (Figure S7), consistent with our previous findings on the levels of pan-BiP in lung tissue (Figure S4). However, knowing that it is not pan- but cs-BiP the one involved in the modulation of ARDS and anti-stress treatment with 4-PBA, we studied interactions of proteins from this cluster with BiP (Hspa5) (Figures 5A, B). Among the proteins from the UPR/stress cluster, we found that BiP interacted with Hsph1, Hspa1a, Hspa1b, Bag3 (all molecular

chaperones with a role in protein refolding and UPR signaling), Nup85 (a nucleoporin involved in CCR2-mediated chemotaxis of monocytes), Ripk1 (the Receptor-interacting serine/threonine-protein kinase 1, a key regulator of TNF-mediated apoptosis, necroptosis and inflammatory pathways, S100a11 (a calcium binding protein inducible by ER stress) and H2-Q6 or HLA-G (a component of the Major Histocompatibility Complex I, G related to diseases like asthma, pre-eclampsia and to the antigen recognition of SARS-CoV-2 (62). Interestingly, when cs-BiP was incorporated to the analysis, RIPK1, which was previously included in the inflammatory cluster (Figure S6A), was then included within the UPR/ER stress cluster (Figure 5A) as interactors of Hspa1b and Hspa5 (BiP), highlighting the blur boundary between inflammation and stress. These interactions suggested a network of proteins that connect a major stress pathway, the UPR signaling, to inflammation and infection.

As anti-stress treatments demonstrated to immunomodulate ARDS inflammatory response we next studied the proteomic changes between lungs challenged with LPS and LPS + 4-PBA to identify proteins involved in the amelioration of the inflammatory response. We found a group of 51 proteins with significant changes between LPS and LPS+4-PBA treated lungs (Figure 5C). We focused our attention in the ones whose levels changed upon LPS challenge and were then restored after 4-PBA treatment, and we identified 12 proteins that followed this pattern (Figures 5–O). Levels of six of these proteins dropped with LPS and returned to normal values after 4-PBA treatment (Figures 5D–I): Pin1 (a peptidyl isomerase with a role in regulation of TP53, stress and cytokine signaling in immune system) (63), Gpm6a, Ephx2, L2hgdh, Dhdh (general metabolic modulators) and Tmed5 (Transmembrane P24 Trafficking protein 5 involved in ER-Golgi trafficking and WNT signaling) (64). The other six proteins had elevated levels upon LPS challenge and returned to low levels with 4-PBA (Figures 5J–O): Ripk1 (the previously described key TNF regulator) (65, 66), Wdr5 (WD Repeat Domain 5, a Cilia associated protein with GO-term related to histone modification and also present in cluster 4 in Figure S6E), Nup85 (the previously described nucleoporin involved in monocyte chemotaxis) (67), Zc3h4 (A Zinc Finger CCHtype Containing 4 protein involved in transcriptional regulation), Lpgat1 (the metabolic enzyme Lysophosphatidylglycerol Acyltransferase 1) and Gng5 (the G protein Subunit Gamma 5 related to immune response through CCR3 signaling) (68). It is interesting to note that within this small group of proteins, three belong to the previously described UPR/Stress cluster (Ripk1, Wdr5, Nup85) and two to the inflammation cluster (Gng5, Lpgat1) (Figure 5), further suggesting the existence of a network of proteins that connect stress and inflammation. Particularly interesting is Ripk1, a kinase activated by SARS-CoV-2 infection in lungs that when inhibited reduces the viral load and mortality in COVID-19 humanized mouse model (69). As observed in our proteomic studies, Ripk1 is the main link between ER stress and inflammation clusters and a direct interactor of BiP.

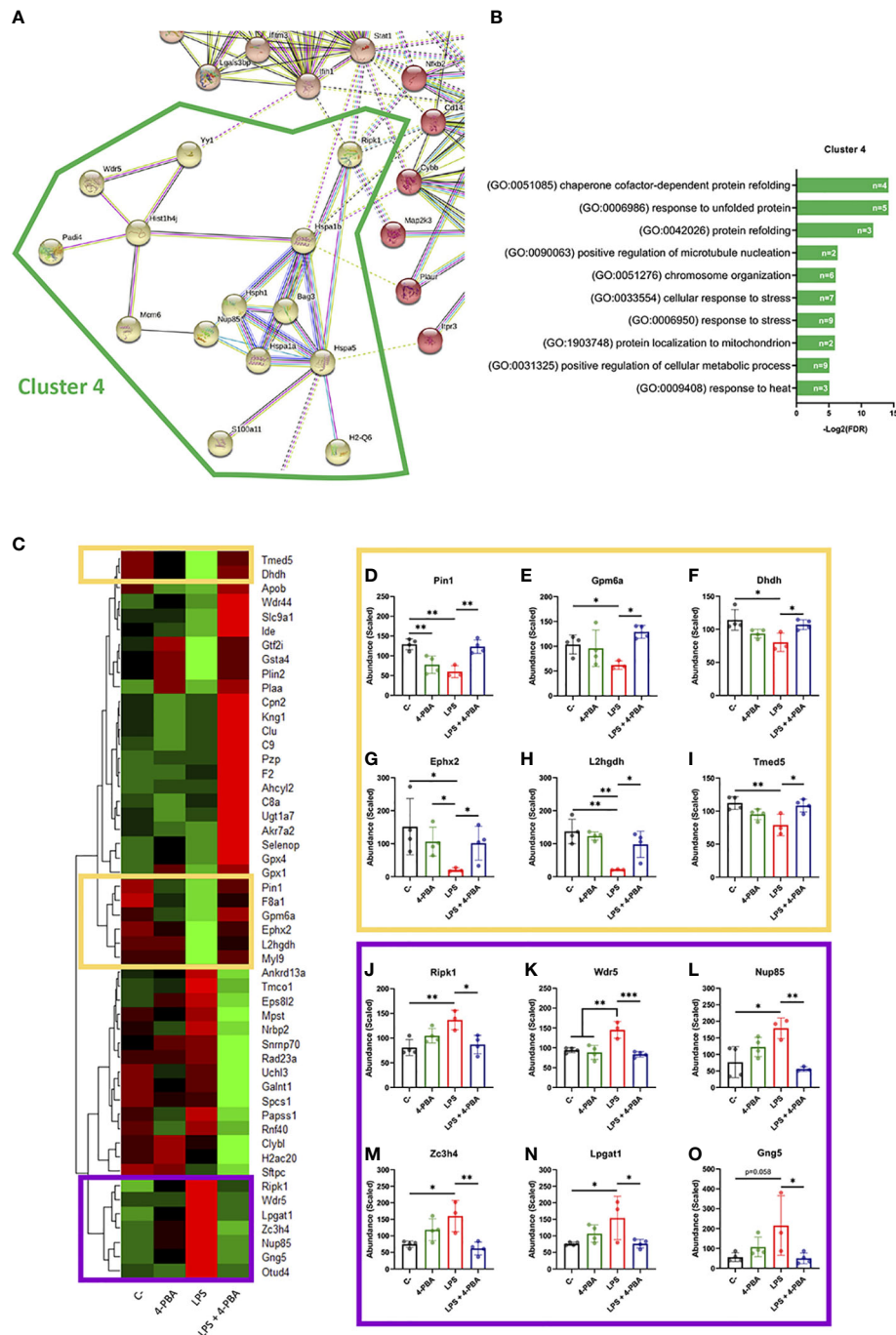


FIGURE 5

Differentially expressed proteins group as UPR/ER stress and inflammatory clusters linked by BiP and Ripk1. (A) StringDB network showing the associations between proteins differentially expressed in response to LPS challenge in mice lungs forming a cluster detected by an unsupervised Markov Cluster Algorithm (MCL). (B) Bar plots showing the Top-10 enriched Biological Processes associated with this cluster ordered by False Discovery Rate. Every single bar indicates the number of proteins associated with every GO-term. (C) Hierarchical clustered heatmap showing relative quantities of the 51 proteins expressed differentially in "LPS" group versus "LPS + 4-PBA" group. (D–O) Proteins with decreased (D–I, yellow squares) or increased (J–O, purple squares) levels after LPS challenge and that were rescued to normal levels after 4-PBA treatment. Bar plots show in detail the mean  $\pm$  SD by treatment for every one of those highlighted proteins. \* $P < 0.05$ , \*\* $P < 0.01$ , \*\*\* $P < 0.001$  indicate statistically significant differences between samples linked with a straight line for a One-Way ANOVA with a Tukey's multiple comparisons test ( $n=4$  for C-, 4-PBA and LPS + 4-PBA groups;  $n=3$  for LPS group).



Overall, our work uncovers a connection between cellular stress represented by BiP and the hyper-inflammatory response induced in ARDS. It defines csBiP as a key modulator of immune lineages and as a biomarker of severity for respiratory infectious diseases such as COVID-19. We also establish a network of proteins that crosstalk between UPR/stress signaling and inflammation and demonstrate the potential of anti-stress therapies with chemical chaperones such as 4-PBA to treat ARDS related diseases.

## Discussion

Our research demonstrates a connection between inflammation and cellular stress through the UPR regulator BiP. Until recently, BiP has been defined as a chaperone assisting protein folding and UPR signaling within the ER compartment, however, this multifunctional protein has also been found to translocate to other cell locations expanding its role from an ER stress regulator to a general cellular stress transducer in the cytoplasm, mitochondria, and cell surface (28, 29). Evidence that cell surface BiP influences ligand and antigen recognition is well documented (30, 70), especially in COVID19, where BiP recognition by SARS-CoV-2 has been recently demonstrated (32, 71, 72). This role, together with the fact that BiP reaches the cell surface upon stress stimulus, makes it a strong candidate to link inflammatory extracellular signals and stress in immune cells. This is supported by several studies that show that stress and inflammation pathways influence each other (21, 22, 45, 73–76). Our results further support this connection by uncovering an inflammation-infection feedback system mediated by the ER stress regulator BiP. Initial infection-inflammatory process induces cellular stress, increasing cell surface BiP in immune lineages responsible for cytokine release and favoring virus entry through overexposed BiP, feeding the inflammatory process into a cytokine storm.

ER or cellular stress have also been related to the mechanism of disease of multiple pathologies (17, 23, 27, 73, 77, 78), including clinical and subclinical manifestations classified as risk factors of COVID-19 (hypertension, diabetes, cardiovascular disease, obesity, autoimmune and respiratory diseases, among others). All these pathologies have been demonstrated to rise BiP levels and show signs of cellular stress, some of them even to be treatable by molecular chaperones (79, 80). As a pre-existing state of cellular stress means abnormal levels of BiP, and BiP is able to feedback the inflammatory response (22, 75, 81), it is no surprise that these risk factors push cells and tissues closer towards the molecular stress threshold that facilitates the hyperinflammatory response during ARDS.

Our results strongly support that BiP levels in blood or in bronchoalveolar fluid can be used as an early severity biomarker of risk of pneumonia in COVID-19 and other respiratory

inflammatory diseases. Statistically, our study of almost 200 patients suggests that any SARS-CoV-2 positive patient that shows BiP values of 300pg/ml or higher in serum at the beginning of the infection has a 100% probability of developing pneumonia. This translates into a powerful prognosis tool, easy to apply in the clinic, however, it is important to note that it does not predict all patients that end up with a severe pneumonia, but a 19,48% (15 of the 77 patients with severe pneumonia in our cohort). Still, this 19,48% represents a risk group of patients where prognosis of development of severe pneumonia could have been applied with absolute certainty. We did not find any indication that BiP performs better as a biomarker of severity compared to IL-6. We believe that the importance of BiP as biomarker lies on its early detection, before the development of the hyperinflammatory response, when IL-6 is elevated, so patients with one of the pulmonary risk factors found in this study (for example EPOC) can be tested with this biomarker to assess the possibility of having a prophylactic treatment (for example 4-PBA) before developing pneumonia.

Experiments with the anti-stress agent 4-PBA indicate that stress does not act as a switch but as a modulator of the inflammatory response with a major significance in the transition from a moderate to severe respiratory disease. Most importantly, 4-PBA experiments suggest that ARDS and the hyperinflammatory response in lungs can be ameliorated by anti-stress drugs through small changes in the cytokine signaling pathways without blocking whole pathways that intervene in the immune response. At this point, it is important to acknowledge the heterogeneity of the inflammatory response, in both the animal model and human patients, replicating a system where small and slightly variable cytokine levels lead to different pathological outputs. Other than that, it remains to be tested is its efficiency in avoiding the development of a severe pneumonia in patients with high levels of BiP in blood, but it is clear that 4-PBA is a strong candidate for the treatment of ARDS and that it seems like a viable option due to the fact that it is an approved drug.

There is still a certain gap in the knowledge about how the localization of BiP at the cell surface translates into changes in the cellular cascades that modulate cytokine pathways. From our proteomic studies, a potential candidate is RIPK1, an intermediary kinase between the UPR/stress proteins and the inflammation and the interferon response. Ripk1 interacts with both Hpsa5 (BiP) and Hpsa1a within this cluster, but it also interacts with Nfkb2 (Nuclear factor NF-kappa-B 2), which is present in many inflammatory and immune pathways (82, 83). RIPK1 seems to act as a bridge between stress and the immune response also through its interactions with CD14 (Monocyte differentiation antigen CD14 (Cd14) that mediates the immune response to bacterial LPS), MAP2K3 (which is activated by cytokines and environmental stress processes), STAT1 (Signal transducer and activator of transcription 1 (Stat1) which

modulates responses to many cytokines and interferons (84)) and IFIH1 (Interferon-induced helicase C domain-containing protein 1 (Ifih1) that acts as a viral sensor and plays a major role in the activation of the antiviral response through an increase in pro-inflammatory cytokines and type I interferons (85)) from clusters 1 and 2 (Figure 5 and S6). This points RIPK1 as a strong candidate to mediate BiP signal transduction in the cell surface of neutrophils and alveolar macrophages while acting as a co-receptor of NFKB/TNF signals (86, 87). Recently, RIPK1 activation was described in human COVID-19 lung samples; inhibition of RIPK1 with the use of small molecules reduced lung viral load and mortality in ACE2 transgenic mice (69, 88). This further supports that the reduction of BiP levels could result beneficial for the treatment of patients with severe COVID-19. Another interesting interactor of BiP during inflammation of ARDS is H2-Q6, a histocompatibility factor that has been related to SARS-CoV-2 recognition (62, 89). This suggests that BiP and H2-Q6 could be favoring virus recognition.

In summary, our research connects stress and inflammation during ARDS in diseases such as COVID-19, it finds a valuable early biomarker of severe pneumonia, suggests a mechanism of severity by csBiP exposure in immune lineages and offers proof-of-concept for a new therapeutic approach through the use of anti-stress drugs.

## Methods

### Patients

Human serum was obtained from 194 confirmed positive patients for SARS-CoV-2 by clinical qPCR test (108 male and 86 females with a mean age of  $64.85 \pm 16.25$  years; ranging between 0 and 94 years). The whole blood samples were collected at the time just after hospital admission at the beginning of the SARS-CoV-2 infection. This cohort included patients with different degree of clinical severity, from asymptomatic to lethal COVID-19 from the first wave of the pandemic (March-June 2020).

We also enrolled 30 healthy patients without any known comorbidities in order to determine the normal range of BiP in blood to compare with COVID-19 patients.

More detailed information about blood donor selection/exclusion criteria can be found in [supplementary document 1](#).

### LPS challenge and 4-PBA treatment

Male wild-type C57BL/6J mice between 8-12 weeks old were used in this study (Charles River laboratories). Mice were kept on a 12h light/dark cycle with free access to food and water. All procedures and animal care follow the guide for the care and use of laboratory and all experimental protocols were approved by

safety and ethics committees of the IBIMA-Bionand Platform Institute for the Animal Research Facility.

Before the challenge, mice were anesthetized with a mixture of ketamine and xylazine (50 and 4 mg/Kg, respectively). Then, 2 mg/Kg of Lipopolysaccharides (LPS) from *E. coli* O111:B4 (L2630, Sigma) diluted in PBS were intranasally administered in 50  $\mu$ L of total volume ( $\approx 50 \mu$ g by animal). Procedure for control mice was identical but instillation was performed with PBS. Then, 200 mg/Kg of Sodium 4-phenylbutyrate (4-PBA) (kindly provided by Scandinavian Formulas) diluted in PBS were administered intraperitoneally at 0, 6 and 8 hours after LPS challenge. Animals that did not receive 4-PBA were treated with the corresponding PBS volume in the same way.

Mice samples were harvested 24 hours after LPS instillation. Mice were euthanized by inhaled isoflurane overdose. Abdominal cavity was opened, blood was collected from the abdominal vena cava and transferred to EDTA pretreated tubes (BD Vacutainer®). Then, the trachea was exposed to perform a bronchoalveolar lavage (BAL) with 800  $\mu$ L of chilled PBS which was carefully infused into the lungs and withdrawn three times. The collected fluid was then centrifuged at 800 xg during 10 minutes at 4 °C. Supernatant (BALF) was stored at -20 °C until posterior measurements. After that, washed lungs were extracted, snap-freeze in liquid nitrogen and stored at -80 °C for posterior molecular and proteomic analyses. Hematological analyses were immediately performed in a DF50 DYMIND hematology analyzer following the manufacturer instructions.

### Cytokines content in BALF

Cytokines content in mice BALF were measured by a custom designed ProcartaPlex multiplex immunoassay (Invitrogen) including the mice analytes: IL-1 $\beta$ , TNF- $\alpha$ , IL-6, IFN- $\gamma$ , IL-17A, MIP-1 $\alpha$ , MCP-3, GM-CSF, IP-10, RANTES, MIG, IL-12p70, IL-18 and MCP-1. Assays were performed following manufacturer instructions using undiluted BALF samples. Measurements were done in the Bio-Plex 200 system and calculations of cytokine content were performed in Bio-Plex Manager 6.0 software (Bio-Rad).

### ELISA

Human circulating BiP from serum samples and BiP content in mice BALF samples were evaluated with commercially available ELISA kits (LS-F11578 and LS-F17959 respectively, from LSBio). Human samples were diluted 1:5 in the supplied buffer whereas mice BALF were performed undiluted. Every single sample and standard were measured in duplicate.

## RT-qPCR

RNA was extracted from lung tissue previously broken up with a mortar and pestle using TRIzol<sup>TM</sup> Reagent (catalog no. 15596026, ThermoFisher). Complementary DNA (cDNA) was prepared from 1 µg of RNA using PrimeScript<sup>TM</sup> RT Master Mix (catalog no. RR036A, Takara). qPCR was performed using TB Green Premix Ex Taq<sup>TM</sup> (catalog no. RR420L, Takara). Gene expression was calculated using the  $2^{-\Delta\Delta CT}$  method of analysis against the stable housekeeping gene TBP. Five biological replicates were performed with three technical replicates each. qPCR primers were: BiP, 5'-TGAAACTGTGGGAGGAGTCA-3' (forward), 5'-TTCAGCTGTCACTCGGAGAA-3' (reverse), TBP, 5'-AGAACAATCCAGACTAGCAGCA-3' (forward), 5'-GGGAACCTCACATCACAGCTC-3' (reverse).

## Western blot

For protein analyses, lung tissue was mechanically broken up with a mortar and pestle and collected in IP lysis buffer (catalog no. 87787, Thermo Fisher Scientific) supplemented with proteinase inhibitors. Concentrations were determined using the Pierce<sup>TM</sup> BCA Protein Assay Kit (catalog no. 23227, ThermoFisher).

For Western blot analyses, protein lysates were separated by electrophoresis on 10% SDS-polyacrylamide gels, transferred to polyvinylidene difluoride membranes, blocked in 5% milk, and probed with primary antibodies: anti-BiP antibody (1:1000; catalog no. 3177, CST), anti-GAPDH (1:2000; catalog no. 2118). Peroxidase-conjugated secondary antibodies (catalog nos. 7071 and 7072, CST) were used, and immunocomplexes were identified using the ECL (enhanced chemiluminescence) Detection Reagent (catalog no. 322009, ThermoFisher). Fiji was used to quantify bands after gel analysis recommendations from ImageJ and (<http://rsb.info.nih.gov/ij/docs/menus/analyze.html#gels>).

## Proteomic analysis by label-free quantification-based mass spectrometry

Mice lungs (n=4 for every treatment group) were mechanically broken up with a mortar and pestle and sonicated for 30 minutes in RIPA buffer to obtain protein extracts. After quantification by BCA method, volumes were adjusted to equalize all concentrations (One sample of the group "LPS" was excluded at this level by abnormally low values). The carried-out protocol was previously described in detail (90) and adapted for lung tissue. Briefly, proteins were stacked in an acrylamide gel, bands were cut and further treated to be reduced with DTT, carbamidomethylated and digested with trypsin overnight. Then, resulting peptides were extracted, purified

and concentrated for next steps and posterior mass spectrometric analysis.

Peptides samples were separated by liquid chromatography in Easy nLC 1200 UHPLC system coupled to a spectrometer coupled to a hybrid quadrupole-linear trap-Orbitrap Q-Exactive HF-X mass spectrometer for the analysis. Protein identification was performed, against the *Mus musculus* protein database of the SwissProt. Raw acquired data were analyzed on the Proteome Discoverer 2.4 platform (all by Thermo Fisher Scientific). Label-free quantification was implemented using the Minora function, setting the following parameters: maximum alignment retention time of 10 min with a minimum signal/noise of 5 for feature linkage mapping. The calculation of the abundances was based on the intensities of the precursor ions. Protein abundance ratios were calculated directly from the pooled abundances. p-Values were calculated by ANOVA based on the abundances of individual proteins or peptides. Only proteins with changes higher than 1.5-fold and with p-Values < 0.05 were considered significantly affected by the different treatments.

Protein-protein interaction of those significantly changed by LPS treatment against the control samples were analyzed and visualized using the online STRING database in order to establish a representative protein network associated with the response to endotoxin insult. Clustering was performed in the same website using the unsupervised MCL clustering tool with an inflation parameter = 1.4 (91). The resultant GO-terms list for the enriched biological processes in every single cluster were ascendent ordered by false discovery rate (FDR) and processed in the Revigo website tool in order to summarize it and removing redundant GO terms (92).

## Flow cytometry

For flow cytometry, independent groups of mice were treated and euthanized following the same aforementioned procedure. In this case, they were bled cutting the inferior vena cava and both lungs were dissected. In these lungs the BAL was not performed in order to maintain the whole interstitial and alveolar populations to be processed for flow cytometry.

Harvested tissues were minced by scissors and digested in DMEM Low glucose (Sigma) + collagenase A (1 mg/mL) (Sigma) + DNase (0.05 mg/mL) (Roche) for 30 minutes at 37 °C in constant orbital agitation. Then, samples were vortexed for 10 seconds and passed through a 70 µm cell strainer to be disaggregated and erythrocytes were removed by incubation with ACK lysis Buffer (Sigma).

After extensive washing in Cell Staining Buffer (BioLegend), obtained single cell suspensions were stained with the fixable viability Zombie Aqua<sup>TM</sup> dye according with the manufacturer instructions (#423101; BioLegend, 1:500).

Then, all samples were treated with anti-CD16/32 (#14-0161-82; 0.5 µg/test, 10 min at 4°C) for Fc-receptor blockage prior to staining procedure. Cells were incubated at 4 °C in the dark for 20 minutes with the following antibodies: Alexa Fluor 488 conjugated anti-GRP78 (#PA1-014A-A488, 1:50), eFluor™ 450 conjugated anti-CD45 (#48-0451-80, 1:100), Alexa Fluor 700 conjugated anti-CD11c (#56-0114-80, 1:50), Allophycocyanin (APC) conjugated Ly6G (#17-9668-80, 1:200) and phycoerythrin (PE) conjugated CD11b (#12-0112-81, 1:100). All the antibodies in this section were purchased from Thermo Fisher Scientific.

Finally, cells were fixed with 4% fresh formaldehyde at RT for 15 minutes, washed extensively and resuspended in Cell Staining Buffer to be evaluated on a BD FACS Aria Fusion flow cytometer (BD Biosciences). Results were analyzed with the software Kaluza (Beckman Coulter). Single stained and FMOs controls were included for every single antibody and for the viability marker in order to make the correspondent compensations and to determine all the cell population gates. Gating strategies are shown in [Supplementary Figure S5](#).

## Statistical analysis

All statistical analyses were performed using GraphPad Prism and SigmaPlot 11.0. Unless stated different, all data are presented as mean ± SEM. Two tailed Student's t-test, two-way ANOVA or ordinary one-way ANOVA with Tukey multiple-comparison test were performed for statistically significant differences among samples. Scatter plot were analyzed by Pearson's correlation coefficient ( $r$  and its related  $P$ -value). Bold line shows the linear regression between the two variables and dotted lines denote the 95% confidence interval. Data sets from mice experiments of cytokines and BiP measurements were evaluated with the ROUT method ( $Q = 1\%$ ) to identify and exclude outlier values from nonlinear regressions (93).

For proteomic analyses, results for *Label Free* protein quantification were generated by the Central Research Support Services from the University of Malaga. From that data, *abundance ratio* between samples from every treatment (calculated as a pairwise ratio) and their associated *p-Values* (from ANOVA *Background-Based* method) were used to classify proteins that significantly change in response to different treatments (Fold change > 1.5 and  $p$ -Value < 0.05). Volcano plots, hierarchical clustered heatmaps and correlation plots were performed in RStudio software.

## Data availability statement

Proteomic datasets are publicly available in PRIDE repository with the following accession reference: PXD037978.

## Ethics statement

The studies involving human participants were reviewed and approved by PEIBA (Junta de Andalucía). The patients/participants provided their written informed consent to participate in this study. The animal study was reviewed and approved by Bionand and University of Malaga Animal research committee.

## Author contributions

Conceptualization: FC, JB and ID. Investigation: GR-L, OP-P, SE. Writing: GR-L, FC and ID. Funding Acquisition: FC, JB and ID. Clinical data acquisition: OP-P, LV and JMR. Mouse model optimization and data acquisition: DV, MC, DB-V, and JP-T. Supervision: FC and ID. All authors contributed to the article and approved the submitted version.

## Funding

This study was supported by Junta de Andalucía (Consejería de Salud y Familia) through CV20-81404 and PIGE-0178-2020. Universidad de Málaga and IBIMA-Plataforma Bionand funds (Plan propio UMA and IBIMA-TECH); Ministerio de Ciencia, Innovación y Tecnología (PID2020-117255-RB100). FC is supported by PCI2021-122094-2B and JMPT by FPU19/06951.

## Acknowledgments

We thank patients from our cohort for their disposition to participate in this study and clinicians that diligently noted all the parameters included in this study. We would also like to thank the Scandinavian Formulas Inc. for kindly providing 4-PBA. Authors thank Casimiro Cardenas (Proteomics service at UMA) and David Navas (Flow cytometry service at UMA) for their technical assistance.

## Conflict of interest

ID and FC declare a patent application for the use of 4-PBA to treat respiratory insufficiency P-585531-EP.

The remaining authors declare that the research was conducted in the absence of any commercial or financial relationships that could be construed as a potential conflict of interest.



## Publisher's note

All claims expressed in this article are solely those of the authors and do not necessarily represent those of their affiliated organizations, or those of the publisher, the editors and the reviewers. Any product that may be evaluated in this article, or claim that may be made by its manufacturer, is not guaranteed or endorsed by the publisher.

## Supplementary material

The Supplementary Material for this article can be found online at: <https://www.frontiersin.org/articles/10.3389/fimmu.2022.1054962/full#supplementary-material>

### SUPPLEMENTARY FIGURE 1

(A–P) Serum BiP levels classified by group of patients/donors. Black lines and whiskers denote the mean  $\pm$  SEM of every data set. Green areas were defined between 5<sup>th</sup> and 95<sup>th</sup> percentiles of healthy donor's data set as normal BiP levels in serum (0 and 181 pg/mL, respectively). \* $P < 0.05$ , \*\* $P < 0.01$ , \*\*\* $P < 0.001$  indicate statistical significant differences between samples for a Two-Tailed unpaired t-Test (A–C, E–L, O, P) and One-Way ANOVA with a Tukey's multiple comparisons test (D, M, N).

### SUPPLEMENTARY FIGURE 2

(A–N) Scatter plots showing the correlation between BiP levels versus different hematological and biochemical parameter levels in COVID-19 patient's blood serum tested by Pearson's correlation coefficient ( $r$  and its related  $P$ -value). Bold line shows the linear regression between the two variables and dotted lines denote the 95% confidence interval.

### SUPPLEMENTARY FIGURE 3

(A–H) Hematological analyses: percentages of neutrophils (A), lymphocytes (B) and monocytes (C), total numbers of white blood cells (WBC) (D), total numbers of neutrophils (E) and total numbers of lymphocytes (F), hematocrit (HCT) (G) and mean corpuscular hemoglobin concentration (MCHC) (H) in total blood obtained from mice challenged with LPS without 4-PBA treatment (LPS,  $n=10$ , graphed

in red) and with 4-PBA treatment (LPS + 4-PBA,  $n=10$ , graphed in blue). Groups of unchallenged mice without 4-PBA (C-,  $n=3$ , graphed in black) and with 4-PBA treatment (4-PBA,  $n=6$ ; graphed in green) were also evaluated. (I) Animal's weight for every experimental group. Colored lines and whiskers denote mean  $\pm$  SEM for every data set. Hash marks indicate significant difference versus C- (\* $P < 0.05$ , \*\* $P < 0.01$ , \*\*\* $P < 0.001$ ) and asterisks between samples linked by a line (\* $P < 0.05$ , \*\* $P < 0.01$ , \*\*\* $P < 0.001$ ) for a Two-way ANOVA followed by Tukey's *post-hoc* test.

### SUPPLEMENTARY FIGURE 4

(A) Quantitative gene expression of Hspa5 (BiP) measured by RT-qPCR. (B, C) Total (pan) levels of BiP protein in lung tissues; western blot (B) and corresponding quantification of protein levels representation (C). No statistical significance was found among the represented conditions.

### SUPPLEMENTARY FIGURE 5

Flow cytometry gating strategy. (A) Representative scatter plots showing FSC-A x SSC-A gating to exclude debris based on size and granularity; (B) FSC-A x FSC-H to exclude doublets. (C) Zombie Aqua™ fixable viability marker to identify live cells (negative for the marker). (D) Staining with CD45 to identify hematopoietic cell lineages. (E) Ly6G was used to identify neutrophils (as Ly6G<sup>+</sup>). (F) Among the Ly6G<sup>+</sup> cells, CD11b x CD11c was used to identify alveolar macrophages and dendritic cells population (as CD11c<sup>+</sup> with variable levels of CD11b) and monocytes as long as other myeloid subsets (as CD11b<sup>+</sup> CD11c<sup>low</sup>). Gates for all viability marker and all antibodies were determined using respective fluorescence minus one (FMO) control.

### SUPPLEMENTARY FIGURE 6

(A) StringDB network (without inclusion of Hspa5) showing the associations between proteins differentially expressed in response to LPS challenge in mice lungs forming 4 principal clusters detected by an unsupervised Markov Cluster Algorithm (MCL). (B–E) Bar plots showing the Top-10 enriched Biological Processes associated with every cluster ordered by False Discovery Rate. Single bars indicate the number of proteins associated with every GO term.

### SUPPLEMENTARY FIGURE 7

BiP Levels measured by proteomic analysis in lung tissues showing the mean  $\pm$  SD of the scaled abundances. There were no statistically significant differences between samples for a One-Way ANOVA with a Tukey's multiple comparisons test ( $n=4$  for C-, 4-PBA and LPS + 4-PBA groups;  $n=3$  for LPS group).

## References

- Huang C, Wang Y, Li X, Ren L, Zhao J, Hu Y, et al. Clinical features of patients infected with 2019 novel coronavirus in wuhan, China. *Lancet* (2020) 395 (10223):497–506. doi: 10.1016/S0140-6736(20)30183-5
- Mehta P, McAuley DF, Brown M, Sanchez E, Tattersall RS, Manson JJ, et al. COVID-19: consider cytokine storm syndromes and immunosuppression. *Lancet (London England)*. (2020) 395(10229):1033–4. doi: 10.1016/S0140-6736(20)30628-0
- Que Y, Hu C, Wan K, Hu P, Wang R, Luo J, et al. Cytokine release syndrome in COVID-19: a major mechanism of morbidity and mortality. *Int Rev Immunol* (2022) 41(2):217–30. doi: 10.1080/08830185.2021.1884248
- Bassetti M, Vena A, Giacobbe DR. The novel Chinese coronavirus (2019-nCoV) infections: Challenges for fighting the storm - bassetti. *Eur J Clin Invest* (2020) 50(3):e13209. doi: 10.1111/eci.13209
- Epidemiological and clinical characteristics of 99 cases of 2019 novel coronavirus pneumonia in wuhan, China: a descriptive study - the lancet . Available at: [https://www.thelancet.com/journals/lancet/article/PIIS0140-6736\(20\)30211-7/fulltext](https://www.thelancet.com/journals/lancet/article/PIIS0140-6736(20)30211-7/fulltext).
- Global percentage of asymptomatic SARS-CoV-2 infections among the tested population and individuals with confirmed COVID-19 diagnosis: A systematic review and meta-analysis | global health | JAMA network open | JAMA network . Available at: <https://jamanetwork.com/journals/jamanetworkopen/fullarticle/2787098>.
- Murray CJL. COVID-19 will continue but the end of the pandemic is near. *Lancet* (2022) 399(10323):417–9. doi: 10.1016/S0140-6736(22)00100-3
- Dong GY, Ding M, Dong X, Jin ZJ, Kursat Azkur A, Azkur D, et al. Risk factors for severe and critically ill COVID-19 patients: A review. *Allergy*. (2021) 76 (2):428–55.
- Liu XQ, Xue S, Xu JB, Ge H, Mao Q, Xu XH, et al. Clinical characteristics and related risk factors of disease severity in 101 COVID-19 patients hospitalized in wuhan, China. *Acta Pharmacol Sin* (2022) 43(1):64–75. doi: 10.1038/s41401-021-00627-2
- Risk factors associated with mortality among patients with COVID-19 in intensive care units in Lombardy, Italy | critical care medicine | JAMA internal medicine | JAMA network. Available at: <https://jamanetwork.com/journals/jamainternalmedicine/fullarticle/2768>.
- Jin JM, Bai P, He W, Fei W, Liu XF, Han DM, et al. Gender differences in patients with COVID-19: Focus on severity and mortality. *Front Public Health* (2020) 8:152. doi: 10.3389/fpubh.2020.00152
- Pobre KFR, Poet GJ, Hendershot LM. The endoplasmic reticulum (ER) chaperone BiP is a master regulator of ER functions: Getting by with a little help from ERdj friends. *J Biol Chem* (2019) 294(6):2098–108. doi: 10.1074/jbc.REV118.002804



13. Gardner BM, Pincus D, Gotthardt K, Gallagher CM, Walter P. Endoplasmic reticulum stress sensing in the unfolded protein response. *Cold Spring Harbor Perspect Biol* (2013) 5(3):a013169. doi: 10.1101/cshperspect.a013169
14. Endoplasmic reticulum stress in liver disease.
15. Tabas I. The role of endoplasmic reticulum stress in the progression of atherosclerosis. *Circ Res* (2010) 107(7):839–50. doi: 10.1161/CIRCRESAHA.110.224766
16. Girona J, Rodríguez-Borjabad C, Ibarretxe D, Vallvé JC, Ferré R, Heras M, et al. The circulating GRP78/BiP is a marker of metabolic diseases and atherosclerosis: Bringing endoplasmic reticulum stress into the clinical scenario. *J Clin Med* (2019) 8(11):1793. doi: 10.3390/jcm8111793
17. Ren J, Bi Y, Sowers JR, Hetz C, Zhang Y. Endoplasmic reticulum stress and unfolded protein response in cardiovascular diseases. *Nat Rev Cardiol* (2021) 18(7):499–521. doi: 10.1038/s41598-021-00511-w
18. Marchetti P, Bugliani M, Lupi R, Marselli L, Masini M, Boggi U, et al. The endoplasmic reticulum in pancreatic beta cells of type 2 diabetes patients. *Diabetologia* (2007) 50:2486–94. doi: 10.1007/s00125-007-0816-8
19. Gopal U, Pizzo SV. Cell surface GRP78 signaling: An emerging role as a transcriptional modulator in cancer. *J Cell Physiol* (2021) 236(4):2352–63. doi: 10.1002/jcp.30030
20. Glucose-regulated proteins in cancer: molecular mechanisms and therapeutic potential | nature reviews cancer . Available at: <https://www.nature.com/articles/nrc3701>.
21. Leonard A, Grose V, Paton AW, Paton JC, Yule DI, Rahman A, et al. Selective inactivation of intracellular BiP/GRP78 attenuates endothelial inflammation and permeability in acute lung injury. *Sci Rep* (2019) 9(1):2096. doi: 10.1038/s41598-018-38312-w
22. Morito D, Nagata K. ER stress proteins in autoimmune and inflammatory diseases. *Front Immunol* (2012) 3. doi: 10.3389/fimmu.2012.00048.
23. Zhang K, Kaufman RJ. From endoplasmic-reticulum stress to the inflammatory response. *Nature* (2008) 454(7203):455–62. doi: 10.1038/nature07203
24. Lee SE, Takagi Y, Nishizaka T, Baek JH, Kim HJ, Lee SH, et al. Subclinical cutaneous inflammation remained after permeability barrier disruption enhances UV sensitivity by altering ER stress responses and topical pseudoceramide prevents them. *Arch Dermatol Res* (2017) 309:541–50. doi: 10.1007/s00403-017-1753-0
25. Evidence that autophagy, but not the unfolded protein response, regulates the expression of IL-23 in the gut of patients with ankylosing spondylitis and subclinical gut inflammation | annals of the rheumatic diseases. Available at: <https://ard.bmj.com/content/73/8/1566.long>.
26. Chung HY, Kim DH, Lee EK, Chung KW, Chung S, Lee B, et al. Redefining chronic inflammation in aging and age-related diseases: Proposal of the senoinflammation concept. *Aging Dis* (2019) 10(2):367–82. doi: 10.14336/AD.2018.0324
27. Hetz C, Saxena S. ER stress and the unfolded protein response in neurodegeneration. *Nat Rev Neurol* (2017) 13(8):477–91. doi: 10.1038/nrneuro.2017.99
28. Quinones QJ, de Ridder GG, Pizzo SV. GRP78: A chaperone with diverse roles beyond the endoplasmic reticulum. *Histol Histopathol* (2008) 23(11):1409–16. doi: 10.14670/HH-23.1409
29. Ni M, Zhang Y, Lee AS. Beyond the endoplasmic reticulum: atypical GRP78 in cell viability, signalling and therapeutic targeting. *Biochem J* (2011) 434(2):181–8. doi: 10.1042/BJ20101569
30. Gonzalez-Gronow M, Selim MA, Papalas J, Pizzo SV. GRP78: a multifunctional receptor on the cell surface. *Antioxidants Redox Signaling* (2009) 11(9):2299–306. doi: 10.1089/ars.2009.2568
31. Gopal U, Pizzo SV. The endoplasmic reticulum chaperone GRP78 also functions as a cell surface signaling receptor. In: *Cell surface GRP78, a new paradigm in signal transduction biology*. (Cambridge, MA: Academic Press (Elsevier)) (2018) 9–40. Available at: <https://linkinghub.elsevier.com/retrieve/pii/B9780128123515000027>.
32. Carlos AJ, Ha DP, Yeh DW, Van Krieken R, Tseng CC, Zhang P, et al. The chaperone GRP78 is a host auxiliary factor for SARS-CoV-2 and GRP78 depleting antibody blocks viral entry and infection. *J Biol Chem* (2021) 296:100759. doi: 10.1016/j.jbc.2021.100759
33. Ibrahim IM, Abdelmalek DH, Elshahat ME, Elfiky AA. COVID-19 spike-host cell receptor GRP78 binding site prediction. *J Infect* (2020) 80(5):554–62. doi: 10.1016/j.jinf.2020.02.026
34. Elfiky AA. Ebola Virus glycoprotein GP1-host cell-surface HSPA5 binding site prediction. *Cell Stress Chaperones*. (2020) 25(3):541–8. doi: 10.1007/s12192-020-01106-z
35. Honda T, Horie M, Daito T, Ikuta K, Tomonaga K. Molecular chaperone BiP interacts with borna disease virus glycoprotein at the cell surface. *J Virol* (2009) 83(23):12622–5. doi: 10.1128/JVI.01201-09
36. Nain M, Mukherjee S, Karmakar SP, Paton AW, Paton JC, Abidin MZ, et al. GRP78 is an important host factor for Japanese encephalitis virus entry and replication in mammalian cells. *J Virol* (2017) 91(6):e02274–16. doi: 10.1128/JVI.02274-16
37. Chen TH, Chiang YH, Hou JN, Cheng CC, Sofiyatun E, Chiu CH, et al. XBP1-mediated BiP/GRP78 upregulation copes with oxidative stress in mosquito cells during dengue 2 virus infection. *BioMed Res Int* (2017) 2017:3519158. doi: 10.1155/2017/3519158
38. Khongwichit S, Sornjai W, Jitobaom K, Greenwood M, Greenwood MP, Hitakarun A, et al. A functional interaction between GRP78 and Zika virus E protein. *Sci Rep* (2021) 11(1):393. doi: 10.1038/s41598-020-79803-z
39. Triantafilou K, Fradelizi D, Wilson K, Triantafilou M. GRP78, a coreceptor for coxsackievirus A9, interacts with major histocompatibility complex class I molecules which mediate virus internalization. *J Virol* (2002) 76(2):633–43. doi: 10.1128/JVI.76.2.633-643.2002
40. Zhang LH, Zhang X. Roles of GRP78 in physiology and cancer. *J Cell Biochem* (2010) 110(6):1299–305. doi: 10.1002/jcb.22679
41. Ibrahim IM, Abdelmalek DH, Elfiky AA. GRP78: A cell's response to stress. *Life Sci* (2019) 226:156–63. doi: 10.1016/j.lfs.2019.04.022
42. Shakya M, Yildirim T, Lindberg I. Increased expression and retention of the secretory chaperone proSAAS following cell stress. *Cell Stress Chaperones*. (2020) 25(6):929–41. doi: 10.1007/s12192-020-01128-7
43. Flores-Diaz M, Higuera JC, Florin I, Okada T, Pollesello P, Bergman T, et al. A cellular UDP-glucose deficiency causes overexpression of glucose/oxygen-regulated proteins independent of the endoplasmic reticulum stress elements. *J Biol Chem* (2004) 279(21):21724–31. doi: 10.1074/jbc.M312791200
44. Chen JC, Wu ML, Huang KC, Lin WW. HMG-CoA reductase inhibitors activate the unfolded protein response and induce cytoprotective GRP78 expression. *Cardiovasc Res* (2008) 80(1):138–50. doi: 10.1093/cvr/cvn160
45. Krupkova O, Sadowska A, Kameda T, Hitzl W, Hausmann ON, Klasek J, et al. p38 MAPK facilitates crosstalk between endoplasmic reticulum stress and IL-6 release in the intervertebral disc. *Front Immunol* (2018) 9:1706. doi: 10.3389/fimmu.2018.01706
46. Sheng M, Huang Z, Pan L, Yu M, Yi C, Teng L, et al. SOCS2 exacerbates myocardial injury induced by ischemia/reperfusion in diabetic mice and H9c2 cells through inhibiting the JAK-STAT-IGF-1 pathway. *Life Sci* (2017) 188:101–9. doi: 10.1016/j.lfs.2017.08.036
47. Kim HJ, Jeong JS, Kim SR, Park SY, Chae HJ, Lee YC. Inhibition of endoplasmic reticulum stress alleviates lipopolysaccharide-induced lung inflammation through modulation of NF- $\kappa$ B/HIF-1 $\alpha$  signaling pathway. *Sci Rep* (2013) 3(1):1142. doi: 10.1038/srep01142
48. Csukasi F, Rico G, Becerra J, Duran I. Should we unstress SARS-CoV-2 infected cells? In: *Cytokine & growth factor reviews* (2020) 54:3–5. doi: 10.1016/j.cytogfr.2020.06.011
49. Duca A, Piva S, Focà E, Latronico N, Rizzi M. Calculated decisions: Brescia-COVID respiratory severity scale (BCRSS)/Algorithm. *Emerg Med Pract* (2020) 22(5 Suppl):CD1–2.
50. Mohammed-Ali Z, Cruz GL, Dickhout JG. Crosstalk between the unfolded protein response and NF- $\kappa$ B-mediated inflammation in the progression of chronic kidney disease. *J Immunol Res* (2015) 2015:428508. doi: 10.1155/2015/428508
51. Southern KW, Murphy J, Sinha IP, Nevitt SJ. Corrector therapies (with or without potentiators) for people with cystic fibrosis with class II CFTR gene variants (most commonly F508del). *Cochrane Database Syst Rev* (2020) 12:CD010966. doi: 10.1002/14651858.CD010966.pub3
52. Vanweert F, Neinst M, Tapia EE, van de Weijer T, Hoeks J, Schrauwen-Hinderling VB, et al. A randomized placebo-controlled clinical trial for pharmacological activation of BCAA catabolism in patients with type 2 diabetes. *Nat Commun* (2022) 13(1):3508. doi: 10.1038/s41467-022-31249-9
53. Collier KA, Valencia H, Newton H, Hade EM, Sborov DW, Cavaliere R, et al. A phase 1 trial of the histone deacetylase inhibitor AR-42 in patients with neurofibromatosis type 2-associated tumors and advanced solid malignancies. *Cancer Chemother Pharmacol* (2021) 87(5):599–611. doi: 10.1007/s00280-020-04229-3
54. Paganoni S, Macklin EA, Hendrix S, Berry JD, Elliott MA, Maiser S, et al. Trial of sodium phenylbutyrate-taurursodiol for amyotrophic lateral sclerosis. *N Engl J Med* (2020) 383(10):919–30. doi: 10.1056/NEJMoa1916945
55. Zeng W, Guo YH, Qi W, Chen JG, Yang LL, Luo ZF, et al. 4-phenylbutyric acid suppresses inflammation through regulation of endoplasmic reticulum stress of endothelial cells stimulated by uremic serum. *Life Sci* (2014) 103(1):15–24. doi: 10.1016/j.lfs.2014.03.007
56. Kolb PS, Ayaub EA, Zhou W, Yum V, Dickhout JG, Ask K. The therapeutic effects of 4-phenylbutyric acid in maintaining proteostasis. *Int J Biochem Cell Biol* (2015) 61:45–52. doi: 10.1016/j.biocel.2015.01.015
57. Zeng M, Sang W, Chen S, Chen R, Zhang H, Xue F, et al. 4-PBA inhibits LPS-induced inflammation through regulating ER stress and autophagy in acute

lung injury models. *Toxicol letters*. (2017) 271:26–37. doi: 10.1016/j.toxlet.2017.02.023

58. Zhang X, Tan Y, Ling Y, Lu G, Liu F, Yi Z, et al. Viral and host factors related to the clinical outcome of COVID-19. *Nature*. (2020) 583(7816):437–40. doi: 10.1038/s41586-020-2355-0

59. Van Krieken R, Tsai YL, Carlos AJ, Ha DP, Lee AS. ER residential chaperone GRP78 unconventionally relocates to the cell surface via endosomal transport. *Cell Mol Life Sci* (2021) 78(12):5179–95. doi: 10.1007/s00018-021-03849-z

60. Three unique interstitial macrophages in the murine lung at steady state | *American journal of respiratory cell and molecular biology*. Available at: <https://www.atsjournals.org/doi/10.1165/rcmb.2016-0361OC>.

61. Duan M, Steinfert DP, Smallwood D, Hew M, Chen W, Ernst M, et al. CD11b immunophenotyping identifies inflammatory profiles in the mouse and human lungs. *Mucosal Immunol* (2016) 9(2):550–63. doi: 10.1038/mi.2015.84

62. Lin A, Yan WH. Perspective of HLA-G induced immunosuppression in SARS-CoV-2 infection. *Front Immunol* (2021) 12:788769. doi: 10.3389/fimmu.2021.788769

63. Bae JS, Noh SJ, Kim KM, Jang KY, Park HS, Chung MJ, et al. PIN1 in hepatocellular carcinoma is associated with TP53 gene status. *Oncol Rep* (2016) 36(4):2405–11. doi: 10.3892/or.2016.5001

64. Buechling T, Chaudhary V, Spirohn K, Weiss M, Boutros M. p24 proteins are required for secretion of wnt ligands. *EMBO Rep* (2011) 12(12):1265–72. doi: 10.1038/embor.2011.212

65. Jaco I, Annibaldi A, Lalaoui N, Wilson R, Tenev T, Laurien L, et al. MK2 phosphorylates RIPK1 to prevent TNF-induced cell death. *Mol Cell* (2017) 66(5):698–710.e5. doi: 10.1016/j.molcel.2017.05.003

66. Ting AT, Bertrand MJM. More to life than NF- $\kappa$ B in TNFR1 signaling. *Trends Immunol* (2016) 37(8):535–45. doi: 10.1016/j.it.2016.06.002

67. Terashima Y, Onai N, Murai M, Enomoto M, Poonpiriya V, Hamada T, et al. Pivotal function for cytoplasmic protein FROUNT in CCR2-mediated monocyte chemotaxis. *Nat Immunol* (2005) 6(8):827–35. doi: 10.1038/ni1222

68. Wang H, Yu L, Cui Y, Huang J. G Protein subunit gamma 5 is a prognostic biomarker and correlated with immune infiltrates in hepatocellular carcinoma. *Dis Markers*. (2022) 2022:1313359. doi: 10.1155/2022/1313359

69. Xu G, Li Y, Zhang S, Peng H, Wang Y, Li D, et al. SARS-CoV-2 promotes RIPK1 activation to facilitate viral propagation. *Cell Res* (2021) 31(12):1230–43. doi: 10.1038/s41422-021-00578-7

70. Hebban N, Epperly R, Vaidya A, Thanekar U, Moore SE, Umeda M, et al. CAR T cells redirected to cell surface GRP78 display robust anti-acute myeloid leukemia activity and do not target hematopoietic progenitor cells. *Nat Commun* (2022) 13(1):587. doi: 10.1038/s41467-022-28243-6

71. Elfiky AA, Ibrahim IM. Host-cell recognition through Cs-GRP78 is enhanced in the new omicron variant of SARS-CoV-2, *in silico* structural point of view. *J Infect* (2022) 84(5):722–46. doi: 10.1016/j.jinf.2022.01.019

72. Puzyrenko A, Jacobs ER, Sun Y, Felix JC, Sheinin Y, Ge L, et al. Pneumocytes are distinguished by highly elevated expression of the ER stress biomarker GRP78, a co-receptor for SARS-CoV-2, in COVID-19 autopsies. *Cell Stress Chaperones*. (2021) 26(5):859–68. doi: 10.1007/s12192-021-01230-4

73. Yoshida H. ER stress and diseases. *FEBS J* (2007) 274(3):630–58. doi: 10.1111/j.1742-4658.2007.05639.x

74. Panayi GS, Corrigan VM. Immunoglobulin heavy-chain-binding protein (BiP): a stress protein that has the potential to be a novel therapy for rheumatoid arthritis. *Biochem Soc Trans* (2014) 42(6):1752–5. doi: 10.1042/BST20140230

75. Ghosh AK, Garg SK, Mau T, O'Brien M, Liu J, Yung R. Elevated endoplasmic reticulum stress response contributes to adipose tissue inflammation in aging. *Journals Gerontology Ser A Biol Sci Med Sci* (2015) 70(11):1320–9. doi: 10.1093/gerona/glu186

76. Zhang Y, Lim C, Sikirzhyski V, Naderi A, Chatzistamou I, Kiaris h. propensity to endoplasmic reticulum stress in deer mouse fibroblasts predicts

skin inflammation and body weight gain. *Dis Models Mech* (2021) 14(10): dmm.049113. doi: 10.1242/dmm.049113

77. Marciniak SJ, Chambers JE, Ron D. Pharmacological targeting of endoplasmic reticulum stress in disease. *Nat Rev Drug Discovery* (2021) 21(2):1–26. doi: 10.1038/s41573-021-00320-3

78. Di Conza G, Ho PC. ER stress responses: An emerging modulator for innate immunity. *Cells*. (2020) 9(3):695. doi: 10.3390/cells9030695

79. Brandvold KR, Morimoto RI. The chemical biology of molecular chaperones—implications for modulation of proteostasis. *J Mol Biol* (2015) 427(18):2931–47. doi: 10.1016/j.jmb.2015.05.010

80. Cao SS, Kaufman RJ. Targeting endoplasmic reticulum stress in metabolic disease. *Expert Opin Ther targets*. (2013) 17(4):437–48. doi: 10.1517/14728222.2013.756471

81. Wang Z, Huang Y, Cheng Y, Tan Y, Wu F, Wu J, et al. Endoplasmic reticulum stress-induced neuronal inflammatory response and apoptosis likely plays a key role in the development of diabetic encephalopathy. *Oncotarget*. (2016) 7(48):78455–72. doi: 10.18632/oncotarget.12925

82. Klemann C, Camacho-Ordóñez N, Yang L, Eskandarian Z, Rojas-Restrepo JL, Frede N, et al. Clinical and immunological phenotype of patients with primary immunodeficiency due to damaging mutations in NFKB2. *Front Immunol* (2019) 10:297. doi: 10.3389/fimmu.2019.00297

83. Chawla M, Mukherjee T, Deka A, Chatterjee B, Sarkar UA, Singh AK, et al. An epithelial Nfkb2 pathway exacerbates intestinal inflammation by supplementing latent RelA dimers to the canonical NF- $\kappa$ B module. *Proc Natl Acad Sci U S A*. (2021) 118(25):e2024828118. doi: 10.1073/pnas.2024828118

84. Mitchell TJ, John S. Signal transducer and activator of transcription (STAT) signalling and T-cell lymphomas. *Immunol* (2005) 114(3):301–12. doi: 10.1111/j.1365-2567.2005.02091.x

85. Type I interferons in infectious disease | *nature reviews immunology*. Available at: <https://www.nature.com/articles/nri3787>.

86. Dondelinger Y, Jouan-Lanhouet S, Divert T, Theatre E, Bertin J, Gough PJ, et al. NF- $\kappa$ B-independent role of IKK $\alpha$ /IKK $\beta$  in preventing RIPK1 kinase-dependent apoptotic and necroptotic cell death during TNF signaling. *Mol Cell* (2015) 60(1):63–76. doi: 10.1016/j.molcel.2015.07.032

87. Yamamoto S, Iwakuma T. RIPK1-TRAF2 interplay on the TNF/NF- $\kappa$ B signaling, cell death, and cancer development in the liver. *translational cancer research* (2017). Available at: <https://tcr.amegroups.com/article/view/13352>.

88. Riebeling T, Jamal K, Wilson R, Kolbrink B, von Samson-Himmelstjerna FA, Moerke C, et al. Primidone blocks RIPK1-driven cell death and inflammation. *Cell Death Differ* (2021) 28(5):1610–26. doi: 10.1038/s41418-020-00690-y

89. Nguyen A, David JK, Maden SK, Wood MA, Weeder BR, Nellore A, et al. Human leukocyte antigen susceptibility map for severe acute respiratory syndrome coronavirus 2. *J Virology*. (2020) 94(13):e00510-20. doi: 10.1128/JVI.00510-20

90. Identification of key molecular biomarkers involved in reactive and neurodegenerative processes present in inherited congenital hydrocephalus | *fluids and barriers of the CNS*. Available at: <https://fluidsbarrierscns.biomedcentral.com/articles/10.1186/s12987-021-00263-2>.

91. Szklarczyk D, Gable AL, Nastou KC, Lyon D, Kirsch R, Pyysalo S, et al. The STRING database in 2021: customizable protein-protein networks, and functional characterization of user-uploaded gene/measurement sets. *Nucleic Acids Res* (2021) 49(D1):D605–12. doi: 10.1093/nar/gkaa1074

92. REVIGO summarizes and visualizes long lists of gene ontology terms | *PLOS ONE*. Available at: <https://journals.plos.org/plosone/article?id=10.1371/journal.pone.0021800>.

93. Motulsky HJ, Brown RE. Detecting outliers when fitting data with nonlinear regression – a new method based on robust nonlinear regression and the false discovery rate. *BMC Bioinf* (2006) 7(1):123. doi: 10.1186/1471-2105-7-123



## OPEN ACCESS

## EDITED BY

Alfonso J. Rodriguez-Morales,  
Fundacion Universitaria Autónoma de  
las Américas, Colombia

## REVIEWED BY

Daniel Gideon,  
Bishop Heber College, India  
Mao Luo,  
Southwest Medical University, China

## \*CORRESPONDENCE

Zhonglei Wang  
wangzl16@tsinghua.org.cn  
Liyan Yang  
yangly@iccas.ac.cn  
Xian-qing Song  
Song\_xianqing@126.com

## SPECIALTY SECTION

This article was submitted to  
Viral Immunology,  
a section of the journal  
Frontiers in Immunology

RECEIVED 09 August 2022

ACCEPTED 21 November 2022

PUBLISHED 06 December 2022

## CITATION

Wang Z, Yang L and Song X-q (2022)  
Oral GS-441524 derivatives: Next-  
generation inhibitors of SARS-CoV-2  
RNA-dependent RNA polymerase.  
*Front. Immunol.* 13:1015355.  
doi: 10.3389/fimmu.2022.1015355

## COPYRIGHT

© 2022 Wang, Yang and Song. This is  
an open-access article distributed under  
the terms of the [Creative Commons  
Attribution License \(CC BY\)](#). The use,  
distribution or reproduction in other  
forums is permitted, provided the  
original author(s) and the copyright  
owner(s) are credited and that the  
original publication in this journal is  
cited, in accordance with accepted  
academic practice. No use,  
distribution or reproduction is  
permitted which does not comply with  
these terms.

# Oral GS-441524 derivatives: Next-generation inhibitors of SARS-CoV-2 RNA-dependent RNA polymerase

Zhonglei Wang<sup>1,2\*</sup>, Liyan Yang<sup>3\*</sup> and Xian-qing Song<sup>4\*</sup>

<sup>1</sup>Key Laboratory of Green Natural Products and Pharmaceutical Intermediates in Colleges and Universities of Shandong Province, School of Chemistry and Chemical Engineering, Qufu Normal University, Qufu, China, <sup>2</sup>School of Pharmaceutical Sciences, Tsinghua University, Beijing, China, <sup>3</sup>Shandong Provincial Key Laboratory of Laser Polarization and Information Technology, School of Physics and Physical Engineering, Qufu Normal University, Qufu, China, <sup>4</sup>General Surgery Department, Ningbo Fourth Hospital, Xiangshan, China

GS-441524, an RNA-dependent RNA polymerase (RdRp) inhibitor, is a 1'-CN-substituted adenine C-nucleoside analog with broad-spectrum antiviral activity. However, the low oral bioavailability of GS-441524 poses a challenge to its anti-SARS-CoV-2 efficacy. Remdesivir, the intravenously administered version (version 1.0) of GS-441524, is the first FDA-approved agent for SARS-CoV-2 treatment. However, clinical trials have presented conflicting evidence on the value of remdesivir in COVID-19. Therefore, oral GS-441524 derivatives (VV116, ATV006, and GS-621763; version 2.0, targeting highly conserved viral RdRp) could be considered as game-changers in treating COVID-19 because oral administration has the potential to maximize clinical benefits, including decreased duration of COVID-19 and reduced post-acute sequelae of SARS-CoV-2 infection, as well as limited side effects such as hepatic accumulation. This review summarizes the current research related to the oral derivatives of GS-441524, and provides important insights into the potential factors underlying the controversial observations regarding the clinical efficacy of remdesivir; overall, it offers an effective launching pad for developing an oral version of GS-441524.

## KEYWORDS

SARS-CoV-2, GS-441524, remdesivir, oral version, VV116, ATV006, GS-621763, COVID-19

## Introduction

With more than 6.5 million deaths worldwide, the coronavirus disease 2019 (COVID-19) pandemic, first identified in late 2019, continues to be the most extraordinary public health burden in 2022 (1). Severe acute respiratory syndrome coronavirus 2 (SARS-CoV-2) causes a wide range of post-acute infection syndromes, including cognitive impairment, dyspnea,

fatigue, headache, and loss of taste or smell (2–5). The scientific community has made significant progress in mitigating the threat of COVID-19 through the discovery and development of myriad vaccines, monoclonal antibodies, traditional medicines, and small-molecule agents (6–9). However, the efficacy of antibodies or vaccines has been affected by the development of SARS-CoV-2 variants (i.e., their drug resistance), global access, sub-optimal administration routes, and heterogeneous responses (10, 11). Briefly, resistant SARS-CoV-2 variants have led to waves of resurgence, exacerbated global anxiety, and challenged global health efforts.

As an acute infectious disease, use of orally bioavailable antivirals at the early stage of SARS-CoV-2 infection would be more beneficial in facilitating early administration to non-hospitalized patients to prevent progression to severe disease; however, antiviral treatment does not provide the best benefits in the late stage in hospitalized patients (12, 13). Therefore, oral antivirals suitable for outpatient treatment are superior to injectable therapies for hospitalized patients. Currently, oral antivirals are critical as pre- and post-exposure prophylaxis. Notably, several orally bioavailable anti-SARS-CoV-2 agents have been approved. Among these, Paxlovid (nirmatrelvir plus ritonavir) from Pfizer and molnupiravir (MK-4482, EIDD-2801) from Merck can effectively reduce the risk of severe COVID-19 or death in patients with mild-to-moderate COVID-19 (14–16). Although these results are appealing, some concerns remain. First, despite a high cure rate with initial therapy, patients treated with Paxlovid and molnupiravir have experienced rebound COVID-19 infections (17, 18). Second, mutations are challenging the efficiency of these small-molecule antivirals. Third, commercialized antivirals remain expensive (around US \$530 for each 5-day course of Paxlovid), particularly, for low and middle-income countries (19, 20). Fourth, the widening use of antivirals can increase the development of drug resistance. Fifth, molnupiravir has mutagenic potential in human cells (21, 22). Based on these concerns, efforts are needed to achieve the desired clinical effects (e.g., tissue-specific localization and enhanced oral bioavailability) of antivirals.

RNA-dependent RNA polymerase (RdRp) is essential in viral RNA synthesis (23–25). Both remdesivir and molnupiravir are FDA-approved SARS-CoV-2 inhibitors that target RdRp. Notably, remdesivir exhibited conflicting impact in clinical trials (26); rebound of COVID-19 infection and mutagenicity may occur in patients receiving molnupiravir (27). In such cases, oral GS-441524 derivatives, with enhanced bioavailability and sufficient safety profile, may be another alternative to consider.

GS-441524, a potent RdRp inhibitor, is a 1'-CN-substituted adenine C-nucleoside ribose analogue that demonstrates *in vitro* broad-spectrum activity against various viruses, including SARS-CoV (half-maximum effective concentration [EC<sub>50</sub>] = 0.18 μM), Middle East respiratory syndrome coronavirus (EC<sub>50</sub> = 0.86 μM), and feline infectious peritonitis virus (EC<sub>50</sub> = 0.78 μM), SARS-CoV-2 (EC<sub>50</sub> = 0.48 μM) (28–31). Cellular uptake depends on

membrane-bound transporters, and GS-441524 is hydrophilic, resulting in a limited ability to transmembrane by diffusion (32). Notably, GS-441524 displayed low oral bioavailability in cynomolgus monkeys ( $F < 8.0\%$ ), in rats ( $F = 16\%$ ) and humans ( $F = 13\%$ ) (33). Other detailed pharmacokinetic properties (such as maximum plasma concentration, terminal half-life, and oral bioavailability) of GS-441524 are shown in Table 1. Also, GS-441524 is stable *in vitro* in liver microsomes, cytoplasm, and hepatocytes across studied species (including rats, monkeys, dogs, and humans) (37). Further, clinical trials have shown that GS-441524 is the major circulating metabolite of remdesivir after IV administration (44). GS-441524 displays a good safety profile without serious adverse effects (45). Therefore, GS-441524 and its prodrugs or analogues provide an excellent option for oral SARS-CoV-2 drug design.

However, the low oral bioavailability of GS-441524 hinders its promising anti-SARS-CoV-2 efficacy (33, 34, 46, 47). As depicted in Figure 1, further optimization of GS-441524 has resulted in the development of the more potent intravenously administered remdesivir (version 1.0 of GS-441524) and orally administered GS-441524 derivatives (version 2.0 of GS-441524). This review summarizes the potential factors underlying controversial observations regarding the clinical efficacy of remdesivir, the intravenously administered version (version 1.0) of GS-441524 and the current research related to the oral versions of GS-441524.

## Inhibitors of SARS-CoV-2 RNA-dependent RNA polymerase

The SARS-CoV-2 genome encodes 29 proteins, including 4 structural proteins, 16 non-structural proteins (replicase proteins; nsp1–nsp16), and 9 accessory proteins (48, 49). These 29 proteins participate in sequential viral adsorption, entry into the target cell, uncoating, replication and transcription, protein synthesis, SARS-CoV-2 assembly and release (50, 51). Among these, nsp constitutes the viral replication and transcription complex (RTC), which plays an essential role in the synthesis of (–)-strand template, (+)-strand genomic RNA and subgenomic mRNAs (52, 53). Nsp12 (RdRp), the core component of RTC, is one of the most conserved catalytic subunits responsible for RNA synthesis (54). In addition, the co-factors nsp7 and nsp8 enhance the enzymatic activity of nsp12 to catalyze viral RNA synthesis (55). Thus, the core polymerase complex nsp12–nsp7–nsp8 could be called the minimal core component of RNA synthesis (56). A schematic diagram of the core RdRp complex shows in Figure 2A. nsp12 contains a right-hand C-terminal RdRp domain with a catalytic cavity (the finger, palm, and thumb subdomains), an N-terminal NiRAN domain (including a novel β-hairpin domain), and an interface domain. In addition, seven conserved motifs (A–G) that mediate template-directed RNA synthesis have been identified in the core RdRp domain (57–59).



TABLE 1 Pharmacokinetic properties of GS-441524, VV116, and related compounds.

Compound	<i>In vivo</i> model	Route of administration	Dose(mg/kg)	Pharmacokinetic parameters				
				AUC <sub>last</sub>	T <sub>1/2</sub> (h)	T <sub>max</sub> (h)	C <sub>max</sub>	F (%)
GS-441524	rat (34, 35)	i.v.	5	11.0 (μM*h)	1.2		10.7 μM	
		p.o.	25	11.7 (μM*h)	1.4	1.0	3.4 μM	21.7
		i.v.	30	591.9 (μg/mL*h)	4.8	0.1	163.6 (μg/mL)	
	CD-1 mice (36)	p.o.	30	28.7 (μg/mL*h)	20.6	0.9	2.7 (μg/mL)	4.8
		i.v.	5	14.8 (μM*h)	2.5	0.08	11.6 μM	
		p.o.	10	16.8 (μM*h)	2.9	1.0	3.3 μM	57.0
	mic (37)	p.o.	10	<2540 (ng/mL*h)	3.9	1.5	582 (ng/mL)	39.0
	rat (37)	p.o.	10	<2170 (ng/mL*h)	3.4	3.8	193 (ng/mL)	33.0
			30	<4220 (ng/mL*h)	3.4	3.8	326 (ng/mL)	21.0
			100	<9560 (ng/mL*h)	4.2	2.3	825 (ng/mL)	15.0
	monkey (37)	p.o.	5	<734 (ng/mL*h)	7.7	2.0	59.4 (ng/mL)	8.3
	dog (37)	p.o.	5	< 19000 (ng/mL*h)	4.1	0.3	6010 (ng/mL)	85.0
	dog (38)	i.v.	2	26.6 (μM*h)	3.6	0.5	1897 (ng/mL)	
		p.o. (solution)	5	61.5 (μM*h)	4.0	0.5	5060 (ng/mL)	92.0
		p.o. (capsule)	6.5	65.6 (μM*h)	3.4	1.0	4580 (ng/mL)	76.0
	patients (39)	p.o. (normal renal function)	100 mg	1582 (ng/mL*h)	25.5	0.5	102 (ng/mL)	–
				1905 (ng/mL*h)	13.3	0.5	157 (ng/mL)	–
		p.o. (impaired renal function)	100 mg	7728 (ng/mL*h)	43.7	12	356 (ng/mL)	–
				11060 (ng/mL*h)	26.2	0.5	563 (ng/mL)	–
		p.o. (impaired renal function receiving CRR)	100 mg	9203 (ng/mL*h)	48.6	0.5	436 (ng/mL)	–
				8213 (ng/mL*h)	37.8	0.5	421 (ng/mL)	–
		p.o. (impaired renal function receiving IHD)	100 mg	25615 (ng/mL*h)	70.4	2.5	1653 (ng/mL)	–
				26950 (ng/mL*h)	–	–	1280 (ng/mL)	–
ATV006	rat (35)	i.v.	5	5.6 (μM*h)	1.5		8.7 μM	
		p.o.	25	22.8 (μM*h)	1.2	0.5	8.2 μM	81.5
	monkey (35)	i.v.	5	20.5 (μM*h)	1.8	0.08	12.8 μM	
			10	12.2 (μM*h)	4.1	1.5	3.7 μM	30.1
GS-621763	ferrets (40)	p.o.	30	80.8 (μM*h)	2.7	4.0	15.8 μM	115.0
GS-621763 ·HBr	mice (31)	i.v.	25	3603 (ng/mL*h)	2.5	–	–	
		p.o.	50	7112 (ng/mL*h)	2.7	0.3	3613 (ng/mL)	98.7
X1	rat (41)	i.v.	2	1724 (ng/mL*h)	6.7		1630 (ng/mL)	
		p.o.	10	1869 (ng/mL*h)	4.5	2.0	246 (ng/mL)	21.7
X2	rat (41)	i.v.	2	1611 (ng/mL*h)	5.0		1570 (ng/mL)	
		p.o.	10	2556 (ng/mL*h)	4.1	2.0	246 (ng/mL)	32.6

(Continued)



TABLE 1 Continued

Compound	In vivo model	Route of administration	Dose(mg/kg)	Pharmacokinetic parameters				
				AUC <sub>last</sub>	T <sub>1/2</sub> (h)	T <sub>max</sub> (h)	C <sub>max</sub>	F (%)
X2-H	monkey (41)	i.v.	5	6814 (ng/mL*h)	1.3		3322 (ng/mL)	
		p.o.	10	1939 (ng/mL*h)	2.0	1.0	941 (ng/mL)	14.2
	mice (31)	i.v.	25	7981 (ng/mL*h)	4.8		–	
		p.o.	50	13817 (ng/mL*h)	2.5	0.4	6677 (ng/mL)	86.6
X3	rat (41)	i.v.	2	1915 (ng/mL*h)	6.7		2520 (ng/mL)	
		p.o.	10	4455 (ng/mL*h)	4.0	0.3	801 (ng/mL)	46.5
	monkey (41)	i.v.	5	6780 (ng/mL*h)	1.4		7766 (ng/mL)	
		p.o.	10	2497 (ng/mL*h)	2.3	1.0	1064 (ng/mL)	18.4
X3-H	mice (31)	i.v.	25	10174 (ng/mL*h)	0.8		–	
		p.o.	50	14565 (ng/mL*h)	1.1	0.3	7879 (ng/mL)	71.6
X6	rat (41)	i.v.	2	1820 (ng/mL*h)	1.3		1693 (ng/mL)	
		p.o.	10	4539 (ng/mL*h)	2.0	0.3	1370 (ng/mL)	49.9
VV116	rat (41)	i.v.	10	4582 (ng/mL*h)	1.4		–	
		p.o.	10	3960 (ng/mL*h)	1.4	1.0	785 (ng/mL)	86.4
			30	10883 (ng/mL*h)	2.1	0.8	2068 (ng/mL)	79.2
			90	32807 (ng/mL*h)	3.6	0.8	6040 (ng/mL)	79.6
		p.o. (multiple)	7*30	7743 (ng/mL*h)	3.9	2.0	1740 (ng/mL)	–
	dogs (41)	i.v.	10	15835 (ng/mL*h)	3.9		–	
		p.o.	10	13845 (ng/mL*h)	4.5	1.0	3218 (ng/mL)	87.4
			20	32206 (ng/mL*h)	4.2	1.1	6633 (ng/mL)	101.7
			40	63289 (ng/mL*h)	4.3	1.1	11058 (ng/mL)	99.9
		p.o. (multiple)	7*20	27372 (ng/mL*h)	4.3	1.2	6317 (ng/mL)	–
	ICR mice (42)	i.v.	5	2341 (ng/mL*h)	1.6		2995 (ng/mL)	
		p.o.	25	12868 (ng/mL*h)	4.5	0.3	6500 (ng/mL)	110.2
	Balb/c mice (42)	p.o.	25	11461 (ng/mL*h)	2.3	0.4	5360 (ng/mL)	–
			50	24594 (ng/mL*h)	3.3	0.4	11617 (ng/mL)	–
			100	47799 (ng/mL*h)	4.3	0.4	24017 (ng/mL)	–
Rat (42)	i.v.		5	1774 (ng/mL*h)	0.7		1923 (ng/mL)	
	p.o.		30	9259 (ng/mL*h)	5.2	0.3	2710 (ng/mL)	87.0

(Continued)

TABLE 1 Continued

Compound	<i>In vivo</i> model	Route of administration	Dose(mg/kg)	Pharmacokinetic parameters				
				AUC <sub>last</sub>	T <sub>1/2</sub> (h)	T <sub>max</sub> (h)	C <sub>max</sub>	F (%)
	healthy subjects (43)	p.o.	20 mg	744 (ng/mL*h)	4.8	1.0	165 (ng/mL)	-
			200 mg	6631 (ng/mL*h)	5.5	1.0	1096 (ng/mL)	-
			400 mg	12759 (ng/mL*h)	6.2	1.5	1898 (ng/mL)	-
			800 mg	25886 (ng/mL*h)	6.8	2.5	2796 (ng/mL)	-
			1200 mg	28057 (ng/mL*h)	7.0	2.0	3086 (ng/mL)	-
		p.o. (multiple)	1*200 mg	4610 (ng/mL*h)	4.7	1.5	858 (ng/mL)	-
			6*200 mg	9384 (ng/mL*h)	7.6	1.0	1131 (ng/mL)	-
			1*400 mg	10351 (ng/mL*h)	4.9	1.5	1968 (ng/mL)	-
			6*400 mg	20774 (ng/mL*h)	8.1	1.0	2304 (ng/mL)	-
			1*600 mg	12871 (ng/mL*h)	5.4	1.5	2418 (ng/mL)	-
			6*400 mg	25077 (ng/mL*h)	7.9	1.5	2842 (ng/mL)	-
		p.o.	400 mg (Fasting)	10443 (ng/mL*h)	5.7	1.5	1523 (ng/mL)	-
			400 mg (Standard meal)	12405 (ng/mL*h)	5.3	3.0	1583 (ng/mL)	-
			400 mg (High-fat meal)	13107 (ng/mL*h)	5.5	2.5	1602 (ng/mL)	-
VV116-H	rat (42)	i.v.	5	1689 (ng/mL*h)	0.7		1997 (ng/mL)	
		p.o.	30	7664 (ng/mL*h)	4.6	1.0	2060 (ng/mL)	75.6

t<sub>1/2</sub>, terminal half-life; C<sub>max</sub>, maximum plasma concentration; T<sub>max</sub>, time to reach C<sub>max</sub>; AUC<sub>last</sub>, area under the concentration–time curve from the time of dosing to the last quantifiable time point; i.v., intravenous administration; p.o., per os; CRRT, continuous renal replacement therapy; IHD, intermittent hemodialysis.

Blocking initial SARS-CoV-2 attachment or entry into the target cell and preventing viral replication by suppressing gene transcription are two optimal therapeutic strategies for drug design (Figure 2B) (60, 61). That is, RdRp is a key target for antiviral inhibitors. The model of remdesivir (the first approved RdRp inhibitor to treat SARS-CoV-2) binding to nsp12 indicates that remdesivir covalently binds to the 1+ position of the template chain at the central channel, thereby terminating chain extension (62, 63). Based on structural similarities (e.g., remdesivir, molnupiravir, sofosbuvir, and AT-527), nucleoside analogs (Figure 2C) are suggested optimal candidates in the search for agents against SARS-CoV-2 (64–70). In brief, the high-resolution crystal structure of SARS-CoV-2 RdRp (PDB ID: 7BTF) has been deciphered, which provides a rational basis for drug design. RdRp plays an essential role in viral RNA synthesis; it is an excellent target in the development of anti-SARS-CoV-2 drugs due to high sequence and structural conservation.

To date, remdesivir, molnupiravir, and paxlovid have been approved for COVID-19 treatment (71). Remdesivir, the first

intravenously administered drug targeting RdRp for SARS-CoV-2 treatment, has yielded contradictory clinical results (26). Concerns over renal toxicity, liver injury, and cardiac safety challenge the safety of remdesivir (72–75). Molnupiravir, developed by Merck and Ridgeback Biotherapeutics, is the first approved oral anti-SARS-CoV-2 therapy, which also targets RdRp (15). Concerningly, molnupiravir can induce mutations in mammalian cells and drive new variants (76–78). The use of molnupiravir has been cautioned by the World Health Organization (79). Paxlovid, a main protease inhibitor, is recognized as having a reasonable safety profile (80–82). However, later studies showed that symptoms might reappear after paxlovid treatment, and are often more severe than the initial bout (83). Consequently, there is still a need for safe and effective oral agents. In such cases, oral GS-441524 derivatives (oral version of remdesivir), with sufficient safety and resistance profile, may be more potent SARS-CoV-2 inhibitors against an expansive range of variants.

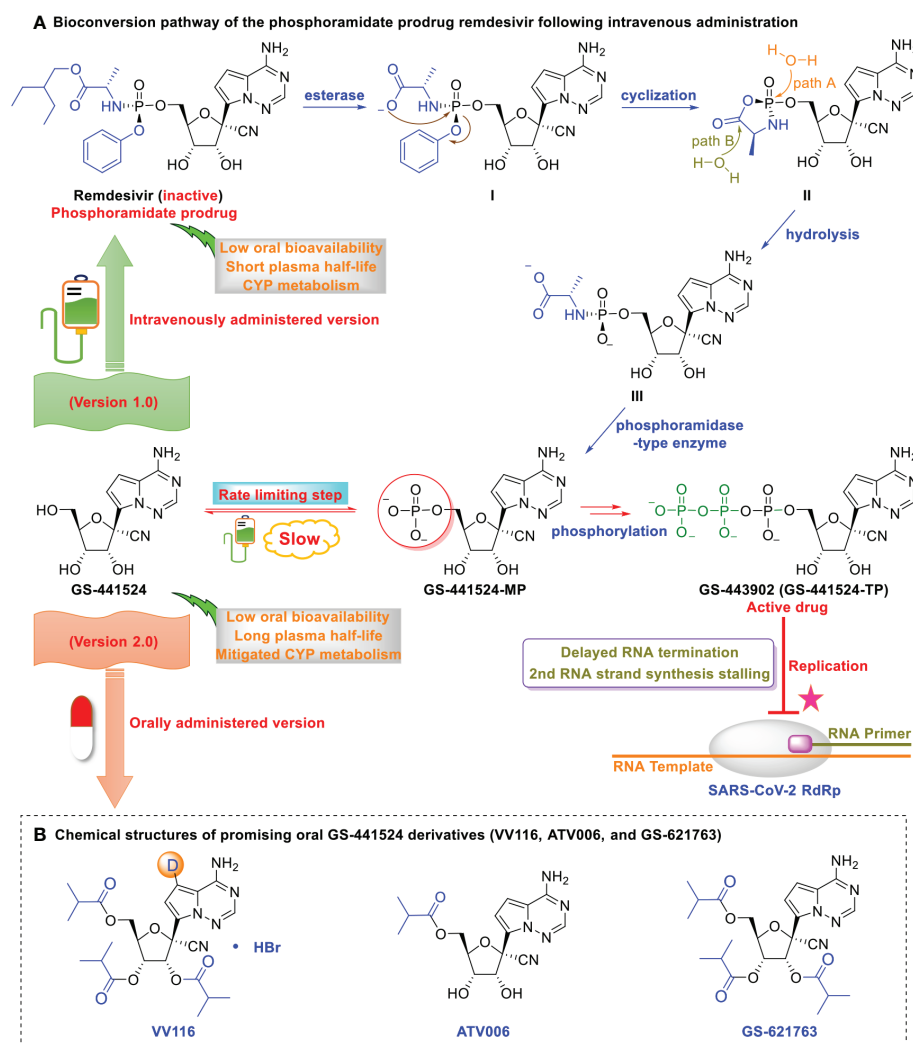


FIGURE 1

Optimization of GS-441524 for intravenous remdesivir and the oral version, VV116. **(A)** Bioconversion pathway of the phosphoramidate prodrug remdesivir following intravenous administration. Low oral bioavailability renders GS-441524 unsuitable as an oral drug. The first phosphorylation is the rate-limiting step of GS-441524, which renders it less efficient as an intravenous drug. GS-441524-based lead optimization resulted in the development of the more potent intravenously administered remdesivir (version 1.0). Following intravenous administration, remdesivir distributes to the lung, where it is rapidly converted into its monophosphate metabolite and efficiently anabolized to the bioactive triphosphate form (GS-443902). However, human microsomal hepatic cytochrome P450 (CYP)-mediated metabolism in the liver and the short plasma half-life of remdesivir renders it unsuitable as an oral drug. **(B)** Chemical structures of promising oral GS-441524 derivatives (VV116, ATV006, and GS-621763). GS-441524 does not undergo human microsomal hepatic cytochrome P450 (CYPs 1A1, 1A2, 3A4, 3A5, 2B6, 2C8, 2C9, 2C19, and 2D6) metabolism and exhibits a long plasma half-life. Further optimization of GS-441524 has resulted in the development of promising orally administered VV116, ATV006, and GS-621763 (version 2.0).

## Remdesivir: The intravenously administered version of GS-441524

Remdesivir (Veklury<sup>®</sup>, GS-5734), the first FDA-approved intravenously administered drug for SARS-CoV-2 treatment, has exhibited broad-spectrum antiviral activity in studies on *in vitro* models, animal models, and preliminary clinical trials (84–86). Remdesivir, having melting point 89.4–90.4° C and molecular formula C<sub>27</sub>H<sub>35</sub>N<sub>6</sub>O<sub>8</sub>P, has generated widespread interest as a anti-COVID-19 drug (87). However, clinical trials

on the value of remdesivir in the treatment of COVID-19 have yielded contradictory results, which have raised several concerns and provided insights.

## Conflicting evidences from clinical trials of remdesivir

To date, several trials have demonstrated promising results with remdesivir. For example, Boglione et al. (88) conducted a

single-centre retrospective observational study (time bias and seroprevalence not discussed) in Italy to evaluate the survival, efficacy, and safety of remdesivir treatment in hospitalized patients with COVID-19. In total, 566 participants with similar baseline characteristics underwent randomization: 163 patients were assigned to receive remdesivir (200 mg on day 1, followed by 100 mg per day on days 2–5) and 403 patients in the control group were randomly assigned to receive lopinavir/ritonavir, darunavir/cobicistat, or hydroxychloroquine. The COVID-19-related mortality rate was significantly lower in the remdesivir group (4 of 163 participants [2.4%]) than in the control group (100 of 403 [24.8%]) ( $p < 0.001$ ). Furthermore, the percentage of patients hospitalised in the intensive care unit was lower in the remdesivir group than in the control group (9.8% [16 of 163] vs. 17.8% [72 of 403],  $p = 0.008$ ). Overall, remdesivir-treated patients had a significantly shorter mean hospitalization time than that of the control group (9.5 vs. 12.5 days,  $p < 0.001$ ). No significant adverse drug events were observed in the remdesivir group. Several other studies have produced results consistent with the findings of the Boglione group (89, 90). For example, Gottlieb et al. (89) showed that the percentage of unvaccinated outpatients with COVID-19 who were hospitalized or died was significantly lower in the remdesivir-treated group (200 mg on day 1, followed by 100 mg on days 2 and 3; 2 of 279 participants [0.7%]) than in the placebo group (15 of 283 [5.3%]; 87% lower).

Notably, the anti-SARS-CoV-2 efficacy of remdesivir has also been questioned, as several other studies have found that it adds no value to COVID-19 treatment (91–94). One large-scale, open-label, randomized trial including 11,330 hospitalized adults with COVID-19 (81% aged  $\leq 70$  years, 38% female) at 405 hospitals in 30 countries was conducted by the World Health Organization to estimate mortality rates. This study indicated that remdesivir did not reduce the mortality rate (remdesivir, 301 of 2743 [11.0%] vs. control, 303 of 2708 [11.2%]) or hospitalisation duration (91). Further, Wang et al. (94) conducted a small-scale, double-blind, multicentre, and randomized placebo controlled trial (ClinicalTrials.gov: NCT04257656) to evaluate the efficacy and safety of remdesivir in adults with severe COVID-19 at 10 hospitals in Hubei, China; however, treatment with the drug was not associated with statistically significant benefits. Considering the available clinical evidence, new strategies (such as optimal delivery of the parent nucleoside into systemic circulation) and further investigations may be required to respond to public concerns and to define how remdesivir is best used.

## Practical limitations and countermeasures of remdesivir

Overall, remdesivir has several practical limitations, which need to be addressed to reinforce the value of antivirals. This

section addresses the other limitations and concerns regarding remdesivir. First, remdesivir shows strong liver-targeting properties. Remdesivir, the McGuigan (ProTide) prodrug, was initially designed for treating hepatitis C virus infection by overcoming the rate-limiting initial phosphorylation step and sustaining a high concentration of biologically active nucleotide triphosphates (NTP) in the liver (95). However, remdesivir (preferential hepatic extraction) may not be suitable for treating COVID-19 because the lungs are the primary site (type II alveolar cells) of SARS-CoV-2 infection and the most affected organs (96, 97).

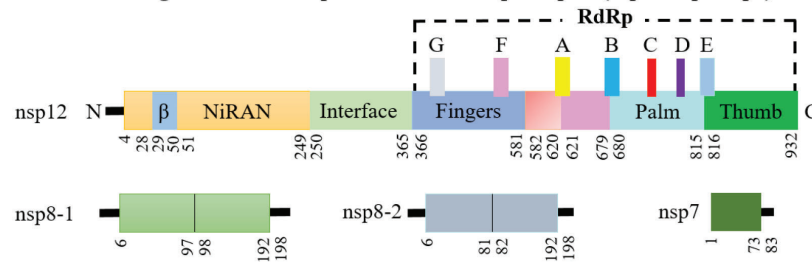
Second, remdesivir is not suitable for oral or buccal delivery. Remdesivir shows rapid clearance (plasma half-life  $< 1$  h) owing to its intrinsic hepatic first-pass metabolism and plasma esterase hydrolysis (98, 99). Short exposure is insufficient to achieve the desired anti-SARS-CoV-2 activity. Therefore, remdesivir is highly recommended for only for intravenous therapy in hospitals, which severely limits its application. Although buccal administration is a potential approach to avoid hepatic first-pass metabolism and enzymatic degradation (100), experimental data indicate that cyclodextrin-enabled buccal administration of remdesivir shows only 10% bioavailability (47), suggesting this strategy faces many challenges.

Third, solid preclinical data (overemphasizing low  $EC_{50}$ ) do not reflect the clinical efficacy of remdesivir. For example, Chiu et al. (101) screened a 5676-compound repurposing library of drugs that have passed Phase I clinical trials to identify anti-SARS-CoV-2 candidates; remdesivir alone ( $EC_{50}$  values of 5.4 and 1.3  $\mu$ M in VeroE6-eGFP and Caco-2 cell lines, respectively) was identified as an optimal drug candidate owing to its excellent pharmacodynamic and safety data. However, cell culture studies do not predict the clinical utility of a drug, and it is inappropriate to overrate the clinical efficacy of remdesivir based on *in vitro* cell culture data regarding its efficacy. Thus, additional models and data on remdesivir antiviral therapy are needed.

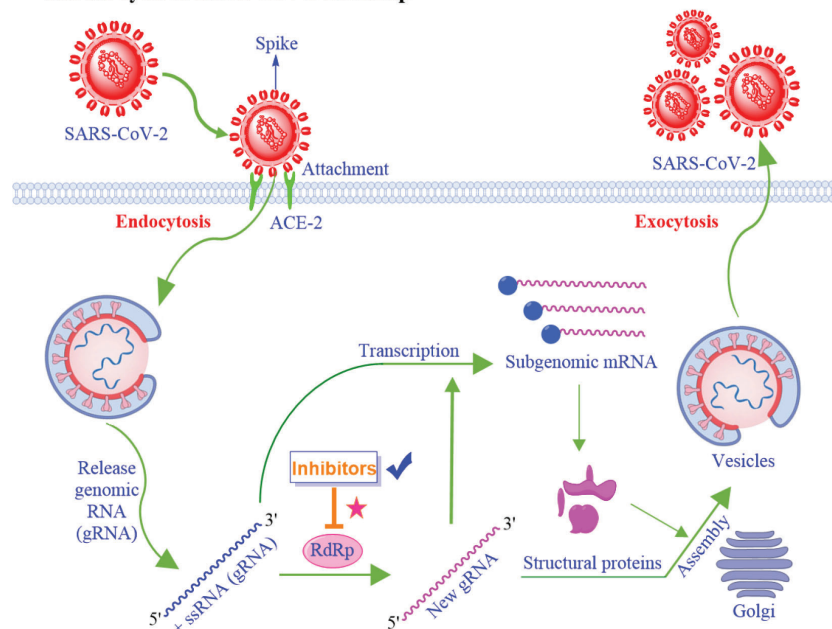
Finally, the long-term safety of remdesivir remains incompletely examined. Current data indicate that non-uniform distribution of remdesivir could result in high drug accumulation and long-term toxicity; for example, remdesivir potentially increases liver transaminases (102) and diminishes the viability of human embryonic stem cells (103) compared to its metabolite, GS-441524. Further, the widespread use of remdesivir in clinical practice raises several concerns regarding the development of drug resistance.

However, the underwhelming clinical performance of remdesivir does not mean that its significance can be disregarded. In contrast, the described limitations provides important insights (such as tissue-specific localization, enhanced oral bioavailability, excellent safety and activity against Omicron variant) to be considered when developing version 2.0 of GS-441524 (targeting highly conserved viral RdRp) for clinical advancement.

### A Schematic diagram for the components of the RdRp complex (nsp12-nsp7-nsp8).



### B The life cycle of SARS-CoV-2 via RdRp



### C Selected RdRp inhibitors

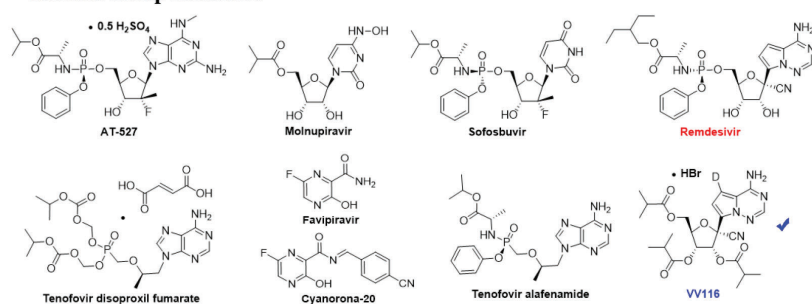


FIGURE 2

The mechanistic diagram of SARS-CoV-2 RNA-dependent RNA polymerase. (A) The schematic diagram for the components of the RdRp complex, containing nsp12, nsp8 and nsp7. The polymerase motif (A to G) and the  $\beta$  hairpin are highlighted. (B) The life cycle of SARS-CoV-2 via RdRp. The life cycle of SARS-CoV-2 involves sequential viral entry into the target cell, uncoating, replication and transcription, protein synthesis, and viral assembly and release. The RdRp is involved in SARS-CoV-2 genomic and subgenomic mRNA synthesis. (C) Chemical structures of selected SARS-CoV-2 RdRp inhibitors (AT-527, Molnupiravir, Sofosbuvir, Tenofovir disoproxil fumarate, Favipiravir, Cyanorona-20, Tenofovir alafenamide, Remdesivir, and VV116) for COVID-19 treatment.



## The orally administered versions of GS-441524

Viral RdRp is as a valuable target for treating COVID-19 because it is highly conserved in SARS-CoV-2 variants (104, 105). Use of orally administered versions of GS-441524 at the early stage of the acute infection would be more beneficial in facilitating early administration to non-hospitalized patients to prevent progression to severe disease. Research has shown that oral GS-441524 derivatives (ATV006, VV116, and GS-621763) obtained through individual alterations could be considered game changers for COVID-19 treatment to maximize clinical benefits, including decreased duration of COVID-19 and reduced post-acute sequelae of SARS-CoV-2 infection, as well as limited side effects such as hepatic accumulation. In the following sections, we describe the currently developed orally administered versions of GS-441524.

### ATV006

GS-441524 has its own advantages, further esterification at the 5'-position yielded mono-isobutyrate ester ATV006 with improved oral bioavailability. Xie et al. (36) showed that GS-441524, a promising RdRp inhibitor, demonstrated adequate intracellular conversion into active triphosphate (GS-443902, 42.7–100 nmol/L) in the lungs of CD-1 mice upon oral administration. Furthermore, GS-441524 does not exhibit preferential hepatic metabolism because it is not a substrate for human microsomal hepatic cytochrome P450 (CYPs 1A1, 1A2, 3A4, 3A5, 2B6, 2C8, 2C9, 2C19, and 2D6) (106). Li et al. (34) demonstrated that GS-441524 potentially alleviated lung inflammation and injury in AAV-hACE2 mice infected with SARS-CoV-2. However, further development of GS-441524 as an oral drug was hindered by its poor oral bioavailability ( $F = 4.84\%$  in rats) (34).

To develop orally bioavailable anti-SARS-CoV-2 inhibitors, Cao et al. (35) synthesised and evaluated a series of GS-441524 derivatives. Among the designs, mono-isobutyryl esterification of the hydroxyl groups on the C5' position (ATV006) showed improved activities against the Delta ( $EC_{50} = 0.349 \mu\text{M}$ , therapeutic index = 366.76) and Omicron ( $EC_{50} = 0.106 \mu\text{M}$ , therapeutic index = 1207.55) variants of SARS-CoV-2 in a Vero E6 cell model (35). In addition, ATV006 displayed excellent oral bioavailability ( $F = 81.5\%$ ), effective blood concentration ( $C_{\text{max}} = 8.2 \mu\text{M}$ ), extensive target distribution (plasma, liver, kidneys, and lung), and potent anti-SARS-CoV-2 efficacy (reduced viral load, inflammatory cytokines, and lung damage) in mouse models (35). Notably, ATV006 and remdesivir could be metabolized to the same active triphosphate form (GS-443902) via different bioconversion pathways (35, 36). ATV006 can be rapidly metabolized to GS-441524 after oral absorption, which is

then intracellularly converted to monophosphate GS-441524-MP through cellular kinases and further metabolized to the bioactive triphosphate GS-443902. In contrast, remdesivir is a monophosphorylated prodrug that does not require the first phosphorylation, which is a rate-limiting step (107). In the context of developing orally bioavailable anti-SARS-CoV-2 inhibitors, ATV006 is still in the experimental stage and has not entered clinical trials. Additional studies are thus required to demonstrate its safety, efficacy, and tolerability.

### VV116

Deuterated GS-441524 derivatives (Figure 3, such as X1-X6, VV116) provide a beneficial strategy for the development and selection of oral antiviral drugs. In medicinal chemistry, deuterium (D) substitution represents a valuable direction because of its potential pharmacokinetic and pharmacodynamic benefits attributed to the kinetic isotope effect (108–110). GS-441524 possesses an electron-rich pyrrolotriazine moiety that is easily oxidized by enzymes. The carbon-deuterium bond is shorter ( $\sim 0.005 \text{ \AA}$ ) than the C–H bond and is more stable under oxidative clearance processes (111, 112). Strategic deuteration could impede metabolic transformations by inhibiting oxidation or ring opening of the pyrrolotriazine moiety, leading to an increase in anti-SARS-CoV-2 activity.

As depicted in Figure 3, lead compound X1 was produced by deuteration and could significantly inhibit viral replication, with an  $EC_{50}$  of  $0.39 \mu\text{M}$  and no observable cytotoxicity (selectivity index [SI] > 1282) (41). However, the oral bioavailability of X1 ( $F = \sim 21.7\%$  in rats) was low because of poor solubility and liposolubility. Further esterification yielded tri-isobutyrate ester X6 ( $F = \sim 50\%$  in rats). The detailed pharmacokinetic properties (such as maximum plasma concentration, terminal half-life, and oral bioavailability) of the related compounds are shown in Table 1.

To better control solubility and oral bioavailability, salification of X6 with hydrobromide proved to be a winning strategy that enhanced the oral bioavailability of VV116 (JT001, renmindevir, on a 10.8 g scale) up to 60% with respect to that of X6 in rats (41). VV116 also displayed excellent oral bioavailability in beagle dogs ( $F = 90\%$ ) and in ICR mice ( $F = 110.2\%$ ). In the mouse model, VV116 showed a dose-dependent anti-SARS-CoV-2 effect (with reduced lung injury), and high doses of VV116 markedly reduced the viral RNA copy number and improved lung histopathology (41). Overall, VV116 displays a good safety profile (high tolerated single doses: > 2.0 g/kg in rats, 1.0 g/kg in Beagle dogs) without adverse effects (14 days, 200 mg/kg in rats, 30 mg/kg in dogs), and indicates no mutagenic effects (41). Further, oral administration of VV116 showed pharmacokinetic advantages relative to its non-deuterated form VV116-H in Sprague Dawley (SD) rats (30.0 mg/kg/day,  $N = 3$ ,  $F = 87.0\%$  vs.  $F = 75.6\%$ ) (42).

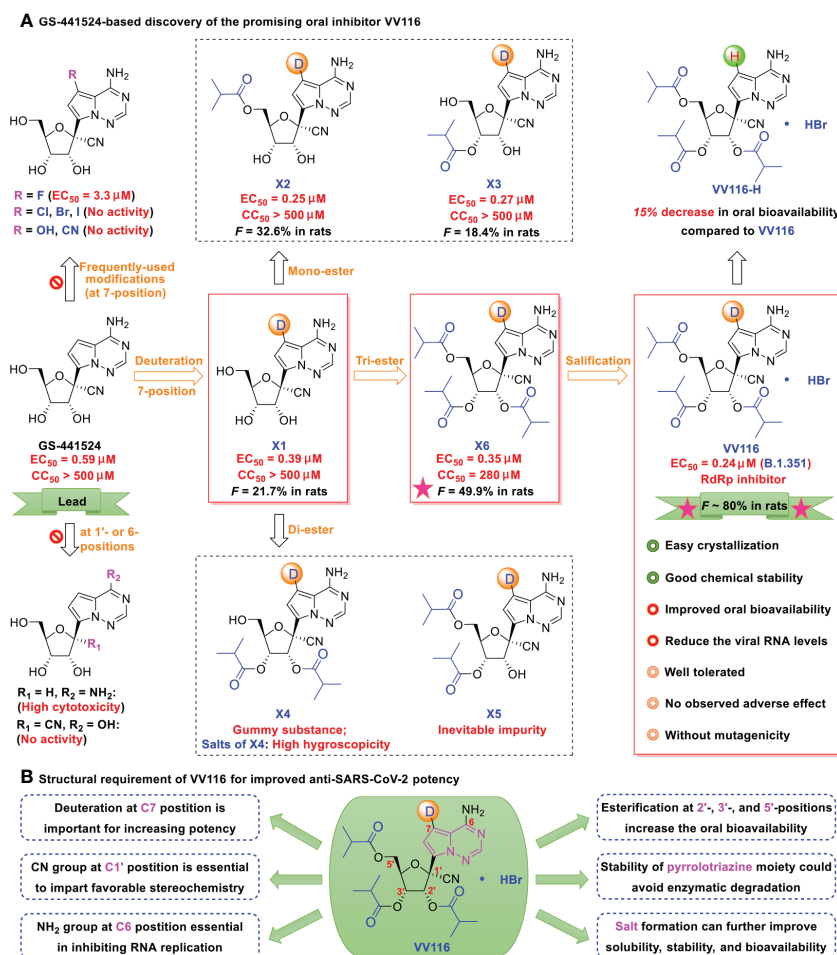


FIGURE 3

(A) GS-441524-based discovery of the promising oral inhibitor VV116. GS-441524 presents a promising drug candidate for further drug development. Several previous failed attempts are summarized: (i) introduction of frequently-used halogen (F, Cl, Br, I), hydroxyl, or cyano groups at the C7-position, resulting in less potent or no anti-SARS-CoV-2 activity, (ii) removal of the cyano group at C1'-position, results in high cytotoxicity, (iii) changing the 6-amino to a hydroxyl, methylation of the 2'- $\alpha$ -hydroxyl, or changing the 2'- $\alpha$ -hydroxyl to fluorine, results in loss of anti-SARS-CoV-2 activity. Promising attempts: deuteration at the C7 position results in strong antiviral activity; induces mono-, di- and tri-esters at the 2', 3', and 5'-positions, and improves oral bioavailability (tri-isobutyrate ester X6 [ $F \sim 50\%$  in rats] was superior to the others in rats); and induces hydrobromide in X6, yielding the promising oral candidate VV116 (white solid, with improved oral bioavailability, good chemical stability; no observed adverse effect, and no mutagenicity). (B) Structural requirement of VV116 for improved anti-SARS-CoV-2 potency.

Fast-spreading SARS-CoV-2 variants cause resurgence of infections raise several concerns (113). However, VV116 was found to retain its anti-viral capacity against the Alpha, Beta, Gamma, Delta, as well as Omicron ( $EC_{90} = 0.30 \mu M$ ) variants of SARS-CoV-2 (114). In terms of the molecular mechanism, VV116 functioned by targeting the highly conserved viral RdRp to block SARS-CoV-2 replication through evading “proofreading” of viral RNA sequences (41). Specifically, the postulated activation pathway of VV116 is divided into four steps: oral absorption, hydrolysis of ester group, phosphorylation (VV116-NTP), and incorporation into the growing SARS-CoV-2 RNA strand. Further, the preference of remdesivir for hepatic extraction can result in high drug

accumulation and long-term toxicity (e.g., elevated liver transaminases) (114), however, the excellent tissue distribution (e.g., single oral administration in rats at 30 mg/kg) of oral VV116 can avoid these liver-targeting problems (Figure 4) (115).

Specifically, in male SD rats and long Evans rats groups, the liver-to-plasma concentration ratios of [ $^{14}C$ ]GS-441524 (the major metabolite of [ $^{14}C$ ]remdesivir) were higher than the lungs-to-plasma concentration ratios by approximately 23 times (SD rats, 1 h), 37 times (SD rats, 4 h), 34 times (Long Evans rats, 1 h), and 58 times (Long Evans rats, 4 h) (116). In contrast, the liver-to-plasma concentration ratios of 116-N1 (the major metabolite of VV116) were higher than the lungs-to-plasma concentration ratios by only 1.8 times (Balb/c mice, 0.25

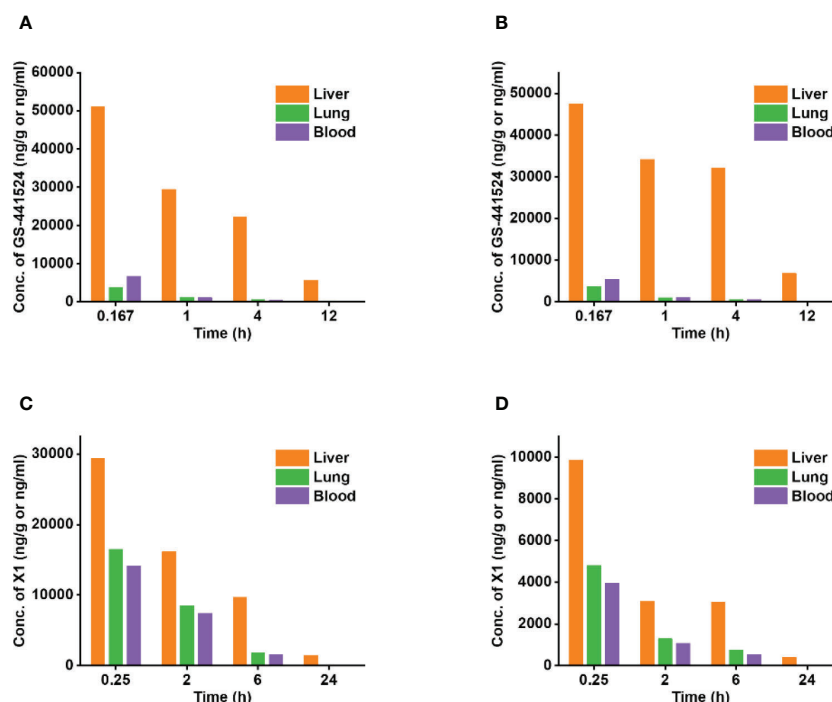


FIGURE 4

The concentration distribution of the key metabolites, GS-441524 and X1, in the liver, lungs, and blood in rats or mice. Oral VV116 administration can circumvent liver-targeting issues. (A) The concentration of  $^{14}\text{C}$ -GS-441524 in the liver, lungs, and blood following intravenous administration of  $^{14}\text{C}$ -remdesivir at a single dose of 10 mg/kg in male SD rats. (B) The concentration of  $^{14}\text{C}$ -GS-441524 in the liver, lungs, and blood following intravenous administration of  $^{14}\text{C}$ -remdesivir at a single dose of 10 mg/kg in male Long Evans rats. (C) The concentration of X1 in the liver, lungs, and blood following oral administration of VV116 at a single dose of 100 mg/kg in Balb/c mice. (D) The concentration of X1 in the liver, lungs, and blood following oral administration of VV116 at a single dose of 30 mg/kg in SD rats.

h), 1.9 times (Balb/c mice, 2 h), 2.1 times (SD rats, 0.25 h), and 2.4 times (SD rats, 2 h) (116). This indicates that in contrast to the high liver-targeting capability of remdesivir, VV116 can effectively circumvent this issue.

Considering the promising therapeutic usage of VV116 against SARS-CoV-2 infection in preclinical studies, Qian et al. (43) further launched three phase I studies of VV16 in Shanghai, China (ClinicalTrials.gov: NCT05227768, NCT05201690, and NCT05221138; Table 2). The result found that VV116 exhibited satisfactory safety, tolerability, and pharmacokinetic properties in 86 healthy subjects (aged 18–45 years, 38 in single ascending-dose study, 36 in multiple ascending-dose study, and 12 in food-effect study). As depicted in Figure 5, VV116 can be efficiently converted to its active triphosphate form following oral administration. Moreover, the area under the curve (AUC) demonstrates that VV116 is quickly absorbed after the first dose with a median  $T_{\max}$  of 1.00–2.50 h, and that 116-N1 is eliminated with a median  $t_{1/2}$  of 4.80–6.95 h (43).

Furthermore, Shen et al. (114) conducted an open, prospective cohort study in China, including 136 hospitalised patients with non-severe COVID-19 caused by the Omicron

variant, 60 of whom patients received VV116 (300 mg, twice daily for 5 days), and found that the viral shedding time of the VV116 group was significantly shorter than that of the control group (8.56 vs. 11.13 days). Nine mild adverse events occurred in the VV116 group, and all resolved without required intervention (114). VV116 targets highly conserved RdRp (only one mutation in nsp12, distant from the RdRp active site), which may explain why it maintains high potency against the Omicron variant (117). Moreover, VV116 has been further investigated in five clinical trials (ClinicalTrials.gov: NCT05242042, NCT05279235, NCT05341609, NCT05355077, and NCT05582629; As depicted in Table 2), and their findings will be disclosed shortly.

## GS-621763

Cox et al. (40) demonstrated that GS-621763 (X6-H; white solid), which is generated by tri-isobutyl esterification of the hydroxyl groups of GS-441524 at the C5', C2', and C3' positions, represents another example of a GS-441524 prodrug with enhanced oral bioavailability, which could significantly reduce the SARS-CoV-2 burden to near-undetectable levels in ferrets

TABLE 2 VV116 in clinical development based on a systematic search of ClinicalTrials.gov (<https://clinicaltrials.gov/>, accessed 31 October, 2022).

Interventions	Principal Investigator	Identifier (year)	Participants	Progress
VV116	Shanghai Xuhui Central Hospital, Shanghai, China	NCT05221138 (2021)	12	Phase I trial exhibited satisfactory safety and tolerability in Chinese healthy subjects after fasting, standard diet or high-fat diet.
VV116 (25 mg Group, 200 mg Group, 400 mg Group, 800 mg Group, 1200 mg Group)	Shanghai Xuhui Central Hospital, Shanghai, China	NCT05227768 (2021)	38	Phase I trial exhibited satisfactory safety and tolerability in Chinese healthy subjects at five dose levels.
VV116 (200 mg Group, 400 mg Group, 600 mg Group)	Shanghai Xuhui Central Hospital, Shanghai, China	NCT05201690 (2021)	36	Phase I trial exhibited satisfactory safety and tolerability in Chinese healthy subjects after multiple ascending doses.
VV116 (200 mg Group, Bid; 400 mg Group, Bid; 600 mg Group, Bid)	Nucleus Network Pty Ltd, Victoria, Australia	NCT05355077 (2022)	27	Phase I trial is in progress for Caucasian healthy subjects.
VV116	Chongqing Public Health Medical Center, Chongqing, China	NCT05242042 (2022)	1310	Phase II/III trial is in progress for the early treatment of patients with mild/moderate COVID-19, at high risk for progression to severe COVID-19, including death.
VV116 Paxlovid	Ruijin Hospital Affiliated to Shanghai Jiao Tong University School of Medicine, Shanghai, China	NCT05341609 (2022)	822	Phase III trial is in progress for the early treatment of patients with mild/moderate COVID-19.
VV116 Favipiravir	Shanghai Public Health Clinical Center, Shanghai, China	NCT05279235 (2022)	640	Phase III trial is in progress for patients with moderate/severe COVID-19.
VV116	Shanghai Vinnerna Biosciences Co., Ltd., Shanghai, China	NCT05582629 (2022)	1200	Phase III trial is in progress for patients with mild/moderate COVID-19

infected with the gamma variant. SARS-CoV-2 infection can have long-term effects on pulmonary and multiple extrapulmonary tissues and organs (118). Schäfer et al. (119) showed that oral delivery of GS-621763 could diminish SARS-CoV-2 replication, improve pulmonary function, and prevent COVID-19 progression in BALB/c model mice. The potential anti-SARS-CoV-2 had been preliminarily revealed, while the safety, efficacy, and pharmacokinetic properties of GS-621763 are still an open question and require additional studies.

Although the potential anti-SARS-CoV-2 had been preliminarily revealed, at the same time, we must understand that oral GS-441524 derivatives (VV116, ATV006, and GS-621763) have not been deeply investigated yet. The clinical data are still limited (only VV116 has entered in clinical development, as shown in (Table 2), we call for more comprehensive studies.

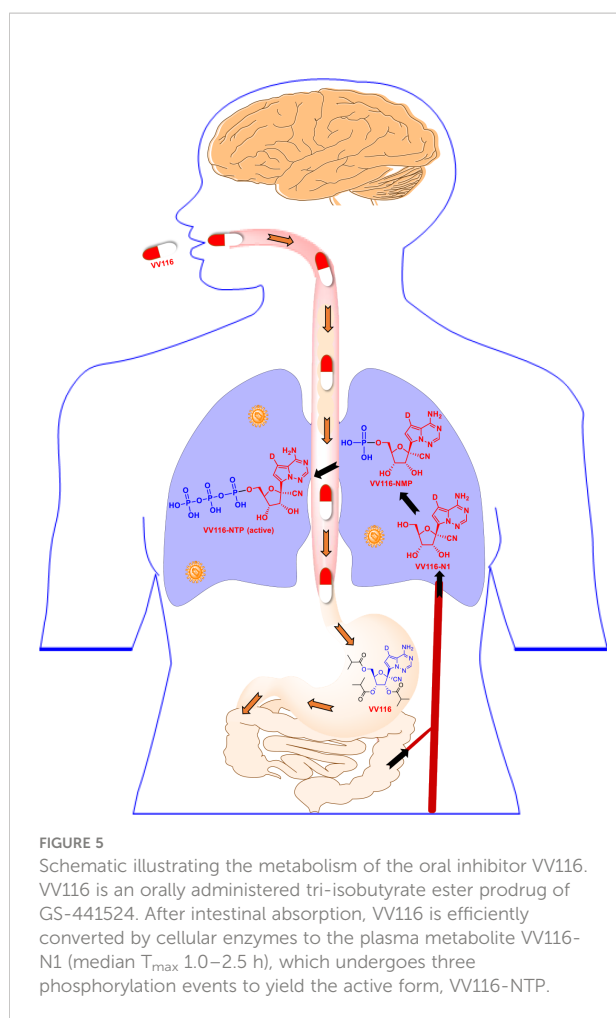
## Conclusion and discussion

Viral RdRp is a valuable target for COVID-19 therapeutic interventions because it is highly conserved among SARS-CoV-2 variants. Oral administration has the potential to maximize clinical benefits, including decreased duration of COVID-19 and reduced post-acute sequelae of SARS-CoV-2 infection, whereas remdesivir (version 1.0 of GS-441524) is only suitable for injection. The currently available data support the exploration of next-generation oral inhibitors of SARS-CoV-2 polymerase (version 2.0, GS-441524) for treating COVID-19.

This exploration could enhance preparedness for future outbreaks of SARS-CoV-2 and improve therapeutic efficacy during the current pandemic. Oral GS-441524 derivatives, including VV116, ATV006, and GS-621763, have potential as the cornerstone of first-line defence against COVID-19.

Specifically, a promising oral version of GS-441524 should have the following key characteristics: (i) enhanced oral bioavailability, tissue-specific localization, and plasma half-life; (ii) sufficient safety (excellent CC<sub>50</sub>) and resistance profile; (iii) significantly reduced viral loads and dramatically decreased lung injury; (iv) maximally maintained antiviral activity against SARS-CoV-2 variants; and (v) large-scale manufacturing ability for increased accessibility and affordability to outpatients (VV116 is easier to synthesize than remdesivir).

Although the potential oral anti-SARS-CoV-2 agents have been preliminarily revealed, the relevant data remain limited, because only VV116 has reached the clinical stage (Table 2). Considering the positive effects of oral GS-441524 derivatives on COVID-19 and the urgent need to explore possible SARS-CoV-2 treatments, it is crucial to systematically elucidate their safety, efficacy, tolerability, and pharmacokinetic properties through large-scale preclinical and clinical studies. Notably, GS-441524 showed high interpatient variability owing to differences in renal function (Table 1) (39), implying that the related pharmacokinetics (including potential efficacy and toxicity) of oral GS-441524 derivatives need to be investigated further to rationally evaluate the possibility of its clinical application and to further guide drug development.



Meanwhile, multiple measures can be considered. Deuterated GS-441524 derivatives provide a beneficial strategy for the development and selection of oral antiviral drugs. Deuteration has gained overwhelming popularity (120). However, owing to synthetic difficulties, only 7-deuterated derivatives of GS-441524 (pyrrolotriazine moiety) have been obtained. Additional site-specific deuterium substitution derivatives need to be synthesized through novel efficient synthetic reactions to exert kinetic isotope effects, enhance oral bioavailability, and exploit SARS-CoV-2-specific antiviral drugs with clinical advantages. Further, optimized drug combinations (such as VV116 + PF-07321332, VV116 + EIDD-2801, VV116 + masitinib, and VV116 + F0213) that target multiple routes can both enhance synergistic efficacy and reduce drug resistance and

toxicity (121–125). However, any potential combination must verify the anticipated synergistic/additive effects and drug-drug interactions through systematic studies. Further, a VV116-based nano delivery system (with enhanced bioavailability, precision, and sustained drug release) can be a good therapeutic alternative for SARS-CoV-2 infection. However, as the relevant studies are limited, this approach should be considered and elucidated further.

With continuing advances, more effective oral GS-441524 derivatives can be developed. However, to date, VV116 is the top contender for clinical development owing to its large-scale manufacturing ability, excellent oral bioavailability and safety profile, reduced viral RNA copies, and improved lung histopathology.

## Author contributions

ZW: Conceptualization, collecting the literatures, writing-original draft, writing-review & editing, visualization, funding acquisition. LY: Conceptualization, writing-review & editing, funding acquisition. X-QS: Collecting the literatures, editing, visualization. All authors contributed to the article and approved the submitted version.

## Funding

This work was supported by Shandong Provincial Natural Science Foundation (ZR2022MH162, ZR2022QE202), the PhD research start-up fund of Qufu Normal University (614901, 615201).

## Conflict of interest

The authors declare that the research was conducted in the absence of any commercial or financial relationships that could be construed as a potential conflict of interest.

## Publisher's note

All claims expressed in this article are solely those of the authors and do not necessarily represent those of their affiliated organizations, or those of the publisher, the editors and the reviewers. Any product that may be evaluated in this article, or claim that may be made by its manufacturer, is not guaranteed or endorsed by the publisher.

## References

1. World Health Organization. WHO coronavirus (COVID-19) dashboard. Available at: <https://covid19.who.int/> (Accessed October 31, 2022).
2. Al-Aly Z, Xie Y, Bowe B. High-dimensional characterization of post-acute sequelae of COVID-19. *Nature* (2021) 594:259–64. doi: 10.1038/s41586-021-03553-9



3. Zhao W, Li H, Li J, Xu B, Xu J. The mechanism of multiple organ dysfunction syndrome in patients with COVID-19. *J Med Virol* (2022) 94(5):1886–92. doi: 10.1002/jmv.27627
4. Nalbandian A, Sehgal K, Gupta A, Madhavan MV, McGroder C, Stevens JS, et al. Post-acute COVID-19 syndrome. *Nat Med* (2021) 27(4):601–15. doi: 10.1038/s41591-021-01283-z
5. Su Y, Yuan D, Chen DG, Ng RH, Wang K, Choi J, et al. Multiple early factors anticipate post-acute COVID-19 sequelae. *Cell* (2022) 185(5):881–95. doi: 10.1016/j.cell.2022.01.014
6. Tuekprakhon A, Nutralai R, Dijokaite-Guraliuc A, Zhou D, Ginn HM, Selvaraj M, et al. Antibody escape of SARS-CoV-2 omicron BA. 4 BA. 5 Vaccine BA. 1 serum. *Cell* (2022) 185(14):2422–33. doi: 10.1016/j.cell.2022.06.005
7. Wang Z, Yang L. Broad-spectrum prodrugs with anti-SARS-CoV-2 activities: Strategies, benefits, and challenges. *J Med Virol* (2022) 94(4):1373–90. doi: 10.1002/jmv.27517
8. Wang Z, Yang L. Chinese Herbal medicine: Fighting SARS-CoV-2 infection on all fronts. *J Ethnopharmacol* (2021) 270:113869. doi: 10.1016/j.jep.2021.113869
9. Riva L, Yuan S, Yin X, Martin-Sancho L, Matsunaga N, Pache L, et al. Discovery of SARS-CoV-2 antiviral drugs through large-scale compound repurposing. *Nature* (2020) 586(7827):113–9. doi: 10.1038/s41586-020-2577-1
10. VanBlargan LA, Errico JM, Halfmann PJ, Zost SJ, Crowe JE, Purcell LA, et al. An infectious SARS-CoV-2 b. 1.1. 529 omicron virus escapes neutralization by therapeutic monoclonal antibodies. *Nat Med* (2022) 28(3):490–5. doi: 10.1038/s41591-021-01678-y
11. Tomalka JA, Suthar MS, Deeks SG, Sekaly RP. Fighting the SARS-CoV-2 pandemic requires a global approach to understanding the heterogeneity of vaccine responses. *Nat Immunol* (2022) 23(3):360–70. doi: 10.1038/s41590-022-01130-4
12. Lo MK, Shrivastava-Ranjan P, Chatterjee P, Flint M, Beadle JR, Valiaeva N, et al. Broad-spectrum *in vitro* antiviral activity of ODBG-P-RVn: An orally-available, lipid-modified monophosphate prodrug of remdesivir parent nucleoside (GS-441524). *Microbiol Spectr.* (2021) 9(3):e01537–21. doi: 10.1128/Spectrum.01537-21
13. Unoh Y, Uehara S, Nakahara K, Nobori H, Yamatsu Y, Yamamoto S, et al. Discovery of s-217622, a noncovalent oral SARS-CoV-2 3CL protease inhibitor clinical candidate for treating COVID-19. *J Med Chem* (2022) 65(9):6499–512. doi: 10.1021/acs.jmedchem.2c00117
14. Sun F, Lin Y, Wang X, Gao Y, Ye S. Paxlovid in patients who are immunocompromised and hospitalised with SARS-CoV-2 infection. *Lancet Infect Dis* (2022) 22(9):1279. doi: 10.1016/S1473-3099(22)00430-3
15. Wang Z, Yang L. In the age of omicron variant: Paxlovid raises new hopes of COVID-19 recovery. *J Med Virol* (2022) 94(5):1766–7. doi: 10.1002/jmv.27540
16. Jayk Bernal A, Gomes da Silva MM, Musungaie DB, Kovalchuk E, Gonzalez A, Delos Reyes V, et al. Molnupiravir for oral treatment of covid-19 in nonhospitalized patients. *New Engl J Med* (2022) 386(6):509–20. doi: 10.1056/NEJMoa2116044
17. Rubin R. From positive to negative to positive again—the mystery of why COVID-19 rebounds in some patients who take paxlovid. *JAMA* (2022) 327(24):2380–2. doi: 10.1001/jama.2022.9925
18. Wang L, Berger NA, Davis PB, Kaelber DC., Volkow ND, Xu R. COVID-19 rebound after paxlovid and molnupiravir during January-June 2022. *medRxiv* (2022). doi: 10.1101/2022.06.21.22276724
19. Burki T. The future of paxlovid for COVID-19. *Lancet Resp Med* (2022) 10(7):e68. doi: 10.1016/S2213-2600(22)00192-8
20. Dal-Ré R, Becker SL, Bottieau E, Holm S. Availability of oral antivirals against SARS-CoV-2 infection and the requirement for an ethical prescribing approach. *Lancet Infect Dis* (2022) 22(8):e231–8. doi: 10.1016/S1473-3099(22)00119-0
21. Zhang X, Horby P, Cao B. COVID-19 can be called a treatable disease only after we have antivirals. *Sci Bull* (2022) 67:999–1002. doi: 10.1016/j.scib.2022.02.011
22. Extance A. Covid-19: What is the evidence for the antiviral molnupiravir? *BMJ* (2022) 377:o926. doi: 10.1136/bmj.o926
23. Bai X, Sun H, Wu S, Li Y, Wang L, Hong B. Identifying small-molecule inhibitors of SARS-CoV-2 RNA-dependent RNA polymerase by establishing a fluorometric assay. *Front Immunol* (2022) 13:844749. doi: 10.3389/fimmu.2022.844749
24. Wang Y, Anirudhan V, Du R, Cui Q, Rong L. RNA-Dependent RNA polymerase of SARS-CoV-2 as a therapeutic target. *J Med Virol* (2021) 93(1):300–10. doi: 10.1002/jmv.26264
25. Wang Z, Yang L, Zhao XE. Co-Crystallization and structure determination: An effective direction for anti-SARS-CoV-2 drug discovery. *Comput Struct Biotec J* (2021) 19:4684–701. doi: 10.1016/j.csbj.2021.08.029
26. Wu Z, Han Z, Liu B, Shen N. Remdesivir in treating hospitalized patients with COVID-19: A renewed review of clinical trials. *Front Pharmacol* (2022) 13:971890. doi: 10.3389/fphar.2022.971890
27. Parums DV. Editorial: Rebound COVID-19 and cessation of antiviral treatment for SARS-CoV-2 with paxlovid and molnupiravir. *Med Sci Monit* (2022) 28:e938532. doi: 10.12659/MSM.938532
28. Cho A, Saunders OL, Butler T, Zhang L, Xu J, Vela JE, et al. Synthesis and antiviral activity of a series of 1'-substituted 4-aza-7,9-dideazaadenosine c-nucleosides. *Bioorg Med Chem Lett* (2012) 22(8):2705–7. doi: 10.1016/j.bmcl.2012.02.105
29. Agostini ML, Andres EL, Sims AC, Graham RL, Sheahan TP, Lu X, et al. Coronavirus susceptibility to the antiviral remdesivir (GS-5734) is mediated by the viral polymerase and the proofreading exoribonuclease. *mBio* (2018) 9(2):e00221–18. doi: 10.1128/mBio.00221-18
30. Murphy BG, Perron M, Murakami E, Bauer K, Park Y, Eckstrand C, et al. The nucleoside analog GS-441524 strongly inhibits feline infectious peritonitis (FIP) virus in tissue culture and experimental cat infection studies. *Vet Microbiol* (2018) 219:226–33. doi: 10.1016/j.vetmic.2018.04.026
31. Wei D, Hu T, Zhang Y, Zheng W, Xue H, Shen J, et al. Potency and pharmacokinetics of GS-441524 derivatives against SARS-CoV-2. *Bioorg Med Chem* (2021) 46:116364. doi: 10.1016/j.bmc.2021.116364
32. Rasmussen HB, Jürgens G, Thomsen R, Taboureau O, Zeth K, Hansen PE, Hansen PR. Cellular uptake and intracellular phosphorylation of GS-441524: Implications for its effectiveness against COVID-19. *Viruses* (2021) 13(7):1369. doi: 10.3390/v13071369
33. Rasmussen HB, Thomsen R, Hansen PR. Nucleoside analog GS-441524: pharmacokinetics in different species, safety, and potential effectiveness against covid-19. *Pharmacol Res Perspe.* (2022) 10(2):e00945. doi: 10.1002/prp2.945
34. Li Y, Cao L, Li G, Cong F, Li Y, Sun J, et al. Remdesivir metabolite GS-441524 effectively inhibits SARS-CoV-2 infection in mouse models. *J Med Chem* (2021) 65(4):2785–93. doi: 10.1021/acs.jmedchem.0c01929
35. Cao L, Li Y, Yang S, Li G, Zhou Q, Sun J, et al. The adenosine analog prodrug ATV006 is orally bioavailable and has preclinical efficacy against parental SARS-CoV-2 and variants. *Sci Transl Med* (2022) 14(661):eabm7621. doi: 10.1126/scitranslmed.abm7621
36. Xie J, Wang Z. Can remdesivir and its parent nucleoside GS-441524 be potential oral drugs? an *in vitro* and *in vivo* DMPK assessment. *Acta Pharm Sin B* (2021) 11(6):1607–16. doi: 10.1016/j.apsb.2021.03.028
37. Wang AQ, Hagen NR, Padilha EC, Yang M, Shah P, Chen CZ, et al. Preclinical pharmacokinetics and *in vitro* properties of GS-441524, a potential oral drug candidate for COVID-19 treatment. *Front Pharmacol* (2022) 13:918083. doi: 10.3389/fphar.2022.918083
38. Yan VC, Pham CD, Yan MJ, Yan AJ, Khadka S, Arthur K, et al. Pharmacokinetics of orally administered GS-441524 in dogs. *bioRxiv* (2021). doi: 10.1101/2021.02.04.429674
39. Choe PG, Jeong SI, Kang CK, Yang L, Lee S, Cho JY, et al. Exploration for the effect of renal function and renal replacement therapy on pharmacokinetics of remdesivir and GS-441524 in patients with COVID-19: A limited case series. *CTS-Clin Transl Sci* (2022) 15(3):732–40. doi: 10.1111/cts.13194
40. Cox RM, Wolf JD, Lieber CM, Sourimant J, Lin MJ, Babusis D, et al. Oral prodrug of remdesivir parent GS-441524 is efficacious against SARS-CoV-2 in ferrets. *Nat Commun* (2021) 12:6415. doi: 10.1038/s41467-021-26760-4
41. Xie Y, Yin W, Zhang Y, Shang W, Wang Z, Luan X, et al. Design and development of an oral remdesivir derivative VV116 against SARS-CoV-2. *Cell Res* (2021) 31(11):1212–4. doi: 10.1038/s41422-021-00570-1
42. Zhang R, Zhang Y, Zheng W, Shang W, Wu Y, Li N, et al. Oral remdesivir derivative VV116 is a potent inhibitor of respiratory syncytial virus with efficacy in mouse model. *Signal Transduct Tar Ther* (2022) 7:123. doi: 10.1038/s41392-022-00963-7
43. Qian HJ, Wang Y, Zhang MQ, Xie YC, Wu QQ, Liang LY, et al. Safety, tolerability, and pharmacokinetics of VV116, an oral nucleoside analog against SARS-CoV-2, in Chinese healthy subjects. *Acta Pharmacol Sin* (2022). doi: 10.1038/s41401-022-00895-6
44. Tempestilli M, Caputi P, Avataneo V, Notari S, Forini O, Scorzolini L, et al. Pharmacokinetics of remdesivir and GS-441524 in two critically ill patients who recovered from COVID-19. *J Antimicrob Chemother* (2020) 75(10):2977–80. doi: 10.1093/jac/dkaa239
45. Krentz D, Zenger K, Alberer M, Felten S, Bergmann M, Dorsch R, et al. Curing cats with feline infectious peritonitis with an oral multi-component drug containing GS-441524. *Viruses* (2021) 13(11):2228. doi: 10.3390/v13112228
46. Mackman RL, Hui HC, Perron M, Murakami E, Palmiotti C, Lee G, et al. Prodrugs of a 1'-CN-4-aza-7, 9-dideazaadenosine c-nucleoside leading to the discovery of remdesivir (GS-5734) as a potent inhibitor of respiratory syncytial

- virus with efficacy in the African green monkey model of RSV. *J Med Chem* (2021) 64(8):5001–17. doi: 10.1021/acs.jmedchem.1c00071
47. Szenté L, Renkecz T, Sirok D, Stáhl J, Hirka G, Puskás I, et al. Comparative bioavailability study following a single dose intravenous and buccal administration of remdesivir in rabbits. *Internat J Pharmaceut* (2022) 620:121739. doi: 10.1016/j.iijpharm.2022.121739
  48. Bai C, Zhong Q, Gao GF. Overview of SARS-CoV-2 genome-encoded proteins. *Sci China Life Sci* (2022) 65:280–94. doi: 10.1007/s11427-021-1964-4
  49. Lou Z, Rao Z. The life of SARS-CoV-2 inside cells: Replication-transcription complex assembly and function. *Annu Rev Biochem* (2022) 91:381–401. doi: 10.1146/annurev-biochem-052521-115653
  50. Yan W, Zheng Y, Zeng X, He B, Cheng W. Structural biology of SARS-CoV-2: Open the door for novel therapies. *Signal Transduct Tar.* (2022) 7:26. doi: 10.1038/s41392-022-00884-5
  51. Duan X, Lacko LA, Chen S. Druggable targets and therapeutic development for COVID-19. *Front Chem* (2022) 10:963701. doi: 10.3389/fchem.2022.963701
  52. Yan L, Zhang Y, Ge J, Zheng L, Gao Y, Wang T, et al. Architecture of a SARS-CoV-2 mini replication and transcription complex. *Nat Commun* (2020) 11:5874. doi: 10.1038/s41467-020-19770-1
  53. Yan L, Ge J, Zheng L, Zhang Y, Gao Y, Wang T, et al. Cryo-EM structure of an extended SARS-CoV-2 replication and transcription complex reveals an intermediate state in cap synthesis. *Cell* (2021) 184(1):184–193.e10. doi: 10.1016/j.cell.2020.11.016
  54. Peng Q, Peng R, Yuan B, Zhao J, Wang M, Wang X, et al. Structural and biochemical characterization of the nsp12-nsp7-nsp8 core polymerase complex from SARS-CoV-2. *Cell Rep* (2020) 31(11):107774. doi: 10.1016/j.celrep.2020.107774
  55. Biswal M, Diggs S, Xu D, Khudaverdyan N, Lu J, Fang J, et al. Two conserved oligomer interfaces of NSP7 and NSP8 underpin the dynamic assembly of SARS-CoV-2 RdRP. *Nucleic Acids Res* (2021) 49(10):5956–66. doi: 10.1093/nar/gkab370
  56. Xu X, Chen Y, Lu X, Zhang W, Fang W, Yuan L, et al. An update on inhibitors targeting RNA-dependent RNA polymerase for COVID-19 treatment: Promises and challenges. *Biochem Pharmacol* (2022) 205:115279. doi: 10.1016/j.bcp.2022.115279
  57. Yin W, Mao C, Luan X, Shen DD, Shen Q, Su H, et al. Structural basis for inhibition of the RNA-dependent RNA polymerase from SARS-CoV-2 by remdesivir. *Science* (2020) 368:1499–504. doi: 10.1126/science.abc1560
  58. Lehmann KC, Gulyaeva A, Zevenhoven-Dobbe JC, Janssen GM, Ruben M, Overkleef HS, et al. Discovery of an essential nucleotidylating activity associated with a newly delineated conserved domain in the RNA polymerase-containing protein of all nidoviruses. *Nucleic Acids Res* (2015) 43:8416–34. doi: 10.1093/nar/gkv838
  59. Gao Y, Yan L, Huang Y, Liu F, Zhao Y, Cao L, et al. Structure of the RNA-dependent RNA polymerase from COVID-19 virus. *Science* (2020) 368:779–82. doi: 10.1126/science.abb7498
  60. Yang H, Rao Z. Structural biology of SARS-CoV-2 and implications for therapeutic development. *Nat Rev Microbiol* (2021) 19:685–700. doi: 10.1038/s41579-021-00630-8
  61. Sumon TA, Hussain MA, Hasan M, Rashid A, Abualreesh MH, Jang WJ, et al. Antiviral peptides from aquatic organisms: Functionality and potential inhibitory effect on SARS-CoV-2. *Aquaculture* (2021) 541:736783. doi: 10.1016/j.aquaculture.2021.736783
  62. Hillen HS, Kokic G, Farnung L, Dienemann C, Tegunov D, Cramer P. Structure of replicating SARS-CoV-2 polymerase. *Nature* (2020) 584:154–6. doi: 10.1038/s41586-020-2368-8
  63. Wang Q, Wu J, Wang H, Gao Y, Liu Q, Mu A, et al. Structural basis for RNA replication by the SARS-CoV-2 polymerase. *Cell* (2020) 182:417–428.e13. doi: 10.1016/j.cell.2020.05.034
  64. Shannon A, Fattorini V, Sama B, Selisko B, Feracci M, Falcou C, et al. Protein-primed RNA synthesis in SARS-CoVs and structural basis for inhibition by AT-527. *bioRxiv* (2021). doi: 10.1101/2021.03.23.436564
  65. Khoo SH, FitzGerald R, Saunders G, Middleton C, Ahmad S, Edwards CJ, et al. Molnupiravir versus placebo in unvaccinated and vaccinated patients with early SARS-CoV-2 infection in the UK (AGILE CST-2): A randomised, placebo-controlled, double-blind, phase 2 trial. *Lancet Infect Dis* (2022). doi: 10.1016/s1473-3099(22)00644-2
  66. Yan L, Huang Y, Ge J, Liu Z, Lu P, Huang B, et al. A mechanism for SARS-CoV-2 RNA capping and its inhibition by nucleotide analogue inhibitors. *Cell* (2022) 185(23):4347–60.e17. doi: 10.1016/j.cell.2022.09.037
  67. Parienti JJ, Prazuck T, Peyro-Saint-Paul L, Fournier A, Valentin C, Brucato S, et al. Effect of tenofovir disoproxil fumarate and emtricitabine on nasopharyngeal SARS-CoV-2 viral load burden amongst outpatients with COVID-19: A pilot, randomized, open-label phase 2 trial. *EclinicalMedicine* (2021) 38:100993. doi: 10.1016/j.eclinm.2021.100993
  68. Chiba S, Kiso M, Nakajima N, Iida S, Maemura T, Kuroda M, et al. Co-Administration of favipiravir and the remdesivir metabolite GS-441524 effectively reduces SARS-CoV-2 replication in the lungs of the syrian hamster model. *oBio* (2022) 13(1):e03044–21. doi: 10.1128/mbio.03044-21
  69. Rabie AM. Cyanorona-20: The first potent SARS-CoV-2 agent. *Int Immunopharmacol.* (2021) 98:107831. doi: 10.1016/j.intimp.2021.107831
  70. Li J, Liu S, Shi J, Zhu HJ. Activation of tenofovir alafenamide and sofosbuvir in the human lung and its implications in the development of nucleoside/nucleotide prodrugs for treating SARS-CoV-2 pulmonary infection. *Pharmaceutics* (2021) 13(10):1656. doi: 10.3390/pharmaceutics13101656
  71. Madariaga-Mazón A, Naveja JJ, Becerra A, Campillo-Balderas JA, Hernández-Morales R, Jácome R, et al. Subtle structural differences of nucleotide analogs may impact SARS-CoV-2 RNA-dependent RNA polymerase and exoribonuclease activity. *Comput Struct Biotech J* (2022) 20:5181–92. doi: 10.1016/j.csbj.2022.08.056
  72. Gérard AO, Laurain A, Fresse A, Parassol N, Muzzzone M, Rocher F, et al. Remdesivir and acute renal failure: A potential safety signal from disproportionality analysis of the WHO safety database. *Clin Pharmacol Ther* (2021) 109:1021–4. doi: 10.1002/cpt.2145
  73. Wong CKH, Au ICH, Cheng WY, Man KK, Lau KT, Mak LY, et al. Remdesivir use and risks of acute kidney injury and acute liver injury among patients hospitalised with COVID-19: A self-controlled case series study. *Aliment Pharm Ther* (2022) 56:121–30. doi: 10.1111/apt.16894
  74. Merches K, Breunig L, Fender J, Brand T, Bätz V, Idel S, et al. The potential of remdesivir to affect function, metabolism and proliferation of cardiac and kidney cells. *vitro. Arch Toxicol* (2022) 96:2341–60. doi: 10.1007/s00204-022-03306-1
  75. Rafaniello C, Ferrajolo C, Sullo MG, Gaio M, Zinzi A, Scavone C, et al. Cardiac events potentially associated to remdesivir: An analysis from the european spontaneous adverse event reporting system. *Pharmaceutics* (2021) 14:611. doi: 10.3390/ph14070611
  76. Nabati M, Parsaee H. Potential cardiotoxic effects of remdesivir on cardiovascular system: A literature review. *Cardiovasc Toxicol* (2022) 22:268. doi: 10.1007/s12012-021-09703-9
  77. Zhou S, Hill CS, Sarkar S, Tse LV, Woodburn BM, Schinazi RF, et al.  $\beta$ -d-N4-hydroxycytidine inhibits SARS-CoV-2 through lethal mutagenesis but is also mutagenic to mammalian cells. *J Infect Dis* (2021) 224:415–9. doi: 10.1093/infdis/jiab247
  78. Hashemian SMR, Pourhanifeh MH, Hamblin MR, Shahrzad MK, Mirzaei H. RdRp inhibitors and COVID-19: Is molnupiravir a good option? *BioMed Pharmacother.* (2022) 146:112517. doi: 10.1016/j.biopha.2021.112517
  79. World Health Organization. *Therapeutics and COVID-19: Living guideline* (2022). Available at: <https://www.who.int/publications/i/item/WHO-2019-nCoV-therapeutics-2022.4> (Accessed October 22, 2022).
  80. Zhong W, Jiang X, Yang X, Feng T, Duan Z, Wang W, et al. The efficacy of paxlovid in elderly patients infected with SARS-CoV-2 omicron variants: Results of a non-randomized clinical trial. *Front Med* (2022) 9:980002. doi: 10.3389/fmed.2022.980002
  81. Malden DE, Hong V, Lewin BJ, Ackerson BK, Lipsitch M, Lewnard JA, et al. Hospitalization and emergency department encounters for COVID-19 after paxlovid treatment-California, December 2021–may 2022. *MMWR-Morbid Mortal W.* (2022) 71(25):830–3. doi: 10.15585/mmwr.mm7125e2
  82. Najjar-Debbiny R, Gronich N, Weber G, Khoury J, Amar M, Stein N, et al. Effectiveness of paxlovid in reducing severe COVID-19 and mortality in high risk patients. *Clin Infect Dis* (2022), ciac443. doi: 10.1093/cid/ciac443
  83. Charness M, Gupta K, Stack G, Strymish J, Adams E, Lindy D, et al. Rapid relapse of symptomatic omicron SARS-CoV-2 infection following early suppression with nirmatrelvir/ritonavir. *Res Square.* (2022). doi: 10.21203/rs.3.rs-1588371/v3
  84. Williamson BN, Feldmann F, Schwarz B, Meade-White K, Porter DP, Schulz J, et al. Clinical benefit of remdesivir in rhesus macaques infected with SARS-CoV-2. *Nature* (2020) 585(7824):273–6. doi: 10.1038/s41586-020-2423-5
  85. Wang Z, Yang L. GS-5734: A potentially approved drug by FDA against SARS-CoV-2. *N J Chem* (2020) 44(29):12417–29. doi: 10.1039/D0NJ02656E
  86. Holshue ML, DeBolt C, Lindquist S, Lofy KH, Wiesman J, Bruce H, et al. First case of 2019 novel coronavirus in the united states. *N Engl J Med* (2020) 382:929–36. doi: 10.1056/NEJMoa2001191
  87. Wang M, Zhang L, Huo X, Zhang Z, Yuan Q, Li P, et al. Catalytic asymmetric synthesis of the anti-COVID-19 drug remdesivir. *Angew Chem Int Ed* (2020) 59:20814–9. doi: 10.1002/anie.202011527
  88. Boglione L, Dodaro V, Meli G, Rostagno R, Poletti F, Moglia R, et al. Remdesivir treatment in hospitalized patients affected by COVID-19 pneumonia: a case-control study. *J Med Virol* (2022) 94(8):3653–60. doi: 10.1002/jmv.27768

89. Gottlieb RL, Vaca CE, Paredes R, Mera J, Webb BJ, Perez G, et al. Early remdesivir to prevent progression to severe covid-19 in outpatients. *N Engl J Med* (2022) 386(4):305–15. doi: 10.1056/NEJMoa2116846
90. Grein J, Ohmagari N, Shin D, Diaz G, Asperges E, Castagna A, et al. Compassionate use of remdesivir for patients with severe covid-19. *N Engl J Med* (2020) 382(24):2327–36. doi: 10.1056/NEJMoa2007016
91. Solidarity Trial Consortium WHO. Repurposed antiviral drugs for Covid-19—interim WHO solidarity trial results. *N Engl J Med* (2021) 384(6):497–511. doi: 10.1056/NEJMoa2023184
92. Ader F, Bouscambert-Duchamp M, Hites M, Peiffer-Smadja N, Poissy J, Belhadi D, et al. Remdesivir plus standard of care versus standard of care alone for the treatment of patients admitted to hospital with COVID-19 (DisCoVeRy): A phase 3, randomised, controlled, open-label trial. *Lancet Infect Dis* (2022) 22(2):209–21. doi: 10.1016/S1473-3099(21)00485-0
93. Solidarity Trial Consortium. Remdesivir WHO. And three other drugs for hospitalised patients with COVID-19: Final results of the WHO solidarity randomised trial and updated meta-analyses. *Lancet* (2022) 399(10339):1941–53. doi: 10.1016/S0140-6736(22)00519-0
94. Wang Y, Zhang D, Du G, Du R, Zhao J, Jin Y, et al. Remdesivir in adults with severe COVID-19: A randomised, double-blind, placebo-controlled, multicentre trial. *Lancet* (2020) 395(10236):1569–78. doi: 10.1016/S0140-6736(20)31022-9
95. Cihlar T, Mackman RL. Journey of remdesivir from the inhibition of hepatitis C virus to the treatment of COVID-19. *Antivir Ther* (2022). doi: 10.1177/13596535221082773
96. Yan VC, Muller FL. Why remdesivir failed: Preclinical assumptions overestimate the clinical efficacy of remdesivir for COVID-19 and ebola. *Antimicrob Agents Ch.* (2021) 65(10):e01117–21. doi: 10.1128/AAC.01117-21
97. Yan VC, Muller FL. Single-cell RNA sequencing supports preferential bioactivation of remdesivir in the liver. *Antimicrob Agents Ch.* (2021) 65(10):e01333–21. doi: 10.1128/AAC.01333-21
98. Zhang F, Li HX, Zhang TT, Xiong Y, Wang HN, Lu ZH, et al. Human carboxylesterase 1A plays a predominant role in the hydrolytic activation of remdesivir in humans. *Chem-Bio Interact* (2022) 351:109744. doi: 10.1016/j.cbi.2021.109744
99. Humeniuk R, Mathias A, Cao H, Osinusi A, Shen G, Chng E, et al. Safety, tolerability, and pharmacokinetics of remdesivir, an antiviral for treatment of COVID-19, in healthy subjects. *Clin Transl Sci* (2020) 13:896–906. doi: 10.1111/cts.12840
100. Hua S. Advances in nanoparticulate drug delivery approaches for sublingual and buccal administration. *Front Pharmacol* (2019) 10:1328. doi: 10.3389/fphar.2019.01328
101. Chiu W, Verschuereen L, Van den Eynde C, Buyck C, De Meyer S, Jochmans D, et al. Development and optimization of a high-throughput screening assay for *in vitro* anti-SARS-CoV-2 activity: Evaluation of 5676 phase 1 passed structures. *J Med Virol* (2022) 94(7):3101–11. doi: 10.1002/jmv.27683
102. Montastruc F, Thuriot S, Durrieu G. Hepatic disorders with the use of remdesivir for coronavirus 2019. *Clin Gastroenterol H.* (2020) 18(12):2835–6. doi: 10.1016/j.cgh.2020.07.050
103. Marikawa Y, Alarcon VB. Remdesivir impairs mouse preimplantation embryo development at therapeutic concentrations. *Reprod Toxicol* (2022) 111:135–47. doi: 10.1016/j.reprotox.2022.05.012
104. Ferner RE, Aronson JK. Remdesivir in covid-19. *BMJ* (2020) 369:m1610. doi: 10.1136/bmj.m1610
105. Emadi MS, Soltani S, Noori B, Zandi M, Shateri Z, Tabibzadeh A, et al. Highly conserve sequences in envelope, nucleoprotein and RNA-dependent RNA polymerase of SARS-CoV-2 in nasopharyngeal samples of the COVID-19 patients; a diagnostic target for further studies. *J Cell Mol Anesth* (2022) 7(2):78–83. doi: 10.22037/jcma.v7i2.36963
106. Yang L, Lin IH, Lin LC, Dalley JW, Tsai TH. Biotransformation and transplacental transfer of the anti-viral remdesivir and predominant metabolite, GS-441524 in pregnant rats. *eBioMedicine* (2022) 81:104095. doi: 10.1016/j.ebiom.2022.104095
107. Wang Z, Yang L. Turning the tide: Natural products and natural-product-inspired chemicals as potential counters to SARS-CoV-2 infection. *Front Pharmacol* (2020) 11:1013. doi: 10.3389/fphar.2020.01013
108. Mullard A. FDA Approves first deuterated drug. *Nat Rev Drug Discovery* (2017) 16(5):305–6. doi: 10.1038/nrd.2017.89
109. Kopf S, Bourriquen F, Li W, Neumann H, Junge K, Beller M. Recent developments for the deuterium and tritium labeling of organic molecules. *Chem Rev* (2022) 122(6):6634–718. doi: 10.1021/acs.chemrev.1c00795
110. Blum E, Zhang J, Zaluski J, Einstein DE, Korshin EE, Kubas A, et al. Rational alteration of pharmacokinetics of chiral fluorinated and deuterated derivatives of emixustat for retinal therapy. *J Med Chem* (2021) 64(12):8287–302. doi: 10.1021/acs.jmedchem.1c00279
111. Gajula SNR, Nadimpalli N, Sonti R. Drug metabolic stability in early drug discovery to develop potential lead compounds. *Drug Metab Rev* (2021) 53(3):459–77. doi: 10.1080/03602532.2021.1970178
112. Pirali T, Serafini M, Cargnin S, Genazzani AA. Applications of deuterium in medicinal chemistry. *J Med Chem* (2019) 62(11):5276–97. doi: 10.1021/acs.jmedchem.8b01808
113. Wang Z, Wang N, Yang L, Song XQ. Bioactive natural products in COVID-19 therapy. *Front Pharmacol* (2022) 13:926507. doi: 10.3389/fphar.2022.926507
114. Shen Y, Ai J, Lin N, Zhang H, Li Y, Wang H, et al. An open, prospective cohort study of VV116 in Chinese participants infected with SARS-CoV-2 omicron variants. *Emerg Microbes Infect* (2022) 11(1):1518–23. doi: 10.1080/22221751.2022.2078230
115. Humeniuk R, Mathias A, Kirby BJ, Lutz JD, Cao H, Osinusi A, et al. Pharmacokinetic, pharmacodynamic, and drug-interaction profile of remdesivir, a SARS-CoV-2 replication inhibitor. *Clin Pharmacokinet* (2021) 60(5):569–83. doi: 10.1007/s40262-021-00984-5
116. Pharmaceuticals and medical devices agency. Tokyo: *Pharmaceuticals and medical devices agency; c2022. Gilead sciences. section 2.6.4 pharmacokinetics written summary of remdesivir common technical document* (2020). Available at: [https://www.pmda.go.jp/drugs/2020/P20200518003/230867000\\_30200AMX00455\\_1100\\_1.pdf](https://www.pmda.go.jp/drugs/2020/P20200518003/230867000_30200AMX00455_1100_1.pdf) (Accessed 8 Aug 2022).
117. Stevens LJ, Pruijssers AJ, Lee HW, Gordon CJ, Tchesnokov EP, Gribble J, et al. Mutations in the SARS-CoV-2 RNA dependent RNA polymerase confer resistance to remdesivir by distinct mechanisms. *Sci Transl Med* (2022) 14(656):eabo0718. doi: 10.1126/scitranslmed.abo0718
118. Wang Z, Yang L. Post-acute sequelae of SARS-CoV-2 infection: A neglected public health issue. *Front Public Health* (2022) 10:908757. doi: 10.3389/fpubh.2022.908757
119. Schäfer A, Martinez DR, Won JJ, Meganck RM, Moreira FR, Brown AJ, et al. Therapeutic treatment with an oral prodrug of the remdesivir parental nucleoside is protective against SARS-CoV-2 pathogenesis in mice. *Sci Transl Med* (2022) 14(643):eabm3410. doi: 10.1126/scitranslmed.abm3410
120. Zheng W, Hu T, Zhang Y, Wei D, Xie Y, Shen J. Synthesis and anti-SARS-CoV-2 activity of deuterated GS-441524 analogs. *Tetrahedron Lett* (2022) 104:154012. doi: 10.1016/j.tetlet.2022.154012
121. Yang L, Wang Z. Natural products, alone or in combination with FDA-approved drugs, to treat COVID-19 and lung cancer. *Biomedicines* (2021) 9:689. doi: 10.3390/biomedicines9060689
122. Lamb YN. Nirmatrelvir plus ritonavir: First approval. *Drugs* (2022) 82:585–91. doi: 10.1007/s40265-022-01692-5
123. Wahl A, Gralinski LE, Johnson CE, Yao W, Kovarova M, Dinno KH, et al. SARS-CoV-2 infection is effectively treated and prevented by EIDD-2801. *Nature* (2021) 591(7850):451–7. doi: 10.1038/s41586-021-03312-w
124. Drayman N, DeMarco JK, Jones KA, Azizi SA, Froggatt HM, Tan K, et al. Masitinib is a broad coronavirus 3CL inhibitor that blocks replication of SARS-CoV-2. *Science* (2021) 373(6557):931–6. doi: 10.1126/science.abg5827
125. Shannon A, Fattorini V, Sama B, Selisko B, Feracci M, Falcou C, et al. A dual mechanism of action of AT-527 against SARS-CoV-2 polymerase. *Nat Commun* (2022) 13:621. doi: 10.1038/s41467-022-28113-1





## OPEN ACCESS

## EDITED BY

Alfonso J. Rodriguez-Morales,  
Fundacion Universitaria Autónoma de  
las Américas, Colombia

## REVIEWED BY

Zhonglei Wang,  
Qufu Normal University, China  
Trina Ekawati Tallei,  
Sam Ratulangi University, Indonesia

## \*CORRESPONDENCE

Hongwei Gao  
✉ gaohongw369@ldu.edu.cn

## SPECIALTY SECTION

This article was submitted to  
Viral Immunology,  
a section of the journal  
Frontiers in Immunology

RECEIVED 09 August 2022

ACCEPTED 05 December 2022

PUBLISHED 23 December 2022

## CITATION

Wang Z, Zhan J and Gao H (2022)  
Computer-aided drug design  
combined network pharmacology to  
explore anti-SARS-CoV-2 or anti-  
inflammatory targets and mechanisms  
of Qingfei Paidu Decoction for  
COVID-19.  
*Front. Immunol.* 13:1015271.  
doi: 10.3389/fimmu.2022.1015271

## COPYRIGHT

© 2022 Wang, Zhan and Gao. This is an  
open-access article distributed under  
the terms of the [Creative Commons  
Attribution License \(CC BY\)](#). The use,  
distribution or reproduction in other  
forums is permitted, provided the  
original author(s) and the copyright  
owner(s) are credited and that the  
original publication in this journal is  
cited, in accordance with accepted  
academic practice. No use,  
distribution or reproduction is  
permitted which does not comply with  
these terms.

# Computer-aided drug design combined network pharmacology to explore anti- SARS-CoV-2 or anti- inflammatory targets and mechanisms of Qingfei Paidu Decoction for COVID-19

Zixuan Wang, Jiuyu Zhan and Hongwei Gao\*

School of Life Science, Ludong University, Yantai, Shandong, China

**Introduction:** Coronavirus Disease-2019 (COVID-19) is an infectious disease caused by SARS-CoV-2. Severe cases of COVID-19 are characterized by an intense inflammatory process that may ultimately lead to organ failure and patient death. Qingfei Paidu Decoction (QFPD), a traditional Chinese medicine (TCM) formula, is widely used in China as anti-SARS-CoV-2 and anti-inflammatory. However, the potential targets and mechanisms for QFPD to exert anti-SARS-CoV-2 or anti-inflammatory effects remain unclear.

**Methods:** In this study, Computer-Aided Drug Design was performed to identify the antiviral or anti-inflammatory components in QFPD and their targets using Discovery Studio 2020 software. We then investigated the mechanisms associated with QFPD for treating COVID-19 with the help of multiple network pharmacology approaches.

**Results and discussion:** By overlapping the targets of QFPD and COVID-19, we discovered 8 common targets (RBP4, IL1RN, TTR, FYN, SFTPD, TP53, SRPK1, and AKT1) of 62 active components in QFPD. These may represent potential targets for QFPD to exert anti-SARS-CoV-2 or anti-inflammatory effects. The result showed that QFPD might have therapeutic effects on COVID-19 by regulating viral infection, immune and inflammation-related pathways. Our work will promote the development of new drugs for COVID-19.

## KEYWORDS

COVID-19, herb, target, active component, anti-inflammatory, anti-SARS-CoV-2

# 1 Introduction

The pandemic of Coronavirus Disease-2019 (COVID-19) has posed an unprecedented crisis to global public health (1–3). The main symptoms of COVID-19 infection are fever, coughing, shortness of breathing and also death (4). Traditional Chinese medicine (TCM) formulas was widely used in China against COVID-19, especially in 2020, in the absence of specific drugs and vaccines (5–7). Based on the current clinical investigation, the treatment of inflammatory storms has been proposed as a critical part of rescuing severe COVID-19 (8–11). Qingfei Paidu Decoction (QFPD) has become one of the most used compounds due to its potential role in the treatment of COVID-19 (12–14). QFPD is composed of 20 herbs (15), namely *Agaric* (Zhuling), *Oriental waterplantain tuber* (Zexie), *Largehead atractylodes rhizome* (Baizhu), *Cassia twig* (Guizhi), *Chinese ephedra herb* (Mahuang), *Semen armeniacae amarum* (Xingren), *Poria cocos* (Fuling), *Chinese thorowax root* (Chaihu), *Baikang skullcap root* (Huangqin), *Pinellinae rhizoma praeparatum* (Jiangbanxia), *Common ginger rhizome* (Shengjiang), *Tatarian aster root and rhizomes* (Ziwan), *Common coltsfoot flower* (Kuandonghua), *Blackberrylily rhizome* (Shegan), *Manchurian wildginger herb* (Xixin), *Common yam rhizome* (Shanyao), *Immature bitter orange* (Zhishi), *Wrinkled gianthysop herb* (Huoxiang), *Dried tangerine peel* (Chenpi), and *Baked radix glycyrrhizae* (Zhigancao). The combination of these herbs is used to reduce mortality and improve cure rates in patients with COVID-19 (16).

Computer-Aided Drug Design (CADD) is a method for developing lead compounds by theoretical calculation, simulation, and prediction of the relationship between drugs and receptors (17). Network pharmacology is a powerful tool to reflect the pharmacological effects and mechanisms of TCM (18–20). The concept of holism for TCM has much in common with the major points of network pharmacology, in which the general “one target, one drug” mode is shifted to a new “multi-target, multi-component” mode (21). The research method of CADD combined with network pharmacology can be used to reveal the mystery of the “multi-target, multi-component and multi-path” of TCM formulas. This method greatly improves the success rate of drug research and saves the cost of drug development.

QFPD has the potential therapeutic effects for COVID-19 intervention in China, but how to take advantage of its anti-SARS-CoV-2 and anti-inflammatory effects deserves further exploration. Therefore, we aim to screen the antiviral or anti-inflammatory components in QFPD and their targets using Discovery Studio 2020 (DS2020) software. We compared the targets regulated by the active components in QFPD with the COVID-19 targets recorded in the Genecards database (<https://www.genecards.org>) and obtained their common targets. With the help of network pharmacology, we investigated how QFPD regulates the body from various aspects through multiple targets and multiple pathways. The results provided some vital

information for the precise clinical medication and improved the therapeutic ability of TCM for COVID-19.

## 2 Experimental section

### 2.1 Screening the active components in QFPD from the database

Most active components of 20 herbs in QFPD were collected through the Traditional Chinese Medicines Database (TCMdb). It was a new tool with 23033 active components to support the modernization of TCM (22–24). In addition, the Traditional Chinese Medicine Systems Pharmacology Database (TCMSP database; <http://tcmssp.com/tcmssp.php>) was used to supplement active components. The TCMSP database integrated active components, relevant diseases, targets, and pharmacokinetic data of drugs, providing a new platform for studying the mechanism of drug action systematically (25). Only components with antiviral or anti-inflammatory effects were retained for later studies.

### 2.2 Ligand preparation and the prediction of absorption, distribution, metabolism, excretion, and toxicity properties

The Prepare Ligands protocol helped to prepare ligands for input components, performing tasks such as removing duplicates, enumerating isomers and tautomers. This study performed the following steps to complete this operation: changing ionization, generating tautomers, generating isomers, and fixing bad valencies. Then, the ligands of active components needed to be minimized in batches by Minimize Ligands protocol before ADMET properties' prediction. ADMET refers to the Absorption, Distribution, Metabolism, Excretion, and Toxicity properties of a molecule within an organism (26, 27). The ADMET properties predicted in this study were hepatotoxicity, Blood-brain barrier penetration (BBB) and Human intestinal absorption (HIA) (28, 29). Optimizing these two properties during early drug discovery was crucial for reducing ADMET problems later in development.

### 2.3 The prediction of toxicological properties and druggability screening

Toxicity Prediction by Komputer Assisted Technology (TOPKAT) accurately and rapidly assessed the toxicity of chemicals based solely on their 2D molecular structure. It could assess the toxicological properties of candidate active components with a range of robust, cross-validated, and Quantitative Structure-Toxicity Relationship (QSTR) models (30). The toxicological properties we predicted in this study were the Ames test, Rodent Carcinogenicity, Aerobic Biodegradability,



and oral LD50 in rats. After the predicted results were obtained, all active components that exceed these four properties' optimal prediction space (OPS) needed to be deleted manually. In order to exclude active components with poor absorption, permeation, and oral bioavailability, it was necessary to ensure that the screened active components comply with Lipinski's rule of five (31) and Veber's rules (32, 33). The active components that did not meet these rules will be automatically deleted at the end of the calculation. The reserved active components had better pharmacokinetic properties and higher bioavailability in the metabolism of organisms.

## 2.4 Performing reverse finding target

The technique of reverse finding target was the core of this study. Reverse finding target process was to match the pharmacophore models with active components which had high credibility after a series of screening. In addition, the matching degree of pharmacophore models and active components can be distinguished by different colors in the "Heat map of Ligand profiler". Generally, the higher the matching between the pharmacophore models and the active components, the higher the confidence of the targets corresponding to the pharmacophore models. Based on these pharmacophore models, we can identify the target proteins regulated by the active components of QFPD. We then used the search function in the Protein Data Bank (PDB) database to convert the target protein names to standard gene names. COVID-19 targets recorded in the Genecards database and QFPD targets regulated by active ingredients in QFPD were compared to get common targets. These common targets represented potential targets for QFPD to exert anti-SARS-CoV-2 or anti-inflammatory effects.

## 2.5 Construction of protein-protein interaction network

The interaction between the targets was illustrated as a PPI network. The construction of the PPI network was realized *via* the Search Tool for the Retrieval of Interacting Genes (STRING; <https://string-db.org/>). It gathered a large number of information resources, mainly for storing PPI data identified by experiments, calculating predicted data, and collecting public text (34).

## 2.6 Construction of "herb-active component-target" interaction network diagram

The "herb-active component-target" interaction network was plotted by the major constituents of QFPD and their

targets using Cytoscape 3.8.0. The network constructed by this information was represented as nodes and edges with related data attributes, which revealed the close relationship between diseases, targets, and drugs, and provided ideas for further study of multi-target and multi-component TCM formula.

## 2.7 Pathway analysis of QFPD

Gene set enrichment analysis (GSEA) was performed on transcriptome sequencing data of COVID-19 from Gene Expression Omnibus (GEO) database using GSEA 4.1.0. The COVID-19 group consisted of 30 samples, which were organized into gene expression matrix. Based on the expression of the target, they were divided into target high expression and low expression groups for GSEA analysis.

The potential targets of QFPD were submitted to DAVID (<https://david.ncifcrf.gov/>) to analyze Gene Ontology (GO) function enrichment and Kyoto Encyclopedia of Genes and Genomes (KEGG) pathway enrichment. GO analysis was involved in terms of cellular component (CC), molecular function (MF), as well as biological process (BP) (35). CC was defined as the active sites of gene products in cells. MF was considered as the biochemical activity. BP involved the contribution of genes or genetic products to biological objectives. KEGG was a highly integrated database for biological interpretation of wholly sequenced genomes through pathway mapping (36).

## 3 Results and discussion

### 3.1 Screening the active components in QFPD from the database

A total of 108 active components in QFPD were selected from TCMdb and TCMSP database based on the above criteria about antiviral or anti-inflammatory effects. The basic information of 108 active components was showed in Table 1.

### 3.2 Ligand preparation and prediction of ADMET properties

Prepare Ligands and Minimize Ligands protocols in DS2020 were used to prepare and minimize the structures of 108 active components, respectively. The results showed that 107 tautomers were produced during the preparation process, so the number of active components reached 215. After minimization, the number of active components remained unchanged. Favorable ADMET properties can be considered as essential nature for a candidate drug. As shown in Figure 1, the green ellipse represents 99% of the absorption confidence interval, and the blue ellipse represents 99%

TABLE 1 Active components in QFPD.

Herb	Active components	Effect	References
Huangqin	Isoscutellarein	antiviral	(37, 38)
	Baicalein	anti-inflammatory	
	Baicalin	anti-inflammatory	
	Eriodictyol	anti-inflammatory	
	Oroxylin A	anti-inflammatory	
	beta-Sitosterol	anti-inflammatory	
	Wogonin	anti-inflammatory	
	Wogonoside	anti-inflammatory	
	Chrysin	anti-inflammatory, antiviral	
Jiangbanxia	beta-Sitosterol	anti-inflammatory	(39)
Kuandonghua	Gallic acid	anti-inflammatory	(40–42)
	Hyperin	anti-inflammatory	
	Rutin	anti-inflammatory, antiviral	
Shegan	Tectoridin	anti-inflammatory	(43, 44)
	Tectorigenin	anti-inflammatory	
	Mangiferin	anti-inflammatory, antiviral	
Xixin	Sesamin	antiviral	(45–47)
	Aristolochic acid	antiviral	
	(+)-Eudesma-4(15),7(11)-dien-8-one	anti-inflammatory	
	Terpinen-4-ol	anti-inflammatory	
Shanyao	beta-Sitosterol	anti-inflammatory	(39)
Zhishi	Tangeretin	antiviral	(48, 49)
	5,7,4'-Trimethoxyflavone	antiviral	
	Hesperidin	antiviral	
	Apigenin-7-O-neohesperidoside	antiviral	
	Lonicerin	anti-inflammatory	
	Naringin	anti-inflammatory, antiviral	
Chenpi	Hesperidin	antiviral	(49, 50)
	Naringin	anti-inflammatory, antiviral	
Huoxiang	Linalool	antiviral	(51–53)
	Pachypodol	antiviral	
	Acacetin	anti-inflammatory	
	Friedelan-3-one	anti-inflammatory	
	beta-Pinene	anti-inflammatory	
(Continued)			

TABLE 1 Continued

Herb	Active components	Effect	References
	beta-Sitosterol	anti-inflammatory	(54, 55)
	Cinnamaldehyde	anti-inflammatory	
Mahuang	Kaempferol	antiviral	
	(4S,5R) Ephedroxane	anti-inflammatory	
	Isoquercitrin	anti-inflammatory	
	N-Methylephedrine	anti-inflammatory	(45, 51, 56)
Shengjiang	Linalool	antiviral	
	6-Dehydrogingerdione	anti-inflammatory	
	10-Dehydrogingerdione	anti-inflammatory	
	Geraniol	anti-inflammatory	
	D-Isoborneol	anti-inflammatory	
	L-Isoborneol	anti-inflammatory	
	Terpinen-4-ol	anti-inflammatory	(51, 57)
Xingren	Linalool	antiviral	
	Dihydroquercetin	anti-inflammatory	
	Eriodictyol	anti-inflammatory	(58, 59)
Ziwan	Quercetin	antiviral	
	Friedelan-3-one	anti-inflammatory	
	Anethole	anti-inflammatory	(60)
Baizhu	Atractylenolide I	anti-inflammatory	
	Atractylone	anti-inflammatory	
	(+)-Eudesma-4(15),7(11)-dien-8-one	anti-inflammatory	(61, 62)
Fuling	Dihydroquercetin	anti-inflammatory	
	Astilbin	anti-inflammatory, antiviral	(39, 63)
Guizhi	2-Methoxycinnamaldehyde	anti-inflammatory	
	beta-Sitosterol	anti-inflammatory	
	Cinnamaldehyde	anti-inflammatory, antiviral	(64)
Zhuling	MAN	anti-inflammatory, antiviral	
	GLA	anti-inflammatory, antiviral	(65–67)
Zexie	Emodin	anti-inflammatory, antiviral	
	HMF	anti-inflammatory, antiviral	
	alpha-D-fructofuranose	anti-inflammatory, antiviral	
	EA-fructofuranoside		

(Continued)

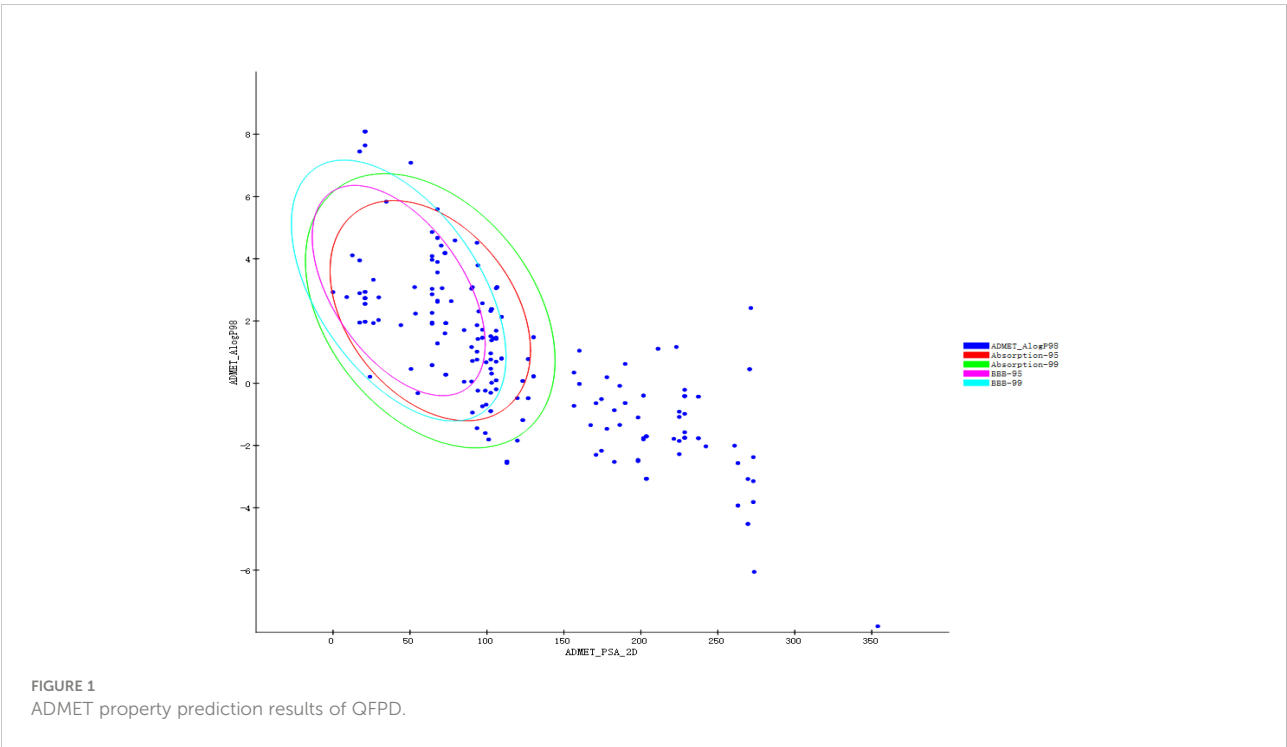
TABLE 1 Continued

Herb	Active components	Effect	References
		anti-inflammatory, antiviral	
	stachyose	anti-inflammatory, antiviral	
	NCA	anti-inflammatory, antiviral	
	1-Monolinolein	anti-inflammatory, antiviral	
	stearic acid	anti-inflammatory, antiviral	
	orientalolf	anti-inflammatory, antiviral	
	Sulfoorientalol C	anti-inflammatory, antiviral	
	raffinose	anti-inflammatory, antiviral	
	(2R,3S,4S,5R)-2-ethoxy-2,5-bis(hydroxymethyl)oxolane-3,4-diol	anti-inflammatory, antiviral	
Zhigancao	3,3'-Dimethylquercetin	antiviral	(11, 39, 41, 68–70)
	Glycycoumarin	antiviral	
	Glepidotin D	antiviral	
	Glycyrrhisoflavone	antiviral	
	Glycyrrhizic acid	antiviral	
	Isolicoflavonol	antiviral	
	Licopyranocoumarin	antiviral	
	6,8-Bis(C-beta-glucosyl)-apigenin	anti-inflammatory	
	Isoliquiritin	anti-inflammatory	
	Isoquercitrin	anti-inflammatory	
	Liquiritic acid	anti-inflammatory	
	Pinocembrin	anti-inflammatory	
	beta-Sitosterol	anti-inflammatory	
	Glycyrrhetic acid	anti-inflammatory	
	Licochalcone A	anti-inflammatory, antiviral	
	Glycyrrhizic acid	anti-inflammatory, antiviral	
	Rutin	anti-inflammatory, antiviral	
Chaihu	Linalool	antiviral	(51, 56, 71–73)
	Saikosaponin C	antiviral	
	Geraniol	anti-inflammatory	
	Isoquercitrin	anti-inflammatory	
(Continued)			

TABLE 1 Continued

Herb	Active components	Effect	References
	Kaempferitrin	anti-inflammatory	
	Oroxylin A	anti-inflammatory	
	Propapyriogenin A2	anti-inflammatory	
	Pulegone	anti-inflammatory	
	Saikosaponin B2	anti-inflammatory	
	Scoparone	anti-inflammatory	
	alpha-Spinasterol	anti-inflammatory	
	Wogonin	anti-inflammatory	
	Saikosaponin D	anti-inflammatory, antiviral	
	Saikosaponin A	anti-inflammatory, antiviral	
	(E)-3-(3,4-Dimethoxyphenyl)-2-propen-1-yl (Z)-2-[(Z)-2-methyl-2-butenoyloxymethyl] butenoate	anti-inflammatory	
	1-(3,4,5-Trimethoxyphenyl)-2-propenyl 2-(2-methyl-2Z-butenoyloxymethyl)-2Z-butenolate	anti-inflammatory	

of the BBB confidence interval. In general, the absorption outside the 99% ellipse tends to drop relatively quickly. If the active component is outside the 99% confidence interval of the BBB model, the prediction of the molecule is considered unreliable. In order to reduce the risk of late-stage attrition, we excluded active components outside the 99% confidence interval of the BBB model and HIA model. In this process, all the active components from the 5 herbs (Jiangbanxia, Chenpi, Fuling, Shanyao, Zhuling) were excluded. In the end, only 97 compounds from 15 herbs were left.





### 3.3 TOPKAT and druggability screening

We checked whether the 97 active components were in the OPS of four toxicological properties (Ames test, Rodent Carcinogenicity, Aerobic Biodegradability, and oral LD50). It can be seen from [Table S1](#) that the number of candidate active components became 68 after excluding active components that did not meet the OPS. Due to the unsatisfactory results of the active components of Kuandonghua and Ziwan, they should not be further studied. In the process of druggability screening, the program automatically eliminated 2 unqualified active components according to Lipinski's rule of five and Veber's rules. Therefore, 66 active components from 13 herbs may become oral drugs.

### 3.4 Reverse finding target

The results showed that the corresponding targets of active components in Guizhi did not have antiviral or anti-inflammatory effects. Therefore, 64 active components from 12 herbs were retained in the reverse finding target process. The structures of 64 active components are shown in [Figure S1](#). It can be seen from [Figure 2](#) that the horizontal axis and the longitudinal axis represent the pharmacophore models and the active components, respectively. The color gradient trend is red, yellow, green, and blue on the Heat map. The pharmacophore models with high and low Fit Value are represented by red and blue, respectively. Red means that the matching degree is good. Based on these pharmacophore models, we found that the possible targets of the 64 active components in QFPD were

Antigen peptide transporter 1 (TAP1), Retinol-binding protein 4 (RBP4), Interleukin 1 receptor antagonist (IL1RN), Centromere-associated protein E (CENPE), Beta-secretase 1 (BACE1), Transthyretin (TTR), Tyrosine-protein kinase Fyn (FYN), Thyroid hormone receptor alpha (THRA), Pulmonary surfactant-associated protein D (SFTPD), Nuclear receptor subfamily 0 group B member 2 (NR0B2), Cellular tumor antigen p53 (TP53), SRSF protein kinase 1 (SRPK1), RAC-alpha serine/threonine-protein kinase (AKT1) and Protein Mdm4 (MDM4). We compared 14 targets regulated by 64 active components in QFPD with the COVID-19 targets recorded in Genecards databases and found the common targets RBP4 (74), IL1RN (8), TTR (75), FYN (76), SFTPD (77), TP53 (78), SRPK1 (79), and AKT1 (80). The information of 8 potential targets is shown in [Table 2](#). FYN, AKT1, SFTPD, SRPK1, and TP53 were SARS-CoV-2 specific targets.

### 3.5 Construction of protein-protein interaction network

PPI network was constructed by String with the potential targets of the 62 active components in QFPD. It can be seen from [Figure 3A](#) that the network contained 8 nodes and 6 edges. The nodes represented the targets, and the edges represented the interactions between the targets. The more edges the node had, the more critical it was in the network. TP53 and AKT1, with a high degree of connectivity, were core genes that may play an essential role in treating COVID-19 with QFPD. The network in [Figure 3B](#) contained 5 nodes and 5 edges. If medium confidence  $\geq 0.4$  was

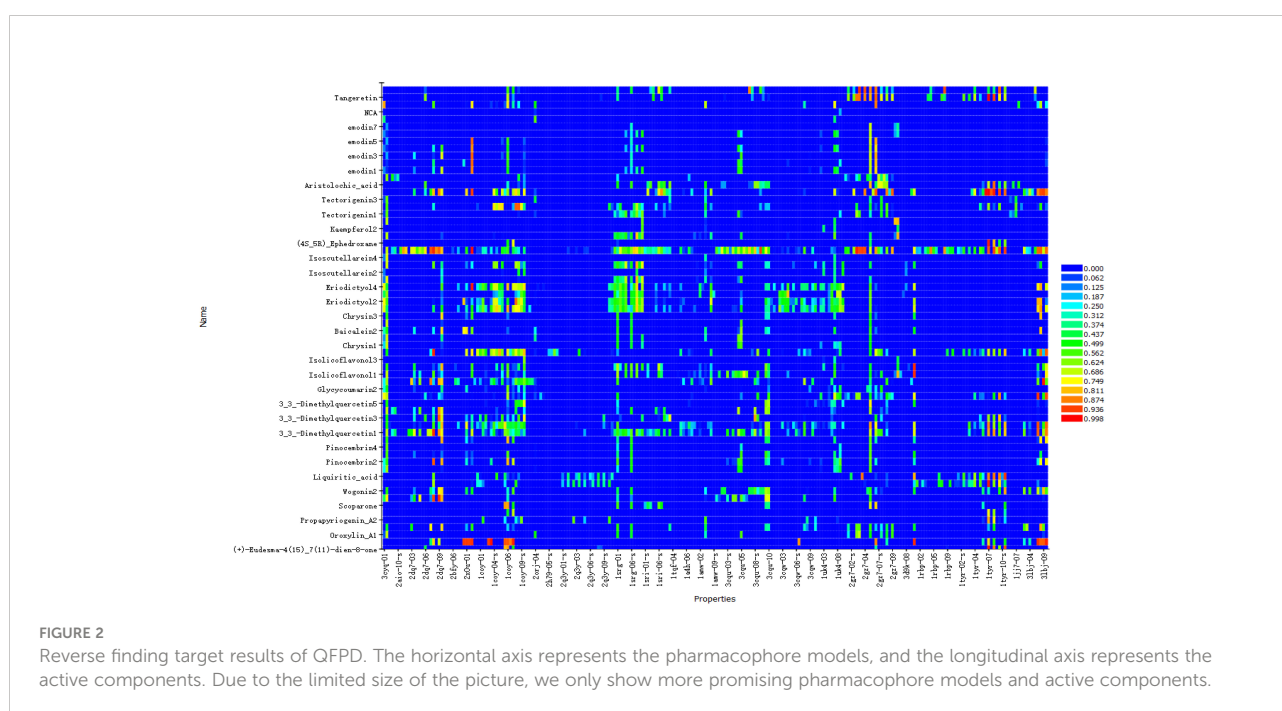


TABLE 2 All pharmacophores and their possible corresponding targets obtained by reverse finding target.

Pharmacophore	Possible target (gene name)	Effect	References
1rbp-02,1rbp-02-s,1rbp-03,1rbp-03-s,1rbp-04,1rbp-04-s,1rbp-05,1rbp-06,1rbp-07-s,1rbp-08,1rbp-08-s,1rbp-09,1rbp-10,1rbp-10-s	1rbp(RBP4)	anti-inflammatory	(74)
1sri-01-s, 1sri-02-s, 1sri-03-s, 1sri-04-s, 1sri-05-s, 1sri-06-s, 1sri-07-s, 1sri-08-s, 1sri-09-s, 1sri-10-s	1sri(IL1RN)	anti-inflammatory	(8)
1tyr-01,1tyr-01-s,1tyr-02,1tyr-02-s,1tyr-03,1tyr-03-s,1tyr-04,1tyr-04-s,1tyr-05,1tyr-05-s,1tyr-06,1tyr-07,1tyr-07-s,1tyr-08,1tyr-08-s,1tyr-09,1tyr-09-s,1tyr-10,1tyr-10-s	1tyr(TTR)	anti-inflammatory	(75)
2dq7-01,2dq7-02,2dq7-02-s,2dq7-03,2dq7-03-s,2dq7-04,2dq7-05,2dq7-05-s,2dq7-06,2dq7-06-s,2dq7-07,2dq7-07-s,2dq7-08,2dq7-09,2dq7-09-s,2dq7-10	2dq7(FYN)	anti-SARS-CoV-2 anti-inflammatory	(76)
3cqu-01,3cqu-01-s,3cqu-02,3cqu-02-s,3cqu-03,3cqu-03-s,3cqu-04,3cqu-04-s,3cqu-05,3cqu-05-s,3cqu-06,3cqu-06-s,3cqu-07,3cqu-07-s,3cqu-08,3cqu-08-s,3cqu-09,3cqu-09-s,3cqu-10,3cqu-10-s	3cqu(AKT1)	anti-SARS-CoV-2 anti-inflammatory	(80)
3cqw-01,3cqw-01-s,3cqw-02,3cqw-03, 3cqw-04, 3cqw-04-s, 3cqw-05, 3cqw-05-s, 3cqw-06, 3cqw-06-s, 3cqw-07, 3cqw-07-s, 3cqw-08, 3cqw-09, 3cqw-10, 3cqw-10-s	3cqw(AKT1)	anti-SARS-CoV-2 anti-inflammatory	(80)
2orj-01,2orj-02,2orj-03,2orj-04	2orj(SFTPD)	anti-SARS-CoV-2 anti-inflammatory	(77)
2x0u-01,2x0u-01-s	2x0u(TP53)	anti-SARS-CoV-2 anti-inflammatory	(78)
2x0v-01,2x0v-01-s	2x0v(TP53)	anti-SARS-CoV-2 anti-inflammatory	(78)
3beg-01,3beg-02	3beg(SRPK1)	anti-SARS-CoV-2	(79)

selected as the screening criteria, the candidate targets were TP53, AKT1, FYN, and SRPK1. If the highest confidence  $\geq 0.9$  was selected as the screening criteria, the candidate targets were TP53, AKT1. The network in Figure 3C contained 7 nodes and 4 edges. If medium confidence  $\geq 0.4$  was selected as the screening criteria, the candidate targets were TP53, AKT1, RBP4, TTR, and FYN. If the highest confidence  $\geq 0.9$  was selected as the screening criteria, the candidate targets were TP53, AKT1, RBP4, and TTR.

### 3.6 Construction of “herb-active component-target” interaction network diagram

As shown in Figure 4, 62 active components from 12 herbs (Mahuang, Zhishi, Huoxiang, Zexie, Shengan, Shengjiang, Chaihu, Huangqin, Xingren, Baizhu, Xixin, and Zhigancao) have anti-SARS-CoV-2 or anti-inflammatory effects. Among

them, Eriodictyol was common in Xixin and Huangqin. Wogonin was common in Chaihu and Huangqin. Geraniol was common in Chaihu and Shengjiang. (+)-Eudesma-4(15),7(11)-dien-8-one was common in Xixin and Baizhu. It can be seen from Table 3 that, Kaempferol2, Kaempferol3, Emodin7, and Isolicoflavonol3 only had anti-SARS-CoV-2 effects, (4S\_5R) Ephedroxane and Pulegone only had anti-inflammatory effects. The other 56 components were both anti-inflammatory and anti-SARS-CoV-2. Among these components, Quercetin, Wogonin, and Emodin were able to interfere with various stages of the coronavirus entry and replication cycle (59, 81, 82). Kaempferol could be used as an antiviral drug against the 3a Channel Protein of Coronavirus (55). Baicalein had a high affinity for SARS-CoV-2 3CLpro (83). They were identified as candidate active components for COVID-19. In addition, each target was bound to two or more active components, indicating that these targets could be affected by multiple active components simultaneously to exert different effects.

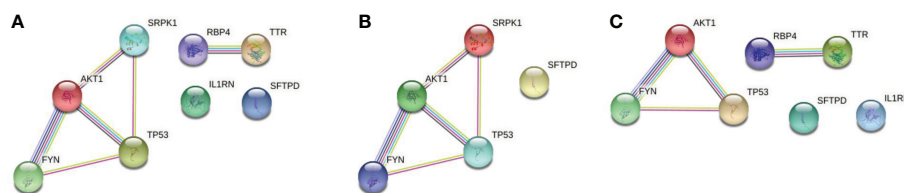


FIGURE 3

(A) PPI network of 8 potential targets. (B) PPI network of the SARS-CoV-2 specific targets. (C) PPI network of the inflammatory targets. Associations are meant to be specific and meaningful, i.e. proteins jointly contribute to a shared function; this does not necessarily mean they are physically binding to each other. The light-blue edges denote known interactions from curated databases. The pink edges show that the known interactions were determined by experimental methods. The yellow edges demonstrate that the predicted interactions arose from text-mining. The black edges denote that the predicted interactions arose from co-expression. The lavender edges show that the predicted interactions arose from protein homology. The dark-blue edges denote that the predicted interactions arose from gene co-occurrence.

### 3.7 Pathway analysis of QFPD

We identified TP53 and AKT1 as core targets based on the PPI network. Therefore, according to the expression of TP53 or AKT1, we divided them into high and low expression groups for GSEA analysis.  $P$ -value  $< 0.05$  was considered statistically significant. Figure 5A showed that 6 significant pathways were enriched in the TP53 high expression group: RNA polymerase, primary immunodeficiency, intestinal immune network for IGA

production, systemic lupus erythematosus, allograft rejection, and autoimmune thyroid disease. 3 pathways were enriched in the TP53 low expression group: O glycan biosynthesis, regulation of autophagy, and long-term potentiation. 20 meaningful pathways were enriched in the AKT1 high expression group. We showed the first six significant enrichments in Figure 5B, which were taste transduction, ECM receptor interaction, focal adhesion, ABC transporters, long term depression, and linoleic acid metabolism. 3 pathways

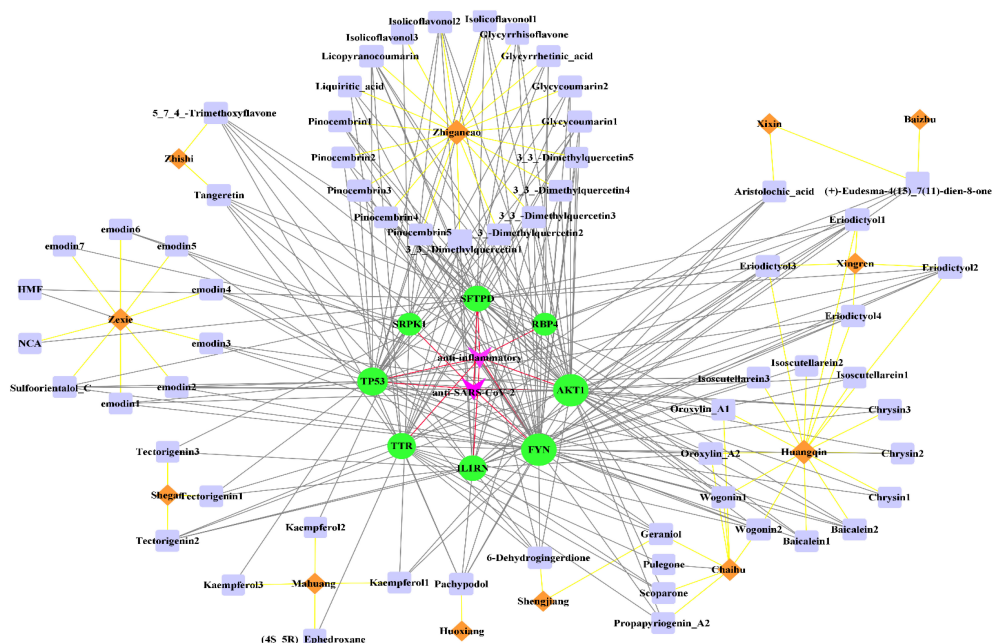


FIGURE 4

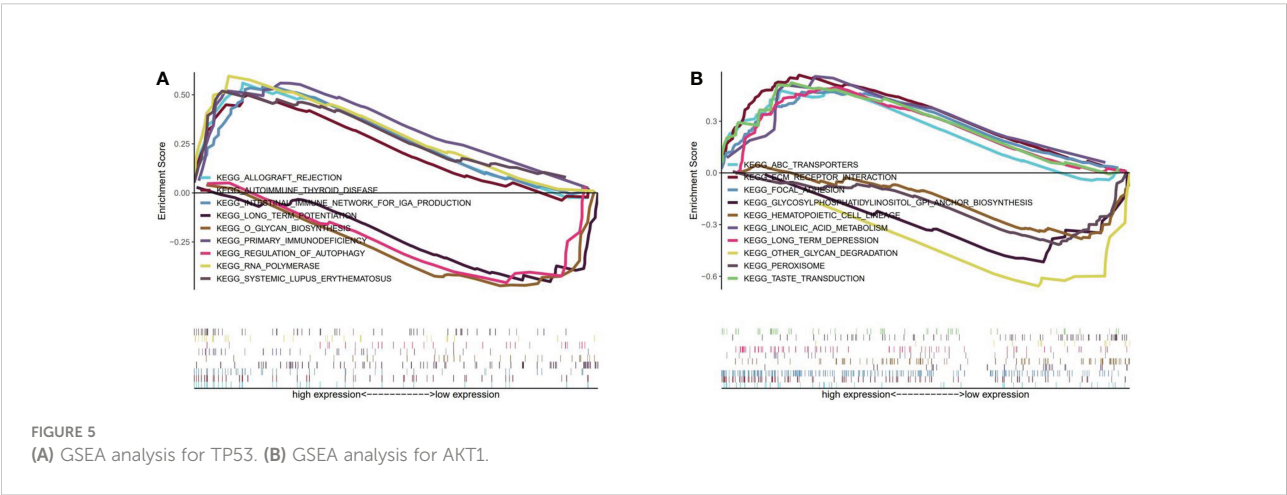
The "herb-active component-target" interaction network diagram for the treatment of COVID-19. 12 herbs (Mahuang, Zhishi, Huoxiang, Xezie, Shengan, Shengjiang, Chaihu, Huangqin, Xingren, Baizhu, Xixin, Zhigancao) in QFPD are marked in orange; 62 active components screened from 12 herbs with anti-SARS-CoV-2 or anti-inflammatory effects are marked in purple; 8 potential targets of QFPD are marked in green, and the properties of the targets are marked in pink. The black line represents that a certain active component comes from a certain herb; the yellow line represents the interaction between the active component and the target, and the red line represents a certain target is against inflammation or SARS-CoV-2.

TABLE 3 62 components determined by multiple computational processes in QFPD.

Active components	Effect
Kaempferol3	anti-SARS-CoV-2
Emodin7	anti-SARS-CoV-2
Kaempferol2	anti-SARS-CoV-2
Isolicoflavonol3	anti-SARS-CoV-2
(4S_5R)_Ephedroxane	anti-inflammatory
Pulegone	anti-inflammatory
Pachypodol	anti-SARS-CoV-2, anti-inflammatory
3_3_-Dimethylquercetin1	anti-SARS-CoV-2, anti-inflammatory
Glycyrrhisoflavone	anti-SARS-CoV-2, anti-inflammatory
Oroxylin_A2	anti-SARS-CoV-2, anti-inflammatory
Wogonin1	anti-SARS-CoV-2, anti-inflammatory
Isolicoflavonol2	anti-SARS-CoV-2, anti-inflammatory
6-Dehydrogingerdione	anti-SARS-CoV-2, anti-inflammatory
Isolicoflavonol1	anti-SARS-CoV-2, anti-inflammatory
3_3_-Dimethylquercetin3	anti-SARS-CoV-2, anti-inflammatory
Baicalein2	anti-SARS-CoV-2, anti-inflammatory
3_3_-Dimethylquercetin4	anti-SARS-CoV-2, anti-inflammatory
Emodin3	anti-SARS-CoV-2, anti-inflammatory
Emodin1	anti-SARS-CoV-2, anti-inflammatory
Wogonin2	anti-SARS-CoV-2, anti-inflammatory
Pinocembrin3	anti-SARS-CoV-2, anti-inflammatory
Glycoumarin2	anti-SARS-CoV-2, anti-inflammatory
3_3_-Dimethylquercetin2	anti-SARS-CoV-2, anti-inflammatory
Eriodictyol2	anti-SARS-CoV-2, anti-inflammatory
Tangeretin	anti-SARS-CoV-2 anti-inflammatory
Aristolochic_acid	anti-SARS-CoV-2, anti-inflammatory
(+)-Eudesma-4(15)_7(11)-dien-8-one	anti-SARS-CoV-2, anti-inflammatory
Glycoumarin1	anti-SARS-CoV-2, anti-inflammatory
5_7_4_-Trimethoxyflavone	anti-SARS-CoV-2, anti-inflammatory
Glycyrrhetic_acid	anti-SARS-CoV-2, anti-inflammatory
Geraniol	anti-SARS-CoV-2, anti-inflammatory
Licopyranocoumarin	anti-SARS-CoV-2, anti-inflammatory
Propapyriogenin_A2	anti-SARS-CoV-2, anti-inflammatory
Pinocembrin2	anti-SARS-CoV-2, anti-inflammatory
Isoscutellarein3	anti-SARS-CoV-2, anti-inflammatory
Liquiritic_acid	anti-SARS-CoV-2, anti-inflammatory
Sulfoorientalol_C	anti-SARS-CoV-2 anti-inflammatory
(Continued)	

TABLE 3 Continued

Active components	Effect
Eriodictyol1	anti-SARS-CoV-2, anti-inflammatory
Emodin2	anti-SARS-CoV-2, anti-inflammatory
Tectorigenin2	anti-SARS-CoV-2, anti-inflammatory
Emodin4	anti-SARS-CoV-2, anti-inflammatory
Pinocembrin5	anti-SARS-CoV-2, anti-inflammatory
Chrysin3	anti-SARS-CoV-2, anti-inflammatory
Eriodictyol4	anti-SARS-CoV-2, anti-inflammatory
Baicalein1	anti-SARS-CoV-2, anti-inflammatory
Isoscutellarein1	anti-SARS-CoV-2, anti-inflammatory
Isoscutellarein2	anti-SARS-CoV-2, anti-inflammatory
Eriodictyol3	anti-SARS-CoV-2, anti-inflammatory
Kaempferol1	anti-SARS-CoV-2 anti-inflammatory
Chrysin1	anti-SARS-CoV-2, anti-inflammatory
Chrysin2	anti-SARS-CoV-2, anti-inflammatory
Pinocembrin1	anti-SARS-CoV-2, anti-inflammatory
Pinocembrin4	anti-SARS-CoV-2, anti-inflammatory
3_3_-Dimethylquercetin5	anti-SARS-CoV-2, anti-inflammatory
HMF	anti-SARS-CoV-2, anti-inflammatory
Oroxylin_A1	anti-SARS-CoV-2, anti-inflammatory
Tectorigenin3	anti-SARS-CoV-2, anti-inflammatory
Tectorigenin1	anti-SARS-CoV-2, anti-inflammatory
NCA	anti-SARS-CoV-2, anti-inflammatory
Emodin5	anti-SARS-CoV-2, anti-inflammatory
Emodin6	anti-SARS-CoV-2, anti-inflammatory
Scoparone	anti-SARS-CoV-2, anti-inflammatory





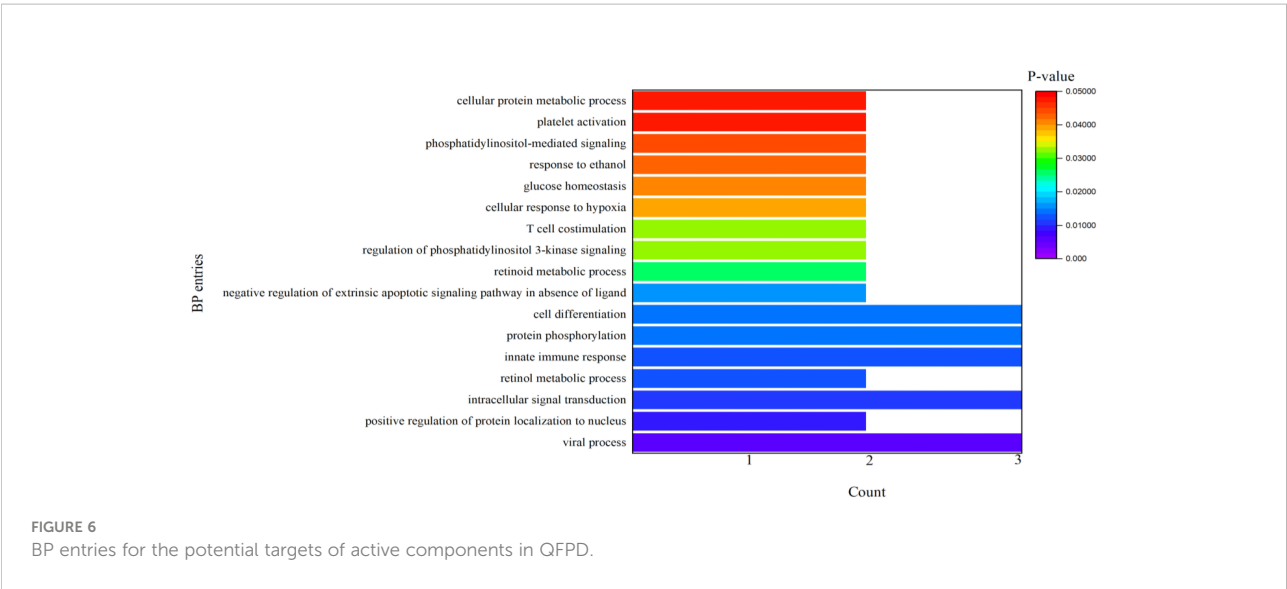
were enriched in the AKT1 low expression group, namely other glycan degradation, glycosylphosphatidylinositol GPI anchor biosynthesis, peroxisome, and hematopoietic cell lineage.

It can be seen from Table 4 that 8 potential targets of QFPD (RBP4, IL1RN, TTR, FYN, SFTPD, TP53, SRPK1, and AKT1) were mainly enriched in 21 BP entries. 17 BP entries were determined with  $P\text{-value} < 0.05$  (Figure 6). The core

BP entries mainly included the viral process, intracellular signal transduction, innate immune response, protein phosphorylation, and cell differentiation. During SARS-CoV-2 infection, the innate immune system experienced substantial disturbance (84). Several of the cytokines involved in the reaction employ a distinct intracellular signaling pathway mediated by Janus kinases (85). Researchers studied the perturbation in protein phosphorylation

TABLE 4 BP, MF and CC entries of GO analysis.

	Item	Count	P-value	Genes
BP	viral process	3	0.0063	FYN, TP53, SRPK1
	intracellular signal transduction	3	0.0111	AKT1, FYN, SRPK1
	innate immune response	3	0.0126	SFTPD, FYN, SRPK1
	protein phosphorylation	3	0.0141	AKT1, FYN, SRPK1
	cell differentiation	3	0.0145	AKT1, FYN, TP53
	positive regulation of protein localization to nucleus	2	0.0087	AKT1, FYN
	retinol metabolic process	2	0.0124	RBP4, TTR
	negative regulation of extrinsic apoptotic signaling pathway in absence of ligand	2	0.0153	AKT1, FYN
	retinoid metabolic process	2	0.0252	RBP4, TTR
	regulation of phosphatidylinositol 3-kinase signaling	2	0.0321	AKT1, FYN
	T cell costimulation	2	0.0321	AKT1, FYN
	cellular response to hypoxia	2	0.0393	AKT1, TP53
	glucose homeostasis	2	0.0414	RBP4, AKT1
	response to ethanol	2	0.0430	RBP4, FYN
	phosphatidylinositol-mediated signaling	2	0.0434	AKT1, FYN
	platelet activation	2	0.0470	AKT1, FYN
	cellular protein metabolic process	2	0.0482	TTR, SFTPD
	regulation of signal transduction by p53 class mediator	2	0.0506	AKT1, TP53
	negative regulation of gene expression	2	0.0557	AKT1, FYN
	cellular response to DNA damage stimulus	2	0.0836	AKT1, TP53
	regulation of apoptotic process	2	0.0855	FYN, TP53
MF	protein binding	8	0.0103	IL1RN, RBP4, TTR, SFTPD, AKT1, FYN, TP53, SRPK1
	identical protein binding	4	0.0027	TTR, AKT1, FYN, TP53
	ATP binding	4	0.0185	AKT1, FYN, TP53, SRPK1
	enzyme binding	3	0.0076	AKT1, FYN, TP53
	protein heterodimerization activity	3	0.0145	RBP4, TTR, TP53
	protein phosphatase 2A binding	2	0.0111	AKT1, TP53
CC	protein complex	4	0.0004	RBP4, TTR, AKT1, TP53
	extracellular space	4	0.0112	IL1RN, RBP4, TTR, SFTPD
	mitochondrion	3	0.0875	AKT1, FYN, TP53
	nuclear matrix	2	0.0367	TP53, SRPK1



during SARS-CoV-2 infection by mass spectrometry, and the results showed that large changes were observed in protein phosphorylation (86). This evidences verified that QFPD regulates diseases through a variety of biological processes. The core MF entries mainly included protein binding, identical protein binding, enzyme binding, and ATP binding. A recent study reported that SARS-CoV-2 enters the host cells through the binding of its spike protein to the cell surface-expressing angiotensin-converting enzyme 2 (ACE2) (87). Therefore, inhibiting the binding of some specific proteins or enzymes may attenuate the progression of COVID-19. The core CC entries mainly included protein complex and extracellular space. The GO analysis results showed that AKT1, FYN, TP53, TTR, and RBP4

were key targets involved in regulation. The KEGG analysis results showed that AKT1, FYN, and TP53 were key targets involved in regulation (Table 5). The top 13 KEGG pathways are shown in Figure 7. The core pathways mainly included Sphingolipid signaling pathway, Fc epsilon RI signaling pathway, Apoptosis, and Measles. Sphingolipids play a vital role in protecting the lung from damages (88). The Fc epsilon RI signaling pathway is associated with cytokine secretion and inflammatory responses (89). Based on previous data, SARS-CoV-2 may have the ability to induce endogenous and exogenous apoptotic pathways and stimulate T cell apoptosis (90). Therefore, we speculate that the active components in QFPD may play an important role in the therapeutic of COVID-19 by multiple pathways.

TABLE 5 13 KEGG pathways.

Pathway	Count	P-value	Genes
Sphingolipid signaling pathway	3	0.0018	AKT1, FYN, TP53
Measles	3	0.0022	AKT1, FYN, TP53
Endometrial cancer	2	0.0299	AKT1, TP53
Non-small cell lung cancer	2	0.0322	AKT1, TP53
Colorectal cancer	2	0.0356	AKT1, TP53
Apoptosis	2	0.0356	AKT1, TP53
Central carbon metabolism in cancer	2	0.0367	AKT1, TP53
Glioma	2	0.0373	AKT1, TP53
Pancreatic cancer	2	0.0373	AKT1, TP53
Fc epsilon RI signaling pathway	2	0.0390	AKT1, FYN
Melanoma	2	0.0407	AKT1, TP53
Chronic myeloid leukemia	2	0.0412	AKT1, TP53
Small cell lung cancer	2	0.0485	AKT1, TP53

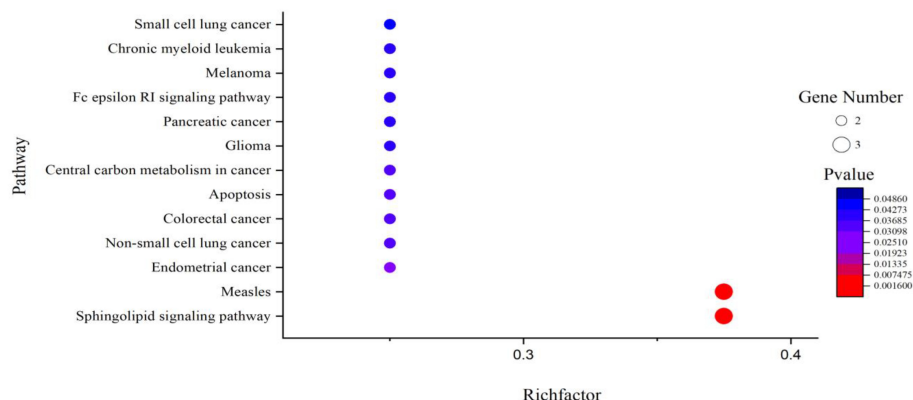


FIGURE 7

KEGG pathway analysis for the SARS-CoV-2 specific targets of active components in QFPD. The rich factor indicates the ratio of the number of target genes belonging to a pathway to the total number of annotated target genes in the pathway. The higher value for this ratio corresponds to a higher level of enrichment. The size and color of the bubble indicates the number and significant characters of target genes that enriched in pathways.

## Conclusion

In this study, we used various network pharmacology methods combined with CADD techniques to reveal the diversity of potential targets and therapeutic pathways for QFPD against COVID-19. We found that RBP4, IL1RN, TTR, FYN, SFTPD, TP53, SRPK1, and AKT1 are highly related to COVID-19. QFPD could act on multiple pathways, including viral process, immunodeficiency, RNA polymerase, Sphingolipid signaling pathway, and taste transduction. The results showed that QFPD has “multi-component, multi-target, and multi-pathway” characteristics in regulating inflammation, viral infection, cellular damage, and immune responses. Our work helps to establish the basic theory of TCM for the treatment of COVID-19.

## Data availability statement

The original contributions presented in the study are included in the article/**Supplementary Material**. Further inquiries can be directed to the corresponding author.

## Author contributions

ZW conducted the literature review, designed the research system, collated data information, and wrote the manuscript. JZ contributed to the manuscript's revision and guided the calculation process. HG contributed to the conception and design of the study. All authors participate in the revision, reading, and approval the submitted version.

## Funding

This work was financially supported by the High-end Talent Team Construction Foundation [Grant No. 108-10000318], the Cooperation Project of University and Local Enterprise in Yantai of Shandong Province (2021XDRHXM23).

## Conflict of interest

The authors declare that the research was conducted in the absence of any commercial or financial relationships that could be construed as a potential conflict of interest.

## Publisher's note

All claims expressed in this article are solely those of the authors and do not necessarily represent those of their affiliated organizations, or those of the publisher, the editors and the reviewers. Any product that may be evaluated in this article, or claim that may be made by its manufacturer, is not guaranteed or endorsed by the publisher.

## Supplementary material

The Supplementary Material for this article can be found online at: <https://www.frontiersin.org/articles/10.3389/fimmu.2022.1015271/full#supplementary-material>

## References

- Pinotti F, Di Domenico L, Ortega E, Mancastroppa M, Pullano G, Valdano E, et al. Tracing and analysis of 288 early SARS-CoV-2 infections outside China: A modeling study. *PLoS Med* (2020) 17:1003193–1003193. doi: 10.1371/journal.pmed.1003193
- Larremore DB, Toomre D, Parker R. Modeling the effectiveness of olfactory testing to limit SARS-CoV-2 transmission. *Nat Commun* (2021) 12:3664–4. doi: 10.1038/s41467-021-23315-5
- Lowery SA, Sariol A, Perlman S. Innate immune and inflammatory responses to SARS-CoV-2: Implications for COVID-19. *Cell Host Microbe* (2021) 29:1052–62. doi: 10.1016/j.chom.2021.05.004
- Amat-Santos JJ, Santos-Martinez S, López-Otero D, Nombela-Franco L, Gutiérrez-Ibanes E, Del Valle R, et al. Ramipril in high-risk patients with COVID-19. *J Am Coll Cardiol* (2020) 76:268–76. doi: 10.1016/j.jacc.2020.05.040
- Li Y, Liu X, Guo L, Li J, Zhong D, Zhang Y, et al. Traditional Chinese herbal medicine for treating novel coronavirus (COVID-19) pneumonia: protocol for a systematic review and meta-analysis. *Systematic Rev* (2020) 9:75–5. doi: 10.1186/s13643-020-01343-4
- Constantinos G, Anna H, Dimitrios K, Taxiarchis P, Vasiliki T. Status of traditional Chinese medicine in Greece and its approach on COVID-19 pandemic. *Chin Med Culture* (2021) 4:78–85. doi: 10.4103/CMAC.CMAC\_16\_21
- Li M, Yang Y, Liu Y, Zheng M, Li J, Chen L, et al. Progress of traditional Chinese medicine treating COVID-19. *World J Traditional Chin Med* (2021) 7:167–83. doi: 10.4103/wjtc.wjtc\_m68\_20
- Fricke-Galindo I, Falfan-Valencia R. Genetics insight for COVID-19 susceptibility and severity: a review. *Front Immunol* (2021) 12:1057–8. doi: 10.3389/fimmu.2021.622176
- Huan-Huan T, Qi L, Pan-Hong J, Xiang-Dong Z. Clinical value of related inflammatory factors in COVID-19. *J Hainan Med Univ* (2021) 27:647–50. doi: 10.13210/j.cnki.jhmu.20210329.001
- Vannucchi AM, Sordi B, Moretti A, Nozzoli C, Poggesi L, Pieralli F, et al. Compassionate use of JAK1/2 inhibitor ruxolitinib for severe COVID-19: a prospective observational study. *Leukemia* (2021) 35:1121–33. doi: 10.1038/s41375-020-01018-y
- Wang Z, Zhang J, Zhan J, Gao H. Screening out anti-inflammatory or antiviral targets in xuanfei baidu tang through a new technique of reverse finding target. *Bioorganic Chem* (2021) 116:105274–4. doi: 10.1016/j.bioorg.2021.105274
- Shi N, Liu B, Liang N, Ma Y, Ge Y, Yi H, et al. Association between early treatment with qingfei paidu decoction and favorable clinical outcomes in patients with COVID-19: a retrospective multicenter cohort study. *Pharmacol Res* (2020) 161:105290–0. doi: 10.1016/j.phrs.2020.105290
- Xin S, Cheng X, Zhu B, Liao X, Yang F, Song L, et al. Clinical retrospective study on the efficacy of qingfei paidu decoction combined with Western medicine for COVID-19 treatment. *Biomed Pharmacother* (2020) 129:110500–0. doi: 10.1016/j.biopha.2020.110500
- Ren W, Ma Y, Wang R, Liang P, Sun Q, Pu Q, et al. Research advance on qingfei paidu decoction in prescription principle, mechanism analysis and clinical application. *Front Pharmacol* (2021) 11:2046–6. doi: 10.3389/fphar.2020.589714
- Gao K, Song YP, Chen H, Zhao LT, Ma L. Therapeutic efficacy of qingfei paidu decoction combined with antiviral drugs in the treatment of corona virus disease 2019: A protocol for systematic review and meta analysis. *Medicine* (2020) 99:20489–9. doi: 10.1097/MD.00000000000020489
- Junhua M, Yang H, Qian C, Qiang G, Yonggang C, Jing A. A retrospective study on the treatment of COVID-19 type common/type severe with qingfei paidu decoction. *Chin J Hosp Pharm* (2020) 40:2152–7. doi: 10.3969/j.issn.2097-0005.2021.12.009
- Silva C.H.T.D.P.D., Silva V, Resende J, Rodrigues PF, Bononi FC, Benevenuto CG, et al. Computer-aided drug design and ADMET predictions for identification and evaluation of novel potential farnesyltransferase inhibitors in cancer therapy. *J Mol Graphics Model* (2010) 28:513–23. doi: 10.1016/j.jmgm.2009.11.011
- Zhang A, Hui S, Yang B, Wang X. Predicting new molecular targets for rhein using network pharmacology. *BMC Syst Biol* (2012) 6:20–0. doi: 10.1186/1752-0509-6-20
- Shao L, Zhang B. Traditional Chinese medicine network pharmacology: theory, methodology and application. *Chin J Natural Medicines* (2013) 11:110–20. doi: 10.1016/S1875-5364(13)60037-0
- Chang-Xiao L, Liu R, Fan H-R, Ng X-F, Xiao X-P, Chen. Network pharmacology bridges traditional application and modern development of traditional Chinese medicine. *Chin Herbal Medicines* (2015) 7:3–17. doi: 10.1016/S1674-6384(15)60014-4
- Yang Y, Ding Z, Wang Y, Zhong R, Feng Y, Xia T, et al. Systems pharmacology reveals the mechanism of activity of physalis alkekengi l. var. franchetii against lipopolysaccharide-induced acute lung injury. *J Cell Mol Med* (2020) 24:5039–56. doi: 10.1111/jcmm.15126
- Liu Y, Sun Y. China Traditional Chinese medicine (TCM) patent database. *World Patent Inf* (2004) 26:91–6. doi: 10.1016/S0172-2190(03)00110-8
- Hsin-Yi C. Discovery of novel insomnia leads from screening traditional Chinese medicine database. *J Biomolecular Structure Dynamics* (2013) 32:776–91. doi: 10.1080/07391102.2013.790849
- Arya H, Coumar MS. Virtual screening of traditional Chinese medicine (TCM) database: identification of fragment-like lead molecules for filariasis target asparaginyl-tRNA synthetase. *J Mol Modeling* (2014) 20:2266–7. doi: 10.1007/s00894-014-2266-9
- Ru J, Li P, Wang J, Zhou W, Li B, Huang C, et al. TCMSP: a database of systems pharmacology for drug discovery from herbal medicines. *J Cheminform* (2014) 6:13–4. doi: 10.1186/1758-2946-6-13
- Ma LY, Zhou QL, Yang XB, Wang HP, Yang XW. Metabolism of 20(S)-ginsenoside Rg2 by rat liver microsomes: Bioactivation to SIRT1-activating metabolites. *Molecules* (2016) 21:757–8. doi: 10.3390/molecules21060757
- Tailong L, Youyong Li, Yunlong S, Dan Li, Huiyong, Sun. ADMET evaluation in drug discovery: 15. accurate prediction of rat oral acute toxicity using relevance vector machine and consensus modeling. *J Cheminformatics* (2016) 8:6–8. doi: 10.1186/s13321-016-0117-7
- Qidwai T. QSAR modeling, docking and ADMET studies for exploration of potential anti-malarial compounds against plasmodium falciparum. *In Silico Pharmacol* (2017) 5:6–7. doi: 10.1007/s40203-017-0026-0
- Alam S, Khan F. Virtual screening, docking, ADMET and system pharmacology studies on garcinia caged xanthone derivatives for anticancer activity. *Sci Rep* (2018) 8:5524–5. doi: 10.1038/s41598-018-23768-7
- Ruiz P, Begliuitti G, Tincher T, Wheeler J, Mumtaz M. Prediction of acute mammalian toxicity using QSAR methods: a case study of sulfur mustard and its breakdown products. *Molecules (Basel Switzerland)* (2012) 17:8982–9001. doi: 10.3390/molecules17088982
- Bahadur Gurung A, Ajmal Ali M, Lee J, Abul Farah M, Mashay Al-Anazi K. Structure-based virtual screening of phytochemicals and repurposing of FDA approved antiviral drugs unravels lead molecules as potential inhibitors of coronavirus 3C-like protease enzyme. *J King Saud University. Sci* (2020) 32:2845–53. doi: 10.1016/j.jksus.2020.07.007
- Alam S, Khan F. 3D-QSAR, docking, ADME/Tox studies on flavone analogs reveal anticancer activity through tankyrase inhibition. *Sci Rep* (2019) 9:5414–4. doi: 10.1038/s41598-019-41984-7
- Zhou Y, Lu X, Yang H, Chen Y, Wang F, Li J, et al. Discovery of selective butyrylcholinesterase (BChE) inhibitors through a combination of computational studies and biological evaluations. *Molecules (Basel Switzerland)* (2019) 24:4217–7. doi: 10.3390/molecules24234217
- Damian S, Andrea F, Stefan W, Kristoffer F, Davide H, Jaime HC, et al. STRING v10: protein–protein interaction networks, integrated over the tree of life. *Nucleic Acids Res* (2015) 43:447–52. doi: 10.1093/nar/gku1003
- Grindrod P, Kibble M. Review of uses of network and graph theory concepts within proteomics. *Expert Rev Proteomics* (2004) 1:229–38. doi: 10.1586/14789450.1.2.229
- Kanehisa M, Goto S, Sato Y, Furumichi M, Tanabe M. KEGG for integration and interpretation of large-scale molecular data sets. *Nucleic Acids Res* (2012) 40:D109–14. doi: 10.1093/nar/gkr988
- Shen Y-C, Chiou W-F, Chou Y-C, Chen C-F. Mechanisms in mediating the anti-inflammatory effects of baicalin and baicalein in human leukocytes. *Eur J Pharmacol* (2003) 465:171–81. doi: 10.1016/S0014-2999(03)01378-5
- Lee JY, Park W. Anti-inflammatory effects of oroxylin A on RAW 264.7 mouse macrophages induced with polyinosinic-polycytidylic acid. *Exp Ther Med* (2016) 12:151–6. doi: 10.3892/etm.2016.3320
- Paniagua-Pérez R, Flores-Mondragón G, Reyes-Legorreta C, Herrera-López B, Cervantes-Hernández I, Madrigal-Santillán O, et al. Evaluation of the anti-inflammatory capacity of beta-sitosterol in rodent assays. *Afr J Traditional Complementary Altern Medicines* (2017) 14:123–30. doi: 10.21010/ajtcam.v14i1.13
- Kroes BV, Van Den Berg A, Van Ufford HQ, Van Dijk H, Labadie R. Anti-inflammatory activity of gallic acid. *Planta Med* (1992) 58:499–504. doi: 10.1055/s-2006-961535
- Selloum L, Bouriche H, Tigrine C, Boudoukha C. Anti-inflammatory effect of rutin on rat paw oedema, and on neutrophils chemotaxis and degranulation. *Exp Toxicologic Pathol* (2003) 54:313–8. doi: 10.1078/0940-2993-00260

42. Lee S, Jung SH, Lee YS, Yamada M, Kim B-K, Ohuchi K, et al. Antiinflammatory activity of hyperin from *Acanthopanax chiisanensis* roots. *Arch Pharmacol Res* (2004) 27:628–32. doi: 10.1007/BF02980162
43. Pan C-H, Kim ES, Jung SH, Nho CW, Lee JK. Tectorigenin inhibits IFN- $\gamma$ /LPS-induced inflammatory responses in murine macrophage RAW 264.7 cells. *Arch Pharmacol Res* (2008) 31:1447–56. doi: 10.1007/s12272-001-2129-7
44. Saha S, Sadhukhan P, Sil PC. Mangiferin: A xanthone with multipotent anti-inflammatory potential. *Biofactors* (2016) 42:459–74. doi: 10.1002/biof.1292
45. Hart P, Brand C, Carson C, Riley T, Prager R, Finlay-Jones J. Terpinen-4-ol, the main component of the essential oil of *Melaleuca alternifolia* (tea tree oil), suppresses inflammatory mediator production by activated human monocytes. *Inflammation Res* (2000) 49:619–26. doi: 10.1007/s000110050639
46. Cosyns J-P. Aristolochic acid and 'Chinese herbs nephropathy'. *Drug Saf* (2003) 26:33–48. doi: 10.2165/00002018-200326010-00004
47. Fanhchaksai K, Kodchakorn K, Pothacharoen P, Kongtawelert P. Effect of sesamin against cytokine production from influenza type A H1N1-induced peripheral blood mononuclear cells: Computational and experimental studies. *In Vitro Cell Dev Biol Anim* (2016) 52:107–19. doi: 10.1007/s11626-015-9950-7
48. Xu J-J, Liu Z, Tang W, Wang G-C, Chung HY, Liu Q-Y, et al. Tangeretin from citrus reticulate inhibits respiratory syncytial virus replication and associated inflammation *in vivo*. *J Agric Food Chem* (2015) 63:9520–7. doi: 10.1021/acs.jafc.5b03482
49. Haggag YA, El-Ashmawy NE, Okasha KM. Is hesperidin essential for prophylaxis and treatment of COVID-19 infection? *Med Hypotheses* (2020) 144:109957–8. doi: 10.1016/j.mehy.2020.109957
50. Tutunchi H, Naeini F, Ostadrahimi A, Hosseinzadeh-Attar MJ. Naringenin, a flavanone with antiviral and anti-inflammatory effects: A promising treatment strategy against COVID-19. *Phytotherapy Res* (2020) 34:3137–47. doi: 10.1002/ptr.6781
51. Chiang LC, Ng LT, Cheng PW, Chiang W, Lin CC. Antiviral activities of extracts and selected pure constituents of *Ocimum basilicum*. *Clin Exp Pharmacol Physiol* (2005) 32:811–6. doi: 10.1111/j.1440-1681.2005.04270.x
52. Bhattacharjee B, Chatterjee J. Identification of proapoptotic, anti-inflammatory, anti-proliferative, anti-invasive and anti-angiogenic targets of essential oils in cardamom by dual reverse virtual screening and binding pose analysis. *Asian Pacific J Cancer Prev* (2013) 14:3735–42. doi: 10.7314/APJCP.2013.14.6.3735
53. Carballo-Villalobos A, González-Trujano M, López-Muñoz F. Evidence of mechanism of action of anti-inflammatory/antinociceptive activities of acetamin. *Eur J Pain* (2014) 18:396–405. doi: 10.1002/j.1532-2149.2013.00378.x
54. Rogerio A, Kanashiro A, Fontanari C, Da Silva E, Lucisano-Valim Y, Soares E, et al. Anti-inflammatory activity of quercetin and isoquercitrin in experimental murine allergic asthma. *Inflammation Res* (2007) 56:402–8. doi: 10.1007/s00011-007-7005-6
55. Schwarz S, Sauter D, Wang K, Zhang R, Sun B, Karioti A, et al. Kaempferol derivatives as antiviral drugs against the 3a channel protein of coronavirus. *Planta Med* (2014) 80:177–82. doi: 10.1055/s-0033-1360277
56. Murbach Teles Andrade BF, Conti BJ, Santiago KB, Fernandes A, Sforzin JM. C ymbopogon martinii essential oil and geraniol at noncytotoxic concentrations exerted immunomodulatory/anti-inflammatory effects in human monocytes. *J Pharm Pharmacol* (2014) 66:1491–6. doi: 10.1111/jphpp.12278
57. Lee JK. Anti-inflammatory effects of eriodictyol in lipopolysaccharide-stimulated raw 264.7 murine macrophages. *Arch Pharmacol Res* (2011) 34:671–9. doi: 10.1007/s12272-011-0418-3
58. Freire RS, Morais SM, Catunda-Junior FEA, Pinheiro DC. Synthesis and antioxidant, anti-inflammatory and gastroprotector activities of anethole and related compounds. *Bioorganic medicinal Chem* (2005) 13:4353–8. doi: 10.1016/j.bmc.2005.03.058
59. Agrawal PK, Agrawal C, Blunden G. Quercetin: antiviral significance and possible COVID-19 integrative considerations. *Natural Product Commun* (2020) 15:1–10. doi: 10.1177/1934578X20976293
60. Sin KS, Kim HP, Lee WC, Pachaly P. Pharmacological activities of the constituents of *Atractylodes rhizomes*. *Arch Pharmacol Res* (1989) 12:236–8. doi: 10.1007/BF02911051
61. Huang H, Cheng Z, Shi H, Xin W, Wang TT, Yu L. Isolation and characterization of two flavonoids, engeletin and astilbin, from the leaves of *Engelhardtia roxburghiana* and their potential anti-inflammatory properties. *J Agric Food Chem* (2011) 59:4562–9. doi: 10.1021/jf2002969
62. Lee CW, Park NH, Kim JW, Um BH, Shpatov A, Shults E, et al. Study of skin anti-ageing and anti-inflammatory effects of dihydroquercetin, natural triterpenoids, and their synthetic derivatives. *Russian J Bioorganic Chem* (2012) 38:328–34. doi: 10.1134/S1068162012030028
63. Hwa JS, Jin YC, Lee YS, Ko YS, Kim YM, Shi LY, et al. 2-methoxycinnamaldehyde from *Cinnamomum cassia* reduces rat myocardial ischemia and reperfusion injury *in vivo* due to HO-1 induction. *J ethnopharmacol* (2012) 139:605–15. doi: 10.1016/j.jep.2011.12.001
64. Kim D-H, Yoo T-H, Lee SH, Kang HY, Nam BY, Kwak SJ, et al. Gamma linolenic acid exerts anti-inflammatory and anti-fibrotic effects in diabetic nephropathy. *Yonsei Med J* (2012) 53:1165–75. doi: 10.3349/ymj.2012.53.6.1165
65. Pan P-H, Lin S-Y, Ou Y-C, Chen W-Y, Chuang Y-H, Yen Y-J, et al. Stearic acid attenuates cholestasis-induced liver injury. *Biochem Biophys Res Commun* (2010) 391:1537–42. doi: 10.1016/j.bbrc.2009.12.119
66. Xia S, Ni Y, Zhou Q, Xiang H, Sui H, Shang D. Emodin attenuates severe acute pancreatitis *via* antioxidant and anti-inflammatory activity. *Inflammation* (2019) 42:2129–38. doi: 10.1007/s10753-019-01077-z
67. Shang X, He X, Liu H, Wen B, Tan T, Xu C, et al. Stachyose prevents intestinal mucosal injury in the immunosuppressed mice. *Starch-Stärke* (2020) 72:1900073–1900074. doi: 10.1002/star.201900073
68. Zhou Y-Z, Li X, Gong W-X, Tian J-S, Gao X-X, Gao L, et al. Protective effect of isoliquiritin against corticosterone-induced neurotoxicity in PC12 cells. *Food Funct* (2017) 8:1235–44. doi: 10.1039/C6FO01503D
69. Abdizadeh R, Hadizadeh F, Abdizadeh T. In silico analysis and identification of antiviral coumarin derivatives against 3-chymotrypsin-like main protease of the novel coronavirus SARS-CoV-2. *Mol Diversity* (2021) 16:1053–76. doi: 10.1007/s11030-021-10230-6
70. Richard SA. Exploring the pivotal immunomodulatory and anti-inflammatory potentials of glycyrrhizic and glycyrrhetic acids. *Mediators Inflammation* (2021) 2021:1–15. doi: 10.1155/2021/6699560
71. Lee JY, Park W. Anti-inflammatory effect of wogonin on RAW 264.7 mouse macrophages induced with polyinosinic-polycytidylic acid. *Molecules* (2015) 20:6888–900. doi: 10.3390/molecules20046888
72. Roy A, Park H-J, Abdul QA, Jung HA, Choi JS. Pulegone exhibits anti-inflammatory activities through the regulation of NF- $\kappa$ B and nrf-2 signaling pathways in LPS-stimulated RAW 264.7 cells. *Natural Product Sci* (2018) 24:28–35. doi: 10.20307/nps.2018.24.1.28
73. Hui Y, Wang X, Yu Z, Fan X, Cui B, Zhao T, et al. Scoparone as a therapeutic drug in liver diseases: Pharmacology, pharmacokinetics and molecular mechanisms of action. *Pharmacol Res* (2020) 160:105170–2. doi: 10.1016/j.phrs.2020.105170
74. Leng L, Li M, Li W, Mou D, Liu G, Ma J, et al. Sera proteomic features of active and recovered COVID-19 patients: potential diagnostic and prognostic biomarkers. *Signal transduction targeted Ther* (2021) 6:1–3. doi: 10.1038/s41392-021-00612-5
75. Tahery N, Khodadost M, Sherafat SJ, Tavirani MR, Ahmadi N, Montazer F, et al. C-reactive protein as a possible marker for severity and mortality of COVID-19 infection. *Gastroenterol Hepatol From Bed to Bench* (2021) 14:S118–22.
76. Vavougiou GD, Breza M, Mavridis T, Krogfelt KA. FYN, SARS-CoV-2, and IFITM3 in the neurobiology of Alzheimer's disease. *Brain Disord* (2021) 3:100022–3. doi: 10.1016/j.dscb.2021.100022
77. Chen L, Zheng S. Understand variability of COVID-19 through population and tissue variations in expression of SARS-CoV-2 host genes. *Inf Med unlocked* (2020) 21:100443–3. doi: 10.1016/j.imu.2020.100443
78. Harford JB, Kim SS, Pirollo KF, Chang EH. TP53 gene therapy as a potential treatment for patients with COVID-19. *Viruses* (2022) 14:739–40. doi: 10.3390/v14040739
79. Savastano A, Ibáñez De Opakua A, Rankovic M, Zwickstetter M. Nucleocapsid protein of SARS-CoV-2 phase separates into RNA-rich polymerase-containing condensates. *Nat Commun* (2020) 11:1–10. doi: 10.1038/s41467-020-19843-1
80. Xia QD, Xun Y, Lu JL, Lu YC, Yang YY, Zhou P, et al. Network pharmacology and molecular docking analyses on Lianhua Qingwen capsule indicate Akt1 is a potential target to treat and prevent COVID-19. *Cell proliferation* (2020) 53:12949–9. doi: 10.1111/cpr.12949
81. Shah T, Shah Z, Xia K-Y, Baloch Z. Therapeutic mechanisms and impact of traditional Chinese medicine on COVID-19 and other influenza diseases. *Pharmacol Research-Modern Chin Med* (2021) 2:100029–9. doi: 10.1016/j.prmcm.2021.100029
82. Zhang X, Gao R, Zhou Z, Tang X, Lin J, Wang L, et al. A network pharmacology based approach for predicting active ingredients and potential mechanism of Lianhuaqingwen capsule in treating COVID-19. *Int J Med Sci* (2021) 18:1866–7. doi: 10.1155/ijms.53685
83. Tao Q, Du J, Li X, Zeng J, Tan B, Xu J, et al. Network pharmacology and molecular docking analysis on molecular targets and mechanisms of huashi baidu formula in the treatment of COVID-19. *Drug Dev Ind Pharm* (2020) 46:1345–53. doi: 10.1080/03639045.2020.1788070



84. Kuri-Cervantes L, Pampena MB, Meng W, Rosenfeld AM, Ittner CA, Weisman AR, et al. Comprehensive mapping of immune perturbations associated with severe COVID-19. *Sci Immunol* (2020) 5:eabd7114. doi: 10.1126/sciimmunol.abd7114
85. Luo W, Li Y-X, Jiang L-J, Chen Q, Wang T, Ye D-W. Targeting JAK-STAT signaling to control cytokine release syndrome in COVID-19. *Trends Pharmacol Sci* (2020) 41:531–43. doi: 10.1016/j.tips.2020.06.007
86. Bouhaddou M, Memon D, Meyer B, White KM, Rezeli VV, Marrero MC, et al. The global phosphorylation landscape of SARS-CoV-2 infection. *Cell* (2020) 182:685–712.e619. doi: 10.1016/j.cell.2020.06.034
87. Kiew L-V, Chang C-Y, Huang S-Y, Wang P-W, Heh C-H, Liu C-T, et al. Development of flexible electrochemical impedance spectroscopy-based biosensing platform for rapid screening of SARS-CoV-2 inhibitors. *Biosensors Bioelectronics* (2021) 183:113213–3. doi: 10.1016/j.bios.2021.113213
88. Abu-Farha M, Thanaraj TA, Qaddoumi MG, Hashem A, Abubaker J, Al-Mulla F. The role of lipid metabolism in COVID-19 virus infection and as a drug target. *Int J Mol Sci* (2020) 21:3544–5. doi: 10.3390/ijms21103544
89. Barh D, Aljabali AA, Tambuwala MM, Tiwari S, Serrano-Aroca Á., Alzahrani KJ, et al. Predicting COVID-19–comorbidity pathway crosstalk-based targets and drugs: towards personalized COVID-19 management. *Biomedicines* (2021) 9:556–8. doi: 10.3390/biomedicines9050556
90. Chu H, Zhou J, Wong BH-Y, Li C, Chan JF-W, Cheng Z-S, et al. Middle East respiratory syndrome coronavirus efficiently infects human primary T lymphocytes and activates the extrinsic and intrinsic apoptosis pathways. *J Infect Dis* (2016) 213:904–14. doi: 10.1093/infdis/jiv380



## OPEN ACCESS

## EDITED BY

Alfonso J. Rodriguez-Morales,  
Fundacion Universitaria Autónoma  
de las Américas,  
Colombia

## REVIEWED BY

Rita Carsetti,  
Bambino Gesù Children's Hospital (IRCCS),  
Italy  
Yuri Battaglia,  
University of Verona,  
Italy  
Pasquale Esposito,  
University of Genoa,  
Italy

## \*CORRESPONDENCE

Andrea Ticinesi  
✉ andrea.ticinesi@unipr.it

## SPECIALTY SECTION

This article was submitted to  
Infectious Diseases: Pathogenesis and Therapy,  
a section of the journal  
Frontiers in Medicine

RECEIVED 30 November 2022

ACCEPTED 11 January 2023

PUBLISHED 01 February 2023

## CITATION

Ticinesi A, Parise A, Nouvenne A, Cerundolo N,  
Prati B, Guerra A, Tuttolomondo D,  
Gaibazzi N and Meschi T (2023) Insights from  
comparison of the clinical presentation and  
outcomes of patients hospitalized with  
COVID-19 in an Italian internal medicine ward  
during first and third wave.  
*Front. Med.* 10:1112728.  
doi: 10.3389/fmed.2023.1112728

## COPYRIGHT

© 2023 Ticinesi, Parise, Nouvenne, Cerundolo,  
Prati, Guerra, Tuttolomondo, Gaibazzi and  
Meschi. This is an open-access article  
distributed under the terms of the [Creative  
Commons Attribution License \(CC BY\)](#). The  
use, distribution or reproduction in other  
forums is permitted, provided the original  
author(s) and the copyright owner(s) are  
credited and that the original publication in this  
journal is cited, in accordance with accepted  
academic practice. No use, distribution or  
reproduction is permitted which does not  
comply with these terms.

# Insights from comparison of the clinical presentation and outcomes of patients hospitalized with COVID-19 in an Italian internal medicine ward during first and third wave

Andrea Ticinesi<sup>1,2\*</sup>, Alberto Parise<sup>2</sup>, Antonio Nouvenne<sup>2</sup>,  
Nicoletta Cerundolo<sup>2</sup>, Beatrice Prati<sup>2</sup>, Angela Guerra<sup>1,2</sup>,  
Domenico Tuttolomondo<sup>1,3</sup>, Nicola Gaibazzi<sup>3</sup> and Tiziana Meschi<sup>1,2</sup>

<sup>1</sup>Department of Medicine and Surgery, University of Parma, Parma, Italy, <sup>2</sup>Geriatric-Rehabilitation Department, Azienda Ospedaliero-Universitaria di Parma, Parma, Italy, <sup>3</sup>Cardiology Unit, Azienda Ospedaliero-Universitaria di Parma, Parma, Italy

**Background:** The reasons of variability of clinical presentation of coronavirus disease-19 (COVID-19) across different pandemic waves are not fully understood, and may include individual risk profile, SARS-CoV-2 lineage and seasonal variations of viral spread. The objective of this retrospective study was to compare the characteristics and outcomes of patients admitted with confirmed coronavirus disease-19 (COVID-19) in the same season during the first (March 2020) and the third pandemic wave (March 2021, dominance of SARS-CoV-2 B.1.1.7 lineage) in an internal medicine ward of a large teaching hospital in Italy.

**Materials and methods:** Data of 769 unvaccinated patients (399 from the first and 370 from the third wave) were collected from clinical records, including symptom type and duration, extension of lung abnormalities on chest computed tomography (CT) and PaO<sub>2</sub>/FiO<sub>2</sub> ratio on admission arterial blood gas analysis.

**Results:** Third wave patients were in average younger (median 65, interquartile range [IQR] 55–75, vs. 72, IQR 61–81 years old,  $p < 0.001$ ), with less comorbidities and better pulmonary (CT visual score median 25, IQR 15–40, vs. 30, IQR 15–50, age- and sex-adjusted  $p = 0.017$ ) and respiratory involvement (PaO<sub>2</sub>/FiO<sub>2</sub> median 288, IQR 237–338, vs. 233, IQR 121–326 mmHg, age- and sex-adjusted  $p < 0.001$ ) than first wave patients. Hospital mortality was lower (19% vs. 36%,  $p < 0.001$ ), but not for subjects over 75 years old (46 vs. 49%). Age, number of chronic illnesses, PCT levels, CT visual score [Odds Ratio (OR) 1.022, 95% confidence interval (CI) 1.009–1.036,  $p < 0.001$ ] and PaO<sub>2</sub>/FiO<sub>2</sub> (OR 0.991, 95% CI 0.988–0.994,  $p < 0.001$ ), but not the pandemic wave, were associated with mortality on stepwise multivariate logistic regression analysis.

**Conclusion:** Despite the higher virulence of B.1.1.7 lineage, we detected milder clinical presentation and improved mortality in patients hospitalized during the third COVID-19 wave, with involvement of younger subjects. The reasons of this discrepancy are unclear, but could involve the population effect of vaccination campaigns, that were being conducted primarily in older frail subjects during the third wave.

## KEYWORDS

SARS-CoV-2, B.1.1.7 lineage, respiratory failure, care improvement, geriatric patients, multimorbidity, vaccine

# 1. Introduction

From February 2020 to May 2021, Italy was struck by three major waves of the coronavirus disease-19 (COVID-19) pandemic, causing peaks of hospital admissions and putting the National Healthcare system under extreme pressure (1). A similar epidemic trend was also observed in other Western countries, especially of the European region, although the magnitude of waves and the response of healthcare systems showed significant differences (1).

Patients who required hospital admission during the first wave were overall characterized by severe respiratory failure, high prevalence of abnormalities on chest imaging and high hospital mortality (2–6). Some reports, however, highlighted differences in the clinical presentation of patients hospitalized for COVID-19 between the earliest and the late phases of the first wave (6, 7). These differences were probably due to improvements in the pre-hospital management and seasonal variations of SARS-CoV-2 transmission and virulence (8). The reduced mortality rates observed in the late phases of the first wave could also depend on improved treatments, particularly the use of intravenous steroids, non-invasive mechanical ventilation and high-flow nasal oxygen delivery devices (9, 10).

Small, but detectable, differences in clinical presentation of COVID-19 cases requiring hospital admission were observed during the second wave in autumn 2020, in comparison with cases from the first wave (11–16). Reduced mortality was also observed, as a result of improved treatment protocols, but not in all studies (17). However, from January 2021 onwards, a novel pandemic wave, sustained by the B.1.1.7 SARS-CoV-2 lineage (alpha variant) rapidly arose. This variant was largely dominant in Italy in March 2021 (18). In other countries, this variant was reported to be associated with increased disease severity and mortality (19, 20). To date, few studies have been focused on the clinical characteristics and outcomes of patients infected during the third pandemic wave in Italy.

Therefore, the aim of this retrospective single-center study was to compare the clinical presentation and outcomes of patients hospitalized with COVID-19 during the same period (March 1–31) of the year 2020 (first wave) and 2021 (third wave) in an internal medicine ward of a teaching hospital in Italy, identifying factors associated with mortality.

# 2. Materials and methods

## 2.1. Patient characteristics and data collection

This study was conducted in an Internal Medicine unit of a large teaching hospital in Northern Italy (Parma University-Hospital), that has been appointed as the main hub for the care of COVID-19 patients of the whole Parma province (approximately 450,000 inhabitants) since the earliest phases of the first wave (21). Two groups of patients hospitalized with COVID-19 in March 2020 and March 2021 were retrospectively enrolled after check for inclusion and exclusion criteria and availability of data on clinical records. The periods of observation were chosen because they corresponded to the first and third wave peaks of the COVID-19 pandemic, respectively, and to avoid confounding by seasonal variations of SARS-CoV-2 virulence and transmission in comparisons.

Only patients aged  $\geq 18$  years old with SARS-CoV-2 infection confirmed by reverse transcriptase polymerase-chain reaction (RT-PCR)

on nasopharyngeal swab performed upon urgent admission were included in the study. Additional inclusion criteria were chest computed tomography (CT) and lab tests including serum C-reactive protein (CRP) performed on the day of admission. Conversely, subjects with missing data on these variables and subjects who were transferred to other wards (i.e., with missing data on outcome) were excluded from the study. The 2021 patients who contracted SARS-CoV-2 infection after having received one or more doses of anti-SARS-CoV-2 vaccine were also excluded.

The records of each participant were reviewed in order to collect demographic data (age and sex), number and types of comorbidities (including hypertension, diabetes, obesity, dyslipidemia, heart diseases, cancer, chronic kidney disease), number of drugs, clinical presentation of COVID-19 (i.e., symptoms and their duration, chest CT abnormalities, vital signs), and the results of lab tests performed on admission, including arterial blood gas analysis, blood cell count, serum creatinine and predicted glomerular filtration rate, D-dimer, CRP and procalcitonin (PCT). The extension of pulmonary infiltrates and abnormalities on chest CT was estimated through calculation of the chest CT visual score, detailed elsewhere (22). Arterial blood oxygen partial pressure and the administered oxygen flow were used to calculate the fractional inspired oxygen saturation (P/F). Data on treatments administered during hospital stay and outcome (survival vs. death) were also collected for all participants.

Ethics Committee approval was obtained (Comitato Etico dell'Area Vasta Emilia Nord, Emilia-Romagna region) under the ID 399/2021/OSS/AOUPR as part of a larger project on clinical and radiological factors associated with mortality in hospitalized COVID-19 patients. All participants, who were contactable by phone or for follow-up reasons, provided written informed consent for participations. For all other cases, the Ethics Committee waived written informed consent collection due to retrospective design of the study.

## 2.2. Statistical analyses

Variables were expressed as median and interquartile range (IQR) or percentages, as appropriate. The characteristics of participants were compared between the 2020 and 2021 groups with the Mann–Whitney or chi-square tests, with adjustment for age and sex with Quade non-parametric ANCOVA (continuous variables) or binary logistic regression (dichotomous variables). The factors independently associated with mortality in both groups were investigated with stepwise multivariate logistic regression models considering participants altogether and after partition by pandemic wave. Age, sex, period of admission, symptom duration, type of symptoms, number of chronic illnesses, obesity, diabetes, hypertension, chronic kidney disease, chronic heart disease, cancer, systolic and diastolic blood pressure, chest CT visual score, P/F on admission arterial blood gas analysis, hemoglobin levels, neutrophil and lymphocyte count, serum creatinine, CRP and PCT were considered as entries in these multivariate models. PCT was either considered as a continuous variable or as classes (class 1:  $< 0.05$  ng/ml; class 2:  $\geq 0.05$  and  $< 0.5$  ng/ml; class 3:  $\geq 0.5$  and  $\leq 2$  ng/ml; class 4:  $> 2$  ng/ml). This partition was applied because, in a study conducted on patients from the first pandemic wave, we demonstrated that admission PCT classes were predictive of survival in oldest old COVID-19 patients (23).

Additional analyses were also made after categorization of participants of both waves by age ( $< 75$  years old vs.  $\geq 75$  years old), for

the known association between age, age-related conditions such as frailty and multimorbidity, and COVID-19 related mortality (6). Finally, the factors independently associated with P/F on admission blood gas analysis were investigated with stepwise multivariate linear regression, for the known prognostic importance of P/F ratio in COVID-19 pneumonia (24).

Analyses were performed with the SPSS statistical package (v. 28, IMB, Armonk, US), considering  $p$  values  $<0.05$  as statistically significant.

### 3. Results

We included in this study 399 patients from the first wave and 370 patients from the third wave. Their clinical characteristics are compared in Table 1. Patients from the third wave were younger, and with less comorbidities than those admitted in the first wave. The clinical presentation of COVID-19 was also different, with increased prevalence of diarrhea (17% vs. 6%) and fatigue (34% vs. 11%) as main symptoms, reduced extension of pulmonary involvement on chest CT (visual score median 25, IQR 15–40, vs. 30, IQR 15–50, age- and sex-adjusted  $p=0.017$ ), improved P/F ratio on blood gas analysis (median 288, IQR 237–338, vs. 233, IQR 121–326 mmHg, age- and sex-adjusted  $p<0.001$ ). These differences were also mirrored by lower levels of CRP and PCT (Table 1).

In spite of this, patients admitted during the third wave experienced significantly higher rates of non-invasive ventilation (NIV) support (28% vs. 14%) and intensive-care unit (ICU) transfer (13% vs. 5%). However, mortality was significantly lower (19% vs. 36%, age- and sex-adjusted  $p<0.001$ ).

On a stepwise multivariate logistic regression model (Table 2), age, the number of chronic illnesses, symptom duration, P/F ratio, chest CT visual score and PCT classes were independently associated with hospital mortality. The period of admission (first or third wave) was included in the multivariate model, but was not independently associated with mortality (Table 2).

In the first wave, age and P/F ratio on admission were the only independent predictors of mortality (Table 3). In the third wave, instead, other factors were involved in addition to age and P/F ratio (Table 3).

Supplementary Tables 1 and 2 show a comparison between patients of the two study periods aged  $<75$  and  $\geq 75$  years old, respectively. While most differences between the 2020 and 2021 groups, shown in Table 1, were confirmed after stratification by age, mortality showed significant improvement in the 2021 group only in patients  $<75$  years old (10% vs. 27%, age- and sex-adjusted  $p<0.001$ ), but not in patients  $\geq 75$  years old (46% vs. 49%, age- and sex-adjusted  $p=0.666$ ).

The association between P/F values on admission arterial blood gas analysis and mortality, according to study period and age range, is depicted in Figure 1. In the 2020 group, increasing P/F values were associated with reduced mortality, although mortality remained higher in subjects  $\geq 75$  years old than in subjects  $<75$  years old for each P/F class (Figure 1). Conversely, in the 2021 group, mortality in subjects  $\geq 75$  years old seemed unrelated with P/F values, while a steep decline was observed in patients  $<75$  years old with  $P/F > 200$  mmHg (Figure 1). Table 4 shows the factors independently associated with P/F values in each age class on stepwise multivariate linear regression models. Admission during the third wave was positively associated with P/F in both subjects aged  $<75$  (standardized  $\beta=0.105$ ,  $p=0.014$ ) and subjects aged 75 or older (standardized  $\beta=0.217$ ,  $p<0.001$ ).

### 4. Discussion

In this retrospective study, we showed that patients admitted for COVID-19 during the third wave in March 2021 had less severe clinical presentation of the disease and reduced mortality, in comparison with patients admitted during the first wave. Patients from the third wave, however, were younger and had less chronic comorbidities.

These findings are apparently in contrast with experimental and epidemiological data suggesting an increased virulence of the B.1.1.7 SARS-CoV-2 lineage (19, 20, 25), that was responsible for the third COVID-19 wave in Italy (18). COVID-19 severity, however, is significantly influenced by age and multimorbidity (3, 6, 26), and an overwhelming majority of older patients dead with COVID-19 had multimorbidity in their personal history (27). Thus, the involvement of a younger and less comorbid population in the COVID-19 pandemic during the third wave could have masked the increased virulence of the B.1.1.7 lineage.

We can hypothesize that this circumstance may have been the result of the anti-SARS-CoV-2 vaccination campaign, that in Italy was started at the end of December 2020 and was initially focused on healthcare professionals and older subjects with frailty (28). By March 2021, when the third wave arose, a significant rate of the older population had been administered anti-SARS-CoV-2 vaccines, though with significant barriers including social disadvantage (29). These vaccines exhibit the maximum effectiveness against SARS-CoV-2 transmission and protection against severe illness for an interval of 6 months after completion of the primary cycle (30), so that we can assume that a significant portion of the frail older population was protected against COVID-19 by March 2021. A recent study conducted in patients with chronic kidney disease undergoing hemodialysis highlighted that vaccination against SARS-CoV-2 was able to modify COVID-19 severity and reduce hospitalization need even in the presence of a condition of extreme vulnerability (31). The different epidemiological characteristics of patients admitted during the third wave could therefore reflect this phenomenon.

Improvements in hospital management of patients could be also responsible for better outcomes in the third wave. In the 2021 group, 96% of patients had received intravenous steroids during hospital stay, in comparison with just 16% in the first wave (Table 1). Intravenous dexamethasone treatment has rapidly gained the role of cornerstone treatment of COVID-19 related interstitial pneumonia, for its capacity of reducing mortality, oxygen supplementation and ventilatory support need (32). Intravenous remdesivir was also commonly used during the third wave, but not in the first one (33). Interestingly, the higher frequencies of NIV support and ICU treatment detected in the third wave (Table 1) could reflect improved management protocols and better understanding of indications and timing of ventilatory escalation in patients with severe respiratory failure. Better supportive care and evidence-based treatment protocols were recognized as the main factors influencing improved outcomes during the third wave also in another study from Italy (34).

Patients admitted during the third wave, however, had not only better outcomes, but also different clinical pictures on hospital admission. During the third wave, the organization of pre-hospital care was improved in comparison with the abrupt emergence of the pandemic. At a community level, medical teams dedicated to home care of COVID-19 patients were formed, prompting early diagnosis and rationalizing pathways of hospital referral for more severe cases (35, 36).

**TABLE 1** Comparison of the main characteristics of COVID-19 presentation and outcomes between patients admitted during the first wave (March 2020,  $n=399$ ) and the third wave (March 2021,  $n=370$ ).

	First wave March 2020 ( $n=399$ )	Third wave March 2021 ( $n=370$ )	$p$	$p^*$
Demography and personal history				
Age, years	72 (61–81)	65 (55–75)	<0.001	–
Females, %	40	40	0.861	–
Chronic illnesses, number	2 (1–4)	2 (1–3)	<0.001	<b>0.023</b>
Hypertension, %	61	52	<b>0.011</b>	0.630
Diabetes, %	22	18	0.139	0.479
Obesity, %	13	15	0.302	0.833
Dyslipidemia, %	21	19	0.624	0.813
Chronic heart disease, %	24	10	<0.001	<0.001
Chronic kidney disease, %	6	2	<b>0.004</b>	<b>0.010</b>
Cancer, %	12	6	<b>0.006</b>	<b>0.021</b>
Drugs, number	3 (1–6)	2 (0–4)	<0.001	<0.001
Clinical presentation upon admission				
Duration of symptoms, days	7 (4–10)	6 (3–9)	0.192	<b>0.017</b>
Fever, %	89	81	<b>0.001</b>	<0.001
Cough, %	53	50	0.421	0.095
Dyspnea, %	49	52	0.291	0.165
Fatigue, %	11	34	<0.001	<0.001
Diarrhea, %	6	17	<0.001	<0.001
Systolic blood pressure, mmHg	130 (120–140)	130 (120–140)	0.948	0.467
Diastolic blood pressure, mmHg	80 (70–80)	80 (70–80)	0.204	0.151
Chest CT visual score, %	30 (15–50)	25 (15–40)	<b>0.009</b>	<b>0.017</b>
P/F ratio, mmHg	233 (121–326)	288 (237–338)	<0.001	<0.001
P/F ratio $\leq$ 100 mmHg, %	20	5	<0.001	<0.001
Blood tests on admission				
Hemoglobin, g/dl	13.8 (12.5–14.9)	13.9 (12.8–15.0)	0.499	0.984
Platelet count, 1,000/mm <sup>3</sup>	195 (152–243)	189 (147–244)	0.716	0.278
Neutrophil count, n/mm <sup>3</sup>	4,721 (3,338–7,284)	4,871 (3,281–6,824)	0.966	0.680
Lymphocyte count, n/mm <sup>3</sup>	893 (630–1,205)	852 (588–1,130)	0.163	<b>0.032</b>
Creatinine, mg/dl	0.9 (0.7–1.2)	0.9 (0.7–1.1)	<b>0.018</b>	0.377
eGFR, ml/min	80 (57–105)	89 (68–113)	<0.001	0.275
D-dimer, ng/ml	922 (600–1,376)	709 (436–1,258)	<0.001	<b>0.022</b>
CRP, mg/L	106 (50–168)	52 (26–96)	<0.001	<0.001
PCT, ng/ml	0.17 (0.09–0.50)	0.09 (0.05–0.23)	<0.001	<0.001
PCT class 1 (<0.05 ng/ml), %	9	22	<0.001	<0.001
PCT class 4 (>2 ng/ml), %	11	3	<0.001	<0.001
Treatments and outcomes				
NIV, %	14	28	<0.001	<0.001
ICU, %	5	13	<0.001	<b>0.002</b>
Intravenous steroids, %	16	96	<0.001	<0.001
Hospital death, %	36	19	<0.001	<0.001
Hospital stay, days	7 (3–12)	14 (9–21)	<0.001	<0.001

Data expressed as median and interquartile range or percentage.  $p$  values calculated with Mann–Whitney or Chi-square test.

\* $p$  adjusted for age and sex with Quade non-parametric ANCOVA or binary logistic regression.  $p$  values < 0.05 are indicated in bold.

CT = computed tomography; P/F = PaO<sub>2</sub>/FiO<sub>2</sub>; eGFR = estimated glomerular filtration rate; CRP = C-reactive protein; PCT = procalcitonin; NIV = non-invasive ventilation; ICU = intensive care unit.



**TABLE 2** Factors associated with hospital mortality on stepwise multivariate logistic regression analysis, considering patients from the first and the third wave altogether.

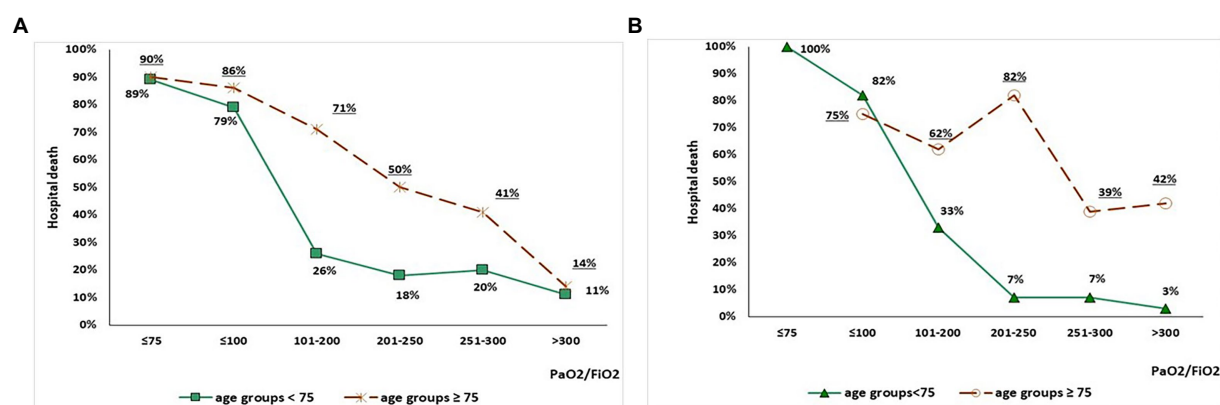
	Odds ratio	95% Confidence interval	<i>p</i>
Age, years	1.061	1.036–1.087	<b>&lt;0.001</b>
Chronic illnesses, number	1.348	1.168–1.555	<b>&lt;0.001</b>
Duration of symptoms, days	0.939	0.889–0.992	<b>0.025</b>
P/F ratio, mmHg	0.991	0.988–0.994	<b>&lt;0.001</b>
Chest CT visual score, %	1.022	1.009–1.036	<b>&lt;0.001</b>
PCT classes, for each incremental class	1.842	1.300–2.610	<b>&lt;0.001</b>

Other variables considered in the model: sex (F vs M), period of admission (third wave vs first wave), fever, cough, dyspnea, fatigue, diarrhea, obesity, diabetes, hypertension, chronic kidney disease, chronic heart disease, cancer, systolic and diastolic blood pressure, hemoglobin, neutrophil count, lymphocyte count, creatinine, C-reactive protein. *p* values < 0.05 are indicated in bold. P/F=PaO<sub>2</sub>/FiO<sub>2</sub>; CT = computed tomography; PCT = procalcitonin.

**TABLE 3** Factors associated with hospital mortality on stepwise multivariate logistic regression analysis, after stratification of participants by COVID-19 wave.

	Odds ratio	95% Confidence interval	WALD	<i>p</i>
First wave, March 2020				
Age, years	1.052	1.022–1.083	12.004	<b>&lt;0.001</b>
P/F ratio, mmHg	0.988	0.984–0.991	53.351	<b>&lt;0.001</b>
Third wave, March 2021				
Age, years	1.094	1.050–1.141	18.176	<b>&lt;0.001</b>
Chronic illnesses, number	1.601	1.275–2.010	16.455	<b>&lt;0.001</b>
Duration of symptoms, days	0.916	0.843–0.996	4.235	<b>0.040</b>
P/F ratio, mmHg	0.991	0.986–0.997	10.509	<b>0.001</b>
Chest CT visual score, %	1.036	1.014–1.059	10.088	<b>0.001</b>
PCT classes, for each incremental class	2.664	1.431–4.961	9.542	<b>0.002</b>

Other variables considered in the model: sex (F vs M), period of admission (third wave vs first wave), fever, cough, dyspnea, fatigue, diarrhea, obesity, diabetes, hypertension, chronic kidney disease, chronic heart disease, cancer, systolic and diastolic blood pressure, hemoglobin, neutrophil count, lymphocyte count, creatinine, C-reactive protein. *p* values < 0.05 are indicated in bold. P/F=PaO<sub>2</sub>/FiO<sub>2</sub>; CT = computed tomography; PCT = procalcitonin.

**FIGURE 1**

Association between P/F values on admission arterial blood gas analysis and mortality in the 2020 group (panel A) and 2021 group (panel B), stratified by age (<75 vs. ≥75 years old).

Home treatment protocols could include administration of anti-inflammatory agents, antivirals or, in selected cases, even corticosteroids (37). These aspects could have influenced the clinical presentation of COVID-19 on admission, with less severe pulmonary involvement and better respiratory exchanges. Similar findings were also observed in

studies comparing the second (autumn 2020) with the first wave (11–16).

The heterogeneity of clinical presentation of SARS-CoV-2 infection, especially with the emergence of novel lineages, should be also considered (38). This characteristic is particularly emphasized in older

**TABLE 4** Stepwise multivariate linear regression models exploring factors independently associated with P/F values in each age class in the studied population of patients from the first and third pandemic wave.

	Standardized beta	T	p
Model 1, patients <75 years old			
Age, years	−0.127	−2.788	<b>0.006</b>
Chronic illnesses, number	−0.097	−2.091	<b>0.037</b>
Presence of dyspnea	−0.120	−2.817	<b>0.005</b>
Period of admission (2021 vs. 2020)	0.105	2.479	<b>0.014</b>
Chest CT visual score, %	−0.463	−10.441	<b>&lt;0.001</b>
Neutrophil count, n/mm <sup>3</sup>	−0.098	−2.287	<b>0.023</b>
Model 2, patients ≥75 years old			
Presence of dyspnea	−0.234	−3.742	<b>&lt;0.001</b>
Period of admission (2021 vs. 2020)	0.217	3.532	<b>&lt;0.001</b>
Chest CT visual score, %	−0.353	−5.212	<b>&lt;0.001</b>
Neutrophil count, n/mm <sup>3</sup>	−0.136	−2.039	<b>0.043</b>

Other variables considered in the model: sex (F vs M), duration of symptoms, fever, cough, fatigue, diarrhea, obesity, diabetes, hypertension, chronic kidney disease, chronic heart disease, cancer, systolic and diastolic blood pressure, hemoglobin, lymphocyte count, creatinine, C-reactive protein, procalcitonin classes. *p* values < 0.05 are indicated in bold. P/F=PaO<sub>2</sub>/FiO<sub>2</sub>.

patients, where the classical association of fever, cough and dyspnea is found less frequently than in younger subjects (39) and extra-pulmonary involvement is more common (40). The demographical differences between the two groups considered in our study could thus contribute to explain also differences in clinical presentation, and not just in outcomes.

Another remarkable finding of our study concerns the outcomes of patients over 75 years old, that were similar between the two considered waves despite significant differences in clinical presentation and improvements in treatment regimens. Namely, in the 2021 group prognosis of subjects over 75 years old was less dependent on respiratory parameters on admission (Figure 1). We can speculate that this phenomenon may be the effect of an increased burden of frailty, influencing weaker response to treatments during the acute phase of the disease (41). Frailty syndrome is in fact one of the main factors influencing adverse outcomes in older subjects with COVID-19 (42).

Unfortunately, frailty was not systematically assessed in all the participants to our study, preventing to include this variable in the analyses. Further limitations include the retrospective design, the exclusion of a large number of patients hospitalized during the first wave for lack of relevant data, and the absence of SARS-CoV-2 genotypization for identification of lineages on nasopharyngeal swabs.

In spite of this, our study provides important insight on the clinical and epidemiological differences of patients hospitalized during the first and third pandemic waves in Italy, eliminating the possible confounding factor of seasonality in SARS-CoV-2 transmission. Although the differences in clinical presentation and outcomes between the third and the first wave allow to advance several epidemiological hypotheses on the evolution of the COVID-19 pandemic, the circumstance that this is a single-center hospital-based study should be also remarked as a limitation. No data were in fact available on the management of patients in the community setting before hospital arrival and on the clinical characteristics of subjects with COVID-19 who did not require hospitalization.

## 5. Conclusion

Patients hospitalized for COVID-19 during the third pandemic wave were younger and had less comorbidities than patients hospitalized during the first wave. Their clinical presentation was also different, with improved P/F ratio on admission and different symptom distribution. Mortality was also improved, but not in patients older than 75 years old. The reasons of these differences, apparently in contrast with the increased reported severity of the SARS-CoV-2 B.1.1.7 lineage, are unclear. They could be related to the effect of vaccination campaigns in older frail subjects, granting protection against severe disease and favoring the spread of the infection among younger unvaccinated subjects, and improvements in pre-hospital and hospital care.

## Data availability statement

The raw data supporting the conclusions of this article will be made available by the authors upon request, without undue reservation.

## Ethics statement

The studies involving human participants were reviewed and approved by Comitato Etico dell'Area Vasta Emilia Nord, Emilia Romagna Region, Italy. The ethics committee waived the requirement of written informed consent for participation.

## Author contributions

AT, DT, and TM: conception and design. AT, AP, AN, NC, BP, and DT: data collection and interpretation. AG: data analysis. AT: manuscript drafting. NG and TM: critical revision for important intellectual content. All authors contributed to the article and approved the submitted version.

## Conflict of interest

The authors declare that the research was conducted in the absence of any commercial or financial relationships that could be construed as a potential conflict of interest.

## Publisher's note

All claims expressed in this article are solely those of the authors and do not necessarily represent those of their affiliated organizations, or those of the publisher, the editors and the reviewers. Any product that may be evaluated in this article, or claim that may be made by its manufacturer, is not guaranteed or endorsed by the publisher.

## Supplementary material

The Supplementary material for this article can be found online at: <https://www.frontiersin.org/articles/10.3389/fmed.2023.1112728/full#supplementary-material>

## References

- Gabutti, C, d'Anchera, E, de Motoli, F, Savio, M, and Stefanati, A. The epidemiological characteristics of the COVID-19 pandemic in Europe: focus on Italy. *Int J Environ Res Public Health*. (2021) 18:2942. doi: 10.3390/ijerph18062942
- Grasselli, G, Zangrillo, A, Zanella, A, Antonelli, M, Cabrini, L, Castelli, A, et al. Baseline characteristics and outcomes of 1591 patients infected with SARS-CoV-2 admitted to ICUs of the Lombardy region, Italy. *JAMA*. (2020) 323:1574–81. doi: 10.1001/jama.2020.5394
- Iaccarino, G, Grassi, G, Borghi, C, Ferri, C, Salvetti, M, Volpe, M, et al. Age and multimorbidity predict death among COVID-19 patients: results of the SARS-RAS study of the Italian Society of Hypertension. *Hypertension*. (2020) 76:366–72. doi: 10.1161/hypertensionaha.120.15324
- Polverino, F, Stern, DA, Ruocco, G, Balestro, E, Bassetti, M, Candelli, M, et al. Comorbidities, cardiovascular therapies, and COVID-19 mortality: a nationwide, Italian observational study (ItaliCO). *Front Cardiovasc Med*. (2020) 7:585866. doi: 10.3389/fcvm.2020.585866
- Okoye, C, Calsolaro, V, Calabrese, AM, Zotti, S, Fedecostante, M, Volpato, S, et al. Determinants of cause-specific mortality and loss of independence in older patients following hospitalization for COVID-19: the GeroCovid outcomes study. *J Clin Med*. (2022) 11:5578. doi: 10.3390/jcm11195578
- Ticinesi, A, Nouvenne, A, Cerundolo, N, Parise, A, Prati, B, Guerra, A, et al. Trends of COVID-19 admissions in an Italian hub during the pandemic peak: large retrospective study focused on older subjects. *J Clin Med*. (2021) 10:1115. doi: 10.3390/jcm10051115
- Gautret, P, Colson, P, Lagier, JC, Camoin-Jau, L, Giraud-Gatineau, A, Boudjema, S, et al. Different pattern of the second outbreak of COVID-19 in Marseille, France. *Int J Infect Dis*. (2021) 102:17–9. doi: 10.1016/j.ijid.2020.10.005
- Byun, WS, Heo, SW, Jo, G, Kim, JW, Kim, S, Lee, S, et al. Is coronavirus disease (COVID-19) seasonal? A critical analysis of empirical and epidemiological studies at global and local scales. *Environ Res*. (2021) 196:110972. doi: 10.1016/j.envres.2021.110972
- Agarwal, A, Rochwerf, B, Lamontagne, F, Siemieniuk, RA, Agoritsas, T, Askie, L, et al. A living WHO guideline on drugs for COVID-19. *BMJ*. (2020) 370:m3379. doi: 10.1136/bmj.m3379
- Gorman, E, Connolly, B, Couper, K, Perkins, GD, and McAuley, DF. Non-invasive respiratory support strategies in COVID-19. *Lancet Respir Med*. (2021) 9:553–6. doi: 10.1016/s2213-2600(21)00168-5
- Meschiari, M, Cozzi-Lepri, A, Tonelli, R, Bacca, E, Menozzi, M, Franceschini, E, et al. First and second waves among hospitalised patients with COVID-19 with severe pneumonia: a comparison of 28-day mortality over the 1-year pandemic in a tertiary university hospital in Italy. *BMJ Open*. (2022) 12:e054069. doi: 10.1136/bmjopen-2021-054069
- Budweiser, S, Baş, Ş, Jörres, RA, Engelhardt, S, Thilo, C, von Delius, S, et al. Comparison of the first and second waves of hospitalized patients with SARS-CoV-2. *Dtsch Arztebl Int*. (2021) 118:326–7. doi: 10.3238/arztebl.m2021.0215
- Blanca, D, Nicolosi, S, Bandera, A, Blasi, F, Mantero, M, Hu, C, et al. Comparison between the first and second COVID-19 waves in internal medicine wards in Milan, Italy: a retrospective observational study. *Intern Emerg Med*. (2022) 17:2219–28. doi: 10.1007/s11739-022-03052-3
- Naushad, VA, Purayil, NK, Chandra, P, Saeed, AAM, Radhakrishnan, P, Varikkodan, I, et al. Comparison of demographic, clinical and laboratory characteristics between first and second COVID-19 waves in a secondary care hospital in Qatar: a retrospective study. *BMJ Open*. (2022) 12:e061610. doi: 10.1136/bmjopen-2022-061610
- Wolfsberg, S, Gregoriano, C, Struja, T, Kutz, A, Koch, D, Bernasconi, L, et al. Comparison of characteristics, predictors and outcomes between the first and second COVID-19 waves in a tertiary care Centre in Switzerland: an observational analysis. *Swiss Med Wkly*. (2021) 151:w20569. doi: 10.4414/smww.2021.20569
- Buttenshon, HN, Lyngaard, V, Sandbøl, SG, Glassou, EA, and Haagerup, A. Comparison of the clinical presentation across two waves of COVID-19: a retrospective cohort study. *BMC Infect Dis*. (2022) 22:423. doi: 10.1186/s12879-022-07413-3
- Carbonell, R, Urgelès, S, Rodríguez, A, Bodí, M, Martín-Loeches, I, Solé-Violán, J, et al. Mortality comparison between the first and second/third waves among 3,795 critical COVID-19 patients with pneumonia admitted to the ICU: a multicenter retrospective cohort study. *Lancet Reg Health Eur*. (2021) 11:100243. doi: 10.1016/j.lanepe.2021.100243
- Istituto Superiore di Sanità (2021). CS N° 20/2021—Covid-19: in Italia la 'variante inglese' all'86,7% Il 4,0% dei casi con quella 'brasiliiana'. *Comunicato* (Italian Language). Available at: <https://www.iss.it/web/guest/primopiano/-/asset-publisher/3f4alMwzN1Z7/content/id/5683229#:~:text=ISS%2C%2030%20marzo%202021%20%2D%20In,sotto%20lo%200%2C%2525>. Accessed on October 25, 2022.
- Fisman, DR, and Tuite, AR. Evaluation of the relative virulence of novel SARS-CoV-2 variants: a retrospective cohort study in Ontario, Canada. *CMAJ*. (2021) 193:E1619–25. doi: 10.1503/cmaj.211248
- Dabrera, G, Allen, H, Zaidi, A, Flannagan, J, Twohig, K, Thelwall, S, et al. Assessment of mortality and hospital admissions associated with confirmed infection with SARS-CoV-2 alpha variant: a matched cohort and time-to-event analysis, England, October to December 2020. *Eur Secur*. (2022) 27:2100377. doi: 10.2807/1560-7917.es.2022.27.20.2100377
- Meschi, T, Rossi, S, Volpi, A, Ferrari, C, Sverzellati, N, Brianti, E, et al. Reorganization of a large academic hospital to face COVID-19 outbreak: the model of Parma, Emilia-Romagna region, Italy. *Eur J Clin Invest*. (2020) 50:e13250. doi: 10.1111/eci.13250
- Nouvenne, A, Zani, MD, Milanese, G, Parise, A, Baciarello, M, Bignami, EG, et al. Lung ultrasound in COVID-19 pneumonia: correlations with chest CT on hospital admission. *Respiration*. (2020) 99:617–24. doi: 10.1159/000509223
- Ticinesi, A, Nouvenne, A, Prati, B, Guida, L, Parise, A, Cerundolo, N, et al. The clinical significance of procalcitonin elevation in patients over 75 years old admitted for COVID-19 pneumonia. *Mediat Inflamm*. (2021) 2021:5593806. doi: 10.1155/2021/5593806
- Bonaventura, A, Mumoli, N, Mazzone, A, Colombo, A, Evangelista, I, Cerutti, S, et al. Correlation of SpO2/FiO2 and PaO2/FiO2 in patients with symptomatic COVID-19: an observational, retrospective study. *Intern Emerg Med*. (2022) 17:1769–75. doi: 10.1007/s11739-022-02981-3
- Davies, NG, Abbott, S, Barnard, RC, Jarvis, CI, Kucharski, AJ, Munday, JD, et al. Estimated transmissibility and impact of SARS-CoV-2 lineage B.1.1.7 in England. *Science*. (2021) 372. doi: 10.1126/science.abg3055
- Marengoni, A, Zucchelli, A, Vetrano, DL, Armellini, A, Botteri, E, Nicosia, F, et al. Beyond chronological age: frailty and multimorbidity predict in-hospital mortality in patients with coronavirus disease 2019. *J Gerontol A Biol Sci Med Sci*. (2021) 76:e38–45. doi: 10.1093/gerona/glaa291
- Vetrano, DL, Tazzeo, C, Palmieri, L, Marengoni, A, Zucchelli, A, Lo Noce, C, et al. Comorbidity status of deceased COVID-19 in-patients in Italy. *Aging Clin Exp Res*. (2021) 33:2361–5. doi: 10.1007/s40520-021-01914-y
- Papini, F, Grassi, N, Guglielmi, G, Gattini, V, Rago, L, Bisordi, C, et al. Covid-19 vaccine management (Comirnaty and mrna-1273 Moderna) in a teaching hospital in Italy: a short report on the vaccination campaign. *Environ Health Prev Med*. (2021) 26:99. doi: 10.1186/s12199-021-01018-z
- Russo, AG, Tunesi, S, Consolazio, D, Decarli, A, and Bergamaschi, W. Evaluation of the anti-COVID-19 vaccination campaign in the metropolitan area of Milan (Lombardy region, northern Italy). *Epidemiol Prev*. (2021) 45:568–79. doi: 10.19191/ep21.6.114
- Feikin, DR, Higdon, MM, Abu-Raddad, LJ, Andrews, N, Araos, R, Goldberg, Y, et al. Duration of effectiveness of vaccines against SARS-CoV-2 infection and COVID-19 disease: results of a systematic review and meta-regression. *Lancet*. (2022) 399:924–44. doi: 10.1016/S0140-6736(22)00152-0
- Espósito, R, Picciotto, D, Cappadona, F, Russo, E, Falqui, V, Conti, NE, et al. The evolving scenario of COVID-19 in hemodialysis patients. *Int J Environ Res Public Health*. (2022) 19:10836. doi: 10.3390/ijerph191710836
- Wagner, C, Griesel, M, Mikolajewska, A, Mueller, A, Nothacker, M, Kley, K, et al. Systemic corticosteroids for the treatment of COVID-19. *Cochrane Database Syst Rev*. (2021) 2021. doi: 10.1002/14651858.cd014963
- Ticinesi, A, Tuttolomondo, D, Nouvenne, A, Parise, A, Cerundolo, N, Prati, B, et al. Co-Administration of Remdesivir and Azithromycin may Protect against intensive care unit admission in COVID-19 pneumonia requiring hospitalization: a real-life observational study. *Antibiotics*. (2022) 11:941. doi: 10.3390/antibiotics11070941
- Leidi, F, Boari, GEM, Scarano, O, Mangili, B, Gorla, B, Corbani, A, et al. Comparison of the characteristics, morbidity and mortality of COVID-19 between first and second/third wave in a hospital setting in Lombardy: a retrospective cohort study. *Intern Emerg Med*. (2022) 17:1941–9. doi: 10.1007/s11739-022-03034-5
- Nouvenne, A, Ticinesi, A, Parise, A, Prati, B, Espósito, M, Cocchi, V, et al. Point-of-care chest ultrasonography as a diagnostic resource for COVID-19 outbreak in nursing homes. *J Am Med Dir Assoc*. (2020) 21:919–23. doi: 10.1016/j.jamda.2020.05.050
- D'Ardes, D, Tana, C, Salzmann, A, Ricci, F, Guagnano, MT, Giamberardino, MA, et al. Ultrasound assessment of SARS-CoV-2 pneumonia: a literature review for the primary care physician. *Ann Med*. (2022) 54:1140–9. doi: 10.1080/07853890.2022.2067896
- Perico, N, Cortinovis, M, Suter, F, and Remuzzi, G. Home as the new frontier for the treatment of COVID-19: the case for anti-inflammatory agents. *Lancet Infect Dis*. (2022) Epub ahead of preprint Aug 25) 23:e22–33. doi: 10.1016/S1473-3099(22)00433-9
- Larsen, JR, Martin, MR, Martin, JD, Hicks, JB, and Kuhn, P. Modelling the onset of symptoms of COVID-19: effects of SARS-CoV-2 variant. *PLoS Comput Biol*. (2021) 17:e1009629. doi: 10.1371/journal.pcbi.1009629
- Trevisan, C, Remelli, F, Fumagalli, S, Mossello, E, Okoye, C, Bellelli, G, et al. COVID-19 as a paradigmatic model of the heterogeneous disease presentation in older people: data from the GeroCovid observational study. *Rejuvenation Res*. (2022) 25:129–40. doi: 10.1089/rej.2021.0063
- Tuttolomondo, D, Frizzelli, A, Aiello, M, Bertorelli, G, Majori, M, and Chetta, A. Beyond lung involvement in COVID-19 patients. *Minerva Med*. (2022) 113:558–68. doi: 10.23736/s0026-4806.20.06719-1
- Hatheway, OL, Mitnitski, A, and Rockwood, K. Frailty affects the initial treatment response and time to recovery of mobility in acutely ill older adults admitted to hospital. *Age Ageing*. (2017) 46:920–5. doi: 10.1093/ageing/afw257
- Kastora, S, Kounidas, G, Perrott, S, Carter, B, Hewitt, J, and Myint, PK. Clinical frailty scale as a point of care prognostic indicator of mortality in COVID-19: a systematic review and meta-analysis. *eClinicalMedicine*. (2021) 36:100896. doi: 10.1016/j.eclim.2021.100896



## OPEN ACCESS

## EDITED BY

Alfonso J. Rodriguez-Morales,  
Fundacion Universitaria Autónoma de las  
Américas, Colombia

## REVIEWED BY

Safaet Alam,  
Bangladesh Council of Scientific and  
Industrial Research (BCSIR), Bangladesh  
Desh Deepak Singh,  
Amity University Rajasthan, India

## \*CORRESPONDENCE

Amit Awasthi

✉ aawasthi@thsti.res.in

Madhu Dikshit

✉ drmadhudikshit@gmail.com;

✉ madhu.dikshit@cdri.res.in

Zaigham Abbas Rizvi

✉ zaigham.abbas15@gmail.com

## SPECIALTY SECTION

This article was submitted to  
Viral Immunology,  
a section of the journal  
Frontiers in Immunology

RECEIVED 05 January 2023

ACCEPTED 20 February 2023

PUBLISHED 07 March 2023

## CITATION

Rizvi ZA, Babele P, Madan U, Sadhu S,  
Tripathy MR, Goswami S, Mani S, Dikshit M  
and Awasthi A (2023) Pharmacological  
potential of *Withania somnifera*  
(L.) Dunal and *Tinospora cordifolia* (Willd.)  
Miers on the experimental models of  
COVID-19, T cell differentiation,  
and neutrophil functions.  
*Front. Immunol.* 14:1138215.  
doi: 10.3389/fimmu.2023.1138215

## COPYRIGHT

© 2023 Rizvi, Babele, Madan, Sadhu,  
Tripathy, Goswami, Mani, Dikshit and  
Awasthi. This is an open-access article  
distributed under the terms of the [Creative  
Commons Attribution License \(CC BY\)](#). The  
use, distribution or reproduction in other  
forums is permitted, provided the original  
author(s) and the copyright owner(s) are  
credited and that the original publication in  
this journal is cited, in accordance with  
accepted academic practice. No use,  
distribution or reproduction is permitted  
which does not comply with these terms.

# Pharmacological potential of *Withania somnifera* (L.) Dunal and *Tinospora cordifolia* (Willd.) Miers on the experimental models of COVID-19, T cell differentiation, and neutrophil functions

Zaigham Abbas Rizvi<sup>1,2\*</sup>, Prabhakar Babele<sup>3</sup>, Upasna Madan<sup>1,2</sup>,  
Srikanth Sadhu<sup>1,2</sup>, Manas Ranjan Tripathy<sup>1,2</sup>,  
Sandeep Goswami<sup>1,2</sup>, Shailendra Mani<sup>3</sup>, Madhu Dikshit<sup>3,4\*</sup>  
and Amit Awasthi<sup>1,2\*</sup>

<sup>1</sup>Immuno-biology Lab, Translational Health Science and Technology Institute, NCR-Biotech Science Cluster, Faridabad, Haryana, India, <sup>2</sup>Immunology-Core Lab, Translational Health Science and Technology Institute, NCR-Biotech Science Cluster, Faridabad, Haryana, India, <sup>3</sup>NCD, Translational Health Science and Technology Institute (THSTI), NCR Biotech Science Cluster, Faridabad, Haryana, India, <sup>4</sup>Pharmacology, CSIR-Central Drug Research Institute, Lucknow, Uttar Pradesh, India

Cytokine release syndrome (CRS) due to severe acute respiratory coronavirus-2 (SARS-CoV-2) infection leads to life-threatening pneumonia which has been associated with coronavirus disease (COVID-19) pathologies. Centuries-old Asian traditional medicines such as *Withania somnifera* (L.) Dunal (WS) and *Tinospora cordifolia* (Willd.) Miers (TC) possess potent immunomodulatory effects and were used by the AYUSH ministry, in India during the COVID-19 pandemic. In the present study, we investigated WS and TC's anti-viral and immunomodulatory efficacy at the human equivalent doses using suitable *in vitro* and *in vivo* models. While both WS and TC showed immuno-modulatory potential, WS showed robust protection against loss in body weight, viral load, and pulmonary pathology in the hamster model of SARS-CoV2. *In vitro* pretreatment of mice and human neutrophils with WS and TC had no adverse effect on PMA, calcium ionophore, and TRLM-induced ROS generation, phagocytosis, bactericidal activity, and NETs formation. Interestingly, WS significantly suppressed the pro-inflammatory cytokines-induced Th1, Th2, and Th17 differentiation. We also used hACE2 transgenic mice to further investigate the efficacy of WS against acute SARS-CoV2 infection. Prophylactic treatment of WS in the hACE2 mice model showed significant protection against body weight loss, inflammation, and the lung viral load. The results obtained indicate that WS promoted the immunosuppressive environment in the hamster and hACE2 transgenic mice models and limited the worsening of the disease by



reducing inflammation, suggesting that WS might be useful against other acute viral infections. The present study thus provides pre-clinical efficacy data to demonstrate a robust protective effect of WS against COVID-19 through its broader immunomodulatory activity

#### KEYWORDS

*Withania somnifera* (Ashwagandha), *Tinospora cordifolia*, SARS-CoV-2, hamster model, T cells, neutrophils, and hACE2 transgenic mice, COVID-19

## Introduction

The first reported case of SARS-CoV-2 was in 2019 and has since then become a predominant cause of global morbidity and mortality (1). COVID-19 was declared a pandemic by the World Health Organization (WHO) in March 2020 demanding the development of therapeutic interventions and vaccine candidates to mitigate COVID-19-related pathology and mortality (2–5). One of the hallmarks of severe COVID-19 is cytokine release syndrome (CRS) which is responsible for elevated pro-inflammatory cytokines in the pulmonary region leading to respiratory distress (6–9). Moreover, attenuated functionality in other major organs or multiple organ failure has also been manifested in a significant number of COVID-19 cases (10–12). Active vaccination strategy helped in alleviating the COVID-19 severity and related death, however, the continuous evolution of the ancestral virus using acquiring mutations led to immune evasion and poorer protection against variants of concern (VoC) and emerging variants of SARS-CoV-2 (13, 14). In addition, COVID-19 vaccines may not be sufficient to confer protection in immunocompromised individuals or the individuals with comorbid conditions. Therapeutic antiviral drugs such as Remdesivir (RDV) and immunosuppression by Dexamethasone (DXM) were the most acceptable therapeutic options against SARS-CoV-2 infection. While DXM was effective in reducing the overall morbidity and mortality arising due to COVID-19 and showed success in clinical trials, a randomized clinical trial of RDV did not show any significant protection in COVID-19 deaths and was marginally successful in giving relief from clinical symptoms (15, 16).

In addition, a major issue with synthetic drugs is also their off-target reactivity limiting their usage in clinical cases. DXM, for example, is a broad immuno-suppressant drug and is known to suppress the overall immune response which may lead to a rise in opportunistic pathogenic infections and other life-threatening complications (17). The alternate strategy of COVID-19 management includes prophylaxis or preventative strategies with immunomodulators to improve immunity against SARS-CoV-2 infection. In this regard, plant-derived immunomodulators have gained considerable interest owing to their prolonged human use and better safety. The emerging line of evidence has shown that the use of herbal extracts from traditional medicine systems might help in mitigating the COVID-19 pathology (18–20). In the current

study, we investigated the efficacy of WS (Ashwagandha), TC (Guduchi), and *Piper longum* L. (Thippali), in the *in vitro* cell-based systems and animal models. WS, a shrub traditionally used in India and other Asian countries, is known to possess immunomodulatory properties. Previous *in-vitro* and *in-vivo* studies have shown that WS could play a role in the regulation of inflammation by suppressing pro-inflammatory cytokines (21–24). More recently, in-silico docking studies showed the potent inhibitory potential of Withanone, an active ingredient of WS, against SARS-CoV-2 virulence proteins such as spike protein (22, 25). Other reports have shown Withaferin A, a bioactive steroidal lactone derived from WS, to be anti-inflammatory by reducing the levels of inflammatory cytokines such as IL-6 and TNF $\alpha$  which is desirable in COVID-19 patients to alleviate pulmonary pathology (26, 27). More recently, we have also characterized the anti-viral component of WS which was found to exhibit potent anti-viral property *in-vitro* (28). Similarly, TC and PL have also been shown to modulate inflammatory responses in various disease conditions. TC, particularly, was found to exert anti-viral activity against SARS-CoV-2 in *in-silico* and *in-vitro* studies (25). However, there is still a lack of evidence on the protective efficacy and immunomodulatory potential of these herbal extracts in the *in-vivo* models of COVID-19.

To address these questions, we used hamster (chronic model) and hACE2.Tg mice (acute model) to evaluate the protective efficacy of WS, TC, and PL and the immunological correlates of protection in COVID-19. Our data from the hamster challenge study showed that prophylactic dosing of WS, but not TC or TC in combination with PL (TC+PL), was able to significantly reduce body weight loss. In line with this, WS dosing showed significantly decreased lung viral load, pulmonary pathology, and suppression of inflammatory cytokine mRNA expression. In contrast, the TC group showed robust anti-inflammatory potential but no viral load and pathology alleviation. Next, we used cellular T-cell assay to show potent inhibition of Th1, Th2, and Th17 differentiation in presence of WS, while TC was found to inhibit Th1, Th2, and Th17 differentiation only at higher doses. To understand the effector immune population, we used hACE2.Tg model and show that WS administration results in boosting the immunosuppressive environment in SARS-CoV-2 infected mice which leads to amelioration of pulmonary pathology and significant protection against COVID-19 morbidity and mortality. Together, we provide data from moderate and acute SARS-CoV-2 animal challenge



studies suggesting robust protective efficacy by prophylactic WS and determining the immune correlates of protection. Our *in-vitro* and *in-vivo* results support the translational value of WS against COVID-19 and provide the basis for further clinical evaluations.

## Materials and methods

WS, TC, and PL extract was provided by National Medicinal Plant Board and was used as per pharmacopeial standards in the current study for both *in-vitro* and *in-vivo* evaluations.

## Animal ethics and biosafety statement

6-8 weeks of K18-humanized ACE2 transgenic mice (hACE2. Tg mice) were initially procured from Jackson's laboratory and then bred and maintained at the small animal facility (SAF), THST. Golden Syrian hamsters (6-9 weeks) were procured from the Central drug research institute (CDRI) and were used for experimentation post-quarantine. The animals were randomly divided into 5 groups based on their body weight viz uninfected (UI), Infected (I), Infected treated with remdesivir (I+RDV), Infected treated with WS (I+WS), Infected treated with TC (I+TC) and infected treated with TC+PL (I+TC+PL). The hamster prophylactic WS, TC or TC+PL group started receiving twice-daily oral doses of 130 mg/kg (0.5% CMC preparation) 5 days before the challenge and continued till the endpoint. The hACE2 transgenic mice group started receiving prophylactic WS, TC or TC+PL group started receiving twice-daily oral doses of 78 mg/kg (0.5% CMC preparation) 5 days before the challenge and continued till the endpoint. The hamster remdesivir control group received 15mpk (subcutaneous: sc) on 1 day before and 1 day after the challenge while hACE2 transgenic mice received 25mpk (intraperitoneal: ip) injections of remdesivir started on the same day of infection and continued till the end point. The animals were shifted to ABSL3 1 day prior to the challenge. Live intranasal infection of SARS-CoV-2 SARS-Related Coronavirus 2, Isolate USA-WA1/2020) 10<sup>5</sup>PFU/100µl (for hamster) and 10<sup>5</sup>PFU/50µl (for mice) or with DMEM mock control was established with the help of catheter under mild anesthetized by using ketamine (150mg/kg) and xylazine (10mg/kg) intraperitoneal injection inside ABSL3 facility (29–34). Experimental protocols related to handling and experimentation was approved by RCGM, institutional biosafety, and IAEC (IAEC/THSTI/105) animal ethics committee.

## Preparation and characterization of WS, TC, PL extract

1g of dry powder of WS (roots), TC (stem), and PL (seeds) were dissolved in 100 ml of water at 37°C overnight in a shaker incubator to obtain the herbal extracts. The following day, the suspended extract was centrifuged at high speed 10000 x g for 30 min. The supernatant thus obtained was filtrated by using a 0.45 filter. The filtrate obtained was assumed to be 100% aqueous extract which was

further diluted in water to achieve a dosing concentration. The filtrate was further used for evaluating the composition and was previously published (28).

## Virus culture and titration

Dulbecco's Modified Eagle Medium (DMEM) complete media containing 4.5 g/L D-glucose, 100,000 U/L Penicillin-Streptomycin, 100 mg/L sodium pyruvate, 25mM HEPES and 2% FBS was used to propagate and titrate SARS-Related Coronavirus 2, Isolate USA-WA1/2020 virus in Vero E6 cell line. The plaque-purified stocks of virus were prepared and used inside at ABSL3 facility at IDRF, THSTI in accordance with the IBSC and RCGM protocols.

## Gross clinical parameters of SARS-CoV2 infection

For mice experiment the endpoint of the study was day 6 post-challenge, while for hamster study the endpoint was 4 days post-challenge. The animal body weight was recorded for everyday post challenge. At the end point all the animals were sacrificed and a necropsy was performed to investigate lungs and spleen. Gross morphological changes were recorded and imaging was performed for excised lungs and spleen. For histological analysis, left lower lobe of the lung was excised and fixed in 10% formalin (31, 33, 35). Lungs were homogenized in Trizol for RNA isolation while spleen was either homogenized (hamster) or used for flow cytometry (hACE2 transgenic mice) (30). The homogenized samples were immediately stored at -80 °C till further use. Serum samples isolated from blood w immediately stored at -80 °C till further use.

## Viral load

Isolated lung was homogenized in 2ml Trizol reagent (Invitrogen) and RNA was isolated by Trizol-Choloform method. Yield of RNA was quantitated by nano-drop and 1 µg of RNA was use to reverse-transcribed to cDNA using the iScript cDNA synthesis kit (BIORAD; #1708891) (Roche). 1:5 diluted cDNAs was used for qPCR by using KAPA SYBR<sup>®</sup> FAST qPCR Master Mix (5X) Universal Kit (KK4600) on Fast 7500 Dx real-time PCR system (Applied Biosystems) and the results were analyzed with SDS2.1 software (30, 33). Briefly, 200 ng of RNA was used as a template for reverse transcription-polymerase chain reaction (RT-PCR). The CDC-approved commercial kit was used for of SARS-CoV-2 N gene: 5'-GACCCCAAAATCAGCGAAAT-3' (Forward), 5'-TCTG GTTACTGCCAGTTGAATCTG-3' (Reverse). Hypoxanthine-guanine phosphoribosyl transferase (HGPRT) gene was used as an endogenous control for normalization through quantitative RT-PCR. The relative expression of each gene was expressed as fold change and was calculated by subtracting the cycling threshold (Ct) value of hypoxanthine-guanine phosphoribosyl transferase (HGPRT-endogenous control gene) from the Ct value of the

target gene ( $\Delta$ CT). Fold change was then calculated according to the formula  $POWER(2, -\Delta$ CT) $\times 10,000$  (36, 37).

## qPCR from splenocytes

RNA isolated from spleen samples were converted into cDNA as described above. Thereafter, the relative expression of each gene was expressed as fold change and was calculated by subtracting the cycling threshold (Ct) value of hypoxanthine-guanine phosphoribosyl transferase (HGPRT-endogenous control gene) from the Ct value of target gene ( $\Delta$ CT). Fold change was then calculated according to the formula  $POWER(2, -\Delta$ CT) $\times 10,000$  (36–38). The list of the primers is provided in Table 1 as follows.

## Histology

Formalin-fixed samples of lungs were embedded in paraffin blocks, sectioned and stained with hematoxylin and eosin dye as previously described (35, 36). Strained lung samples were then analysed and imaged at 40X. Histological assessment for pathological features was done by professional histologist in a blinded manner and scoring was carried out on a scale of 0–5 (where 0 indicated the absence of histological feature while 5

indicated the highest score). Disease index score was calculated by the addition of all the individual histological scores.

## In vitro differentiation of T cells

The single cell suspension was prepared from spleen and lymph nodes of 6–8 weeks old C57BL/6 mice. The cells were activated using soluble anti-CD3 (2ug/ml) and differentiated into Th1 conditions by adding recombinant mouse IL-12 (15ng/ml) cytokine or Th2 conditions by adding recombinant mouse IL-4 (15ng/ml) cytokine or Th17 conditions by adding TGF-beta (2ng/ml) plus IL-6 cytokine (25ng/ml) (37, 39). WS or TC was added in concentrations ranging from 10ug/ml to 1000ug/ml at the start of culture. Cells were harvested after 72 hours of culture. Intracellular cytokine staining was performed to check the expression of IFN-gamma, IL-4 and IL-17 cytokine for Th1, Th2 and Th17 cells respectively.

## Intracellular cytokine staining

Surface markers were stained for 15–20 min in room temperature in PBS with 1% FBS, then were fixed in Cytofix and permeabilized with Perm/Wash Buffer using Fixation Permeabilization solution kit and stained anti-IL-17A; anti-IFN-gamma, anti-IL-4 diluted in Perm/Wash buffer. All antibodies were used in 1:500 dilution. The cells were then taken for flow cytometry using BD FACS-CantoII and data was analyzed with FlowJo software (32, 36, 37).

## Isolation of murine BMDNs and human peripheral neutrophils

Murine BMDNs were isolated according to the method described by Rizvi et al., 2022 from long bones of C57BL/6 wild-type male mice (12–16 weeks, 20–25 g) (31). After flushing the long bones with HBSS + 0.1% BSA, BMDNs were collected between the 81% and 62% layers of the Percoll (Sigma GE17-0891-02) density gradient. Cell viability and purity were checked by Trypan blue and anti-Ly6G (Thermo 14-5931-82) and anti-CD11b (Thermo 14-0112-82) antibodies, respectively. Similarly, human PMNs were also isolated from the peripheral blood of healthy individuals, after sedimenting the RBCs with 6% dextran at 37°C. Isolated neutrophils were assessed by CD15 (Thermo 14-0159-82) labeling for their purity. All the studies on mice were approved by the institutional animal (THSTI/105) and human (THS1.8.1/100) ethical committees, DBT-THSTI, Faridabad.

## Cell viability assay

Different concentrations of the extracts, ranging from 100–1000  $\mu$ g/ml were used to determine, if any, cytotoxicity on

TABLE 1 Mouse qPCR primers.

Gene	Forward	Reverse
HGPRT	GATAGATCCACTCCC ATAACTG	TACCTTCAACAATCAAGA CATTC
tryptase $\beta$ 2	TCGCCACTGTATCCCC TGAA	CTAGGCACCCTTGACTT TGC
chymase	ATGAACCACCCTCGG ACACT	AGAAGGGGGCTTTGCAT TCC
muc1	CGGAAGAACTATGGG CAGCT	GCCACTACTGGGTTGGTG TAAG
Sftp-D	TGAGCATGACAGACG TGGAC	GGCTTAGAACTCGCAGA CGA
Eotaxin	ATGTGCTCTCAGGTC ATCGC	TCCTCAGTTGTCCCCAT CCT
PAI-1	CCGTGGAACCAGAAC GAGAT	ACCAGAATGAGGCGTGT CAG
IFN $\gamma$	TGTTGCTCTGCCTCA CTCAGG	AAGACGAGGTCCCTCCA TTC
TNF $\alpha$	AGAATCCGGGCAGG TCTACT	TATCCCGGCAGCTTGTG TTT
IL13	AAATGGCGGGTTCT GTGC	AATATCCTCTGGGTCTTGTAG ATGG
IL17A	ATGTCCAAACACTGAG GCCAA	GCGAAGTGGATCTGTTGA GGT
IL10	GGTTGCCAAACCTTATC AGAA ATG	TTCACCTGTTCCACAGCC TTG
IL6	GGACAATGACTATGTGT TGTTAGAA	AGGCAAAATTTCCCAATTGTATC CAG

neutrophils up to 240 min (40).  $1.0 \times 10^6$  per ml cells were incubated with propidium iodide (PI, 50  $\mu\text{g/ml}$ , Sigma P4170) for 15 min and analyzed on BD FACS Canto cell analyzer (BD Biosciences, USA).

## Intracellular ROS and mtROS analysis

Both cytosolic and mitochondrial ROS were measured with DCFH-DA (10  $\mu\text{M}$ , Sigma D6883) and MitoSOX (10  $\mu\text{M}$ , Thermo M36008), respectively as previously reported (40). Extract pre-incubated cells ( $1.0 \times 10^6$  cells/ml) were treated with different interventions such as TRLM (10  $\mu\text{M}$ , MedChem HY-109104), PMA (10–100 nM, Sigma P1585), A23187 (1–5  $\mu\text{M}$ , Sigma C5149), ionomycin (1–4  $\mu\text{M}$ , Sigma I9657), NAC (10  $\mu\text{M}$ , Sigma A9165), and MitoTEMPO (10  $\mu\text{M}$ , Sigma SML0737). DMSO (0.1%) was used as a control. A minimum of 10,000 events were acquired for each sample using BD FACS Canto II.

## NETosis assay

$5.0 \times 10^4$  cells were incubated with both the extract for 60 min at 37°C, followed by treatment with TRLM (10  $\mu\text{M}$ ), PMA (10  $\mu\text{M}$ ), A23187 (1  $\mu\text{M}$ ), ionomycin (1  $\mu\text{M}$ ), or vehicle (DMSO 0.1%). SYTOX Green (100 nM, Thermo S7020) was used to monitor the fluorescence at different time periods up to 240 min in a plate reader at 37°C (Synergy 2; BioTek) as described earlier (Rizvi et al., 2022). Additionally, immunofluorescence images were also developed using anti-MPO (Santa Cruz Sc390109) and anti-H4Cit3 (Sigma 07-596) antibodies by confocal microscope (Olympus FV3000) at 100X resolution.

## Phagocytosis and bactericidal assay

Phagocytosis was accessed by adding PE-labelled latex beads (Sigma L2778) to extract pre-treated PMNs ( $1.0 \times 10^4$ ) at a 1:50 ratio using FACS (41). The bactericidal activity of neutrophils was accessed by first incubating the cells with extracts and then treating them with kanamycin-resistant *E. coli* for 30 min at 37°C. Internalized bacteria were plated on LB agar after the lysis of PMNs. The killing activity is expressed as a percent of CFU in the presence/absence of PMNs.

## Statistical analysis

All the experiments have been carried out independently in triplicate. Results are being expressed as mean  $\pm$  SEM. Multiple group comparisons have been performed using one-way ANOVA followed by the Bonferroni test using GraphPad Prism 8. The differences have been considered as statistically significant when the *p*-value was  $< 0.05$ .

## Results

### Prophylactic use of WS, but not TC, limits SARS-CoV-2-induced pulmonary pathology in hamsters

To determine and evaluate the therapeutic potential of WS and TC (two commonly used traditional herbs) against COVID-19, we used a previously established hamster model for SARS-CoV-2 infection which has been shown to mimic moderate COVID-19 pathology (30, 31, 33, 42, 43). The dosing regimen involved prophylactic intra-gastric administration of WS, TC, or TC+PL for 5 days before intranasal SARS-CoV-2 challenge in hamsters which was continued till the end point of the study (4 days post-infection, dpi). RDV was used as a prototypic anti-viral as a positive control to compare the *in vivo* results. Though, RDV in clinical trials results in marginal protection against morbidity, in animal studies RDV has been shown to provide robust protection against COVID-19. The schematic summary of the dosing regimen and study design is shown in Figure 1A. Our hamster challenge data indicated that prophylactic dosing of WS was able to significantly reduce the body mass loss following SARS-CoV-2 infection as compared to the (I+WS). This protection against mass loss was found to be similar to that of the RDV-treated group (Figure 1B). However, both TC and TC+PL treated groups showed 4–8% body mass loss at 4 dpi when compared to the uninfected group (UI) (Figure 1B). Since protection in body mass loss is correlated with the decreased lung viral load and pathology, we next examined the gross morphological manifestation in excised lungs post necropsy and the corresponding lung viral load. Our data show significantly reduced pathological features and relative N gene expression in the lungs in the WS treatment group, as compared to the infected group, which was similar to the reduction seen in the RDV group. The TC and TC+PL group showed no significant reduction in the pathology and viral load in the lungs (Figures 1C, D).

In a significant percentage of clinical cases, COVID-19 is characterized by inflammation in the lungs leading to pneumonitis and cellular injury (44). We, therefore, set out to understand the degree of protection in pulmonary pathology by WS, TC, and TC+PL groups. Blinded-random histopathological assessment of the lung sections by a trained pathologist showed robust overall protection in the hamsters receiving WS in terms of overall mitigation in pneumonitis, bronchitis, epithelial injury, lung injury, and inflammation score which was Together, we provide pre-clinical data from mild and severe infection models suggesting robust protection by WS against COVID-19 through its broader immunomodulatory activity. Our study supports the evaluation of WS alone or as a formulation for therapeutic intervention against acute viral infections.

Similar to the degree of protection in the RDV-treated group. TC and TC+PL groups, however, failed to alleviate the overall pathological score of the lungs (Figures 1E, F). Next, to understand the mechanism we evaluated the expression of genes involved in lung injury. Chymase and tryptase are effector enzymes secreted by mast cells that have been implicated in COVID-19 pulmonary



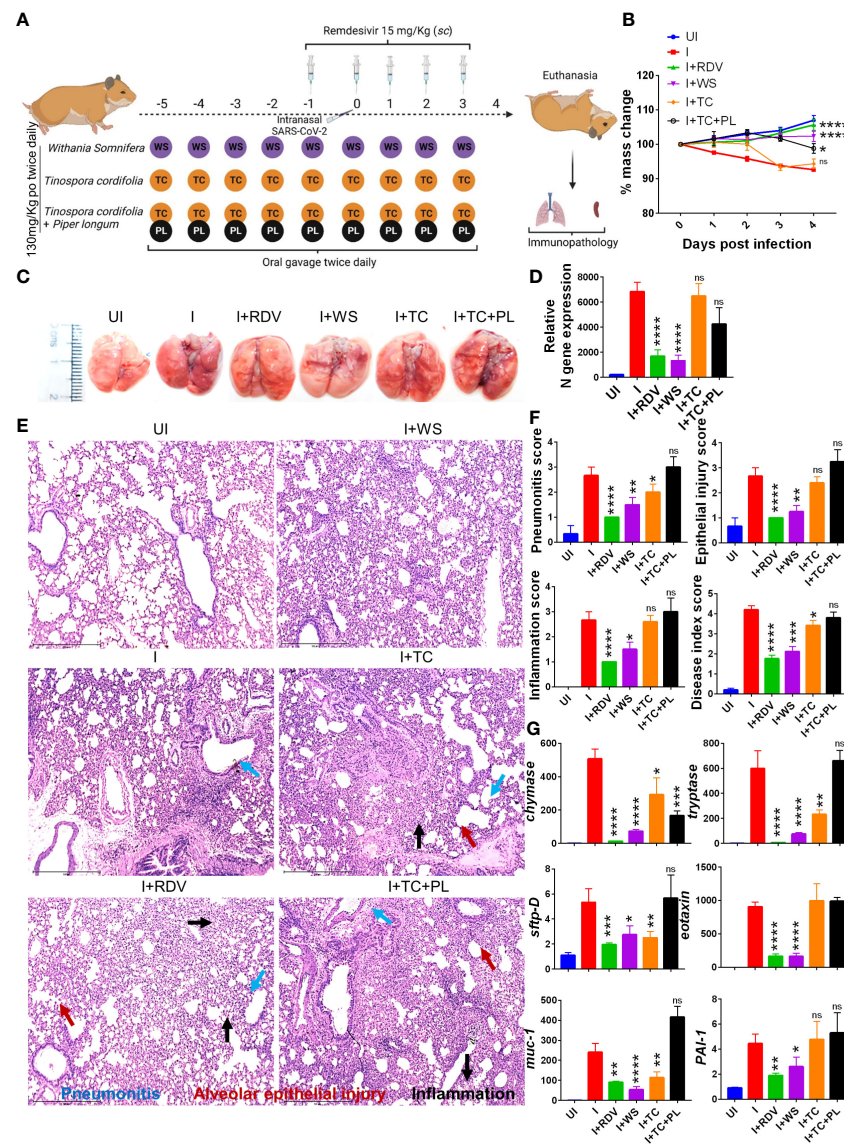


FIGURE 1

Prophylactic efficacy of selected herbal extract on the SARS-CoV-2 infected hamsters. (A) Schematic representation of dosing regimen for prophylactic treatment of WS, TC or TC in combination with PL, positive control remdesivir (RDV), infection control (I) or uninfected hamster group. All the animals except the uninfected control was intranasally challenged with  $10^5$  pfu SARS-CoV-2 on day 0 and sacrificed on 4-day post infection (dpi). (B) Body mass of the animals were monitored post challenge and was plotted as %age change as compared to its day 0 body mass. (C) Representative images of harvested lungs post necropsy. (D) Relative viral load by N gene expression by qPCR shown as bar graph mean  $\pm$  SEM. Histological analysis of left lung lower lobe was carried out post necropsy. The samples were fixed in 10% neutral formalin solution, paraffin embedded, sectioned and hematoxylin (H) & eosin (E) stained. Stained sections were then imaged at 10X and assessed by trained pathologist for histological features. (E) Representative images of HE stained lungs showing pneumonitis (blue), bronchitis (red), epithelial injury (green) and inflammation (yellow). (F) Blinded pathological score for pneumonitis, bronchitis, lung injury, epithelial injury and inflammation as assessed by trained pathologist. (G) mRNA expression of key genes involved in cellular injury of lungs. For each experiment N=5. One way-Anova using non-parametric Kruskal-Wallis test for multiple comparison. \*P < 0.05, \*\*P < 0.01, \*\*\*P < 0.001, \*\*\*\*P < 0.0001.

pathology (45, 46). On the other hand, secretion of mucin-1 (muc1) and surfactant protein D (sftp-D) are important defense mechanisms in the lungs against pathogenic infection, while elevated plasminogen activator inhibitor-I (PAI-1) is a risk factor for thrombosis and has been shown to be correlated with COVID-19 severity (30). Eotaxin is a lung injury-associated gene whose lung expression is upregulated in the case of severe COVID-19 (30, 47). Our data showed that both WS and TC were able to significantly decrease the mRNA expression of chymase, trypsin, sftpD, and

muc1, though the fold change inhibition observed in the WS group was dramatically more prominent than that observed in the TC group. Notably, WS, but not TC, group showed a decrease in exotoxin and PAI as well (Figure 1G). However, the combinatorial effect of TC with PL showed no alleviation in the gene expression markers for lung injury. In conclusion, we show that hamsters receiving prophylactic dosing of WS but not TC or TC in combination with PL alleviates the pulmonary pathology induced by COVID-19.

## Prophylactic WS promotes the anti-inflammatory response to COVID-19

During the active phase of SARS-CoV-2 infection, immune cells are recruited in the lungs leading to an aggressive inflammatory response that is correlated to morbidity and mortality (44). Previous studies have shown that the inflammatory profile of the lungs corroborates well with the inflammatory profile of the spleen in COVID-19 animal models (30, 31). Furthermore, splenomegaly has been shown to be one of the crucial COVID-19 severity indicators in the hamster model (30). In line with the previously published reports, we found a significant increase in the spleen length and mass in the infected hamsters while the hamsters receiving WS and RDV showed a significant reduction in the body spleen length and mass increase as compared to the infected control (Figures 2A, B). Severe COVID-19 patients have elevated pro-inflammatory cytokines and diminished anti-inflammatory cytokines levels. Therapeutic drugs such as DXM which were successful in decreasing the pro-inflammatory cytokines were found to be effective in clinical trials. Therefore, we tested the immunomodulatory potential of WS, TC, and TC+PL in SARS-CoV-2-infected hamsters. Our mRNA expression data from the spleen shows that both WS and TC showed potent anti-inflammatory potential in lowering the expression of *IL-6*, *IL4*, *IL13*, and *TNF- $\alpha$* . Notably, WS showed inhibitory potential for *IL-17* cytokine which is pathogenic for pulmonary injury, and significantly boosted the expression of *IL-10* cytokine and *foxp3* transcription factor which are crucial for the induction of regulatory T cells (Tregs) (Figures 2C, D). There were no significant changes observed in the expression of *IFN- $\gamma$*  cytokine and *t-bet* transcription factor which is responsible for the induction of Th1 response. The TC+PL group also showed non-significant modulations compared to the I group. Together, we found both WS and TC to show immunomodulatory potential in COVID-19 hamsters. WS was more potent in the induction of anti-inflammatory response.

## Effect on TRLM-PMA/ionophore-stimulated ROS and mtROS production in human PMNs and murine BMDNs

Neutrophils engage the pathogens by TLRs *via* recognizing PAMPs: among the discovered TLRs, endosomal TLR 7/8 binds viral single-stranded RNA as in SARS-CoV-2. Various TLR7/8 agonists induce neutrophil activation (48) however, little is known about a putative link between TLR7/8 signaling and neutrophil responses. In the present study, we found a significant increase in different neutrophil functions against priming of TLR7/8 by TRLM prior induction with PMA and/or ionophores.

WS and TC have been extensively characterized elsewhere as an alternative or complementary remedy for oxidative and inflammatory diseases owing to the presence of a range of alkaloids, polyphenols, terpenes, flavonoids, coumarins and other phytochemicals. Therefore, to determine the effect of WS and TC on ROS and mtROS production, DCF-DA and mitoTEMPO were added respectively, to the cells followed by priming with TRLM and

induction with PMA and ionophores. A marked decrease in ROS production in TC-treated PMNs, from 43% (50  $\mu$ g/ml) to 52% (100  $\mu$ g/ml,  $p < 0.05$ ) was observed when stimulated with TRLM-PMA whereas TRLM-ionomycin led to a decrease of 35% at 50  $\mu$ g/ml and 49% at 100  $\mu$ g/ml,  $p < 0.05$  (Figures 3A, B). WS also had similar effects in limiting the formation of superoxide anions elicited by TRLM-PMA (19% at 50  $\mu$ g/ml and 30% at 100  $\mu$ g/ml,  $p < 0.05$ ) or TRLM-ionomycin (maximum decrease of 21% at 100  $\mu$ g/ml,  $p < 0.05$ ) (Figures 3C, D). A similar trend was also seen in murine datasets (Figures S1A–D). Further, the ability of TC, 100  $\mu$ g/ml to inhibit mtROS production in PMNs revealed a 40% and 23% reduction with TRLM-PMA and TRLM-ionomycin respectively (Figures 3E–F). A somewhat lower percent reduction was seen in WS-exposed cells with TRLM-PMA (19%), and TRLM-ionomycin (12%) at 100  $\mu$ g/ml of WS (Figures 3G, H). Similar to the TC and WS effect on PMNs, murine cells also showed more potent inhibition on TRLM-PMA mediated cytosolic and mitochondrial radical production (Figures S1E–H). Notably, WS and TC both were comparatively more efficient in reducing PMA-mediated ROS and mtROS production in neutrophils from humans or mice.

## Effect on NETosis in human PMNs and murine BMDNs

Since sera and postmortem lung biopsies from COVID-19 patients have a high concentration of NET components especially in the inflammatory interstitial lesions and airways (49), elucidating their detailed mechanism could be highly useful. Although NETs formation has been considered a defensive microbicidal phenomenon to exterminate the invading foreign pathogens (50) but a loss of its control and their persistent presence in inflammation results in host tissue damage.

A steep rise in NETosis of more than 50% was observed in PMNs primed with TRLM before exposing PMA or ionophores. Supplementing the cells with TC but not WS could inhibit double-stranded DNA release, a hallmark for NETs formation. TC exhibited an inhibitory effect on NETs in a concentration-dependent manner. A low concentration of TC has no significant effect on the inhibition of NETs in neutrophils, however, higher concentrations exerted an inhibitory effect on the release of dsDNA. PMA-induced NETosis in human PMNs was reduced from 13% to 25% after treatment with 100 and 300  $\mu$ g/ml,  $p < 0.05$  of TC respectively (Figure 4A). In contrast, with TRLM-ionomycin stimulation TC did not exert a noticeable reduction in DNA release; a maximum of 15% inhibition was seen at 300  $\mu$ g/ml (Figure 4B). Treatment of cells with WS did not reveal a significant down-regulation of NETosis (Figures 4C, D). Further, similar effects were replicated in the mouse model also using murine BMDNs as shown in Figures S1I–L. Our immunofluorescence images further corroborated the fluorimetry data. Figures 4E, F showed that the pre-treatment of PMNs with 300  $\mu$ g/ml TC prevented the diffused and web-like state of TRLM-PMA treated cells as evidenced by the reduction of percent NETs forming cells, MPO, and H4Cit3 expression. Incubation of TC with the TRLM-ionomycin group did not result in much elimination of characteristic DNA fibers extrusion, except with shrinkage of nuclear diameter. Results obtained thus



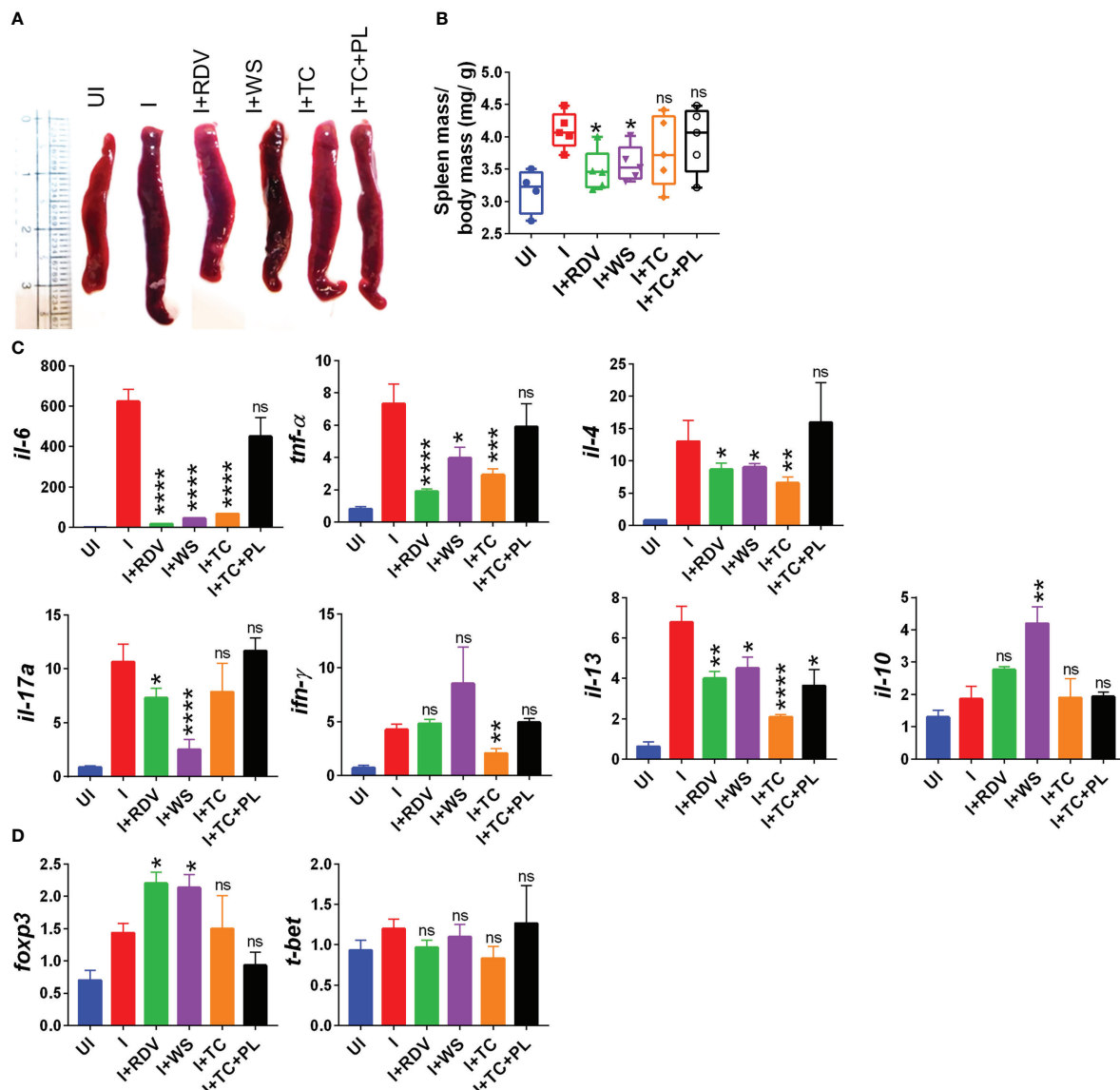


FIGURE 2

Immunomodulatory effects of WS or TC on the infected hamsters. Immunomodulatory activity of prophylactic treatment of WS or TC on infected vs uninfected hamsters were studied. (A) representative spleen images harvested post necropsy. (B) changes in spleen mass to body mass ratio for different groups (C) modulation in the mRNA expression of pro-inflammatory cytokines and (D) transcription factors. For each experiment N=5. One way-Anova using non-parametric Kruskal-Wallis test for multiple comparisons. \*P < 0.05, \*\*P < 0.01, \*\*\*P < 0.001, \*\*\*\*P < 0.0001.

indicate that TC might contribute to the regulation of neutrophil NETs formation *via* modulating the PMA-mediated signaling pathways involved in NETosis.

## Effect of WS on phagocytosis by human PMNs

In addition to degranulation and NETs, phagocytosis is another critical anti-microbial function of neutrophils. The measurable effect of WS and TC on neutrophils led us to study the role of these extracts on the phagocytic potential of these immune first responders. TC and WS showed a modest reduction of 17% and 13% ( $p < 0.05$ ), respectively only at the high concentration (300  $\mu\text{g}/\text{ml}$ , Figures S2A, B), while 1–100  $\mu\text{g}/$

ml of both the herbal extracts did not elicit any noticeable change. Also, pre-treatment of human peripheral neutrophils with TC and WS did not impart any significant effect on the killing activities of phagocytes; approximately 74% and 41% reduction in *E. coli* growth was observed when bacteria were incubated with TC and WS-treated PMNs, respectively (Figures S2C, D).

## Effect of WS, and TC on Th1, Th2, and Th17 polarization

T helper cell subset responses determine the clinical outcome of SARS-CoV-2 infection (51, 52). An appropriate Th1 cell response is required to clear the virus when the infection is initially established.

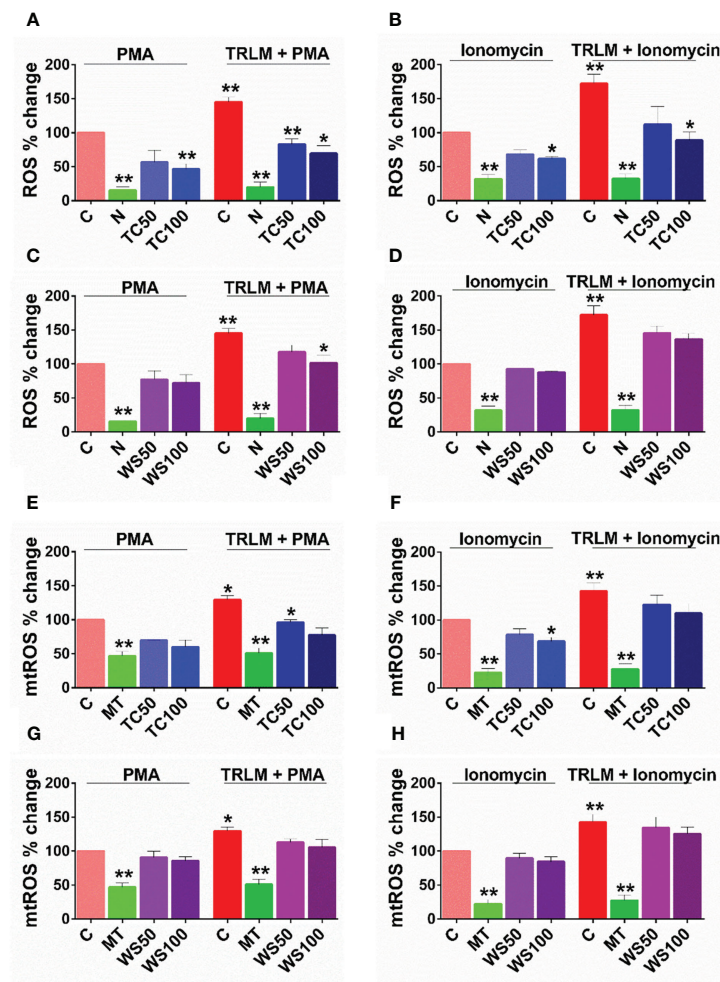


FIGURE 3

Effect of WS and TC on TRLM primed-PMA/ionomycin induced NETs formation in human PMNs. After pre-incubation with different concentrations TC and WS, PMNs were treated with TRLM (10 µg/ml) for 30 min and stimulated with sub-maximal concentration of PMA (12.5 nM) and ionomycin (2 µM) for 30 min. SYTOX Green (100 nM) was used to monitor extracellular DNA release using a plate reader (A, B: TC; C, D: WS). Total MFI in each experimental condition is expressed as Mean ± SEM of min 3 experiments. NETosis in human PMNs was also monitored using immunofluorescence imaging with DAPI (blue), anti-MPO antibody (green), and anti-H4Cit3 antibody (red, E–H). Representative fields are shown at 100X with a scale bar of 10 µm. Bar diagram represents quantification of percent NETs forming cells as calculated from five transects from three independent experiments. Statistical analysis consisted of one-way ANOVA followed by Bonferroni's test (\*p < 0.05, \*\*p < 0.01, vs respective control groups; C, control; V, VAS2870; D, Diltiazem; WS100, WS 100 µg/ml; WS300, WS 300 µg/ml; TC100, TC 100 µg/ml; TC300, TC 300 µg/ml).

However, prolonged Th1 cell activation precedes cytokine storm and priming of Th2 responses, leading to a poor prognosis (51, 53). Patients with severe Covid infection show high levels of IL-17 and GM-CSF (44, 54). Th17 cells lead to the recruitment of neutrophils and increase vascular permeability and leakage, causing lung damage (55). Thus, preventing the hyperactivation of pro-inflammatory T cells (Th1, Th2, and Th17) will help reduce the disease's severity. To study the immunomodulatory role of WS, we studied the effect on *in vitro* differentiation of different Th cell subsets like Th1, Th2, and Th17 cells (Figure 1). WS showed effective inhibition in the differentiation of Th1, Th2, and Th17 cells with an increase in doses (Figures 5A–I). IC50 values were calculated to compare its efficacy in inhibiting different Th cell subsets. The IC50 value of WS for Th1, Th2, and Th17 cells inhibition were 490.9 µg/ml, 185.8 µg/ml, and 488.7 µg/ml respectively (Figures 5C, F, I). These observations show that WS

is a more potent inhibitor of Th2 cells, followed by Th17 and Th1 cells. We also studied the effect of TC on *in vitro* differentiation of helper T cell subsets Th1, Th2, and Th17 cells (Supplementary Figures S3A–I). It showed a marginal inhibition of Th1, Th2, and Th17 cells with an increase in doses. The IC50 value of TC for Th1, Th2, and Th17 cells inhibition was 1294 µg/ml, 1330 µg/ml, and 1679 µg/ml (Supplementary Figures S3A–I). These observations show that TC is not as good an inhibitor of pro-inflammatory T-cell differentiation as compared to WS. DXM was used as a positive control since it is a well-known immunosuppressive drug (Supplementary Figures S4A–I). IC50 values of DXM were 517.6 nM, 1364 pM, and 3162 pM for Th1, Th2, and Th17 cells respectively (Supplementary Figures S4A–I). Together, through our *in-vitro* assay, we show that WS exhibits immune-suppressive potential and could inhibit the differentiation of Th1, Th2, and Th17 cells similar to the DXM-mediated inhibition.

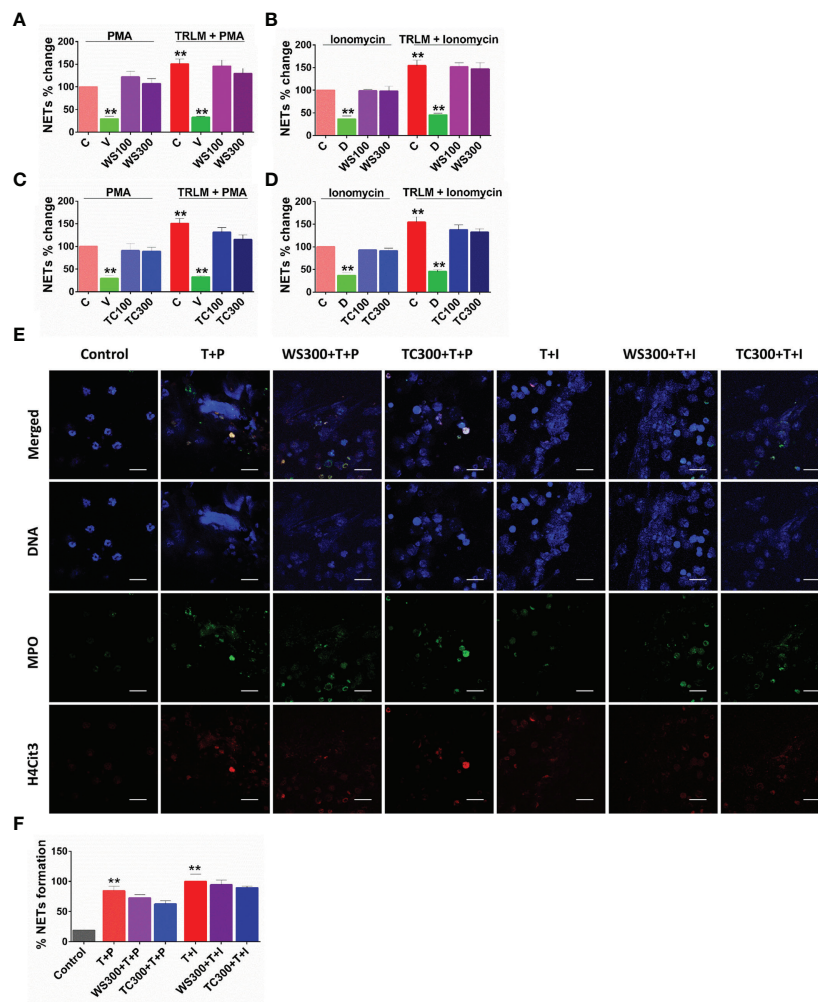


FIGURE 4

Effect of WS and TC on TRLM primed-PMA/ionomycin induced cytosolic ROS and mtROS production in human PMNs. PMNs pre-incubated at different concentrations of TC and WS were treated with TRLM (10  $\mu$ g/ml) for 30 min and stimulated with sub-maximal concentration of PMA (12.5 nM) and ionomycin (2  $\mu$ M) for 30 min. DCF-DA (10  $\mu$ M) and MitoSOX (10  $\mu$ M) were used for cytosolic ROS and mtROS detection, respectively using flow cytometry. All the data are represented as Mean  $\pm$  SEM,  $n$  = min 3 per group, and statistical analysis consisted of one-way ANOVA followed by Bonferroni's test (A–F) (\*\* $p$  < 0.01, vs respective control groups; C, control; N, N-acetyl cysteine; MT, MitoTEMPO; WS50, WS 50  $\mu$ g/ml; WS100, WS 100  $\mu$ g/ml; TC50, TC 50  $\mu$ g/ml; TC100, TC 100  $\mu$ g/ml).

## WS mitigates COVID-19 pathology and improves overall survival in hACE2.Tg mice

Screening of anti-viral or immunomodulatory drugs against COVID-19 has so far relied on two *in vivo* models viz hamster and hACE2.Tg mice model both of which mimic clinical symptoms of COVID-19 yet significantly differ in the disease pathology (30, 31, 43, 56). While hamsters have been shown to develop mild to moderate COVID-19 pathology following intranasal infection and mimic the majority of the clinical cases, hACE2.Tg mice, on the other hand, are a lethal model for SARS-CoV-2 infection and result in severe respiratory distress leading to 100% mortality by 6–8 days post-infection (dpi). In order to understand the protective efficacy of WS during acute infection, which is known to occur in a less but a significant number of clinical cases, we used hACE2.Tg mice model (Figure 6A). TC and TC+PL were not evaluated in hACE2.Tg mice, since they did not show significant protection in the hamster model

previously. Our data from hACE2.Tg mice challenge study showed about 8–10% recovery in the body mass in the WS-treated group as compared to the I control (Figure 6B). The overall survival of the hACE2.Tg mice improved by 2 days in WS treated group which was marginal yet significant as compared to the I control (Figure 6C). We next examined the gross morphological changes, viral load and pathological features in the excised lungs post necropsy on 6 dpi. Our data show that the WS group showed significant alleviation in gross morphological changes and lung viral load in the WS group as compared to the I control (Figures 6D, E). The H & E histopathological assessment results showed robust protection in the overall pathological scores in the WS group as compared to the I control (Figures 6F, G). RDV group showed log10 2-fold decreased lung viral load, however, the pathological disease index score of RDV and WS was found to be similar. Taken together, we found significant mitigation in COVID-19 pathology and lung viral load in the WS group which is reminiscent of robust protective efficacy.

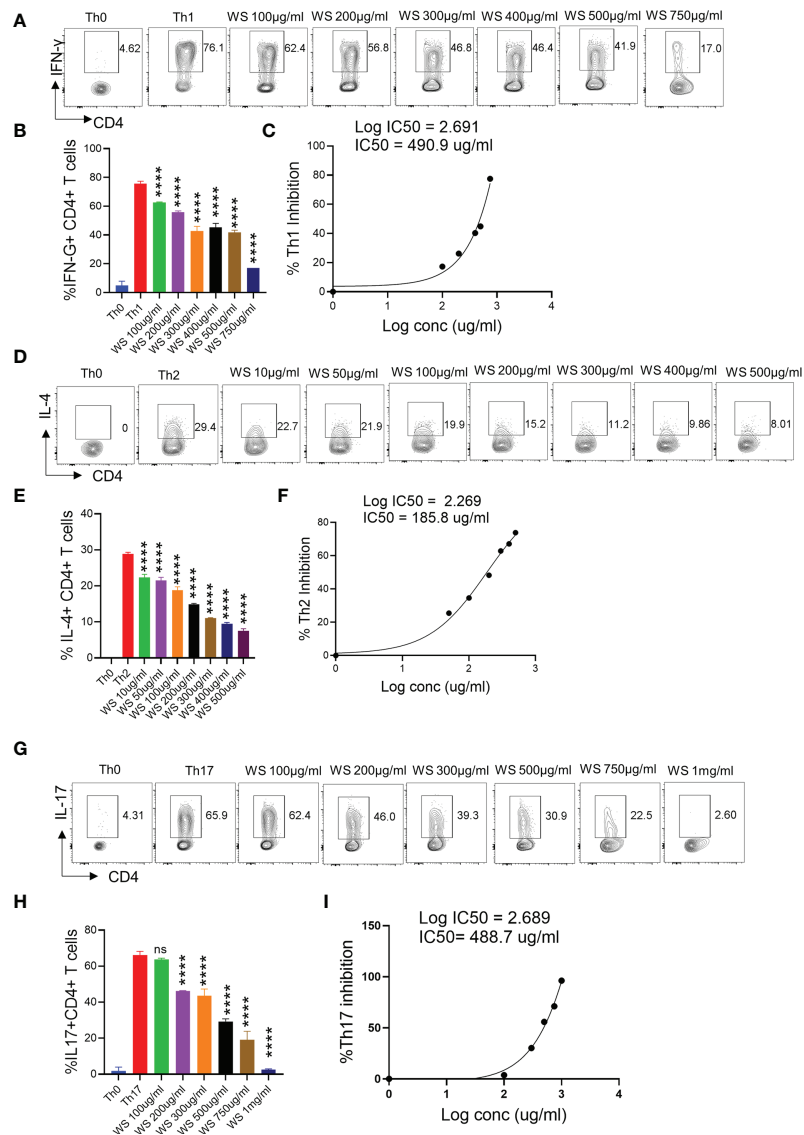


FIGURE 5

Dose kinetics of WS response on *in vitro* differentiation of Th1, Th2 and Th17 cells from naïve CD4+ T cells. Sorted naïve CD4+ T cells from mouse spleen and lymph nodes were activated using soluble anti-CD3 antibody and differentiated into helper T (Th)2 (A, B), Th17 cells (D, E) and Th1 subtypes (G, H) by using different cytokines viz recombinant mouse IL-4; TGF-β + IL-6 and IL-12 cytokines respectively. WS was added in concentrations ranging from 10μg/ml to 1000μg/ml initially at the time of cell seeding. After 72 h of incubation IL-4, IL-17 and IFN-γ production was measured respectively for Th2, Th17 and Th1 cells by intracellular cytokine staining. IC50 values were calculated using Graph pad prism software (C, F, I). \*\*\*\*P < 0.0001 by one-way ANOVA.

## WS treatment results in the boosting of MDSCs in hACE2.Tg mice

COVID-19 is characterized by lymphopenia resulting in dysregulation of immune profile and function (57). To test the immunomodulatory potential of WS in mice infected with SARS-CoV-2, we carried out flow cytometry-based immunophenotyping of the major immune population in WS treated vs non-treated group. In line with the previously published reports, our data from lymph-node cells shows that intranasal SARS-CoV-2 infection causes severe lymphopenia in hACE2.Tg mice were characterized by a significant decrease in lymphocytes (CD45+), total T cells (CD3+) cells, T helper cells (CD4+), and cytotoxic T (CD8+) cells (Figures 7A–C). This

skewed immune profile was rescued in the RDV group. WS group also showed recovery in depleted CD45+ cells but failed to show any significant recovery in T cell frequency. In addition to T cell depletion, COVID-19 is also characterized by a high frequency of inflammatory monocytes and myeloid-derived suppressor cells (MDSCs) in clinical cases (58). In line with this, we found a high frequency of monocytes in the lymph nodes in I control which was significantly reduced in WS or RDV-treated group. Moreover, the high levels of MDSCs were significantly suppressed in both WS and RDV groups. However, we did not find any observable difference in the percentage frequency of NK, NKT, macrophages, or neutrophils (Figures 7D–E). Taken together, we found that WS-treated mice show a rescuing effect in the dysregulated immune profile following SARS-CoV-2 infection.



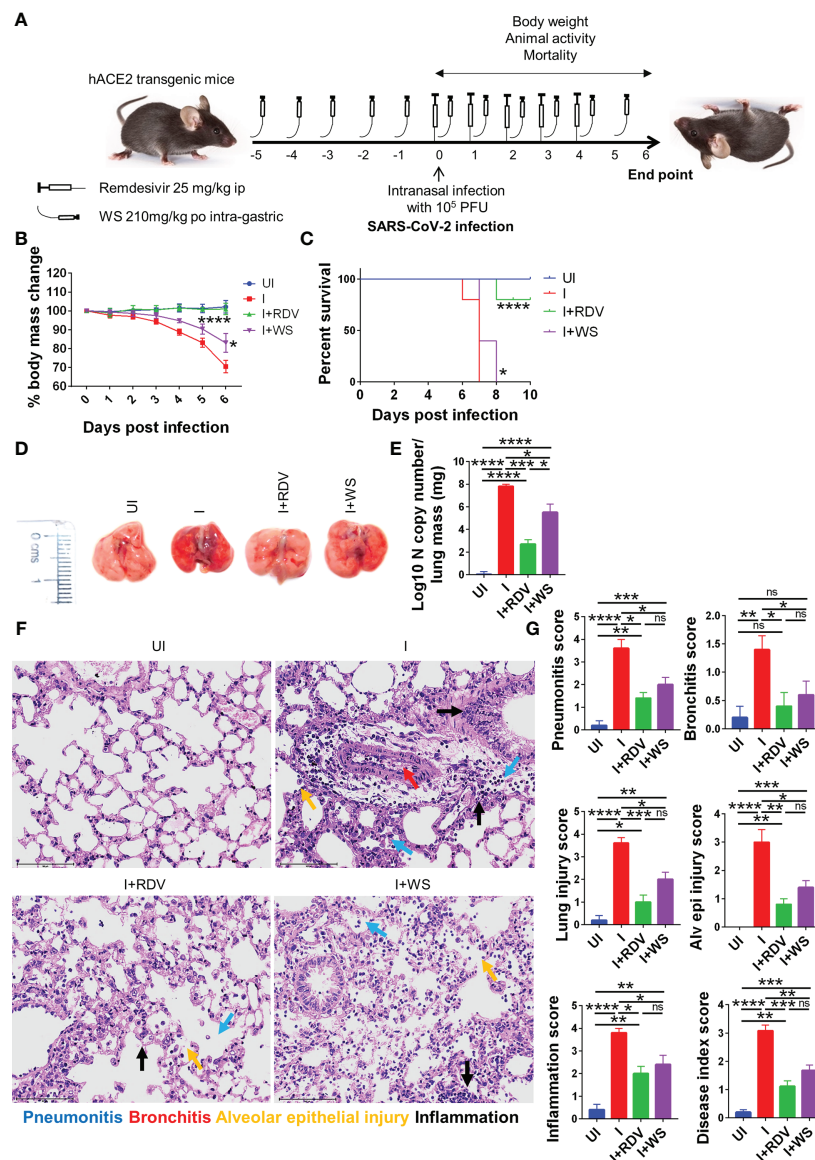


FIGURE 6

Assessment of protective efficacy of WS in acute SARS-CoV-2 infection model of hACE2 transgenic mice. To evaluate the effect of prophylactic treatment of WS on severe SARS-CoV-2 infection, we used hACE2 mice model for acute infection and compared it with RDV control. (A) Schematic representation showing treatment regimen for WS and RDV. Mice were intranasally infected with SARS-CoV-2 and (B) %age changes in body mass and (C) mortality was monitored and plotted. (D) Representative excised lung images 6 days post infection (E) Lung viral load presented as Log<sub>10</sub> N copy number (F) Lower lung lobe was used for HE staining (G) and assessed for pathological features by blinded scoring by trained pathologist. For each experiment N=5. One way-Anova using non-parametric Kruskal-Wallis test for multiple comparisons. \*P < 0.05, \*\*P < 0.01, \*\*\*P < 0.001, \*\*\*\*P < 0.0001.

## WS effectively inhibits inflammatory cytokine in hACE2.Tg mice

In order to understand the immunomodulatory potential of WS in the *in-vivo* settings, we performed intracellular cytokine staining (ICS) of phorbol myristate acetate (PMA), Ionomycin-activated lymph-node cells isolated from challenged hACE2.Tg mice. Based on the results obtained from ICS, we did not find any difference in Th1 (CD4+IFN $\gamma$ +) and Th2 (CD4+IL-4+) response in the WS group, however, there was 2-3-folds inhibition of Th17 cells (CD4

+IL17A+) and TNF $\alpha$  secreting CD4+ T cells in WS group as compared to the I control (Figures 8A–D). We also studied the effector cytokine response in CD8+ T cells and NK cells compartment. Effector cytotoxic response is correlated with improved survival and morbidity in COVID-19 cases, while NK cell activity is crucial for early viral clearance and immunity. Our data shows WS did not significantly modulate the cytokine profile of CD8+ and NK cells, when compared to the I control profile (Supplementary Figures S5A–G). However, we did see significant inhibition in the CD8+IFN $\gamma$ + T cell response in presence of WS *in-*



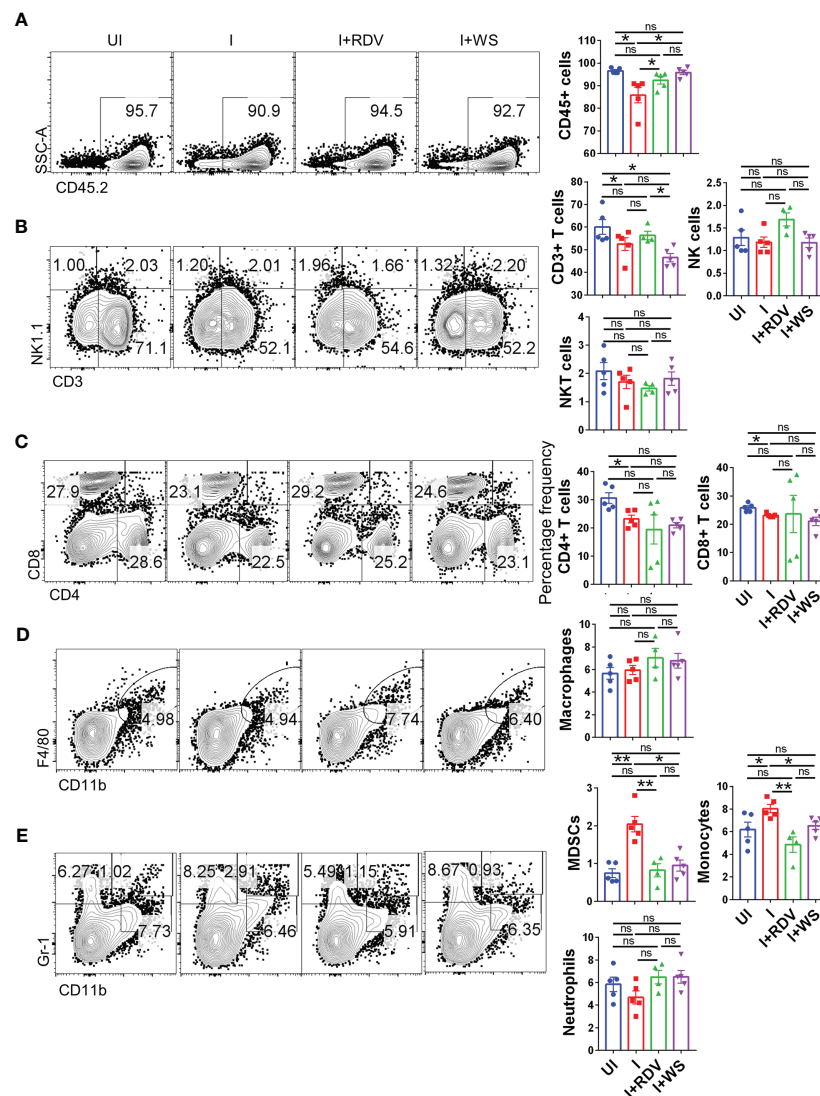


FIGURE 7

Changes in the major immune populations of infected hACE2 mice with or without treatment. Flow cytometry-based quantitation was done to evaluate changes in the major immune population in the lymph nodes of sacrificed animals at 6 dpi. The % age frequency was plotted as bar graph along with the representative contour plot (A) CD45+ population (B) CD3+ T lymphocytes, NK cells and NKT cells (C) CD4+ T helper cells and CD8+ T cytotoxic cells (D) Macrophages (E) Monocytes, neutrophils and MDSCs population. For each experiment N=5. One way-Anova using non-parametric Kruskal-Wallis test for multiple comparisons. \*P < 0.05, \*\*P < 0.01.

*vivo*. Taken together, CD4+ T cell-specific inhibition was mediated by WS *in-vivo*, while cytokine response in the cytotoxic T cell compartment was relatively unaltered.

## WS mitigates COVID-19 pathology in the animal model by anti-inflammatory response

In summary, we show by using two animal models viz hamster and hACE2.Tg mice that animals receiving prophylactic treatment of WS were broadly protected against COVID-19 both in terms of pulmonary pathology and lung viral load. This protection was further shown to be associated with immunosuppressive activity

by WS, especially in the CD4+ T cells effector response both *in-vitro* and *in-vivo* (Figure 9).

## Discussion

Since its first reported case, COVID-19 has led to an unprecedented number of clinical cases and mortality warranting urgent prophylactic and therapeutic interventions. The vaccination strategy was found to be largely useful against the SARS-CoV-2 ancestral strain, however, the subsequent rise in mutant strains led to immune evasion and decreased efficacy of vaccines (13, 14). So far only a few therapeutic drugs have been approved by FDA for COVID-19, while new drugs based on chemical entities require

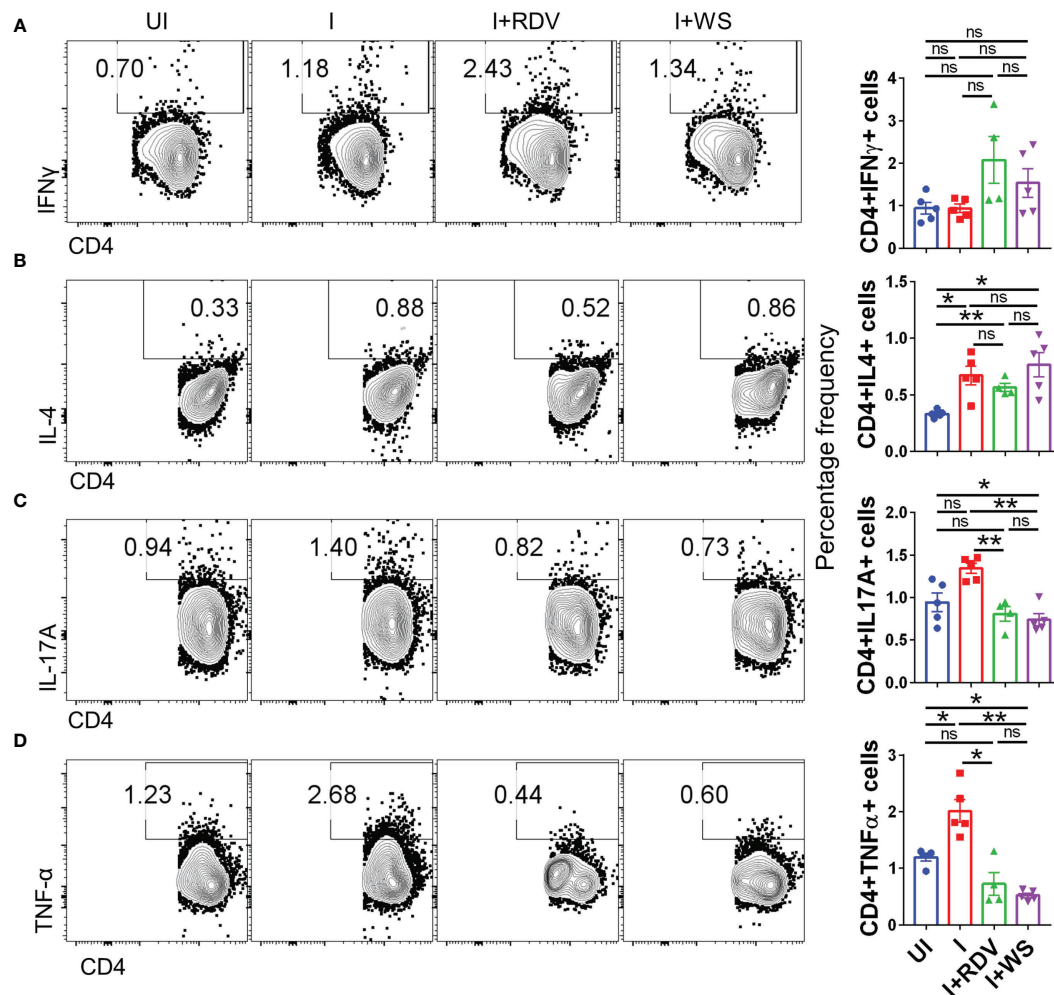


FIGURE 8

Changes in the effector cytokines of CD4+ T cells of infected hACE2 mice with or without treatment. Flow cytometry-based quantitation was done to evaluate changes in the major immune population in the lymph nodes of sacrificed animals at 6 dpi. The % age frequency was plotted as bar graph along with the representative contour plot (A) CD4+IFN $\gamma$ + cells (B) CD4+IL4+ cells (C) CD4+IL17A+ cells (D) CD4+TNF $\alpha$ + cells for each experiment N=5. One way-Anova using non-parametric Kruskal-Wallis test for multiple comparison. \*P < 0.05, \*\*P < 0.01.

relatively more time for development and are also associated with off-target or safety concerns (5). Interventions based on time-tested herbal extracts have offered an exciting alternate strategy due to their prolonged human use, acceptance, and safety as well as efficacy against infectious diseases (19, 59).

In the current study, we used well-characterized extracts of WS and TC two commonly used Asian traditional medicines to investigate their protective effect against COVID-19 by using hamster and hACE2.Tg mice model. WS contains a large number of phytoconstituents including steroids, alkaloids, saponins, glycosides, volatile oils, sitosterols, and others with various pharmacological activities (60). Various chemical constituents such as diterpenoid lactones, glycosides, steroids, sesquiterpenoid, phenolics, aliphatic compounds, essential oils, fatty acids, and polysaccharides are present in TC with known biological activities (61).

Various groups have shown that WS constituents could act as a potent inhibitor of SARS-CoV-2. *In silico* studies have shown that Withanone interacts and blocks the activity of both spike

glycoprotein and 3CLpro protease which are crucial for virus entry and replication (62). Furthermore, the detailed interactive sites of Withanone and its non-covalent interactions were also elucidated suggesting that Withanone/WS could exhibit protective efficacy *in-vivo* (26). Withaferin A, which is another Withanolide derived from WS, has also been shown to possess anti-viral and immunomodulatory activity as per the *in-silico* studies (26). A detailed characterization of the active ingredients of WS along with other herbal extracts was reported recently by our group, in which the *in-vitro* anti-viral activity of WS extract components was shown for the first time (28). On the other hand, TC, another important herbal extract, has also been previously used and shown to have anti-viral potential through docking studies (25). Though there existed *in-silico* evidence supporting the rationale that WS and TC may be helpful drug candidates for anti-viral activity against SARS-CoV-2, these observations lacked experimental animal model efficacy studies. Moreover, a recently published report by Kataria S et al, 2022 found that Ayurvedic formulation containing TC and PL in addition to the first line of treatment for COVID-19 was

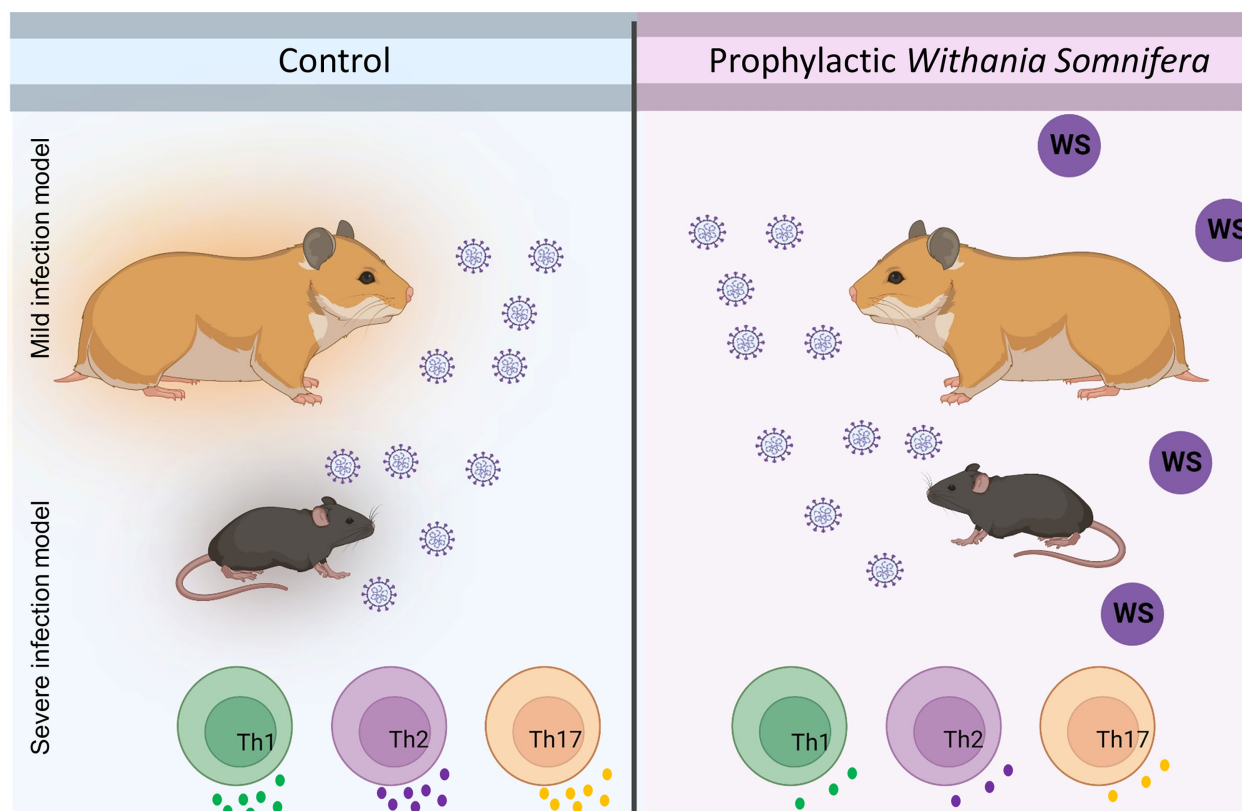


FIGURE 9  
Summary figure highlighting the study design and novel findings from the study.

beneficial in reducing the duration of hospitalization and time of recovery for COVID-19 patients warranting studies aimed at evaluating the combinatorial effect of TC and PL in the *in-vivo* model. However, the immunological correlates of protection elicited by WS or TC, if any, against COVID-19 have also been investigated.

In the hamster COVID-19 model, WS showed robust rescuing in the loss of body weight and pulmonary pathologies which were comparable to the RDV group validating the protective efficacy of WS. Notably, the WS group showed a 7-8 folds decrease in the lung viral load of infected hamsters while no protection was seen in other groups viz TC and TC+PL. It is, therefore, reasonable to argue that WS could inhibit the SARS-CoV-2 entry by blocking its interactive sites as shown previously through *in-silico* studies. However, *in-vitro* validation of the anti-viral potential of WS warrants further examination. Moreover, the decrease in lung viral load also led to the overall recovery of the pulmonary pathology in the WS group. The immunomodulatory potential of Withanolides has been well documented and has been shown to promote an anti-inflammatory environment (22). In line with this, we found that WS-treated hamsters exhibited a significant reduction in the mRNA expression of pro-inflammatory cytokines and boosted the expression of anti-inflammatory cytokines and transcription factors in the hamsters infected with SARS-CoV-2. Since the inflammatory response has been implicated in pulmonary pathology, increased risk of hospitalization and mortality, it could be argued that the anti-

inflammatory potential of WS could be the basis of protection together with its anti-viral activity. This was an important finding which showed in parts that WS in COVID-19 led to immunomodulatory effects beneficial for recovery.

The other major arm of immunity that plays a key role in the COVID-19 protective response is the adaptive immune response mediated by T & B cells. Due to a lack of antibody resources for the hamsters to study cellular immunological response, we used hACE2.Tg mice to study the immunological response following infection and the effect of WS (32, 56). Our hACE2.Tg mice data gave two crucial insights, it showed that the WS group may not be fully protected in severe COVID-19 cases as infected hACE2.Tg mice though marginally protected ultimately died following SARS-CoV-2 infection. It is likely that the WS-mediated SARS-CoV-2 inhibition through spike interaction and other entry protease inhibition might not be sufficient to prevent the viral entry and multiplication into the hACE2-expressing lung epithelial cells and therefore might allow virus entry and replication leading to disease pathology. However, notably, the overall pulmonary pathology as examined by histopathological assessment did show significantly less lung injury. Two, immunophenotyping data from hACE2.Tg mice showed recovery from the lymphopenia and dysregulated immune profile in the WS group. Interestingly, we found that the effector cytokine response specific to Th cells was specifically inhibited in presence of WS both *in-vitro* and *in-vivo*. Though, WS exhibited inhibition of the differentiation of Th1, Th2, and

Th17 cells *in-vitro*, in the infected hACE2.Tg mice WS treated only showed significant inhibition in Th17 and TNF $\alpha$  secreting CD4+ T cells. Notably, heightened TNF $\alpha$  levels have been correlated with a higher risk of mortality in COVID-19 cases and were associated with cellular injury. Since WS inhibitory potential was specific for CD4+ T cells and not CD8+ T cells or NK cells it is a possibility that WS may be interfering with Th cell activation signaling or downstream signaling involved in the effector response. In addition, WS was also found to suppress the frequency of MDSCs and monocytes which have been shown to promote COVID-19 severity. It is a possibility that the immunomodulatory effect of WS could be acting through both innate and adaptive arm of immunity. Extensive and meticulously designed studies are needed to investigate further the molecular basis for this specificity.

In the infected mice, we did not find any modulation in the neutrophil number. In infected human subjects, however, the neutrophil number is enhanced and NETosis has been linked with thrombosis in COVID-19 pathologies. We, therefore, performed *in vitro* studies on mice BMDNs and human neutrophils. To further look into the possible mechanism of protection, we carried out a detailed investigation of immunological changes. In one part of the study, TRLM primed and PMA and calcium ionophores-induced neutrophil functions were studied in the presence of WS and TC. The ROS generation pathways in the neutrophils have been classically mediated either by NOX2-dependent *via* the activation of protein kinase C (63, 64) or NOX2-independent by calcium-activated small conductance potassium channel (SK3) and/or non-selective mitochondrial permeability transition pore (mPTP) in inducing mtROS production *via* intracellular Ca<sup>2+</sup> flux (65, 66). Additionally, many reports had also postulated the crosstalk of NOX2 activation and mtROS production and thus represents a feed-forward vicious cycle for ROS generation in oxidative stress (67). By using mitochondrial-targeted inhibitors of NOX2, Vorobjeva et al. (2020) showed the involvement of both NOX2-derived ROS and mtROS in NETosis in human PMNs (66). We also observed a large amount of ROS and mtROS production induced by PMA and/or ionophores. WS and TC have been known to contain anti-oxidants with potent free-radical scavenging abilities. We found a significant reduction in the oxidative stress in TC and WS pretreated cells as demonstrated by their ability to suppress both ROS and mtROS. However, the anti-oxidant properties of both WS and TC were comparatively more pronounced in the case of PMA than ionophores. This indicates a putative role of WS and TC primarily as the NOX2-targeted effector, however, the inhibitory effect of these herbal extracts on the mtROS – NOX2 feed-forward cycle cannot be omitted.

NETosis is a distinct process of cell death unlike necrosis, apoptosis, or necroptosis (50); the molecular processes involved in NETosis are now better understood (66, 68). NETs are characterized by initial morphological changes and histone modifications followed by mechanical changes leading to chromatin decondensation and an irreversible rupture of nuclear and cell envelope (Neubert et al., 2018). Moreover, Awasthi et al. (2016) had reported the involvement of TLRs in NETosis; they have found that blocking TLR-2 and -6 with specific antibodies could significantly inhibit oxLDL induced

NETosis (69). In agreement with this, we have also found a notable reduction in NETs formation in TC pre-treated cells in response to TRLM primed and PMA/calcium ionophores activation. We found that TC predominantly inhibited neutrophil NOX-2 activity as evidenced by immunolabeling of MPO and citrullinated histones. NOX-2 is the most abundant protein and an important source of superoxide radicals in neutrophils that mediate PMA-induced NETosis. Since TC preferentially inhibited ROS, mtROS, and NETs production largely stimulated by PMA, we postulate that TC antagonizes an upstream component at the early stage of NOX2-mediated NETosis.

Neutrophils are the first phagocytic cells to reach the site of infection or injury (70). WS and TC did not reveal any significant adversity on phagocytosis by neutrophils when these were pre-treated with up to 300  $\mu$ g/ml concentrations of the extracts; however, a low of 20% was observed with TC. Moreover, the intracellular bactericidal capacity of neutrophils also did not show any notable change with the extracts. Together, these results suggested that modulation of neutrophil functionality could be one of the contributing factors for WS-mediated protection against COVID-19.

## Future prospects

Our results provide the first direct evidence that prophylactic WS administration is affecting in mitigating the pathology of COVID-19 which is mediated by the anti-inflammatory potential of WS through suppression of effector T helper cell response. Though there is pool of literature available based on computational analysis as well as *in-vitro* activity suggesting the active pharmaceutical ingredients of WS which may be essential for these immunomodulatory potentials, but lacks data from animal studies. Future experiments should be designed to investigate and decipher the therapeutically potential of WS ingredient and to optimize its dosage which could be taken for randomized clinical trials. Moreover, the pharmacological potential of WS in combination with COVID-19 anti-viral drug or vaccine candidates could be exploited to better understand the synergistic effect of the treatment. In addition, future proof of concept studies could be designed for other infectious diseases which are known to cause cytokine release syndrome such as Influenza, to test if it helps mitigate the disease.

## Conclusion

Though ancient knowledge of medicinal potential of herbs existed in Ayurvedic science since long we did not have much scientific evidence about its protective/preventative efficacy from animal studies and more so on COVID19. In this study, by combining hamster and hACE2 transgenic mice model we provide direct evidence that prophylactic treatment of WS mitigates COVID19 through its anti-inflammatory properties. Our findings are important in the context of a continuously evolving virus that leads to immune evasion by previous



vaccination and warrants a more robust therapeutic approach against emerging variants of SARS-CoV-2. We also defined the immunological correlates of protection based on *in-vitro* and *in-vivo* studies and believe that the potent anti-inflammatory potential of WS could be further exploited against other infectious diseases and inflammatory disorders (one such clinical trial, CTRI/2021/06/034496, for this is already conducted in India for WS). Finally, our study supports the use of WS to prevent COVID-19 pathologies and may also be evaluated for its efficacy against other viral infections.

## Data availability statement

The original contributions presented in the study are included in the article/**Supplementary Material**. Further inquiries can be directed to the corresponding authors.

## Ethics statement

The animal study was reviewed and approved by Institutional animal ethics committee (IAEC) THSTI.

## Author contributions

Conceived, designed, and supervised the study: MD, AA. Performed the experiments: ZR, PB, SS, UM. ABSL3 experiment: ZR, MT. FACS: PB and UM. qPCR: ZR. Viral load: ZR. Histology: ZR. Confocal microscopy: PB. Analyzed the data: ZR, PB, and UM. Contributed reagents/materials/analysis tools: MD, AA. Wrote the manuscript: ZR, PB, AA, MD. All authors contributed to the article and approved the submitted version.

## Funding

The authors express their gratitude to the Ministry of AYUSH and the Department of Biotechnology (DBT), Government of India for joint funding to carry out the research work presented in this manuscript (Grant Nos: BT/ PR40738/TRM/120/486/2020 and A.11019/03/2020-NMPB-IV-A). Financial support from THSTI core to AA is acknowledged. MD also acknowledges the financial support from SERB (JBR/2020/000034) and CCRAS (HQ-PROJ011/ 20/2022-PROJ).

## Acknowledgments

We greatly acknowledge the support and critical inputs of Dr. Pramod Kumar Garg in the manuscript. We thank IDRf (THSTI) for the support at the ABSL3 facility. Prabhanjan and Jitender for providing technical support. Small animal facility and Immunology Core for providing support in experimentation. Hamsters were procured from CDRI, Lucknow. ILBS for support in histological analysis and assessment. The following reagent was deposited by the

Centers for Disease Control and Prevention and obtained through BEI Resources, NIAID, NIH: SARS Related Coronavirus 2, Isolate USA-WA1/2020, NR-52281.

## Conflict of interest

The authors declare that the research was conducted in the absence of any commercial or financial relationships that could be construed as a potential conflict of interest.

## Publisher's note

All claims expressed in this article are solely those of the authors and do not necessarily represent those of their affiliated organizations, or those of the publisher, the editors and the reviewers. Any product that may be evaluated in this article, or claim that may be made by its manufacturer, is not guaranteed or endorsed by the publisher.

## Supplementary material

The Supplementary Material for this article can be found online at: <https://www.frontiersin.org/articles/10.3389/fimmu.2023.1138215/full#supplementary-material>

### SUPPLEMENTARY FIGURE 1

Effect of WS and TC on PMA/A23187 induced cytosolic ROS and mtROS production in mice BMDNs. BMDNs pre-incubated at different concentrations of TC and WS were stimulated with optimal concentration of PMA (100 nM) and A23187 (10  $\mu$ M) for 30 min. DCF-DA (10  $\mu$ M) and MitoSOX (10  $\mu$ M) were used for cytosolic ROS and mtROS detection, respectively using flow cytometry. BMDNs pre-incubated at different concentrations of TC and WS were stimulated with optimal concentration of PMA (100 nM) and A23187 (10  $\mu$ M) for 30 min. SYTOX Green (100 nM) was used to monitor extracellular DNA release using a plate reader (A, B: TC; C, D: WS). Total MFI in each experimental condition is expressed as Mean  $\pm$  SEM of min 3 experiments. All the data are represented as Mean  $\pm$  SEM, n = min 3 per group, and statistical analysis consisted of one-way ANOVA followed by Bonferroni's test (\*p < 0.05, \*\*p < 0.01, \*\*\*p < 0.001 vs respective control groups; #p < 0.05, ##p < 0.01 vs PMA/A23187 treated groups). C, control; N, N-acetyl cysteine; MT, MitoTEMPO. C, control; V, VAS2870; D, Diltiazem. Cytotoxic potential of WS and TC on human PMNs and murine BMDNs. Percent cell death was obtained by flow cytometry using PI (10  $\mu$ g/ml). Doxorubicin (10  $\mu$ M) was used as a positive control (100%).

### SUPPLEMENTARY FIGURE 2

Effect of WS and TC on phagocytosis and bactericidal activity of human PMNs. (A, B) Human PMNs were incubated with different concentrations of WS and TC before adding PE-labelled latex beads for phagocytic assay. Fluorescent signal was quenched using trypan blue (0.4%) before acquiring in FACS cell analyzer. (C, D) Effect of GG on bactericidal activity of human PMNs. Cells were pre-treated with 300  $\mu$ g/ml of WS and TC before incubating with kanamycin-resistant *E. coli*. The direct effect of WS and TC on *E. coli* growth was also monitored by incubating bacteria with 300  $\mu$ g/ml concentration for 30 min. \*\*p < 0.01 vs control groups; ##p < 0.01 vs GG treated groups. All the data are represented as Mean  $\pm$  SEM, n = min 3 per group, and statistical analysis consisted of one-way ANOVA followed by Bonferroni's test. C, control; WS300, WS 300  $\mu$ g/ml; TC300, TC 300  $\mu$ g/ml.

### SUPPLEMENTARY FIGURE 3

Immunosuppressive effect of *Tinospora cordifolia* (Willd.) Miers on *in vitro* differentiation of Th1, Th2 and Th17 cells. Naïve CD4+ T cells were sorted from mice spleen and lymph nodes and were activated by soluble anti-CD3 antibody. Cells were then differentiated into helper T (Th) 2 (A, B), Th17 cells



(D, E) and Th1 conditions (G, H) using recombinant mouse IL-4; TGF- $\beta$  + IL-6 and IL-12 cytokines respectively in presence or absence of dexamethasone (doses ranging from 1pM to 20uM). Differentiated cells at 72 hours were quantitated by performing intracellular cytokine staining for IL-4, IL-17 and IFN- $\gamma$  production. IC50 values were calculated using Graph pad prism software (C, F, I). \*P < 0.05, \*\*P < 0.01, \*\*\*P < 0.001, \*\*\*\*P < 0.0001 by one-way ANOVA.

#### SUPPLEMENTARY FIGURE 4

Immunosuppressive effect of Dexamethasone on *in vitro* differentiation of Th1, Th2 and Th17 cells. Naïve CD4+ T cells were sorted from mice spleen and lymph nodes and were activated by soluble anti-CD3 antibody. Cells were then differentiated into helper T (Th) 2 (A, B), Th17 cells (D, E) and Th1 conditions (G, H) using recombinant mouse IL-4; TGF- $\beta$  + IL-6 and IL-12 cytokines respectively in presence or absence of dexamethasone (doses ranging from 1pM to 20uM). Differentiated cells at 72 hours were

quantitated by performing intracellular cytokine staining for IL-4, IL-17 and IFN- $\gamma$  production. IC50 values were calculated using Graph pad prism software (C, F, I). \*P < 0.05, \*\*P < 0.01, \*\*\*P < 0.001, \*\*\*\*P < 0.0001 by one-way ANOVA.

#### SUPPLEMENTARY FIGURE 5

Changes in the effector cytokines of CD8+ T and NK cells of infected hACE2 mice with or without treatment. Flow cytometry-based quantitation was done to evaluate changes in the major immune population in the lymph nodes of sacrificed animals at 6 dpi. The % age frequency was plotted as bar graph along with the representative contour plot (A) CD8+GzB+ cells (B) CD8+Prf-1+ cells (C) CD8+TNF $\alpha$ + cells (D) CD8+IFN $\gamma$ + cells (E) CD8+IL4+ cells (F) CD8+IL17A+ cells (G) CD3-NK1.1+ IFN $\gamma$ + cell population. Granzyme (GzB), Perforin (Prf-1). For each experiment N=5. One way-Anova using non-parametric Kruskal-Wallis test for multiple comparisons. \*P < 0.05, \*\*P < 0.01.

## References

- Global Burden of Disease Long COVID Collaborators. Estimated global proportions of individuals with persistent fatigue, cognitive, and respiratory symptom clusters following symptomatic COVID-19 in 2020 and 2021. *JAMA* (2022) 328:1604–15. doi: 10.1001/jama.2022.18931
- Jackson LA, Anderson EJ, Roupel NG, Roberts PC, Makhene M, Coler RN, et al. An mRNA vaccine against SARS-CoV-2 — preliminary report. *New Engl J Med* (2020) 383:1920–31. doi: 10.1056/NEJMoa2022483
- Tostanoski LH, Wegmann F, Martinot AJ, Loos C, McMahan K, Mercado NB, et al. Ad26 vaccine protects against SARS-CoV-2 severe clinical disease in hamsters. *Nat Med* (2020) 26(11):1694–700. doi: 10.1038/s41591-020-1070-6
- Forni G, Mantovani A. COVID-19 vaccines: Where we stand and challenges ahead. *Cell Death Differ* (2021) 28:626–39. doi: 10.1038/s41418-020-00720-9
- Niknam Z, Jafari A, Golchin A, Danesh Pouya F, Nemati M, Rezaei-Tavirani M, et al. Potential therapeutic options for COVID-19: An update on current evidence. *Eur J Med Res* (2022) 27:6. doi: 10.1186/s40001-021-00626-3
- Gibson PG, Qin L, Puah SH. COVID-19 acute respiratory distress syndrome (ARDS): Clinical features and differences from typical pre-COVID-19 ARDS. *Med J Aust* (2020) 213:54–56.e1. doi: 10.5694/mja2.50674
- Guan W-J, Ni Z-Y, Hu Y, Liang W-H, Ou C-Q, He J-X, et al. Clinical characteristics of coronavirus disease 2019 in China. *N Engl J Med* (2020) 382:1708–20. doi: 10.1056/NEJMoa2002032
- Leng L, Cao R, Ma J, Mou D, Zhu Y, Li W, et al. Pathological features of COVID-19-associated lung injury: A preliminary proteomics report based on clinical samples. *Signal Transduct Targeted Ther* (2021) 5:1–9. doi: 10.1038/s41392-020-00355-9
- Chen Y, Li L. SARS-CoV-2: Virus dynamics and host response. *Lancet Infect Dis* (2020) 20:515–6. doi: 10.1016/S1473-3099(20)30235-8
- Nishiga M, Wang DW, Han Y, Lewis DB, Wu JC. COVID-19 and cardiovascular disease: from basic mechanisms to clinical perspectives. *Nat Rev Cardiol* (2020) 17:543–58. doi: 10.1038/s41569-020-0413-9
- Neurath MF. COVID-19 and immunomodulation in IBD. *Gut* (2020) 69:1335–42. doi: 10.1136/gutjnl-2020-321269
- Wu Y, Xu X, Chen Z, Duan J, Hashimoto K, Yang L, et al. Nervous system involvement after infection with COVID-19 and other coronaviruses. *Brain Behav Immun* (2020) 87:18–22. doi: 10.1016/j.bbi.2020.03.031
- Cao Y, Wang J, Jian F, Xiao T, Song W, Yisimayi A, et al. Omicron escapes the majority of existing SARS-CoV-2 neutralizing antibodies. *Nature* (2022) 602:657–63. doi: 10.1038/s41586-021-04385-3
- McCallum M, Walls AC, Sprouse KR, Bowen JE, Rosen LE, Dang HV, et al. Molecular basis of immune evasion by the delta and kappa SARS-CoV-2 variants. *Science* (2021) 374:1621–6. doi: 10.1126/science.abl8506
- Beigel JH, Tomashek KM, Dodd LE, Mehta AK, Zingman BS, Kalil AC, et al. Remdesivir for the treatment of covid-19 — final report. *New Engl J Med* (2020) 383:1813–26. doi: 10.1056/NEJMoa2007764
- RECOVERY Collaborative Group, Horby P, Lim WS, Emberson JR, Mafham M, Bell JL, et al. Dexamethasone in hospitalized patients with covid-19. *N Engl J Med* (2021) 384:693–704. doi: 10.1056/NEJMoa2021436
- Cain DW, Cidlowski JA. After 62 years of regulating immunity, dexamethasone meets COVID-19. *Nat Rev Immunol* (2020) 20:587–8. doi: 10.1038/s41577-020-00421-x
- Ang L, Song E, Lee HW, Lee MS. Herbal medicine for the treatment of coronavirus disease 2019 (COVID-19): A systematic review and meta-analysis of randomized controlled trials. *J Clin Med* (2020) 9:1583. doi: 10.3390/jcm9051583
- Jan J-T, Cheng T-JR, Juang Y-P, Ma H-H, Wu Y-T, Yang W-B, et al. Identification of existing pharmaceuticals and herbal medicines as inhibitors of SARS-CoV-2 infection. *PNAS* (2021) 118. doi: 10.1073/pnas.2021579118
- Benarba B, Pandiella A. Medicinal plants as sources of active molecules against COVID-19. *Front Pharmacol* (2020) 11:1189. doi: 10.3389/fphar.2020.01189
- Pandey A, Bani S, Dutt P, Kumar Satti N, Avtar Suri K, Nabi Qazi G. Multifunctional neuroprotective effect of withanone, a compound from withania somnifera roots in alleviating cognitive dysfunction. *Cytokine* (2018) 102:211–21. doi: 10.1016/j.cyto.2017.10.019
- Khanal P, Chikhale R, Dey YN, Pasha I, Chand S, Gurav N, et al. Withanolides from withania somnifera as an immunity booster and their therapeutic options against COVID-19. *J Biomol Structure Dyn* (2022) 40:5295–308. doi: 10.1080/07391102.2020.1869588
- Parihar S. Anti-viral activity of withania somnifera phytoconstituents against corona virus (SARS-CoV-2). *J Pharmacovigilance Drug Res* (2022) 3:22–6. doi: 10.53411/jpadr.2022.3.2.5
- Singh M, Jayant K, Singh D, Bhutani S, Poddar NK, Chaudhary AA, et al. Withania somnifera (L.) dunal (Ashwagandha) for the possible therapeutics and clinical management of SARS-CoV-2 infection: Plant-based drug discovery and targeted therapy. *Front Cell Infect Microbiol* (2022) 12:933824. doi: 10.3389/fcimb.2022.933824
- Shree P, Mishra P, Selvaraj C, Singh SK, Chaube R, Garg N, et al. Targeting COVID-19 (SARS-CoV-2) main protease through active phytochemicals of ayurvedic medicinal plants – withania somnifera (Ashwagandha), tinospora cordifolia (Giloy) and ocimum sanctum (Tulsi) – a molecular docking study. *J Biomol Struct Dyn* (2022) 40(1):190–203. doi: 10.1080/07391102.2020.1810778
- Kumar V, Dhanjal JK, Bhargava P, Kaul A, Wang J, Zhang H, et al. Withanone and withaferin-a are predicted to interact with transmembrane protease serine 2 (TMPRSS2) and block entry of SARS-CoV-2 into cells. *J Biomol Struct Dyn* (2022) 40:1–13. doi: 10.1080/07391102.2020.1775704
- Kumano K, Kanak MA, Saravanan PB, Blanck JP, Liu Y, Vasu S, et al. Withaferin a inhibits lymphocyte proliferation, dendritic cell maturation *in vitro* and prolongs islet allograft survival. *Sci Rep* (2021) 11:10661. doi: 10.1038/s41598-021-90181-y
- Kasarla SS, Borse SP, Kumar Y, Sharma N, Dikshit M. *In vitro* effect of withania somnifera, AYUSH-64, and remdesivir on the activity of CYP-450 enzymes: Implications for possible herb-drug interactions in the management of COVID-19. *Front Pharmacol* (2022) 13:973768. doi: 10.3389/fphar.2022.973768
- Parray HA, Narayanan N, Garg S, Rizvi ZA, Shrivastava T, Kushwaha S, et al. A broadly neutralizing monoclonal antibody overcomes the mutational landscape of emerging SARS-CoV-2 variants of concern. *PLoS Pathog* (2022) 18:e1010994. doi: 10.1371/journal.ppat.1010994
- Rizvi ZA, Dalal R, Sadhu S, Binayke A, Dandotiya J, Kumar Y, et al. Golden Syrian hamster as a model to study cardiovascular complications associated with SARS-CoV-2 infection. *eLife* (2022) 11:e73522. doi: 10.7554/eLife.73522
- Rizvi ZA, Babel P, Sadhu S, Madan U, Tripathy MR, Goswami S, et al. Prophylactic treatment of glycyrrhiza glabra mitigates COVID-19 pathology through inhibition of pro-inflammatory cytokines in the hamster model and NETosis. *Front Immunol* (2022) 13:945583. doi: 10.3389/fimmu.2022.945583
- Rizvi ZA, Sadhu S, Dandotiya J, Binyaka A, Sharma P, Singh V, et al. SARS-CoV-2 and its variants, but not omicron, induces thymic atrophy and impaired T cell development. (2022). doi: 10.1101/2022.04.07.487556

33. Rizvi ZA, Tripathy MR, Sharma N, Goswami S, Srikanth N, Sastry JLN, et al. Effect of prophylactic use of intranasal oil formulations in the hamster model of COVID-19. *Front Pharmacol* (2021) 12:746729. doi: 10.3389/fphar.2021.746729
34. Hingankar N, Deshpande S, Das P, Rizvi ZA, Wibmer CK, Mashilo P, et al. A combination of potentially neutralizing monoclonal antibodies isolated from an Indian convalescent donor protects against the SARS-CoV-2 delta variant. *PLoS Pathog* (2022) 18:e1010465. doi: 10.1371/journal.ppat.1010465
35. Rizvi ZA, Puri N, Saxena RK. Evidence of CD1d pathway of lipid antigen presentation in mouse primary lung epithelial cells and its up-regulation upon mycobacterium bovis BCG infection. *PLoS One* (2018) 13:e0210116. doi: 10.1371/journal.pone.0210116
36. Rizvi ZA, Dalal R, Sadhu S, Kumar Y, Kumar S, Gupta SK, et al. High-salt diet mediates interplay between NK cells and gut microbiota to induce potent tumor immunity. *Sci Adv* (2021) 7:eabg5016. doi: 10.1126/sciadv.abg5016
37. Roy S, Rizvi ZA, Clarke AJ, Macdonald F, Pandey A, Zaiss DMW, et al. EGFR-HIF1 $\alpha$  signaling positively regulates the differentiation of IL-9 producing T helper cells. *Nat Commun* (2021) 12:3182. doi: 10.1038/s41467-021-23042-x
38. Sadhu S, Rizvi ZA, Pandey RP, Dalal R, Rathore DK, Kumar B, et al. Gefitinib results in robust host-directed immunity against salmonella infection through proteo-metabolomic reprogramming. *Front Immunol* (2021) 12:648710. doi: 10.3389/fimmu.2021.648710
39. Malik S, Sadhu S, Elesela S, Pandey RP, Chawla AS, Sharma D, et al. Transcription factor Foxo1 is essential for IL-9 induction in T helper cells. *Nat Commun* (2017) 8:815. doi: 10.1038/s41467-017-00674-6
40. Singh AK, Awasthi D, Dubey M, Nagarkoti S, Kumar A, Chandra T, et al. High oxidative stress adversely affects NF $\kappa$ B mediated induction of inducible nitric oxide synthase in human neutrophils: Implications in chronic myeloid leukemia. *Nitric Oxide* (2016) 58:28–41. doi: 10.1016/j.niox.2016.06.002
41. Jyoti A, Singh AK, Dubey M, Kumar S, Saluja R, Keshari RS, et al. Interaction of inducible nitric oxide synthase with Rac2 regulates reactive oxygen and nitrogen species generation in the human neutrophil phagosomes: Implication in microbial killing. *Antioxid Redox Signaling* (2014) 20:417–31. doi: 10.1089/ars.2012.4970
42. Chan JF-W, Zhang AJ, Yuan S, Poon VK-M, Chan CC-S, Lee AC-Y, et al. Simulation of the clinical and pathological manifestations of coronavirus disease 2019 (COVID-19) in a golden Syrian hamster model: Implications for disease pathogenesis and transmissibility. *Clin Infect Dis* (2020) 71:2428–46. doi: 10.1093/cid/ciaa325
43. Sia SF, Yan L-M, Chin AWH, Fung K, Choy K-T, Wong AYL, et al. Pathogenesis and transmission of SARS-CoV-2 in golden hamsters. *Nature* (2020) 583(7818):1–7. doi: 10.1038/s41586-020-2342-5
44. Del Valle DM, Kim-Schulze S, Huang H-H, Beckmann ND, Nirenberg S, Wang B, et al. An inflammatory cytokine signature predicts COVID-19 severity and survival. *Nat Med* (2020) 26:1636–43. doi: 10.1038/s41591-020-1051-9
45. Afrin LB, Weinstock LB, Molderings GJ. Covid-19 hyperinflammation and post-Covid-19 illness may be rooted in mast cell activation syndrome. *Int J Infect Dis* (2020) 100:327–32. doi: 10.1016/j.ijid.2020.09.016
46. Caughey GH. Mast cell tryptases and chymases in inflammation and host defense. *Immunol Rev* (2007) 217:141–54. doi: 10.1111/j.1600-065X.2007.00509.x
47. Guo RF, Lentsch AB, Warner RL, Huber-Lang M, Sarma JV, Hlaing T, et al. Regulatory effects of eotaxin on acute lung inflammatory injury. *J Immunol* (2001) 166:5208–18. doi: 10.4049/jimmunol.166.8.5208
48. Makni-Maalej K, Boussetta T, Hurtado-Nedelec M, Belambri SA, Gougerot-Pocidallo M-A, El-Benna J. The TLR7/8 agonist CL097 primes N-Formyl-Methionyl-Leucyl-Phenylalanine-stimulated NADPH oxidase activation in human neutrophils: Critical role of p47phox phosphorylation and the proline isomerase Pin1. *J Immunol* (2012) 189:4657–65. doi: 10.4049/jimmunol.1201007
49. Radermecker C, Detrembleur N, Guiot J, Cavalier E, Henket M, d'Emal C, et al. Neutrophil extracellular traps infiltrate the lung airway, interstitial, and vascular compartments in severe COVID-19. *J Exp Med* (2020) 217:e20201012. doi: 10.1084/jem.20201012
50. Kenny EF, Herzig A, Krüger R, Muth A, Mondal S, Thompson PR, et al. Diverse stimuli engage different neutrophil extracellular trap pathways. *eLife* (2017) 6:e24437. doi: 10.7554/eLife.24437
51. Gil-Etayo FJ, Suárez-Fernández P, Cabrera-Marante O, Arroyo D, Garcinuño S, Naranjo L, et al. T-Helper cell subset response is a determining factor in COVID-19 progression. *Front Cell Infect Microbiol* (2021) 11:624483. doi: 10.3389/fcimb.2021.624483
52. Grifoni A, Weiskopf D, Ramirez SI, Mateus J, Dan JM, Moderbacher CR, et al. Targets of T cell responses to SARS-CoV-2 coronavirus in humans with COVID-19 disease and unexposed individuals. *Cell* (2020) 181:1489–501. doi: 10.1016/j.cell.2020.05.015
53. Roncati L, Nasillo V, Lusenti B, Riva G. Signals of Th2 immune response from COVID-19 patients requiring intensive care. *Ann Hematol* (2020) 99:1419–20. doi: 10.1007/s00277-020-04066-7
54. Martonik D, Parfieniuk-Kowerda A, Rogalska M, Flisiak R. The role of Th17 response in COVID-19. *Cells* (2021) 10:1550. doi: 10.3390/cells10061550
55. Allegra A, Di Gioacchino M, Tonacci A, Musolino C, Gangemi S. Immunopathology of SARS-CoV-2 infection: Immune cells and mediators, prognostic factors, and immune-therapeutic implications. *Int J Mol Sci* (2020) 21:E4782. doi: 10.3390/ijms21134782
56. Winkler ES, Bailey AL, Kafai NM, Nair S, McCune BT, Yu J, et al. SARS-CoV-2 infection of human ACE2-transgenic mice causes severe lung inflammation and impaired function. *Nat Immunol* (2020) 21:1327–35. doi: 10.1038/s41590-020-0778-2
57. Tan L, Wang Q, Zhang D, Ding J, Huang Q, Tang Y-Q, et al. Lymphopenia predicts disease severity of COVID-19: a descriptive and predictive study. *Sig Transduct Target Ther* (2020) 5:1–3. doi: 10.1038/s41392-020-0148-4
58. Sacchi A, Grassi G, Bordini V, Lorenzini P, Cimini E, Casetti R, et al. Early expansion of myeloid-derived suppressor cells inhibits SARS-CoV-2 specific T-cell response and may predict fatal COVID-19 outcome. *Cell Death Dis* (2020) 11:1–9. doi: 10.1038/s41419-020-03125-1
59. Matveeva T, Khafizova G, Sokornova S. In search of herbal anti-SARS-Cov2 compounds. *Front Plant Sci* (2020) 11:589998. doi: 10.3389/fpls.2020.589998
60. Kashyap VK, Peasah-Darkwah G, Dhasmana A, Jaggi M, Yallapu MM, Chauhan SC. Withania somnifera: Progress towards a pharmaceutical agent for immunomodulation and cancer therapeutics. *Pharmaceutics* (2022) 14:611. doi: 10.3390/pharmaceutics14030611
61. Sharma P, Dwivedee BP, Bisht D, Dash AK, Kumar D. The chemical constituents and diverse pharmacological importance of *inospora cordifolia*. *Heliyon* (2019) 5:e02437. doi: 10.1016/j.heliyon.2019.e02437
62. Patil VS, Hupparage VB, Malgi AP, Deshpande SH, Patil SA, Mallapur SP. Dual inhibition of COVID-19 spike glycoprotein and main protease 3CLpro by withanone from *withania somnifera*. *Chin Herbal Medicines* (2021) 13:359–69. doi: 10.1016/j.chmed.2021.06.002
63. Kumar S, Dikshit M. Metabolic insight of neutrophils in health and disease. *Front Immunol* (2019) 10:2099. doi: 10.3389/fimmu.2019.02099
64. Parker H, Albrett AM, Kettle AJ, Winterbourn CC. Myeloperoxidase associated with neutrophil extracellular traps is active and mediates bacterial killing in the presence of hydrogen peroxide. *J Leukoc Biol* (2012) 91:369–76. doi: 10.1189/jlb.0711387
65. Douda DN, Khan MA, Grasemann H, Palaniyar N. SK3 channel and mitochondrial ROS mediate NADPH oxidase-independent NETosis induced by calcium influx. *Proc Natl Acad Sci* (2015) 112:2817–22. doi: 10.1073/pnas.1414055112
66. Vorobjeva NV, Chernyak BV. NETosis: Molecular mechanisms, role in physiology and pathology. *Biochem Moscow* (2020) 85:1178–90. doi: 10.1134/S0006297920100065
67. Dikalov SI, Kirilyuk IA, Voinov M, Grigor'ev IA. EPR detection of cellular and mitochondrial superoxide using cyclic hydroxylamines. *Free Radical Res* (2011) 45:417–30. doi: 10.3109/10715762.2010.540242
68. Zhu Y, Chen X, Liu X. NETosis and neutrophil extracellular traps in COVID-19: Immunothrombosis and beyond. *Front Immunol* (2022) 13:838011. doi: 10.3389/fimmu.2022.838011
69. Awasthi D, Nagarkoti S, Kumar A, Dubey M, Singh AK, Pathak P, et al. Oxidized LDL induced extracellular trap formation in human neutrophils via TLR-PKC-IRAK-MAPK and NADPH-oxidase activation. *Free Radical Biol Med* (2016) 93:190–203. doi: 10.1016/j.freeradbiomed.2016.01.004
70. Nagarkoti S, Sadaf S, Awasthi D, Chandra T, Jagavelu K, Kumar S, et al. L-arginine and tetrahydrobiopterin supported nitric oxide production is crucial for the microbicidal activity of neutrophils. *Free Radical Res* (2019) 53:281–92. doi: 10.1080/10715762.2019.1566605

## Glossary

ABSL3	animal biosafety level 3
COVID-19	coronavirus disease 19, set of clinical pathologies following of coronavirus infection
CRS	cytokine release syndrome
DXM	Dexamethasone
FACS	fluorescence activated cell sorting
hACE2 mice	Transgenic mice developed by knocking in humanized ACE2 receptors under the influence of the K18 promoter
Hamster	golden Syrian hamster, the animal model used for COVID-19 study
Herbal extract	Aqueous Extract of herbs that have been used in the study
I	Infected
I+TC	infected animals receiving TC
I+TC+PL	infected animals receiving TC in combination with PL
I+WS	infected animals receiving WS
IFN $\gamma$	interferon gamma
IL6	interleukin 6
mtROS	ROS generated in mitochondria
Muc-1	mucin 1 gene
NET	neutrophil extracellular traps
Pathology	clinical features of the disease that can be used for diagnosis and examination
Pfu	plaque forming unit
PL	<i>Piper longum</i> (L.)
qPCR	quantitative PCR
RDV	remdesivir
ROS	reactive oxygen species
SARS-CoV-2	severe acute respiratory syndrome coronavirus 2, the virus responsible for COVID-19.
Sftp-D	surfactant protein D
T helper cells	component of cell-mediated immunity which express CD4 marker
TC	<i>Tinospora cordifolia</i> (Willd.) Miers
Th1 cells	Subset of CD4+ T helper cells which are important for anti-viral immunity
Th17 cell	subset of CD4+ T helper cells which are important of inflammation and autoimmunity
Th2 cells	subset of CD4+ T helper cells which are important for extra cellular pathogens
TNF $\alpha$	tumor necrosis factor alpha
UI	uninfected
WS	<i>Withania somnifera</i> (L.) Dunal



## OPEN ACCESS

## EDITED BY

Alfonso J. Rodriguez-Morales,  
Fundacion Universitaria Autónoma de las  
Américas, Colombia

## REVIEWED BY

Wentao Li,  
Huazhong Agricultural University, China  
Hang Yang,  
Wuhan Institute of Virology (CAS), China

## \*CORRESPONDENCE

Latifa Zekri

✉ latifa.zekri@ifiz.uni-tuebingen.de

<sup>†</sup>These authors share last authorship

## SPECIALTY SECTION

This article was submitted to  
Viral Immunology,  
a section of the journal  
Frontiers in Immunology

RECEIVED 30 November 2022

ACCEPTED 22 February 2023

PUBLISHED 08 March 2023

## CITATION

Zekri L, Ruetalo N, Christie M, Walker C,  
Manz T, Rammensee H-G, Salih HR,  
Schindler M and Jung G (2023) Novel  
ACE2 fusion protein with adapting activity  
against SARS-CoV-2 variants *in vitro*.  
*Front. Immunol.* 14:1112505.  
doi: 10.3389/fimmu.2023.1112505

## COPYRIGHT

© 2023 Zekri, Ruetalo, Christie, Walker,  
Manz, Rammensee, Salih, Schindler and  
Jung. This is an open-access article  
distributed under the terms of the [Creative  
Commons Attribution License \(CC BY\)](#). The  
use, distribution or reproduction in other  
forums is permitted, provided the original  
author(s) and the copyright owner(s) are  
credited and that the original publication in  
this journal is cited, in accordance with  
accepted academic practice. No use,  
distribution or reproduction is permitted  
which does not comply with these terms.

# Novel ACE2 fusion protein with adapting activity against SARS-CoV-2 variants *in vitro*

Latifa Zekri<sup>1,2,3,4\*</sup>, Natalia Ruetalo<sup>5</sup>, Mary Christie<sup>6</sup>,  
Carolyn Walker<sup>1,2</sup>, Timo Manz<sup>1,2</sup>, Hans-Georg Rammensee<sup>1,2,4</sup>,  
Helmut R. Salih<sup>2,3,4</sup>, Michael Schindler<sup>5†</sup> and Gundram Jung<sup>1,2,4†</sup>

<sup>1</sup>Department of Immunology, Institute for Cell Biology, Eberhard Karls Universität Tübingen, Tübingen, Germany, <sup>2</sup>German Cancer Research Center (DKFZ) Partner Site Tübingen, German Cancer Consortium (DKTK), Tübingen, Germany, <sup>3</sup>Clinical Collaboration Unit Translational Immunology, Department of Internal Medicine, University Hospital Tübingen, Tübingen, Germany, <sup>4</sup>Cluster of Excellence iFIT (EXC 2180) "Image-Guided and Functionally Instructed Tumor Therapies", University of Tübingen, Tübingen, Germany, <sup>5</sup>Institute for Medical Virology and Epidemiology, University Hospital Tübingen, Tübingen, Germany, <sup>6</sup>School of Life and Environmental Sciences and School of Life of Medical Sciences, The University of Sydney, Sydney, NSW, Australia

Despite the successful development of vaccines and neutralizing antibodies to limit the spread of severe acute respiratory syndrome coronavirus 2 (SARS-CoV-2), emerging variants prolong the pandemic and emphasize the persistent need to develop effective antiviral treatment regimens. Recombinant antibodies directed to the original SARS-CoV-2 have been successfully used to treat established viral disease. However, emerging viral variants escape the recognition by those antibodies. Here we report the engineering of an optimized ACE2 fusion protein, designated ACE2-M, which comprises a human IgG1 Fc domain with abrogated Fc-receptor binding linked to a catalytically-inactive ACE2 extracellular domain that displays increased apparent affinity to the B.1 spike protein. The affinity and neutralization capacity of ACE2-M is unaffected or even enhanced by mutations present in the spike protein of viral variants. In contrast, a recombinant neutralizing reference antibody, as well as antibodies present in the sera of vaccinated individuals, lose activity against such variants. With its potential to resist viral immune escape ACE2-M appears to be particularly valuable in the context of pandemic preparedness towards newly emerging coronaviruses.

## KEYWORDS

SARS-CoV-2 therapy, ACE-2, neutralizing antibodies, immune escape, fusion protein

## 1 Introduction

In the past two years, the Coronavirus disease 2019 (COVID-19) pandemic has claimed several millions of lives worldwide and has caused enormous -and unprecedented- social and economic damage (1, 2). Fortunately -and unprecedented as well- efficient vaccines have been developed and administered to millions of individuals in less than two years, and currently it appears that vaccination has become the cornerstone for the control of the pandemic worldwide (1, 3).



In the face of this truly remarkable success, the development of reagents for the treatment of established viral infections remains challenging. A growing understanding and appropriate treatment of the hyper-inflammatory and -coagulatory states occurring in the course of moderate and severe disease resulted in a significant reduction in mortality rates in treated patients. In addition, reagents with direct antiviral activity have been developed. Such reagents can be divided into two classes, small molecules with antiviral activity and neutralizing antiviral antibodies. For the latter, the tools of modern recombinant antibody technology, i. e., phage display, and single-cell cloning, have been used to generate optimized monoclonal antibodies with potent neutralizing capacity, directed to the receptor-binding domain (RBD) of the viral spike protein (S-protein) that binds to the ACE2 receptor on target cells (4–8). Several of these reagents have received approval for use during the early stages of infection. As of today, however, their activity in more advanced stages has been limited. Indeed, antibody-dependent enhancement (ADE), e.g., by non-neutralizing antibodies binding to viral particles, was reported to promote their Fc-mediated uptake by cells carrying Fc-receptors (FcRs), such as alveolar macrophages (9, 10).

However, a major limitation for the therapeutic activity of antibodies are recent mutations in SARS-CoV-2 variants that not only confer enhanced affinity to ACE2 and thus increased infectivity but also prevent the binding of antibodies raised against the B.1 S-protein (11–13).

A recombinant antibody approved for treatment of limited disease, REGN 10933 (14) exemplifies this strikingly. It strongly binds to the RBD of the B.1 S-protein but fails to bind to the S-protein encoded by known variants of concern (VOCs), such as the Beta and Omicron variants. The latter escapes effective neutralization by five of seven mAbs approved for treatment of COVID-19 (15–17). At the same time, the S-protein of the Omicron variant gained affinity towards the ACE2 protein (18, 19), resulting in increased infectivity.

In principle, the conceptual weakness of neutralizing antibodies directed to the RBD domain of the S-protein discussed above might be overcome by recombinant Fc-based fusion proteins comprising the “natural” binding partner of the RBD domain, the ACE2 protein. In contrast to RBD binding antibodies, the neutralizing capacity of such proteins would not be impaired but rather strengthened by affinity gaining mutations in the RBD. Moreover, since the RBD ACE2 interaction is mediated by a dimeric form of ACE2, an Fc based format may promote ACE2 dimerization (20). Despite this conceptual advantage, the construction of such fusion proteins faces challenges as well: first, the affinity of recombinant ACE2 to viral S-proteins is lower than that of most antibodies. Second, the enzymatic activity of physiologically expressed ACE2 is critical for the proper function of the renin-angiotensin-aldosterone system (RAAS). This system is of vital importance, among others, for blood pressure regulation, and high doses of enzymatically active protein might induce uncontrollable side effects. Although it has been suggested that ACE2 may function as a “rescue protein” in the course of the SARS-CoV-2 infection (21), we share the view expressed in a paper Khodarahmi et al. (22), that recommend the use of enzymatically inactive ACE2 if blockade of the S-protein is intended.

Based on the considerations outlined above, we have constructed and characterized an ACE2-Fc fusion protein designated ACE2-M, that carries mutations to:

- i. abrogate FcR binding and complement activation by the Fc domain
- ii. deplete enzymatic activity of the ACE2 protein
- iii. enhance the apparent affinity of the ACE2 S-protein interaction

Here we evaluate the capability of ACE2-M to bind and to neutralize various virus variants. This activity was benchmarked against the therapeutic antibody REGN 10933 and the serum of vaccinated individuals.

## 2 Materials and methods

### 2.1 Generation and production of ACE2 fusion proteins and REGN 10933

The human ACE2 extracellular domain (aa 18-740; Gene ID: 59272) and the variable domain sequences of the REGN 10933 antibody (14) were codon-optimized for expression by Chinese hamster cells using the GeneArt GeneOptimizer tool (Thermo Fisher Scientific, Regensburg, Germany). VH, VL, and ACE2 sequences (ACE2 wild-type (ACE2) or the indicated mutants, ACE2-RR, ACE2-K, ACE2-M) were synthesized *de novo* at GeneArt (Thermo Fisher Scientific, Regensburg, Germany). ACE-2 coding sequences were fused at their C-terminus to a human Igγ1 Hinge- Fc domain via a flexible (GGGGS)<sup>3</sup> linker. Modifications in the CH2 domain consisting of the amino acid substitutions and deletions E233P; L234V; L235A; ΔG236; D265G; A327Q; A330S (EU index), which abrogate FcR binding and complement fixation, were introduced as described (23). REGN 10933 variable sequences were inserted into a human Igγ1 backbone comprising CH1-CH2-CH3- or CK-constant domain sequences as described (23). All constructs were transiently transfected and produced using the ExpiCHO<sup>TM</sup> Expression System (Thermo Fisher Scientific, Regensburg, Germany) according to the manufacturer's instructions and were then purified by HiTrap<sup>TM</sup> MabSelect<sup>TM</sup> SuRe columns (Cytiva, Freiburg, Germany), before being subjected to preparative and analytical size exclusion chromatography (SEC) using HiLoad<sup>TM</sup> 16/600 Superdex 200 pg and Superdex<sup>TM</sup> 200 Increase 10/300 GL columns (Cytiva Freiburg, Germany), respectively. Endotoxin levels of samples, as determined by a limulus amoebocyte lysate assay (Endosafe<sup>®</sup> Charles River, Charleston, SC), were < 0.5 EU/ml. Sodium dodecyl sulfate-polyacrylamide gel electrophoresis (SDS-PAGE) was performed as previously described (23).

### 2.2 Spike proteins

SARS-CoV-2 full-length trimeric spike proteins corresponding to the B.1 (B.1.126), Alpha (B.1.1.7), Beta (B.1.351), Gamma (P.1),



and Delta (B.1.617.2) were purchased from BioServ, (Sheffield, UK). The Trimeric S-protein corresponding to Omicron (B.1.1.529) or Omicron subvariant BA.5 and BQ1.1 were obtained from Sino Biological (Beijing, China).

## 2.3 ACE2 catalytic activity assay

Enzymatic activity of ACE2 fusion proteins was measured using the ACE2 Activity Assay Kit (Fluorometric) (BioVision, Milpitas, CA) according to the manufacturer's instructions. The proteins were diluted in assay buffer to 22.7, 4.54, and 0.91 nM final concentration. Fluorescence was measured using a Wallac 1420 Victor 2 Multi-Label Counter (Perkin-Elmer, Waltham, MA).

## 2.4 Competitive ELISA

The indicated S trimeric proteins were coated on 96-well plates at 1 µg/ml, 4°C overnight. After washing, wells were blocked with PBS containing 3% BSA for 1 hour at room temperature. Next, a serial dilution of the indicated ACE2 fusion proteins, REGN 10933 or serum antibodies were pre-mixed with 150 nM of His-tagged ACE2 wild-type protein (BioLegend, San Diego, CA) and added to the plates. In case of the Omicron variants (Sino Biological), the His-tagged ACE2 protein was additionally biotinylated using the One-Step Biotinylation Kit (Miltenyi, Cologne, Germany) according to the manufacturer's instructions. For visualization, a Penta-His HRP conjugate (1:1000) (Qiagen, Hilden, Germany) or mouse anti-Biotin HRP conjugate (1:1000) (Invitrogen, Waltham, MA) were used. Unbound HRP-conjugated antibodies were removed by washing, TMB substrate was added, and absorbance was measured at 450nm.

## 2.5 Determination of anti-spike antibodies in the sera of vaccine recipients

Sera were collected from 8 healthy donors (25-65 years of age). All donors received a first dose of Vaxzevria vaccine and then a second dose of Comirnaty or Spikevax. Sera were collected 40-45 days after the second dose and anti-SARS-CoV-2 antibody concentrations were measured using the Euroimmun Anti-SARS CoV-2 ELISA IgG kit (Euroimmun, Luebeck, Germany). Briefly, serum samples were diluted at 1:100 and 1:1000 and ELISA was performed following manufacturer's instructions. A titration of a reference neutralizing antibody (REGN 10933) was used to calibrate the assay.

## 2.6 Measurement of fusion- and spike protein interaction by biolayer interferometry

Trimeric S-proteins were analyzed for their binding to ACE2-RR or ACE2-M fusion proteins using an Octet HTX system (Sartorius, Goettingen, Germany). Assays were run with a sensor offset of 3 mm

and an acquisition rate of 5 Hz on AHC biosensors in 16-channel mode. Microplates were loaded with 60 µL per well of assay buffer consisting of PBS with 0.05% Tween-20 and 0.1% BSA. Sensors were equilibrated in assay buffer for 10 min. Following a baseline step of 60s, the analyte S-proteins were loaded for 120 s. Association was measured for 150s and dissociation for 300s. Regeneration of the sensors was performed using 10 mM Glycine pH 1.5. Data evaluation was done using Octet Analysis HT Software. The reference subtraction was performed to consider the potential dissociation of analyte loaded onto the biosensor. Data traces were aligned to the baseline, followed by an inter-step correction for the dissociation step. Savitzky-Golay filtering was applied to the data and the curves were fitted globally using a 1:1 binding model (with Rmax unlinked by sensor).

## 2.7 Viruses

All experiments with SARS-CoV-2 viruses were conducted in a Biosafety Level 3 laboratory at the University Hospital Tübingen. The SARS-CoV-2 strain icSARS-CoV-2-mNG (24) was obtained from the World Center for Emerging Viruses and Arboviruses (WRCEVA) of the UTMB (University of Texas Medical Branch, Galveston, TX, USA). SARS-CoV-2 B.1.126 (parental D614G), referred as B.1, and SARS-CoV-2 B.1.351 (Beta), were isolated from patient samples and variant identity was confirmed by next-generation sequencing of the entire viral genome as described before (25, 26). SARS-CoV-2 B.1.1.529 (Omicron) was isolated from a throat swab collected in December 2021 at the Institute for Medical Virology and Epidemiology of Viral Diseases, University Hospital Tübingen, from a PCR-positive patient. Fifty microliters of patient material were diluted in medium and used directly to inoculate 150,000 Caco-2 cells in a six-well plate. 48 hours post-infection (hpi), the supernatant was collected, centrifuged, and stored at -80°C. After two consecutive passages, an RNA sample from the supernatant was prepared, and NGS confirmed that the clinical isolate belongs to the lineage B.1.1.529. All virus stocks were generated in Caco-2 cells collecting supernatants 48-72 hpi. Multiplicity of infection determination (MOI) was conducted by titration using serial dilutions of both virus stocks. The number of infectious virus particles per ml was calculated as  $(\text{MOI} \times \text{cell number}) / (\text{infection volume})$ , where  $\text{MOI} = -\ln(1 - \text{infection rate})$ .

## 2.8 Virus neutralization assay

Caco-2 (Human Colorectal adenocarcinoma, ATCC HTB-37) cells were cultured at 37°C with 5% CO<sub>2</sub> in DMEM containing 10% FCS, 2 mM L-glutamine, 100 mg/ml penicillin-streptomycin and 1% NEAA. Neutralization assays using clinical isolates were performed as described in Wagner et al., 2021. Briefly, cells were co-incubated with the clinical isolate SARS-CoV-2 B.1.126, SARS-CoV-2 B.1.351 (Beta), or SARS-CoV-2 B.1.1.529 (Omicron), at MOI of 0.7-4.0, and serial dilutions of the ACE2 protein designs. 48 hpi, cells were fixed with 80% acetone, and immunofluorescence (IF) staining was performed using an anti-SARS-CoV-2 nucleocapsid antibody (GeneTex, Cat No. GTX135357) and goat

anti-rabbit Alexa594-conjugated secondary antibody. Cells were counterstained with DAPI solution and images were taken with the Cytation3 (BioTek). Infection rates were calculated as the ratio of Alexa594-positive over DAPI-positive cells, which were automatically counted by the Gen5 software (BioTek). Inhibitory concentration 50 (IC<sub>50</sub>) was calculated as the half-maximal inhibitory dose using four-parameter nonlinear regression (GraphPad Prism).

## 2.9 Binding of ACE2 fusion proteins to SARS-CoV-2 infected cells

For binding experiments,  $3 \times 10^6$  Caco-2 cells were seeded in a T75 flask the day before infection, in a medium containing 5% FCS. Cells were infected with SARS-CoV-2-mNG, and 48 hpi cells were detached from the flask using Accutase, fixed with 2% PFA for 10 minutes at 37°C, and resuspended in FACS buffer (PBS, 1%FCS).  $1 \times 10^6$  cells in 100  $\mu$ L in FACS buffer were distributed in a U-shape 96-well plate. The plate was centrifuged at 600 g for 5 min and the buffer was removed by a fast decant. Cells were incubated for 1h at 4°C using 50  $\mu$ L of 3-fold serial dilutions of ACE2 protein or REGN 10933, tested from 40  $\mu$ g/ml following 12 dilution points. Cells were washed with 150  $\mu$ L of FACS buffer/well, centrifuged, and the supernatant decanted. The washing step was repeated using 200  $\mu$ L of FACS buffer/well. Subsequently, cells were incubated with 50  $\mu$ L of a 1:200 dilution of the Secondary AB- R-Phycoerythrin (PE) conjugated affinity pure F(ab')<sub>2</sub> Fragment Goat-anti Human IgG-Fc gamma fragment (Jackson-Immuno) for 30 minutes at 4°C. The two washing steps were repeated, and the cells were resuspended using 100  $\mu$ L of FACS buffer/well. Controls included: mock-infected cells incubated with the highest and lower protein concentrations; infected cells non-incubated as well as infected cells stained only with the secondary antibody. Alternatively, Caco-2 cells were infected with SARS-CoV-2 parental or Omicron variants and the same protocol described above was followed. After incubation with PE-secondary antibody, cells were permeabilized with 80% Acetone for 5 minutes at room temperature, washed as described before and immunofluorescence (IF) staining was performed using an anti-SARS-CoV-2 nucleocapsid antibody (GeneTex, Cat No. GTX135357) (1:1000, 1 h) and goat anti-rabbit Alexa594-conjugated secondary antibody (1:2000, 1 h). After the final washing steps, the cells were analyzed using a MACSQuant VYB (Miltenyi). FACS analysis was performed with MACS Quantify Software (Miltenyi) and Flowlogic (Miltenyi-Inivai).

## 3 Results and discussion

### 3.1 Construction and characterization of ACE2-M

ACE2 fusion proteins were constructed by fusing the ACE2 extracellular domain to a human IgG1 Fc fragment that was originally developed to prevent binding to FcRs by T cell

activating bispecific antibodies. This modification consists of 6 mutations and one deletion in the CH2 domain of the human IgG1 Fc domain that completely abrogates binding to FcRs and ablates complement activation (23).

To avoid the introduction of undesired peptidase activity, two catalytically-inactive forms of ACE2 were generated. The first mutant, ACE2-RR, contains two substitutions in the catalytic pocket, H374R, and H378R, that prevent zinc binding within the active site of the protein (27). The second mutant, ACE2-K, has a single mutation at position 273 (R273K), which is critical for enzymatic activity (28). Fc-fusion proteins constructed with either of the two variants show the size expected for a dimeric molecule as demonstrated by SDS-PAGE and size exclusion chromatography (Supplementary Figures 1A–C). In contrast to ACE2-RR, ACE2-K retained some residual enzymatic activity and showed a slight loss in binding affinity to recombinant trimeric parental S-protein as measured by enzyme-linked immunosorbent assay (ELISA) (Supplementary Figures 1D, E). Thus, the ACE2-RR version of the fusion protein was selected for further modification.

To enhance binding to the S-protein, we introduced three additional mutations to the ACE2-RR-Fc fusion protein that are located at the S-protein binding surface of ACE2: T27Y, L79Y, and N330Y (Figures 1A, B). These mutations are similar to an ACE2 variant described by Chan and collaborators (29). ACE2-M, was produced as a stable dimer and had no detectable enzymatic activity (Figures 1C–E).

We next measured the binding affinity of recombinant trimeric S-protein and ACE2-M by ELISA, which was benchmarked against an Fc-fusion protein comprising the wild type ACE2 protein, as well as against the reference antibody REGN10933. In this assay, ACE2-M showed a 4-fold higher binding affinity than wild-type ACE2 fusion protein (Figure 1F). Interestingly, the apparent binding affinity measured by flow cytometry of Caco-2 cells infected with a recombinant parental virus resulted in a greater than 18-fold affinity enhancement (Figure 1G). In both assays, the S-protein apparent binding affinity of ACE2-M and REGN 10933 was similar. The differences between the affinities of antibodies and fusion proteins to S-proteins coated to an ELISA plate compared with those embedded in the membrane of a virus-infected cell are noteworthy. Obviously, binding to infected cells resembles the “physiological state” more closely, and may predict different neutralization capacities of the various fusion proteins more reliably as demonstrated below.

To test whether ACE2-M retains binding to the globally spreading SARS-CoV-2 VOCs Alpha (B.1.1.7), Beta (B.1.351), Gamma (P.1), Delta (B.1.617.2), and Omicron (B.1.1.529), structural analysis of ACE2-M and the respective S-RBD variants was performed (Supplementary Figure 2). This analysis revealed that the affinity-enhancing mutations introduced into the ACE2-M protein appear to be spared by the viral escape mechanism, probably because they form part of the RBD-binding interface. Those observations were further confirmed by measuring the binding kinetics of ACE2-M to all variants by biolayer interferometry technology (BLI). The results depicted in Supplementary Figure 3 demonstrate a superior apparent binding

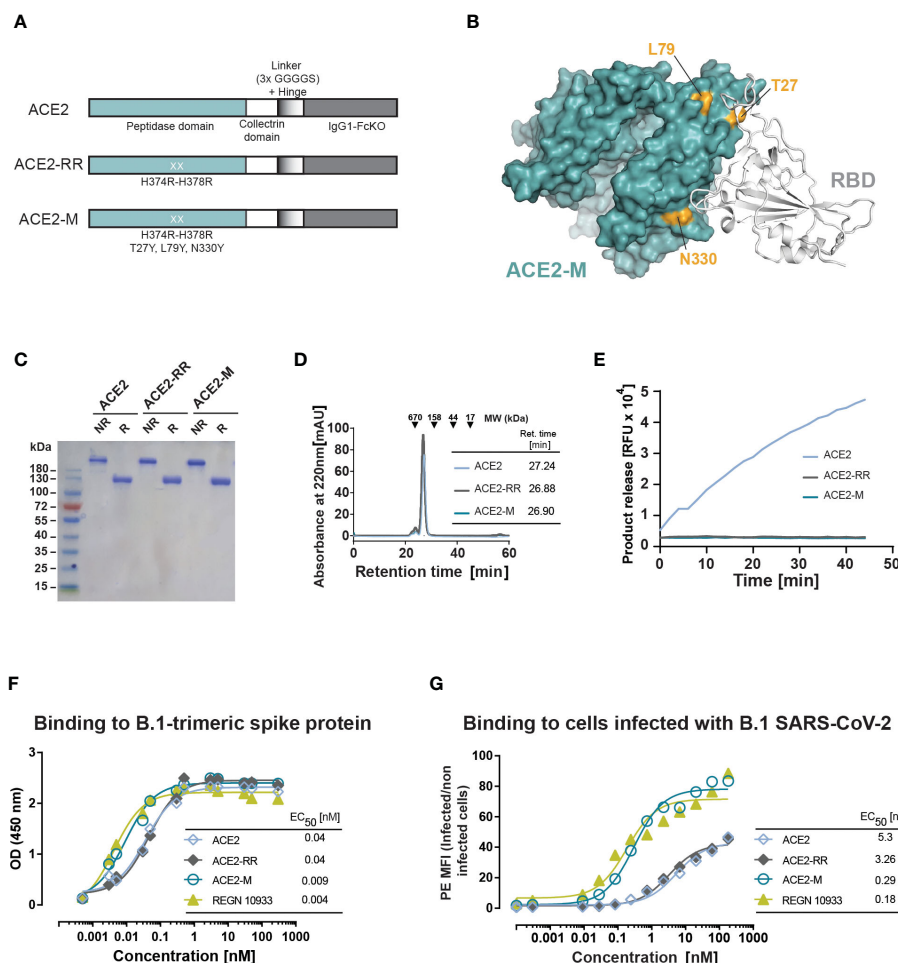


FIGURE 1

Design and biochemical characterization of ACE2-M. (A) Schematic representation of the ACE2 molecules used in this study. The ACE2 extracellular domain, comprising peptidase and collectrin domains, was fused to an IgG1-Hinge-Fc-Ko domain via a flexible linker (GGGGS)<sub>3</sub> (ACE2 version). The H374R-H378R mutations were introduced to abolish ACE2 enzymatic activity (ACE2-RR version). Additional mutations were introduced to increase binding to the S-protein as indicated in (A, B). (B) Structure of ACE2 in complex with S-RBD (using PDB 6M0J) with residues substituted in ACE2-M highlighted in gold. (C) Coomassie-stained gel of the three generated fusion proteins. NR, non-reduced; R, reduced. (D) Superposed analytic chromatography profiles of the ACE2 proteins run on a Superdex S200 Increase 10/300GL column. The table indicates the corresponding retention times. (E) Enzymatic activity of the ACE2 fusion proteins (4.5 nM) as measured by cleavage of a fluorescent peptide substrate. (F) Binding of the fusion proteins and REGN 10933 to B.1 trimeric S-protein determined by ELISA. Results represent the standard deviation (SD) of  $n=3$ . EC<sub>50</sub> as calculated by the GraphPad software. (G) Binding of the fusion proteins and REGN 10933 to Caco-2 cells infected with the recombinant infectious clone SARS-CoV-2 that expresses the mNeonGreen as a reporter gene. Binding was assessed by flow cytometry.

affinity of ACE2-M to spike variants. Again, the differences in affinities were less pronounced compared to those observed by flow cytometry of infected cells (Figure 1G).

### 3.2 ACE2-M resists viral escape, in contrast to REGN 10933

Next, we tested the ability of ACE2-RR, ACE2-M, and REGN 10933 to inhibit binding of ACE2 to various S-proteins by competition ELISA. To this end, the fusion proteins and REGN 10933 were mixed with a saturating amount of His-tagged-ACE2 protein before binding to immobilized S-proteins was determined. In line with the BLI results, we observed an improved inhibition of binding by ACE2-M to all S-proteins (Figure 2A). In contrast,

REGN 10933 failed to inhibit ACE2 binding to Beta, Gamma, and Omicron S-proteins. These results are consistent with previously published data, suggesting that the reduced binding of REGN 10933 to certain S variants is likely due to mutations in amino acids K417 and E484 of the S-protein (30, 31), found in the Beta, Gamma, and Omicron variants.

Likewise, binding of ACE2 fusion proteins and REGN 10933 antibody to Caco-2 cells infected with authentic SARS-CoV-2 natural isolates corresponding to the parental strain (D614G) and Omicron (B.1.1.529) showed similar results (Supplementary Figure 4). REGN 10933 bound with high affinity to Caco-2 cells infected with the parental virus, in line with the results obtained with the recombinant virus in Figure 1G. However, REGN 10933 failed to bind to Caco-2 cells infected with the Omicron virus. In contrast, ACE2-M retains high-affinity binding to Caco-2 cells

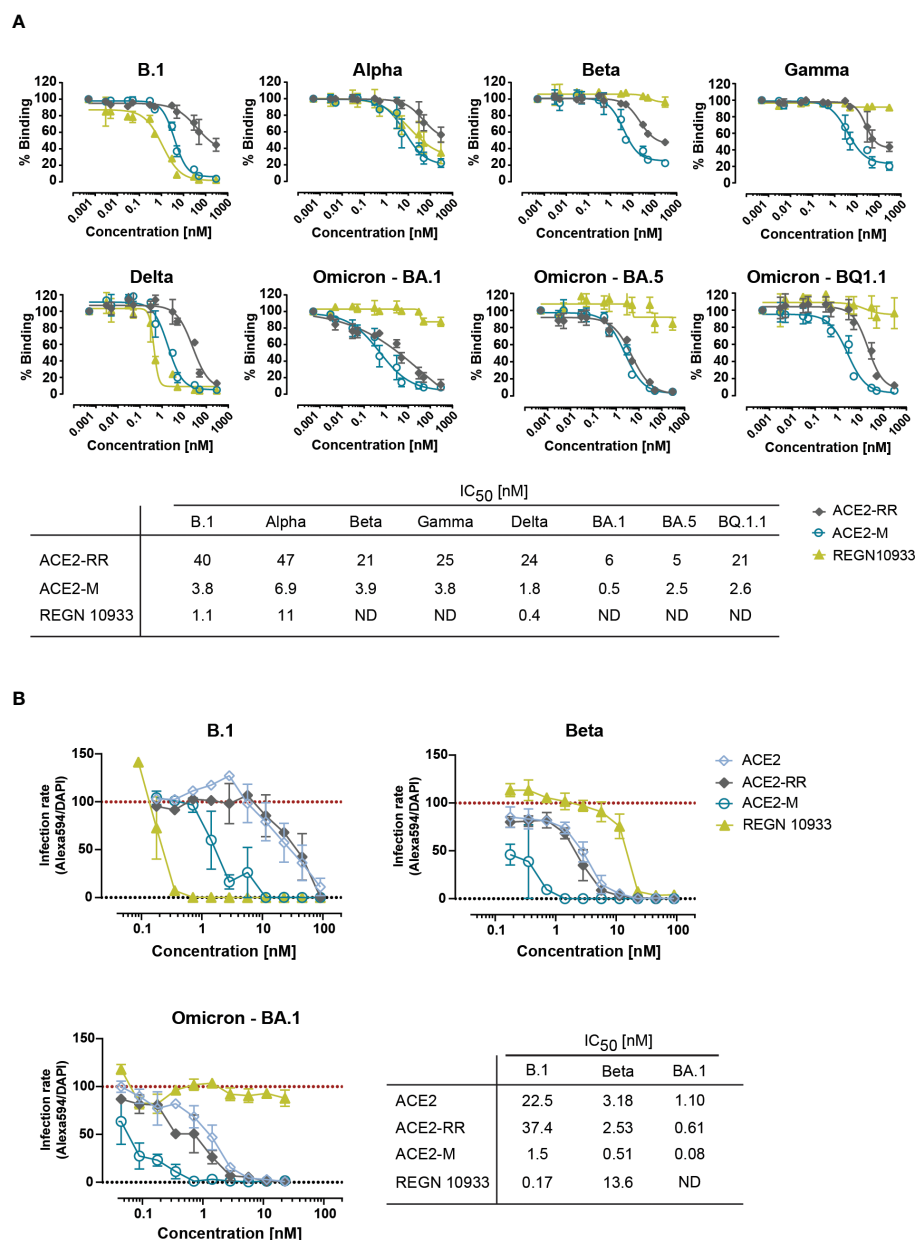


FIGURE 2

Competitive binding of fusion proteins and REGN 10933 to ACE2 and their capacity to neutralize parental and SARS-CoV-2 VOCs. **(A)** Competitive ELISA was performed by immobilizing the indicated full length S-proteins. The results depicted show the binding of 150 nM of His-tagged ACE2 wild-type protein, that was competed with the indicated concentrations of the ACE2 fusion molecules or REGN 10933 antibody. The error bars represent the SD of two independent experiments with technical replicates. The IC<sub>50</sub> values summarized in the table were calculated using the GraphPad software. ND: Not detected. **(B)** Neutralization capacity was determined as described in material and methods. Briefly, Caco-2 cells were infected with the indicated clinical isolates of SARS-CoV-2. Infection rates, calculated as the number of infected cells (Alexa594+) over the total number of cells (DAPI+), were normalized to virus-only infection control. Mean and SEM values are calculated from three independent experiments with technical duplicates. Neutralization assay corresponding IC<sub>50</sub> values were calculated using GraphPad software. ND, Not detectable.

infected with either isolate. Unexpectedly, we observed a 4-fold lower MFI for binding to cells infected with Omicron vs. parental virus. This observation could be explained by the reduced replication capacity recently described for Omicron variant (32–34). The reduced replication seems to be due to the inefficient use of the cellular protease TMPRSS2, which promotes cell entry through plasma membrane fusion (33). We speculate that reduced replication in Caco-2 cells may result in a decreased expression of S-proteins on the cell surface.

To investigate the efficacy of ACE2-M in preventing viral infection, we performed a neutralization assay in Caco-2 cells using SARS-CoV-2 natural isolates from the parental B.1 as well as Beta, and Omicron strains. ACE2-M neutralized all SARS-CoV-2 infected cells at picomolar concentrations (Figure 2B and Supplementary Figure 5). ACE2-M activity was greater against Omicron than against the Beta variant or the parental B.1. In contrast, the activity of REGN 10933 against the Beta and Omicron variants was reduced and undetectable, respectively. Altogether, our

results demonstrate that binding of ACE2-M to S-variants (vs. parental) is preserved or enhanced (in case of Omicron), while it is weakened or lost in the case of REGN 10933. Thus, these results confirm our “founding hypothesis” for the construction of ACE2 fusion proteins, namely that viral variants will mutate “away” from recognition by antibodies but “towards” recognition by ACE2 fusion proteins and hence to neutralization by such proteins.

### 3.3 SARS-CoV-2 VOCs are able to evade vaccine-elicited antibodies but not ACE2-M

To evaluate the binding efficiency of antibodies generated by active immunization to parental, Beta, Delta, and Omicron trimeric S-proteins, sera from 8 healthy fully vaccinated donors were used and evaluated in a competitive ELISA similar to that described above in Figure 2A. Similar to REGN 10933, antibodies present in the post-vaccination sera showed a reduction in binding to Beta, Delta, and, to a greater extent, to Omicron S-proteins (Figure 3A). These results suggest that antibodies generated after active immunization against the parental S-protein are less effective against new variants in accordance with recent reports (35–40).

Next, we defined the required amount of neutralizing antibodies and ACE2-M protein, to achieve a complete inhibition of binding to S-proteins. To this end, SARS-CoV-2 antibody concentrations present in the sera of vaccinated donors were quantified, adjusted, and compared in a competitive ELISA to the ACE2-M protein. Our results, depicted in Figure 3B, show that ACE2-M, at a

concentration of 1  $\mu\text{g/ml}$ , achieved almost complete binding inhibition of ACE2 wild type to all S-variants, however, only a partial binding inhibition could be obtained with antibodies in the various sera. Of note, a serum concentration of 1  $\mu\text{g/ml}$  is easily reached during treatment of antiviral disease with suitable monoclonal antibodies (41, 42).

We have demonstrated that ACE2 fusion proteins are not subject to immune escape exerted by variants of the S-protein in line with recent publications (43–46). In fact, variants with increased affinity such as Omicron variants (BA.1, BA.5 and BQ.1.1), are neutralized more effectively than the parental B.1. Recently, alternative receptors have been reported to interact with the SARS-CoV-2 virus (47–51). In cells with low ACE2 expression, it is thought that SARS-CoV-2 can enter the cells *via* several alternative receptors, but the entry mechanism remains to be defined. Although there is no direct evidence that SARS-CoV-2 escapes ACE2 treatment, the fact that the highly transmissible variant Omicron BA.1 has evolved to be less dependent on TMPRSS2, raises the possibility that alternative SARS-CoV-2 mutations may also contribute to viral evolution and may cause ACE2 immune escape.

To our knowledge, ACE2-M is the first engineered ACE2 fusion molecule combining modifications for Fc-attenuation, enzymatic depletion, and ACE2 affinity enhancement. Although animal studies are required to conclusively evaluate the importance of enzymatic depletion and Fc-attenuation, this molecule provides an important additional option for treatment of COVID-19 and other coronaviruses that use the ACE2 protein as entry receptor.

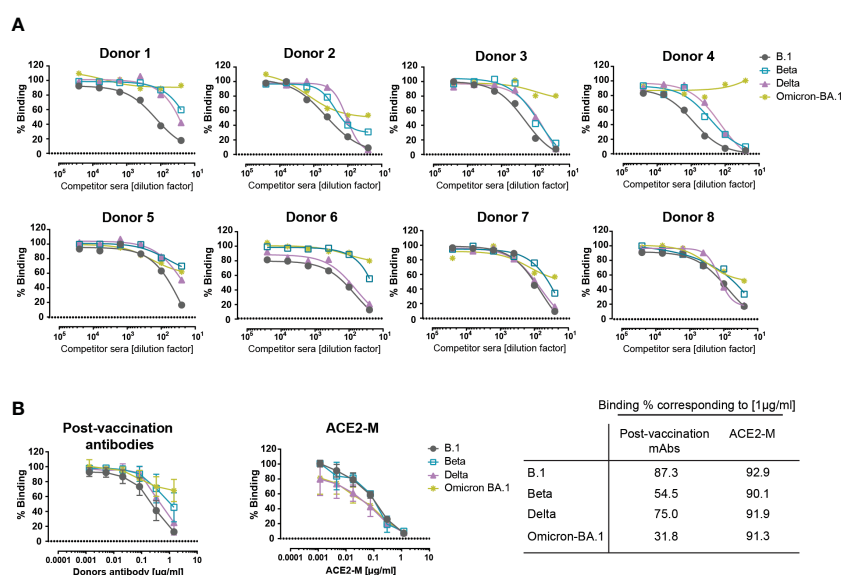


FIGURE 3

Competitive binding of antibodies in the sera of vaccinated donors and ACE2-M to various spike proteins. (A) Similar competition ELISA assay to the one described in Figure 1A was performed with sera from 8 healthy vaccinated individuals. Each serum sample was diluted in a range of 1/25 to 1/25600 and tested against His-tagged ACE2 for binding to SARS-CoV-2 B.1, Beta, Delta, and Omicron – BA.1 S-protein variants. (B) SARS-CoV-2 antibodies were quantified in donor sera using the Euroimmun ELISA. Equal amounts of antibody or ACE2-M were diluted in SARS-CoV-2 negative serum and tested in a competition ELISA for their ability to compete with wild-type ACE2-His for S-protein binding. The table summarizes the percentage binding achieved by a protein concentration of 1  $\mu\text{g/ml}$ .



## Data availability statement

The original contributions presented in the study are included in the article/Supplementary Material. Further inquiries can be directed to the corresponding author.

## Ethics statement

The studies involving human participants were reviewed and approved by ethics committee of the Faculty of Medicine of the Eberhard Karls Universität Tübingen and of the University Hospital Tübingen. The patients/participants provided their written informed consent to participate in this study.

## Author contributions

GJ and LZ designed the study. LZ, NR, MS and GJ designed and interpreted the results. LZ produced and characterized ACE2 fusion proteins. MC designed the affinity matured mutant and performed structural analysis. LZ and CW performed the *in vitro* binding and competition assays. NR performed the binding analysis on virus-infected cells and neutralization assays. TM and LZ conducted BLI analysis. HS and H-GR contributed to interpretation of the experimental results. LZ wrote the manuscript. GJ, MS, MC and NR critically revised the manuscript. All authors read and accepted the submitted manuscript.

## Funding

This project was funded by the German Cancer Consortium (DKTK).

## Acknowledgments

The authors thank Beate Pömmel, Andrea Dobler and Ilona Hagelstein for expert technical assistance.

## Conflict of interest

GJ, LZ, HS, MS, NR and MC are listed as inventors on the patent application “Modified ACE2 proteins with improved activity against SARS-CoV-2”, EP22198499, applicant German Cancer Research Center, Heidelberg and University of Tübingen, Germany.

The remaining authors declare that the research was conducted in the absence of any commercial or financial relationships that could be construed as a potential conflict of interest.

## Publisher's note

All claims expressed in this article are solely those of the authors and do not necessarily represent those of their affiliated organizations, or those of the publisher, the editors and the reviewers. Any product that may be evaluated in this article, or claim that may be made by its manufacturer, is not guaranteed or endorsed by the publisher.

## Supplementary material

The Supplementary Material for this article can be found online at: <https://www.frontiersin.org/articles/10.3389/fimmu.2023.1112505/full#supplementary-material>

## References

- Anderson RM, Vegvari C, Hollingsworth TD, Pi L, Madder R, Ng CW, et al. The SARS-CoV-2 pandemic: Remaining uncertainties in our understanding of the epidemiology and transmission dynamics of the virus, and challenges to be overcome. *Interface Focus* (2021) 11(6):20210008. doi: 10.1098/rsfs.2021.0008
- Cascella M, Rajnik M, Aleem A, Dulebohn SC, Di Napoli R. Features, evaluation, and treatment of coronavirus (COVID-19). In: *StatPearls [Internet]*. Treasure Island (FL): StatPearls Publishing (2022).
- Kumar S, Caliskan DM, Janowski J, Faist A, Conrad BCG, Lange J, et al. Beyond vaccines: Clinical status of prospective COVID-19 therapeutics. *Front Immunol* (2021) 12:752227. doi: 10.3389/fimmu.2021.752227
- Baum A, Fulton BO, Wloga E, Copin R, Pascal KE, Russo V, et al. Antibody cocktail to SARS-CoV-2 spike protein prevents rapid mutational escape seen with individual antibodies. *Science* (2020) 369(6506):1014–8. doi: 10.1126/science.abd0831
- Bertoglio F, Fuhner V, Ruschig M, Heine PA, Abassi L, Klunemann T, et al. A SARS-CoV-2 neutralizing antibody selected from COVID-19 patients binds to the ACE2-RBD interface and is tolerant to most known RBD mutations. *Cell Rep* (2021) 36(4):109433. doi: 10.1016/j.celrep.2021.109433
- Chen P, Nirula A, Heller B, Gottlieb RL, Boscia J, Morris J, et al. SARS-CoV-2 neutralizing antibody LY-CoV555 in outpatients with covid-19. *N Engl J Med* (2021) 384(3):229–37. doi: 10.1056/NEJMoa2029849
- Gottlieb RL, Nirula A, Chen P, Boscia J, Heller B, Morris J, et al. Effect of bamlanivimab as monotherapy or in combination with etesevimab on viral load in patients with mild to moderate COVID-19: A randomized clinical trial. *JAMA* (2021) 325(7):632–44. doi: 10.1001/jama.2021.0202
- Weinreich DM, Sivapalasingam S, Norton T, Ali S, Gao H, Bhore R, et al. REGN-COV2, a neutralizing antibody cocktail, in outpatients with covid-19. *N Engl J Med* (2021) 384(3):238–51. doi: 10.1056/NEJMoa2035002
- Liu L, Wei Q, Lin Q, Fang J, Wang H, Kwok H, et al. Anti-spike IgG causes severe acute lung injury by skewing macrophage responses during acute SARS-CoV infection. *JCI Insight* (2019) 4(4):e123158. doi: 10.1172/jci.insight.123158
- Nouailles G, Wyler E, Pennitz P, Postmus D, Vladimirova D, Kazmierski J, et al. Temporal omics analysis in Syrian hamsters unravel cellular effector responses to moderate COVID-19. *Nat Commun* (2021) 12(1):4869. doi: 10.1038/s41467-021-25030-7
- Harvey WT, Carabelli AM, Jackson B, Gupta RK, Thomson EC, Harrison EM, et al. SARS-CoV-2 variants, spike mutations and immune escape. *Nat Rev Microbiol* (2021) 19(7):409–24. doi: 10.1038/s41579-021-00573-0
- Hu J, Peng P, Cao X, Wu K, Chen J, Wang K, et al. Increased immune escape of the new SARS-CoV-2 variant of concern omicron. *Cell Mol Immunol* (2022) 19(2):293–5. doi: 10.1038/s41423-021-00836-z
- Ao D, Lan T, He X, Liu J, Chen L, Baptista-Hon DT, et al. SARS-CoV-2 omicron variant: Immune escape and vaccine development. *MedComm* (2022) 3(1):e126. doi: 10.1002/mco2.126
- Hansen J, Baum A, Pascal KE, Russo V, Giordano S, Wloga E, et al. Studies in humanized mice and convalescent humans yield a SARS-CoV-2 antibody cocktail. *Science* (2020) 369(6506):1010–4. doi: 10.1126/science.abd0827
- Cameron E, Bowen JE, Rosen LE, Saliba C, Zepeda SK, Culap K, et al. Broadly neutralizing antibodies overcome SARS-CoV-2 omicron antigenic shift. *Nature* (2022) 602(7898):664–70. doi: 10.1038/s41586-021-04386-2

16. McCallum M, Czudnochowski N, Rosen LE, Zepeda SK, Bowen JE, Walls AC, et al. Structural basis of SARS-CoV-2 omicron immune evasion and receptor engagement. *Science* (2022) 375(6583):864–8. doi: 10.1126/science.abn8652
17. VanBlargan LA, Errico JM, Halfmann PJ, Zost SJ, Crowe JE Jr., Purcell LA, et al. An infectious SARS-CoV-2 B.1.1.529 omicron virus escapes neutralization by therapeutic monoclonal antibodies. *Nat Med* (2022) 28(3):490–5. doi: 10.1038/s41591-021-01678-y
18. Han Y, Wang Z, Wei Z, Schapiro I, Li J. Binding affinity and mechanisms of SARS-CoV-2 variants. *Comput Struct Biotechnol J* (2021) 19:4184–91. doi: 10.1016/j.csbj.2021.07.026
19. Han P, Su C, Zhang Y, Bai C, Zheng A, Qiao C, et al. Molecular insights into receptor binding of recent emerging SARS-CoV-2 variants. *Nat Commun* (2021) 12(1):6103. doi: 10.1038/s41467-021-26401-w
20. Yan R, Zhang Y, Li Y, Xia L, Guo Y, Zhou Q. Structural basis for the recognition of SARS-CoV-2 by full-length human ACE2. *Science* (2020) 367(6485):1444–8. doi: 10.1126/science.abb2762
21. Zoufaly A, Poglitsch M, Aberle JH, Hoepfer W, Seitz T, Traugott M, et al. Human recombinant soluble ACE2 in severe COVID-19. *Lancet Respir Med* (2020) 8(11):1154–8. doi: 10.1016/S2213-2600(20)30418-5
22. Khodarahmi R, Sayad B, Sobhani M. The ACE2 as a “rescue protein” or “suspect enzyme” in COVID-19: possible application of the “engineered inactive hrsACE2” as a safer therapeutic agent in the treatment of SARS-CoV-2 infection. *J Iran Chem Soc* (2020) 18(3):495–502. doi: 10.1007/s13738-020-02049-z
23. Zekri L, Vogt F, Osburg L, Muller S, Kauer J, Manz T, et al. An IgG-based bispecific antibody for improved dual targeting in PSMA-positive cancer. *EMBO Mol Med* (2021) 13(2):e11902. doi: 10.15252/emmm.201911902
24. Xie X, Muruato A, Lokugamage KG, Narayanan K, Zhang X, Zou J, et al. An infectious cDNA clone of SARS-CoV-2. *Cell Host Microbe* (2020) 27(5):841–8.e3. doi: 10.1016/j.chom.2020.04.004
25. Ruetalo N, Businger R, Althaus K, Fink S, Ruoff F, Pogoda M, et al. Antibody response against SARS-CoV-2 and seasonal coronaviruses in nonhospitalized COVID-19 patients. *mSphere* (2021) 6(1):e01145–20. doi: 10.1128/mSphere.01145-20
26. Becker M, Strengert M, Junker D, Kaiser PD, Kerrinnes T, Traenkle B, et al. Exploring beyond clinical routine SARS-CoV-2 serology using MultiCoV-ab to evaluate endemic coronavirus cross-reactivity. *Nat Commun* (2021) 12(1):1152. doi: 10.1038/s41467-021-20973-3
27. Towler P, Staker B, Prasad SG, Menon S, Tang J, Parsons T, et al. ACE2 X-ray structures reveal a large hinge-bending motion important for inhibitor binding and catalysis. *J Biol Chem* (2004) 279(17):17996–8007. doi: 10.1074/jbc.M311191200
28. Guy JL, Jackson RM, Jensen HA, Hooper NM, Turner AJ. Identification of critical active-site residues in angiotensin-converting enzyme-2 (ACE2) by site-directed mutagenesis. *FEBS J* (2005) 272(14):3512–20. doi: 10.1111/j.1742-4658.2005.04756.x
29. Chan KK, Dorosky D, Sharma P, Abbasi SA, Dye JM, Kranz DM, et al. Engineering human ACE2 to optimize binding to the spike protein of SARS coronavirus 2. *Science* (2020) 369(6508):1261–5. doi: 10.1126/science.abc0870
30. Starr TN, Greaney AJ, Addetia A, Hannon WW, Choudhary MC, Dingens AS, et al. Prospective mapping of viral mutations that escape antibodies used to treat COVID-19. *Science* (2021) 371(6531):850–4. doi: 10.1126/science.abc9302
31. Wang P, Nair MS, Liu L, Iketani S, Luo Y, Guo Y, et al. Antibody resistance of SARS-CoV-2 variants B.1.351 and B.1.1.7. *Nature* (2021) 593(7857):130–5. doi: 10.1038/s41586-021-03398-2
32. Shuai H, Chan JF, Hu B, Chai Y, Yuen TT, Yin F, et al. Attenuated replication and pathogenicity of SARS-CoV-2 B.1.1.529 omicron. *Nature* (2022) 603(7902):693–9. doi: 10.1038/s41586-022-04442-5
33. Meng B, Abdullahi A, Ferreira I, Goonawardane N, Saito A, Kimura I, et al. Altered TMPRSS2 usage by SARS-CoV-2 omicron impacts infectivity and fusogenicity. *Nature* (2022) 603(7902):706–14. doi: 10.1038/s41586-022-04474-x
34. Bojkova D, Widera M, Ciesek S, Wass MN, Michaelis M, Cinatl J Jr. Reduced interferon antagonism but similar drug sensitivity in omicron variant compared to delta variant of SARS-CoV-2 isolates. *Cell Res* (2022) 32(3):319–21. doi: 10.1038/s41422-022-00619-9
35. Cele S, Jackson L, Khoury DS, Khan K, Moyo-Gwete T, Tegally H, et al. Omicron extensively but incompletely escapes pfizer BNT162b2 neutralization. *Nature* (2022) 602(7898):654–6. doi: 10.1038/s41586-021-04387-1
36. Zhang L, Li Q, Liang Z, Li T, Liu S, Cui Q, et al. The significant immune escape of pseudotyped SARS-CoV-2 variant omicron. *Emerg Microbes Infect* (2022) 11(1):1–5. doi: 10.1080/22221751.2021.2017757
37. Dejnirattisai W, Shaw RH, Supasa P, Liu C, Stuart AS, Pollard AJ, et al. Reduced neutralisation of SARS-CoV-2 omicron B.1.1.529 variant by post-immunisation serum. *Lancet* (2022) 399(10321):234–6. doi: 10.1016/S0140-6736(21)02844-0
38. Edara VV, Manning KE, Ellis M, Lai L, Moore KM, Foster SL, et al. mRNA-1273 and BNT162b2 mRNA vaccines have reduced neutralizing activity against the SARS-CoV-2 omicron variant. *bioRxiv* (2021). doi: 10.1101/2021.12.20.473557
39. Cao Y, Wang J, Jian F, Xiao T, Song W, Yisimayi A, et al. Omicron escapes the majority of existing SARS-CoV-2 neutralizing antibodies. *Nature* (2022) 602(7898):657–63. doi: 10.1038/s41586-021-04385-3
40. VanBlargan L, Errico J, Halfmann P, Zost S, Crowe J, Purcell L, et al. An infectious SARS-CoV-2 B.1.1.529 omicron virus escapes neutralization by therapeutic monoclonal antibodies. *Res Sq* (2021). doi: 10.21203/rs.3.rs-1175516/v1
41. Maruyama T, Rodriguez LL, Jahrling PB, Sanchez A, Khan AS, Nichol ST, et al. Ebola Virus can be effectively neutralized by antibody produced in natural human infection. *J Virol* (1999) 73(7):6024–30. doi: 10.1128/JVI.73.7.6024-6030.1999
42. Reuter SE, Evans AM, Ward MB. Reducing palivizumab dose requirements through rational dose regimen design. *CPT Pharmacometrics Syst Pharmacol* (2019) 8(1):26–33. doi: 10.1002/psp4.12364
43. Tsai TI, Khalili JS, Gilchrist M, Waight AB, Cohen D, Zhuo S, et al. ACE2-fc fusion protein overcomes viral escape by potentially neutralizing SARS-CoV-2 variants of concern. *Antiviral Res* (2022) 199:105271. doi: 10.1016/j.antiviral.2022.105271
44. Chen Y, Sun L, Ullah I, Beaudoin-Bussieres G, Anand SP, Hederman AP, et al. Engineered ACE2-fc counters murine lethal SARS-CoV-2 infection through direct neutralization and fc-effector activities. *Sci Adv* (2022) 8(28):eabn4188. doi: 10.1126/sciadv.abn4188
45. Leach A, Ilca FT, Akbar Z, Ferrari M, Bentley EM, Mattiuzzo G, et al. A tetrameric ACE2 protein broadly neutralizes SARS-CoV-2 spike variants of concern with elevated potency. *Antiviral Res* (2021) 194:105147. doi: 10.1016/j.antiviral.2021.105147
46. Tang H, Gao L, Wu Z, Meng F, Zhao X, Shao Y, et al. Multiple SARS-CoV-2 variants exhibit variable target cell infectivity and ability to evade antibody neutralization. *Front Immunol* (2022) 13:836232. doi: 10.3389/fimmu.2022.836232
47. Wang K, Chen W, Zhang Z, Deng Y, Lian JQ, Du P, et al. CD147-spike protein is a novel route for SARS-CoV-2 infection to host cells. *Signal Transduct Target Ther* (2020) 5(1):283. doi: 10.1038/s41392-020-00426-x
48. Wang S, Qiu Z, Hou Y, Deng X, Xu W, Zheng T, et al. AXL is a candidate receptor for SARS-CoV-2 that promotes infection of pulmonary and bronchial epithelial cells. *Cell Res* (2021) 31(2):126–40. doi: 10.1038/s41422-020-00460-y
49. Gu Y, Cao J, Zhang X, Gao H, Wang Y, Wang J, et al. Receptome profiling identifies KREMEN1 and ASGR1 as alternative functional receptors of SARS-CoV-2. *Cell Res* (2022) 32(1):24–37. doi: 10.1038/s41422-021-00595-6
50. Hoffmann D, Mereiter S, Jin Oh Y, Monteil V, Elder E, Zhu R, et al. Identification of lectin receptors for conserved SARS-CoV-2 glycosylation sites. *EMBO J* (2021) 40(19):e108375. doi: 10.15252/embj.2021108375
51. Zhu S, Liu Y, Zhou Z, Zhang Z, Xiao X, Liu Z, et al. Genome-wide CRISPR activation screen identifies candidate receptors for SARS-CoV-2 entry. *Sci China Life Sci* (2022) 65(4):701–17. doi: 10.1007/s11427-021-1990-5



## OPEN ACCESS

## EDITED BY

Alfonso J. Rodriguez-Morales,  
Fundacion Universitaria Autónoma de las  
Américas, Colombia

## REVIEWED BY

Fahad S. Alshehri,  
Umm Al Qura University, Saudi Arabia  
Rajashri R. Naik,  
Al-Ahliyya Amman University, Jordan  
Engy Elekhawy,  
Tanta University, Egypt

## \*CORRESPONDENCE

Aleksandra Zielińska  
✉ aleksandra.zielinska@igcz.poznan.pl  
Piotr Eder  
✉ piotred@ump.edu.pl  
Eliana B. Souto  
✉ ebsouto@ff.up.pt

<sup>†</sup>These authors have contributed  
equally to this work

## SPECIALTY SECTION

This article was submitted to  
Viral Immunology,  
a section of the journal  
Frontiers in Immunology

RECEIVED 19 January 2023

ACCEPTED 06 March 2023

PUBLISHED 22 March 2023

## CITATION

Zielińska A, Eder P, Karczewski J, Szalata M,  
Hryhorowicz S, Wielgus K, Szalata M,  
Dobrowolska A, Atanasov AG, Stomski R  
and Souto EB (2023) Tocilizumab-coated  
solid lipid nanoparticles loaded with  
cannabidiol as a novel drug delivery  
strategy for treating COVID-19: A review.  
*Front. Immunol.* 14:1147991.  
doi: 10.3389/fimmu.2023.1147991

## COPYRIGHT

© 2023 Zielińska, Eder, Karczewski, Szalata,  
Hryhorowicz, Wielgus, Szalata, Dobrowolska,  
Atanasov, Stomski and Souto. This is an  
open-access article distributed under the  
terms of the [Creative Commons Attribution  
License \(CC BY\)](#). The use, distribution or  
reproduction in other forums is permitted,  
provided the original author(s) and the  
copyright owner(s) are credited and that  
the original publication in this journal is  
cited, in accordance with accepted  
academic practice. No use, distribution or  
reproduction is permitted which does not  
comply with these terms.

# Tocilizumab-coated solid lipid nanoparticles loaded with cannabidiol as a novel drug delivery strategy for treating COVID-19: A review

Aleksandra Zielińska <sup>1†</sup>, Piotr Eder <sup>2†</sup>, Jacek Karczewski <sup>3</sup>,  
Marlena Szalata <sup>4</sup>, Szymon Hryhorowicz <sup>1</sup>,  
Karolina Wielgus <sup>5</sup>, Milena Szalata <sup>6</sup>,  
Agnieszka Dobrowolska <sup>2</sup>, Atanas G. Atanasov <sup>7,8,9</sup>,  
Ryszard Stomski <sup>1</sup> and Eliana B. Souto <sup>10,11\*</sup>

<sup>1</sup>Institute of Human Genetics, Polish Academy of Sciences Poznan, Poznan, Poland, <sup>2</sup>Department of Gastroenterology, Dietetics, and Internal Diseases, Poznan University of Medical Sciences, Poznan, Poland, <sup>3</sup>Department of Environmental Medicine/Department of Gastroenterology, Human Nutrition and Internal Medicine, Poznan University of Medical Sciences, Poznan, Poland, <sup>4</sup>Department of Biochemistry and Biotechnology, Poznań University of Life Sciences, Poznań, Poland, <sup>5</sup>Department of Pediatric Gastroenterology and Metabolic Diseases, Poznan University of Medical Sciences, Poznan, Poland, <sup>6</sup>Department of Biotechnology, Institute of Natural Fibres and Medicinal Plants National Research Institute, Poznan, Poland, <sup>7</sup>Institute of Genetics and Animal Biotechnology, Magdalena, Poland, <sup>8</sup>Institute of Neurobiology, Bulgarian Academy of Sciences, Sofia, Bulgaria, <sup>9</sup>Department of Pharmacognosy, University of Vienna, Vienna, Austria, <sup>10</sup>UCIBIO – Applied Molecular Biosciences Unit, MEDTECH, Laboratory of Pharmaceutical Technology, Department of Drug Sciences, Faculty of Pharmacy, University of Porto, Porto, Portugal, <sup>11</sup>Associate Laboratory i4HB – Institute for Health and Bioeconomy, Faculty of Pharmacy, University of Porto, Porto, Portugal

Commonly used clinical strategies against coronavirus disease 19 (COVID-19), including the potential role of monoclonal antibodies for site-specific targeted drug delivery, are discussed here. Solid lipid nanoparticles (SLN) tailored with tocilizumab (TCZ) and loading cannabidiol (CBD) are proposed for the treatment of COVID-19 by oral route. TCZ, as a humanized IgG1 monoclonal antibody and an interleukin-6 (IL-6) receptor agonist, can attenuate cytokine storm in patients infected with SARS-CoV-2. CBD (an anti-inflammatory cannabinoid and TCZ agonist) alleviates anxiety, schizophrenia, and depression. CBD, obtained from *Cannabis sativa* L., is known to modulate gene expression and inflammation and also shows anti-cancer and anti-inflammatory properties. It has also been recognized to modulate angiotensin-converting enzyme II (ACE2) expression in SARS-CoV-2 target tissues. It has already been proven that immunosuppressive drugs targeting the IL-6 receptor may ameliorate lethal inflammatory responses in COVID-19 patients. TCZ, as an immunosuppressive drug, is mainly used to treat rheumatoid arthritis, although several attempts have been made to use it in the active hyperinflammatory phase of COVID-19, with promising outcomes. TCZ is currently administered intravenously. In this review, we discuss the potential advances on the use of SLN for oral administration of TCZ-tailored CBD-loaded SLN, as an innovative platform for managing SARS-CoV-2 and related infections.

## KEYWORDS

COVID-19, solid lipid nanoparticles (SLN), tocilizumab (TCZ), cannabidiol (CBD), cytokine storm, oral drug therapy

## 1 Highlights

- Tocilizumab (TCZ) attenuates cytokine storm in SARS-CoV-2-infected patients;
- Cannabidiol (CBD) promotes alleviation of anxiety, schizophrenia and depression;
- High levels of CBD from *Cannabis sativa* L. may be used to modulate angiotensin-converting enzyme II (ACE2) expression in SARS-CoV-2 target tissues;
- Dual TCZ and CBD-loading in lipid nanoparticles may ameliorate lethal inflammatory responses in COVID-19 patients;
- Lipid nanoparticles are suitable for orally-administered TNF- $\alpha$  inhibitors.

## 2 COVID-19 – Current therapies and promising drugs

Coronavirus disease-2019 (COVID-19) is caused by the severe acute respiratory syndrome (SARS) coronavirus-2 (SARS-CoV-2). It was first reported in Wuhan, China, in November 2019, when the outbreak was dated. Based on scientific reports, this acute infection is related to a cytokine storm, causing symptoms such as fever, cough, and muscle pain. In most severe cases, bilateral interstitial pneumonia with ground-glass opacity and focal chest infiltrates can be observed by using computerized tomography scans (1).

Despite the urgent need for specified therapeutic intervention, there are no effective antiviral drugs or vaccines against SARS-CoV-2. In October 2020, FDA approved remdesivir as the first promising antiviral drug to treat COVID-19 patients (2, 3). Previously, this antiviral drug has been applied to treat hepatitis C and was also used against Ebola. In the EU, remdesivir is now licensed to treat COVID-19 in adults and adolescents with pneumonia requiring supplemental oxygen (4).

Studies demonstrate that hospitalized COVID-19 patients with a lower respiratory tract infection in the remdesivir group recovered faster than patients in the placebo group (5). However, the clinical status of the patients within the 10-day course of remdesivir did not have any statistical improvement compared to standard care at 11 days after initiation of treatment in the case of moderate COVID-19. On the other hand, patients randomized to a 5-day treatment with remdesivir have shown a statistically significant difference compared to standard care. The obtained clinical importance was unreliable (6). To sum up, the first randomized trial indicated that remdesivir has no significant clinical values. In contrast, the numerical reduction in time to clinical improvement points out the need for more research investment (7).

Even though hydroxychloroquine, lopinavir/ritonavir, and interferon were also proposed against SARS-CoV2 (8), research is still ongoing on more effective treatments. Among available

therapeutic regimens, the most common drugs are those used for autoimmune diseases, antiviral agents, and antibodies from people who have recovered from COVID-19. It is worth underlining that due to the reproduction of viruses, an efficient antiviral drug should be able to target the specific part of its life cycle necessary. Moreover, antiviral agents must be able to kill viruses without killing human cells.

Still, plenty of ongoing clinical trials of COVID-19 treatment are performed worldwide. In June 2020, the European Medicines Agency (EMA) announced negotiations with the developers of 132 potential COVID-19 therapies (9). Different drugs listed in Table 1 have been mentioned among possible medications for treating COVID-19.

The need for drug repurposing has increased to prompt an efficient way to fight against SARS-CoV-2. Various drug repurposing screenings have chosen several potential drug candidates against COVID-19, but no one is fully efficient.

In this review, we discuss the studies that have implemented tocilizumab (TCZ) as an anti-IL-6 receptor antibody in COVID-19 treatment, proposing a new TCZ-coated platform for the targeted delivery of CBD. Many already published results indicate that the combination of dual delivery TCZ and CBD may aid in the recovery of patients with COVID-19 and reduce mortality. A novel approach is therefore discussed here, exploiting opportunities associated with linking nanocarriers loaded with TCZ and its agonist – CBD. Both drugs can inhibit IL-6, a major inflammatory cytokine involved in cytokine release syndrome (CRS) in various inflammatory conditions (56). Therefore, this dual-drug delivery system may have a crucial meaning in the mechanism of SARS-CoV-2 infections.

## 3 Clinical view of COVID-19

The SARS-CoV-2 virus has already infected millions of people worldwide and has led to numerous deaths. COVID-19 was firstly recognized and described in November 2019 in Wuhan (Hubei Province, China) during a series of cases that initiated the pandemic of this disease (57). The transmission of infection is primarily by droplet infection (58). Still, the SARS-CoV-2 virus is also noted in the stool, suggesting that the gastrointestinal tract is the second - after the respiratory system - target site for initial viral replication (59). The natural course of COVID-19 can be split into three stages of development: early, pulmonary, and hyperinflammatory. Each phase, presented in Figure 1, has slightly different clinical characteristics and minor differences in the proposed treatment algorithms (60). Many infected patients are asymptomatic, augmenting the spread of the virus (61). When symptomatic, cough, fever, fatigue, and dyspnoea are the most frequent manifestations of COVID-19; however, some people develop serious complications resulting in death. People with reduced immunity are at the highest risk of more severe side effects attributed to the infection, such as dysfunction of specific organs or even respiratory failure (61).



TABLE 1 Identification of the potential drugs for treating COVID-19.

	Drug Name	Previous use	Evidence of efficacy against COVID-19	Ref.
ANTIVIRALS	Remdesivir	Hepatitis C and Ebola	Remdesivir was higher-efficient than placebo regarding the time shortened to recovery in hospitalized COVID-19 patients.	(4, 5, 8)
	Chloroquine/hydroxychloroquine	Malaria	Daily hydroxychloroquine is ineffective in protecting exposed hospital-based healthcare workers from contracting SARS-CoV-2 infection, but the trial has been suspended.	(10, 11)
	Lopinavir/ritonavir combination	HIV infection, when combined with other antiretrovirals	Initial results may suggest that the impact of lopinavir/ritonavir has inconceivable or no effect on mortality in hospitalized COVID-19 patients.	(12, 13)
	Favipiravir	Influenza, coronavirus ( <i>in vitro</i> )	Favipiravir combined with tocilizumab can effectively reduce the mortality of COVID-19.	(14, 15)
	Umifenovir	Influenza (Russia and China)	There is no supporting evidence of use in patients with COVID-19; no evidence of improvement. SARS-CoV-2 clearance in non-ICU patients. Need for randomized control clinical trial for efficacy assessment of umifenovir.	(16, 17)
	Ribavirin	Hepatitis C, respiratory syncytial virus (RSV), and bronchiolitis	Early treatment with triple antiviral therapy, consisting of IFN beta-1b, lopinavir-ritonavir, and ribavirin, reduces the duration of viral shedding in patients with mild to moderate COVID-19. Only ribavirin did not lower the mortality rate compared with the control group.	(18–20)
	Molnupiravir (also known as MK-4482 or EIDD-2801)	RNA viruses (broad spectrum), including Influenza, coronaviruses (SARS, MERS, and SARS-CoV-2)	Trials have shown that it may reduce mortality and speed recovery in COVID-19 patients.	(21)
	Niclosamide	Anthelmintic drug; effective agent against various viral infections, such as SARS-CoV, MERS-CoV, ZIKV, HCV	Niclosamide has been shown to have inhibitory activity on the replication of SARS-CoV. It enables the entry of SARS-CoV-2 by altering endosomal pH and restraining virus replication by inhibiting autophagy.	(22–24)
IMMUNEMODULATORS	Oseltamivir	Influenza A and B	Early oseltamivir administration, combined with antibacterial therapy, may lower the duration of fever in COVID-19-suspected outpatients without hypoxia.	(25)
	Dexamethasone	Reduction of inflammation by mimicking anti-inflammatory hormones produced by the body	Dexamethasone reduces 28-day mortality among those receiving invasive mechanical ventilation or oxygen at randomization. However, it is not among patients not receiving respiratory support.	(26)
	Hydrocortisone	Reduction of inflammation by mimicking anti-inflammatory for adrenocortical insufficiency, rheumatoid arthritis, dermatitis, asthma, chronic obstructive pulmonary disorder	Evidence regarding corticosteroid use against SARS-CoV-2 is limited; low-dose hydrocortisone has not significantly prevented death or continued respiratory support for severe COVID-19 patients.	(27, 28)
	Azithromycin	Macrolide antibiotic; activity against, e.g., influenza A and zika	In patients with severe COVID-19, azithromycin, including caring treatment with hydroxychloroquine, has not improved clinical outcomes.	(29)
	Tocilizumab	Rheumatoid arthritis, Systemic juvenile idiopathic arthritis	Tocilizumab reduces the need for non-invasive ventilation, improving the clinical diagnosis of COVID-19 patients and reducing the risk of death by day 14 (although not mortality by day 28).	(14, 30)
	Sarilumab	Rheumatoid arthritis	Sarilumab has shown unclear efficacy results in the ongoing trial of hospitalized patients with severe or critical respiratory illness secondary to COVID-19.	(31, 32)
	Canakinumab	Inhibits IL-1; recommended to treat periodic fever syndromes and gouty arthritis	It has been used to treat cytokine release syndrome in severely ill COVID-19 patients.	(33, 34)
	Anakinra	Inhibits IL-1; for the treatment of rheumatoid arthritis	Using to reduce the cause of acute respiratory distress syndrome (ARDS) in COVID-19 patients.	(35, 36)
	Baricitinib	Janus-associated tyrosine kinase (JAK1 and JAK2 inhibitor); Rheumatoid arthritis	Baricitinib can reduce the cytokine-release syndrome associated with COVID-19; It has reduced the COVID-19 mortality rate in a retrospective multicenter trial.	(37, 38)
	Ruxolitinib	Inhibitor of JAK 1/JAK 2 and indicated for specialist treatments, such as in blood diseases	Using ruxolitinib, a direct block of the SARS-CoV-2 enters the cell has been noticed. Although there is a risk of adverse effects (opportunistic infections to the immunosuppression must also be considered), it significantly impacts overcoming complications due to immune hyperactivation by the JAK/STAT signaling pathway.	(39–41)
	Acalabrutinib	Lymphocytic leukemia	It decreases inflammation and improves outcomes in severe COVID-19 patients.	(42)

(Continued)



TABLE 1 Continued

	Drug Name	Previous use	Evidence of efficacy against COVID-19	Ref.
	Ravulizumab	Regularly used in blood diseases where complement activation destroys red blood cells.	III-phase of ongoing randomized and controlled trials to assess the safety and efficacy of ravulizumab in COVID-19 patients with severe pneumonia or ARDS.	(43, 44)
	Infliximab	Rheumatoid arthritis, Inflammatory bowel disease (IBD)	Under investigation on its use in the management of inflammation associated with COVID-19.	(45)
	Adalimumab	Rheumatoid arthritis, Inflammatory bowel disease (IBD)	Recent studies have shown that COVID-19 patients were more rarely treated in hospitals due to taking anti-TNF drugs for other conditions.	(46, 47)
	Namulumab	Rheumatoid arthritis; Ankylosing spondylitis	It has been shown to have already approved the safety profile from its use in ongoing clinical trials.	(47–49)
	Otilimab	Arthritis	IV-phase of ongoing randomized, double-blind, placebo-controlled trials to determine the safety and efficacy of otilimab in COVID-19 patients with severe pneumonia. It has already shown promising results during the initial developmental phases.	(48, 50)
	Lenzilumab	Recombinant monoclonal antibody targeting human GM-CSF, with a potential role in the pathogenesis of COVID-19-related immune hyper-response	III-phase of therapy randomized and controlled trials to determine its use as sequenced therapy with CAR-T treatments. Obtained results have shown the higher effectiveness of tocilizumab than lenzilumab in managing this cytokine-mediated syndrome in treating COVID-19.	(48, 51)
	Leronlimab	A promising therapy in the treatment of triple-negative breast cancer and HIV infection	Ongoing trials to detect the safety and efficacy of leronlimab in COVID-19 patients.	(52)
	Bamlanivimab (LY-CoV555)	A potent neutralizing IgG <sub>1</sub> monoclonal antibody to target the spike protein of SARS-CoV-2	One of three doses (2800 mg) of bamlanivimab can accelerate the natural decline in viral load over time in mild or moderate COVID-19 patients.	(53–55)
	Etesevimab (LY-CoV016)	Targeting SARS-CoV-2 spike protein and blocking the binding of the virus to the ACE2 host cell surface receptor	Ongoing trials to identify the safety and efficacy of etesevimbab in patients with mild to moderate COVID-19. <i>In vivo</i> studies have shown that it may be efficient for prophylactic and therapeutic venues against SARS-CoV-2 infection by reducing viral load, symptoms, and COVID-19-related hospitalization.	(54)

Bold values refer to ongoing clinical trials.

In many cases, COVID-19 can cause some other less typical clinical manifestations (57). Very often, anxiety is the accompanying symptom. As the expression of specific receptor proteins for the SARS-CoV-2 virus is exceptionally high in intestinal epithelial cells, symptoms at the gastrointestinal level (e.g., diarrhea, abdominal pain, and nausea) are also commonly reported, especially in the early stages of the disease (59, 62). The risk factors for a severe course of the illness with dynamic progression to the hyperinflammatory phase, the clinical manifestation of which is acute respiratory distress syndrome, circulatory failure, and shock, are still not fully understood. The most crucial pathophysiological phenomenon responsible for these processes is the cytokine-associated toxicity resulting from SARS-CoV-2 virus infection (58). One of the critical directions of research into an effective COVID-19 therapy is the search for drugs that can inhibit and prevent the uncontrolled production of pro-inflammatory cytokines, showing significant potential to damage tissues, including respiratory diseases. Cytokine-associated toxicity or cytokine release syndrome (CRS) is mainly associated with pro-inflammatory cytokine IL-6 released in severe COVID-19 infections. Cytokine IL-6 initiates the CRS in the MAPK/NF-κB-IL-6 or JAK-STAT pathway (63), and as an infection trigger, IL-6

has been associated with the symptom progression in this disease (64). The cytokine-associated toxicity has been regarded as the most typical marker of the severity of COVID-19 infection and high mortality risk (65).

As the number of patients infected with the SARS-CoV-2 virus continues to grow worldwide, there is still a need to introduce an effective therapy that can provide effective treatment in all phases of the infection and especially prevent the progression of COVID-19 into clinical forms that constitute a direct threat to the patient's life.

## 4 Gene delivery and therapy in SARS-CoV-2 infection

The genome sequence of SARS-CoV-2, shown in Figure 2, shows a very high similarity to SARS-CoV-2. Therefore, 3D homology sequence lines were used to analyze potential antiviral properties based on databases of over 32 000. Recognized medicinal plants and substances used in Chinese medicine are listed in Table 2 (67).

The genome of the SARS-CoV-2 virus distinguishes genes encoding structural proteins that make up the virus particle, including spike proteins (S protein) essential for infection, as well

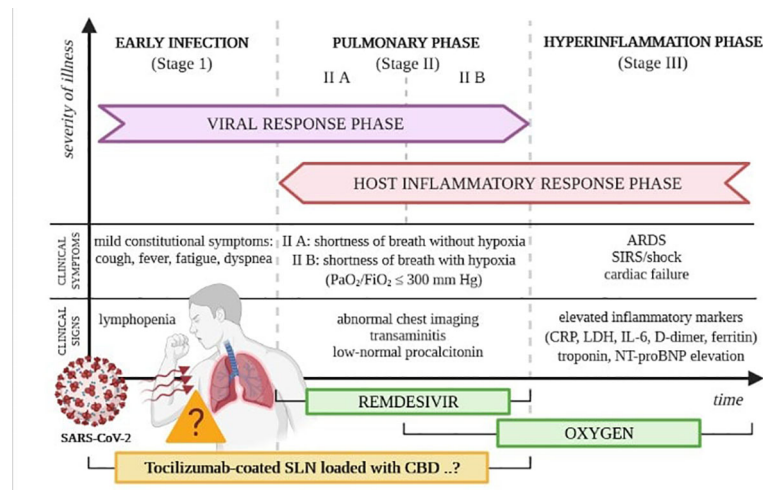


FIGURE 1

Phases of the clinical course of COVID-19. Own drawing, based on (60).

as envelope proteins (E), nucleocapsid proteins (N) and membrane proteins (M) (66). The SARS-CoV-2 virus also contains sequences encoding non-structural proteins (NSP), which inhibit the host's innate immune response to infection through the activity of papain-like protease (PLP) encoded by the NSP3 sequence and 3CL protease encoded by the NSP5 sequence, located in the gene designated as ORF1a. The virus has its RNA polymerase (RdRP) that is RNA-dependent (NSP12) and an RNA helicase (NSP13) located within the ORF1b gene. One of the tasks of the 16 non-structural proteins involves the transcription and translation of the genome (RTC replication-transcription complex).

Substances with an antiviral activity that inhibit the main proteases of the SARS-CoV-2 virus (Mpro) can be searched among bioactive compounds from medicinal plants using a molecular docking strategy. Khaerunnis et al. informed that nelfinavir and lopinavir can treat SARS-CoV-2 infection. In

addition, the main protease activity is inhibited by apigenin-7-glucoside, curcumin, demethoxycurcumin, catechin, epicatechin-gallate, and oleuropein, luteolin-7-glucoside has been shown, which can be used in therapy (68).

Further work has identified other low-risk drugs that can inhibit the activity of the COVID-19 protease due to its ability to bind to it. They are also characterized by high affinity, suggesting the potential for use in treating viral infection. Among the proposed substances, bilobalide and citral can be distinguished, in addition, to forskolin, ginkgolide A, menthol, or noscaphine, salvinorin A and beta selinene and thymoquinone (69). An interesting substance of plant origin is cannabidiol (CBD), which may be used for immunological health support and possible substance protection from infection. The anti-inflammatory effect was found in various immune-mediated disorders, including autoimmune conditions and neurodegeneration. Since cannabidiol can support the body during infection against pathogens,

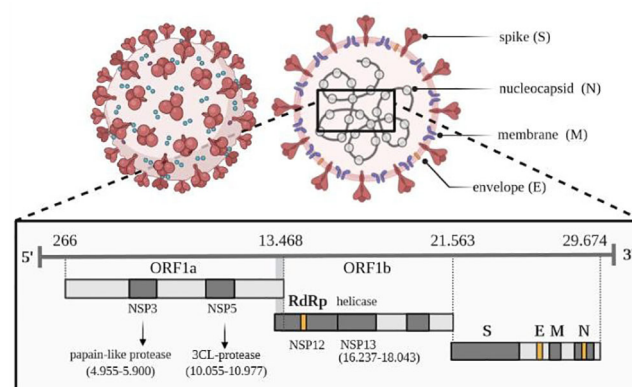


FIGURE 2

Viral genome of SARS-CoV-2. Own drawing, based on (66).

TABLE 2 Selected plant substances with potential antiviral activity.

Common name	Latin name	Active compound
Edible amaranth Chinese amaranth Amarante Douteuse	<i>Amaranthus tricolor</i> L.	Amaranthin
Siebold Ash Japanese Flowering Ash Chinese Flowering Ash	<i>Fraxinus sieboldiana</i> Blume	Calceolarioside B
Indian gooseberry	<i>Phyllanthus emblica</i> L.	(2S)-Eriodictyol 7-O-(6"-O-galloyl)-beta-D-glucopyranoside
Common bean	<i>Phaseolus vulgaris</i> L.	3,5,7,3',4',5'-hexahydroxy flavanone-3-O-beta-D-glucopyranoside
Chinese liquorice Gan cao	<i>Glycyrrhiza uralensis</i> Fisch.	Licoleafol
Wax myrtle Southern wax myrtle, southern bayberry	<i>Myrica cerifera</i> L.	Myricitrin
Tea tree Tea Plant Assam tea	<i>Camellia sinensis</i> (L.) Kuntze	Myricetin 3-O-beta-D-glucopyranoside
Mojave indigo bush California Indigobush Mojave Dalea,	<i>Psoralea argophylla</i> (Torr. ex A. Gray) Barneby	5,7,3',4'-Tetrahydroxy-2'-(3,3-dimethylallyl) isoflavone
Marubio oscuro	<i>Hyptis atrorubens</i> Poit.	Methyl rosmarinat

it is assumed that it can play a similar role in COVID-19 disease. Cannabidiol reduces the secretion of cytokines, leading to a decrease in the level of chemokines.

Moreover, the anti-inflammatory effect is associated with limiting cell-mediated immunity with the participation of effector T cells. Similarly, in the central nervous system, it also modulates the activity of microglial cells (70, 71). This information is interesting within the problem of cytokine storm, which strongly influences the odds ratio of survival of affected COVID-19 patients. The main conclusion of many papers is the need for proper analysis of the influence of cannabidiol and tetrahydrocannabinol (THC) as potential therapeutic substances with antiviral properties (71–73).

Patients infected with SARS-CoV2 are treated with various drugs that reduce excessive inflammation associated with the enormous secretion of cytokines. The most commonly used are interleukin inhibitors, Janus kinase inhibitors, corticosteroids, convalescent Plasma, interferons, nitric oxide, statins, and adjunctive nutritional therapies, including zinc and vitamin D (47, 74, 75).

One of the drugs under investigation is tocilizumab (Actemra). This IL-6 inhibitor participates in several phase III clinical trials, all randomized (for participants and investigators) and double-blind. For example, clinical trials in patients with COVID-19 pneumonia, COVACTA, and EMPACTA, included an analysis of tocilizumab and a placebo, and REMDACTA additionally included an analysis of remdesivir. Preliminary results of clinical trials are encouraging (76–78).

An essential part of any therapy is the successful delivery of a drug or new gene construct, for example, based on genome editing,

to the destination. Still, the big challenge is how to deliver the therapeutic protein to the specific compartment of the target cell (79). Nanocarriers based on lipids, polymers, graphene, or gold have been proposed. It is assumed that using nanoparticles based on lipids and polymers does not stimulate the immune system's response and does not cause additional problems for cells or tissues (80).

After administration *via* systemic injection or by oral route, numerous obstacles must be overcome before reaching specific cell types or cellular compartments. One possibility is to put a drug, nucleic acids, or proteins into a nanoparticle shell, preventing aggregation, immune clearance, kidney removal, or premature release. It is assumed that the carrier, e.g., non-viral nanoparticle, and the transferred payload/cargo should be compatible in electrostatic charge. On the surface of the shell, additional targeting ligands may improve delivery precision. The next step will cover crossing the cell membrane of the target cell, which may be overcome by bombardment, using guiding peptides, or even *via* endocytosis. The developed formulations have to escape endosomes. After that, they may stay in the cytoplasm or journey to the nucleus. At each point, the risk of degradation has to be considered. For the delivery of nucleic acids, viral vectors (e.g., lentiviruses and adeno-associated viruses), are used. Due to problems related to their limited loading capacity, the possibility to increase immune response connected with mutagenesis and carcinogenesis, and issues with up-scaling, other delivery systems are being proposed. Nonviral vectors use lipids and/or polymers as nanocarriers and may deliver large cargo (81, 82). The choice of a virus-based or a non-viral vector will depend on the load we want to transfer to the cell rather than on the vector itself.

For lipid-based nanoparticles, synthetic lipids containing disulfide bonds, which will break after exposition to the reducing environment in the cell and release the nanoparticle contents, have been proposed (81). Another study used a covalently cross-linked thin polymer carrier that can be removed by glutathione (GSH) to deliver a Cas9 ribonucleoprotein complex for *in vivo* genome editing. The presence on the surface of the additional nanocapsule peptides may guide the whole structure to the destination cells. Inside the cell, cytosolic glutathione may disrupt the shell releasing the cargo (82).

Biocompatible carriers such as lipid and polymeric nanoparticles, peptide/protein and messenger RNA complexes, and other biomaterials have recently been used for *in vivo* protection and delivery of various loads (83, 84). For the formulation of lipid-like nanoparticles like cationic lipids, such as DOTAP and DOTMA, and ionizable lipid derivatives such as TT3, 5A2-SC8, LP-01, cKK-E12, and A18-Iso5-2 DC18 to improve the efficiency and lowering toxicity *in vivo* (83).

Polymeric carriers are of great interest due to their ease of uptake by cells, the ability to combine with proteins, and the ability to form complex systems with biologically active biodegradable substances. Carriers often show the ability to bind to the cell surface; such endocytic uptake is due to their functionalization/modification. Perfluorocarbon nanoemulsions (PFCs) more and more often are used in medicine, enabling the response to emerging stimuli, taking part in the active prevention and control of hemorrhage, actively participating in the transport of oxygen as synthetic artificial blood or in tissue ischemia (79). Such substances are sensitive to ultrasound, which allows them to be tracked and activate selected proteins at the expected target sites. This strategy may find application in the tightly controlled delivery of antibodies.

Cell and gene therapies aim to replace a defective gene. New medicines can be used in the treatment of a whole range of common diseases of great social importance, often with a complex genetic background (e.g., cancer, heart disease, or diabetes), conditioned by single genes (e.g., cystic fibrosis, hemophilia) and infections caused by viruses (e.g., AIDS). Cell and gene therapies still need to be fully commercialized and may be available only as part of a clinical trial, but already some treatments are marketed. Gene therapy possibility as the replacement of a diseased gene variant was mentioned in 1972. Still, it has taken years since the first gene therapy, Gendicine, for skin cancer was commercialized in China in 2003. FDA approved the first gene therapy in 2017. Since the first gene therapy patient Jesse Gelsinger died in 1999 (the ornithine transcarbamylase gene using a recombinant adenovirus), gene therapy may become a reality due to knowledge of the human genome, availability of precise and efficient tools for genes edition, and using of better delivery methods. Currently, several gene therapy products are commercially available, approved by the relevant agencies (Europe: European Medicines Agency, U.S.: Food and Drug Administration); advanced therapy medicines include Kymriah, Luxturna, Tecartus, Yescarta, as well as Zolgensma. Gene therapy aims to cure diseases caused by defined single-gene mutations mainly. Cell-specific delivery and immunogenicity remain challenges in gene therapy. Gene or drug

transfer can be based on two strategies that enable the introduction of permanent changes by incorporating them into the genome or obtaining a transient effect; the first often use modified viruses, and the second can use lipid nanoparticles. After using adenovirus as a delivery vector, nowadays mainly for *in vivo* gene therapy, adeno-associated viruses (AAVs) are used and *in vitro* modification lentiviruses, for example, in chimeric antigen receptor (CAR) T cells (85, 86). Scientists also focused on decreasing the toxicity of viral vectors by limiting viral dosage by using capsids with increased efficiency of cell penetration, or the possibility of modifying virus expression specific for target tissues, or increasing the purity of the virus injected.

Gene therapy is not only strictly focused on gene delivery; there are attempts to cure polygenic disorders by delivering proteins for disease treatment (87). Another approach involves using a modifier gene platform and providing a functional copy of the gene encoding the retina-specific nuclear receptor *NR2E3* using the Adeno-Associated Virus AAV platform for gene therapy instead of correcting the damaged gene (88), changing disease phenotype.

It is also interesting to use specific receptors activated only by dedicated active substances (DREADD) for non-invasive and longitudinal tracking of neuron activity (89). Gene therapy may establish resistance to infectious diseases, and fragments of the SARS-CoV-2 sequence may be delivered within an AAV capsid (vaccine AACOVID). Production of antibodies against the adeno-associated virus may be prevented by endopeptidase imlifidase (IdeS) expression without disrupting B lymphocytes (90). The availability of therapy is limited in price.

Gene therapies are available on the market offer insertion of correct genes: Gendicine (China), Glybera (EU), and Imlygic (China, US, and EU); delivery of the DNA for drug production: Holoclar (EU), Kymriah (US and EU), Luxturna (US and EU), Strimvelis (EU), Yescarta (US, EU, in China under clinical trials), Zolgensma (US), Zynteglo (EU); gene interference: Defitelio (US and EU), Exondys 51 (US), Kynamro (US), Macugen (US) and Spinraza (US).

Gene therapy strategies include replacing entire genes with normal genes, repairing a mutated gene fragment, or making abnormal cells more recognizable by the immune system so they can be effectively removed from the body. Problematic is the delivery of genes using a carrier, usually a viral vector, because viruses can recognize specific cells and introduce genetic material into the cell. Another vehicle may include using of stem cells or liposomes. The risk of gene therapy may be associated with the occurrence of an inappropriate reaction of the immune system, the impact on non-target cells, the appearance of infection with the virus used as a carrier, and even the development of cancer. Liposomal carriers are now very often analyzed. Due to COVID-19, many clinical trials are delayed, but new challenging options are concentrated on producing vaccines and finding new drugs against SARS-CoV-2 using an available portfolio of viral vectors. Usually, adeno-associated virus (AAV) may be chosen to deliver spike protein fragments. Using nanolipids as delivery vectors is also auspicious, not only to transport vaccines but also to deliver specific drugs.

WHO reports 42 candidate vaccines under clinical evaluation: 13 working with protein subunit, 10 using Non-Replicating Viral Vectors, 7 Inactivated, 6 RNA, 4 DNA, and two virus-like particles (VLP). Other 151 candidate vaccines are in preclinical evaluation and use mainly protein subunits (54), Non-Replicating Viral Vectors (18), RNA (18), Replicating Viral Vectors (18), virus-like particles VLP (14), DNA (13), Inactivated (11), Live weakened viruses (3), Replication-competent bacterial vector (1) and based on the use of T cells (1). Only 10 developers/manufacturers of the COVID-19 vaccine have passed phase 3 clinical trials. Among them, the following centers can be distinguished: ii) Sinovac, ii) Wuhan Institute of Biological Products in cooperation with Sinopharm, iii) Beijing Institute of Biological Products in cooperation with Sinopharm as well as iv) CanSino Biological Inc. together with the Beijing Institute of Biotechnology, the following centers can be distinguished: v) the University of Oxford in cooperation with AstraZeneca, vi) Gamaleya Research Institute, vii) Janssen Pharmaceutical Companies, viii) Novavax, ix) Moderna with the National Institute of Allergy and Infectious Diseases (NIAID), and v) BioNTech in cooperation with the Chinese company Fosun Pharma and Pfizer.

The SARS-CoV-2 coronavirus can infect cells with angiotensin-converting enzyme 2 (ACE2) receptors on their surface. It also uses type II transmembrane serine protease TMPRSS2, penetrating, among others, lung epithelial and lung endothelial cells, macrophages, or monocytes. Additionally, coronavirus may use antibody-dependent enhancement (ADE) for infection of cells with a lower level of ACE2 and TMPRSS2 receptors (91). Such a possibility may be connected with problems finding a good strategy for producing vaccines against coronavirus (92). The main aim should be focused on the preparation of specific therapies against SARS-CoV2, including RNA interference (RNAi) (93, 94), small interfering RNA (siRNAs) (95), RNA aptamers, Ribozymes, antisense RNA (ASOs), and oligonucleotide therapeutics (96–99). The ideal vaccine has to be immunogenic with minimal side effects. Production of the vaccine should be efficient and affordable, with the possibility of easy scale-up in full compliance with the principles of good manufacturing practice (GMP). Moreover, the vaccine must not lead to adverse post-vaccination reactions, including antibody-dependent aggravation of infection (100). Conventional methods of obtaining vaccines allow for their effective production. Inactivated vaccines can be used based on attenuated viruses and those using immunogenic subunits. Still, they are associated with the possibility of problems involving strain specificity, risks of viral interference, cross-immunity, allergenicity, or triggering only partially of the immune response. Using genetic vaccines (naked DNA or RNA) like replication-defective recombinant adenoviruses may overcome limitations, be more safely, cost-effective, and quicker, and induce an innate and adaptive immune response, including activation of T cells and antibodies. There is also no problem with the derivation of nucleic acids-based vaccine using antigens sequence and choose fragment, generating better immunological response (88, 100, 101). Genetic vaccines based on DNA and RNA still have some limitations, such as lower immunogenicity. Still, high

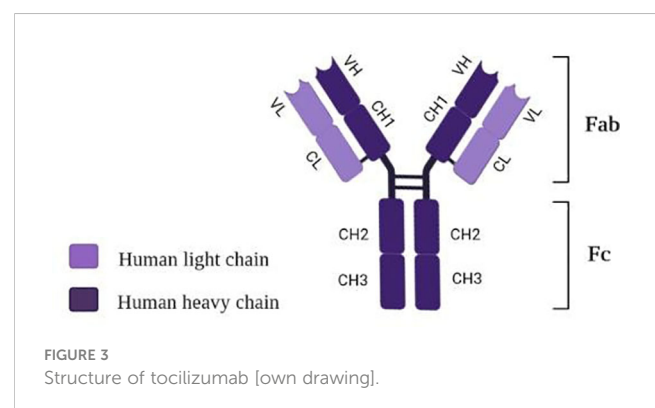
reproducibility, low costs, and relatively short production time are promising (101, 102).

The nucleic acid-based molecules/drugs may influence viral infection by regulating transcription or post-transcriptional processes, leading to the overexpression of protective genes and silencing damaged genes (103, 104). The main types of nucleic acid-based vaccines are DNA and RNA vaccines outlining in detail the mode of action, evidence supporting a therapeutic strategy based on nucleic acids, the use of new research and development solutions, emerging patents, vaccines for SARS-CoV-2 based on the use of DNA and RNA; clinical trials, expenditures related to the development and production of the vaccine and the pros and cons of vaccines based on mRNA and DNA against SARS-CoV-2 were presented in the paper prepared by Piyush et al. (2020) (103).

## 5 Chemical structure, properties, and medical application of tocilizumab

Tocilizumab (TCZ), also known as atlizumab (RoActemra®), is known as a humanized IgG<sub>1</sub> monoclonal antibody targeting interleukin-6 (IL-6) receptor (105). The structure of TCZ is schematically shown in Figure 3. The antibody consists of two heavy chains (dark violet) containing a variable VH domain and constant domains CH1, CH2, and CH3. In comparison, two light chains (light violet) consist of a variable VL domain and constant CL. Moreover, an antigen-binding fragment (Fab) and a fragment responsible for antibody effectors' functions (Fc) are distinguished in the structure of this immunosuppressive drug (106).

Tocilizumab binds with high affinity with both soluble receptors for IL-6 (SIL-6R) and membrane-bound IL-6 receptor (mIL-6R), as well as it inhibits JAK-STAT or MAPK/NF-κB-IL-6 signaling pathway (107, 108). In addition, TCZ can block cytokine storm syndrome (63) and inhibit intracellular signaling in cells expressing soluble gp130 protein (sgp130, Figure 4) (109). Currently, this FDA-approved drug commonly used so far in treating rheumatoid arthritis and juvenile idiopathic arthritis is administered intravenously (107, 110) only in hospital conditions, which is a great difficulty in its use during a pandemic.





## 5.1 Tocilizumab in the treatment of cytokine-associated toxicity in COVID-19 patients

Several attempts have been made to use tocilizumab in the active hyperinflammatory phase of COVID-19 (63, 111, 112). Exaggerated immune response to infection with the SARS-CoV-2 virus contributes to respiratory distress and multi-organ failure (113). It is caused by the elicitation of the so-called cytokine storm (114) (Figure 4). The results of recent scientific reports have shown that TCZ therapy in COVID-19 can drive a significant reduction in the inflammatory process. It can be explained by the induction of apoptosis of immunocompetent cells in affected tissues and by inhibiting proinflammatory cytokine release (115–117). Although the results are promising, previous studies of cytokine storm associated with other coronavirus and influenza virus infections and CAR (chimeric antigen receptor)-T cell therapy have also proven high levels of interleukin (IL)-6 and other cytokines (113, 114).

The study by Guo et al. (2020) has shown that immunosuppressive drugs targeting the IL-6 receptor, such as TCZ, can ameliorate lethal inflammatory responses in COVID-19 patients (118). The research has proven that the inflammatory cascade caused by excessive immune responses correlated with the death rate of COVID-19 (83, 119). As a result of SARS-CoV-2 infection, an increase in plasma concentrations of several inflammatory cytokines was observed, besides tumor necrosis factor  $\alpha$  (TNF- $\alpha$ ), interleukins (IL-2, -6, -7, -10), granulocyte-macrophage colony-stimulating factor (GM-CSF), and granulocyte colony-stimulating factor (G-CSF) (118).

Since tocilizumab has been considered effective for treating severe cytokine-release syndrome (120), this immunosuppressive drug has also been applied to treat selected COVID-19 patients (121). Other results have shown that pathogenic T cells and peripheral inflammatory monocytes may induce cytokine-associated toxicity in patients infected with SARS-CoV-2. However, the administration of tocilizumab decreased the patient's body temperature within 24 hours, and a visible reduction of oxygen inhalation in COVID-19 patients within less than a week of treatment (122). Although it was shown that TCZ might efficiently attenuate the cytokine cascade in COVID-19 patients, no single-cell-level analysis explaining these phenomena has been performed so far. This study would help to disclose the tocilizumab mode of action in the context of a characteristic COVID-19-induced activation of an inflammatory storm (118).

Xu et al. (2020) conducted an uncontrolled study using TCZ as IL-6 blocker in 21 COVID-19 patients with the most common symptoms. All patients required supplemental oxygen (2 were on ventilators), had worsening ground-glass opacities on chest computed tomography, and showed deterioration of other clinical and laboratory measures (122). It is worth underlining that within 24 hours of TCZ therapy beginning, fevers and increased C-reactive protein levels significantly resolved, while all pro-inflammatory cytokines (especially IL-6) declined. Furthermore, there was no urgent need to use oxygen in 15 patients. In all patients, oxygen saturation levels were improved (122).

One of the most extensive studies regarding the use of tocilizumab in COVID-19 patients was conducted in Northern Italy and reported by Guaraldi et al. (2020) (105). SARS-CoV-2-infected patients were administered 8 mg/kg (up to 800 mg) of TCZ

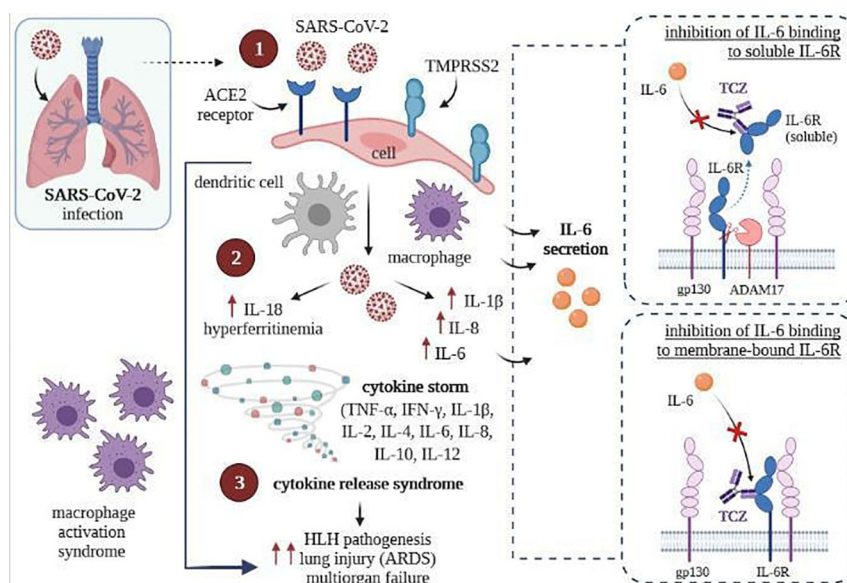


FIGURE 4

SARS-CoV-2 infection (left) and inhibition of intracellular signaling in cells by TCZ, resulting express of gp130 (right) [own drawing]. (1) Virus entry and infection of pneumocytes expressing the ACE2 receptor, recruiting antigen-presenting cells (dendritic cells and macrophages) into the lungs; (2) Activation of the NLRP4 inflammasome, which causes the overproduction of IL1 $\beta$  and IL 18, and causes the secretion of IL6 and ferritin by macrophages; (3) Upregulation resulting in cytokine release syndrome and macrophage recruitment to the lungs, contributing to ARDS.

intravenously or 162 mg subcutaneously in two simultaneous doses (81 mg per thigh). Both amounts were based on pharmacokinetic data and were intended to mimic peak plasma concentration (111). Patients who received tocilizumab were compared with a control group with the same inclusion and exclusion criteria. However, the main limitation of this study was that patients and controls were not randomly chosen, thus making it impossible to compare the obtained results and draw reliable conclusions.

Another study has identified the outcomes among SARS-CoV-2-infected patients treated with tocilizumab to target cytokine storms (112). The results helped set specific criteria to define the cytokine storm in all SARS-CoV-2-RNA-positive patients. Moreover, it has been shown that early identification and inhibition of cytokine storms before intubation is much more significant than any anti-inflammatory treatment. Cytokine storm duration should be included, while randomized controlled trials based on targeted anti-cytokine and corticosteroids may also be considered (109, 112, 123).

## 6 The impact of the endocannabinoid system on COVID-19

Emerging reports on the production of endocannabinoids in the respiratory system and cannabinoid-induced bronchial dilatation allow conclusions about the potential therapeutic use of cannabinoids in treating respiratory diseases, including acute respiratory failure syndrome in severe COVID-19 patients (124). Despite the identification of the first strains of human coronavirus in the 1960s and the molecular similarity of SARS-CoV to SARS-CoV-2, no studies have been conducted to prove the effect of cannabinoids on this family of single-stranded RNA viruses so far. There was also no objective evidence of the therapeutic, anti-inflammatory effects of cannabidiol (CBD) and delta-9-tetrahydrocannabinol ( $\Delta^9$ -THC), the two main cannabinoids would contribute to promote or prevent the application of cannabinoids as compounds to the fight against the virus. Nonetheless, it seems that THC, CBD, or other cannabinoids can act as immune modulators, which could be helpful in the treatment of viral infections, especially those where we have a pathogenic host-inflammatory response, as with SARS-CoV-2 (125).

Infection caused by SARS-CoV-2 leads, for reasons not fully explained, to the overproduction of inflammatory cytokines (mainly from immune cells) with a wide range of biological activity, which is caused by various infections and loss of unfavorable influence on the immune system. On the other hand, these cytokines positively influence different immune cells, guiding them to the inflammation sites, which causes an exponential increase in inflammation, leading to continuous extreme activation of the autoimmune system. This mechanism is called a cytokine storm, a significant cause of acute respiratory distress syndrome, systemic inflammatory response, and multi-organ failure (126). It is suggested that cannabinoids could be part of two schemes to treat these acute inflammatory reactions. The first, with non-steroidal anti-inflammatory drugs (NSAIDs) targeting the

immune system, which hurt antiviral therapies due to NSAIDs interactions and weakening the immune response to acute viral infections leading to disease progression, while the second, with drugs specifically binding to pro-inflammatory cytokine receptors, such as tocilizumab that inhibits the transmission of the signals through IL-6 receptors leading to a weakening of IL-6 activity.

## 7 Cannabinoids and their influence on the treatment of COVID-19

Cannabidiol (CBD;  $C_{21}H_{30}O_2$ ) is a phytocannabinoid without psychoactive activities produced by *Cannabis Sativa* L. and has a structural similarity to  $\Delta^9$ -tetrahydrocannabinol (THC;  $C_{21}H_{30}O_2$ ), the primary psychotropic congener of this cannabis plant. Both cannabinoids are lipophilic compounds characterized by long half-life, bioaccumulation, and shared common metabolic pathways within the cytochrome family, drug carriers, and plasma protein binding substrates (127). Both of them also have anti-inflammatory activity and possible antiviral potential. Nonetheless, the majority of studies indicate the immunosuppressive and anti-inflammatory effects of cannabidiol in various immunological reactions and inflammations (70). CBD, unlike THC, is a non-toxic compound with a high safety margin and drug tolerance, even at doses up to 1500 mg/day. Recently, it was demonstrated that cannabidiol has anti-inflammatory effects in chronic inflammatory diseases preclinical models, apoptotic effects on the mammalian cells (70), or effects that contribute to the host of the viral infection response (128, 129).

Interleukin-6 is effectively suppressed by cannabidiol in numerous models of inflammation, including diabetes, asthma, pancreatitis, and hepatitis. *In vivo*, cannabidiol use resulted in an IL-6 decrease in ex vivo lipopolysaccharide-stimulated peritoneal macrophages in acute pancreatitis and bronchial-alveolar lavage fluid in lipopolysaccharide-induced pneumonia. Also, in mice with the induced asthma-like disease, IL-4, IL-5, and IL-13 cytokines and chemokines caused in the lungs of mice were shown to be suppressed by CBD (70). Cannabidiol decreased lung inflammation in asthma and acute pneumonia mouse models by inhibiting the production of pro-inflammatory cytokines by immune cells and suppressing the exuberant immune response (130, 131). Nichols and Kaplan (2020) (70) have shown that CBD inhibits the production of pro-inflammatory cytokines such as interleukin IL-1 $\alpha$  and  $\beta$ , IL-2, IL-6, IL-17A interferon- $\gamma$  inducible protein 10, monocyte chemoattractant protein-1, tumor necrosis factor - $\alpha$  and macrophage inflammatory protein-1 $\alpha$ , which are associated with the occurrence of polyorgan inflammation and high mortality caused by SARS-CoV-2 (70). The current research results point out that CBD's immunotherapeutic and anti-inflammatory properties may limit the cytokine storm and reduce the effects of exaggerated inflammation in patients with severe respiratory tract viral infections and ARDS often associated with COVID-19 (124).

To date, no studies about interactions between drugs used to treat SARS-CoV-2 infection and CBD have been published, but

considering the inhibition of interleukin 6 receptor by Tocilizumab and the anti-inflammatory role of cannabidiol in the treatment of severe respiratory viral infections, a synergic, significant effect of these compounds on the reduction of inflammation in the acute course of COVID-19 can be expected (Figure 5).

The constant mutations of SARS-CoV-2 make it imperative to identify an effective medication for patients suffering from COVID-19. The possibility of using cannabinoids to treat severe cases of this disease is increasingly being discussed.

The novel coronavirus binds to cellular receptors *via* angiotensin-converting enzyme 2 (ACE2), characteristic of pulmonary tissue, oral and nasal mucosa, kidneys, IG, and testicles. Furthermore, smokers and patients with chronic obstructive pulmonary disease have been reported to be more susceptible to COVID-19 and develop a severe form of the illness, as they present a high level of ACE2 expression. Therefore, it is believed that ACE2 expression in the oral, respiratory, and intestinal epithelium may provide SARS-CoV-2 with a vital entry point into the host cells, and ACE2 modulation in these tissues may limit SARS-CoV-2 binding to ACE2 receptors and thus reduce susceptibility to COVID-19 (57, 132–134). A study by Wang et al. on artificial human 3D models of the tissues mentioned above allowed these authors to identify 13 extracts from *Cannabis sativa* with a significant amount of CBD, which affects the expression of the ACE2 gene and the level of the ACE2 protein. Preliminary experiments also demonstrated that the extracts studied may decrease the concentration of the transmembrane protease serine 2 (TMPRSS2), a protein essential in the process of the viruses entering into cells (57).

The cannabinoid system consists of two cannabinoid receptors: CB1, present in the central nervous system (CNS), and CB2, in the immune system. Various ligands activate cannabinoid receptors: endogenous (anandamide, AEA; 2-arachidonoylglycerol, 2-AG), exogenous (e.g., phytocannabinoids from *Cannabis sativa* L.), or synthetic (135). The most critical phytocannabinoids include psychoactive delta-9-tetrahydrocannabinol (THC) and non-psychoactive cannabidiol (CBD). In contrast to THC, a partial antagonist of both CB1 and CB2 receptors, CBD is a partial

antagonist of CB2 and only a weak antagonist of CB1 (136–138). Other cannabinoids are found in dried cannabis in much lower amounts. Cannabigerol and cannabichromene inhibit AEA reuptake (139). The MOA of numerous other phytocannabinoids, such as cannabidivarin, cannabidiol, or cannabielsoin, has not been fully explored yet (138). When developing an adequate preparation based on cannabis flower extracts, it must be remembered that cannabis contains over 100 identified cannabinoids,  $\Delta^9$ -THC and CBD being the best-known ones, and other compounds like terpenes (140, 141). Terpenes and cannabinoids may interact with each other, affecting a given extract's overall therapeutic effect. It is assumed that a quote is more potent than a single compound; therefore, it is essential to study the impact of a whole extract obtained from a plant rather than a single compound (142, 143). It has been known that anandamide (AEA) endocannabinoid, an endogenous antagonist with a high affinity to CB1, decreases IL-6 production. In contrast, THC, a partial antagonist of CB1 and CB2, inhibits IL-12 and IFN- $\gamma$  release (144–148). Another phytocannabinoid (E)- $\beta$ -caryophyllene [(E)-BCP], as a functional antagonist of CB2, inhibits both the production of pro-inflammatory cytokines in the peripheral blood induced by lipopolysaccharides (LPS) and the LPS-incited phosphorylation of Erk1/2 and JNK1/2 in monocytes (149–151). CBD impedes the expression of IL-6, IL-8, and TNF- $\alpha$  in *in vitro* models of allergic contact dermatitis and bone and joint inflammation. On the other hand, delta-9-tetrahydrocannabinol reduces the release of TNF- $\alpha$ , IL-1 $\beta$ , IL-6, and IL-8 in MG63 cells incited with LPS, which points to an essential role of the CB2 receptor in the anti-inflammatory response (152, 153). COVID-19 patients show macrophages, monocytes, and low levels of lymphocytes accountable for acute lung injury and leading to acute respiratory distress syndrome or even death. There are two groups of macrophages involved in the inflammatory response, cytokine production, phagocytosis, cell proliferation, and tissue repair: classically activated macrophages (M1) and alternatively activated macrophages (M2) (154–157). CB2 receptors are known as macrophage polarization regulators in inflammation. The use of an antagonist reduces the proliferation of inflammation-stimulating macrophages (M1) and increases the

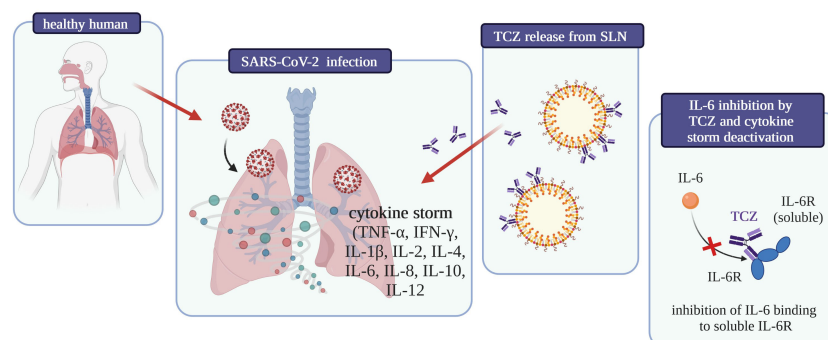


FIGURE 5

Graphical summary of the influence on COVID-19 treatment of tocilizumab-coated solid lipid nanoparticles [own drawing].

commonness of the second type of macrophages, which have an opposite effect (M2) (148, 158).

In SARS-CoV2 infection, there is a change in cytokine production, very similar to a cytokine storm, accompanied by excessive release of immune cells. Mesenchymal stromal cells (MSCs) have an anti-inflammatory effect. Their use may decrease the production of inflammatory-inducing compounds, which could improve the condition of the lungs previously damaged by, e.g., the flu virus (64, 159–161). MSCs raise the level of peripheral lymphocytes, simultaneously lowering the number of immune cells producing cytokines. Furthermore, MSCs produce leukemia inhibitory factor (LIF), which helps counteract the cytokine storm in viral pneumonia and stimulates CB2 receptors (162–164). The proposed MSC treatment for COVID-19 patients and proper stimulation of CB2 receptors will allow for the repair of damaged stem cells and immune response stimulation. It has been observed that MSCs do not stimulate the synthesis of ACE2 and TMPRSS2 proteins, which are associated with SARS-CoV-2 infection (165–167).

It was demonstrated that, in comparison to women, men are more prone to SARS-CoV-2 infection, which lower estrogen concentrations could explain. This beneficial property of estrogens and the immunosuppressive effect, which reduces excessive inflammation, may be associated with the CB2 cannabinoid receptor, a well-known immune response modulator (168–172).

Selective stimulation of CB2 may limit inflammation in COVID-19 patients through inflammatory cascade control in several checkpoints by reducing cytokine production, limiting immune cell proliferation, or producing antibodies, thus eliminating acute immune response (148, 173, 174). Currently, there are no CB2 antagonists approved for human use. Therefore, while searching for a commercially available CB2 receptor inhibitor is ongoing, treatment with CBD may be an alternative solution for COVID-19 patients (148).

Numerous experimental studies on rodents have shown that CB1 activation is essential for an effective immune response in bacterial infections, whereas CB2 activation prevents further damage caused by inflammation in sepsis due to an immunosuppressive effect (175). El Biali et al. (2020) (175) report a few human studies identifying potential relationships between the endocannabinoid system and the immune response. For instance, it was found that a genetic polymorphism in CB2 (CBQ63R), which reduces CB2 responses, can be linked with a higher probability of hospitalization in small children infected with RSV ( $n = 83$ ), with the risk of developing severe ARTI being two times higher in allele Q carriers (OR = 2.148; 95% CI: 1.09–4.22), and three times higher in the carriers of the QQ genotype (OR = 3.28; 95% CI: 1.22–8.71) (175, 176).

The FDA approved two forms of delta-9-tetrahydrocannabinol (dronabinol and nabilone) for treating some of the adverse effects of chemotherapy (i.e., nausea and vomiting) and for recovery of the appetite in wasting diseases like AIDS. In 2018, CBD was permitted for

treating two types of pediatric epilepsy: Dravet syndrome and Lennox-Gastaut syndrome. Apart from these four indications, the most solid evidence of using cannabinoids with desired therapeutic outcomes is observed in chronic pain (including neuropathic pain) and MS-related muscle spasticity (125). Numerous *in vitro* and *in vivo* studies on animal and human cells suggest that CBD has an immunosuppressive and anti-inflammatory effect through direct inhibition of microglial cells and T cells, induction of apoptosis in regulatory T cells, or through myeloid-derived regulatory T cell induction (70). *In vitro* studies in animals suggest that *Cannabis sativa* extracts have an anti-bacterial and limited anti-fungal properties (177). A study conducted among healthy volunteers ( $n = 10$ ) demonstrated that a dose of 30 mg of water-soluble or fat-soluble CBD significantly decreased the TNF level in peripheral blood mononuclear cells stimulated with bacterial lipopolysaccharide (178).

To date, there have been no studies investigating the effect of cannabinoids on SARS-CoV-2 infection. Furthermore, there is no epidemiological data on COVID-19 incidence in people using cannabinoids for medical or recreational purposes. A paper by Esposito lists four features of CBD that warrant its use, namely: 1) *Cannabis sativa* extracts have been proven to regulate the expression of two receptors that are of crucial importance for SARS-CoV-2 in a cellular model, 2) it has been demonstrated that CBD has an extensive range of immunomodulatory and anti-inflammatory effects, which may reduce the over-production of that leads to acute lung injury, 3) as a PPAR $\gamma$  antagonist, CBD may present a direct anti-viral effect, 4) as a PPAR $\gamma$  antagonist, CBD may inhibit the process of pulmonary fibrosis (179).

The characteristic feature of severe SARS-CoV-2 infection is the uncontrolled release of cytokines IL-1 $\beta$ , IL-6, and CCL2, and pro-inflammatory molecules, together with a decrease in the number of NK (natural killer) cells that may cause the cytokine storm. There is much to suggest that the severe course of infection does not stem from the viremia *per se* but depends on the degree of immune dysregulation. To limit mortality in severe cases of COVID-19, it is necessary to develop new therapeutic options to mitigate the cytokine storm (180). Esposito et al. (2020) indicate that due to the rapid spread of the pandemic, the ideal drug candidate should already be used in treating other diseases, have a good safety profile, and act to mitigate the cytokine storm through immunomodulation rather than immunosuppression (179). Recently, it was shown that *Cannabis sativa* extracts with a high concentration of CBD down-regulate the activity of ACE2 and TMPRSS2 enzymes, which are vital for SARS-CoV-2 to enter the human body (181). In recent years, CBD has been the subject of much research due to its broad spectrum of therapeutic effects, including anti-seizure, calming, sleep-inducing, anti-psychotic, anti-cancer, anti-inflammatory, and neuroprotective effects (182). What has been emphasized is the lack of adverse psychotropic effects of cannabidiol and its favorable safety profile in humans (182). The pharmacological activity of CBD was tested in patients suffering from various conditions, including respiratory diseases characterized by acute lung injury (179). CBD effect on adenosine A2A receptors limited



leukocyte migration to the lungs, which was accompanied by a significant decrease in pro-inflammatory cytokine (TNF- $\alpha$  and IL-6) and chemokine (MCP-1/MIP-2/CXCL2) release, thus clearly improving the compromised lung function (131, 183).

CBD has also been studied as a molecule with a potential anti-viral effect. CBD acts by interacting with nuclear hormone receptors PPAR. It was shown that down-regulation of PPAR $\gamma$  expression by alveolar macrophages significantly reduces lung inflammation and enhances regeneration after viral respiratory tract infections (184). Preventive and therapeutic administration of PPAR $\gamma$  antagonists decreased morbidity and mortality related to influenza A virus infection (185). However, the use of full PPAR $\gamma$  agonists has several adverse effects, including the risk of cardiovascular complications, cardiac insufficiency, and stroke. It needs to be verified whether CBD, as a weak antagonist of PPAR $\gamma$ , could be used without causing such adverse effects (179). There is no direct proof of the anti-viral activity of cannabinoids in viral infections. Such products have been described *in vitro* studies. Lowe et al. demonstrated an anti-viral effect of CBD against the hepatitis C virus (HCV), but not against HBV, in cell lines for producing these viruses (128). Anti-viral activity of CBD was also confirmed against Kaposi's sarcoma-associated herpesvirus (KSHV) in a model of KSHV-infected human dermal microvascular endothelial cells (HMVECs) (129). In yet another study, CBD mitigated the effects of neuroinflammation induced by Theiler's murine encephalomyelitis virus (TMEV) (186). Respiratory syncytial virus (RSV) used in the mouse model has indicated that CB2 activation reduced infection symptoms, and CB1 antagonist administration alleviated pulmonary complications (176).

Research has shown that CBD is a reasonably safe molecule (187). In the case of COVID-19 patients, it is essential to establish the toxicity profile of CBD when administered concomitantly with other drugs used in the current anti-COVID-19 protocols.

First, pharmacokinetic (PK) and pharmacodynamic (PD) interactions between cannabinoids and experimental COVID-19 drugs must be determined. Both  $\Delta^9$ -THC and CBD are lipophilic, highly protein-bound molecules. They have a long half-life, undergo bioaccumulation, and share metabolic pathways with cytochrome P450, drug transporters (e.g., breast cancer resistance protein), and substrates that bind to plasma proteins (127). Furthermore, PK (e.g., warfarin and clobazam) and PD (e.g., valproic acid) interactions were described for THC and CBD (188). Land et al. (2020) (127) compiled a table with 16 compounds examined for their potential use in COVID-19 treatment and their possible pharmacokinetic or pharmacodynamic interactions with cannabinoids.

They found that most candidate drugs could interact with THC and CBD. The authors propose that COVID-19 patients should be asked about their use of substances containing cannabinoids, as these may significantly affect their reaction to the selected treatment method (127).

Esposito points to the possibility of testing the therapeutic potential of CBD in COVID-19 patients at the beginning of the disease to suppress the cytokine storm, prevent the danger of respiratory failure, or assess the effect of CBD on pulmonary fibrosis. The central aspect of being clarified is dosing. In the case of HIV and post-Ebola syndrome, CBD was used as an agent controlling immune activation at doses of 10–20 mg  $\cdot$  kg $^{-1}$   $\cdot$  day $^{-1}$  and 1.7–10 mg  $\cdot$  kg $^{-1}$   $\cdot$  day $^{-1}$  (100 mg  $\cdot$  day $^{-1}$  titrating up to 600 mg  $\cdot$  day $^{-1}$ ) (189, 190).

The results of pre-clinical studies are encouraging. However, evidence is needed to approve cannabidiol as a supportive drug in COVID-19 treatment.

## 8 Lipid nanoparticles as carriers for proteins and monoclonal antibodies

Lipid nanoparticles (LNPs) are composed of biodegradable and biocompatible lipids (191, 192), and they can be successfully proposed to encapsulate proteins (193–198). The literature describes two classical types of lipid nanoparticles, namely:

- **solid lipid nanoparticles (SLN)**, so-called “1st generation”,
- **nanostructured lipid carriers (NLC)**, so-called “2nd generation”.

SLN and NLC are known to increase the bioavailability of loaded drugs administered by different routes (199, 200). In contrast to SLN, the lipid matrix of NLC consists of a mixture of solid and liquid lipids (that melt above 40°C). The matrix originates a less-ordered matrix with the capacity to load a higher drug amount than SLN, preventing its leakage during storage and allowing a more flexible drug release modulation (201). SLN contains only solid lipids in its matrix, offering the capacity to modulate the release profile of loaded drugs. SLN and NLC require surfactants (e.g., poloxamers, tweens) to stabilize the lipid matrices in aqueous dispersion (202, 203). Acylglycerols, waxes, fatty acids, and hard fats are the most commonly used lipids that should be approved by the Food and Drug Administration (191, 204).

### 8.1 Drug release form of SLN

There are three basic types of SLN, defined by the location of the drug in the lipid matrix (205, 206). Loaded drugs can be placed between fatty acid chains or between lipid layers. The final drug location affects its release mechanism from the lipid matrices (198).

The SLN type I is defined as the homogeneous matrix model, in which the drug is molecularly dispersed in the lipid core or amorphous clusters. This model is obtained when applying the hot, high-pressure homogenization (HPH) in an optimized drug and lipid ratio or when using the cold HPH. Due to their structure, SLN type I can show controlled release properties.

The SLN type II, or drug-enriched shell model, is obtained when applying the hot HPH technique and the low drug concentration in the melted lipid. During the cooling of the homogenized nanoemulsion, the lipid molecules precipitate first. Then, they lead to a steadily increasing drug concentration in the remaining lipid melt with an increased fraction of solidified lipid. A drug-free (or drug-reduced) lipid core is formed; when the drug reaches its saturation solubility in the remaining melt, an outer shell will solidify, containing both drug and lipid. This model is not suitable for prolonged drug release.

Nonetheless, it may be used to obtain a burst release of medicine and the occlusive properties of the lipid core. The SLN type III, or



drug-enriched core model, is formed when the drug concentration is relatively close to or at its saturation solubility in the lipid melt. Under the nanoemulsion cooling, the drug's solubility will decrease when the saturation solubility is exceeded. This model is also helpful for prolonged-release purposes (204, 207–209). SLN work as an absorption enhancer when orally administered (206, 210, 211). Types of SLN that can be obtained have been shown schematically in Figure 6.

## 8.2 TCZ-coated SLN loaded with CBD

The use of CBD-based SLN as potential TCZ carriers for oral administration is mainly associated with the safety of LNPs and their ability to faster enteral administration with the increased bioavailability of both hydrophilic and lipophilic active substances. On the other hand, understanding the impact of the size and shape of LNPs on their distribution in the intestine can be used in developing improved drug delivery systems to treat COVID-19. The biodegradable lipid matrix of SLN undergoes enzymatic decomposition into components naturally occurring in the human body (191). The novel approach proposed by the authors is the oral form administration of TCZ and CBD simultaneously, which can significantly improve the comfort of patients who have previously used regular intravenous injections of mAb. Moreover, the obtained SLN may be an ideal carrier for TCZ/CBD because of the ability of LNPs to modify drug release, increase bioavailability and thus regulate pharmacological activity (212). The selection of the type of lipids to be used for the production of SLN is governed by the solubility of CBD in the solid lipid. We have recently developed a stabilized SLN formulation based on glycerol behenate for the loading of CBD. The surface tailoring with the mAb is usually carried out by biotinylation as described by Souto et al. (2019) (213). Due to the potential of SLN to delay drug release, there is a high probability of optimizing these nanocarriers for drug release in the colon, thereby protecting the gastrointestinal tract against the

destructive influence of COVID-19 at the initial phase. It is worth underlining that a final enteric formulation would be developed for the delayed release of the actives into the colon by encapsulating drugs-loaded LNPs in gastro-resistant capsules to prevent earlier degradation of nanoparticles in the stomach (214).

The development of surface-modified SLN formulations for targeted delivery to the colon requires the production of gastro-resistant capsules in which the TCZ-coated CBD-loaded SLN dispersions are loaded. Enteric coatings for colonic administration exploit the pH differences along the gastrointestinal tract to release the drug only when reaching pH 6.0–7.0 in the colon. Polymethacrylates (e.g., Eudragit® brands) are typical polymers that coat tablets and capsules to protect the drugs from gastric and small intestinal pathways. They are commonly found in commercially available pharmaceutical formulations for ulcerative colitis and Crohn's disease (215).

The combination of SLN and electroporation has been proposed to enhance drug transport to the colon. Cyanine-type IR 780 and the flavonoid derivative baicalein were co-loaded into SLN for both imaging and therapy of colorectal carcinoma (216). The authors reported that the presence of flavonoids contributed to reducing the dose and, thus, cytotoxicity in chemotherapy. Electroporation generates external electric field pulses and increases cell membrane permeability, which offers the opportunity for intracellular trafficking of the cargo (217). The p53 and manganese superoxide dismutase expression was significantly increased by electroporation, with substantially higher cytotoxicity.

## 9 Conclusion

In this review, scientific evidence is given about the added value of using cannabidiol (CBD) for the management SARS-CoV-2 infection. CBD was found to down-regulate the activity of ACE2 and TMPRSS2 enzymes, both governing the entry of SARS-CoV-2 in the human body.

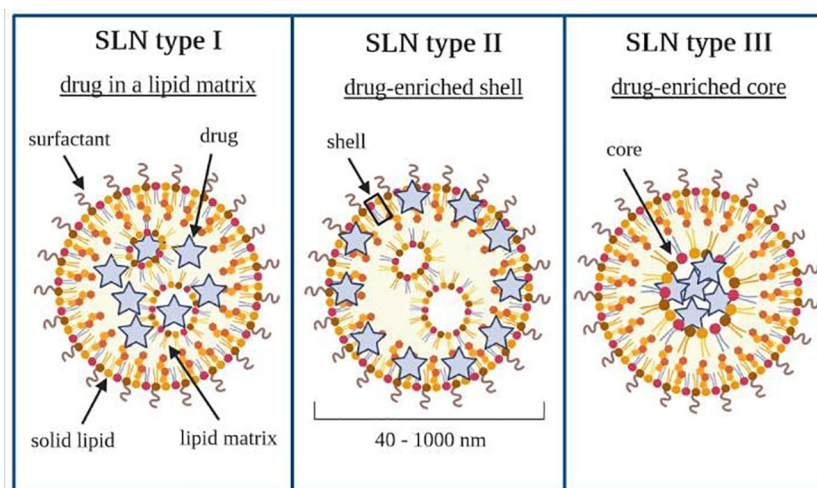


FIGURE 6  
Types of solid lipid nanoparticles. Own drawing based on (206).

Besides reducing the secretion of cytokines, cannabidiol also promotes body protection against several pathogenic infections and is also expected to can play a similar role against COVID-19. On the other hand, solid lipid nanoparticles (SLN) are ideal carriers for the oral administration of drugs, provided that lipids are known to be absorption enhancers in the gastrointestinal tract. Given its lipophilic character, CBD is an appropriate candidate to be loaded into SLN. A synergistic effect is expected with the combination of tocilizumab (TCZ), as this monoclonal antibody is an anti-IL-6 receptor antibody in COVID-19 treatment. Indeed, cytokine-associated toxicity is linked to pro-inflammatory cytokine IL-6 released in severe COVID-19 infections. An innovative approach is thus proposed by exploiting the advantages of coating SLN with mAb for site specific targeting. To obtain a suitable pharmaceutical dosage form for the oral administration of TCZ-coated CBD-loaded SLN, further studies are suggested towards the optimization of gastro-resistant gelatin capsules in which the lipid nanoparticle formulations can be encapsulated.

## Author contributions

AZ, PE, JK, and EBS were responsible for conceptualizing the manuscript. AZ, PE, JK, MaS, SH, KW, MiS, and EBS were responsible for writing and editing the paper. AD, AGA, RS, and ES were responsible for reviewing, while AZ was responsible for the visualization of the manuscript. All authors have made substantial contributions to the conception and design of the paper, drafting the article and revising it critically for important intellectual content, and final approval of the version to be submitted. All authors contributed to the article and approved the submitted version.

## Funding

This research was also supported by the National Centre for Research and Development (grant number INNOMED/I/

11/NCBR/2014) from the Innovative Economy Operational Programme funds within the framework of the European Regional Development Fund.

## Acknowledgments

EBS acknowledged the national funds from FCT—Fundação para a Ciência e a Tecnologia, I.P., in the scope of the project UIDP/04378/2020 and UIDB/04378/2020 of the Research Unit on Applied Molecular Biosciences—UCIBIO and the project LA/P/0140/2020 of the Associate Laboratory Institute for Health and Bioeconomy—i4HB.

## Conflict of interest

The authors declare that the research was conducted in the absence of any commercial or financial relationships that could be construed as a potential conflict of interest.

## Publisher's note

All claims expressed in this article are solely those of the authors and do not necessarily represent those of their affiliated organizations, or those of the publisher, the editors and the reviewers. Any product that may be evaluated in this article, or claim that may be made by its manufacturer, is not guaranteed or endorsed by the publisher.

## Supplementary material

The Supplementary Material for this article can be found online at: <https://www.frontiersin.org/articles/10.3389/fimmu.2023.1147991/full#supplementary-material>

## References

1. Rothan HA, Byrareddy SN. The epidemiology and pathogenesis of coronavirus disease (Covid-19) outbreak. *J Autoimmun* (2020) 109:102433. doi: 10.1016/j.jaut.2020.102433
2. Agrawal M, Saraf S, Saraf S, Murty US, Kurundkar SB, Roy D, et al. In-line treatments and clinical initiatives to fight against covid-19 outbreak. *Respir Med* (2020) 106:192.
3. Malin JJ, Suárez I, Priesner V, Fätkenheuer G, Rybníček J. Remdesivir against covid-19 and other viral diseases. *Clin Microbiol Rev* (2020) 34(1):e00162–20. doi: 10.1128/CMR.00162-20
4. Eastman RT, Roth JS, Brimacombe KR, Simeonov A, Shen M, Patnaik S, et al. Remdesivir: A review of its discovery and development leading to emergency use authorization for treatment of covid-19. *ACS Cent Sci* (2020). doi: 10.20944/preprints202004.0299.v1
5. Beigel JH, Tomashek KM, Dodd LE, Mehta AK, Zingman BS, Kalil AC, et al. Remdesivir for the treatment of covid-19. *New Engl J Med* (2020). doi: 10.1056/NEJMoa2007764
6. Spinner CD, Gottlieb RL, Criner GJ, López JRA, Cattelan AM, Viladomiu AS, et al. Effect of remdesivir vs standard care on clinical status at 11 days in patients with moderate covid-19: A randomized clinical trial. *Jama* (2020) 324(11):1048–57. doi: 10.1001/jama.2020.16349
7. Wang Y, Zhang D, Du G, Du R, Zhao J, Jin Y, et al. Remdesivir in adults with severe covid-19: A randomised, double-blind, placebo-controlled, multicentre trial. *Lancet* (2020).
8. Organization WH. Solidarity” clinical trial for covid-19 treatments, in: *World health organization (WHO) situation reports* (2020). Geneva: WHO (Accessed 5 Apr 2020).
9. Aditya NP, Vathsala PG, Vieira V, Murthy RS, Souto EB. Advances in nanomedicines for malaria treatment. *Adv Colloid Interface Sci* (2013) 201–202:1–17. doi: 10.1016/j.cis.2013.10.014
10. Abella BS, Jolkovsky EL, Biney BT, Uspal JE, Hyman MC, Frank I, et al. Efficacy and safety of hydroxychloroquine vs placebo for pre-exposure sars-Cov-2 prophylaxis among health care workers: A randomized clinical trial. *JAMA Internal Med* (2020). doi: 10.1001/jamainternmed.2020.6319
11. Axfors C, Schmitt AM, Janiaud P, van't Hooft J, Abd-El Salam S, Abdo EF, et al. Mortality outcomes with hydroxychloroquine and chloroquine in covid-19: An international collaborative meta-analysis of randomized trials. *Nat Commun* (2021) 12(1):2349. doi: 10.1038/s41467-021-22446-z
12. Horby PW, Mafham M, Bell JL, Linsell L, Staplin N, Emberson J, et al. Lopinavir–ritonavir in patients admitted to hospital with covid-19 (Recovery): A randomised, controlled, open-label, platform trial. *Lancet* (2020) 396(10259):1345–52. doi: 10.1016/S0140-6736(20)32013-4

13. Cao B, Wang Y, Wen D, Liu W, Wang J, Fan G, et al. A trial of lopinavir-ritonavir in adults hospitalized with severe covid-19. *New Engl J Med* (2020) 382 (19):1787–99. doi: 10.1056/NEJMoa2001282
14. Zhao H, Zhu Q, Zhang C, Li J, Wei M, Qin Y, et al. Tocilizumab combined with favipiravir in the treatment of covid-19: A multicenter trial in a small sample size. *Biomed Pharmacother* (2020) 133:110825. doi: 10.1016/j.biopha.2020.110825
15. Drożdżał S, Rosik J, Lechowicz K, Machaj F, Kotfis K, Ghavami S, et al. Fda approved drugs with pharmacotherapeutic potential for sars-Cov-2 (Covid-19) therapy. *Drug Resist Updates* (2020) 100719.
16. Huang D, Yu H, Wang T, Yang H, Yao R, Liang Z. Efficacy and safety of umifenovir for coronavirus disease 2019 (Covid-19): A systematic review and meta-analysis. *J Med Virol* (2020). doi: 10.1002/jmv.26256
17. Lian N, Xie H, Lin S, Huang J, Zhao J, Lin Q. Umifenovir treatment is not associated with improved outcomes in patients with coronavirus disease 2019: A retrospective study. *Clin Microbiol Infect* (2020).
18. Hung IF-N, Lung K-C, Tso EY-K, Liu R, Chung TW-H, Chu M-Y, et al. Triple combination of interferon beta-1b, lopinavir-ritonavir, and ribavirin in the treatment of patients admitted to hospital with covid-19: An open-label, randomised, phase 2 trial. *Lancet* (2020) 395(10238):1695–704. doi: 10.1016/S0140-6736(20)31042-4
19. Tong S, Su Y, Yu Y, Wu C, Chen J, Wang S, et al. Ribavirin therapy for severe covid-19: A retrospective cohort study. *Int J Antimicrob Agents* (2020) 56(3):106114.
20. Khalili JS, Zhu H, Mak NSA, Yan Y, Zhu Y. Novel coronavirus treatment with ribavirin: Groundwork for an evaluation concerning covid-19. *J Med Virol* (2020).
21. Corum J, Wu KJ, Zimmer C. Coronavirus drug and treatment tracker. *New York Times* (2020).
22. Chang Y-W, Yeh T-K, Lin K-T, Chen W-C, Yao H-T. Pharmacokinetics of anti-Sars-Cov agent niclosamide and its analogs in rats. *J Food Drug Anal* (2006) 14(4). doi: 10.38212/2224-6614.2464
23. Wu C-J, Jan J-T, Chen C-M, Hsieh H-P, Hwang D-R, Liu H-W, et al. Inhibition of severe acute respiratory syndrome coronavirus replication by niclosamide. *Antimicrobial Agents Chemother* (2004) 48(7):2693–6. doi: 10.1128/AAC.48.7.2693-2696.2004
24. Pindiprolu SKS, Pindiprolu SH. Plausible mechanisms of niclosamide as an antiviral agent against covid-19. *Med Hypotheses* (2020) 109765. doi: 10.1016/j.mehy.2020.109765
25. Chiba S. Effect of early oseltamivir on covid-19-Suspected outpatients without hypoxia. (2020).
26. Horby P, Lim WS, Emberson JR, Mafham M, Bell JL, Linsell L, et al. Dexamethasone in hospitalized patients with covid-19-Preliminary report. *New Engl J Med* (2020). doi: 10.1101/2020.06.22.20137273
27. Angus DC, Derde L, Al-Beidh F, Annane D, Arabi Y, Beane A, et al. Effect of hydrocortisone on mortality and organ support in patients with severe covid-19: The remap-cap covid-19 corticosteroid domain randomized clinical trial. *Jama* (2020) 324 (13):1317–29.
28. Dequin P-F, Heming N, Meziani F, Plantefève G, Voiriot G, Badié J, et al. Effect of hydrocortisone on 21-day mortality or respiratory support among critically ill patients with covid-19: A randomized clinical trial. *Jama* (2020) 324(13):1298–306. doi: 10.1001/jama.2020.16761
29. Furtado RH, Berwanger O, Fonseca HA, Corrêa TD, Ferraz LR, Lapa MG, et al. Azithromycin in addition to standard of care versus standard of care alone in the treatment of patients admitted to the hospital with severe covid-19 in Brazil (Coalition ii): A randomised clinical trial. *Lancet* (2020) 396(10256):959–67. doi: 10.1016/S0140-6736(20)31862-6
30. Hermine O, Mariette X, Tharaux P-L, Resche-Rigon M, Porcher R, Ravaut P. Effect of tocilizumab vs usual care in adults hospitalized with covid-19 and moderate or severe pneumonia: A randomized clinical trial. *JAMA Internal Med* (2020). doi: 10.1001/jamainternmed.2021.2209
31. Alvi MM, Sivasankaran S, Singh M. Pharmacological and non-pharmacological efforts at prevention, mitigation, and treatment for covid-19. *J Drug Target* (2020) 28(7-8):742–54. doi: 10.1080/1061186X.2020.1793990
32. Chakraborty C, Sharma AR, Bhattacharya M, Sharma G, Lee SS, Agoramoorthy G. Covid-19: Consider IL6 receptor antagonist for the therapy of cytokine storm syndrome in sars-Cov-2 infected patients. *J Med Virol* (2020). doi: 10.1002/jmv.26078
33. Caracciolo M, Macheda S, Labate D, Tescione M, La Scala S, Vadalà E, et al. Case report: Canakinumab for the treatment of a patient with covid-19 acute respiratory distress syndrome. *Front Immunol* (2020) 11:1942. doi: 10.3389/fimmu.2020.01942
34. Sheng CC, Sahoo D, Dugar S, Prada RA, Wang TKM, Abou Hassan OK, et al. Canakinumab to reduce deterioration of cardiac and respiratory function in sars-Cov-2 associated myocardial injury with heightened inflammation (Canakinumab in covid-19 cardiac injury: The three c study). *Clin Cardiol* (2020) 43(10):1055–63. doi: 10.1002/clc.23451
35. Navarro-Millán I, Sattui SE, Lakhanpal A, Zisa D, Siegel CH, Crow MK. Use of anakinra to prevent mechanical ventilation in severe covid-19: A case series. *Arthritis Rheumatol* (2020). doi: 10.1002/art.41422
36. Cavalli G, De Luca G, Campochiaro C, Della-Torre E, Ripa M, Canetti D, et al. Interleukin-1 blockade with high-dose anakinra in patients with covid-19, acute respiratory distress syndrome, and hyperinflammation: A retrospective cohort study. *Lancet Rheumatol* (2020). doi: 10.1016/S2665-9913(20)30127-2
37. Cantini F, Niccoli L, Nannini C, Matarrese D, Di Natale ME, Lotti P, et al. Beneficial impact of baricitinib in covid-19 moderate pneumonia; multicentre study. *J Infect* (2020) 81(4):647–79. doi: 10.1016/j.jinf.2020.06.052
38. Favalli EG, Biggoggero M, Maioli G, Caporali R. Baricitinib for covid-19: A suitable treatment? *Lancet Infect Dis* (2020).
39. Yezeswaram S, Smith P, Burn T, Covington M, Juvekar A, Li Y, et al. Inhibition of cytokine signaling by ruxolitinib and implications for covid-19 treatment. *Clin Immunol* (2020), 108517.
40. Bagca BG, Avci CB. The potential of Jak/Stat pathway inhibition by ruxolitinib in the treatment of covid-19. *Cytokine Growth Factor Rev* (2020) 54:51.
41. Cao Y, Wei J, Zou L, Jiang T, Wang G, Chen L, et al. Ruxolitinib in treatment of severe coronavirus disease 2019 (Covid-19): A multicenter, single-blind, randomized controlled trial. *J Allergy Clin Immunol* (2020).
42. Roschewski M, Lionakis MS, Sharman JP, Roswarski J, Goy A, Monticelli MA, et al. Inhibition of bruton tyrosine kinase in patients with severe covid-19. *Sci Immunol* (2020);5(48).
43. Jodele S, Köhl J. Tackling covid-19 infection through complement-targeted immunotherapy. *Br J Pharmacol* (2020). doi: 10.1111/bph.15187
44. Smith K, Pace A, Ortiz S, Kazani S, Rottinghaus S. A phase 3 open-label, randomized, controlled study to evaluate the efficacy and safety of intravenously administered ravulizumab compared with best supportive care in patients with covid-19 severe pneumonia, acute lung injury, or acute respiratory distress syndrome: A structured summary of a study protocol for a randomised controlled trial. *Trials* (2020) 21(1):639. doi: 10.1186/s13063-020-04548-z
45. Bezzio C, Manes G, Bini F, Pellegrini L, Saibeni S. Infliximab for severe ulcerative colitis and subsequent sars-Cov-2 pneumonia: A stone for two birds. *Gut* (2020). doi: 10.1136/gutjnl-2020-321760
46. Tursi A, Angarano G, Monno L, Saracino A, Signorile F, Ricciardi A, et al. Covid-19 infection in crohn's disease under treatment with adalimumab. *Gut* (2020) 69 (7):1364–5. doi: 10.1136/gutjnl-2020-321240
47. Rizk JG, Kalantar-Zadeh K, Mehra MR, Lavie CJ, Rizk Y, Forthall DN. Pharmacologic-immunomodulatory therapy in covid-19. *Drugs* (2020) 80(13):1267–92. doi: 10.1007/s40265-020-01367-z
48. J Gómez-Rial M-T. A strategy targeting monocyte-macrophage differentiation to avoid pulmonary complications in sars-Cov2 infection. In: *Clinical immunology*. Orlando, Fla (2020).
49. Bonaventura A, Vecchié A, Wang TS, Lee E, Cremer PC, Carey B, et al. Targeting gm-csf in covid-19 pneumonia: Rationale and strategies. *Front Immunol* (2020) 11:1625. doi: 10.3389/fimmu.2020.01625
50. Mehta P, Porter JC, Manson JJ, Isaacs JD, Openshaw PJM, McInnes IB, et al. Therapeutic blockade of granulocyte macrophage colony-stimulating factor in covid-19-Associated hyperinflammation: Challenges and opportunities. *Lancet Respir Med* (2020) 8(8):822–30. doi: 10.1016/S2213-2600(20)30267-8
51. Melody M, Nelson J, Hastings J, Propst J, Smerina M, Mendez J, et al. Case report: Use of lenzilumab and tocilizumab for the treatment of coronavirus disease 2019. *Immunotherapy* (2020) 12(15):1121–6. doi: 10.2217/imt-2020-0136
52. Yang B, Fulcher JA, Ahn J, Berro M, Goodman-Meza D, Dhody K, et al. Clinical characteristics and outcomes of covid-19 patients receiving compassionate use leronlimab. *Clin Infect Dis An Off Publ Infect Dis Soc America* (2020). doi: 10.1093/cid/ciaa1583
53. Mahase E. Covid-19: Fda authorises neutralising antibody bamlanivimab for non-admitted patients. *BMJ* (2020) 371:m4362. doi: 10.1136/bmj.m4362
54. Mahase E. Covid-19: Experts advise cautious optimism for neutralising antibodies after early results. *BMJ* (2020) 371:m3937. doi: 10.1136/bmj.m3937
55. Chen P, Nirula A, Heller B, Gottlieb RL, Boscia J, Morris J, et al. Sars-Cov-2 neutralizing antibody ly-Cov555 in outpatients with covid-19. *N Engl J Med* (2020). doi: 10.1056/NEJMoa2029849
56. Zhang C, Wu Z, Li J-W, Zhao H, Wang G-Q. The cytokine release syndrome (CrS) of severe covid-19 and interleukin-6 receptor (IL-6r) antagonist tocilizumab may be the key to reduce the mortality. *Int J Antimicrob Agents* (2020) 105954.
57. Mo P, Xing Y, Xiao Y, Deng L, Zhao Q, Wang H, et al. Clinical characteristics of refractory covid-19 pneumonia in wuhan, China. *Clin Infect Dis* (2020) 73(11):e4208–e4213. doi: 10.1093/cid/ciaa270
58. Ragab D, Salah Eldin H, Taieim M, Khattab R, Salem R. The covid-19 cytokine storm; what we know so far. *Front Immunol* (2020) 11:1446. doi: 10.3389/fimmu.2020.01446
59. Guan W-j, Ni Z-y, Hu Y, Liang W-h, Ou C-q, He J-x, et al. Clinical characteristics of coronavirus disease 2019 in China. *New Engl J Med* (2020) 382 (18):1708–20.
60. Siddiqi HK, Mehra MR. Covid-19 illness in native and immunosuppressed states: A clinical–therapeutic staging proposal. *J Heart Lung Transplant* (2020) 39(5):405.
61. Ali A, Kamjani MH, Kesselman MM. The role of tocilizumab in cytokine storm and improving outcomes in covid-19. *Recent Pat Antiinfect Drug Discov* (2020).
62. Goyal P, Choi JJ, Pinheiro LC, Schenck EJ, Chen R, Jabri A, et al. Clinical characteristics of covid-19 in new York city. *New Engl J Med* (2020).
63. Saha A, Sharma AR, Bhattacharya M, Sharma G, Lee S-S, Chakraborty C. Tocilizumab: A therapeutic option for the treatment of cytokine storm syndrome in covid-19. *Arch Med Res* (2020).



64. Mehta P, McAuley DF, Brown M, Sanchez E, Tattersall RS, Manson JJ, et al. Covid-19: Consider cytokine storm syndromes and immunosuppression. *Lancet (London England)* (2020) 395(10229):1033. doi: 10.1016/S0140-6736(20)30628-0
65. Narain S, Stefanov DG, Chau AS, Weber AG, Marder G, Kaplan B, et al. Comparative survival analysis of immunomodulatory therapy for coronavirus disease 2019 cytokine storm. *Chest* (2020). doi: 10.2139/ssrn.3627337
66. Alanagreh L, Alzoughool F, Atoum M. The human coronavirus disease covid-19: Its origin, characteristics, and insights into potential drugs and its mechanisms. *Pathogens* (2020) 9(5):331. doi: 10.3390/pathogens9050331
67. Ul Qamar TM, Alqahtani SM, Alamri MA, Chen LL. Structural basis of SARS-CoV-2 3CLpro and anti-COVID-19 drug discovery from medicinal plants. *J Pharm Anal* (2020) 10(4):313–9. doi: 10.1016/j.jppha.2020.03.009
68. Khaerunnisa S, Kurniawan H, Awaluddin R, Suhartati S, Soetjipto S. Potential inhibitor of covid-19 main protease (Mpro) from several medicinal plant compounds by molecular docking study. *Preprints* (2020) 20944:1–14. doi: 10.20944/preprints202003.0226.v1
69. Shaghghi N. Molecular docking study of novel covid-19 protease with low risk terpenoid compounds of plants. *ChemRxiv* (2020) 10:1–9. doi: 10.26434/chemrxiv.11935722.v1
70. Nichols JM, Kaplan BL. Immune responses regulated by cannabidiol. *Cannabis Cannabinoid Res* (2020) 5(1):12–31. doi: 10.1089/can.2018.0073
71. Brown JD. Cannabidiol as prophylaxis for sars-cov-2 and covid-19? unfounded claims versus potential risks of medications during the pandemic. *Res Soc Administrative Pharmacy: RSAP* (2021) 17(1):2053. doi: 10.1016/j.sapharm.2020.03.020
72. Nelson KM, Bisson J, Singh G, Graham JG, Chen S-N, Friesen JB, et al. The essential medicinal chemistry of cannabidiol (Cbd). *J Med Chem* (2020) 63(21):12137–55. doi: 10.1021/acs.jmedchem.0c00724
73. Costiniuk CT, Jenabian M-A. Acute inflammation and pathogenesis of sars-cov-2 infection: Cannabidiol as a potential anti-inflammatory treatment? *Cytokine Growth Factor Rev* (2020) 53:63–65. doi: 10.1016/j.cytogfr.2020.05.008
74. Ingraham NE, Lotfi-Emran S, Thielen BK, Techar K, Morris RS, Holtan SG, et al. Immunomodulation in covid-19. *Lancet Respir Med* (2020) 8(6):544–6. doi: 10.1016/S2213-2600(20)30226-5
75. Cennimo D. Coronavirus disease 2019 (Covid-19) treatment & management: Approach considerations, medical care, prevention. *Medscape Online* (2020). Available at: <https://emedicine.medscape.com/article/2500114-treatment?reg=1>.
76. Rosas IO, Bräu N, Waters M, Go RC, Malhotra A, Hunter BD, et al. Tocilizumab in patients hospitalized with COVID-19 pneumonia: Efficacy, safety, viral clearance, and antibody response from a randomised controlled trial (COVACTA). *EclinicalMedicine* (2022) 47:101409. doi: 10.1016/j.eclinm.2022.101409
77. Salama C, Han J, Yau L, Reiss WG, Kramer B, Neidhart JD, et al. Tocilizumab in patients hospitalized with Covid-19 pneumonia. *N Engl J Med* (2021) 384(1):20–30. doi: 10.1056/NEJMoa2030340
78. Price CC, Altice FL, Shyr Y, Koff A, Pischel L, Goshua G, et al. Tocilizumab treatment for cytokine release syndrome in hospitalized patients with coronavirus disease 2019: Survival and clinical outcomes. *Chest* (2020) 158(4):1397–408. doi: 10.1016/j.chest.2020.06.006
79. Sloand JN, Nguyen TT, Zinck SA, Cook EC, Zimudzi TJ, Showalter SA, et al. Ultrasound-guided cytosolic protein delivery Via transient fluoros masks. *ACS Nano* (2020) 14(4):4061–73. doi: 10.1021/acsnano.9b08745
80. Mayer K. Nonviral crispr delivery vehicles lay the smart siege: Lipid and polymer-based nanoparticles trust in guile more than force, so they're less likely to arouse immune resistance or wreak collateral damage. *Genet Eng Biotechnol News* (2020) 40(S4):S15–S9. doi: 10.1089/gen.40.S4.05
81. Liu J, Chang J, Jiang Y, Meng X, Sun T, Mao L, et al. Fast and efficient Crispr/Cas9 genome editing in vivo enabled by bioreducible lipid and messenger rna nanoparticles. *Adv Mater* (2019) 31(33):1902575. doi: 10.1002/adma.201902575
82. Chen G, Abdeen AA, Wang Y, Shahi PK, Robertson S, Xie R, et al. A biodegradable nanocapsule delivers a Cas9 ribonucleoprotein complex for in vivo genome editing. *Nat Nanotechnol* (2019) 14(10):974–80. doi: 10.1038/s41565-019-0539-2
83. Zhang X, Zhao W, Nguyen GN, Zhang C, Zeng C, Yan J, et al. Functionalized lipid-like nanoparticles for in vivo mrna delivery and base editing. *Sci Adv* (2020) 6(34):eabc2315. doi: 10.1126/sciadv.abc2315
84. Souto EB, Souto SB, Zielińska A, Durazzo A, Lucarini M, Santini A, et al. Perillaldehyde 1,2-epoxide loaded sln-tailored mab: Production, physicochemical characterization and in vitro cytotoxicity profile in mcf-7 cell lines. *Pharmaceutics* (2020) 12(2):161. doi: 10.3390/pharmaceutics12020161
85. Brantly ML, Chulay JD, Wang L, Mueller C, Humphries M, Spencer LT, et al. Sustained transgene expression despite T lymphocyte responses in a clinical trial of Raav1-aat gene therapy. *Proc Natl Acad Sci* (2009) 106(38):16363–8. doi: 10.1073/pnas.0904514106
86. Keeler AM, Flotte TR. Recombinant adeno-associated virus gene therapy in light of luxturna (and zolgensma and glybera): Where are we, and how did we get here? *Annu Rev Virol* (2019) 6:601–21. doi: 10.1146/annurev-virology-092818-015530
87. Samanta A, Aziz AA, Jhingan M, Singh SR, Khanani A, Chhablani J. Emerging therapies in neovascular age-related macular degeneration in 2020. *Asia-Pac J Ophthalmol* (2020) 9(3):250–9. doi: 10.1097/APO.0000000000000291
88. Li S, Datta S, Brabbitt E, Love Z, Woytowicz V, Flattery K, et al. Nr2e3 is a genetic modifier that rescues retinal degeneration and promotes homeostasis in multiple models of retinitis pigmentosa. *Gene Ther* (2021) 28(5):223–41. doi: 10.1038/s41434-020-0134-z
89. Bonaventura J, Eldridge MA, Hu F, Gomez JL, Sanchez-Soto M, Abramyan AM, et al. High-potency ligands for dread imaging and activation in rodents and monkeys. *Nat Commun* (2019) 10(1):1–12. doi: 10.1038/s41467-019-12236-z
90. Leborgne C, Barbon E, Alexander JM, Hanby H, Delignat S, Cohen DM, et al. Igg-cleaving endopeptidase enables in vivo gene therapy in the presence of anti-aav neutralizing antibodies. *Nat Med* (2020) 26(7):1096–101. doi: 10.1038/s41591-020-0911-7
91. Pedersen NC. An update on feline infectious peritonitis: Virology and immunopathogenesis. *Vet J* (2014) 201(2):123–32. doi: 10.1016/j.tvjl.2014.04.017
92. Morris KV. The improbability of the rapid development of a vaccine for sars-cov-2. *Mol Ther* (2020) 28(7):1548–9. doi: 10.1016/j.ymthe.2020.06.005
93. Tang Q, Li B, Woodle M, Lu PY. Application of sirna against sars in the rhesus macaque model. *Rnai* (2008) 442:139–58. doi: 10.1007/978-1-59745-191-8\_11
94. Casucci M, Falcone L, Camisa B, Norelli M, Porcellini S, Stornaiuolo A, et al. Extracellular ngfr spacers allow efficient tracking and enrichment of fully functional car-T cells Co-expressing a suicide gene. *Front Immunol* (2018) 9:507. doi: 10.3389/fimmu.2018.00507
95. Wu C-J, Huang H-W, Liu C-Y, Hong C-F, Chan Y-L. Inhibition of sars-cov replication by sirna. *Antiviral Res* (2005) 65(1):45–8. doi: 10.1016/j.antiviral.2004.09.005
96. Ahn D-G, Lee W, Choi J-K, Kim S-J, Plant EP, Almazán F, et al. Interference of ribosomal frameshifting by antisense peptide nucleic acids suppresses sars coronavirus replication. *Antiviral Res* (2011) 91(1):1–10. doi: 10.1016/j.antiviral.2011.04.009
97. Shi Y, Luo H, Jia J, Xiong J, Yang D, Huang B, et al. Antisense downregulation of sars-cov gene expression in vero E6 cells. *J Gene Med* (2005) 7(1):97–107. doi: 10.1002/jgm.640
98. Peebles L. News feature: Avoiding pitfalls in the pursuit of a covid-19 vaccine. *Proc Natl Acad Sci* (2020) 117(15):8218–21. doi: 10.1073/pnas.2005456117
99. Donia A, Bokhari H. Rna interference as a promising treatment against sars-cov-2. *Int Microbiol* (2021) 24(1):123–4. doi: 10.1007/s10123-020-00146-w
100. Conforti A, Marra E, Roscilli G, Palombo F, Ciliberto G, Aurisicchio L. Are genetic vaccines the right weapon against covid-19? *Mol Ther* (2020) 28(7):1555–6. doi: 10.1016/j.ymthe.2020.06.007
101. Liu MA. A comparison of plasmid DNA and mrna as vaccine technologies. *Vaccines* (2019) 7(2):37. doi: 10.3390/vaccines7020037
102. Lurie N, Saville M, Hatchett R, Halton J. Developing covid-19 vaccines at pandemic speed. *New Engl J Med* (2020) 382(21):1969–73. doi: 10.1056/NEJMp2005630
103. Piyush R, Rajarshi K, Chatterjee A, Khan R, Ray S. Nucleic acid-based therapy for coronavirus disease 2019. *Heliyon* (2020) 6(9):e05007. doi: 10.1016/j.heliyon.2020.e05007
104. Chen J, Tang Y, Liu Y, Dou Y. Nucleic acid-based therapeutics for pulmonary diseases. *AAPS PharmSciTech* (2018) 19(8):3670–80. doi: 10.1208/s12249-018-1183-0
105. Guaraldi G, Meschieri M, Cozzi-Lepri A, Milic J, Tonelli R, Menozzi M, et al. Tocilizumab in patients with severe covid-19: A retrospective cohort study. *Lancet Rheumatol* (2020) 2(8):e474–e84. doi: 10.1016/S2665-9913(20)30173-9
106. Łodyga M, Eder P, Bartnik W, Gonciarz M, Kłopotka M, Linke K, et al. New pharmaceuticals in inflammatory bowel disease. *Przegląd Gastroenterol* (2015) 10(2):57.
107. Hennigan S, Kavanaugh A. Interleukin-6 inhibitors in the treatment of rheumatoid arthritis. *Ther Clin Risk Manage* (2008) 4(4):767.
108. Consortium I-RMRA. The interleukin-6 receptor as a target for prevention of coronary heart disease: A mendelian randomisation analysis. *Lancet* (2012) 379(9822):1214–24.
109. Bhaskar S, Sinha A, Banach M, Mittoo S, Weissert R, Kass JS, et al. Cytokine storm in Covid-19-immunopathological mechanisms, clinical considerations, and therapeutic approaches: The reprogram consortium position paper. *Front Immunol* (2020) 11:1648. doi: 10.3389/fimmu.2020.01648
110. Scott LJ. Tocilizumab: A review in rheumatoid arthritis. *Drugs* (2017) 77(17):1865–79. doi: 10.1007/s40265-017-0829-7
111. Schuler GS. Can tocilizumab calm the cytokine storm of covid-19? *Lancet Rheumatol* (2020) 2(8):e449–e51. doi: 10.1016/S2665-9913(20)30210-1
112. Langer-Gould A, Smith JB, Gonzales EG, Castillo RD, Figueroa JG, Ramanathan A, et al. Early identification of covid-19 cytokine storm and treatment with anakinra or tocilizumab. *Int J Infect Dis* (2020) 99:291–7. doi: 10.1016/j.ijid.2020.07.081
113. Wang H, Ma S. The cytokine storm and factors determining the sequence and severity of organ dysfunction in multiple organ dysfunction syndrome. *Am J Emerg Med* (2008) 26(6):711–5. doi: 10.1016/j.ajem.2007.10.031
114. Hirano T, Murakami M. Covid-19: A new virus, but a familiar receptor and cytokine release syndrome. *Immunity* (2020). doi: 10.1016/j.immuni.2020.04.003
115. Afif W, Loftus EV Jr., Faubion WA, Kane SV, Bruining DH, Hanson KA, et al. Clinical utility of measuring infliximab and human anti-chimeric antibody

concentrations in patients with inflammatory bowel disease. *Am J Gastroenterol* (2010) 105(5):1133. doi: 10.1038/ajg.2010.9

116. Roblin X, Marotte H, Leclerc M, Del Tedesco E, Phelip J, Peyrin-Biroulet L, et al. Combination of c-reactive protein, infliximab trough levels, and stable but not transient antibodies to infliximab are associated with loss of response to infliximab in inflammatory bowel disease. *J Crohn's Colitis* (2015) 9(7):525–31. doi: 10.1093/ecco-jcc/jjv061

117. Jürgens M, John JMM, Cleynen I, Schnitzler F, Fidler H, van Moerkercke W, et al. Levels of c-reactive protein are associated with response to infliximab therapy in patients with Crohn's disease. *Clin Gastroenterol Hepatol* (2011) 9(5):421–7.e1. doi: 10.1016/j.cgh.2011.02.008

118. Guo C, Li B, Ma H, Wang X, Cai P, Yu Q, et al. Single-cell analysis of two severe COVID-19 patients reveals a monocyte-associated and tocilizumab-responding cytokine storm. *Nat Commun* (2020) 11(1):1–11. doi: 10.1038/s41467-020-17834-w

119. Wang C, Xie J, Zhao L, Fei X, Zhang H, Tan Y, et al. Alveolar macrophage dysfunction and cytokine storm in the pathogenesis of two severe COVID-19 patients. *EBioMedicine* (2020) 57:102833. doi: 10.1016/j.ebiom.2020.102833

120. Kotch C, Barrett D, Teachey DT. Tocilizumab for the treatment of chimeric antigen receptor T cell-induced cytokine release syndrome. *Expert Rev Clin Immunol* (2019) 15(8):813–22. doi: 10.1080/1744666X.2019.1629904

121. Moore JB, June CH. Cytokine release syndrome in severe COVID-19. *Science* (2020) 368(6490):473–4. doi: 10.1126/science.abb8925

122. Xu X, Han M, Li T, Sun W, Wang D, Fu B, et al. Effective treatment of severe COVID-19 patients with tocilizumab. *Proc Natl Acad Sci* (2020) 117(20):10970–5.

123. Tang Y, Liu J, Zhang D, Xu Z, Ji J, Wen C. Cytokine storm in COVID-19: The current evidence and treatment strategies. *Front Immunol* (2020) 11:1708.

124. Khodadadi H, Salles ÉL, Jarrahi A, Chibane F, Costigliola V, Yu JC, et al. Cannabidiol modulates cytokine storm in acute respiratory distress syndrome induced by simulated viral infection using synthetic RNA. *Cannabis Cannabinoid Res* (2020) 5(3):197–201. doi: 10.1089/can.2020.0043

125. Hill KP. Cannabinoids and the coronavirus. *Cannabis Cannabinoid Res* (2020). doi: 10.1089/can.2020.0035

126. Song P, Li W, Xie J, Hou Y, You C. Cytokine storm induced by SARS-CoV-2. *Clin Chim Acta* (2020). doi: 10.1016/j.cca.2020.06.017

127. Land MH, MacNair L, Thomas BF, Peters EN, Bonn-Miller MO. Letter to the Editor: Possible drug–drug interactions between cannabinoids and candidate COVID-19 drugs. *Cannabis Cannabinoid Res* (2020) 5(4):340–3. doi: 10.1089/can.2020.0054

128. Lowe HI, Toyang NJ, McLaughlin W. Potential of cannabidiol for the treatment of viral hepatitis. *Pharmacogn Res* (2017) 9(1):116. doi: 10.4103/0974-8490.199780

129. Maor Y, Yu J, Kuzontkoski PM, Dezube BJ, Zhang X, Groopman JE. Cannabidiol inhibits growth and induces programmed cell death in Kaposi sarcoma-associated herpesvirus-infected endothelium. *Genes Cancer* (2012) 3(7–8):512–20. doi: 10.1177/1947601912466556

130. Vuolo F, Abreu SC, Michels M, Xisto DG, Blanco NG, Hallak JE, et al. Cannabidiol reduces airway inflammation and fibrosis in experimental allergic asthma. *Eur J Pharmacol* (2019) 843:251–9. doi: 10.1016/j.ejphar.2018.11.029

131. Ribeiro A, Almeida V, Costola-de-Souza C, Ferraz-de-Paula V, Pinheiro M, Vitoretti L, et al. Cannabidiol improves lung function and inflammation in mice submitted to LPS-induced acute lung injury. *Immunopharmacol Immunotoxicol* (2015) 37(1):35–41. doi: 10.3109/08923973.2014.976794

132. Turner AJ, Hiscox JA, Hooper NM. ACE2: From vasopeptidase to SARS virus receptor. *Trends Pharmacol Sci* (2004) 25(6):291–4. doi: 10.1016/j.tips.2004.04.001

133. Zou X, Chen K, Zou J, Han P, Hao J, Han Z. Single-cell RNA-seq data analysis on the receptor ACE2 expression reveals the potential risk of different human organs vulnerable to 2019-nCoV infection. *Front Med* (2020), 1–8. doi: 10.1007/s11684-020-0754-0

134. Xu H, Zhong L, Deng J, Peng J, Dan H, Zeng X, et al. High expression of ACE2 receptor of 2019-nCoV on the epithelial cells of oral mucosa. *Int J Oral Sci* (2020) 12(1):1–5. doi: 10.1038/s41368-020-0074-x

135. Hernández-Cervantes R, Méndez-Díaz M, Prospéro-García Ó, Morales-Montor J. Immunoregulatory role of cannabinoids during infectious disease. *Neuroimmunomodulation* (2017) 24(4–5):183–99. doi: 10.1159/000481824

136. Pertwee RG. *Cannabinoids [Handbook of experimental pharmacology 168]*. Berlin Heidelberg: Springer-Verlag (2005).

137. Pisanti S, Malfitano AM, Ciaglia E, Lamberti A, Ranieri R, Cuomo G, et al. Cannabidiol: State of the art and new challenges for therapeutic applications. *Pharmacol Ther* (2017) 175:133–50. doi: 10.1016/j.pharmthera.2017.02.041

138. Morales P, Hurst DP, Reggio PH. Molecular targets of the phytocannabinoids: A complex picture. In: Kinghorn A, Falk H, Gibbons S, Kobayashi J (eds) *Phytocannabinoids. Progress in the Chemistry of Organic Natural Products*. Cham: Springer (2017) 103:103–31. doi: 10.1007/978-3-319-45541-9\_4

139. De Petrocellis L, Ligresti A, Moriello AS, Allarà M, Bisogno T, Petrosino S, et al. Effects of cannabinoids and cannabinoid-enriched cannabis extracts on TRP channels and endocannabinoid metabolic enzymes. *Br J Pharmacol* (2011) 163(7):1479–94. doi: 10.1111/j.1476-5381.2010.01166.x

140. Aizpurua-Olaizola O, Soydaner U, Özütürk E, Schibano D, Simsir Y, Navarro P, et al. Evolution of the cannabinoid and terpene content during the growth of cannabis sativa plants from different chemotypes. *J Nat Prod* (2016) 79(2):324–31. doi: 10.1021/acs.jnatprod.5b00949

141. Russo EB. Taming THC: Potential cannabis synergy and phytocannabinoid-terpenoid entourage effects. *Br J Pharmacol* (2011) 163(7):1344–64. doi: 10.1111/j.1476-5381.2011.01238.x

142. Ligresti A, Moriello AS, Starowicz K, Matias I, Pisanti S, De Petrocellis L, et al. Antitumor activity of plant cannabinoids with emphasis on the effect of cannabidiol on human breast carcinoma. *J Pharmacol Exp Ther* (2006) 318(3):1375–87. doi: 10.1124/jpet.106.105247

143. De Petrocellis L, Ligresti A, Schiano Moriello A, Iappelli M, Verde R, Stott CG, et al. Non-THC cannabinoids inhibit prostate carcinoma growth in vitro and in vivo: Pro-apoptotic effects and underlying mechanisms. *Br J Pharmacol* (2013) 168(1):79–102. doi: 10.1111/j.1476-5381.2012.02027.x

144. Ruan Q, Yang K, Wang W, Jiang L, Song J. Clinical predictors of mortality due to COVID-19 based on an analysis of data of 150 patients from Wuhan, China. *Intensive Care Med* (2020) 46(5):846–8. doi: 10.1007/s00134-020-05991-x

145. Shakoory B, Carcillo JA, Chatham WW, Amdur RL, Zhao H, Dinarello CA, et al. Interleukin-1 receptor blockade is associated with reduced mortality in sepsis patients with features of the macrophage activation syndrome: Re-analysis of a prior phase III trial. *Crit Care Med* (2016) 44(2):275. doi: 10.1097/CCM.0000000000001402

146. Chang YH, Lee ST, Lin WW. Effects of cannabinoids on LPS-stimulated inflammatory mediator release from macrophages: Involvement of eicosanoids. *J Cell Biochem* (2001) 81(4):715–23. doi: 10.1002/jcb.1103

147. Klein TW, Cabral GA. Cannabinoid-induced immune suppression and modulation of antigen-presenting cells. *J Neuroimmune Pharmacol* (2006) 1(1):50. doi: 10.1007/s11481-005-9007-x

148. Rossi F, Tortora C, Argenziano M, Di Paola A, Punzo F. Cannabinoid receptor type 2: A possible target in SARS-CoV-2 (COVID-19) infection? *Int J Mol Sci* (2020) 21(11):3809. doi: 10.3390/ijms21113809

149. Sardinha J, Kelly M, Zhou J, Lehmann C. Experimental cannabinoid 2 receptor-mediated immune modulation in sepsis. *Mediators Inflamm* (2014) 2014:978678. doi: 10.1155/2014/978678

150. Youssef DA, El-Fayoumi HM, Mahmoud MF. Beta-caryophyllene protects against diet-induced dyslipidemia and vascular inflammation in rats: Involvement of CB2 and PPAR-γ receptors. *Chemico-Biol Interact* (2019) 297:16–24. doi: 10.1016/j.cbi.2018.10.010

151. Gertsch J, Leonti M, Raduner S, Racz I, Chen J-Z, Xie X-Q, et al. Beta-caryophyllene is a dietary cannabinoid. *Proc Natl Acad Sci* (2008) 105(26):9099–104. doi: 10.1073/pnas.0803601105

152. Petrosino S, Verde R, Vaia M, Allarà M, Iuvone T, Di Marzo V. Anti-inflammatory properties of cannabidiol, a nonpsychotropic cannabinoid, in experimental allergic contact dermatitis. *J Pharmacol Exp Ther* (2018) 365(3):652–63. doi: 10.1124/jpet.117.244368

153. Yang L, Li F-F, Han Y-C, Jia B, Ding Y. Cannabinoid receptor CB2 is involved in tetrahydrocannabinol-induced anti-inflammation against lipopolysaccharide in mg-63 cells. *Mediators Inflamm* (2015) 2015:362126. doi: 10.1155/2015/362126

154. Channappanavar R, Perlman S. Pathogenic human coronavirus infections: Causes and consequences of cytokine storm and immunopathology. *Semin Immunopathol* (2017) 39(5):529–39. doi: 10.1007/s00281-017-0629-x

155. Snyder RJ, Lantis J, Kirsner RS, Shah V, Molyneaux M, Carter MJ. Macrophages: A review of their role in wound healing and their therapeutic use. *Wound Repair Regen* (2016) 24(4):613–29. doi: 10.1111/wrr.12444

156. Punzo F, Bellini G, Tortora C, Di Pinto D, Argenziano M, Pota E, et al. Mifamurtide and Tam-like compounds: Effect on proliferation, migration and differentiation of osteosarcoma cells. *Oncotarget* (2020) 11(7):687. doi: 10.18632/oncotarget.27479

157. Du Y, Ren P, Wang Q, Jiang S-K, Zhang M, Li J-Y, et al. Cannabinoid 2 receptor attenuates inflammation during skin wound healing by inhibiting M1 macrophages rather than activating M2 macrophages. *J Inflamm* (2018) 15(1):1–12. doi: 10.1186/s12950-018-0201-z

158. Braun M, Khan ZT, Khan MB, Kumar M, Ward A, Achyut BR, et al. Selective activation of cannabinoid receptor-2 reduces neuroinflammation after traumatic brain injury via alternative macrophage polarization. *Brain Behav Immun* (2018) 68:224–37. doi: 10.1016/j.bbi.2017.10.021

159. Stanc N, Ingo D, Conforti A, Rossella V, Tomao L, Pitisci A, et al. Biological and functional characterization of bone marrow-derived mesenchymal stromal cells from patients affected by primary immunodeficiency. *Sci Rep* (2017) 7(1):1–13. doi: 10.1038/s41598-017-08550-5

160. Gao F, Chiu S, Motan D, Zhang Z, Chen L, Ji H, et al. Mesenchymal stem cells and immunomodulation: Current status and future prospects. *Cell Death Dis* (2016) 7(1):e2062–e. doi: 10.1038/cddis.2015.327

161. Chen J, Hu C, Chen L, Tang L, Zhu Y, Xu X, et al. Clinical study of mesenchymal stem cell treating acute respiratory distress syndrome induced by epidemic influenza A (H7N9) infection, a hint for COVID-19 treatment. *Engineering* (2020) 6(10):1153–61. doi: 10.1016/j.eng.2020.02.006

162. Leng Z, Zhu R, Hou W, Feng Y, Yang Y, Han Q, et al. Transplantation of ACE2 (–) mesenchymal stem cells improves the outcome of patients with COVID-19 pneumonia. *Aging Dis* (2020) 11:216–28. doi: 10.14336/AD.2020.0228

163. Shetty AK. Mesenchymal stem cell infusion shows promise for combating coronavirus (COVID-19)-induced pneumonia. *Aging Dis* (2020) 11(2):462. doi: 10.14336/AD.2020.0301



164. Foronjy RF, Dabo AJ, Cummins N, Geraghty P. Leukemia inhibitory factor protects the lung during respiratory syncytial viral infection. *BMC Immunol* (2014) 15(1):41. doi: 10.1186/s12865-014-0041-4
165. Golchin A, Farahany TZ, Khojasteh A, Soleimanifar F, Ardashirylajimi A. The clinical trials of mesenchymal stem cell therapy in skin diseases: An update and concise review. *Curr Stem Cell Res Ther* (2019) 14(1):22–33. doi: 10.2174/1574888X13666180913123424
166. Chen L, Qu J, Xiang C. The multi-functional roles of menstrual blood-derived stem cells in regenerative medicine. *Stem Cell Res Ther* (2019) 10(1):1–10. doi: 10.1186/s13287-018-1105-9
167. Metcalfe SM. Mesenchymal stem cells and management of covid-19 pneumonia. *Med Drug Discov* (2020) 5:100019. doi: 10.1016/j.medidd.2020.100019
168. Franks LN, Ford BM, Prather PL. Selective estrogen receptor modulators: Cannabinoid receptor inverse agonists with differential Cb1 and Cb2 selectivity. *Front Pharmacol* (2016) 7:503. doi: 10.3389/fphar.2016.00503
169. Kumar P, Song Z-H. Identification of raloxifene as a novel Cb2 inverse agonist. *Biochem Biophys Res Commun* (2013) 435(1):76–81. doi: 10.1016/j.bbrc.2013.04.040
170. Dobovišek L, Hojnik M, Ferik P. Overlapping molecular pathways between cannabinoid receptors type 1 and 2 and Estrogens/Androgens on the periphery and their involvement in the pathogenesis of common diseases. *Int J Mol Med* (2016) 38(6):1642–51. doi: 10.3892/ijmm.2016.2779
171. Peretz J, Pekosz A, Lane AP, Klein SL. Estrogenic compounds reduce influenza A virus replication in primary human nasal epithelial cells derived from female, but not Male, donors. *Am J Physiology-Lung Cell Mol Physiol* (2016) 310(5):L415–L25. doi: 10.1152/ajplung.00398.2015
172. Channappanavar R, Fett C, Mack M, Ten Eyck PP, Meyerholz DK, Perlman S. Sex-based differences in susceptibility to severe acute respiratory syndrome coronavirus infection. *J Immunol* (2017) 198(10):4046–53. doi: 10.4049/jimmunol.1601896
173. Rockwell CE, Raman P, Kaplan BL, Kaminski NE. A cox-2 metabolite of the endogenous cannabinoid, 2-arachidonol glycerol, mediates suppression of il-2 secretion in activated jurkat T cells. *Biochem Pharmacol* (2008) 76(3):353–61. doi: 10.1016/j.bcp.2008.05.005
174. Carayon P, Marchand J, Dussosoy D, Derocq J-M, Jbilo O, Bord A, et al. Modulation and functional involvement of Cb2 peripheral cannabinoid receptors during b-cell differentiation. *Blood J Am Soc Hematol* (1998) 92(10):3605–15. doi: 10.1182/blood.V92.10.3605
175. El Biali M, Broers B, Besson M, Demeules J. Cannabinoids and covid-19. *Med Cannabis Cannabinoids* (2020) 3(2):111–5. doi: 10.1159/000510799
176. Tahamtan A, Samieipoor Y, Nayeri FS, Rahbarimanesh AA, Izadi A, Rashidi-Nezhad A, et al. Effects of cannabinoid receptor type 2 in respiratory syncytial virus infection in human subjects and mice. *Virulence* (2018) 9(1):217–30. doi: 10.1080/21505594.2017.1389369
177. Farha MA, El-Halfawy OM, Gale RT, MacNair CR, Carfrae LA, Zhang X, et al. Uncovering the hidden antibiotic potential of cannabis. *ACS Infect Dis* (2020) 6(3):338–46. doi: 10.1021/acinfeddis.9b00419
178. Hobbs JM, Vazquez AR, Remijan ND, Trotter RE, McMillan TV, Freedman KE, et al. Evaluation of pharmacokinetics and acute anti-inflammatory potential of two oral cannabidiol preparations in healthy adults. *Phytother Res* (2020) 34(7):1696–1703. doi: 10.1002/ptr.6651
179. Esposito G, Pesce M, Seguela L, Sanseverino W, Lu J, Corpetti C, et al. The potential of cannabidiol in the covid-19 pandemic: A hypothesis letter. *Br J Pharmacol* (2020) 177(21):4967–70. doi: 10.22541/au.158894349.98427987
180. Huang C, Wang Y, Li X, Ren L, Zhao J, Hu Y, et al. Clinical features of patients infected with 2019 novel coronavirus in wuhan, China. *Lancet* (2020) 395(10223):497–506. doi: 10.1016/S0140-6736(20)30183-5
181. Wang B, Kovalchuk A, Li D, Ilnytskyi Y, Kovalchuk I, Kovalchuk O. In search of preventative strategies: Novel anti-inflammatory high-cbd cannabis sativa extracts modulate Ace2 expression in covid-19 gateway tissues. *Aging (Albany NY)* (2020) 12(22):22425–44. doi: 10.20944/preprints202004.0315.v1
182. Iffland K, Grotenhermen F. An update on safety and side effects of cannabidiol: A review of clinical data and relevant animal studies. *Cannabis Cannabinoid Res* (2017) 2(1):139–54. doi: 10.1089/can.2016.0034
183. Ribeiro A, Ferraz-de-Paula V, Pinheiro ML, Vitoretti LB, Mariano-Souza DP, Quinteiro-Filho WM, et al. Cannabidiol, a non-psychotropic plant-derived cannabinoid, decreases inflammation in a murine model of acute lung injury: Role for the adenosine A2a receptor. *Eur J Pharmacol* (2012) 678(1–3):78–85. doi: 10.1016/j.ejphar.2011.12.043
184. Huang S, Goplen NP, Zhu B, Cheon IS, Son Y, Wang Z, et al. Macrophage ppar- $\gamma$  suppresses long-term lung fibrotic sequelae following acute influenza infection. *PLoS One* (2019) 14(10):e0223430. doi: 10.1371/journal.pone.0223430
185. Bassaganya-Riera J, Song R, Roberts PC, Hontecillas R. Ppar- $\gamma$  activation as an anti-inflammatory therapy for respiratory virus infections. *Viral Immunol* (2010) 23(4):343–52. doi: 10.1089/vim.2010.0016
186. Mecha M, Feliú A, Iñigo P, Mestre L, Carrillo-Salinas F, Guaza C. Cannabidiol provides long-lasting protection against the deleterious effects of inflammation in a viral model of multiple sclerosis: A role for A2a receptors. *Neurobiol Dis* (2013) 59:141–50. doi: 10.1016/j.nbd.2013.06.016
187. Millar SA, Stone N, Bellman Z, Yates A, England T, O'Sullivan S. A systematic review of cannabidiol dosing in clinical populations. *Br J Clin Pharmacol* (2019) 85(9):1888–900. doi: 10.1111/bcp.14038
188. Foster BC, Abramovici H, Harris CS. Cannabis and cannabinoids: Kinetics and interactions. *Am J Med* (2019) 132(11):1266–70. doi: 10.1016/j.amjmed.2019.05.017
189. Costiniuk CT, Sanezi Z, Routy J-P, Margolese S, Mandarino E, Singer J, et al. Oral cannabinoids in people living with hiv on effective antiretroviral therapy: Ctn Pt028—study protocol for a pilot randomised trial to assess safety, tolerability and effect on immune activation. *BMJ Open* (2019) 9(1):e024793. doi: 10.1136/bmjopen-2018-024793
190. Reznik SE, Gardner EL, Ashby CR Jr. Cannabidiol: A potential treatment for post Ebola syndrome? *Int J Infect Dis* (2016) 52:74–6. doi: 10.1016/j.ijid.2016.09.020
191. Doktorovová S, Kovačević AB, Garcia ML, Souto EB. Preclinical safety of solid lipid nanoparticles and nanostructured lipid carriers: Current evidence from in vitro and in vivo evaluation. *Eur J Pharmaceut Biopharmaceut* (2016) 108:235–52. doi: 10.1016/j.ejpb.2016.08.001
192. Doktorovová S, Souto EB, Silva AM. Nanotoxicology applied to solid lipid nanoparticles and nanostructured lipid carriers—a systematic review of in vitro data. *Eur J Pharmaceut Biopharmaceut* (2014) 87(1):1–18. doi: 10.1016/j.ejpb.2014.02.005
193. Almeida AJ, Souto E. Solid lipid nanoparticles as a drug delivery system for peptides and proteins. *Adv Drug Deliv Rev* (2007) 59(6):478–90. doi: 10.1016/j.addr.2007.04.007
194. Martins S, Costa-Lima S, Carneiro T, Cordeiro-da-Silva A, Souto E, Ferreira D. Solid lipid nanoparticles as intracellular drug transporters: An investigation of the uptake mechanism and pathway. *Int J Pharmaceut* (2012) 430(1–2):216–27. doi: 10.1016/j.jipharm.2012.03.032
195. Martins S, Sarmiento B, Ferreira DC, Souto EB. Lipid-based colloidal carriers for peptide and protein delivery—liposomes versus lipid nanoparticles. *Int J nanomed* (2007) 2(4):595.
196. Martins S, Silva A, Ferreira D, Souto E. Improving oral absorption of samon calcitonin by trimyristin lipid nanoparticles. *J Biomed Nanotechnol* (2009) 5(1):76–83. doi: 10.1166/jbn.2009.443
197. Figueiro J, Gonzalez-Mira E, Martins-Lopes P, Egea M, Garcia M, Souto S, et al. A novel lipid nanocarrier for insulin delivery: Production, characterization and toxicity testing. *Pharm Dev Technol* (2013) 18(3):545–9. doi: 10.3109/10837450.2011.591804
198. Patel M, Souto EB, Singh KK. Advances in brain drug targeting and delivery: Limitations and challenges of solid lipid nanoparticles. *Expert Opin Drug Deliv* (2013) 10(7):889–905. doi: 10.1517/17425247.2013.784742
199. Souto E, Müller R. Cosmetic features and applications of lipid nanoparticles (Sln<sup>®</sup>, nlc<sup>®</sup>). *Int J Cosmetic Sci* (2008) 30(3):157–65. doi: 10.1111/j.1468-2494.2008.00433.x
200. Souto EB, Müller RH. Lipid nanoparticles: Effect on bioavailability and pharmacokinetic changes. In: *Drug delivery*. Springer (2010). p. 115–41.
201. Souto E, Wissing S, Barbosa C, Müller R. Development of a controlled release formulation based on sln and nlc for topical clotrimazole delivery. *Int J Pharmaceut* (2004) 278(1):71–7. doi: 10.1016/j.jipharm.2004.02.032
202. Saupe A, Wissing SA, Lenk A, Schmidt C, Müller RH. Solid lipid nanoparticles (Sln) and nanostructured lipid carriers (Nlc)—structural investigations on two different carrier systems. *Bio-medical Mater Eng* (2005) 15(5):393–402.
203. Teeranachadeekul V, Müller RH, Junyaprasert VB. Encapsulation of ascorbyl palmitate in nanostructured lipid carriers (Nlc)—effects of formulation parameters on physicochemical stability. *Int J Pharmaceut* (2007) 340(1):198–206. doi: 10.1016/j.jipharm.2007.03.022
204. Souto EB, Figueiro JF, Müller RH. Solid lipid nanoparticles (Sln<sup>TM</sup>). In: *Fundamentals of pharmaceutical nanoscience*. Springer (2013). p. 91–116.
205. Souto E, Almeida A, Müller R. Lipid nanoparticles (Sln<sup>®</sup>, nlc<sup>®</sup>) for cutaneous drug delivery: Structure, protection and skin effects. *J Biomed Nanotechnol* (2007) 3(4):317–31. doi: 10.1166/jbn.2007.049
206. Zielińska A, Nowak I. Solid lipid nanoparticles and nanostructured lipid carriers as novel carriers for cosmetic ingredients. In: *Nanobiomaterials in galenic formulations and cosmetics*. Elsevier (2016). p. 231–55.
207. Zielińska A, Ferreira NR, Durazzo A, Lucarini M, Cicero N, Mamouni SE, et al. Development and optimization of alpha-Pinene-Loaded solid lipid nanoparticles (Sln) using experimental factorial design and dispersion analysis. *Molecules* (2019) 24(15):2683.
208. Souto EB, Doktorovová S, Zielińska A, Silva AM. Key production parameters for the development of solid lipid nanoparticles by high shear homogenization. *Pharm Dev Technol* (2019) 24(9):1181–5. doi: 10.1080/10837450.2019.1647235
209. Souto EB, Zielińska A, Souto SB, Durazzo A, Lucarini M, Santini A, et al. (+)-limonene 1, 2-Epoxy-Loaded slns: Evaluation of drug release, antioxidant activity, and cytotoxicity in an hacat cell line. *Int J Mol Sci* (2020) 21(4):1449. doi: 10.3390/ijms21041449
210. Singh KK, Vingkar SK. Formulation, antimalarial activity and biodistribution of oral lipid nanoemulsion of primaquine. *Int J Pharmaceut* (2008) 347(1–2):136–43. doi: 10.1016/j.jipharm.2007.06.035
211. Patil HG, Tiwari RV, Repka MA, Singh KK. Formulation and development of orodispersible sustained release tablet of domperidone. *Drug Dev Ind Pharm* (2016) 42(6):906–15. doi: 10.3109/03639045.2015.1088864

212. Joshi M, Patravale V. Nanostructured lipid carrier (NLC) based gel of celecoxib. *Int J Pharmaceut* (2008) 346(1):124–32. doi: 10.1016/j.ijpharm.2007.05.060
213. Souto EB, Doktorovova S, Campos JR, Martins-Lopes P, Silva AM. Surface-tailored anti-Her2/Neu-Solid lipid nanoparticles for site-specific targeting mcf-7 and bt-474 breast cancer cells. *Eur J Pharm Sci* (2019) 128:27–35. doi: 10.1016/j.ejps.2018.11.022
214. Eder P, Zielińska A, Karczewski J, Dobrowolska A, Slomski R, Souto EB. How could nanobiotechnology improve treatment outcomes of anti-Tnf- $\alpha$  therapy in inflammatory bowel disease? current knowledge, future directions. *J Nanobiotechnol* (2021) 19(1):346. doi: 10.1186/s12951-021-01090-1
215. Maroni A, Moutaharrik S, Zema L, Gazzaniga A. Enteric coatings for colonic drug delivery: State of the art. *Expert Opin Drug Deliv* (2017) 14(9):1027–9. doi: 10.1080/17425247.2017.1360864
216. Kulbacka J, Pucek A, Kotulska M, Dubińska-Magiera M, Rossowska J, Rols M-P, et al. Electroporation and lipid nanoparticles with cyanine ir-780 and flavonoids as efficient vectors to enhanced drug delivery in colon cancer. *Bioelectrochemistry* (2016) 110:19–31. doi: 10.1016/j.bioelechem.2016.02.013
217. Geng T, Lu C. Microfluidic electroporation for cellular analysis and delivery. *Lab Chip* (2013) 13(19):3803–21. doi: 10.1039/c3lc50566a



## OPEN ACCESS

## EDITED BY

Alfonso J. Rodriguez-Morales,  
Fundacion Universitaria Autónoma de las  
Américas, Colombia

## REVIEWED BY

Sabeena Mustafa,  
King Abdullah International Medical  
Research Center (KAIMRC), Saudi Arabia  
Shaban Ahmad,  
Jamia Millia Islamia, India

## \*CORRESPONDENCE

Zhiwang Li

✉ lizhiwanghn@163.com

<sup>†</sup>These authors have contributed  
equally to this work and share  
first authorship

RECEIVED 27 January 2023

ACCEPTED 27 April 2023

PUBLISHED 16 May 2023

## CITATION

Li P, Li T, Zhang Z, Dai X, Zeng B, Li Z and  
Li Z (2023) Bioinformatics and system  
biology approach to identify the influences  
among COVID-19, ARDS and sepsis.  
*Front. Immunol.* 14:1152186.  
doi: 10.3389/fimmu.2023.1152186

## COPYRIGHT

© 2023 Li, Li, Zhang, Dai, Zeng, Li and Li.  
This is an open-access article distributed  
under the terms of the [Creative Commons  
Attribution License \(CC BY\)](#). The use,  
distribution or reproduction in other  
forums is permitted, provided the original  
author(s) and the copyright owner(s) are  
credited and that the original publication in  
this journal is cited, in accordance with  
accepted academic practice. No use,  
distribution or reproduction is permitted  
which does not comply with these terms.

# Bioinformatics and system biology approach to identify the influences among COVID-19, ARDS and sepsis

Peiyu Li<sup>1,2†</sup>, Tao Li<sup>3,4†</sup>, Zhiming Zhang<sup>5</sup>, Xingui Dai<sup>3</sup>, Bin Zeng<sup>5</sup>,  
Zhen Li<sup>5</sup> and Zhiwang Li<sup>5\*</sup>

<sup>1</sup>Department of Gastroenterology, The First People's Hospital of Chenzhou, Chenzhou, Hunan, China,

<sup>2</sup>The First Clinical Medical College of Jinan University, Guangzhou, Guangdong, China, <sup>3</sup>Department of Critical Care Medicine, The First People's Hospital of Chenzhou, Chenzhou, Hunan, China,

<sup>4</sup>Hengyang Medical College, University of South China, Hengyang, Hunan, China, <sup>5</sup>Department of Anesthesiology, The First People's Hospital of Chenzhou, Chenzhou, Hunan, China

**Background** Severe coronavirus disease 2019 (COVID -19) has led to severe pneumonia or acute respiratory distress syndrome (ARDS) worldwide. we have noted that many critically ill patients with COVID-19 present with typical sepsis-related clinical manifestations, including multiple organ dysfunction syndrome, coagulopathy, and septic shock. The molecular mechanisms that underlie COVID-19, ARDS and sepsis are not well understood. The objectives of this study were to analyze potential molecular mechanisms and identify potential drugs for the treatment of COVID-19, ARDS and sepsis using bioinformatics and a systems biology approach. **Methods** Three RNA-seq datasets (GSE171110, GSE76293 and GSE137342) from Gene Expression Omnibus (GEO) were employed to detect mutual differentially expressed genes (DEGs) for the patients with the COVID-19, ARDS and sepsis for functional enrichment, pathway analysis, and candidate drugs analysis. **Results** We obtained 110 common DEGs among COVID-19, ARDS and sepsis. ARG1, FCGR1A, MPO, and TLR5 are the most influential hub genes. The infection and immune-related pathways and functions are the main pathways and molecular functions of these three diseases. FOXC1, YY1, GATA2, FOXL, STAT1 and STAT3 are important TFs for COVID-19. mir-335-5p, miR-335-5p and hsa-mir-26a-5p were associated with COVID-19. Finally, the hub genes retrieved from the DSigDB database indicate multiple drug molecules and drug-targets interaction. **Conclusion** We performed a functional analysis under ontology terms and pathway analysis and found some common associations among COVID-19, ARDS and sepsis. Transcription factors–genes interaction, protein–drug interactions, and DEGs–miRNAs coregulatory network with common DEGs were also identified on the datasets. We believe that the candidate drugs obtained in this study may contribute to the effective treatment of COVID-19.

## KEYWORDS

COVID-19, ARDS, sepsis, differentially expressed genes, gene ontology, protein-protein interaction, drug molecule

## Introduction

Coronavirus disease 19 (COVID-19) is a novel infectious disease caused by severe acute respiratory syndrome coronavirus 2 (SARS-CoV-2) (1, 2). The lung is the organ most severely affected by SARS-CoV-2. Patients with COVID-19 autoimmune diseases (3) may develop severe pneumonia or acute respiratory distress syndrome (ARDS). The pathophysiology of those two diseases are characterized by diffuse alveolar damage, exudation, and accompanied by extensive immune cell infiltration and inflammatory cytokine expression (4). If the inflammation is further aggravated, the extrapulmonary organ damage is serious, manifested as multiple organ dysfunction and systemic inflammatory response, its symptoms include cold limbs, microcirculatory dysfunction, weak peripheral pulse, oxidative stress injury, and cytokine storm. This is very similar to sepsis (5). Consideration of severe COVID-19 disease as a sepsis syndrome has relevance and may assist in terms of determining treatments (6).

Sepsis, a systemic inflammatory response syndrome (SIRS) caused by infection, is a common and critical disease with characteristics of high incidence, complex pathogenesis, severe illness, and high mortality (7, 8). In 2016, sepsis3.0 was released (9), which defined sepsis as a clinical syndrome of maladjusted host immune response triggered by infection and manifested as life-threatening organ dysfunction resulting from it. Sepsis is characterized by uncontrolled inflammation and overproduction of reactive oxygen and nitrogen species (RONS), which in turn leads to cell and tissue destruction, immune system dysfunction and pronounced hematopathology, eventually leading to multiple organ failure syndrome (MODS) (10).

Acute respiratory distress syndrome (ARDS) is a serious respiratory disease secondary to trauma, shock, infection and other non-cardiogenic diseases. ARDS is one of the most common and serious complications in the development of sepsis

(11). The mortality rate of ARDS is as high as 30%-40% (11). People with COVID-19 who have an autoimmune disease may develop severe pneumonia or ARDS (3).

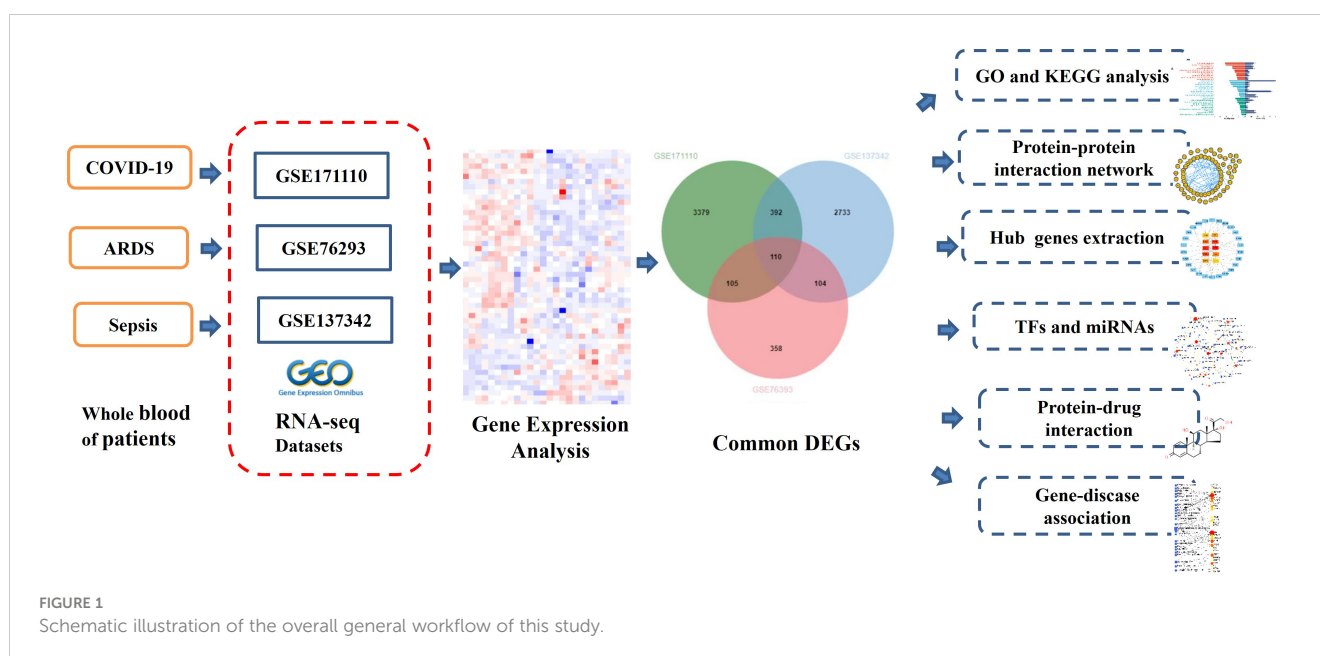
Given the similarities between COVID-19, ARDS, and sepsis, it is necessary to understand the biological links and underlying molecular mechanisms between the three diseases in order to provide new insights into the pathogenesis of COVID-19 and to search for potential therapeutic agents for patients with COVID-19 or those with COVID-19 secondary to ARDS and sepsis.

In this study, three datasets were used to discover the biological relationship among COVID-19, ARDS and sepsis. The three datasets are GSE171110, GSE76293 and GSE137342. Initially, DEGs were identified for datasets and then found common DEGs among the three diseases. The enrichment pathways and biological functions of the common DEGs were analyzed, and the biological processes involved in them were studied. The central gene was extracted from common DEGs, which is an important component of potential drugs. Protein-protein interaction networks (PPIs) are designed by common DEGs to collect central genes. Here, we also trace transcriptional regulators against DEGs similar to GSE171110, GSE76293, and GSE137342. Finally, possible drugs are predicted. The sequential workflow of our research is presented in Figure 1.

## Materials and methods

### Collection of the datasets

To analyze shared genetic interrelations and potential therapeutic targets among COVID-19, ARDS and sepsis, we obtained both microarray and RNA-seq datasets from the Gene Expression Omnibus (GEO) database of the National Center for Biotechnology Information (NCBI) (<https://www.ncbi.nlm.nih.gov/geo/>). The GEO accession ID of the COVID-19 dataset was



GSE171110, which included transcriptional profiling from 78 samples (44 COVID-19 samples and 10 healthy control samples, with samples collected from whole blood). GSE171110 was based on the Illumina HiSeq 2500 (Homo sapiens) (GPL16791) platform for extracting RNA sequence analysis. The ARDS dataset was (GEO accession ID: GSE76293) of whole blood containing 12 ARDS patients and 12 healthy controls, which is based on Affymetrix Human Genome U133 Plus 2.0 Array (GPL570) platform. Similarly, the sepsis dataset (GEO accession ID: GSE137342) included array-based gene expression profiles of whole blood from 43 sepsis patients and 12 healthy individuals. Table 1 shows the basic information of the three datasets.

## Identification of DEGs and common DEGs among COVID-19, ARDS and sepsis

Identification of DEGs for GSE171110, GSE76293 and GSE137342 datasets was the main task of our research. The DEGs for GSE171110 were identified by using the limma package of R programming language. Data generated by microarray analysis were retrieved through DESeq2 and limma package. DEGs for GSE76293 and GSE137342 datasets were analyzed through GEO2R (<https://www.ncbi.nlm.nih.gov/geo/geo2r/>) web tool which also uses limma package for identifying DEGs. Benjamini–Hochberg false discovery rate (FDR) method was applied to discover genes which were statistically significant and limited false positives. Genes that met the cut-off criteria, adjust P-values <0.01 and  $|\log_2FC| \geq 1.0$ , were considered as DEGs. Statistical analysis was carried out for each dataset, and the common DEGs of GSE171110, GSE76293 and GSE137342 datasets were obtained using an online VENN analysis tool called Jvenn (<http://jvenn.toulouse.inra.fr/app/index.html>). Volcano plots were drawn using to show the differential genes in the three datasets.

## Gene ontology and pathway enrichment analysis of DEGs

Gene set enrichment analysis undertakes target gene sets to help understand the general biological functions and chromosomes' positions. Gene ontology (GO) analysis is a common useful method for functional enrichment analysis (12), which can be classified into biological process (BP), cellular composition (CC) and molecular function (MF). Kyoto Encyclopedia of Genes and Genomes (KEGG) pathway was used for metabolic pathway enrichment analysis and contains considerable utility of genomic analysis (13). GO analysis and KEGG pathway enrichment analysis

of DEGs in this study was performed using the DAVID database for annotation, visualization and integrated discovery tools (<https://david.ncifcrf.gov/>). The adjusted P value <0.01 was considered statistically significant GO terms and pathways.

## Protein-protein interaction networks and hub genes extraction

The evaluation and analysis of PPI network are fundamental and key to illustrating the molecular mechanisms of key cellular activities. In our study, the PPI networks on common DEGs were identified, and associations between different diseases were found from the perspective of protein interactions. The search tool for the retrieval of interacting genes database called STRING (<https://www.string-db.org/>) was used to construct the PPI network of proteins derived from shared DEGs among COVID-19, ARDS and sepsis. STRING aims to integrate all known and predicted associations between proteins, including both physical interactions as well as functional associations. This experiment set the medium confidence score of 0.500 to generate the PPI network of common DEGs. The confidence score was also used for the current PPIs network with a medium confidence score of 0.400.

Subsequently, we consume our PPI network into Cytoscape (v.3.9, <https://cytoscape.org/>) for a superior visual representation and further PPI network studies. Then, Cytohubba, a plugin in Cytoscape (<https://apps.cytoscape.org/apps/cytohubba>), was used to calculate the hub genes in the PPI network. Cytohubba can sequence and extract the central or target elements of a biological networks based on different network characteristics. Cytohubba has 11 methods for topological analysis from various viewpoints, and Maximal Clique Centrality (MCC) is the best of them, and the MCC function of Cytohubba was carried out to confirm the top 10 hub genes.

## Identification of transcription factors and miRNAs

Transcription factors (TFs) are proteins that attach to particular genes and control the rate of transcription of genetic information (14). MicroRNAs (miRNAs) are a class of short, endogenously initiated and non-coding RNAs that strive to attach with gene transcripts to affect protein expression; hence, TFs and miRNAs are essential for molecular insights. We used the NetworkAnalyst platform (<https://www.networkanalyst.ca/>) to construct TF–DEG and DEG–miRNA regulatory networks to analyze relevant TFs and miRNAs. NetworkAnalyst is an extensive online platform for meta-

TABLE 1 Overview of datasets with their geo-features and their quantitative measurements in this analysis.

Disease name	GEO accession	GEO platform	Total DEGs count	Up regulated DEGs count	Down regulated DEGs count
SARS-CoV-2	GSE171110	GPL16791	3986	2620	1366
ARDS	GSE76293	GPL570	677	346	331
Sepsis	GSE137342	GPL10558	3339	3309	30



analyzing gene expression data and gaining insights into biological mechanisms, roles, and interpretations. The TF–DEG network was established using the JASPAR database. JASPAR is a publicly available resource for TFs of multiple species in six major taxa. Besides, the DEG–miRNA network was established using the TarBase database. Tarbase and mirTarbase are the main experimental validity databases for miRNAs–target interacting with target genes. We have extracted miRNAs with common DEGs focused on topological analysis from both Tarbase and mirTarbase.

## Drug prediction analysis

Protein–drug interaction (PDI) prediction and drug molecular recognition based on target genes are essential. Potential drug molecules were predicted using the Drug Signatures database (DSigDB) *via* gene set enrichment network tool Enrichr based on the common DEGs of COVID-19, ARDS and sepsis. Enrichr contains a large number of different gene set collections available for analysis, which can be used to explore gene-set enrichment across a genome-wide scale. DSigDB is a web-based resource that contains relevant information about drugs and their target genes for enrichment analysis. This database currently has 22,527 gene sets, including 17,389 drugs and 19,531 genes (15).

## Gene–disease association analysis

DisGeNET is a knowledge management database of gene–disease associations based on various biomedical aspects of diseases, which synchronizes relationships from several origins. It provides and highlights new insights into human genetic disorders. We also examined the gene–disease relationship through NetworkAnalyst using the DisGeNET database to find related diseases and their chronic complications with common DEGs.

## Result

### Identification of DEGs and common DEGs among COVID-19, ARDS and sepsis

Firstly, 3986 genes were differentially expressed for COVID-19 from GSE171110, including 2620 up-regulated and 1366 down-regulated genes exposure. In the same way, we identified 677 DEGs (346 up-regulated and 331 down-regulated) in GSE76293 and 3339 DEGs (3309 up-regulated and 30 down-regulated) in GSE137342. The three volcano plots in Figure 2 visually demonstrated the overall picture of transcribed gene expression for COVID-19, ARDS and sepsis, where red and blue dots indicated up-regulated and down-regulated genes with significant differences, respectively (Figures 2A–C). we identified the 110 common DEGs among GSE171110, GSE76293 and GSE137342 (Figure 2D). There were some mechanistic commonalities and interaction among COVID-19, ARDS and sepsis, the results of differential expression analysis suggested.

## Gene ontology and pathway enrichment analysis

GO analysis included biological process, cell composition, and molecular function. The GO database was selected as an annotation source. Table 2 showed the top 10 items in the categories of biological processes, molecular functions, and cell components. Figure 3A also showed the top 10 GO terms for molecular function, biological process, and cell compartment, respectively. The differentially expressed genes were significantly enriched in inflammatory response in the subset of BP, enriched in the plasma membrane in the subset of CC, and enriched in catalytic activity in the subset of MF, which were all involved into immunotherapy related functional enrichment.

KEGG pathway analysis revealed the following top 10 pathways: Hematopoietic cell lineage, Legionellosis, Pantothenate and CoA biosynthesis, Inflammatory bowel disease, Leishmaniasis, Drug metabolism–other enzymes, Th1 and Th2 cell differentiation, Staphylococcus aureus infection, Viral protein interaction with cytokine and cytokine receptor and Th17 cell differentiation. Table 3 listed the KEGG enrichment pathways generated from the selected dataset. For a more detailed illustration, the pathway enrichment analysis was showed in the bubble graphs (Figure 3B).

## Classification of hub proteins and submodule

The PPI network of common DEGs included 110 nodes and 105 edges, as shown in Figure 4A. Based on PPI network analysis, we identified the top 10 DEGs as the most influential genes by using the Cytohubba plugin in Cytoscape. The hub genes were namely LCN2, HP, ARG1, MPO, CD163, CD4, FCGR1A, CR1, C3AR1, and TLR5. These hub genes could serve as potential biomarkers and potentially new therapeutic strategies for studying disease. The expanded network of hub – gene interactions derived from the PPI network was shown in Figure 4B.

## Construction of regulatory networks

TFs regulators interaction with the common DEGs was pictured in Figure 5. From the Figure 5, KCNJ15, SMARCD3, LILRA5, GAS7 and HMGB2 were more abundant in the highly expressed DEGs as these genes have a higher degree in the TF–gene interactions network. TFs such as FOXC1, GATA2, YY1, FOXL1, FOXO3, STAT1 and STAT3 were more significant than others as presented in the same Figure 5.

The interactions of miRNAs regulators with common DEGs was showed in the Figure 6. In the Figure 6, blue squares represented miRNAs and red circles represented DEGs. Our results showed that ACVR1B, MTF1, CD4, MAPK14, DACH1, KIF1B, GAS7 and CYP1B1 were the hub genes of this network, with the five genes most involved in miRNAs. Besides, we also detected the significant hub miRNAs from the miRNAs–gene interaction network, namely mir-335-5p, hsa-mir-26a-5p, hsa-mir-200b-3p,

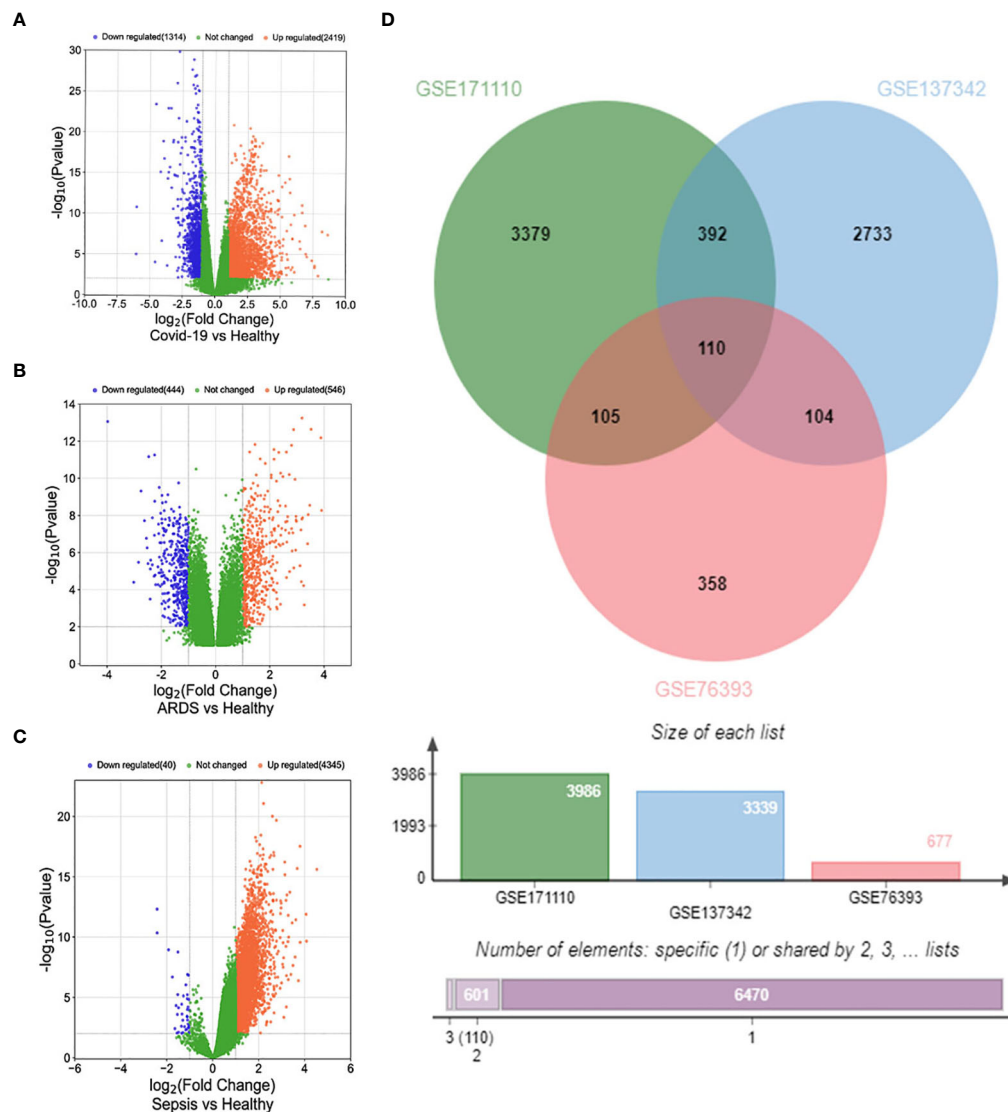


FIGURE 2

Volcano plots exhibit DEGs of (A) COVID-19, (B) ARDS and (C) sepsis. (D) The Venn diagram depicts the common DEGs among COVID-19, ARDS and sepsis.

hsa-mir-194-5p, hsa-mir-192-5p, hsa-mir-143-3p and hsa-mir-520f-3p.

## Identification of candidate drugs

Based on transcriptome signatures, we identified 10 possible drug molecules using Enrichr from the DSigDB database. The top 10 chemical compounds were extracted based on their P-value. These 10 possible drug molecules included isoflupredone, etynodiol, fludroxycortide, flunisolide, halcinonide, flumetasone, diflorasone, ribavirin, gabexate and alclometasone (Table 4).

## Identification of disease association

From the analysis of the gene-disease association by Network Analyst (16), we noticed that major depressive disorder,

cardiovascular diseases, mental depression, hypertensive disease, autosomal recessive predisposition, anemia, liver diseases, schizophrenia and liver cirrhosis are most coordinated to our reported hub genes, and even among COVID-19, ARDS and sepsis. The gene-disease association was shown in Figure 7.

## Discussion

Most patients with severely ill COVID-19 eventually develop typical septic shock manifestations, including cold limbs, microcirculatory dysfunction, peripheral pulse weak, oxidative stress injury, and cytokine storm (17). These symptoms and serological markers are present in both ARDS and sepsis patients (18). ARDS induced by COVID-19 can progress to sepsis (17).

The results of our GO analysis from the DAVID show that inflammatory response (14 genes), defense response to bacterium (11 genes), immune response (12 genes) and innate immune

TABLE 2 Ontological analysis of common DEGs among COVID-19, ARDS and sepsis.

Category	GO ID	Term	P Value	Genes
GO Biological Process	GO:0006954	inflammatory response	3.72E-07	ORM1, SLC11A1, PPBP, NLRC4, LTB4R, TPST1, IL18RAP, AIM2, VNN1, C3AR1, TLR5, IL18R1, CCR3, NAIP
	GO:0042742	defense response to bacterium	6.19E-07	CLEC4D, ANXA3, SLC11A1, HP, LCN2, PPBP, NLRC4, FCGR1A, TLR5, MPO, NAIP
	GO:0006955	immune response	7.58E-05	HLA-DMA, CD4, CLEC4D, IL18RAP, AIM2, SLC11A1, FCGR1A, CST7, CD24, CCR3, IL18R1, LTB4R
	GO:0045087	innate immune response	1.00E-04	ARG1, DEFA4, HMGB2, NLRC4, SRPK1, LILRA5, AIM2, VNN1, LCN2, FCGR1A, TLR5, NAIP, CD177
	GO:0032731	positive regulation of interleukin-1 beta production	4.33E-04	ORM1, AIM2, NLRC4, NAIP, LILRA5
	GO:0071222	cellular response to lipopolysaccharide	6.54E-04	ARG1, DEFA4, HMGB2, LCN2, PPBP, MAPK14, TLR5
	GO:0006953	acute-phase response	0.00153779	CD163, ORM1, HP, LCN2
	GO:0032496	response to lipopolysaccharide	0.001675603	SLC11A1, MGST1, HMGB2, ALPL, IRAK3, MPO
	GO:0002221	pattern recognition receptor signaling pathway	0.002197244	AIM2, NLRC4, NAIP
	GO:0008584	male gonad development	0.003271334	KCNE1, HMGB2, CYP1B1, INSL3, TLR5
GO Cellular Component	GO:0005886	plasma membrane	7.35E-06	KCNE1, FCMR, MGST1, GPR84, ACVR1B, CACNA1E, CD3D, ETS2, LTB4R, LILRA5, ASGR2, MUC1, IL18RAP, PSTPIP2, GRB10, C3AR1, FLVCR2, STOM, CLEC1B, FCGR1A, CCR3, ATP9A, CD177, CD163, CR1, SORT1, ANXA3, SLC11A1, KREMEN1, KCNJ15, AGTRAP, IRAK3, MCEMP1, OLFM4, BMX, SRPK1, F5, CD4, CLEC4D, VNN1, RAB13, TMEM119, SLC26A8, ALPL, RGL4, TLR5, IL18R1, GAS7
	GO:0035580	specific granule lumen	1.70E-05	ORM1, ARG1, DEFA4, HP, LCN2, OLFM4
	GO:0070821	tertiary granule membrane	3.76E-05	CLEC4D, SLC11A1, STOM, MCEMP1, GPR84, CD177
	GO:0035579	specific granule membrane	1.08E-04	CLEC4D, C3AR1, STOM, MCEMP1, GPR84, CD177
	GO:1904724	tertiary granule lumen	0.002875622	ORM1, HP, PPBP, OLFM4
	GO:0035577	azurophil granule membrane	0.003344588	VNN1, MGST1, C3AR1, STOM
	GO:0016021	integral component of membrane	0.006490311	KCNE1, FCMR, MGST1, TMTC1, CD3D, LTB4R, PHTF1, LILRA5, ASGR2, HLA-DMA, MUC1, ZDHHC19, APMAP, C3AR1, CYP1B1, FLVCR2, FCGR1A, SLC37A3, CCR3, ATP9A, CD163, CR1, SORT1, SLC11A1, CSGALNACT2, KREMEN1, KCNJ15, KLHL2, AGTRAP, MCEMP1, FRMD3, CD4, CLEC4D, VNN1, TMEM119, SLC26A8, RGL4, ST6GALNAC3, TLR5, IL18R1, GRINA
	GO:0045092	interleukin-18 receptor complex	0.010283955	IL18RAP, IL18R1
	GO:0005887	integral component of plasma membrane	0.010415288	CD163, CR1, SLC11A1, KCNJ15, GPR84, ACVR1B, LTB4R, MUC1, CD4, C3AR1, SLC26A8, STOM, FCGR1A, CLEC1B, TLR5, CCR3
	GO:0005615	extracellular space	0.020503922	ORM1, CR1, ARG1, DEFA4, HP, HMGB2, PPBP, OLFM4, CST7, MPO, F5, LILRA5, MUC1, LCN2, STOM, ALPL, FAM20A, INSL3

(Continued)

TABLE 2 Continued

Category	GO ID	Term	P Value	Genes
GO Molecular Function	GO:0003824	catalytic activity	8.57E-04	PFKFB2, DDAH2, ECHDC3, UPP1, OLFM4, BCAT1
	GO:0042803	protein homodimerization activity	0.002126894	TPST1, CD4, TP53I3, GADD45A, DEFA4, SLC11A1, STOM, IRAK3, NLRC4, CST7, GYG1, UPB1
	GO:0004888	transmembrane signaling receptor activity	0.004116847	CD4, FCMR, FCGR1A, CLEC1B, TLR5, CD3D
	GO:0042008	interleukin-18 receptor activity	0.011098693	IL18RAP, IL18R1
	GO:0003873	6-phosphofructo-2-kinase activity	0.022075366	PFKFB2, PFKFB3
	GO:0002020	protease binding	0.024084899	LCN2, INSL3, ATP9A, CD177
	GO:0004331	fructose-2,6-bisphosphate 2-phosphatase activity	0.02751836	PFKFB2, PFKFB3
	GO:0005524	ATP binding	0.047221652	PFKFB2, PFKFB3, TDRD9, IRAK3, NLRC4, BMX, MAPK14, OPLAH, ACVR1B, SRPK1, PGS1, MKNK1, KIF1B, NAIP, ATP9A
	GO:0042802	identical protein binding	0.052207838	ARG1, MGST1, KLHL2, AGTRAP, MCEMP1, NLRC4, OPLAH, CD3D, CD4, AIM2, GRB10, LCN2, STOM, UPP1, BCAT1, GAS7
	GO:0061809	NAD <sup>+</sup> nucleotidase, cyclic ADP-ribose generating	0.085446381	IL18RAP, IL18R1

Top 10 terms of each category are listed.

response (13 genes) are among the top GO terms. Innate immune cell hyperactivation plays a critical role in the pathogenesis of severe COVID-19 (19). Studies have shown that the infection mediated immuno-compromised state can result in poor clinical morbidity and a high risk of fatal pneumonia (20). In the molecular function experiment, catalytic activity, protein homodimerization activity and transmembrane signaling receptor activity are three top GO pathways. According to the cellular component, top GO terms are plasma membrane, specific granule lumen, tertiary granule membrane and specific granule membrane.

By identifying the KEGG pathways for 110 common DEGs, similar pathways were identified for COVID-19, ARDS, and sepsis. Some patients experiencing severe COVID-19, the disease caused by the SARS-CoV-2 beta coronavirus, develop what is sometimes described as a “cytokine storm” or “cytokine release syndrome” (21). These cytokines produce eosinopenia and lymphocytopenia characterized by low counts of eosinophils, CD8<sup>+</sup> T cells, natural killer (NK) and naïve T-helper cells, simultaneously inducing naïve B-cell activation, increased T-helper cell 17 (Th17) lymphocyte differentiation and the stimulation of monocyte and neutrophil recruitment (18, 22).

The top hub proteins indicate different diseases, most risk factors for the COVID-19, ARDS and sepsis. A total of 10 hub-proteins (LCN2, HP, ARG1, MPO, CD163, CD4, FCGR1A, CR1, C3AR1 and TLR5) identified involved in these diseases. ARG1 can be released to the extracellular microenvironment during inflammatory conditions, e.g., asthma and infectious diseases

(23). FCGR1A has been proposed as an attractive target for immunotherapy by various workers (24). Research shows that infiltrating neutrophils, a hallmark of COVID-19, can release myeloperoxidase (MPO), which can activate several pathways that lead to elevated cytokines and production of ROS such as hypochlorous acid (HOCl), superoxide (O<sub>2</sub><sup>•-</sup>), and hydrogen peroxide (H<sub>2</sub>O<sub>2</sub>) (25). Another possible facet of the observed pathophysiology in critical cases of COVID-19 is a decline in nitric oxide (NO) and combined with the effect of excessive ROS on the structure and function of hemoglobin (Hb) could impact pulmonary and peripheral circulation, possibly eventually leading to critical or fatal hypoxia (26). Chakraborty recommend the use of active immunomodulation through TLR5 and activation of the innate immune to fight against SARS-CoV-2 as the main entry point of this virus is angiotensin-converting enzyme 2 receptor respiratory in epithelial cells (27).

To understand how common DEGs regulate COVID-19 (or ARDS, sepsis) at the transcriptional level, the interactions among TFs, miRNAs and genes were investigated *via* web tools. The identified TFs, such as FOXC1, GATA2, YY1, FOXL1, FOXO3, STAT1 and STAT3, are associated with COVID-19. In previous bioinformatics analysis, Ahmed (28) and Islam et al. (29) both found that FOXC1, YY1, GATA2, and FOXL1 are important TFs for COVID-19. Coincidentally, Lu Lu also found that FOXC1, YY1, GATA2 and FOXL1 are important TFs for COVID-19 (30). After a careful review of the scientific literature, we realized that COVID-19 is a disease caused by a catastrophic cascade of failures stemming

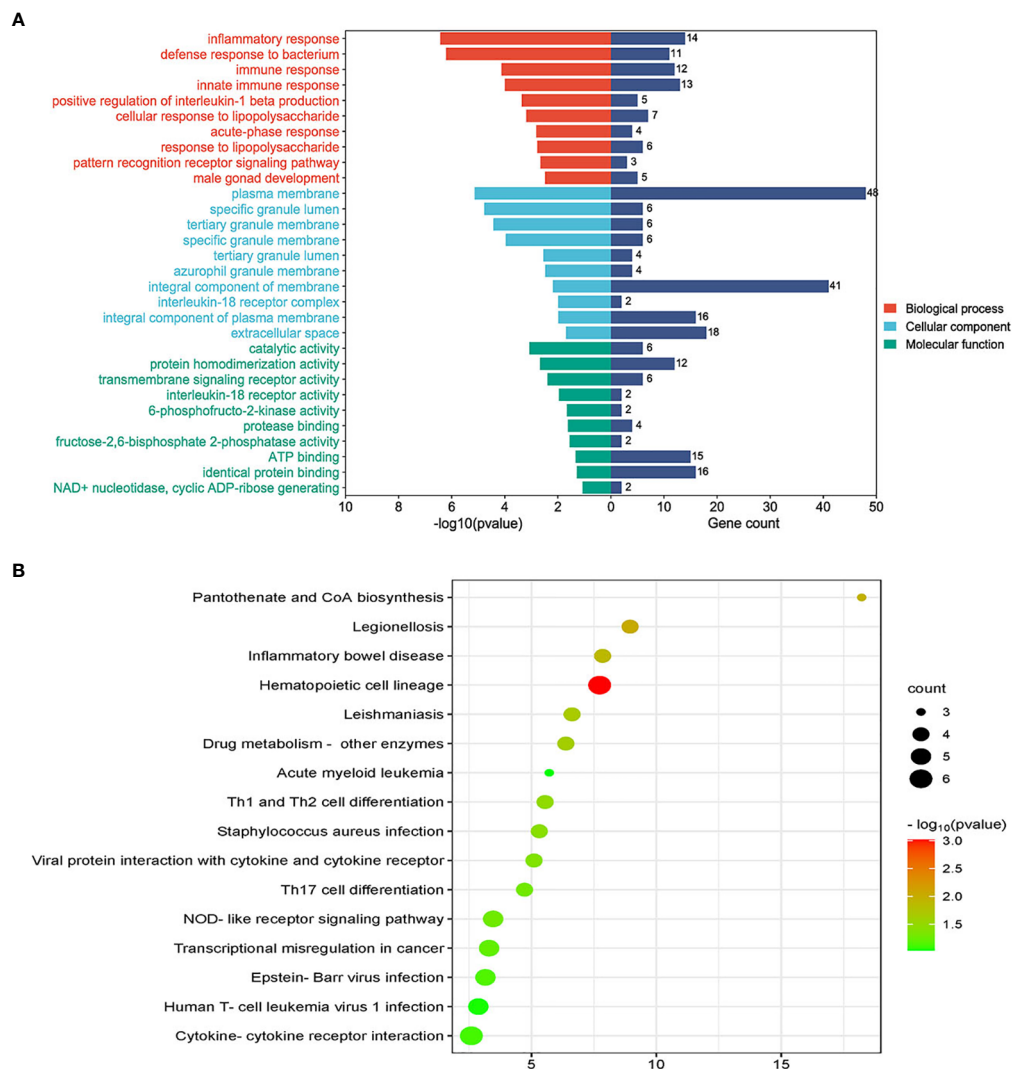


FIGURE 3

(A) The bar graphs of the ontological analysis of the common DEGs among COVID-19, ARDS and sepsis. (B) Bubble graphs indicate the results for KEGG analysis based on the common DEGs among COVID-19, ARDS and sepsis.

TABLE 3 Pathway enrichment analysis of common DEGs among COVID-19, ARDS and sepsis.

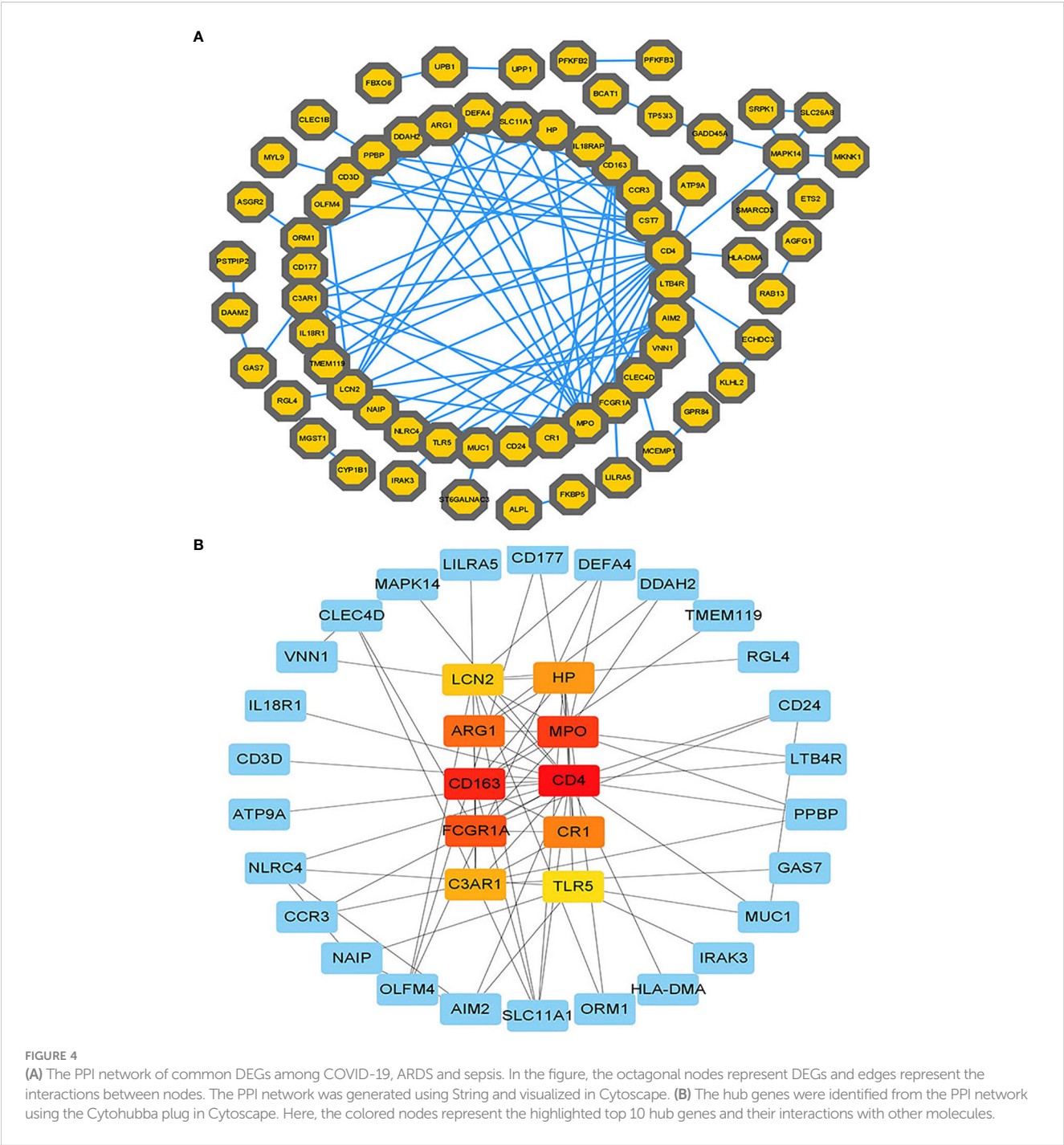
Category	Pathways	P Value	Genes
KEGG_PATHWAY	Hematopoietic cell lineage	9.55E-04	HLA-DMA, CD4, CR1, FCGR1A, CD24, CD3D
	Legionellosis	0.009529899	CR1, NLR4, TLR5, NAIP
	Pantothenate and CoA biosynthesis	0.011199108	VNN1, BCAT1, UPB1
	Inflammatory bowel disease	0.013620921	HLA-DMA, IL18RAP, TLR5, IL18R1
	Leishmaniasis	0.021374347	HLA-DMA, CR1, FCGR1A, MAPK14
	Drug metabolism - other enzymes	0.023620807	MGST1, UPP1, MPO, UPB1
	Th1 and Th2 cell differentiation	0.033841345	HLA-DMA, CD4, MAPK14, CD3D
	Staphylococcus aureus infection	0.037683794	HLA-DMA, DEFA4, C3AR1, FCGR1A
	Viral protein interaction with cytokine and cytokine receptor	0.041740915	IL18RAP, PPBP, CCR3, IL18R1
	Th17 cell differentiation	0.050488231	HLA-DMA, CD4, MAPK14, CD3D

(Continued)



TABLE 3 Continued

Category	Pathways	P Value	Genes
	NOD-like receptor signaling pathway	0.053210438	AIM2, DEFA4, NLR4, MAPK14, NAIP
	Transcriptional misregulation in cancer	0.061334532	CCNA1, GADD45A, DEFA4, FCGR1A, MPO
	Epstein-Barr virus infection	0.070083846	CCNA1, HLA-DMA, GADD45A, MAPK14, CD3D
	Cytokine-cytokine receptor interaction	0.076591926	CD4, IL18RAP, PPBP, ACVR1B, CCR3, IL18R1
	Human T-cell leukemia virus 1 infection	0.091699112	CCNA1, HLA-DMA, CD4, CD3D, ETS2
	Acute myeloid leukemia	0.094203186	CCNA1, FCGR1A, MPO



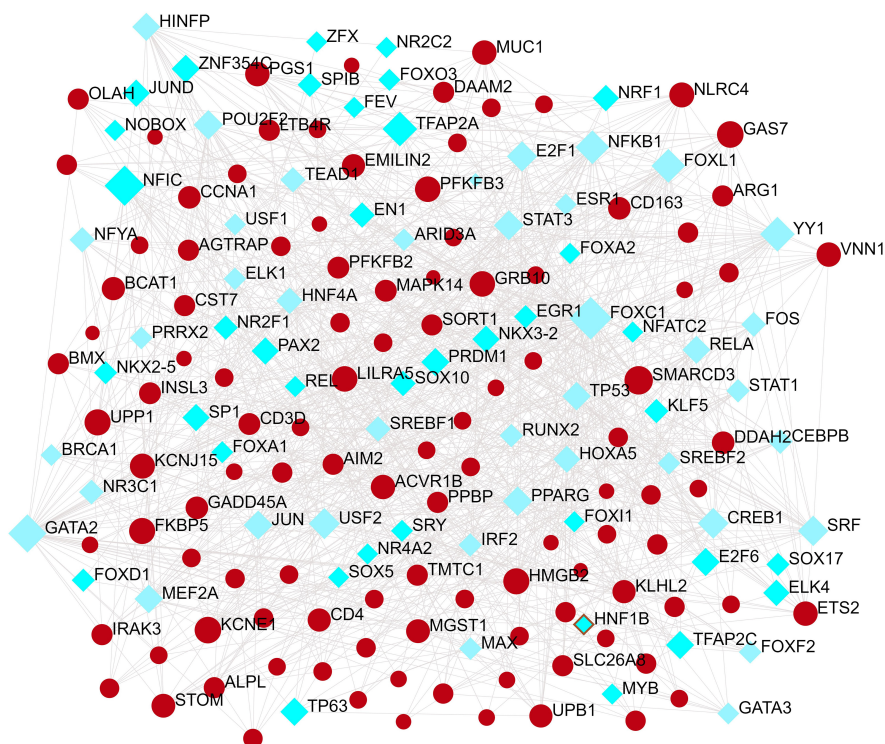


FIGURE 5

The Network Analyst created an interconnected regulatory interaction network of DEG-TFs. In it, blue square nodes represent TFs, gene symbols interact with TFs as yellow circle nodes.

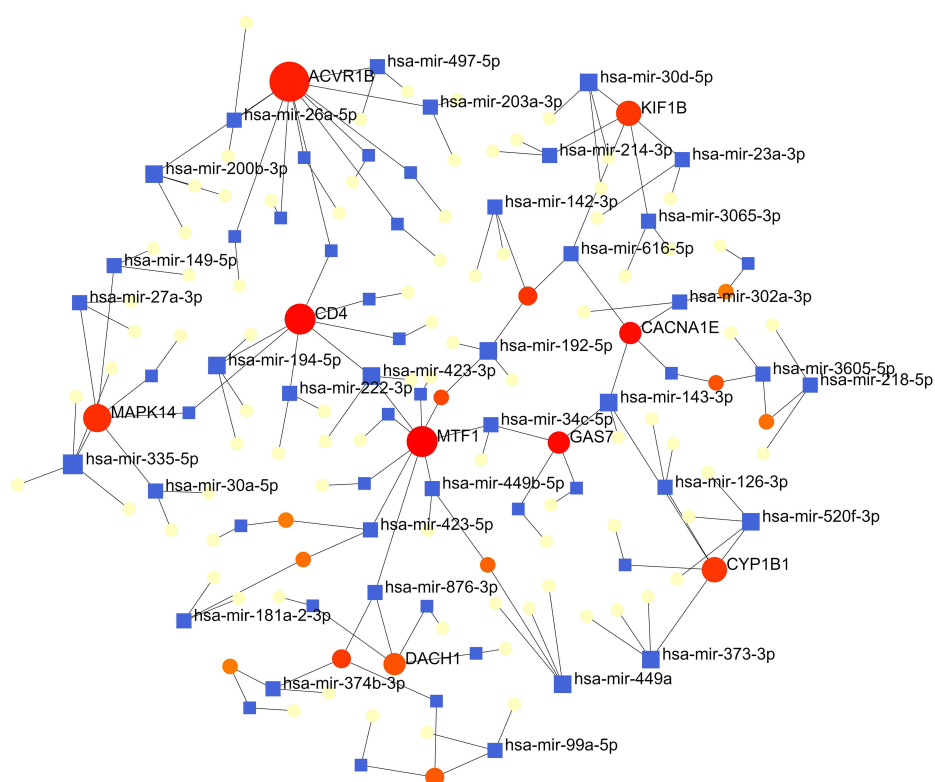
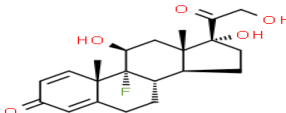
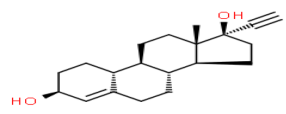
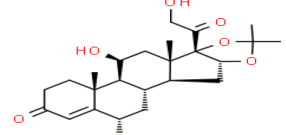
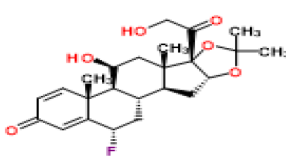
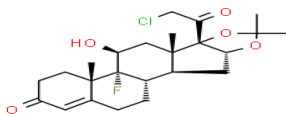
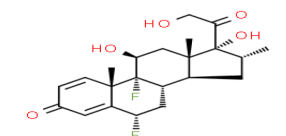
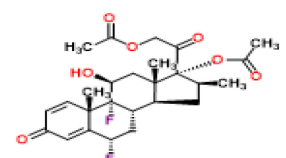
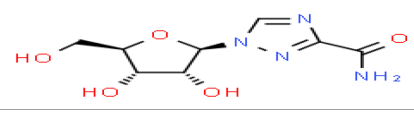
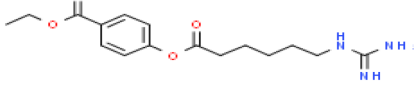
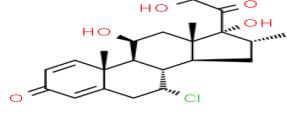


FIGURE 6

The interconnected regulatory interaction network of DEGs-miRNAs. blue squares represented miRNA s, while red circles represented DEGs.

TABLE 4 List of the suggested drugs for COVID-19.

Term	P-value	Chemical Formula	Structure
isoflupredone HL60 UP	2.76E-11	C <sub>21</sub> H <sub>27</sub> FO <sub>5</sub>	
etynodiol HL60 UP	6.10E-11	C <sub>20</sub> H <sub>28</sub> O <sub>2</sub>	
fludroxycortide HL60 UP	1.35E-10	C <sub>24</sub> H <sub>33</sub> FO <sub>6</sub>	
flunisolide HL60 UP	5.08E-09	C <sub>24</sub> H <sub>31</sub> FO <sub>6</sub>	
halcinonide HL60 UP	6.50E-09	C <sub>24</sub> H <sub>32</sub> ClFO <sub>5</sub>	
flumetasone HL60 UP	8.23E-09	C <sub>22</sub> H <sub>28</sub> F <sub>2</sub> O <sub>5</sub>	
diflorasone HL60 UP	1.03E-08	C <sub>26</sub> H <sub>32</sub> F <sub>2</sub> O <sub>7</sub>	
ribavirin HL60 UP	1.03E-08	C <sub>8</sub> H <sub>12</sub> N <sub>4</sub> O <sub>5</sub>	
gabexate HL60 UP	1.29E-08	C <sub>16</sub> H <sub>23</sub> N <sub>3</sub> O <sub>4</sub>	
alclometasone HL60 UP	2.86E-08	C <sub>22</sub> H <sub>29</sub> ClO <sub>5</sub>	

from the SARS-CoV-2-mediated dysregulation of STATs. Specifically, the dysfunctions of STAT1 and STAT3 induced by SARS-CoV-2 proteins may be the foundation of severe COVID-19 pathophysiology (31).

Our results also showed that the regulatory relationship between miRNAs (mir-335-5p, hsa-mir-26a-5p, hsa-mir-200b-3p, hsa-mir-194-5p, hsa-mir-192-5p, hsa-mir-143-3p and hsa-mir-520f-3p) and genes (ACVR1B, MTF1, CD4, MAPK14,

DACH1, KIF1B, GAS7 and CYP1B1) that may play important roles in COVID-19, ARDS and sepsis. It was worth noting that Huan Hu et al. predicted that mir-335-5p associated with different genes from COVID-19 (7). Laura Teodori et al. showed through bioinformatics analysis that miR-335-5p are regulated by Spike, ACE and histone deacetylation (HDAC) pathway (32). Upregulation of hsa-mir-26a-5p expression was significantly associated with inflammatory responses and

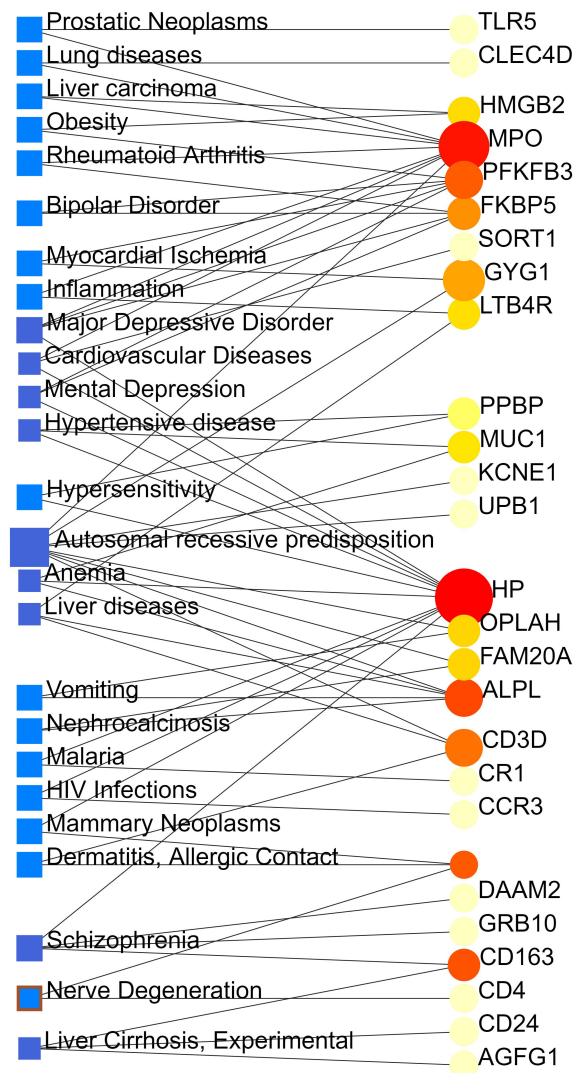


FIGURE 7

The gene-disease association network represents diseases associated with common DEGs. The disorders depicted by the square node and also its subsequent gene symbols are defined by the circular node.

cytokine - and chemokine-mediated signaling pathways in the sera of lactating mothers with type 1 diabetes (33).

We performed gene-disease (GD) analyses and predicted significant DEGs associations with different diseases. Diseases enriched by these DEGs include: major depressive disorder, mental depression, schizophrenia, cardiovascular diseases, hypertensive disease, anemia, liver diseases and liver cirrhosis. Recent studies have proven that people with mental illness, especially depression and schizophrenia, are at high risk of being infected by COVID-19 (34). According to the Clinical Bulletin of the American College of Cardiology (ACC), the mortality rate for patients with coexisting hypertension or cardiovascular disease COVID-19 was 6.0% and 10.5%, respectively (35). Besides, 16.7% of patients face arrhythmia, and 7.2% developed acute cardiac problems with COVID 19-associated complications (36). A study reported that 2–11% of COVID-19 patients had primary chronic liver disease (37). Of those diagnosed with COVID-19, about one-third of cirrhosis patients die within 10 days, and two-thirds of

cirrhosis patients died before admission to the intensive care unit (38).

The current crisis of the COVID-19 pandemic around the world has been devastating as many lives have been lost to the novel SARS CoV-2 virus. Thus, There are bioinformatics studies that aim to identify promising treatment options for COVID-19 through computational drug reuse. Alfred Olaoluwa Akinlalu's study predicted that ethynodiol diacetate exhibited better binding energy and pharmacokinetic properties than the off-Wlabel reference drugs (hydroxychloroquine, lopinavir and remdesivir) which has been currently investigated for the treatment of COVID-19 (39). Giuseppe Nunnari has highlighted Flunisolide, Thalidomide, Lenalidomide, Desoximetasone, xylazine, and salmeterol as potential drugs against SARS-CoV (40). Seyedeh Zahra Mousavi's research showed that HDAC inhibitors can be an effective drug against COVID-19 (41). The mechanism of action needs further investigation.



## Conclusions

We performed a functional analysis under ontology terms and pathway analysis and found some common associations among COVID-19, ARDS and sepsis. Transcription factors–genes interaction, protein–drug interactions, and DEGs–miRNAs coregulatory network with common DEGs also identified on the datasets. We believe that the candidate drugs obtained in this study may contribute to the effective treatment of COVID-19. So, our identified genes can be a novel therapeutic target for COVID-19 vaccine development.

## Data availability statement

Publicly available datasets were analyzed in this study. The data could be downloaded from the GEO database of the National Center for Biotechnology Information (NCBI) (<https://www.ncbi.nlm.nih.gov/geo/>), accession numbers GSE171110, GSE76293, and GSE137342.

## Author contributions

ZhiL conceived and designed the study. PL and TL provided equal contributions to research design, data analysis, and article writing. ZZ and XD helped to write the manuscript. All authors contributed to the article and approved the submitted version.

## References

1. Lu R, Zhao X, Li J, Niu P, Yang B, Wu H, et al. Genomic characterisation and epidemiology of 2019 novel coronavirus: implications for virus origins and receptor binding. *Lancet* (2020) 395(10224):565–74. doi: 10.1016/S0140-6736(20)30251-8
2. Finkel Y, Mizrahi O, Nachshon A, Weingarten-Gabbay S, Morgenstern D, Yahalom-Ronen Y, et al. The coding capacity of SARS-CoV-2. *Nature* (2021) 589(7840):125–30. doi: 10.1038/s41586-020-2739-1
3. Hu H, Tang N, Zhang F, Li L, Li L. Bioinformatics and system biology approach to identify the influences of COVID-19 on rheumatoid arthritis. *Front Immunol* (2022) 13:860676. doi: 10.3389/fimmu.2022.860676
4. Remy KE, Brakenridge SC, Francois B, Daix T, Deutschman CS, Monneret G, et al. Immunotherapies for COVID-19: lessons learned from sepsis. *Lancet Respir Med* (2020) 8(10):946–9. doi: 10.1016/S2213-2600(20)30217-4
5. Yao XH, Luo T, Shi Y, He ZC, Tang R, Zhang PP, et al. A cohort autopsy study defines COVID-19 systemic pathogenesis. *Cell Res* (2021) 31(8):836–46. doi: 10.1038/s41422-021-00523-8
6. Kocak TZ, Kayaaslan B, Mer M. COVID-19 and sepsis. *Turk J Med Sci* (2021) 51(SI-1):3301–11. doi: 10.3906/sag-2108-239
7. Shane AL, Sanchez PJ, Stoll BJ, sepsis. *Lancet* (2017) 390(10104):1770–80.
8. Chen AX, Simpson SQ, Pallin DJ, Med SGNE. (2019) . 380(14):1369–71.
9. Guo FM, Qiu HB. [Definition and diagnosis of sepsis 3.0]. *Zhonghua Nei Ke Za Zhi* (2016) 55(6):420–2. doi: 10.3760/cma.j.issn.
10. Singer M, Deutschman CS, Seymour CW, Shankar-Hari M, Annane D, et al. The third international consensus definitions for sepsis and septic shock (Sepsis-3). *JAMA* (2016) 315(8):801–10. doi: 10.1001/jama.2016.0287
11. Li W, Li D, Chen Y, Abudou H, Wang H, Cai J, et al. Classic signaling pathways in alveolar injury and repair involved in sepsis-induced ALI/ARDS: new research progress and prospect. *Dis Markers* 2022. (2022) p:6362344. doi: 10.1155/2022/6362344
12. . Gene Ontology Consortium. Gene Ontology Consortium: going forward. *Nucleic Acids Res* (2015) 43(Database issue):D1049–56. doi: 10.1093/nar/gku1179
13. Kanehisa M, Goto S. KEGG: kyoto encyclopedia of genes and genomes. *Nucleic Acids Res* (2000) 28(1):27–30. doi: 10.1093/nar/28.1.27
14. Caramori G, Casolari P, Adcock I. Role of transcription factors in the pathogenesis of asthma and COPD. *Cell Commun Adhes* (2013) 20(1-2):21–40. doi: 10.3109/15419061.2013.775257
15. Yoo M, Shin J, Kim J, Ryall KA, Lee K, Lee S, et al. DSigDB: drug signatures database for gene set analysis. *Bioinformatics* (2015) 31(18):3069–71. doi: 10.1093/bioinformatics/btv313
16. Zhou G, Soufan O, Ewald J, Hancock REW, Basu N, Xia J, et al. NetworkAnalyst 3.0: a visual analytics platform for comprehensive gene expression profiling and meta-analysis. *Nucleic Acids Res* (2019) 47(W1):W234–41. doi: 10.1093/nar/gkz240
17. Wiersinga WJ, Rhodes A, Cheng AC, Peacock SJ, Prescott HC. Pathophysiology, transmission, diagnosis, and treatment of coronavirus disease 2019 (COVID-19) A review. *JAMA* (2020) 324(8):782–93. doi: 10.1001/jama.2020.12839
18. Coperchini F, Chiovato L, Croce L, Magri F, Rotondi M. The cytokine storm in COVID-19: an overview of the involvement of the chemokine/chemokine-receptor system. *Cytokine Growth Factor Rev* (2020) 53:25–32. doi: 10.1016/j.cytogfr.2020.05.003
19. Vabret N, Britton GJ, Gruber C, Hegde S, Kim J, Kuksin M, et al. Immunology of COVID-19: current state of the science. *Immunity* (2020) 52(6):910–41. doi: 10.1016/j.immuni.2020.05.002
20. Muralidar S, Ambi SV, Sekaran S, Krishnan UM. The emergence of COVID-19 as a global pandemic: understanding the epidemiology, immune response and potential therapeutic targets of SARS-CoV-2. *Biochimie* (2020) 179:85–100. doi: 10.1016/j.biochi.2020.09.018
21. Root-Bernstein R. Innate receptor activation patterns involving TLR and NLR synergisms in COVID-19, ALI/ARDS and sepsis cytokine storms: a review and model

## Funding

This work was supported by the Natural Science Foundation of Hunan Province (No. 2022JJ40006) and the scientific research project of The First People's Hospital of Chenzhou (No. N2021-14). This work was also supported by the scientific research project of The First People's Hospital of Chenzhou (No.CZYY202207), the key research and development project of chenzhou (No.2020013), the Technology Research and Development Center of chenzhou (2021) and the Science and Technology Key Development Project of Chenzhou City (No. ZDYF2020012).

## Conflict of interest

The authors declare that the research was conducted in the absence of any commercial or financial relationships that could be construed as a potential conflict of interest.

## Publisher's note

All claims expressed in this article are solely those of the authors and do not necessarily represent those of their affiliated organizations, or those of the publisher, the editors and the reviewers. Any product that may be evaluated in this article, or claim that may be made by its manufacturer, is not guaranteed or endorsed by the publisher.



making novel predictions and therapeutic suggestions. *Int J Mol Sci* (2021) 22(4):2108. doi: 10.3390/ijms22042108

22. Ye Q, Wang B, Mao J. The pathogenesis and treatment of the 'Cytokine storm' in COVID-19. *J Infect* (2020) 80(6):607–13. doi: 10.1016/j.jinf.2020.03.037

23. Burrack KS, Tan JJ, McCarthy MK, Her Z, Berger JN, Ng LF, et al. Myeloid cell Arg1 inhibits control of arthritogenic alphavirus infection by suppressing antiviral T cells. *PLoS Pathog* (2015) 11(10):e1005191. doi: 10.1371/journal.ppat.1005191

24. Dhanalakshmi M, Das K, Pandya M, Shah S, Gadnaya A, Dave S, et al. Artificial neural network-based study predicts GS-441524 as a potential inhibitor of SARS-CoV-2 activator protein furin: a polypharmacology approach. *Appl Biochem Biotechnol* (2022) 194(10):4511–29. doi: 10.1007/s12010-022-03928-2

25. Tang D, Comish P, Kang R. The hallmarks of COVID-19 disease. *PLoS Pathog* (2020) 16(5):e1008536. doi: 10.1371/journal.ppat.1008536

26. Goud PT, Bai D, Abu-Soud HM. (2021) A multiple-hit hypothesis involving reactive oxygen species and myeloperoxidase explains clinical deterioration and fatality in Covid-19. *Int J Biol Sci* 17 (1):62–72. doi: 10.7150/ijbs.51811

27. Chakraborty C, Sharma AR, Bhattacharya M, Sharma G, Lee SS, Agoramoorthy G. Consider TLR5 for new therapeutic development against COVID-19. *J Med Virol* (2020) 92(11):2314–5. doi: 10.1002/jmv.25997

28. Ahmed FF, Reza MS, Sarker MS, Islam MS, Mosharaf MP, Hasan S, et al. Identification of host transcriptome-guided repurposable drugs for SARS-CoV-1 infections and their validation with SARS-CoV-2 infections by using the integrated bioinformatics approaches. *PLoS One* (2022) 17(4):e0266124. doi: 10.1371/journal.pone.0266124

29. Islam T, Rahman MR, Aydin B, Beklen H, Arga KY, Shahjahan M. Integrative transcriptomics analysis of lung epithelial cells and identification of repurposable drug candidates for COVID-19. *Eur J Pharmacol* (2020) 887:173594. doi: 10.1016/j.ejphar.2020.173594

30. Lu L, Liu LR, Gui R, Dong H, Su YR, Zhou XH, et al. Discovering common pathogenetic processes between COVID-19 and sepsis by bioinformatics and system biology approach. *Front Immunol* (2022) 13:975848. doi: 10.3389/fimmu.2022.975848

31. Teodori L, Sestili P, Madiati V, Coppari S, Fraternali D, Rocchi MBL, et al. MicroRNAs bioinformatics analyses identifying HDAC pathway as a putative target for existing anti-COVID-19 therapeutics. *Front Pharmacol* (2020) 11:582003. doi: 10.3389/fphar.2020.582003

32. Frorup C, Mirza AH, Yarani R, Nielsen LB, Mathiesen ER, Damm P, et al. Plasma exosome-enriched extracellular vesicles from lactating mothers with type 1 diabetes contain aberrant levels of miRNAs during the postpartum period. *Front Immunol* (2021) 12:744509. doi: 10.3389/fimmu.2021.744509

33. Mahmud SMH, Al-Mustanjid M, Akter F, Rahman MS, Ahmed K, Rahman MH, et al. Bioinformatics and system biology approach to identify the influences of SARS-CoV-2 infections to idiopathic pulmonary fibrosis and chronic obstructive pulmonary disease patients. *Brief Bioinform* (2021) 22(5):115. doi: 10.1093/bib/bbab115

34. Fang L, Karakiulakis G, Roth M. Are patients with hypertension and diabetes mellitus at increased risk for COVID-19 infection? *Lancet Respir Med* (2020) 8(4):e21. doi: 10.1016/S2213-2600(20)30116-8

35. Wang D, Hu B, Hu C, Zhu F, Liu X, Zhang J, et al. Clinical characteristics of 138 hospitalized patients with 2019 novel coronavirus-infected pneumonia in Wuhan, China. *JAMA* (2020) 323(11):1061–9. doi: 10.1001/jama.2020.1585

36. Jothimani D, Venugopal R, Abedin MF, Kaliamoorthy I, Rela M. COVID-19 and the liver. *J Hepatol* (2020) 73(5):1231–40. doi: 10.1016/j.jhep.2020.06.006

37. Sansoe G, Aragno M, Wong F. COVID-19 and liver cirrhosis: focus on the nonclassical renin-angiotensin system and implications for therapy. *Hepatology* (2021) 74(2):1074–80. doi: 10.1002/hep.31728

38. Akinlalu AO, Chamundi A, Yakumbur DT, Afolayan FID, Duru IA, Arowosegbe MA, et al. Repurposing FDA-approved drugs against multiple proteins of SARS-CoV-2: an in silico study. *Sci Afr* (2021) 13:e00845. doi: 10.1016/j.sciaf.2021.e00845

39. Nunnari G, Sanfilippo C, Castrogiovanni P, Imbesi R, Li Volti G, Barbagallo I, et al. Network perturbation analysis in human bronchial epithelial cells following SARS-CoV2 infection. *Exp Cell Res* (2020) 395(2):112204. doi: 10.1016/j.yexcr.2020.112204

40. Mousavi SZ, Rahmani M, Sami A. A connectivity map-based drug repurposing study and integrative analysis of transcriptomic profiling of SARS-CoV-2 infection. *Infect Genet Evol* (2020) 86:104610. doi: 10.1016/j.meegid.2020.104610

41. Matsuyama T, Kubli SP, Yoshinaga SK, Pfeffer K, Mak TW. An aberrant STAT pathway is central to COVID-19. *Cell Death Differ* (2020) 27(12):3209–25. doi: 10.1038/s41418-020-00633-7



## OPEN ACCESS

## EDITED BY

Alfonso J. Rodriguez-Morales,  
Fundacion Universitaria Autónoma de las  
Américas, Colombia

## REVIEWED BY

Armeen Poor,  
Metropolitan Hospital Center,  
United States  
Orlando Pérez-Nieto,  
Hospital General San Juan del Río,  
Mexico

## \*CORRESPONDENCE

Shiqing Liu,  
✉ liushiqing@csu.edu.cn

RECEIVED 28 January 2023

ACCEPTED 09 August 2023

PUBLISHED 24 August 2023

## CITATION

Chen X, Peng C, Xiao Y and Liu S (2023),  
Construction and application of prone  
position ventilation management scheme  
for severe COVID-19 patients.  
*Front. Physiol.* 14:1152723.  
doi: 10.3389/fphys.2023.1152723

## COPYRIGHT

© 2023 Chen, Peng, Xiao and Liu. This is  
an open-access article distributed under  
the terms of the [Creative Commons  
Attribution License \(CC BY\)](#). The use,  
distribution or reproduction in other  
forums is permitted, provided the original  
author(s) and the copyright owner(s) are  
credited and that the original publication  
in this journal is cited, in accordance with  
accepted academic practice. No use,  
distribution or reproduction is permitted  
which does not comply with these terms.

# Construction and application of prone position ventilation management scheme for severe COVID-19 patients

Xiuwen Chen<sup>1,2,3,4</sup>, Cao Peng<sup>1,5</sup>, Yao Xiao<sup>4</sup> and Shiqing Liu<sup>4,6,7\*</sup>

<sup>1</sup>Teaching and Research Section of Clinical Nursing, Xiangya Hospital, Central South University, Changsha, China, <sup>2</sup>Department of Operating Room, Xiangya Hospital, Central South University, Changsha, China, <sup>3</sup>Xiangya Nursing School, Central South University, Changsha, China, <sup>4</sup>National Clinical Research Center for Geriatric Disorders, Xiangya Hospital, Central South University, Changsha, China, <sup>5</sup>Department of Intensive Care Unit, Xiangya Hospital, Central South University, Changsha, China, <sup>6</sup>Department of Respiratory Medicine, Xiangya Hospital, Central South University, Changsha, China, <sup>7</sup>Xiangya Lung Cancer Center, Central South University, Changsha, China

**Background:** Prone position ventilation (PPV) can significantly improve oxygenation index and blood oxygen saturation in most (70%–80%) patients with acute respiratory distress syndrome. However, although PPV is not an invasive procedure, there are many potential PPV-related complications, such as nerve compression, crush injury, venous stasis (e.g., facial oedema), pressure sores, retinal damage, vomiting, and arrhythmia, with an incidence of up to 56.9%. Nursing managers have focused on reducing the occurrence of PPV-related complications and improving safety.

**Objective:** To construct a prone ventilation management scheme for patients with severe coronavirus disease 2019 (COVID-19) and analyse its application effect.

**Methods:** Based on a previous evidence-based study combined with the COVID-19 Diagnosis and Treatment Protocol (Trial Edition 9), a prone ventilation management protocol for severe COVID-19 was formulated and applied to COVID-19 patients in the intensive care unit of a designated hospital. A prospective self-control study was used to compare changes in the oxygenation index and other outcome indicators before and after the intervention.

**Results:** The oxygenation index of patients after intervention ( $321.22 \pm 19.77$  mmHg) was significantly higher ( $p < 0.05$ ) than before intervention ( $151.59 \pm 35.49$  mmHg). The difference in oxygenation index in different prone position ventilation durations was statistically significant ( $p < 0.05$ ). Nursing quality evaluation indicators showed that the implementation rate of gastric residual volume assessment was 100% and the incidence of occupational exposure and cross-infection was 0%; the incidences of pressure ulcers, drug extravasation, and facial oedema were 13.64% (3/22), 4.54% (1/22), and 4.54% (1/22), respectively. The incidence of unplanned extubation, aspiration, and falls/falls was 0%.

## KEYWORDS

prone position ventilation, oxygenation index, nursing quality, management, COVID-19

# 1 Introduction

Prone position ventilation (PPV), in which patients are mechanically ventilated from the prone position, was first developed in the 1970s as a way to improve the oxygenation method for acute respiratory distress syndrome (ARDS) (Petrone et al., 2021). Multiple randomised controlled studies have shown that prone ventilation can reduce the pleural pressure gradient of patients, restore ventilation in the dorsal segment of the lung, significantly improve the oxygenation index and blood oxygen saturation of patients, and reduce 28-day mortality (Munshi et al., 2017a; Douglas et al., 2021). Since the onset of the coronavirus disease 2019 (COVID-19), the outbreak has spread rapidly, leading to a global pandemic. In 2022, due to the characteristics of high infectivity, occultness, and fast transmission rate, the Omicron variant of the novel coronavirus circulating in Shanghai is widely susceptible to infection, especially in the older adults, who are prone to develop into severe and critical forms with high severity and fatality rates (Cai et al., 2022; Zhang et al., 2022). Sparing no effort to treat critically ill patients, improving the treatment rate, and reducing the case fatality rate has become important. Severe and critically ill patients should be treated in a standard prone position for no less than 12 h a day, according to the ninth version of the Diagnosis and Treatment Protocol for the novel coronavirus pneumonia. Therefore, standard and scientific PPV is the premise of ensuring the effectiveness of treatment and patient safety.

However, although PPV is not an invasive procedure, it is complex and has many potential complications. Several studies have shown that PPV can lead to complications such as stress injury, unplanned extubation, falls, aspiration, and arrhythmia, with an incidence as high as 56.9% (Malhotra and Kacmarek, 2020; Moore et al., 2020). In addition, Liu et al. (Liu et al., 2018) pointed out that the prone ventilation treatment rate of patients with severe ARDS in China was only 8.7%, and the high complication rate and low compliance were related to the lack of standardised surgical procedures. In recent years, clinical studies on PPV have mainly focused on the application effect of PPV in different populations and diseases and the analysis of its haemodynamic effect on patients (Huang et al., 2021; Lu et al., 2021). Nursing studies are mostly fragments of experience or summary, and there is still a lack of standard preventive measures and management plans for the whole process, not to say, related nursing guidelines or expert consensus to standardise the implementation of clinical PPV. Therefore, this study intended to develop management plans based on previous evidence-based PPV studies (Peng et al., 2021) and combined them with the characteristics of PPV in patients with severe novel coronavirus pneumonia to provide a basis and empirical reference for clinical nursing.

# 2 Methods

## 2.1 Construction of PPV management scheme for severe COVID-19

### 2.1.1 Build a research team

The research team consisted of 12 members, including seven senior titles, three intermediate titles, one junior title, and one

master's degree student. It consisted of three experts in prone ventilation medicine, three in critical care medicine, one respiratory therapist, one evidence-based nursing expert, one scientific research nurse, two clinical nurses, and one graduate student. Specialists, respiratory therapists, and research nurses were primarily responsible for the development of management plans. Clinical nurses are responsible for personnel training, quality control, and program implementation. The research nurse was responsible for the overall project progress control and liaison consultations. The graduate students were responsible for collecting clinical data and outcome indicators. The research team regularly organised group meetings to implement the project's progress, and the members worked closely with each other.

## 2.2 Develop a PPV management plan for severe COVID-19

This study was based on the previous PPV evidence-based research (Peng et al., 2021), combined with the Diagnosis and Treatment Protocol for Novel Coronavirus Pneumonia (Trial Ninth Edition). The management scheme of PPV was constructed from the aspects of standard operating flow, checklist, complication prevention, risk emergency plan, lung ultrasound-guided nursing flow and quality supervision, etc.

### 2.2.1 Standard operating procedures

- (1) Self-protection: Medical personnel should adopt protective measures in accordance with secondary protection standards.
- (2) Medical evaluation: Evaluation of indications, contraindications, and informed consent. Indications: Common, severe, and critically ill patients with high-risk factors for severe COVID-19 and rapid disease progression. Contraindications: cervical spine injury, unstable fracture, heart surgery/post-traumatic thoracotomy within 24 h after heart surgery, severe haemodynamic instability, increased intracranial pressure, pregnancy, etc. cannot tolerate the prone position. Prior to prone ventilation, authorised informed consent was required.
- (3) Nursing evaluation: Check the doctor's orders and evaluate the patient's vital signs, pipelines (arterial catheterisation, venous access, gastric tube, urinary tube, etc.), Richmond Agitation-Sedation Scale (RASS), gastric residual volume (suspension of enteral nutrient pumping, gastric residual volume), body weight, turning direction, and skin integrity.
- (4) Materials: Prepare the rescue truck, turning sheet, closed sputum suction tube, electrode, extension tube, soft pillow, and pressure-relief tape.
- (5) Personnel preparation: Every turn requires at least five teams of doctors, nurses, and respiratory therapists to work together, the role that team members introduce themselves and show, respiratory therapists, standing on the patient's head to be responsible for the overall coordination, and patients with both need to have at least two staff, according to the number of patients with weight gain.
- (6) Airway/respiration: The ventilator should be as close to the patient's side as possible. A difficult airway intubation cart (bag) and negative pressure suction were placed in the standby state, and the results of laryngoscopy and length of endotracheal intubation were checked again. Fixation or binding of tracheal

**TABLE 1 Checklist for prone position ventilation operations.**

Table 1 Checklist for prone position intubation operations															
Project	Content of verification												Results of verification	Signature	
1	Evaluate and check doctor's orders														
2	Materials: 3 soft pillows, 1 silicone pillow, 2 nursing pads, 1 medium sheet, 1 set of closed sputum suction tubes, 5 ECG electrodes, 3 cotton pads, intubation cart (bag) and rescue cart														
3	Patient preparation: intravenous access, ECG monitoring, indwelling gastric tube and urinary tube, an indwelling catheter for measuring pressure, ensure that all tubes are long enough and properly fixed														
4	Check catheter position, stop nasal feeding, evacuate gastric residual, determine turning direction, administer pure oxygen, record ventilator parameters														
5	Team members take the position, release the electrodes, cuff, and gown, move the patient to the edge of the bed (proximal side), extend the distal arm naturally, and press it under the ipsilateral hip														
6	Place a soft pillow on the abdomen and chest, cover the chest of the patient with a medium sheet, wrap the distal arm, and press them together under the patient														
7	Put the patient in the lateral decubitus position, pull the medium sheet edge under the distal hand horizontally, and another team member pulls the proximal side medium sheet edge to turn the patient over and move the patient to the centre. The member standing on the head protects the patient's cervical vertebra and maintains the pipeline unobstructed, and connects the ECG monitoring														
8	Maintain the patient's upper body breaststroke position with the right hand slightly raised and the right leg slightly bent to promote comfort and protect the skin														
9	Adjust the bed to head high and feet low, clean up the secretions from the mouth and nose, arrange the pipes, and properly fix it														
10	Arrange the bed unit, record the vital signs and adjust the parameters of the ventilator														
11	Assist the patient to turn his face to the opposite side every 2 h, change the position of hands and feet at the same time, suction sputum as needed, slow nasal feeding, and close observation														
	Direction	R	L	R	L	R	L	R	L	R	L	R			L
	Time														
	Signature														
12	At the end of the prone position, arrange all the pipes, remove the electrodes, take off the hospital gown, remove all pillows under the patient, and place both hands and feet on the floor until completely supine														
13	The person standing at the head fixed the breathing line and endotracheal tube and maintained the functional position of each line to prevent slip. The team members moved the patient to face the side of the bed, put the far arm under the patient, held the opposite medium sheet, supported the shoulder and hip, and synchronously turned the patient back to a supine position														
14	Intimate electrodes put on a gown, record vital signs														
15	Clean up the secretions from the mouth and nose, arrange the pipes and fix them properly														
Note															

tubes; Oxygenate the patient with 100% oxygen; monitor tidal volume and inspiratory pressure; perform an arterial blood gas test, and record the results.

- (7) Supine position to prone position: Start a timeout. Timeout refers to a pause before surgery. Perform a procedural check before the official turn to ensure that the team members are ready; try to stay away from the patient's airway to reduce the risk of occupational exposure; loosen the cover, spread the rollover sheet, stick the decompression tape, prepare the head soft pillow; remove electrode sheet; fold the patient's arm under the buttocks, palm facing forward, turn over the single wrap; turn over to the other side and stick the electrode sheet; the patient was turned over on the anteroposterior side with a single turn; head ring pad or face pad decompression, so that the patient's arm in a swimming position, shoulder abduction 80°, elbow bending 90°; tidy the bed unit, cushion soft pillow, pay attention to

privacy and heat preservation; keep head high and foot low, the head height of 30°; The length of prone position was recorded and each shift was handed over to continue treatment and nursing. The entire turning process was gentle, avoided large movements, and reduced the risk of aerosol transmission.

- (8) Prone to supine position: Adjust the bed to a horizontal position, undress, and check the length of the catheter. Remove soft pillows. Turn to your side with your arms in front of you and wrap the rollover sheet. Subsequently, the electrode sheet was removed. An electrode sheet was attached to one side of the electrode. The patient returned to the supine position with a roll sheet. Clear respiratory tract, tidy bed unit, and record.

### 2.2.2 Operation check sheet

A checklist for prone ventilation operations was developed and implemented as shown in [Table 1](#).

TABLE 2 Summary of evidence on the prevention of complications related to prone position ventilation.

Complications	Content of evidence	Recommended level
Stress-induced injury	It is recommended to evaluate the risk of stress-induced injury before prone position ventilation (Moore et al., 2020)	A
	Regularly assess high-risk areas in the prone position, including cheeks, auricle, clavicle, chest, breast, pubic symphysis, iliac crest, male genitalia, knees and toes. To assess changes in skin and tissue integrity, colour, temperature, hardness and humidity, and to assess the grading of pressed red or damaged skin (Malhotra and Kacmarek, 2020; Peng et al., 2021)	A
	It is recommended to prophylactically apply transparent film dressing, foam dressing, hydrocolloid dressing, etc., in high-risk or key compression parts (Malhotra and Kacmarek, 2020; Peng et al., 2021)	A
Unplanned extubation	A special person is responsible for tube management during a position change. For patients who receive extracorporeal membrane oxygenation (ECMO) treatment, it is recommended that an additional person be assigned to manage the ECMO tube during the process of turning over (Intensive Care Society and Faculty of Intensive Care Medicine, 2019)	B
	Ensure that all conduits are reserved for adequate length, and use extension tubing if necessary (Tissue Viability Society, 2020)	A
	It is suggested to have double fixation of the tube and reasonably restrain the patient (Intensive Care Society and Faculty of Intensive Care Medicine, 2019)	B
Oedema of the face	The head direction should be changed every 2 h, the head ring pad or facial pad should be used for decompression, and the protective pad with adsorption function should be placed under the head to reduce the stimulation of oral or nasal secretions on the skin (Intensive Care Society and Faculty of Intensive Care Medicine, 2019; Tissue Viability Society, 2020)	A
	The patient's eyes are closed and protected with gauze or film to ensure that the eyelashes face outward to avoid direct eye pressure (Intensive Care Society and Faculty of Intensive Care Medicine, 2019)	A
	In the prone position, the head is high and the feet are low, and the head of the bed is kept at 30° to reduce head and face oedema (Intensive Care Society and Faculty of Intensive Care Medicine, 2019)	A
Aspiration	Before the position change, the enteral nutrient solution pumping was suspended, and the gastric residual volume was evacuated (Intensive Care Society and Faculty of Intensive Care Medicine, 2019)	A
	It is recommended to evaluate gastric residual volume in each class (Intensive Care Society and Faculty of Intensive Care Medicine, 2019)	B

### 2.2.3 Complication prevention and risk emergency plan

According to the 6s model (Xie et al., 2021) of evidence-based resources from the top down to the principle of computer retrieval PPV-associated complication prevention guidelines, system evaluation, project, etc., evidence extraction prevents stress damage (Malhotra and Kacmarek, 2020; Moore et al., 2020; Peng et al., 2021), planned extubation (Intensive Care Society and Faculty of Intensive Care Medicine, 2019; Tissue Viability Society, 2020), and facial oedema (Intensive Care Society and Faculty of Intensive Care Medicine, 2019; Tissue Viability Society, 2020), evidence of common complications such as aspiration (Intensive Care Society and Faculty of Intensive Care Medicine, 2019) (Table 2), and the brainstorming method is used to formulate the corresponding risk contingency plans. Meanwhile, according to the characteristics of the transmission of the novel coronavirus, an occupational exposure disposal system and procedures for medical staff in the isolation ward of the novel coronavirus were formulated.

### 2.2.4 Nursing process guided by lung ultrasound

Lung re-expansion in the gravity-dependent area was evaluated using severe ultrasound to guide the treatment time and frequency of prone ventilation. At the same time, the effectiveness of prone ventilation was predicted by the semi-quantitative lung ultrasound score, and *in vitro* treatment, turning over, back-patting, and mechanical sputum drainage were also guided. In addition, prone ventilation often requires deep sedation or muscle relaxation therapy, which may affect circulation. In this study, the team

used ultrasound to evaluate and monitor the haemodynamics of patients and selected the appropriate cardiac output for patients, thus playing a role in protecting pulmonary circulation.

### 2.2.5 Quality supervision

The Donabedian structure-process outcome model was adopted as the theoretical framework, and two rounds of the Delphi method of expert correspondence consultation were used to determine the evaluation indices of prone ventilation nursing quality in patients with severe novel coronavirus pneumonia. Quality supervision was carried out on the entire prone ventilation process of patients with severe novel coronavirus pneumonia from three dimensions: structure, process, and result.

## 3 Clinical application of prone ventilation management scheme in patients with severe novel coronavirus pneumonia

### 3.1 Sample

In April 2022, under the deployment of the National Health Commission and Shanghai Municipal Health Commission, the third batch of medical teams from Hunan Province took over the medical treatment, nursing, infection prevention, and control work of the intensive care unit (ICU) of a designated hospital for treating



COVID-19 in Shanghai. This study included patients with severe novel coronavirus pneumonia who were admitted to the ICU as the research object. Inclusion criteria were as follows: 1) age >18 years; 2) any of the following: ① shortness of breath, RR  $\geq 30$  times/min; ② in the resting state, the oxygen saturation <93%; ③ partial pressure of oxygen (PaO<sub>2</sub>)/concentration of oxygen (FiO<sub>2</sub>)  $\leq 300$  mmHg (1 mmHg = 0.133 kPa); ④ progressive aggravation of clinical symptoms, lung imaging shows an obvious progression of the lesion >50% within 24–48 h; 3) the time of prone position ventilation being intubated  $\geq 12$  h; 4) patients or family members signed informed consent. The sample size was calculated using the method of estimating the sample size of the paired design,  $n = [(\alpha + \beta)\sigma d/\delta]^2$ , where  $\delta$  is the required differentiation,  $\sigma d$  is the population standard deviation of each pair difference. Referring to the previous study (Douglas et al., 2021), where the oxygenation index  $\sigma d$  was 147 and  $\delta$  was 107, the sample size was calculated to be 16, and a 10% loss of follow-up was considered. Therefore, the required sample size was 19.

## 3.2 Research methods

A prospective self before and after the control study was used to manage the subjects meeting the inclusion criteria strictly in accordance with the prone position ventilation management scheme for severe novel coronavirus pneumonia, and the changes in various outcome indicators before and after intervention were compared to evaluate the effect. To ensure the homogeneity of intervention quality, all members of the medical team were trained by two specialist nurses in the form of Tencent conferences, face-to-face meetings, and operation demonstrations. The training content covers management schemes such as the standard operating flow of prone ventilation, checklist, complication prevention, risk emergency plan, lung ultrasound-guided nursing flow, and quality supervision. Nursing personnel could only participate in the study after they passed the assessment.

## 3.3 Effect evaluation index and data collection method

The oxygenation index, also known as the ventilation/perfusion index, was calculated as arterial oxygen partial pressure (PaO<sub>2</sub>)/oxygen absorption concentration (FiO<sub>2</sub>)  $\times 100\%$ . In this study, the oxygenation index of patients was obtained by blood gas extraction before prone position ventilation, 8, 12, and 16 h after treatment to evaluate the changes in oxygenation before and after prone position ventilation. At the same time, the incidence of occupational exposure, incidence of cross-infection, execution rate of gastric residual volume assessment, incidence of stress injury, incidence of unplanned extubation, incidence of facial oedema, aspiration, drug exosmosis, and fall/fall incidence were analysed.

## 3.4 Statistical methods

SPSS 22.0 software was used for data entry and statistical analysis. The measurement data were described by mean  $\pm$  SD

and analysed using the t-test or variance analysis. The data were described by frequency and percentage and analysed statistically by chi-square test, Fisher's exact probability test, or rank sum test. Statistical inference was performed according to a test level of  $\alpha = 0.05$ . The  $p$ -value was a bilateral probability value, and  $p < 0.05$  meant that the difference was statistically significant.

# 4 Results

## 4.1 General data analysis

A total of 22 severely ill patients with prone ventilation were included, including nine males and 13 females. There were 2 cases of the normal type, 15 cases of the severe type, and 5 cases of the critical type. The patients were aged between 68 and 96 ( $85.82 \pm 8.20$ ) years, and the RASS score before prone ventilation was  $-5$  to  $-3$  ( $-4.41 \pm 0.59$ ) points. Acute physiology and chronic health evaluation II (APACHE II) was 13–23 ( $19.05 \pm 2.34$ ) minutes, the total duration of prone ventilation was 19.00–52.00 ( $34.14 \pm 8.22$ ) h, an average of 12.67–22.00 ( $16.83 \pm 2.46$ ) h per day. In addition to the novel coronavirus pneumonia, admission diagnosis also included hypertension, diabetes, coronary heart disease, sequelae of cerebral infarction, cirrhosis, epilepsy, sequelae of intracerebral haemorrhage, intracerebral haemorrhage in the basal ganglia area breaking into the ventricle, and renal failure (Supplementary Table S1).

## 4.2 Trend of oxygenation index before and after prone ventilation treatment

The oxygenation index of patients with severe novel coronavirus pneumonia after intervention with the prone ventilation management scheme ( $321.22 \pm 19.77$  mmHg) was significantly higher than that before intervention ( $151.59 \pm 35.49$  mmHg), and the difference was statistically significant ( $p < 0.05$ ). A comparison of the oxygenation index of ventilation duration in different prone positions is shown in Table 3, and the results show that with an increase in ventilation duration in the prone position, the oxygenation index of patients showed a significant linear growth trend ( $p < 0.05$ ).

## 4.3 Analysis of nursing quality evaluation index

Twenty-two patients were turned from the supine to the prone position 45 times. The implementation rate of the gastric residual volume assessment before position conversion was 100%. The incidence of occupational exposure and cross-infection during the operation for position conversion was 0%. The incidence rates of ventilation-related complications in the prone position were 13.64% (3/22) for pressure injury, 4.54% (1/22) for drug exosmosis, 4.54% (1/22) for facial oedema, and 0% for unplanned extubation, aspiration, and fall/fall.

TABLE 3 Trend of oxygenation index before and after prone position ventilation (PPV) treatment (n = 22).

	Before PPV treatment	PPV treatment for 8 h	PPV treatment for 12 h	PPV treatment for 16 h	After PPV treatment	F	P
Oxygenation index (mmHg)	151.59 ± 35.49	203.72 ± 38.65	264.95 ± 34.13	315.31 ± 21.05	321.22 ± 19.77	206.707	0.000

## 5 Discussion

### 5.1 The oxygenation index of patients with severe novel coronavirus pneumonia varies with the time of prone position

The lungs of patients with severe novel coronavirus pneumonia mainly exhibit bilateral diffuse alveolar injury with fibrous mucinous exudation. Patients with ARDS experience hypoxia, which can lead to multiple organ dysfunction and even death. Therefore, reducing hypoxia is a key factor in the treatment of COVID-19 patients. Several multi-centre, prospective, randomised controlled studies (Guérin et al., 2013; Munshi et al., 2017b) have shown that prone ventilation can not only improve the oxygenation of patients but also significantly reduce the mortality of 28 and 90 days for patients with severe ARDS by extending prone ventilation at an early stage. In this study, prone ventilation was used as the main measure to “advance the threshold” in the treatment of severe novel coronavirus pneumonia. The early intervention significantly improved the oxygenation index of patients with severe novel coronavirus pneumonia, and the average oxygenation index was greater than 300 mmHg, which was highly recognised by experts in the medical treatment group of the Joint Prevention and Control Mechanism of The State Council. It was also introduced and promoted in the training sessions of designated and makeshift hospitals in Shanghai, which confirmed the importance of prone ventilation in the treatment of novel coronavirus pneumonia. In addition, the results of this study showed that there were significant differences in the oxygenation index of patients with severe novel coronavirus pneumonia with different prone position ventilation durations, and with the increase in prone position ventilation duration, the oxygenation index of patients showed a significant linear growth trend. Therefore, it is important to standardise and implement the length of the prone position in the treatment of prone ventilation. It is recommended that all designated hospitals strictly comply with the Diagnosis and Treatment Protocol for Novel Coronavirus Pneumonia (Trial Version 9) and ensure that the prone position is treated for at least 12 h per day. The 2019 International Guidelines Official Guidelines: Management of Acute Respiratory Distress Syndrome (Papazian et al., 2019) strongly recommends that ARDS patients with an oxygenation index less than 150 mmHg should continue prone ventilation for at least 16 h. In this study, the average duration of prone ventilation for patients with severe novel coronavirus pneumonia was 16.83 h per day. This also indicates that the implementation of the management scheme in this study improves compliance with prone ventilation therapy to a certain extent.

### 5.2 The prone position ventilation management scheme for severe novel coronavirus pneumonia can standardise the implementation of clinical PPV

This study, according to the results of prone position ventilation in patients with gastric residual position prior to the conversion of quantitative evaluation are enforced is 100%. The incidence of complications related to aspiration-prone position ventilation was 0%, suggesting that the correct nursing assessment is the precondition for the implementation of prone position ventilation, evaluation, and risk assessment in addition to skin prone position ventilation duct outside the risk assessment which still needs to focus on assessing gastric residual volume and reducing the incidence of complications, such as aspiration. Because of the new coronavirus infectious pneumonia, we have put the severe new coronavirus pneumonia nursing quality evaluation index in prone position ventilation and invited fixed-point hospital joint experts to write to the circuit court sense of experts. This has increased the incidence of occupational exposure and cross-infection incidence of outcome indicators, and the results showed that the incidence was 0%, suggesting that the implementation of this program has strengthened the implementation of infection prevention and control measures. Second, according to the results of prone position ventilation duct complications related to the highest stress injury, has to do with Moore (Moore et al., 2020), such as the results are consistent, analyse the causes, and possible thinning and senile patients with skin and associated with basic diseases such as diabetes; further prompt medical personnel need to be strengthened in the prone position treatment in patients with skin protection. It is recommended to use the Braden stress injury risk scale for daily assessment, and formulate corresponding nursing measures according to the assessment results. The Omicron variant of the novel coronavirus circulating in Shanghai is highly contagious, and most severe novel coronavirus pneumonia cases occur in older adults patients. The average age of severe patients included in this study was 85.82 years, and most of them were complicated with basic diseases such as hypertension, diabetes, coronary heart disease, and cerebral infarction, most of whom were physically disabled, which brought great challenges to treatment and nursing. But this study through the formulation and application of severe new coronavirus pneumonia patients prone position ventilation management scheme, to the largest extent, reduces the prone position ventilation related nursing security incidents, visible, severe new coronavirus pneumonia patients prone position ventilation management consultation can standardise the prone position ventilation operation process, operation checklist and nursing quality evaluation index. It is beneficial to improve nursing quality and promote patient safety.

## Conclusion

This study was based on previous evidence-based research, combining the Chinese diagnosis and treatment plan for COVID-19 (Trial Version 9), from the prone position ventilation operation flow, operation checklist, complications, risk prevention, emergency plan, lung ultrasound guidance of nursing process, and quality supervision critical aspects such as building a new coronavirus pneumonia prone position ventilation management solution. The application of this scheme can standardise and promote the implementation of PPV for severe novel coronavirus pneumonia, improve the quality of care, and improve the prognosis of patients. The evaluation index of nursing quality can facilitate a more objective and comprehensive clinical evaluation of the nursing quality of prone position ventilation for severe novel coronavirus pneumonia, and achieve continuous quality improvement. However, this study has the following limitations: 1) small sample size; 2) given ethical reasons, no control group was set up; only before and after the study subjects themselves were compared. Because the severity of the disease is not completely consistent in the comparison, it is difficult to ensure consistency of the starting points of the two stages, which may affect the comparability of the two stages. Therefore, the results of this study need to be further verified.

## Data availability statement

The original contributions presented in the study are included in the article/**Supplementary Material**, further inquiries can be directed to the corresponding author.

## Ethics statement

The studies involving human participants were reviewed and approved by the Human Ethics, Committee of Xiangya Hospital. The patients/participants provided their written informed consent to participate in this study.

## Author contributions

XC conceptualised and designed the study, carried out the analyses, interpreted the data, drafted the initial manuscript, and

approved the final manuscript to be submitted; YX and SL contributed to the project design, assisted in the interpretation of the results, revised the manuscript, and approved the final manuscript to be submitted; CP participated in data collection and the interpretation of the results, and approved the final manuscript to be submitted; All authors contributed to the article and approved the submitted version.

## Funding

This work was supported by the Scientific Research Project of the Chinese Nursing Association (ZHKYQ202107), the Project Program of the National Clinical Research Center for Geriatric Disorders (2022LNJJ19), National Multidisciplinary Cooperative Diagnosis and Treatment Capacity Building Project for Major Diseases (z027002) and Xiangya clinical big data project of Central South University (Clinical big data project of lung cancer).

## Conflict of interest

The authors declare that the research was conducted in the absence of any commercial or financial relationships that could be construed as a potential conflict of interest.

## Publisher's note

All claims expressed in this article are solely those of the authors and do not necessarily represent those of their affiliated organizations, or those of the publisher, the editors and the reviewers. Any product that may be evaluated in this article, or claim that may be made by its manufacturer, is not guaranteed or endorsed by the publisher.

## Supplementary material

The Supplementary Material for this article can be found online at: <https://www.frontiersin.org/articles/10.3389/fphys.2023.1152723/full#supplementary-material>

## References

- Cai, J., Deng, X., Yang, J., Sun, K., Liu, H., Chen, Z., et al. (2022). Modeling transmission of SARS-CoV-2 omicron in China. *Nat. Med.* 28 (7), 1468–1475. doi:10.1038/s41591-022-01855-7
- Douglas, I. S., Rosenthal, C. A., Swanson, D. D., Hiller, T., Oakes, J., Bach, J., et al. (2021). Safety and outcomes of prolonged usual care prone position mechanical ventilation to treat acute coronavirus disease 2019 hypoxemic respiratory failure. *Crit. Care Med.* 49 (3), 490–502. doi:10.1097/CCM.0000000000004818
- Guérin, C., Reigner, J., Richard, J. C., Beuret, P., Gacouin, A., Boulain, T., et al. (2013). Prone positioning in severe acute respiratory distress syndrome. *N. Engl. J. Med.* 368 (23), 2159–2168. doi:10.1056/NEJMoa1214103
- Huang, C. Y., Tsai, Y. L., and Lin, C. K. (2021). The prone position ventilation (PPV) as an approach in pregnancy with acute respiratory distress syndrome (ARDS). *Taiwan J. Obstet. Gynecol.* 60 (3), 574–576. doi:10.1016/j.tjog.2021.03.036
- Intensive Care Society and Faculty of Intensive Care Medicine (2019). *Prone positioning in adult critical care*. Available at: [https://www.ficm.ac.uk/sites/default/files/prone\\_position\\_in\\_adult\\_critical\\_care\\_2019.pdf](https://www.ficm.ac.uk/sites/default/files/prone_position_in_adult_critical_care_2019.pdf).
- Liu, L., Yang, Y., Gao, Z., Li, M., Mu, X., Ma, X., et al. (2018). Practice of diagnosis and management of acute respiratory distress syndrome in mainland China: A cross-sectional study. *J. Thorac. Dis.* 10 (9), 5394–5404. doi:10.21037/jtd.2018.08.137
- Lu, H., Zhang, P., Liu, X., Jin, L., and Zhu, H. (2021). Effect of prone position ventilation on right heart function in patients with acute respiratory distress syndrome. *Clin. Respir. J.* 15 (11), 1229–1238. doi:10.1111/crj.13431
- Malhotra, A., and Kacmarek, R. M. (2020). *Prone ventilation for adult patients with acute respiratory distress syndrome [EB/OL]*. [2022-11-18]. Available at: <http://222.247.54.203:1057/contents/prone-ventilation-for-adult-patients-with-acute-respiratory-distress-syndrome?search=pressure%20sores%20and%20prone%20ventilation&source=Out%20of%20date%20-%20zh-Hans&selectedTitle=1~150>.

- Moore, Z., Patton, D., Avsar, P., McEvoy, N. L., Curley, G., Budri, A., et al. (2020). Prevention of pressure ulcers among individuals cared for in the prone position: lessons for the COVID-19 emergency. *J. Wound Care* 29 (6), 312–320. doi:10.12968/jowc.2020.29.6.312
- Munshi, L., Del, S. L., Adhikari, N., Hodgson, C. L., Wunsch, H., Meade, M. O., et al. (2017a). Prone position for acute respiratory distress syndrome. A systematic review and meta-analysis. *Ann. Am. Thorac. Soc.* 14 (4), S280–S288. doi:10.1513/AnnalsATS.201704-343OT
- Munshi, L., Del Sorbo, L., Adhikari, N. K. J., Hodgson, C. L., Wunsch, H., Meade, M. O., et al. (2017b). Prone position for acute respiratory distress syndrome. A systematic review and meta-analysis. *Ann. Am. Thorac. Soc.* 14 (4), S280–S288. doi:10.1513/AnnalsATS.201704-343OT
- Papazian, L., Aubron, C., and Brochard, L. (2019). Formal guidelines: management of acute respiratory distress syndrome[J]. *Ann. Intensive Care* 9 (1), 1–18. doi:10.1186/s13613-019-0540-9
- Peng, C., Chen, X., and Ren, H. (2021). Evidence summary for prevention of pressure ulcer in patients with prone position ventilation[J]. *Chin. J. Nurs. Educ.* 18 (10), 935–941.
- Petrone, P., Brathwaite, C., and Joseph, D. K. (2021). Prone ventilation as treatment of acute respiratory distress syndrome related to COVID-19. *Eur. J. Trauma Emerg. Surg.* 47 (4), 1017–1022. doi:10.1007/s00068-020-01542-7
- Tissue Viability Society (2020). *Pressure ulcer prevention guidance when nursing patients in the prone position*. Available at: <https://tvs.org.uk/wp-content/uploads/2020/05/Pressure-ulcer-prevention-guidance-when-proning-patients-V5-17th-April-2020-1.pdf>.
- Xie, H. F., Feng, M., Cao, S. M., Jia, Y. Y., Gao, P., and Wang, S. H. (2021). Evidence summary for nonsurgical prevention and management of parastomal hernia in patients with enterostomy. *Am. J. Transl. Res.* 13 (11), 13173–13182.
- Zhang, X., Zhang, W., and Chen, S. (2022). Shanghai's life-saving efforts against the current omicron wave of the COVID-19 pandemic. *Lancet* 399 (10340), 2011–2012. doi:10.1016/S0140-6736(22)00838-8



## OPEN ACCESS

## EDITED BY

Alfonso J. Rodriguez-Morales,  
Fundacion Universitaria Autónoma  
de las Américas, Colombia

## REVIEWED BY

İlhami Çelik,  
University of Health Sciences, Türkiye  
Maja Cupic,  
University of Belgrade, Serbia

## \*CORRESPONDENCE

Kon Ken Wong  
✉ wkk@ppukm.ukm.edu.my

<sup>†</sup>These authors have contributed  
equally to this work and share  
first authorship

RECEIVED 16 November 2022

ACCEPTED 28 July 2023

PUBLISHED 28 August 2023

## CITATION

Liew MNY, Kua KP, Lee SWH and Wong KK  
(2023) SARS-CoV-2 neutralizing antibody  
bebtelovimab – a systematic scoping  
review and meta-analysis.  
*Front. Immunol.* 14:1100263.  
doi: 10.3389/fimmu.2023.1100263

## COPYRIGHT

© 2023 Liew, Kua, Lee and Wong. This is an  
open-access article distributed under the  
terms of the [Creative Commons Attribution  
License \(CC BY\)](#). The use, distribution or  
reproduction in other forums is permitted,  
provided the original author(s) and the  
copyright owner(s) are credited and that  
the original publication in this journal is  
cited, in accordance with accepted  
academic practice. No use, distribution or  
reproduction is permitted which does not  
comply with these terms.

# SARS-CoV-2 neutralizing antibody bebtelovimab – a systematic scoping review and meta-analysis

Mabel Nyit Yi Liew<sup>1†</sup>, Kok Pim Kua<sup>1†</sup>, Shaun Wen Huey Lee<sup>2,3,4,5,6</sup>  
and Kon Ken Wong<sup>7\*</sup>

<sup>1</sup>Pharmacy Unit, Puchong Health Clinic, Petaling District Health Office, Ministry of Health Malaysia, Petaling, Selangor, Malaysia, <sup>2</sup>School of Pharmacy, Monash University, Subang Jaya, Selangor, Malaysia, <sup>3</sup>Health and Well-being Cluster, Monash University, Subang Jaya, Selangor, Malaysia, <sup>4</sup>Gerontechnology Laboratory, Monash University, Bandar Sunway, Selangor, Malaysia, <sup>5</sup>Faculty of Health and Medical Sciences, Taylor's University, Subang Jaya, Selangor, Malaysia, <sup>6</sup>Center for Global Health, Perelman School of Medicine, University of Pennsylvania, Philadelphia, PA, United States, <sup>7</sup>Department of Medical Microbiology & Immunology, Faculty of Medicine, Universiti Kebangsaan Malaysia, Kuala Lumpur, Malaysia

**Introduction:** The COVID-19 pandemic is a major global public health crisis. More than 2 years into the pandemic, effective therapeutic options remain limited due to rapid viral evolution. Stemming from the emergence of multiple variants, several monoclonal antibodies are no longer suitable for clinical use. This scoping review aimed to summarize the preclinical and clinical evidence for bebtelovimab in treating newly emerging SARS-CoV-2 variants.

**Methods:** We systematically searched five electronic databases (PubMed, CENTRAL, Embase, Global Health, and PsycINFO) from date of inception to September 30, 2022, for studies reporting on the effect of bebtelovimab in SARS-CoV-2 infection, using a combination of search terms around —bebtelovimab||, —LY-CoV1404||, —LY3853113||, and —coronavirus infection||. All citations were screened independently by two researchers. Data were extracted and thematically analyzed based on study design by adhering to the stipulated scoping review approaches.

**Results:** Thirty-nine studies were included, thirty-four non-clinical studies were narratively synthesized, and five clinical studies were meta-analyzed. The non-clinical studies revealed bebtelovimab not only potently neutralized wide-type SARS-CoV-2 and existing variants of concern such as B.1.1.7 (Alpha), B.1.351 (Beta), P.1 (Gamma), and B.1.617.2 (Delta), but also retained appreciable activity against Omicron lineages, including BA.2.75, BA.4, BA.4.6, and BA.5. Unlike other monoclonal antibodies, bebtelovimab was able to bind to epitope of the SARS-CoV-2 S protein by exploiting loop mobility or by minimizing side-chain interactions. Pooled analysis from clinical studies depicted that the rates of hospitalization, ICU admission, and death were similar between bebtelovimab



and other COVID-19 therapies. Bebtelovimab was associated with a low incidence of treatment-emergent adverse events.

**Conclusion:** Preclinical evidence suggests bebtelovimab be a potential treatment for COVID-19 amidst viral evolution. Bebtelovimab has comparable efficacy to other COVID-19 therapies without evident safety concerns.

#### KEYWORDS

bebtelovimab, monoclonal antibody, SARS-CoV-2, COVID-19, omicron, variant, neutralization, spike protein

## 1 Introduction

The COVID-19 pandemic is the most significant global public health crisis of this generation, resulting in a high estimated excess mortality rate across the globe (1). Older adults and individuals with multimorbidity are predominantly vulnerable to the severe clinical course of COVID-19, in-hospital complications, and death (2). While several vaccines have been proven to be highly effective in reducing the incidence of hospitalization and death attributed to numerous causative SARS-CoV-2 variants (3), there has been significant hesitancy among the population with vaccine uptake, thus hampering the attainment of vaccination coverage required for population immunity (4). Furthermore, given the increased risks of COVID-19 infection and severe disease associated with inactivated whole-virus vaccines (5), the widespread use in many countries worldwide, particularly in crowded low- and middle-income countries that bear potentially higher risks of emerging SARS-CoV-2 variants becoming the epicenter for further spread and health care crisis warrants the need of effective therapeutic interventions to prevent severe disease progression, hospitalization, and mortality.

A growing body of evidence shows that monoclonal antibody therapies significantly reduce the risk of hospitalization of COVID-19 when administered early (6). Monoclonal antibodies are the largest class of biologicals for use in clinical practice, comprising a myriad of structures, ranging from small fragments to intact, modified, or unmodified immunoglobulins, all of which possess an antigen-binding domain (7). The emergence and proliferation of SARS-CoV-2 variants have been demonstrated to impair the efficacy of monoclonal antibody therapies due to the occurrence of mutations in the antigenic supersite of N-terminal domain or the ACE2-binding site (receptor-binding motif) of SARS-CoV-2, both major binding targets of the neutralizing monoclonal antibodies (8). To date, five types of anti-SARS-CoV-2 antibody drugs have been developed, namely bebtelovimab, bamlanivimab plus etesevimab, casirivimab plus imdevimab, sotrovimab, and tixagevimab-cilgavimab (9).

Of note, circulating variants of concern in the communities affect the effectiveness of each anti-SARS-CoV-2 monoclonal antibody therapy. The emergence and proliferation of SARS-CoV-2 B.1.1.529 Omicron virus has rendered specific monoclonal antibodies ineffective due to a marked reduction in neutralizing

activity (10). A live virus focus reduction neutralization test depicts that combinations of monoclonal antibodies, including bamlanivimab plus etesevimab, casirivimab plus imdevimab, as well as tixagevimab-cilgavimab have neutralizing activity against early strain and the Alpha and Delta variants. Nonetheless, etesevimab plus bamlanivimab exhibits dramatically decreased activity against Gamma variant and exerts no inhibitory effect against Omicron and Beta variants. On the other hand, casirivimab plus imdevimab shows efficacy against Beta and Gamma variants, whilst losing neutralizing activity against Omicron. Tixagevimab-cilgavimab elicits inhibitory activity against Beta, Gamma, and Omicron variants, but the titer of monoclonal antibodies required for a 50% reduction in the number of infectious foci (FRNT<sub>50</sub> or sometimes also referred to as IC<sub>50</sub>) is 24.8 to 142.9 higher for Omicron than for Beta or Gamma. Likewise, sotrovimab remains to have neutralizing activity against Beta, Gamma, and Omicron variants, but nevertheless, the FRNT<sub>50</sub> value is 3.7 to 198.2 higher for Omicron than for Beta or Gamma (11).

In another experiment, etesevimab plus bamlanivimab is found to have no neutralizing activity against Omicron/BA.2. Casirivimab plus imdevimab can inhibit Omicron/BA.2, but no neutralizing activity is demonstrated against Omicron/BA.1 or Omicron/BA.1.1. Tixagevimab-cilgavimab retains activity against Omicron/BA.2. Sotrovimab has been depicted to have lower neutralizing activity against Omicron/BA.2 compared to Omicron/BA.1, Omicron/BA.1.1, and the ancestral strain. The FRNT<sub>50</sub> value of each of these monoclonal antibodies is considerably higher for Omicron/BA.2 in comparison with the ancestral strain and other variants of concern (12).

In view of the global dominance of the Omicron variant and the diminished therapeutic effect against the newly emerged variant, the United States National Institutes of Health (NIH) COVID-19 Treatment Guidelines Panel no longer recommends the use of bamlanivimab plus etesevimab, casirivimab plus imdevimab, or sotrovimab for the treatment of COVID-19. At present, tixagevimab-cilgavimab is shown to be safe and efficacious as pre-exposure prophylaxis and potential treatment for mild to moderate COVID-19 (13). On the other hand, bebtelovimab, being the sole monoclonal antibody that remains effective *in vitro* against all circulating Omicron subvariants (14), is approved by the United States Food and Drug Administration (FDA) and the NIH COVID-

19 Treatment Guidelines Panel as a therapeutic option in high-risk patients with COVID-19 (9, 15).

One of the strategies to ascertain the role of bebtelovimab in mild to moderate COVID-19 infection is evidence synthesis using existing literature to inform and design studies of this promising therapy. Recognizing this gap, a scoping review is performed to identify and delineate of the current state of research evidence on the effect of bebtelovimab on COVID-19. The findings of the review will be utilized to inform future research within the theme of human IgG1 monoclonal SARS-CoV-2 antibody and possibly other research groups examining biologic drugs and lay a cornerstone of the foundation for formulating laboratory guidance and clinical tools for biomedical researchers to work on therapeutic options for COVID-19 patients.

## 2 Methods

### 2.1 Overview

We conducted a systematic search to identify the preclinical and clinical evidence concerning the therapeutic effects of bebtelovimab in COVID-19. The scoping review was done in accordance with the Preferred Reporting Items for Systematic Review and Meta-Analysis Extension for Scoping Reviews (PRISMA-ScR) (16) and the Joanna Briggs Institute (JBI) (17). Our aim was to present a rigorous, comprehensive, systematic approach to synthesize the current heterogeneous literature to ascertain gaps in knowledge and provide an effective summary for practitioners and guide researchers across the disciplines ranging from the laboratory bench to real-world clinical environment. The synthesis of evidence focused on *in vitro* studies, *in vivo* studies, clinical trials, and modeling studies that investigated the effect of bebtelovimab on SARS-CoV-2 infection.

### 2.2 Search strategy and selection criteria

We searched five electronic bibliographic databases, namely PubMed, Cochrane Central Register of Controlled Trials (CENTRAL), Embase, Global Health, and PsycINFO, for articles published in English from database inception until September 30, 2022 using a combination of search terms relating to bebtelovimab and COVID-19, as provided in the Appendix. Reference lists and tracked citations of retrieved articles were scrutinized to locate relevant publications not detected during the database searches. Preprint servers of bioRxiv and medRxiv were also searched for additional studies. Authors were contacted for further information that was not available in the published material (18).

Publications were deemed eligible for inclusion if they reported on preclinical or clinical findings regarding the use of bebtelovimab in SARS-CoV-2 infection. Studies were excluded if they reported aggregation of outcomes from different monoclonal SARS-CoV-2 antibody therapies but did not evaluate an actual or specific impact of bebtelovimab.

### 2.3 Article selection

All citations were imported into EndNote (version X9) reference management software and duplicates were removed. Study selection was undertaken by two reviewers and occurred in two stages, comprising initial title and abstract screening, followed by full-text review. In each stage, two reviewers independently evaluated each study against a set of pre-specified inclusion and exclusion criteria to determine whether it should move forward. Any incongruences were resolved through discussion, or, in the case of no consensus, a third reviewer was involved.

### 2.4 Data analysis

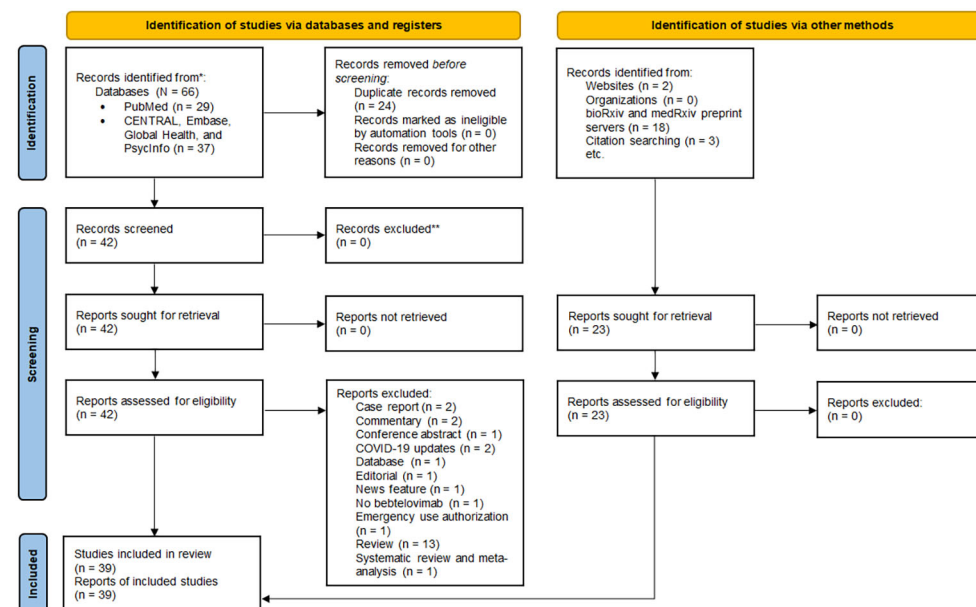
A standardized data extraction form was developed and independently piloted using Microsoft Word. Data from included studies such as details of therapeutic intervention, study characteristics and design, data for our focal outcomes, analytical methods, results, as well as individual study strengths and limitations were independently extracted by two reviewers. The complete data extraction was verified by a third reviewer. All findings were subsequently collated and summarized through the description of narrative synthesis approach. In light of variability in the study designs, we did not plan to formally appraise the methodological quality of the included studies. However, we did provide comments on the limitations of the studies. We also estimated summary risk ratio (RR) using pairwise random-effects meta-analysis.

## 3 Results

The database search yielded 66 records, of which 24 duplicate records were removed. 23 additional articles were identified by manual searching. Hence, 65 full-text articles were assessed for eligibility, of which 39 were included in the review (Figure 1). 34 studies were non-clinical research (19–52), encompassing *in vitro* virus neutralization experiments (19–50), immunoinformatic analysis (51), and deep mutational scanning (52). The remaining 5 studies were clinical research (18, 53–56), comprising randomized controlled trial (53) and retrospective cohort studies (18, 54–56). 17 studies were conducted in the United States (28, 30, 34, 35, 38, 42, 45, 49, 50, 56), 8 in China (19, 23–26, 31, 48), 7 in Europe (20–22, 29, 36, 37, 41), 4 in Japan (39, 40, 46, 47), 2 in India (32, 51), and 1 across three countries, namely United States, Argentina, and Puerto Rico (53). A summary of the main characteristics of each individual study is outlined in Tables 1, 2.

### 3.1 Non-clinical studies

The *in vitro* study conducted by Iketani and co-authors investigated the different therapeutic monoclonal antibodies and found that 17 out of 19 of them had diminished neutralization potency against Omicron BA.2 variant (30). Bebtelovimab



\*Consider, if feasible to do so, reporting the number of records identified from each database or register searched (rather than the total number across all databases/registers).  
\*\*If automation tools were used, indicate how many records were excluded by a human and how many were excluded by automation tools.

FIGURE 1

PRISMA 2020 flow diagram for new systematic review which included searches of databases, registers, and other sources.

TABLE 1 Characteristics and results of included non-clinical studies.

Study (year), country	Virus type <sup>a</sup>	Cell line	Inoculum <sup>b</sup>	Incubation (hours)	Control	Variants	Main findings
Ai, et al. (2022), China (19)	PV (VSV)	Vero	NA	24	B	BA.1, BA.1.1, BA.2, BA.3	Bebtelovimab maintained its neutralization potency against all Omicron sublineages tested.
Andreano, et al. (2022), Italy (20)	Infectious	Vero	NR	72 – 96	B	BA.1, BA.2, BA.4, BA.5	Bebtelovimab had high neutralization potency against all Omicron sublineages, showing an IC <sub>100</sub> of 11.1, 15.6, 44.2, and 62.5 ng/ml against Omicron BA.1, BA.2, BA.4, and BA.5 respectively.
Arora, et al. (2022), Germany (21)	PV (VSV)	Vero	NA	16 – 18	B.1	BA.1, BA.2, BA.2.12.1, BA.4, BA.5	Bebtelovimab neutralized all emerging Omicron subvariants tested with similarly high efficacy.
Bruehl, et al. (2022), France (22)	Infectious	U2OS-ACE2 GFP1-10 or GFP11	NA	18	B.1.617.2	BA.2, BA.4, BA.5	Bebtelovimab remained fully active against Omicron BA.2, BA.4, and BA.5. Bebtelovimab displayed similar levels of binding and activation of NK-mediated antibody-dependent cellular cytotoxicity against all strains.
Cao, et al. (2022), China (23–26)	PV (VSV)	Huh-7	10 <sup>3</sup>	24	B.1	BA.1, BA.1.1, BA.2, BA.2.12.1, BA.2.13, BA.2.74, BA.2.75, BA.2.75.2, BA.2.75.4, BA.2.76, BA.2.77, BA.2.79, BA.3, BA.2.38, BA.2.38.1, BA.4, BA.4.6, BA.5, BA.5.1.12, BA.5.2.7, BA.5.5.1, BA.5.6.2, BF.16, BL.1	Bebtelovimab showed potent neutralizing activity against the majority of assayed Omicron subvariants, except BA.2.38.1, BA.5.2.7, and BA.5.6.2.

(Continued)

TABLE 1 Continued

Study (year), country	Virus type <sup>a</sup>	Cell line	Inoculum <sup>b</sup>	Incubation (hours)	Control	Variants	Main findings
Chakraborty, et al. (2022), India (51)	NA	NA	NA	NA	B	BA.1, BA.2, BA.2.12.1, BA.3, BA.4, BA.5	Immunoinformatics simulation depicted L452R/Q498R double mutations in Omicron subvariants caused an approximately 6% reduction in binding affinities of bebtelovimab.
Duerr, et al. (2022), USA (27)	PV (HIV) and Infectious	293T-ACE2 Vero/TMPRSS2	0.2 MOI 100 – 180 PFU	NA	B.1	AY.45, BA.1, BA.2, AY.45-BA.1	Neutralization assays using infectious and pseudotyped viruses depicted bebtelovimab retained activity against all variants tested.
Fan, et al. (2022), USA (28)	PV (HIV)	293T-ACE2	NA	48	B.1	BA.1, BA.2	Bebtelovimab retained at least partial efficacy against Omicron variants by targeting a Class 3 receptor-binding domain epitope adjacent to the BA.1 and BA.2 mutations.
Gruell, et al. (2022), Germany (29)	PV (HIV)	293T-ACE2	NA	48	B.1	BA.2, BA.2.12.1, BA.2.75, BA.4, BA.5	Bebtelovimab demonstrated high BA.2.75 neutralizing potency (IC <sub>50</sub> = 7.0 ng/ml), although the activity was lower than that against the other variants.
Iketani, et al. (2022), USA (30)	PV (VSV)	Vero	NA	12	B.1	BA.1, BA.1.1, BA.2	Bebtelovimab adequately treated all assayed Omicron sublineages, with IC <sub>50</sub> of approximately 5 ng/ml.
Jian, et al. (2022), China (31)	PV (VSV)	Huh-7	NA	24	B.1	BA.4, BA.4.6, BA.4.7, BA.5, BA.5.9	Bebtelovimab remained potent against R346-mutated BA.4 and BA.5 subvariants.
Kumar, et al. (2022), India (32)	Infectious	Vero/TMPRSS2	1×10 <sup>2</sup> PFU	16 – 40	WA1 isolate	B.1.1.7, B.1.351, P.1, B.1.617.2, BA.1, BA.2	Bebtelovimab showed binding and neutralization potential to Omicron and its sublineages.
Li, et al. (2022), China (33)	Infectious	HEK293F	NA	60	B	BA.1, BA.2, BA.3, BA.4	Bebtelovimab preserved neutralizing activity against all Omicron sublineages tested. None of the four Omicron mutations, namely N440K, G446S, Q498R, and N501Y was found to disrupt the interaction with bebtelovimab, thus indicating its broad neutralizing activity.
Lusvarghi, et al. (2022), USA (34)	PV (HIV)	293T-ACE2-TMPRSS2	1×10 <sup>5</sup> – 5×10 <sup>5</sup> RLU	48	B.1	BA.1	Bebtelovimab maintained potency against BA.1 (IC <sub>50</sub> = 3.2 ng/ml) comparable to B.1 (IC <sub>50</sub> = 1.3 ng/ml), whereas antibody cocktail containing bebtelovimab, bamlanivimab, and etesevimab merely retained partial potency (IC <sub>50</sub> = 32.5 ng/ml).
Misasi, et al. (2022), USA (35)	PV (VSV)	293T-ACE2-TMPRSS2	NA	72	B.1	B.1.351, B.1.617.2, BA.1, BA.2, BA.2.12.1, BA.4, BA.5	Bebtelovimab remained active against all variants tested. However, it fully escaped antibody neutralization within two to three rounds of repeated infection <i>in vitro</i> .
Sheward, et al. (2022), Sweden (37)	PV (HIV)	293T-ACE2	1×10 <sup>5</sup> RLU	48	B.1	BA.2, BA.2.75, BA.5	Bebtelovimab could neutralize BA.2.75 (IC <sub>50</sub> = 15 ng/ml), but the potency was reduced by 7-fold as compared to B.1 (IC <sub>50</sub> = 2 ng/ml).
Sheward, et al. (2022), Sweden (36)	PV (HIV)	293T-ACE2	1×10 <sup>5</sup> RLU	44 – 48	B.1	BA.2.10.4, BA.2.75.2, BA.4.6, BA.5	Bebtelovimab potently neutralized all emerging Omicron sublineages tested.
Starr, et al. (2022), USA (52)	NA	NA	NA	NA	B	BA.1, BA.2	Deep mutational scanning revealed a broadening of the sites of escape from bebtelovimab binding BA.1 and BA.2 compared to the ancestral strain ascribable to mutations at residues K444, V445, P499, and G446.

(Continued)

TABLE 1 Continued

Study (year), country	Virus type <sup>a</sup>	Cell line	Inoculum <sup>b</sup>	Incubation (hours)	Control	Variants	Main findings
Syed, et al. (2022), USA (38)	Infectious	293T-ACE2/ACE2-TMPRSS2 and Vero-E6	50 PFU	72	WA1 isolate	B.1.617.2, B.1.1.529	Bebtelovimab had potent neutralization activity against all variants tested, with IC <sub>50</sub> of less than 10 ng/ml.
Takashita, et al. (2022), Japan (39)	Infectious	Vero-hACE2-TMPRSS2	1×10 <sup>3</sup> FFU	18	NC002 isolate	BA.1.1, BA.1, BA.2, BA.2.12.1, BA.4, BA.5	Bebtelovimab efficiently neutralized BA.2.12.1, BA.4, and BA.5, with similar IC <sub>50</sub> values as the ancestral strain.
Takashita, et al. (2022), Japan (40)	Infectious	Vero-hACE2-TMPRSS2	1×10 <sup>3</sup> FFU	18	NC002 isolate	BA.2, BA.2.75, BA.5	Bebtelovimab efficiently neutralized BA.2.75 (IC <sub>50</sub> = 6.21 ng/ml), however, this value was 4.4-fold higher compared to the ancestral strain.
Turelli, et al. (2022), Switzerland (41)	PV (HIV) and Infectious	Vero-E6/Calu-3	3×10 <sup>3</sup> PFU	48	B.1	B.1.1.7, B.1.351, P.1, B.1.617.2, BA.1, BA.2, BA.4, BA.5	Bebtelovimab displayed good action against BA.4 and BA.5, with IC <sub>50</sub> values of 12 ng/ml and 15 ng/ml respectively. In the Delta variant, spike mutations K444T, V445G, and G446V conferred resistance to bebtelovimab. In the Omicron BA.4 variant, mutations in the spike protein, namely K444T, V445G, and P499H suppressed neutralization activity of bebtelovimab.
Wang, et al. (2022), USA (42)	PV (VSV)	Vero-E6 and HEK293T	NA	24	B	BA.1, BA.1.1, BA.2, BA.2.12.1, BA.4, BA.5	Bebtelovimab retained exquisite <i>in vitro</i> potency against BA.2.12.1, BA.4, and BA.5, with IC <sub>50</sub> below 3 ng/ml.
Wang, et al. (2022), USA (43)	PV (VSV)	Vero-E6 and HEK293T	NA	24	B.1	BA.2, BA.2.12.1, BA.2.75, BA.4, BA.5	Bebtelovimab retained potent neutralizing activity against all Omicron subvariants, with IC <sub>50</sub> below 10 ng/ml. BA.2.75 demonstrated slight resistance to bebtelovimab, albeit modestly at a 3.7-fold loss in neutralization.
Wang, et al. (2022), USA (44)	PV (VSV)	Vero-E6 and HEK293T	NA	24	B.1	BA.2, BA.4, BA.4.6, BA.4.7, BA.5, BA.5.9, BA.4/5-R346T, BA.4/5-R346S, BA.4/5-N658S	Bebtelovimab retained potent activity against all circulating forms of Omicron subvariants.
Westendorf, et al. (2022), USA (45)	PV (VSV) and Infectious	293T-ACE2/ACE2-TMPRSS2 and Vero-E6	NA	72	B.1	B.1.1.7, B.1.351, P.1, B.1.617.2, B.1.526, B.1.427/B.1.429, BA.1, BA.2	Bebtelovimab bound and potently neutralized all variants tested.
Yamasoba, et al. (2022), Japan (46)	PV (HIV)	HOS-ACE2-TMPRSS2	2 × 10 <sup>4</sup> RLU	48	B.1.1	BA.1, BA.2, B.1.617.2, BA.2.11, BA.2.12.1, BA.4, BA.5	Bebtelovimab was approximately 2 times more effective against BA.2 and all Omicron subvariants tested as compared to wild-type virus.
Yamasoba, et al. (2022), Japan (47)	PV (HIV)	HOS-ACE2-TMPRSS2	2.5 × 10 <sup>4</sup> RLU	48	B.1.1	BA.2, BA.2.75, BA.4, BA.5	Bebtelovimab demonstrated strong antiviral effect against BA.2, BA.4, and BA.5. In comparison, BA.2.75 showed about a 20 to 25-fold resistance to neutralization, suggesting that bebtelovimab may not be a good choice to treat BA.2.75 infection.
Zhang, et al. (2022), China (48)	Infectious	Vero	600 PFU/ml	96	WIV04 isolate	B.1.617.2, BA.1	Bebtelovimab exhibited neutralizing potency against wild-type (IC <sub>50</sub> = 40.9 ng/ml), B.1.617.2 (IC <sub>50</sub> = 50.8 ng/ml), and BA.1 (IC <sub>50</sub> = 17.3 ng/ml).

(Continued)



TABLE 1 Continued

Study (year), country	Virus type <sup>a</sup>	Cell line	Inoculum <sup>b</sup>	Incubation (hours)	Control	Variants	Main findings
Zhou, et al. (2022), USA (49)	PV (HIV)	293T-ACE2-TMPRSS2	NA	72	B.1	B.1.1.7, B.1.351, P.1, B.1.617.2, BA.1	Bebtelovimab retained binding and potent neutralization of all variants assessed, including BA.1 and BA.2 sublineages (IC <sub>50</sub> = 5.1 and 0.6 ng/ml respectively).
Zhou, et al. (2022), USA (50)	PV (HIV)	293T-ACE2	0.2 MOI	48	B.1	B.1.617.2, BA.1, BA.2	Bebtelovimab potentially neutralized all variants tested, including BA.1 (IC <sub>50</sub> = 26.2 ng/ml), BA.2 (IC <sub>50</sub> = 11.5 ng/ml), and individual point mutated BA.2 viruses (IC <sub>50</sub> range = 2.8 – 11.7 ng/ml).

<sup>a</sup>PV, pseudotyped virus; HIV, human immunodeficiency virus; VSV, vesicular stomatitis virus; MLV, murine leukemia virus.

<sup>b</sup>The preclinical studies reported inoculum as 50% tissue culture infectious doses (TCID<sub>50</sub>), relative light units (RLU), plaque forming units (PFU), focus forming units (FFU), or transducing units (TU). The clinical study reported inoculum as multiplicity of infection (MOI).

TABLE 2 Characteristics and results of included clinical studies.

Study (year), country	Study design	Study population	Age group (years)	Active treatment	Control treatment	Dominant variant	Main findings
Chen, et al. (2022), USA (18)	Retrospective cohort study	Individuals with COVID-19 infection before receiving tixagevimab-cilgavimab (n=121)  Individuals with breakthrough COVID-19 infection following receipt of tixagevimab-cilgavimab (n=102)	Median: 54.5 (Range: 18 – 79)  Median: 60.5 (Range: 25 – 99)	Bebtelovimab (n=34), sotrovimab (n=58), casirivimab-imdevimab (n=10), nirmatrelvir-ritonavir (n=46), or remdesivir (n=39)	No treatment (n=36)	BA.1 (prior to tixagevimab-cilgavimab prophylaxis)  BA.5 (after tixagevimab-cilgavimab prophylaxis)	Among patients who developed COVID-19 infection prior to tixagevimab-cilgavimab, 36 (29.8%) were hospitalized, including 8 (6.6%) required ICU admission. No COVID-related deaths occurred.  Among patients who developed COVID-19 after receiving tixagevimab-cilgavimab, 6 (5.9%) were hospitalized, but none was admitted to ICU. There was no COVID-related mortality. 34 patients (33.3%) received bebtelovimab, of whom only one was hospitalized, with a length of stay of 12 days.
Dougan, et al. (2022), USA, Argentina, and Puerto Rico (53)	Randomized controlled trial	Ambulatory patients presenting with mild-to-moderate COVID-19 within 3 days of laboratory-confirmed diagnosis (n=714)	Median: 35 [low-risk cohort]  Median: 48.5 – 52.5 [high-risk cohort]	Intravenous bebtelovimab 175 mg over 6.5 minutes (n=125) [low-risk cohort] Intravenous bebtelovimab 175 mg over 30 seconds (n=100) [high-risk cohort]	Placebo (n=128) or intravenous bebtelovimab 175 mg plus bamlanivimab 700 mg plus etesevimab 1400 mg over 6.5 minutes (n=127) [low-risk cohort]  Intravenous bebtelovimab 175 mg plus bamlanivimab 700 mg plus etesevimab 1400 mg over	Ancestral strains of SARS-CoV-2 (low-risk cohort)  Alpha, gamma, delta, and mu lineages (high-risk cohort)	Among low-risk patients, bebtelovimab monotherapy resulted in a greater viral clearance, a reduction in time to sustained symptom resolution, and a similar rate of treatment-emergent adverse events compared to placebo or combination therapy of bebtelovimab plus bamlanivimab plus etesevimab. The incidence of COVID-19-related hospitalization or all-cause deaths by day 29 were similar between treatment groups. 1 death due to COVID-19 on day 5 was reported in a patient who received combination therapy of bebtelovimab plus bamlanivimab plus etesevimab.  Among high-risk patients, there were no treatment comparisons made. The proportion of patients with treatment-emergent adverse events was 14.7% in high-risk patients treated with bebtelovimab or combination therapy. Serious adverse events were reported in 2.1% of high-risk patients, including one death due to cerebrovascular accident.

(Continued)

TABLE 2 Continued

Study (year), country	Study design	Study population	Age group (years)	Active treatment	Control treatment	Dominant variant	Main findings
					30 seconds or 6.5 minutes (n=226) [high-risk cohort]		
Razonable, et al. (2022), USA (54)	Retrospective cohort study	High-risk patients with a positive SARS-CoV-2 polymerase chain reaction or antigen test (n=3607)	Median: 66.2 (IQR: 52.5 – 74.7)	Intravenous bebtelovimab 175 mg over 1 minute (n=2833)	Oral nirmatrelvir (150 or 300 mg) plus ritonavir (100 mg) twice daily for a total of 5 days (n=774)	BA.2	Rates of progression to severe illness and ICU admission were similar between bebtelovimab cohort and nirmatrelvir-ritonavir cohort.
Shertel, et al. (2022), USA (55)	Retrospective cohort study	Solid organ transplant recipients who were treated with Bebtelovimab after being tested positive for COVID-19 (n=25)	Median: 52 ((IQR: 44 – 67)	Bebtelovimab (n=25)	NA	BA.1, BA.2	During 1-month of follow-up period, 2 patients required hospital admission. No cases of acute allograft rejection or death were observed.
Yetmar, et al. (2022), USA (56)	Retrospective cohort study	Solid organ transplant recipients diagnosed with mild-to-moderate COVID-19 (n=361)	Mean: 57.7 ± 14.6	Intravenous bebtelovimab 175 mg over 1 minute (n=92)	Intravenous sotrovimab 500 mg (n=269)	BA.2	Hospitalization rates for COVID-19 were similar between bebtelovimab group and sotrovimab group. 3 patients were admitted to ICU, all of whom received sotrovimab. 4 patients died within 30 days of COVID-19 diagnosis, 2 from each treatment group.

demonstrated a consistent and high neutralizing potency against all Omicron subvariants despite the difference in antigenicity displayed. A research by Arora and team also yielded results which echoed the similarly high efficacy of bebtelovimab against all Omicron subvariants (21). Another finding by Westendorf and colleagues suggested that bebtelovimab potentially neutralized all documented variants of concern, including the dominant Omicron variant and its sublineages circulating globally. The study reported that the bebtelovimab Fab fragment bound to the S protein of the D614G variant with high affinity, with no loss of binding potency to variants of concern such as B.1.1.7 (Alpha) and B.1.351 (Beta), as well as all tested SARS-CoV-2 viruses that had mutations in the N-terminal domain, receptor-binding domain, and the receptor-binding motif (45). Pseudotyped virus neutralization assay confirmed that bebtelovimab retained effect against Alpha, Beta, Gamma, Delta, Epsilon, Delta-Omicron recombinant, and Omicron sublineages, including BA.1.1, BA.2.12.1, BA.2.75, BA.4.6, BA.4.7, and BA.5.9 (19, 21, 23–31, 34–37, 41–47, 49, 50). Likewise, positive results were observed in live virus neutralization assay (Supplementary Table 1) (20, 22, 27, 32, 33, 38–41, 45, 48). Bebtelovimab was the only monoclonal antibody that exhibited good potency against most Omicron variants, except BA.2.38.1, BA.5.2.7, and BA.5.6.2 (23).

Structurally, bebtelovimab bound to the receptor-binding domain epitope on the S protein of SARS-CoV-2 that was less inclined to mutations (19, 45). Bebtelovimab was minimally impacted by the mutational changes in Omicron variants (28, 49, 50). Docking of bebtelovimab onto Omicron's receptor-binding domain detected four amino acid substitutions at the edge of its epitope. Bebtelovimab had minimal side-chain interactions with 3 of the residues (i.e. K440, R498, and Y501) and the loop containing S446 (fourth residue) had conformational flexibility that could facilitate binding of bebtelovimab to the viral spike protein (49). Furthermore, mutations in the Omicron (i.e. N440K, G446S, Q498R, and N501Y) did not affect the interaction with bebtelovimab. Amino acid residues of BA.2 (i.e. Lys440 and Arg498) were found to form H-bonds with Tyr35 and Thr96 of bebtelovimab, whereas a common mutation in BA.1 and BA.3 (i.e. G446S) might cause interaction between Ser446 and Arg60 of heavy chain in bebtelovimab (33). Contrariwise, L452R/Q498R double mutations in Omicron variants could result in an approximately 6% decrease in binding affinities for bebtelovimab (51). A broadening of sites of escape from binding by bebtelovimab were also detected in Omicron BA.1 and BA.2 attributable to mutations at residues K444, V445, P499 and G446, indicating a lower binding affinity of bebtelovimab for Omicron (52).

Bebtelovimab antibody cocktail did not result in an increased potency or synergistic effect against Omicron (49). Complementary findings from an experiment led by Lusvarghi demonstrated bebtelovimab's potency against Omicron BA.1 comparable to B.1, while antibody cocktail containing bebtelovimab, bamlanivimab, and etesevimab merely retained partial potency (34).

## 3.2 Clinical studies

A randomized clinical trial evaluated the safety and efficacy of bebtelovimab in COVID-19 patients. In the Phase 1 part of the study, Dougan and co-investigators examined ascending doses and infusion rates of intravenous administration of bebtelovimab in 40 patients with low risk of developing severe COVID-19. Pharmacokinetics and pharmacodynamics modeling determined that target therapeutic doses of bebtelovimab 175 mg, bamlanivimab 700 mg, and etesevimab 1400 mg would result in a drug concentration for optimal viral load reduction (53).

Phase 2 of the study examined 380 patients at low risk for severe COVID-19 randomized 1:1:1 to placebo, bebtelovimab 175 mg, or combination therapy of bebtelovimab 175 mg, bamlanivimab 700 mg, and etesevimab 1400 mg, with another 150 high-risk patients randomized 2:1 to bebtelovimab 175 mg or combination therapy of bebtelovimab, bamlanivimab, and etesevimab. An additional treatment arm allocated combination therapy to 176 patients based on the Centers for Disease Control and Prevention (CDC) updated criteria for high-risk. Viral dynamic modeling depicted no discernable difference in viral load reduction between bebtelovimab monotherapy or in combination with bamlanivimab and etesevimab. A simulation developed from the trial demonstrated that older patients over 70 years of age benefited more from the administration of bebtelovimab monotherapy in view of a larger decline from baseline in the viral load. In terms of efficacy, bebtelovimab and combination therapy arms had a lower proportion of patients with persistently high viral load at Day 7 but did not reach statistical significance ( $p = 0.097$  for bebtelovimab versus placebo;  $p = 0.132$  for bebtelovimab plus bamlanivimab plus etesevimab versus placebo). A marked reduction in viral load from baseline to Day 11 was shown in patients in bebtelovimab ( $p = 0.006$ ) and combination therapy ( $p = 0.043$ ) groups compared to placebo. The median time to resolution of symptoms was two days shorter with bebtelovimab monotherapy than with placebo ( $p = 0.003$ ). The incidence of COVID-19-related hospitalization and all-cause mortality by day 29 were similar across treatment groups (1.6% for bebtelovimab; 2.4% for bebtelovimab plus bamlanivimab plus etesevimab; 1.6% for placebo). In high-risk patients, there were no significant differences in viral load, symptom resolution, COVID-19 hospital admission, and mortality among two groups of patients treated with bebtelovimab alone or in conjunction with bamlanivimab and etesevimab (53).

Post-treatment follow-up assessments were carried out in both parts of the trial. Phase 1 identified no reports of COVID-19-related hospitalizations or mortality and increasing doses and infusion rates of bebtelovimab were not correlated with higher rates of

treatment-emergent adverse events through at least 24 to 48 hours. No deaths, severe adverse events, or treatment discontinuations occurred. In Phase 2, no discontinuations were ascribed to treatment-emergent adverse events among low-risk patients. The majority of adverse events were mild or moderate, and there was no significant between-group difference in the overall rates (8.8% for bebtelovimab; 12.6% for bebtelovimab plus bamlanivimab plus etesevimab; 7.8% for placebo). In high-risk patients, only one serious adverse event (cerebrovascular accident) resulted in death among recipients of bebtelovimab monotherapy. Similarly, the majority of adverse events were mild or moderate, with overall rates that did not differ significantly between groups (20.0% for bebtelovimab; 16.0% for bebtelovimab plus bamlanivimab plus etesevimab; 11.4% for bebtelovimab plus bamlanivimab plus etesevimab in CDC expanded criteria patients). Two patients who received combination therapy had infusion-related reactions that resolved upon treatment withdrawal, whereas no anaphylactic reaction occurred among patients receiving bebtelovimab alone (53).

A further live virus neutralization assay in the trial depicted combination therapy of bebtelovimab and bamlanivimab had negligible or no neutralizing activity against Omicron variant ( $IC_{99} > 10,000$  ng/ml), while bebtelovimab monotherapy neutralized Omicron variant with a  $IC_{99}$  value of less than 2.44 ng/ml, indicating a comparable or greater potency as that of Delta and WA1 isolates (53).

Two retrospective cohort studies of solid organ transplant patients showed bebtelovimab maintained activity against Omicron BA.1 or BA.2 subvariants (55, 56). The rates of hospitalization, intensive care unit admission, and mortality were similar between bebtelovimab and sotrovimab cohorts (56). Shertel and co-workers reported that only 2 of 25 (8.0%) bebtelovimab-treated patients required hospitalization, of whom one needed remdesivir plus dexamethasone therapy due to worsening oxygenation and another experienced obstructive uropathy and acute kidney injury without any symptoms of upper or lower respiratory tract infection. No deaths and acute allograft rejection were observed during the follow-up (55).

Another retrospective cohort study demonstrated that patients who were given bebtelovimab treatment were significantly older and had more underlying comorbidities than those receiving nirmatrelvir-ritonavir. Notwithstanding the increased risk, bebtelovimab cohort showed similar rates of progression to severe disease, ICU admission, and mortality compared to nirmatrelvir-ritonavir cohort (54). Moreover, Chen and colleagues found patients who contracted COVID-19 following tixagevimab-cilgavimab prophylaxis were less likely to require hospital admission than those without prophylaxis. Only 1 of 34 (2.9%) bebtelovimab-treated patients was hospitalized, and none ended in ICU or death (18).

Pooling of results from the clinical studies depicted no discernable differences in terms of hospital admissions (RR: 1.00, 95% CI: 0.47 – 2.13,  $p = 1.00$ ), ICU admissions (RR: 1.08, 95% CI: 0.33 – 3.58,  $p = 0.90$ ), and death (RR: 3.60, 95% CI: 0.85 – 15.17,  $p = 0.08$ ) between patients receiving bebtelovimab and patients receiving other COVID-19 therapies (Figure 2). Inspection of the

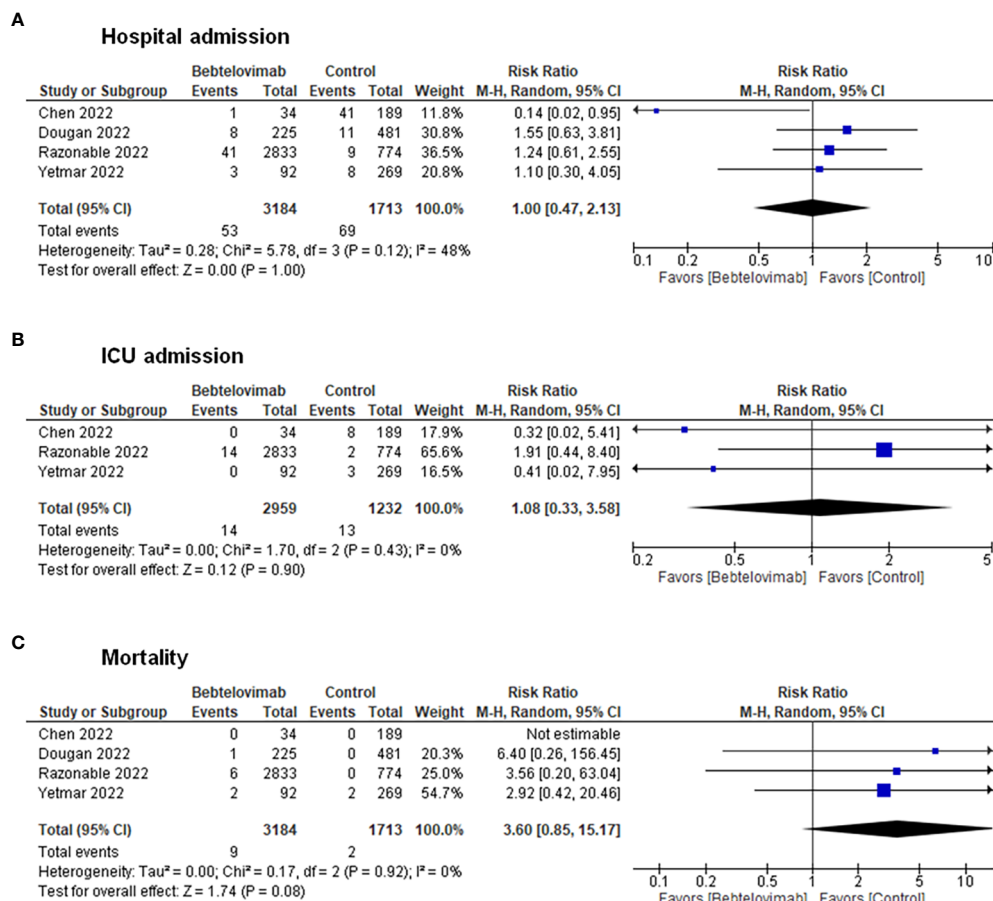


FIGURE 2

Effects of bebtelovimab compared to control on (A) COVID-19-related hospital admission, (B) intensive care unit admission, and (C) mortality.

funnel plots noted some degree of asymmetry for the three clinical outcomes, suggesting the presence of small-study effects and publication bias (Supplementary Figure 1).

## 4 Discussion

The rapid evolution of the SARS-CoV-2 virus continues to challenge our global effort to curb the COVID-19 pandemic. Several clinically available monoclonal antibodies, such as bamlanivimab plus etesevimab, casirivimab plus imdevimab, and sotrovimab are no longer recommended as the treatment for COVID-19 due to a lack of effectiveness against the widely circulating Omicron subvariants. Up till November 2022, bebtelovimab is the sole monoclonal antibody authorized as a treatment for mild to moderate COVID-19 in non-hospitalized patients (9). Our evidence synthesis highlights the therapeutic role of bebtelovimab in COVID-19 infection based on preclinical data depicting its retained potent neutralization against all currently known variants of concern (VOC), along with studies that have demonstrated its clinical safety and efficacy in association with a greater viral clearance and shorter period for symptom resolution. The rate and severity of treatment-emergent adverse events

resulting from the use of bebtelovimab are evidenced to be similar to those of placebo and existing monoclonal antibodies in treating both low-risk and high-risk patients. Meta-analyses of clinical studies show no significant differences in risks of COVID-19 hospitalization, ICU admission, or death between patients treated with bebtelovimab and other COVID-19 therapies.

Bebtelovimab, a fully human immunoglobulin G1 (IgG1) monoclonal SARS-CoV-2 antibody, works by targeting the SARS-CoV-2 spike (S) protein's receptor-binding domain, thereby hindering the spike protein interaction with ACE2 and subsequent viral entry into host cells (45). The *in vitro* efficacy of bebtelovimab is conferred by its ability to bind to an epitope of the SARS-CoV-2 S protein with amino acids that are rarely mutated, as documented in the Global Initiative on Sharing All Influenza Data (GISAID) EpiCoV database (45, 49). Bebtelovimab overcomes mutation-induced structural alterations of the COVID-19 variants by exploiting loop mobility and by minimizing side-chain interactions (49). Overall, there are also consistent findings from clinical studies that demonstrate the effectiveness of bebtelovimab for the treatment of patients infected with SARS-CoV-2 variants (18, 53–56). The collated significant data of this review, in the context of laboratory research and clinical trials, indicate that bebtelovimab is a promising therapeutic option against COVID-

19 and newly emerging Omicron sublineages. Our results broadly concur with a recent prediction analysis that bebtelovimab can maintain detectable *in vitro* neutralization against Omicron subvariants such as BA.1, BA.2, BA.4, and BA.5, as well as have a 70.1% (95% CI: 61.9 – 76.8,  $p < 0.0001$ ) therapeutic efficacy when administered to ambulant COVID-19 positive individuals in preventing illness progression to hospitalization (57).

Monoclonal antibodies have propelled to the forefront in the investigations of pharmacological approaches to treating COVID-19 infection as they are the only appropriate options for clinical use in pediatric patients. Several existing anti-SARS-CoV-2 monoclonal antibodies have been reported to be well-tolerated and raise no safety concerns in children of age between 24 days and 18 years old (58). Whilst bebtelovimab is approved for use in non-hospitalized patients aged 12 years or older, the therapeutic decision to use it across all age pediatric groups should be individualized by incorporating risk factors of progression to severe COVID-19 in the risk-benefit judgment (59). Its indication for a broad population of patients across age groups renders it to be a potential therapeutic strategy to vaccinations and other COVID-19 therapies, especially among those who have underlying immunocompromising condition or multimorbidity, have intolerable adverse effects to COVID-19 vaccination, or are not yet eligible for COVID-19 vaccination.

In tandem with the appearance of multi-mutational SARS-CoV-2 variants such as Delta and Omicron lineages, it is important to enhance the efficacy of bebtelovimab and other potential monoclonal antibodies to overcome new variants that evade natural immunity responses (60). During the period of Delta variant predominance, an existing neutralizing monoclonal antibody sotrovimab resulted in 89% reduction in all-cause mortality and 63% in hospitalization at 28 days compared to untreated patients (61). However, during the period in which Omicron BA.2 was the dominant variant, individuals receiving sotrovimab were associated with higher rates of progression to severe, critical, or fatal COVID-19 (62). Collectively, these real-world findings stand in concurrence with *in vitro* evidence that sotrovimab potently neutralized Omicron B.1.1.529 and BA.1 variants but had low neutralizing activity against Omicron BA.2 and its sublineages (12, 30). Concerning bebtelovimab, the best *in vitro* and clinical data available at present highlight its substantial neutralizing activity against all known SARS-CoV-2 variants, including the Omicron and its new subvariants such as BA.2.75, BA.4, and BA.5, and patients administering bebtelovimab have shown a faster decay in virus titer than placebo. The time frames for clinical studies included in this review comprise pre-Omicron era (53) and Omicron variant (BA.1, BA.2, and BA.5) predominance period (18, 54–56). We could reasonably anticipate that the data carry prominent clinical implications for curbing severe COVID-19 illnesses arising from the current sublineages of the Omicron variant and are likely to resonate with growing evidence from future large-scale randomized controlled trials and real-world studies to recommend the use of bebtelovimab in a broader range of patients. Whilst bebtelovimab appears to be well tolerated in our review, case reports have documented that a patient experienced sinus bradycardia-mediated cardiac arrest immediately

following infusion of bebtelovimab (63) and another patient developed colitis 10 days after the use of bebtelovimab (64). Post-marketing surveillance for adverse events and *ad hoc* safety studies are henceforth crucial for earlier detection of safety issues and preventing patients from unnecessary harm (65). Besides, continued laboratory investigations are critical to develop anti-SARS-CoV-2 monoclonal antibodies with better efficacy, safety, and developability features (66). Albeit dedicated wet-lab preclinical research is warranted, this gap can be addressed more rapidly by adding a bioengineering and viral molecular evolution lens to existing lines of research. Instead of just combining different neutralizing monoclonal antibodies, targeting mutated S protein with multivalent nanobody conjugates that can precisely display neutralizing antibodies against SARS-CoV-2 variants has been suggested to have the potential for enhancing the antiviral efficacy (67). However, a recent retrospective cohort study revealed evidence of lack of treatment efficacy among patients infected with SARS-CoV-2 Omicron BA.2, BA.2.12.1, and BA.5 subvariants (68). Hence, well-designed real-world evidence observational studies are important to confirm the efficacy and usage of bebtelovimab. Of note, a next-generation monoclonal antibody may play a pivotal role in inducing rapid immunomodulation and limiting the course of illness, for instance, in debilitating multisystem inflammatory syndrome in children associated with COVID-19 considering the vast potential for improved outcomes with the use of single or combination immunotherapies (69, 70).

Key strengths of our study encompass adherence to scoping review methods, comprehensive search strategy, and inclusion criteria without restrictions on publication status. Limitations of our review are the inclusion of articles published in English only. Supplementary preclinical research is needed to develop neutralizing monoclonal antibodies with optimized clinical efficacy against the evolving variants. The evidence synthesized by this review and the gaps in knowledge reveal that future clinical studies are necessary to foster a deeper understanding of the safety and efficacy of bebtelovimab across different age groups or clinical characteristics, particularly pediatric population and persons with multiple high-risk conditions or comorbidities, the optimal time to initiate treatment, the impact of bebtelovimab on clinical outcomes among patients having previously immunized with different vaccine types or heterologous vaccination regimens, and how Immunocompromised individuals would benefit from additional doses of bebtelovimab in the event of COVID-19 breakthrough infection. The clinical trial included in our review was limited by the exclusive geographical enrollment of patients in North and Latin America, collection of placebo-controlled data among patients at low risk for severe COVID-19, lack of power to assess improvements in clinical outcomes among patients with active treatment before the emergence of Omicron subvariants, use of viral surrogate markers in low-risk younger or healthier subjects for efficacy evaluation, and absence of patient-level clinical data to determine the efficacy of bebtelovimab in patients with symptomatic Omicron infection (53). The retrospective cohort studies had inherent limitations, such as inability to account for sources of residual confounding and selection bias, absence of an



untreated control group, and the potential of misclassification bias resulting from administrative data ascertainment, variation in completeness of documentation, inclusion of patients solely in the United States, and lack of laboratory values and biomarkers to better characterize the disease severity. Therefore, further large multinational clinical studies are warranted to resolve these limitations, increase generalizability and evaluate the clinical efficacy and safety of bebtelovimab in diverse patient populations.

## 5 Conclusion

The currently available evidence supports the clinical use of bebtelovimab for patients with SARS-CoV-2 infection who are at increased risk of progression to severe illnesses. With relatively similar pharmacological properties as other previously approved anti-SARS-CoV-2 monoclonal antibodies, bebtelovimab possesses superiority in terms of the ability to neutralize presently circulating Omicron subvariants and different variants of interest. The favorable preclinical and clinical results justify its potential to reserve an active therapeutic role despite the evolutionary trajectories of SARS-CoV-2.

## Data availability statement

The original contributions presented in the study are included in the article/**Supplementary Material**. Further inquiries can be directed to the corresponding author.

## Author contributions

ML – Article selection, data analysis, data interpretation, validation, and writing the original draft. KK – Literature search, study design, article selection, data analysis, data interpretation,

validation, and writing the original draft. SL – Literature search, study design, and writing the review & editing. KW – Conceptualization, provision of funding for open-access publishing, project administration, resources, and review. All authors contributed to the article and approved the submitted version.

## Funding

ML, KK, and SL receive no funding for this research. KW gets a sponsorship from his department to pay for the article publishing charge.

## Conflict of interest

The authors declare that the research was conducted in the absence of any commercial or financial relationships that could be construed as a potential conflict of interest.

## Publisher's note

All claims expressed in this article are solely those of the authors and do not necessarily represent those of their affiliated organizations, or those of the publisher, the editors and the reviewers. Any product that may be evaluated in this article, or claim that may be made by its manufacturer, is not guaranteed or endorsed by the publisher.

## Supplementary material

The Supplementary Material for this article can be found online at: <https://www.frontiersin.org/articles/10.3389/fimmu.2023.1100263/full#supplementary-material>

## References

1. COVID-19 Excess Mortality Collaborators. Estimating excess mortality due to the COVID-19 pandemic: A systematic analysis of COVID-19-related mortality, 2020–21. *Lancet* (2022) 399(10334):1513–36.
2. Drake TM, Riad AM, Fairfield CJ, Egan C, Knight SR, Pius R, et al. Characterisation of in-hospital complications associated with COVID-19 using the ISARIC WHO Clinical Characterisation Protocol UK: A prospective, multicentre cohort study. *Lancet* (2021) 398(10296):223–37. doi: 10.1016/S0140-6736(21)00799-6
3. Atmar RL, Lyke KE, Deming ME, Jackson LA, Branche AR, El Sahly HM, et al. Homologous and heterologous COVID-19 booster vaccinations. *N Engl J Med* (2022) 386(11):1046–57. doi: 10.1056/NEJMoa2116414
4. Paul E, Steptoe A, Fancourt D. Attitudes towards vaccines and intention to vaccinate against COVID-19: Implications for public health communications. *Lancet Reg Health Eur* (2021) 1:100012. doi: 10.1016/j.lanepe.2020.100012
5. Premikha M, Chiew CJ, Wei WE, Leo YS, Ong B, Lye DC, et al. Comparative effectiveness of mRNA and inactivated whole virus vaccines against COVID-19 infection and severe disease in Singapore. *Clin Infect Dis* (2022) 75(8):1442–5. doi: 10.1093/cid/ciac288
6. Gupta A, Gonzalez-Rojas Y, Juarez E, Crespo Casal M, Moya J, Falci DR, et al. Early treatment for COVID-19 with SARS-CoV-2 neutralizing antibody sotrovimab. *N Engl J Med* (2021) 385(21):1941–50. doi: 10.1056/NEJMoa2107934
7. Balocco R, De Sousa Guimaraes Koch S, Thorpe R, Weisser K, Malan S. New INN nomenclature for monoclonal antibodies. *Lancet* (2022) 399(10319):24. doi: 10.1016/S0140-6736(21)02732-X
8. Shang J, Ye G, Shi K, Wan Y, Luo C, Aihara H, et al. Structural basis of receptor recognition by SARS-CoV-2. *Nature* (2020) 581(7807):221–4. doi: 10.1038/s41586-020-2179-y
9. COVID-19 treatment guidelines: Anti-SARS-CoV-2 monoclonal antibodies. National Institutes of Health. Available at: <https://www.covid19treatmentguidelines.nih.gov/therapies/anti-sars-cov-2-antibody-products/anti-sars-cov-2-monoclonal-antibodies/> (Accessed 4 July 2022).
10. VanBlargan LA, Errico JM, Halfmann PJ, Zost SJ, Crowe JE, Purcell LA, et al. An infectious SARS-CoV-2 B.1.1.529 Omicron virus escapes neutralization by therapeutic monoclonal antibodies. *Nat Med* (2022) 28(3):490–5.
11. Takashita E, Kinoshita N, Yamayoshi S, Sakai-Tagawa Y, Fujisaki S, Ito M, et al. Efficacy of antibodies and antiviral drugs against COVID-19 Omicron variant. *N Engl J Med* (2022) 386(10):995–8. doi: 10.1056/NEJMc2119407
12. Takashita E, Kinoshita N, Yamayoshi S, Sakai-Tagawa Y, Fujisaki S, Ito M, et al. Efficacy of antiviral agents against the SARS-CoV-2 Omicron subvariant BA. 2. *N Engl J Med* (2022) 386(15):1475–7. doi: 10.1056/NEJMc2201933

13. Levin MJ, Ustianowski A, De Wit S, Launay O, Avila M, Templeton A, et al. Intramuscular AZD7442 (tixagevimab-cilgavimab) for prevention of COVID-19. *N Engl J Med* (2022) 386(23):2188–200. doi: 10.1056/NEJMoa2116620
14. Tao K, Tzou PL, Kosakovsky Pond SL, Ioannidis JPA, Shafer RW. Susceptibility of SARS-CoV-2 omicron variants to therapeutic monoclonal antibodies: systematic review and meta-analysis. *Microbiol Spectr* (2022):e0092622. doi: 10.1128/spectrum.00926-22
15. Focosi D, McConnell S, Casadevall A, Cappello E, Valdiserra G, Tuccori M. Monoclonal antibody therapies against SARS-CoV-2. *Lancet Infect Dis*. (2022)
16. Tricco AC, Lillie E, Zarin W, O'Brien KK, Colquhoun H, Levac D, et al. PRISMA extension for scoping reviews (PRISMA-ScR): Checklist and explanation. *Ann Intern Med* (2018) 169(7):467–73. doi: 10.7326/M18-0850
17. Peters MDJ, Marnie C, Tricco AC, Pollock D, Munn Z, Alexander L, et al. Updated methodological guidance for the conduct of scoping reviews. *JBI Evid Synth* (2020) 18(10):2119–26. doi: 10.1111/24718188.1200167
18. Chen B, Haste N, Binkin N, Law N, Horton LE, Yam N, et al. Real world effectiveness of tixagevimab/cilgavimab (Evusheld) in the Omicron era. *medRxiv* (2022) 2022:2009.2016.22280034. doi: 10.1101/2022.09.16.22280034
19. Ai J, Wang X, He X, Zhao X, Zhang Y, Jiang Y, et al. Antibody evasion of SARS-CoV-2 Omicron BA.1, BA.1.1, BA.2, and BA.3 sub-lineages. *Cell Host Microbe* (2022) 30(8):1077–83. doi: 10.1016/j.chom.2022.04.07.487489
20. Andreano E, Paciello I, Pierleoni G, Maccari G, Antonelli G, Abbiento V, et al. mRNA vaccines and hybrid immunity use different B cell germlines to neutralize Omicron BA.4 and BA.5. *bioRxiv* (2022) 2022:2008.004.502828. doi: 10.1101/2022.08.04.502828
21. Arora P, Kempf A, Nehlmeier I, Schulz SR, Cossmann A, Stankov MV, et al. Augmented neutralisation resistance of emerging Omicron subvariants BA.2.12.1, BA.4, and BA.5. *Lancet Infect Dis* (2022) 22(8):1117–8. doi: 10.1016/S1473-3099(22)00422-4
22. Bruel T, Stéfic K, Nguyen Y, Toniutti D, Staropoli I, Porrot F, et al. Longitudinal analysis of serum neutralization of SARS-CoV-2 Omicron BA.2, BA.4 and BA.5 in patients receiving monoclonal antibodies. *medRxiv* (2022) 2022:2008.2012.22278699. doi: 10.1101/2022.08.04.22278699
23. Cao Y, Jian F, Wang J, Yu Y, Song W, Yisimayi A, et al. Imprinted SARS-CoV-2 humoral immunity induces convergent Omicron RBD evolution. *bioRxiv* (2022) 2022:2009.2015.507787. doi: 10.1038/s41586-022-05644-7
24. Cao Y, Song W, Wang L, Liu Yue P, Jian C, F, et al. Characterizations of enhanced infectivity and antibody evasion of Omicron BA.2.75. *bioRxiv* (2022) 2022:2007.2018.500332. doi: 10.1016/j.chom.2022.09.018
25. Cao Y, Yisimayi A, Jian F, Jian F, Yisimayi A, Yue C, et al. BA.2.12.1, BA.4 and BA.5 escape antibodies elicited by Omicron infection. *Nature* (2022) 608(7923):593–602. doi: 10.1011/2022.04.30.489997
26. Cao Y, Yu Y, Song W, Dimartino D, Marier C, Zappile P, et al. Neutralizing antibody evasion and receptor binding features of SARS-CoV-2 Omicron BA.2.75. *bioRxiv* (2022) 2022:2007.2018.500332. doi: 10.1016/j.chom.2022.09.018
27. Duerr R, Zhou H, Tada T, Hung AF, Keeffe JR, Gnanapragasam PNP, et al. Delta-Omicron recombinant escapes therapeutic antibody neutralization. *bioRxiv* (2022) 2022:2004.2006.487325. doi: 10.1101/2022.04.06.487325
28. Fan C, Cohen AA, Park M, Hillus D, Sander LE, Kurth F, et al. Neutralizing monoclonal antibodies elicited by mosaic RBD nanoparticles bind conserved sarbecovirus epitopes. *bioRxiv* (2022) 55(12):2419–35. doi: 10.1101/2022.06.28.497989
29. Gruell H, Vanshylla K, Tober-Lau P, Hillus D, Sander LE, Kurth F, et al. Neutralisation sensitivity of the SARS-CoV-2 Omicron BA.2.75 sublineage. *Lancet Infect Dis* (2022) 22(10):1422–3. doi: 10.1016/2022.08.04.502609
30. Iketani S, Liu L, Guo Y, Liu L, Chan JF, Huang Y, et al. Antibody evasion properties of SARS-CoV-2 Omicron sublineages. *Nature* (2022) 604(7906):553–6. doi: 10.1038/s41586-022-04594-4
31. Jian F, Yu Y, Song W, Yisimayi A, Yu L, Gao Y, et al. Further humoral immunity evasion of emerging SARS-CoV-2 BA.4 and BA.5 subvariants. *bioRxiv* (2022) 2022:2008.2009.503384. doi: 10.1101/2022.08.04.502609
32. Kumar S, Patel A, Lai L, Chakravarthy C, Valanparambil R, Reddy ES, et al. Structural insights for neutralization of BA.1 and BA.2 Omicron variants by a broadly neutralizing SARS-CoV-2 antibody. *bioRxiv* (2022) 8(40):eadd2032. doi: 10.1101/2022.05.13.491770
33. Li Y, Shen Y, Zhang Y, Yan R. Structural basis for the enhanced infectivity and immune evasion of Omicron subvariants. *bioRxiv* (2022) 15(6). doi: 10.1101/2022.07.13.499586
34. Lusvarghi S, Pollett SD, Neerukonda SN, Wang W, Wang R, Vassell R, et al. SARS-CoV-2 BA.1 variant is neutralized by vaccine booster-elicited serum but evades most convalescent serum and therapeutic antibodies. *Sci Transl Med* (2022) 14(645):eabn8543. doi: 10.1101/2022.07.13.499586
35. Misasi J, Wei RR, Wang L, Pegu A, Wei CJ, Oloniniyi OK, et al. A multispecific antibody confers pan-reactive SARS-CoV-2 neutralization and prevents immune escape. *bioRxiv* (2022) 2022:2007.2029.502029. doi: 10.1101/2022.07.13.499586
36. Sheward DJ, Kim C, Fischbach J, Sato K, Muschiol S, Ehling RA, et al. Omicron sublineage BA.2.75.2 exhibits extensive escape from neutralising antibodies. *bioRxiv* (2022) 2022:2009.2016.508299. doi: 10.1101/2022.07.13.499586
37. Sheward DJ, Kim C, Fischbach J, Muschiol S, Ehling RA, Björkström NK, et al. Evasion of neutralizing antibodies by Omicron sublineage BA.2.75. *bioRxiv* (2022) 22(10):1421–2. doi: 10.1101/2022.07.19.500716
38. Syed AM, Ciling A, Taha TY, Chen IP, Khalid MM, Sreekumar B, et al. Omicron mutations enhance infectivity and reduce antibody neutralization of SARS-CoV-2 virus-like particles. *Proc Natl Acad Sci USA* (2022) 119(31):e2200592119. doi: 10.1073/pnas.2200592119
39. Takashita E, Yamayoshi S, Simon V, van Bakel H, Sordillo EM, Pekosz A, et al. Efficacy of antibodies and antiviral drugs against Omicron BA.2.12.1, BA.4, and BA.5 subvariants. *N Engl J Med* (2022) 387(5):468–70. doi: 10.1056/NEJMc2207519
40. Takashita E, Yamayoshi S, Fukushima S, Suzuki T, Maeda K, Sakai-Tagawa Y, et al. Efficacy of antiviral agents against the Omicron subvariant BA.2.75. *N Engl J Med* (2022) 387(13):1236–8. doi: 10.1056/NEJMc2209952
41. Turelli P, Fenwick C, Raclot C, Genet V, Pantaleo G, Trono D. P2G3 human monoclonal antibody neutralizes SARS-CoV-2 Omicron subvariants including BA.4 and BA.5 and bebtelovimab escape mutants. *bioRxiv* (2022). doi: 10.1101/2022.07.28.501852
42. Wang Q, Guo Y, Iketani S, Nair MS, Li Z, Mohri H, et al. Antibody evasion by SARS-CoV-2 Omicron subvariants BA.2.12.1, BA.4, & BA.5. *Nature* (2022) 608(7923):603–8. doi: 10.1101/2022.05.26.493517
43. Wang Q, Iketani S, Li Z, Guo Y, Yeh AY, Liu M, et al. Antigenic characterization of the SARS-CoV-2 Omicron subvariant BA.2.75. *Cell Host Microbe* (2022) 30(11):1512–7. doi: 10.1016/j.chom.2022.07.31.502235
44. Wang Q, Li Z, Ho J, Guo Y, Yeh AY, Mohri H, et al. Resistance of SARS-CoV-2 Omicron subvariant BA.4.6 to antibody neutralization. *bioRxiv* (2022) 2022:2009.2005.506628. doi: 10.1101/2022.05.26.493517
45. Westendorff K, Zentelis S, Wang L, Foster D, Vaillancourt P, Wiggins M, et al. LY-CoV1404 (bebtelovimab) potentially neutralizes SARS-CoV-2 variants. *Cell Rep* (2022) 39(7):110812. doi: 10.1016/j.celrep.2022.110812
46. Yamasoba D, Kosugi Y, Kimura I, Fujita S, Urie K, Ito J, et al. Neutralisation sensitivity of SARS-CoV-2 Omicron subvariants to therapeutic monoclonal antibodies. *Lancet Infect Dis* (2022) 22(7):942–3. doi: 10.1016/2022.07.14.500041
47. Yamasoba D, Kimura I, Kosugi Y, Urie K, Fujita S, Ito J, et al. Neutralization sensitivity of Omicron BA.2.75 to therapeutic monoclonal antibodies. *bioRxiv* (2022). doi: 10.1101/2022.07.14.500041
48. Zhang X, Luo F, Zhang H, Guo H, Zhou J, Li T, et al. A cocktail containing two synergistic antibodies broadly neutralizes SARS-CoV-2 and its variants including Omicron BA.1 and BA.2. *bioRxiv* (2022). doi: 10.1101/2022.04.26.489529
49. Zhou T, Wang L, Misasi J, Pegu A, Zhang Y, Harris DR, et al. Structural basis for potent antibody neutralization of SARS-CoV-2 variants including B.1.1.529. *Science* (2022) 376(6591):eabn8897. doi: 10.1126/science.abn8897
50. Zhou H, Dcosta BM, Landau NR, Tada T. Resistance of SARS-CoV-2 Omicron BA.1 and BA.2 variants to vaccine-elicited sera and therapeutic monoclonal antibodies. *Viruses* (2022) 14(6). doi: 10.3390/v14061334
51. Chakraborty S, Saha A, Saha C, Ghosh S, Mondal T. Decoding the effects of spike receptor binding domain mutations on antibody escape abilities of omicron variants. *Biochem Biophys Res Commun* (2022) 627:168–75. doi: 10.1016/j.bbrc.2022.08.050
52. Starr TN, Greaney AJ, Stewart CM, Walls AC, Hannon WW, Veelsler D, et al. Deep mutational scans for ACE2 binding, RBD expression, and antibody escape in the SARS-CoV-2 Omicron BA.1 and BA.2 receptor-binding domains. *bioRxiv* (2022) 2022:2009.2020.508745. doi: 10.1101/2022.03.10.22272100
53. Dougan M, Azizad M, Chen P, Feldman B, Frieman M, Igbinadolor A, et al. Bebtelovimab, alone or together with bamlanivimab and etesevimab, as a broadly neutralizing monoclonal antibody treatment for mild to moderate, ambulatory COVID-19. *medRxiv* (2022). doi: 10.1101/2022.03.10.22272100
54. Razonable RR, O'Horo JC, Hanson SN, Arndt RF, Speicher LL, Seville TA, et al. Outcomes of bebtelovimab treatment is comparable to ritonavir-boosted nirmatrelvir among high-risk patients with Coronavirus Disease-2019 during SARS-CoV-2 BA.2 Omicron Epoch. *J Infect Dis* (2022) 226(10):1683–7. doi: 10.1093/infdis/jiac346
55. Shertel T, Lange NW, Salerno DM, Hedvat J, Jennings DL, Choe JY, et al. Bebtelovimab for treatment of COVID-19 in ambulatory solid organ transplant recipients. *Transplantation* (2022) 106(10):e463–4. doi: 10.1097/TP.0000000000004278
56. Yetmar ZA, Beam E, O'Horo JC, Seville MT, Brumble L, Ganesh R, et al. Outcomes of bebtelovimab and sotrovimab treatment of solid organ transplant recipients with mild-to-moderate coronavirus disease 2019 during the Omicron epoch. *Transpl Infect Dis* (2022):e13901. doi: 10.1111/tid.13901
57. Stadler E, Chai KL, Schlub TE, Cromer D, Polizzotto MN, Kent SJ, et al. Determinants of passive antibody efficacy in SARS-CoV-2 infection. *medRxiv* (2022). doi: 10.1101/2022.03.21.22272672
58. Romani L, Calò Carducci FI, Chiurciu S, Cursi L, De Luca M, Di Giuseppe M, et al. Safety of monoclonal antibodies in children affected by SARS-CoV-2 infection. *Children (Basel)* (2022) 9(3):369. doi: 10.3390/children9030369
59. Management strategies in children and adolescents with mild to moderate COVID-19. American Academy of Pediatrics. Available at: <https://www.aap.org/en/pages/2019-novel-coronavirus-covid-19-infections/clinical-guidance/outpatient-covid-19-management-strategies-in-children-and-adolescents/> (Accessed 1 July 2022).
60. Andreano E, Rappuoli R. SARS-CoV-2 escaped natural immunity, raising questions about vaccines and therapies. *Nat Med* (2021) 27(5):759–61. doi: 10.1038/s41591-021-01347-0
61. Aggarwal NR, Beaty LE, Bennett TD, Carlson NE, Davis CB, Kwan BM, et al. Real-world evidence of the neutralizing monoclonal antibody sotrovimab for preventing hospitalization and mortality in COVID-19 outpatients. *J Infect Dis* (2022) 226(12):2129–36. doi: 10.1101/2022.04.03.22273360

62. Zaqout A, Almaslamani MA, Chemaitelly H, Hashim SA, Ittaman A, Alimam A, et al. Effectiveness of the neutralizing antibody sotrovimab among high-risk patients with mild to moderate SARS-CoV-2 in Qatar. *medRxiv* (2022) 124:96–103. doi: 10.1101/2022.04.21.22274060
63. Georges C, Haider H, Rana V, Asghar Z, Kewalramani A, Kuschner Z. Bebtelovimab-induced bradycardia leading to cardiac arrest. *Crit Care Explor* (2022) 4(8):e0747. doi: 10.1097/CCE.0000000000000747
64. Gill R, Siau E. Colitis after SARS-coV-2 infection. *Cureus* (2022) 14(7):e26532. doi: 10.7759/cureus.26532
65. Smith SW. Sidelining safety — The FDA's inadequate response to the IOM. *N Engl J Med* (2007) 357(10):960–3. doi: 10.1056/NEJMp078157
66. Wang B, Gallolu Kankanamalage S, Dong J, Liu Y. Optimization of therapeutic antibodies. *Antib Ther* (2021) 4(1):45–54. doi: 10.1093/abt/tbab003
67. Huang X, Kon E, Han X, Zhang X, Kong N, Mitchell MJ, et al. Nanotechnology-based strategies against SARS-CoV-2 variants. *Nat Nanotechnol* (2022) 17(10):1027–37. doi: 10.1038/s41565-022-01174-5
68. Sridhara S, Gungor AB, Erol H, KAl-Obaidi M, Zangeneh TT, Bedrick EJ, et al. Lack of effectiveness of Bebtelovimab monoclonal antibody among high-risk patients with SARS-Cov-2 Omicron during BA.2, BA.2.12.1 and BA.5 subvariants dominated era. *PLoS One* (2023) 18(4):e0279326. doi: 10.1371/journal.pone.0279326
69. DeBiasi RL. Immunotherapy for MIS-C - IVIG, glucocorticoids, and biologics. *N Engl J Med* (2021) 385(1):74–5. doi: 10.1056/NEJMe2108276
70. Channon-Wells S, Vito O, McArdle AJ, Seaby EG, Patel H, Shah P, et al. Immunoglobulin, glucocorticoid, or combination therapy for multisystem inflammatory syndrome in children: a propensity-weighted cohort study. *The Lancet Rheumatol* (2023) 5(4):e184–99. doi: 10.1016/S2665-9913(23)00029-2

## Appendix

### Search strategy

#### PubMed, CENTRAL, Embase, Global Health, and PsycInfo

(2019 corona virus) OR (2019 coronavirus) OR (2019 CoV) OR (2019CoV) OR (2019nCoV) OR (2019-nCoV) OR (betacoronavirus) OR (betacoronavir\*) OR (corona virus disease 2019) OR (corona virus\*) OR (coronavir\*) OR (coronavirus disease 2019) OR (coronavirus infection) OR (coronavirus infections) OR (cov 19) OR (CoV 2) OR (Cov19) OR (CoV2) OR (COVID 19) OR (COVID 2019) OR (COVID19) OR (COVID-19) OR (COVID2019) OR (COVID-2019) OR (nCoV) OR (new corona virus) OR (new coronavirus) OR (novel corona virus) OR (novel coronavir\*) OR (novel coronavirus) OR (novel CoV) OR (respiratory distress syndrome) OR (sars virus) OR (sars-coronavirus-2) OR (sarscov2) OR (SARSCoV2) OR (SARS-CoV2) OR (SARS-CoV-2) OR (SARS-CoV-2 variant) OR (SARS-CoV-2 variants) OR (severe acute respiratory syndrome) OR (severe acute respiratory syndrome coronavirus 2) AND (bebtelovimab) OR (LY-CoV1404) OR (LY3853113)Preprint servers of bioRxiv and medRxiv (bebtelovimab) OR (LY-CoV1404) OR (LY3853113).

# Frontiers in Immunology

Explores novel approaches and diagnoses to treat immune disorders.

The official journal of the International Union of Immunological Societies (IUIS) and the most cited in its field, leading the way for research across basic, translational and clinical immunology.

## Discover the latest Research Topics

[See more →](#)

### Frontiers

Avenue du Tribunal-Fédéral 34  
1005 Lausanne, Switzerland  
[frontiersin.org](https://frontiersin.org)

### Contact us

+41 (0)21 510 17 00  
[frontiersin.org/about/contact](https://frontiersin.org/about/contact)

